HR. 1603

ERDA Symposium Series 43

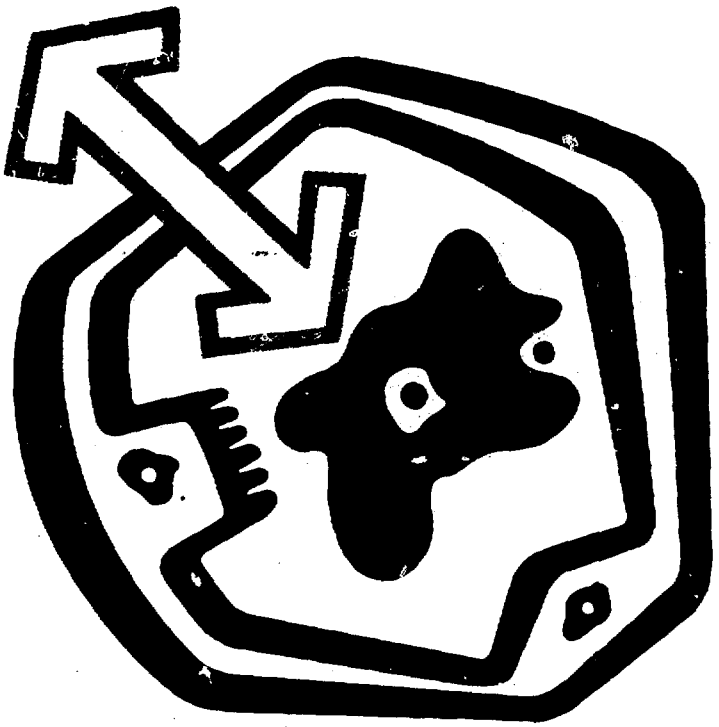

Pulmonary Macrophage and Epithelial Cells

Technical Information Center
Energy Research and Development Administration

CONF-760927

Pulmonary Macrophage and Epithelial Cells

Proceedings of the
Sixteenth Annual Hanford Biology Symposium
at Richland, Washington, September 27—29, 1976

Sponsored by
Division of Biomedical and Environmental Research
Energy Research and Development Administration
and
Pacific Northwest Laboratories
Battelle Memorial Institute

Editors
C. L. Sanders
R. P. Schneider
G. E. Dagle
H. A. Ragan
Pacific Northwest Laboratories

1977

Published by
Technical Information Center
Energy Research and Development Administration

Library of Congress Cataloging in Publication Data

Hanford Biology Symposium, 16th, Richland, Wash., 1976.
Pulmonary macrophage and epithelial cells.

(ERDA symposium series ; 43)
"CONF-760927."
Includes bibliographical references and index.
1. Macrophages—Congresses. 2. Epithelium—Congresses. 3. Lungs—Congresses. I. Sanders, Charles Leonard, 1938- II. United States. Energy Research and Development Administration. Division of Biomedical and Environmental Research. III. Battelle Memorial Institute, Columbus, Ohio. Pacific Northwest Laboratories, Richland, Wash. IV. Title. V. Series: United States. Energy Research and Development Administration. ERDA symposium series ; 43.
[DNLM: 1. Macrophages—Congresses. 2. Lung—Congresses. 3. Epithelial cells—Congresses. W3 HA21 1976p / WF600 H238 1976p]
QR185.8.M3H36 1976 599'.02 77-12024
ISBN 0-87079-204-0

Available as CONF-760927 for $12.50 from

National Technical Information Service
U. S. Department of Commerce
Springfield, Virginia 22161

ERDA Distribution Category UC-48

September 1977

PREFACE

The purpose of this symposium was to assemble reports of current research on the function of, and injury to, selected cell types in mammalian lungs. It has become increasingly apparent that biochemical and functional measurements of whole lung as indices of normal or pathological physiology are frequently of limited value. More than 40 presently recognized cell types are distributed unevenly in the lungs. For studying mechanisms it is necessary to refine the methods used to investigate lungs so that individual cell types are literally, or functionally, isolated for examination.

Pulmonary macrophages are unique in relative ease of the isolation, which has resulted in more rapid progress toward understanding their cell function. Methods for isolating and culturing type II alveolar and endothelial cells are currently being developed; some of these are described in this symposium.

The emphasis of the symposium was on bactericidal, phagocytic, chemotactic, and cytokinetic properties of macrophages; on the biochemistry, fine structure, and cytochemistry of pulmonary epithelium and endothelium; and on techniques of pulmonary cell isolation and study. These experimental approaches were used to better understand the pathophysiological reaction of macrophages and epithelial cells to such diverse toxicants as cotton and asbestos dust, irradiation, oxidant gases, and heavy metals.

We are grateful to the authors and other participants who contributed to the success of this symposium. Special appreciation goes to Judith A. Rising, symposium secretary, to Glenn Horstman, in charge of symposium arrangements, and to Mary N. Hill and Jean Smith of the Editorial Branch, ERDA Technical Infor-

mation Center, Oak Ridge, Tenn., who edited and coordinated the publication of these proceedings.

C. L. Sanders
R. P. Schneider

Cochairmen

CONTENTS

Increased Pulmonary Disease Mediated Through Altered Bacterial Defenses

DONALD E. GARDNER and JUDITH A. GRAHAM
Clinical Studies Division, Health Effects Research Laboratory,
Research Triangle Park, North Carolina

ABSTRACT

The process of infection has been defined as an interaction of a host, a microbe, and the environment. In the natural environment, healthy individuals exist in equilibrium with potentially pathogenic microorganisms. Using this concept, an animal-model system was developed to study the effects of pollutants that can affect this equilibrium and result in acute pulmonary disease. Increase of mortality from exposure to several pathogenic organisms has been reported for a variety of animal species after exposure to ozone, nitrogen dioxide, and a variety of trace metals.

There are a number of possible mechanisms by which the lung can become more vulnerable to microorganisms. These include (1) reduction in deposition or retention of bacteria, (2) slowing of physical removal of bacterial cells by the mucociliary mechanism, (3) dysfunction of the alveolar macrophages, (4) alteration of the acellular lining material (surfactant) of the deep lung, (5) the presence of edema fluid or inflammatory exudate in the airway, and (6) pulmonary immunosuppression. The influence of environmental pollutants on each of these factors is discussed.

For many years it has been apparent that most infectious disease states are not the result of a simple one-to-one cause and effect relationship but instead are a reflection of several different influences acting on the host simultaneously. Establishing an infectious disease requires not only a specific microorganism but additional factors that would render a particular individual vulnerable to microbial invasion. Various factors that weaken host resistance, such as stress,[1-4] preexisting disease,[5] dietary deficiencies,[6] etc., can modify the pathogenesis of the infection. Thus disease is a product of multiple

factors, and the interaction of these factors with the prime etiologic agent has been described as the principle of multiple causality.

Traditionally, environmental toxicologists have been primarily concerned with measuring and describing effects of such single toxic agents[7-11] as O_3, SO_2, and NO_2. More recently, studies have begun to examine the role of multiple pollutants as a modifier of host resistance to experimental infection.

Owing to the inherent problems associated with the study of the effects of pollutants on the susceptibility of the human respiratory system to microbial infection, animal-model systems have been developed to investigate various hypotheses that can later, through appropriate epidemiological surveys, be tested on man. The animal model for this microbe—host interaction system must be a sensitive one for measuring the subtle effects resulting from inhalation of toxic substances. The model should therefore reflect a summation of the varied responses of the respiratory tract, which may include edema, cellular disruption, reduced macrophage function, inflammation, and immunosuppression. The influence of atmospheric pollutants on the microbe—host interaction is difficult to predict because the test substance may increase, decrease, or have no effect on the susceptibility of the host to infection. Also, the host response is dependent on several conditions: (1) the concentration of the pollutant, (2) the physiological state of the host and of the microbial development on and in the host, and (3) the length of time between pollutant exposure and microbial exposure.

A number of different experimental approaches have been used to demonstrate the potential of chemical agents for altering host susceptibility to respiratory infectious agents. One of the most sensitive methods is used by a number of laboratories, including ours, and is called the infectivity model (Fig. 1). Briefly, animals are randomly selected for exposure either to filtered room air or to the test substance. After the cessation of this exposure, the animals from both chambers are combined into a third chamber where they are exposed for approximately 15 min to an aerosol of viable microorganisms. In our laboratory, we routinely use *Streptococcus pyogenes*, Group C. At the termination of this exposure, some animals from each group are sacrificed, and, using standard microbiological techniques, the number of inhaled microorganisms at 0 hr is determined. The remainder of the animals are returned to clean filtered room air, and the rate of mortality in the two groups is determined during a 15-day holding period. The control mortality, which reflects the natural resistance of the host to the infectious agent, is approximately 15 to 20%. This system can also be expanded

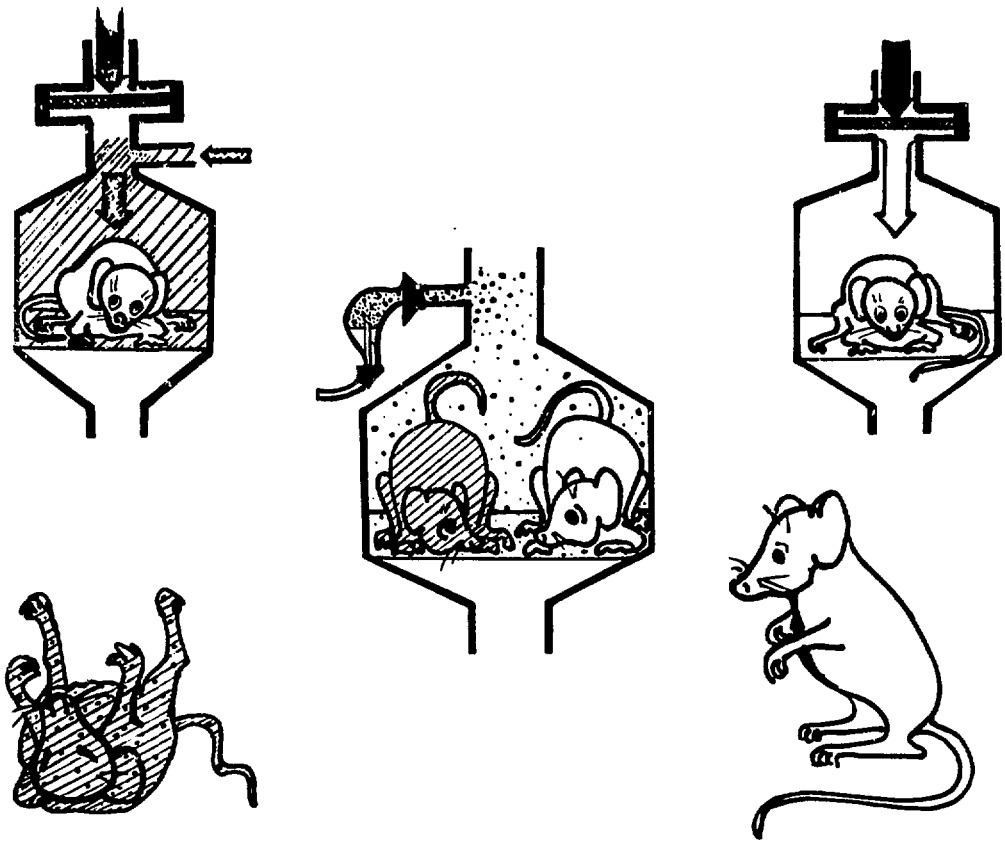

Fig. 1 Infectivity model. Upper left, mouse exposed to pollutant. Upper right, mouse exposed to clean air. Center, pollutant-exposed and air-treated mice challenged with aerosols of bacteria. Lower left, mortality of pollutant-exposed mouse. Lower right, survival of air-exposed mouse.

to permit observation of altered pathogenic modes, relative mean survival time, and cytological indices of isolated lung cells.

For an effective infectivity-model system, the microorganism must fulfill certain criteria. The infectivity model must cause a rather low mortality rate in animals not exposed to the toxicant, and the mortality rate must not be greatly influenced by small variations of bacterial doses or virulence from test to test. Methods must be available for consistently administering the organisms in an aerosol at a concentration and size necessary for pulmonary deposition and for measuring the bacterial dose.

This infectivity-model system, using a number of different microorganisms (*Diplococcus*, *Klebsiella*, *Streptococcus*, influenza virus), has been successfully used with a variety of animal species,

including the mouse,[7-11] rat,[12] hamster[13] and squirrel monkey.[14] Inhalation of a number of noxious gases has been shown to increase mortality in this system.[7-11] As shown in Fig. 2, NO_2 exposure strikingly enhances mortality in mice exposed to streptococci. This family of curves illustrates how the enhancement in mortality can be related to the duration of a continuous exposure at different concentrations of NO_2. Similar studies were performed by Ehrlich,[15] who exposed three species of laboratory animals to NO_2 with a subsequent challenge with *Klebsiella pneumoniae*. Nitrogen dioxide was toxic for all species, and the results also indicate the resistance of each species to the gas and bacteria. Mice were the most sensitive, as evidenced by the data, which showed significant excess mortality at $\geq$ 6.58 mg/m^3 (3.5 ppm). Squirrel monkeys were the least sensitive, with 94.05 mg/m^3 (50 ppm) required for significant effect. Hamsters, which exhibited enhanced mortality at $\geq$ 65.83 mg/m^3 (3.5 ppm), had intermediate sensitivity.

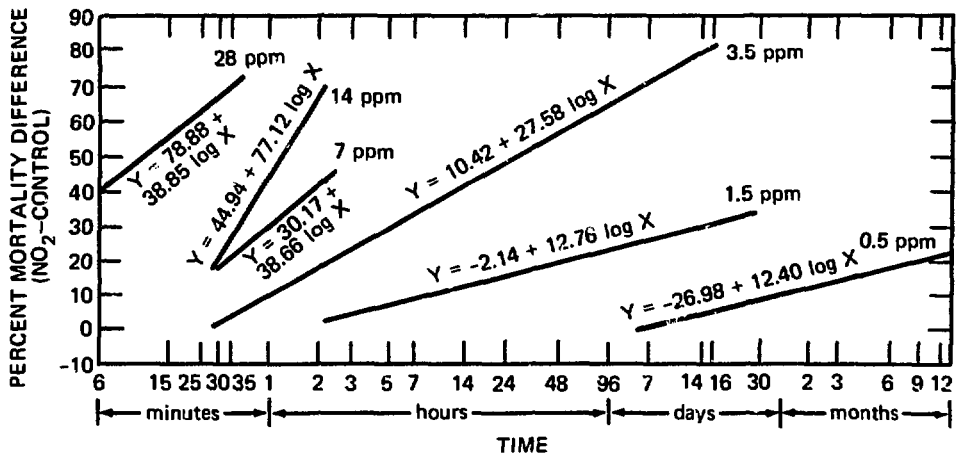

Fig. 2 Percent mortality of mice versus length of continuous exposure to various NO_2 concentrations prior to challenge with streptococci.

Using the infectivity model,[7] experimenters found that exposure of mice to an O_3 concentration between 196 and 392 μg/m^3 (0.1 and 0.2 ppm) and higher for 3 hr also elicits enhancement of mortality (Fig. 3). Various environmental stresses have been shown to further enhance the O_3 effect. Exposure to either reduced or elevated temperatures after a bacterial aerosol challenge results in greater mortality than was produced by either treatment alone.[16]

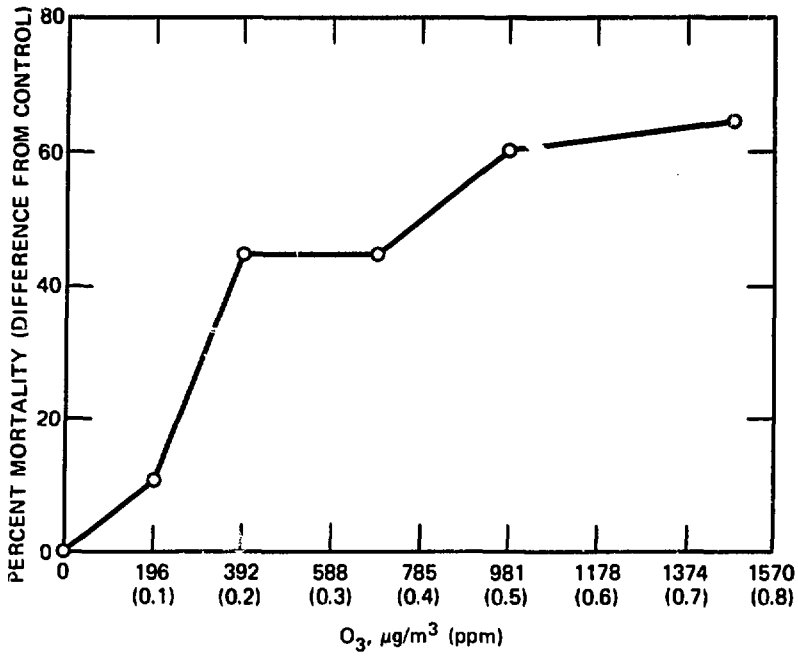

Fig. 3 Effect of a 3-hr exposure to various concentrations of O_3 on mice challenged with aerosols of *Streptococcus*.

Exercise during the exposure of the test animals to either O_3 or NO_2 also appears to enhance the toxicity of the pollutant, as evidenced by increased mortality rates due to infection.[4] Figure 4 illustrates the effect of exercise on mice exposed to NO_2.

Exposure to aerosols of such trace metals[17-19] as $NiCl_2$, PtO_2, and $CdCl_2$ also has a marked proclivity to reduce the ability of the lung to defend itself against microbial insults. As Fig. 5 indicates, an increase of approximately 20% ($p < 0.05$) in percent mortality above controls was observed following a 2-hr exposure to 100 μg Cd/m^3, whereas, with $NiCl_2$, a concentration of 500 μg Ni/m^3 was necessary to obtain a significant increase in mortality. Even though $NiCl_2$ also enhanced the mortality rate, the mechanism of toxicity appears to be somewhat different. When animals that were challenged with viable streptococci immediately were compared to those exposed to the bacteria 24 hr following the nickel treatment, a significantly greater enhancement of mortality was observed in the 24-hr group. No such delay in time effect was observed in the experiment using cadmium.

If host defense mechanisms are functioning normally, there is rapid inactivation of inhaled bacteria that have penetrated and been deposited at the alveolar level.[20-26] However, quite the opposite occurs in pollutant-exposed animals. The number of microbes in the

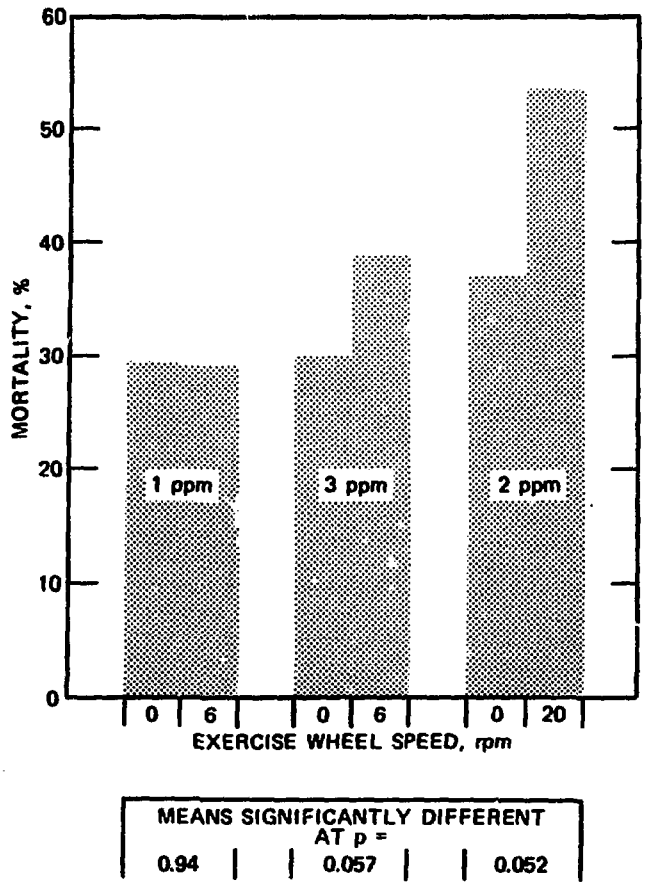

Fig. 4 Influence of exercise on NO_2 toxicity using the infectivity-model system. Mice were exposed to various concentrations of NO_2 for 3 hr, with and without exercise (running on a wheel at the indicated rpm) prior to an aerosol of *Streptococcus*.

lungs of exposed mice quickly multiply and soon increase beyond the original number deposited[7,17,19] (Fig. 6). This acceleration in the rate of bacterial growth has been attributed to the pollutant's alteration of the capability of the lungs to destroy bacteria so as to permit those with pathogenic potential to multiply and produce disease. Such a concept is supported by the work of Goldstein et al.,[21-23] who exposed mice to O_3 and NO_2 alone and together and to aerosols of radiolabeled staphylococci. Their results indicate that these pollutants are capable of reducing the bactericidal activity of the lung. Higher O_3 levels actually resulted in a net multiplication of bacteria. Thus the role of environmental agents in the pathogenesis of infectious pulmonary disease may be mediated through an

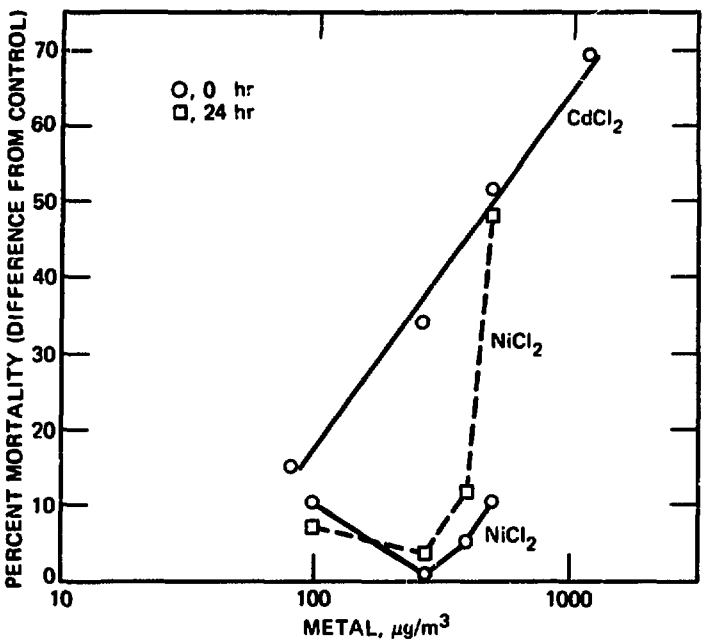

Fig. 5 Toxicity of a 2-hr aerosol exposure to various concentrations of $CdCl_2$ and $NiCl_2$ using the infectivity-model system. ○, mice challenged with an aerosol of *Streptococcus* immediately following metal exposure. □, mice challenged with an aerosol of *Streptococcus* 24 hr following metal exposure.

impairment of integrated pulmonary-host defense functions that maintain sterility in the deep lung.

A number of possible mechanisms can be proposed which might aid in explaining how gaseous and particulate pollutants reduce the ability of the lung to defend itself against the growth of these inhaled microbes. These mechanisms include (1) production of edema, (2) reduction in physical removal by mucociliary mechanisms, and/or (3) alteration of specific cellular defense mechanisms. Each of these possible mechanisms has been studied, and the data obtained provide information that aids in explaining the enhancement of infectivity phenomena.

First, if the test substance caused an influx of edema fluid into the lung, this would provide an ideal culture medium for microbial growth. Tests were designed to determine if edema might play a major role in the enhancement of pulmonary infection. These experiments used O_3, which has been shown to be edemagenic and which also causes enhancement of infections. This study was based on findings of numerous investigators who have reported that, by

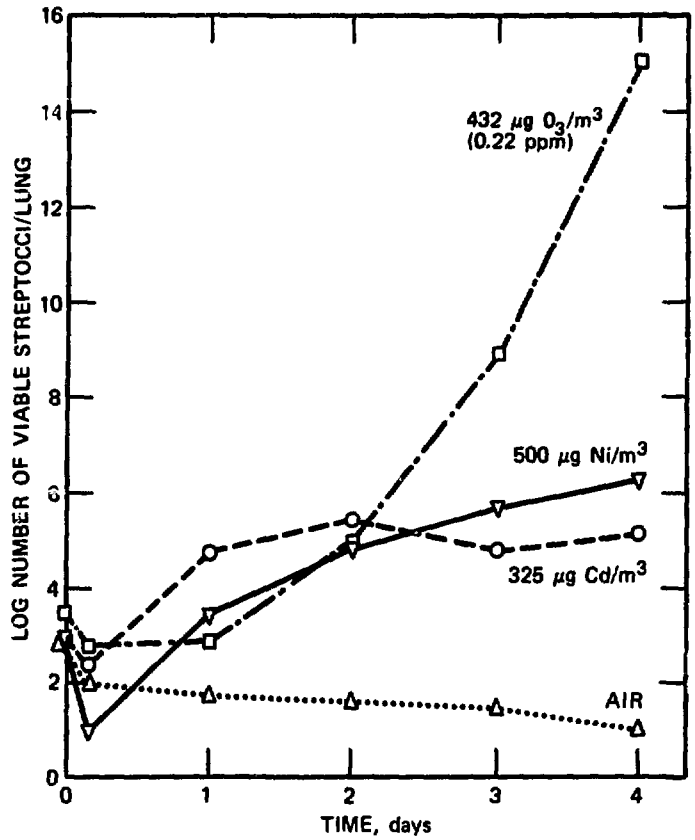

Fig. 6 Growth of streptococci in the lungs of mice exposed to O_3 for 3 hr, metal aerosols for 2 hr, or air for 2 hr prior to challenge with aerosols of bacteria.

repeating O_3 exposures, a protective state (tolerance) against the subsequent production of edema[3,27,28] can be produced. In these classical studies, preexposure to a tolerant dose of O_3 protects the animal from death due to exposure to an acute toxic concentration of O_3 by significantly reducing edemagenesis.[29,30] When experiments were conducted to detect changes in infectivity with a system designed to elicit tolerance, the tolerant animals showed only partial reductions in mortality, compared to animals receiving a single O_3 exposure. Figure 7 illustrates that the mortality is reduced only about one-half in animals preexposed to a tolerant dose of O_3 at a concentration of 588 $\mu g/m^3$ (0.3 ppm) or higher. At 196 $\mu g/m^3$ (0.1 ppm), there is no significant difference imparted by the preparatory or tolerance-eliciting exposure. These results differ significantly from the classical criteria of edema formation used in tolerance studies.

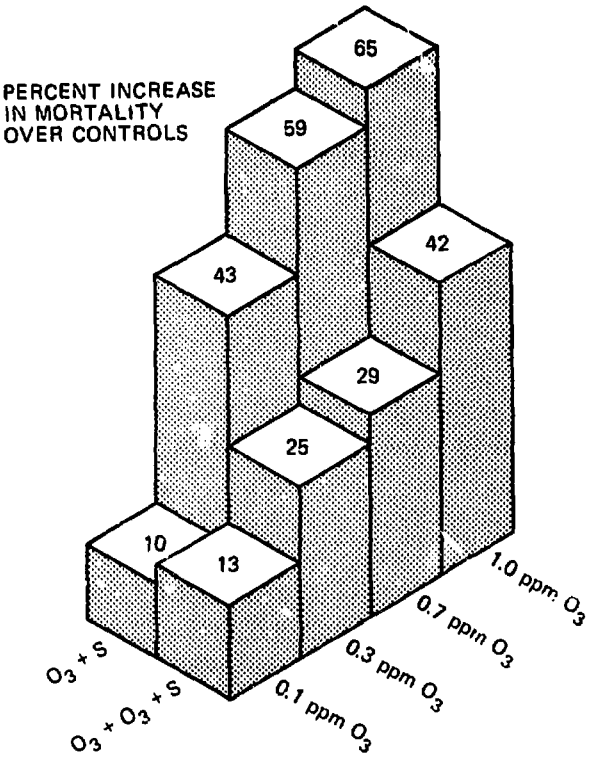

Fig. 7 Influence of a tolerance-inducing dose of O_3 on the infectivity-model system at various O_3 concentrations. O_3 + S, 3 hr of O_3 prior to streptococcal challenge. O_3 + O_3 + S, 3 hr of O_3, 24 hr of clean air, and 3 hr of O_3 prior to streptococcal challenge.

If tolerance were as effective in preventing pulmonary infection as it is in preventing edema, a complete protection against mortality should be evident. That is, the percent increase in mortality over non-O_3-exposed controls should be essentially zero. The data suggest that, since there is partial protection, O_3 may be affecting specific body defenses (possibly alveolar macrophages) which are not protected by the phenomenon of tolerance. This is in agreement with earlier studies by Gardner et al.[31] which showed that preexposure to O_3 produced a tolerance against pulmonary edema but had no protective effect against the cytotoxic effects of O_3 on alveolar macrophages, such as reduction in numbers, viability, and hydrolytic enzyme activities. Another reason why edema does not appear to be solely responsible for the microbial growth in the lung is that enhancement of respiratory infections has been shown at levels[7] lower than those which produce edema in experimental animals.[32]

A second mechanism by which environmental contaminants may impair host defenses possibly occurs through the alteration of the mucociliary escalator, which could lead to increased bacterial burdens in the lung. Adalis et al.[33,34] studied the beating frequency of cilia isolated from the trachea of hamsters that were exposed to aerosols of $CdCl_2$ or $NiCl_2$. Although these metals reduced the ciliary activity, the metal concentrations that produced these effects were lower than the concentrations that enhance mortality in the infectivity model. Thus the slowing of ciliary beating does not appear to be the sole cause of the increased bacterial growth observed in the infectivity system. The lack of relationship between defects in the mucociliary escalator and increased bacterial growth is also evident from studies by other investigators, such as Rylander,[35] Kim et al.,[24] Kass, Green, and Goldstein,[20] Goldstein, Lippert, and Warshauer,[26] and Green and Goldstein.[25] Green and Kass,[36] using radiolabeled microorganisms, found that physical removal could account for only a small fraction (15 to 20%) of the total bacteria cleared from the lung over a 4-hr period. These studies clearly demonstrate that the loss of viable microorganisms results primarily from in situ bactericidal activity rather than from mechanical removal.

After we discount the defects in the physical removal and the edema production as the only causes of enhanced bacterial growth in the lungs of pollutant-exposed animals, just one major protective mechanism remains—that of biological clearance. This type of clearance primarily reflects the role of the alveolar macrophage. An interesting in vivo model described by Green and Goldstein[25] and Kim et al.[24] supports this classical contention. In this system, mice were exposed to aerosols of *Staphylococcus aureus*, and the intra- or extracellular locations of bacteria were determined histologically in the right lung, and the number of viable organisms were determined bacteriologically in the left lung. These investigators showed that phagocytosis of the staphylococci by alveolar macrophages precedes and roughly parallels the actual clearance of the bacteria for a time period of less than 2.5 hr. After this time, phagocytosis reaches a plateau, whereas bactericidal activity continues to increase. Since the alveolar macrophage is therefore primarily responsible for biological clearance, bacterial growth in the lungs due to pollutant exposure is probably a reflection of decreased pulmonary bactericidal ability, which, in turn, is caused by dysfunction of alveolar macrophages.

Pollutant-exposed alveolar macrophages have been the subject of intensive investigation. Aranyi et al.[37] and Waters et al.[38] used scanning electron-microscopy techniques to demonstrate direct

surface alteration of alveolar macrophages caused by exposure to O_3, NO_2, O_2 and a number of trace metals.

Figure 8 illustrates membrane alterations of alveolar macrophages exposed to O_3 and NO_2. The authors conclude that such morphological data may be useful in detecting changes that precede cell death. Experiments conducted in our laboratory have indicated that in vivo exposure to such pollutants as O_3 (Refs. 7 and 39), NO_2 (Ref. 40), and $CdCl_2$ (Ref. 19) have the potential to produce decrements in number, viability, phagocytic activity, and enzymatic activity in macrophages obtained by pulmonary lavage. Bingham et al.[41,42] measured the total number of available alveolar macrophages lavaged from rats exposed to $PbCl_2$, $NiCl_2$, Pb_2O_3, and NiO. The NiO produced a significant increase in the number of free cells, and the Pb_2O_3 resulted in fewer cells. The other two substances did not significantly change the number of available cells.

In vitro studies performed on alveolar macrophages have substantiated many of the above cytotoxic effects with O_3 (Ref. 43), cigarette smoke (Ref. 44), V_2O_5 (Refs. 38, 45, and 46), $MnCl_2$ (Refs. 38 and 45), $NiCl_2$ (Refs. 38 and 45), $CdCl_2$ (Refs. 38 and 45), $CrCl_3$ (Refs. 38 and 45), NO_2 (Refs. 47 and 48), and ethanol (Ref. 49).

In addition to the direct action of the pollutant on the alveolar macrophages, it is also possible that some pollutant toxicity to the alveolar macrophages could be mediated through an indirect effect. Gil and Weibel[50] demonstrated that, within the lung, the alveolar macrophages and the acellular lining substance are intimately associated. Alveolar macrophages appear to be immersed in this substance. Figure 9 is a dose-response curve that illustrates the effect of the in vivo action of O_3 on the stability of alveolar macrophages in vitro.[51] When normal alveolar macrophages are resuspended in normal acellular lavage fluid, the number of cells remain relatively stable (15% lysis) over a 4.5-hr test period. However, if these same normal cells are placed in lavage fluid from animals exposed to O_3 for 3 hr, an increase in cell lysis occurs over the 4.5-hr test period. If both the macrophages and the lavage fluid are from animals exposed to O_3, then stability is severely affected. Figure 10 illustrates that similar effects can be produced when normal lavage fluid is exposed in vitro to O_3 for 30 min. For these in vitro experiments to be valid, the measured response must be due to the action of O_3 on the fluid itself and not due merely to the physical action of bubbling. Table 1 shows the percent of alveolar macrophages remaining after various times when other gases (room air, nitrogen, carbon dioxide) were bubbled through the lavage fluid for a 30-min period. There was no statistically significant difference between normal lavage fluid and

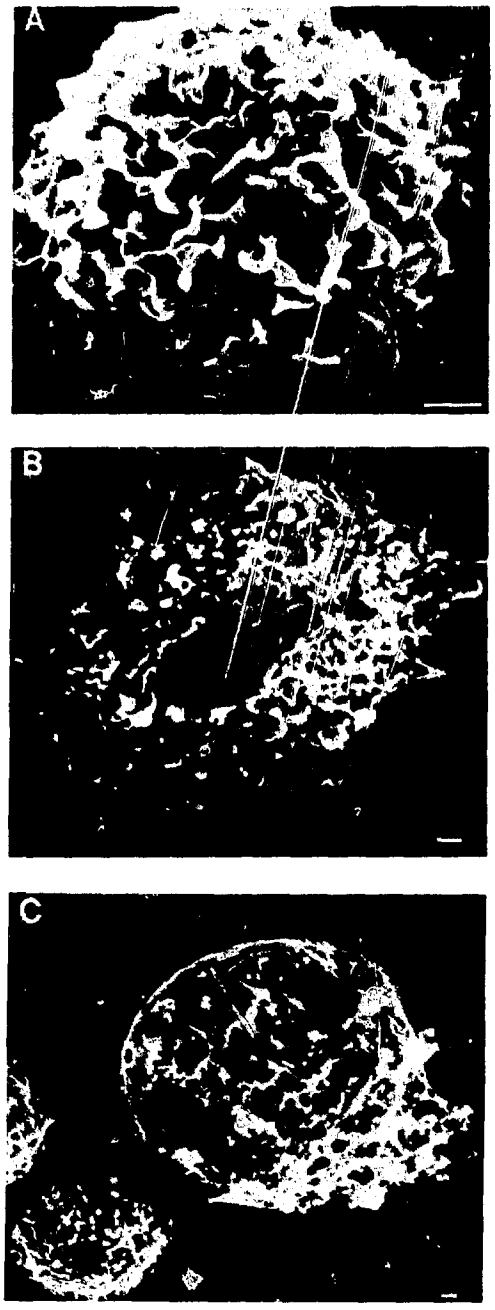

Fig. 8 Scanning electron-microscopic view of alveolar macrophages. Bars represent 1 μm. (A) Alveolar macrophages from a mouse exposed to filtered air. (B) Alveolar macrophages from a mouse exposed to 940.5 $\mu g/m^3$ (0.5 ppm NO_2) continuously for 21 wk with 1-hr peaks of 3762 $\mu g/m^3$ (2 ppm NO_2) five times a week. (C) Alveolar macrophages from a rabbit exposed to 5780 $\mu g/m^3$ (3 ppm O_3) for 3 hr.

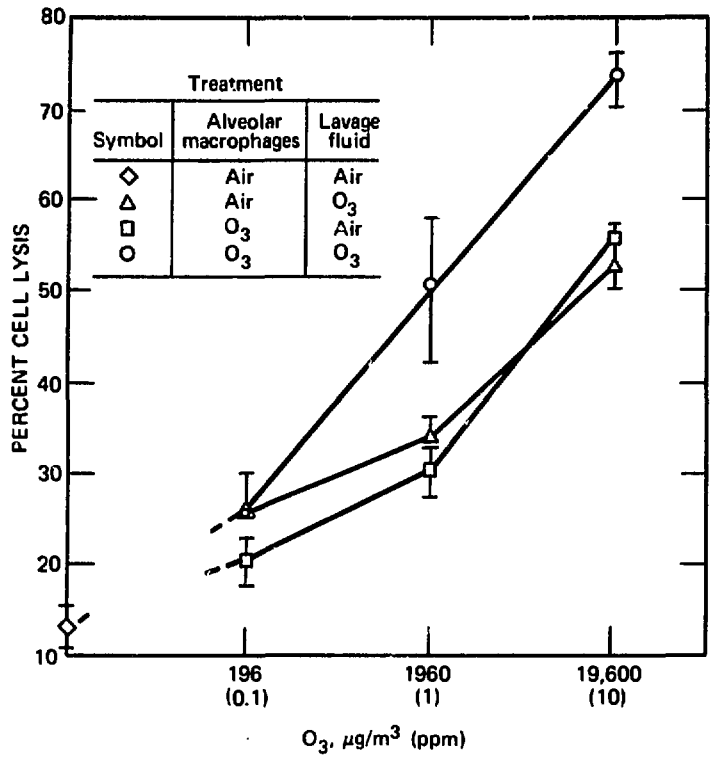

Fig. 9 Influence of various concentrations of O_3 on the percent cell lysis of alveolar macrophages from air- and O_3-exposed rabbits maintained in pulmonary lavage fluids from both air- and O_3-exposed rabbits. Animals were exposed for 3 hr. Points on the graph are mean level ± standard error.

lavage fluid exposed to nitrogen or carbon dioxide. The exposure to filtered room air appeared to affect the stability of the alveolar macrophage, but not to the same extent as O_3. Thus the increase in cell lysis appears to be due to the direct action of O_3 on the protective factor, which, in turn, results in secondary lysis of the alveolar macrophages.

Studies were also conducted to determine what effect the lavage fluid might have on the ability of the alveolar macrophage to phagocytize yeast cells (*Saccharomyces cerevisiae*)[5 1] (Table 2). Normal macrophages that were suspended in saline phagocytized the least (31%), but, as was expected, the phagocytosis was improved by the addition of 20% rabbit serum to the physiological saline. There was no significant difference in the phagocytic ability of alveolar macrophages in normal lavage fluid, as compared to in vitro O_3-treated (19,600 $\mu g/m^3$, 10 ppm) lavage fluid. The alveolar

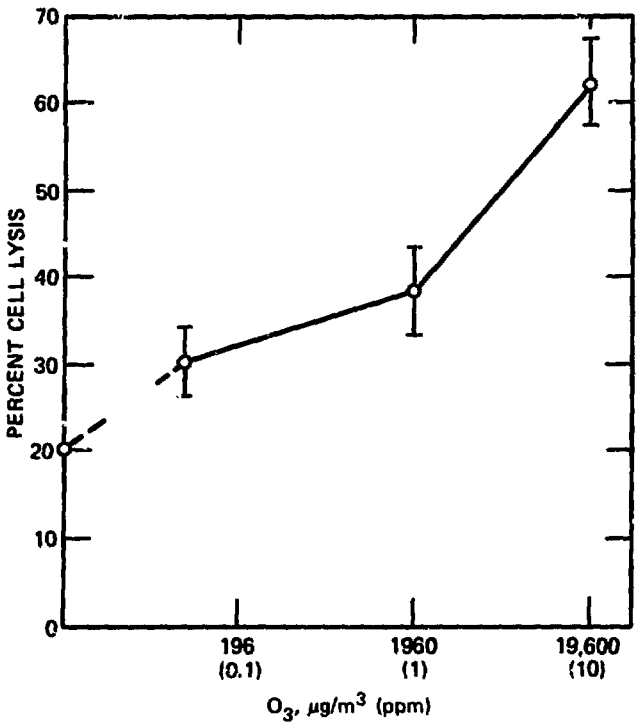

Fig. 10 Percent cell lysis of alveolar macrophages from air-exposed rabbits maintained in pulmonary lavage fluid treated with the indicated concentrations of O_3 for 30 min.

TABLE 1

INTEGRITY OF ALVEOLAR MACROPHAGES FROM NORMAL RABBITS MAINTAINED IN NORMAL LAVAGE FLUID TREATED WITH DIFFERENT GASES FOR 30 min

(Values Are Expressed as Mean ± Standard Error)

Suspended in	Percent of cells remaining at 4.5 hr
L.F.*	81.0 ± 1.2
L.F. + N_2	76.6 ± 3.6
L.F. + CO_2	76.6 ± 1.7
L.F. + room air	68.5 ± 4.0
L.F. + O_3	35.0 ± 4.0

*L.F. = lavage fluid.

TABLE 2

PHAGOCYTIC CAPABILITY OF NORMAL ALVEOLAR MACROPHAGES MAINTAINED IN VARIOUS LAVAGE FLUIDS

(Values Are Expressed as Mean Level ± S.E.*)

Normal cells suspended in	10^6 alveolar macrophages per milliliter ($\bar{X}$† ± S.E.)		Percent of alveolar macrophages remaining at 1 hr ($\bar{X}$ ± S.E.)	Alveolar macrophages/yeast ratio ($\bar{X}$ ± S.E.)		Percent of alveolar macrophages with yeast ($\bar{X}$ ± S.E.)
	0 hr	1 hr		0 hr	1 hr	
Normal L.F.‡	3.63 ± 0.30	3.23 ± 0.31	88.5 ± 1.7	1:26 ± 3	1:29 ± 3	43.8 ± 3.4
Ozone L.F. in vivo	3.54 ± 0.26	2.71 ± 0.27	76.1 ± 2.8	1:26 ± 3	1:35 ± 4	80.8 ± 3.8
Ozone L.F. in vitro	2.92 ± 0.45	2.90 ± 0.29	72.2 ± 1.9	1:34 ± 6	1:47 ± 8	46.2 ± 8.1
Saline	2.55 ± 0.38	1.69 ± 0.31	66.8 ± 6.8	1:41 ± 10	1:66 ± 14	30.8 ± 3.6
Saline + 20% rabbit serum	2.42 ± 0.11	2.2 ± 0.11	90.9 ± 0.4	1:40 ± 2	1:44 ± 2	58.5 ± 3.9

*S.E. = standard error.
†$\bar{X}$ = mean level.
‡L.F. = lavage fluid.

macrophages exhibiting the greatest phagocytic activity (81%) were those normal macrophages which were maintained in lavage fluid harvested from rabbits exposed to 19,600 $\mu g/m^3$ (10 ppm) of O_3 for 2.5 hr. This twofold increase in phagocytosis, as compared to those suspended in normal or in vitro-treated lavage fluid, was thought to be due to an increased protein content of the edema fluid, a typical pulmonary response to this high level of O_3. As this experiment showed, the addition of serum to physiological saline increased the phagocytic ability from 31 to 58%. It was interesting to observe that exposure to O_3 did not adversely affect the phagocytic functioning of normal alveolar macrophages in vitro, but it must be pointed out that, in obtaining the phagocytic index, only remaining intact macrophages were counted. As Table 2 shows, the alveolar macrophages that were held either in O_3-treated lavage fluid or in saline had fewer cells remaining, as compared to those alveolar macrophages which were held in normal lavage fluid.

Other studies have been conducted with this pulmonary protective factor. The data of LaForce, Keely, and Huber[52] suggest that this protective factor can also stimulate the bactericidal activity of alveolar macrophages against *Staphylococcus aureus*. Without the isolated alveolar lining material, no bactericidal effect could be shown. From these studies it becomes important for toxicologists to consider the interaction of environmental pollutants with the intrapulmonary milieu, as well as the cells in the lung, before assuming that the pollutant has a direct action on the alveolar macrophages.

Most of the foregoing discussion has centered on the "classical" role of alveolar macrophage phagocytosis and bacterial lysis, but the possible role of pollutant-induced immunosuppression cannot be ignored; the possible importance of the immune system to pulmonary defense must be considered. Although the actual role of the alveolar macrophages in the pulmonary immune system is still a matter of debate, several investigations provide data on this topic. Seeger and Oppenheim,[53] and Ulrich[54] have demonstrated that alveolar macrophages can enhance immune responses of lymphocytes. Other work by Martin and Laughter[55] showed that alveolar macrophages from cigarette smokers were less able to stimulate lymphocyte activity. Most of the knowledge in the area of pollutant effect on the respiratory immune system is derived from the work of Zarkower,[56] who exposed mice to various air pollutants prior to an aerosol immunization with *Escherichia coli*. Long-term exposure to SO_2 and carbon and to carbon + SO_2 reduced serum antibody titers, and, in addition, the treatment of carbon + SO_2 caused a reduction

in antibody-producing cells in the mediastinal lymph nodes that drain the lung. Miller and Zarkower[5 7] also reported that aerosols of SiO_2 were capable of reducing the functioning of lymphocytes and the number of antibody-forming cells in the mediastinal lymph nodes, and, again, serum antibody titers were reduced. Since this silica-dust treatment also depressed phagocytosis by alveolar macrophages, it is possible that some of these immunosuppressive effects were mediated through the cytotoxic effects of SiO_2 on alveolar macrophages.

Perhaps the difficulty in determining the actual mechanism responsible for the pollutant-induced increase of bacterial growth in the lung and subsequent mortality observed in the infectivity-model system is because there are many possible causes for this phenomenon. It is probable that the large number of pathophysiological changes that occur following pollutant exposure can alter an individual's homeostatic balance, yielding a reduced capacity to recuperate from pulmonary infectious challenges.

As is obvious from this discussion, much more information is needed to determine the total range of the functions of alveolar macrophages and the impact of pollutants on these essential cells.

The papers presented at this symposium and in this session will elucidate some of these problem areas. Many of the papers describe investigations of the mechanisms involved in several macrophage functions. The secretory role of alveolar macrophages was studied from the standpoint of release of any possible chemotactic factors and lysosomal enzymes. This latter research has a bearing on another paper in these proceedings which describes the extracellular lysis of bacteria by secreted lysozyme. One work dealing with the renewal of alveolar macrophage populations is also reported.

The results from these research efforts are particularly relevant to the understanding of pollutant effects on the alveolar macrophage, which is the subject of a number of other papers in these proceedings. Phagocytic functioning was investigated following exposure of alveolar macrophages to cigarette smoke and tobacco substitutes and to fly-ash particles coated with metal oxides. Alveolar macrophages from O_3- and NO_2-treated animals were used in studies of membrane receptors, which may be involved in cell recognition and phagocytosis. Other research described involved such parameters as cytostructure, enzymes, tritiated thymidine uptake, and numbers of alveolar macrophages in animals exposed to both clean air and NO_2.

The work reported at this session presents interesting and important information on the functioning of the alveolar macro-

phages and the serious hazards that pollutants present to these important cells. As with all excellent research, we will leave here with more questions than answers, but we still will have advanced ourselves on the continuum of knowledge.

REFERENCES

1. G. M. Green, Lung Defense Mechanisms, *Med. Clin. North Am.*, 57: 547-562 (1973).
2. G. M. Green and E. H. Kass, The Influence of Bacterial Species on Pulmonary Resistance to Infection in Mice Subjected to Hypoxia, Godstress and Ethanolic Intoxication, *Br. Pathol.*, 46: 360-366 (1965).
3. H. R. Stokinger, W. D. Wagner, and P. G. Wright, Studies of O_3 Toxicity. I. Potentiating Effects of Exercise and Tolerance Development, *Arch. Ind. Health*, 14: 158 (1956).
4. D. E. Gardner, J. W. Illing, F. J. Miller, and D. L. Coffin, Enhancement of Effect of Exposure to Ozone and Nitrogen Dioxide by Exercise (abstract), *Toxicol. Appl. Pharmacol.*, 29: 129 (1974).
5. E. Goldstein, G. M. Green, and C. Seamans, Effect of Acidosis on Pulmonary Bacteriocidal Function, *J. Lab. Clin. Med.*, 75: 912-923 (1970).
6. D. Warshauer, E. Goldstein, P. D. Hoeprich, and W. Lippert, Effect of Vitamin E and O_3 on the Pulmonary Antibacterial Defense Mechanism, *J. Lab. Clin. Med.*, 83: 228-240 (1974).
7. D. L. Coffin and D. E. Gardner, Interaction of Biological Agents and Chemical Air Pollutants, *Ann. Occup. Hyg.*, 15: 219-234 (1972).
8. G. A. Fairchild, J. Roan, and J. McCarroll, Effect of Sulfur Dioxide on the Pathogenesis of Murine Influenza Infection, *Arch. Environ. Health*, 25: 174-182 (1972).
9. M. R. Purvis and R. Ehrlich, Effect of Atmospheric Pollutants on Susceptibility to Respiratory Infection. II. Effect of Nitrogen Dioxide, *J. Infect. Dis.*, 113: 72-76 (1963).
10. R. Ehrlich, Effect of Air Pollutants on Respiratory Infection, *Arch. Environ. Health*, 6: 638-642 (1963).
11. D. L. Coffin, D. E. Gardner, and E. J. Blommer, Time—Dose Response in an Infectivity Model System, *Environ. Health Perspect.*, 13: 11-15 (1976).
12. Earl Blommer, personal communication, Environmental Protection Agency, Health Effects Research Laboratory, 1976.
13. R. Ehrlich, Effect of Nitrogen Dioxide on Resistance to Respiratory Infection, *Bacteriol. Rev.*, 30: 604-614 (1966).
14. M. C. Henry, J. Findlay, J. Spangler, and R. Ehrlich, Chronic Toxicity of NO_2 in Squirrel Monkeys, *Arch. Environ. Health*, 20: 566-570 (1970).
15. R. Ehrlich, Interaction Between Nitrogen Dioxide Exposure and Respiratory Infection, Scientific Seminar on Automotive Pollutants, EPA Publication No. 600/9-75-003, Environmental Protection Agency, 1975.
16. D. L. Coffin and E. J. Blommer, Acute Toxicity of Irradiated Auto Exhaust. Its Indication by Enhancement of Mortality from Streptococcal Pneumonia, *Arch. Environ. Health*, 15: 36-38 (1967).
17. B. Adkins and D. E. Gardner, Effect of Nickel on the Enhancement of Induced Streptococcal Infections, *Proc. Am. Soc. Microbiol.* (abstract B-45): 18 (1976).

18. J. D. Fenters, S. Vana, R. Ehrlich, and D. E. Gardner, Effect of Platinum and Palladium in a Mouse Infectivity Model, in Proceedings of the International Conference on Heavy Metals in the Environment, Ottawa, Canada, 1975.
19. D. E. Gardner, F. J. Miller, J. W. Illing, and J. M. Kirtz, Alterations in Bacterial Defense Mechanisms of the Lung Induced by Inhalation of Cadmium, *Bulletin Europeén de Physiopathologie Respiratoire*, 13: 157-174 (1977).
20. E. H. Kass, G. M. Green, and E. Goldstein, Mechanisms of Antibacterial Action in the Respiratory System, *Bacteriol. Rev.*, 30: 488-497 (1966).
21. E. Goldstein, W. S. Tyler, P. D. Hoeprich, and M. C. Eagle, Ozone and the Antibacterial Defense Mechanisms of the Murine Lung, *Arch. Intern. Med.*, 127: 1099-1102 (1971).
22. E. Goldstein, M. C. Eagle, and P. D. Hoeprich, Effect of Nitrogen Dioxide on Pulmonary Bacterial Defense Mechanisms, *Arch. Environ. Health*, 26: 202-204 (1973).
23. E. Goldstein, D. Warshauer, W. Lippert, and B. Tarkington, Ozone and Nitrogen Dioxide Exposure. Murine Pulmonary Defense Mechanisms, *Arch. Environ. Health*, 28: 85-90 (1974).
24. M. Kim, E. Goldstein, J. P. Lewis, W. Lippert, and D. Warshauer, Murine Pulmonary Alveolar Macrophages: Rates of Bacterial Ingestion, Inactivation and Destruction, *J. Infect. Dis.*, 133: 310-320 (1976).
25. G. M. Green and E. Goldstein, A Method for Quantitating Intrapulmonary Bacterial Inactivation in Individual Animals, *J. Lab. Clin. Med.*, 68: 669-677 (1966).
26. F. Goldstein, W. Lippert, and D. Warshauer, Pulmonary Alveolar Macrophage: Defender Against Bacterial Infection of the Lung, *J. Clin. Invest.*, 54: 519-528 (1974).
27. F. J. Fairchild II, Tolerance Mechanisms. Determinants of Lung Responses to Injurious Agents, *Arch. Environ. Health*, 74: 111-126 (1967).
28. D. L. Coffin and D. E. Gardner, Role of Tolerance in Protection of the Lung Against Secondary Insults, in Proceedings of the International Symposium of Occupational Physicians of the Chemical Industry, Ludwigshafen, Germany, 1972, pp. 344-364.
29. H. R. Stokinger and L. D. Scheel, Ozone Toxicity: Immunochemical and Tolerance-Producing Aspects, *Arch. Environ. Health*, 4: 327-334 (1962).
30. R. N. Matzen, Development of Tolerance to Ozone in Reference to Pulmonary Edema, *Am. J. Physiol.*, 190: 84-88 (1957).
31. D. E. Gardner, T. R. Lewis, S. M. Alpert, D. J. Hurst, and D. L. Coffin, The Role of Tolerance in Pulmonary Defense Mechanisms, *Arch. Environ. Health*, 25: 432-438 (1972).
32. S. M. Alpert, B. B. Schwartz, S. D. Lee, and T. R. Lewis, Alveolar Protein Accumulation: A Sensitive Indicator of Low Level Oxidant Toxicity, *Arch. Intern. Med.*, 128: 69-73 (1971).
33. D. Adalis, D. E. Gardner, F. J. Miller, and D. L. Coffin, Toxic Effects of Cadmium on Ciliary Activity Using a Tracheal Ring Model System, *Environ. Res.* (in press).
34. D. Adalis, F. J. Miller, and D. E. Gardner, Cytotoxic Effects of Nickel on Hamster Tracheal Ring Organ Cultures, in preparation.
35. R. Rylander, Pulmonary Defense Mechanisms to Airborne Bacteria, *Acta Physiol. Scand. (Suppl.)*, 306: 1-89 (1968).

36. G. M. Green and E. H. Kass, Factors Influencing the Clearance of Bacteria by the Lung, *J. Clin. Invest.*, 43: 769-776 (1964).
37. C. Aranyi, J. Fenters, R. Ehrlich, and D. E. Gardner, Scanning Electron Microscopy of Alveolar Macrophages After Exposure to Oxygen, Nitrogen Dioxide, and Ozone, *Environ. Health Perspect.* (in press).
38. M. D. Waters, D. E. Gardner, C. Aranyi, and D. L. Coffin, Metal Toxicity for Rabbit Alveolar Macrophages In Vitro, *Environ. Res.*, 9: 32-47 (1975).
39. D. J. Hurst, D. E. Gardner, and D. L. Coffin, Effect of Ozone on Acid Hydrolases of the Pulmonary Alveolar Macrophage, *J. Reticuloendothel. Soc.*, 8: 288-300 (1970).
40. D. E. Gardner, R. S. Holzman, and D. L. Coffin, Effects of Nitrogen Dioxide on Pulmonary Cell Population, *J. Bacteriol.*, 98: 1041-1043 (1969).
41. E. Bingham, W. Barclay, M. Zerwas, K. Stemmer, and P. Taylor, Responses of Alveolar Macrophages to Metals. I. Inhalation of Lead and Nickel, *Arch. Environ. Health*, 25: 406-414 (1972).
42. E. Bingham, Trace Amounts of Lead in the Lung, in Trace Substances in Environmental Health. III, D. D. Hemphill (Ed.), pp. 83-90, University of Missouri, Columbia, 1969.
43. D. Hurst and D. L. Coffin, Effects of Ozone on Lysosomal Hydrolases of Alveolar Macrophages In Vitro, *Arch. Intern. Med.*, 127: 1059-1063 (1971).
44. G. M. Green and D. Carolin, The Depressant Effect of Cigarette Smoke on the In Vitro Antibacterial Activity of Alveolar Macrophages, *New Engl. J. Med.*, 276: 421-427 (1967).
45. J. A. Graham, D. E. Gardner, M. D. Waters, and D. L. Coffin, Effect of Trace Metals on Phagocytosis by Alveolar Macrophages, *Infect. Immun.*, 11: 1278-1283 (1975).
46. M. D. Waters, D. E. Gardner, and D. L. Coffin, Cytotoxic Effects of Vanadium on Rabbit Alveolar Macrophages In Vitro, *Toxicol. Appl. Pharmacol.*, 28: 253-263 (1974).
47. C. Voisin, C. Aerts, and J. L. Houdret, Method for Studying the Effects of NO_2 on Guinea Pig Alveolar Macrophages Surviving In Vitro, *Rev. Fr. Mal. Respir. (Paris), (Suppl. 1)*: 93-97 (1974).
48. C. L. Vassallo, B. M. Domm, R. H. Poe, M. L. Doncombe, and J. B. L. Gee, NO_2 Gas and NO_2^- Effects on Alveolar Macrophage Phagocytosis and Metabolism, *Arch. Environ. Health*, 26: 270-274 (1973).
49. J. B. L. Gee, J. Kaskin, M. P. Duncombe, and C. L. Vassallo, The Effects of Ethanol on Some Metabolic Features of Phagocytosis in the Alveolar Macrophage, *J. Reticuloendothel. Soc.*, 15: 61-68 (1974).
50. J. Gil and E. R. Weibel, Improvements in Demonstration of Lining Layer of Lung Alveoli by Electron Microscopy, *Resp. Physiol.*, 8: 13-36 (1970).
51. D. E. Gardner, Environmental Influences on Living Alveolar Macrophages (Thesis), University of Cincinnati, 1971.
52. F. M. LaForce, W. J. Keely, and G. L. Huber, Inactivation of Staphylococci by Alveolar Macrophages with Preliminary Observations on the Importance of Alveolar Lining Material, *Am. Rev. Respir. Dis.*, 108: 784-790 (1973).
53. R. C. Seeger and J. J. Oppenheim, Synergistic Interaction of Macrophages and Lymphocytes in Antigen-Induced Transformation of Lymphocytes, *J. Exp. Med.*, 132: 44-65 (1970).
54. F. Ulrich, Lymphocyte Activating Factor from Alveolar Macrophages: Some Effects on Mitogen Stimulated Thymocytes, *Fed. Proc.* (abstract 411), 35: 280 (1976).

55. R. R. Martin and A. H. Laughter, Pulmonary Alveolar Macrophages Can Mediate Immune Responses, *Fed. Proc.* (abstract 2811), 35: 716 (1976).
56. A. Zarkower, Alterations in Antibody Response Induced by Chronic Inhalation of SO_2 and Carbon, *Arch. Environ. Health*, 25: 45-50 (1972).
57. S. D. Miller and A. Zarkower, Alterations of Murine Immunologic Responses After Silica Dust Inhalation, *J. Immunol.*, 113: 1533-1543 (1974).

Bactericidal Mechanisms in Rat Alveolar Macrophages

W. DOUGLAS BIGGAR and JENNIFER M. STURGESS
Departments of Pediatrics, Immunology, and Pathology, The Hospital for Sick Children, Toronto, Canada

ABSTRACT

The bactericidal mechanisms in rat alveolar macrophages have been examined. Cytochemical techniques were used to study peroxidase activity in alveolar macrophages and to compare the peroxidase activity to that in blood neutrophils. No significant peroxidase was detected in alveolar macrophages, whereas blood neutrophils showed abundant peroxidase activity in primary lysosomal granules and in phagosomes following particle ingestion. Because of these observations, functional studies of myeloperoxidase and hydrogen peroxide were pursued. Iodination of zymosan particles, a peroxidase and hydrogen peroxide-dependent reaction, did not occur in alveolar macrophages. Peroxidase was then inserted into the phagocytic vacuole of alveolar macrophages by allowing the cells to ingest peroxidase-coated zymosan particles, and the iodination reaction was reexamined. Iodination of peroxidase-coated zymosan particles was not significantly increased. These observations suggested that hydrogen peroxide production in the region of the phagocytic vacuole might not be increased with phagocytosis as it is in blood neutrophils. Hydrogen peroxide release by alveolar macrophages, demonstrated cytochemically, was similar in resting cells and during active phagocytosis. These results and the observed failure of alveolar macrophages to show increased tetrazolium dye reduction following phagocytosis suggested that peroxidase—hydrogen peroxide mediated bactericidal reactions may not be important in alveolar macrophages. Lysozyme-dependent bacterial killing appeared to be more significant. Alveolar macrophages contained 10-fold more lysozyme than blood neutrophils. The killing of *Micrococcus lysodeikticus*, a lysozyme-dependent event, was significantly greater by alveolar macrophages than by neutrophils. This reaction was shown to be dependent on lysozyme and to occur extracellularly. These results suggest that, in contrast to neutrophils, where oxidative-dependent bactericidal mechanisms appear to be important for microbial killing, alveolar macrophages may use, at least in part, lysozyme-dependent bactericidal mechanisms to contribute to pulmonary defenses.

Alveolar macrophages contribute to pulmonary defenses against a variety of external stimuli. As phagocytic cells, alveolar macrophages and blood neutrophils are known to share some characteristics. However, little is known about the cellular events of either cell type, which are important for bacterial killing. For neutrophils, the increased oxidative metabolism that accompanies phagocytosis is considered important for host defense.[1] This increased oxidative metabolism includes increased oxygen consumption,[2,3] increased hexose monophosphate pathway activity,[2] and increased hydrogen peroxide production.[4]

One mechanism, which is considered to be of primary importance for the microbicidal activity of neutrophils against bacteria, fungi, viruses, and perhaps tumor cells, uses hydrogen peroxide, myeloperoxidase, and a suitable oxidizable substrate.[1,5,6] In the phagocytic vacuole, increased quantities of hydrogen peroxide are released and react with myeloperoxidase, which has been "deposited" into the phagocytic vacuole after lysosomal degranulation, and with a suitable oxidizable substrate. When iodide is used as the oxidizable substrate, a microbicidal iodination reaction occurs. The importance of peroxidative metabolism is perhaps best illustrated in man, by patients whose leukocytes are deficient in hydrogen peroxide[7] or myeloperoxidase.[8] For example, leukocytes from patients with chronic granulomatous disease do not show increased oxidative metabolism and hydrogen peroxide production following phagocytosis and are unable to kill certain strains of bacteria normally.

MICROBICIDAL MECHANISMS OF ALVEOLAR MACROPHAGES

Microbicidal activity of alveolar macrophages has been studied with biochemical, bacteriologic, and electron microscopic techniques. We have examined both oxidative (hydrogen peroxide and myeloperoxidase) and nonoxidative (lysozyme) bactericidal mechanisms in alveolar macrophages. In each case the alveolar macrophage has been examined in parallel with blood neutrophils.

Peroxidase

Small quantities of peroxidase have been reported in pulmonary aspirates containing alveolar macrophages by biochemical techniques,[9] although peroxidase has not been localized specifically to the alveolar macrophage. Peroxidase can be demonstrated cytochemically in lysosomal granules from blood neutrophils, eosin-

ophils, and monocytes and from peritoneal macrophages. We have examined alveolar macrophages for intracellular peroxidase with cytochemical techniques.

The diaminobenzidine technique[10] to localize sites of peroxidase activity with the electron microscope was selected both for its sensitivity and for its ability to detect several enzymes with peroxidative activity. This technique permitted the identification of the cells collected at bronchial lavage and the exclusion of cells other than alveolar macrophages from this study.

The cytochemical studies of alveolar macrophages failed to detect any significant quantity of enzymes with peroxidase activity either in association with intracellular membranes or in lysosomal granules of rat or rabbit alveolar macrophages (Fig. 1).

The secondary lysosomes and residual bodies of alveolar macrophages contained osmiophilic lamellar structures with a dark–light banding pattern typical of condensed phospholipids. Peroxidase activity was not present among these secondary lysosomes since incubation of alveolar macrophages with diaminobenzidine, with or without hydrogen peroxide, showed no change in osmiophilic reaction and since the metabolic inhibitors, aminotriazole and potassium cyanide, did not affect the reaction.[11]

Under similar experimental conditions a very strong peroxidase reaction was present in the cytoplasmic granules of polymorphonuclear leukocytes (Fig. 2). After lysosomal fusion the reaction product was released into the space between the ingested particle and the limiting membrane of the vacuole. The specificity of this reaction was confirmed by omitting hydrogen peroxide from the incubation mixture and by observing a slight and then a more dramatic reduction in the reaction product in the presence of aminotriazole and potassium cyanide, respectively.

These studies would suggest that, for the alveolar macrophage either at rest or during in vitro phagocytosis, neither peroxidase nor catalase, which has peroxidative activity in low concentrations of hydrogen peroxide, is available to the phagocytic vacuole in amounts detectable by this cytochemical method. Thus, in contrast to neutrophils, peroxidase may not play a primary role in microbial killing by alveolar macrophages.

Iodination

In neutrophils the burst of oxidative metabolism and degranulation accompanying phagocytosis is thought to provide the agents necessary for bacterial killing within the phagocytic vacuole. Hydrogen peroxide alone has some bactericidal activity, but, when

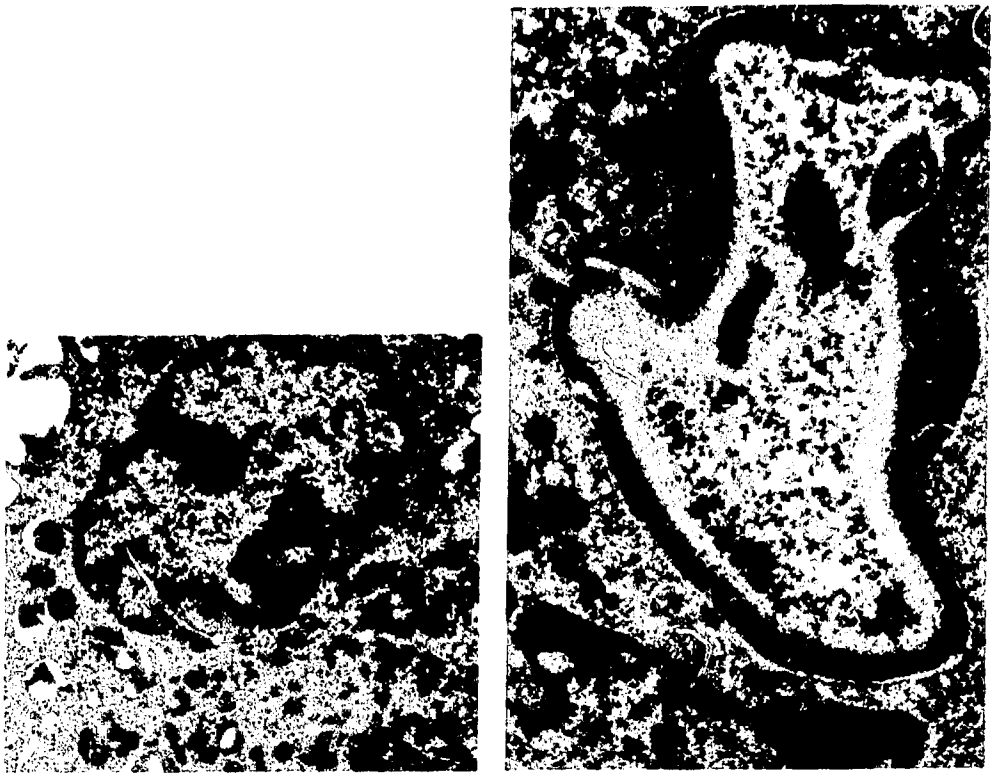

(a) (b)

Fig. 1 (a) Alveolar macrophage reacted with diaminobenzidine to show peroxidase activity. No reaction product is observed in the cytoplasm. Osmiophilic bodies are occasionally observed, but these represent condensed phospholipid structures with a lamellar arrangement which react strongly with osmium tetroxide in the absence of diaminobenzidine. (Magnification, 4000 X .)

(b) Alveolar macrophage incubated with zymosan for 30 min and then reacted with diaminobenzidine. No peroxidase activity is found in the cytoplasm or associated with the phagocytic vacuole. (Magnification, 12,000 X .)

hydrogen peroxide acts in concert with myeloperoxidase and a suitable oxidizable substrate (iodide or chloride), this bactericidal activity is markedly enhanced. When the oxidizable substrate is ^{125}I, an iodination reaction occurs. Iodination by intact cells can be quantitated by the conversion of ^{125}I to a trichloroacetic acid-precipitable form.[12] Since iodination of microorganisms occurs within the phagocytic vacuole and requires myeloperoxidase, hydrogen peroxide, and ^{125}I, this reaction was used to probe some of the biochemical events taking place within the phagocytic vacuole.

Fig. 2 (a) Blood neutrophils reacted to show peroxidase activity. Intense reaction product is observed over the larger granules (arrows), which indicates the presence of peroxidase activity in these lysosomal granules. (Magnification, 2600 X.)

(b) Blood neutrophils incubated with zymosan for 30 min and then reacted with diaminobenzidine. Peroxidase is present in cytoplasmic granules, which fuse with the phagocytic vacuole and release the peroxidase into the phagocytic vacuole (arrows). (Magnification, 18,000 X.)

Under experimental conditions suitable for iodination by neutrophils,[1,2] alveolar macrophages did not iodinate zymosan particles (Table 1). This observation could be explained by insufficient myeloperoxidase and/or insufficient hydrogen peroxide within the phagocytic vacuole.

The observation might also be explained by an inefficient delivery of hydrogen peroxide and/or peroxidase to the phagocytic vacuole after particle ingestion. For an evaluation of these possibilities, the cells were allowed to ingest peroxidase-coated zymosan particles and

TABLE 1

IODINATION BY ALVEOLAR MACROPHAGES AND NEUTROPHILS

Culture components	^{125}I Iodide bounds*
Alveolar macrophages	730 ± 106†
Alveolar macrophages + control zymosan	744 ± 86
Alveolar macrophages + peroxidase-coated zymosan‡	817 ± 69
Neutrophils + control zymosan	151,600 ± 16,000
Control zymosan + H_2O_2, 1 μmol/ml	222 ± 12§
Alveolar macrophages + control zymosan + H_2O_2, 1 μmol/ml	814 ± 73
Alveolar macrophages + peroxidase-coated zymosan + H_2O_2, 1 μmol/ml	2,651 ± 103
Peroxidase-coated zymosan ± H_2O_2, 1 μmol/ml	1,970 ± 54§

*Counts per minute per 10^7 cells per 60 min of incubation except as noted in § below.

†Mean ± standard error for at least three experiments.

‡Peroxidase coated to zymosan particles by glutaraldehyde.

§Counts per minute of incubation in the absence of phagocytes.

then, after peroxidase had been inserted into the phagocytic vacuole,[13] iodination was examined. If significant iodination occurred, then the absence of stimulated iodination after ingestion of control zymosan might be explained by a deficiency of peroxidase or peroxidase-like enzymes (e.g., catalase) in the phagocytic vacuole. As shown in Table 1, no significant increase in iodination was observed after phagocytosis of peroxidase-coated particles, which suggests that hydrogen peroxide may be rate limiting for the iodination reaction.

Tetrazolium dye reduction provided a second metabolic probe for examining the phagocytic vacuole. When neutrophils ingest bacteria or zymosan in the presence of tetrazolium dyes, the dye enters the phagocytic vacuole with the particle and is reduced to a blue formazan precipitate.[14]

Blood neutrophils of patients with chronic granulomatous disease do not increase oxygen consumption after phagocytosis[1] and do not show increased tetrazolium dye reduction.[15] Since studies of the capacity of alveolar macrophages to iodinate ingested particles suggested that hydrogen peroxide was not readily available to the phagocytic vacuole, tetrazolium dye reduction by alveolar macrophages was investigated. In contrast to neutrophils, no increase in

tetrazolium dye reduction was measurable after phagocytosis by alveolar macrophages.

Hydrogen Peroxide

To pursue this question of oxidative mechanisms, we have used a cytochemical technique[16] to compare hydrogen peroxide production in rat alveolar macrophages and rat neutrophils at rest and active phagocytosis.[17] The isolated cells were incubated and agitated in a medium containing cerium chloride and reduced nicotinamide adenine dinucleotide (NADH) in Tris-maleate buffer, pH 7.5, at 37°C for 20 min. Cells were then fixed in glutaraldehyde and processed for electron microscopy. Cerous ions in the presence of hydrogen peroxide precipitate as cerium perhydroxide, an electron-dense material.

Resting alveolar macrophages exhibit a uniform dense reaction at the cell surface. Cerium appears to stimulate endocytic activity in these cells, as evidenced by the increased numbers of pinocytotic vesicles and channels near the cell surface, which were also lined with abundant reaction product. During phagocytosis of latex particles, reaction product is present on the cell surface, but the intensity was similar to that seen in alveolar macrophages at rest (Fig. 3). Reaction product is also observed in many of the phagosomes, which demonstrate their continuity with the cell surface (Fig. 4). Controls in which NADH is omitted from the incubation medium show marked reduction of reaction product.

Resting neutrophils show little surface deposition of cerium except occasionally in surface indentations and small vesicles close to the cell surface. Rat neutrophils activity ingest latex particles at the cell surface but show little reaction on cell membrane that is not associated with latex particles (Fig. 5). Reaction product heavily lines the channels and indentations from the cell surface and phagosomes. Controls that lack NADH in the incubation mixture show little deposition of cerium in cells at rest or during active phagocytosis.

These observations demonstrate that rat neutrophils secrete little hydrogen peroxide at rest, whereas during particle ingestion hydrogen peroxide production is stimulated, particularly at sites where the latex is in contact with the cell membrane. By contrast, alveolar macrophages at rest show more reaction product than neutrophils, and reaction product is distributed over the entire cell surface. Following particle ingestion, hydrogen peroxide production does not appear to be stimulated in alveolar macrophages as it is in neutrophils (Fig. 6).

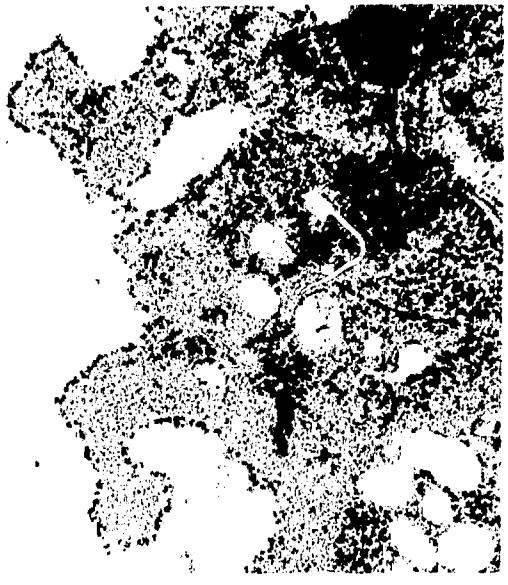

Fig. 3 Resting alveolar macrophage reacted with cerium and NADH to demonstrate hydrogen peroxide release. Reaction product is observed at the cell surface and lining pinocytotic vesicles and channels (arrows). (Magnification, 32,000 X.)

Fig. 4 Alveolar macrophage (during active phagocytosis of latex particles) reacted with cerium to demonstrate hydrogen peroxide release. Reaction product at the cell surface is observed during phagocytosis of latex particles and also lines some phagosomes that are in continuity with the cell surface. Other phagosomes show no reaction product. The intensity of the reaction product at the cell surface is similar to that observed in the resting alveolar macrophage. (Magnification, 37,000 X.)

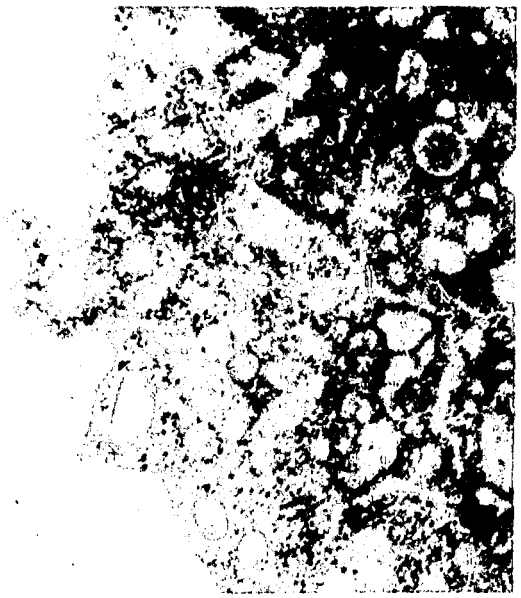

Fig. 5 Blood neutrophils (at rest) reacted with cerium to demonstrate hydrogen peroxide release. Little or no reaction product is observed at the cell surfaces. Occasional pinocytotic vesicles are lined with reaction product. (Magnification, 24,000 X.)

Fig. 6 Blood neutrophils (during active phagocytosis of latex particles) reacted with cerium to demonstrate hydrogen peroxide release. Reaction product is observed at the cell surface surrounding latex particles in contact with the cell surface and around the latex particles within some phagosomes. (Magnification, 19,000 X.)

Thus these experiments suggest that, although there is increased oxidative metabolism by alveolar macrophages after phagocytosis,[18,19] hydrogen peroxide and superoxide anion may not be readily available to the phagocytic vacuole for bacterial killing.

Lysozyme

Rat alveolar macrophages contain significantly greater quantities of lysozyme (10.7 ± 0.7 $\mu g/10^6$ cells) than rat neutrophils (0.87 ± 0.13 $\mu g/10^6$ cells). A typical experiment to compare the bactericidal capacity of alveolar macrophages for *Micrococcus lysodeikticus* to that of neutrophils is illustrated in Fig. 7. After only 10 min of incubation, alveolar macrophages kill greater than one-half the bacteria, and by 30 min no viable bacteria remained. By contrast, bacterial killing by neutrophils is significantly less; i.e., approximately 50% of the bacteria are killed by 30 min. So that the requirement of lysozyme for bacterial killing by alveolar macrophages could be examined, specific rabbit anti-rat lysozyme serum (a generous gift of Dr. E. Osserman) is added to the incubation mixture containing cells plus bacteria. Under these experimental conditions complete inhibition of bacterial killing by alveolar macrophages occurs.

Peritoneal macrophages synthesize and secrete large amounts of lysozyme in vitro.[20,21] However, when the cells are exposed to latex particles, no increase in lysozyme release is observed.[20] Since our results with alveolar macrophages suggested that lysozyme release might be increased following particle exposure, lysozyme release by alveolar macrophages associated with phagocytosis was studied. In the absence of any particles, 6.4% of the intracellular lysozyme is released from alveolar macrophages in 30 min. When latex or zymosan particles are added to the alveolar macrophages, lysozyme release significantly increases (20 and 15%, respectively).[22] These results illustrate yet another difference between alveolar macrophages and peritoneal macrophages.

Of particular importance is that, when the bactericidal event is examined by electron microscopy, lysis of *Micrococcus lysodeikticus* by alveolar macrophages is observed extracellularly within 5 min of incubation. We observe stripping of surface material followed by a progressive loss in granularity and electron density. By 20 to 30 min, bacterial lysis is complete, and only fragments of bacterial membranes are visible. These reactions are illustrated in Fig. 8. Phagocytosis of viable appearing bacteria is only rarely observed. Following bacterial lysis outside the cells, the bacterial "skeletons" are then ingested.

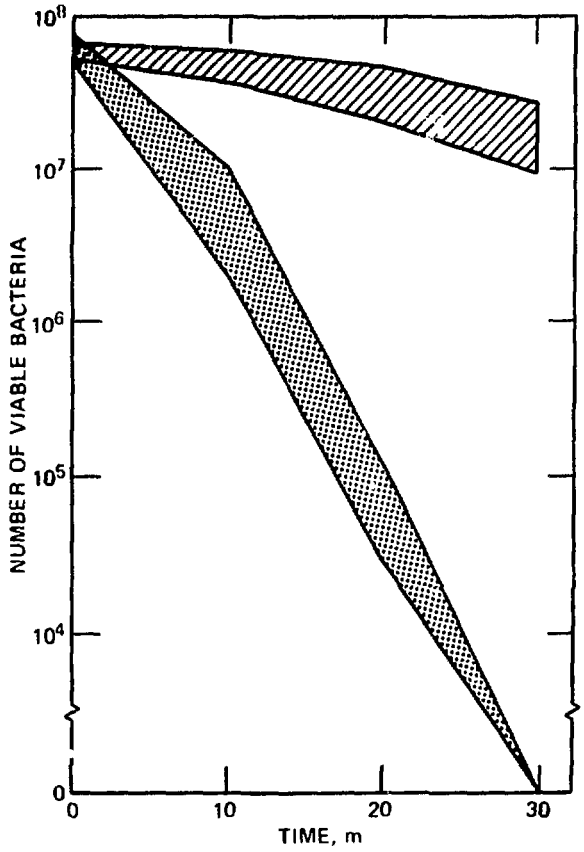

Fig. 7 Viable bacterial counts after incubation for 10, 20, and 30 min with *Micrococcus lysodeikticus*, alveolar macrophages (▒▒▒), and blood neutrophils (▨▨▨).

An important question remains as to whether lysozyme is the only secretory product of alveolar macrophages that is involved in the bactericidal event. Antibody and complement are not present in these experiments; however, other intracellular factors may be released by alveolar macrophages which might also contribute to bacterial killing. Although the bactericidal spectrum of lysozyme by itself is somewhat narrow when examined in vitro, respiratory tract secretions, immunoglobulins, cellular lysosomal hydrolases, and a variety of other substances found within the tracheobronchial tree may collaborate with lysozyme to enhance its microbicidal potential in vivo.

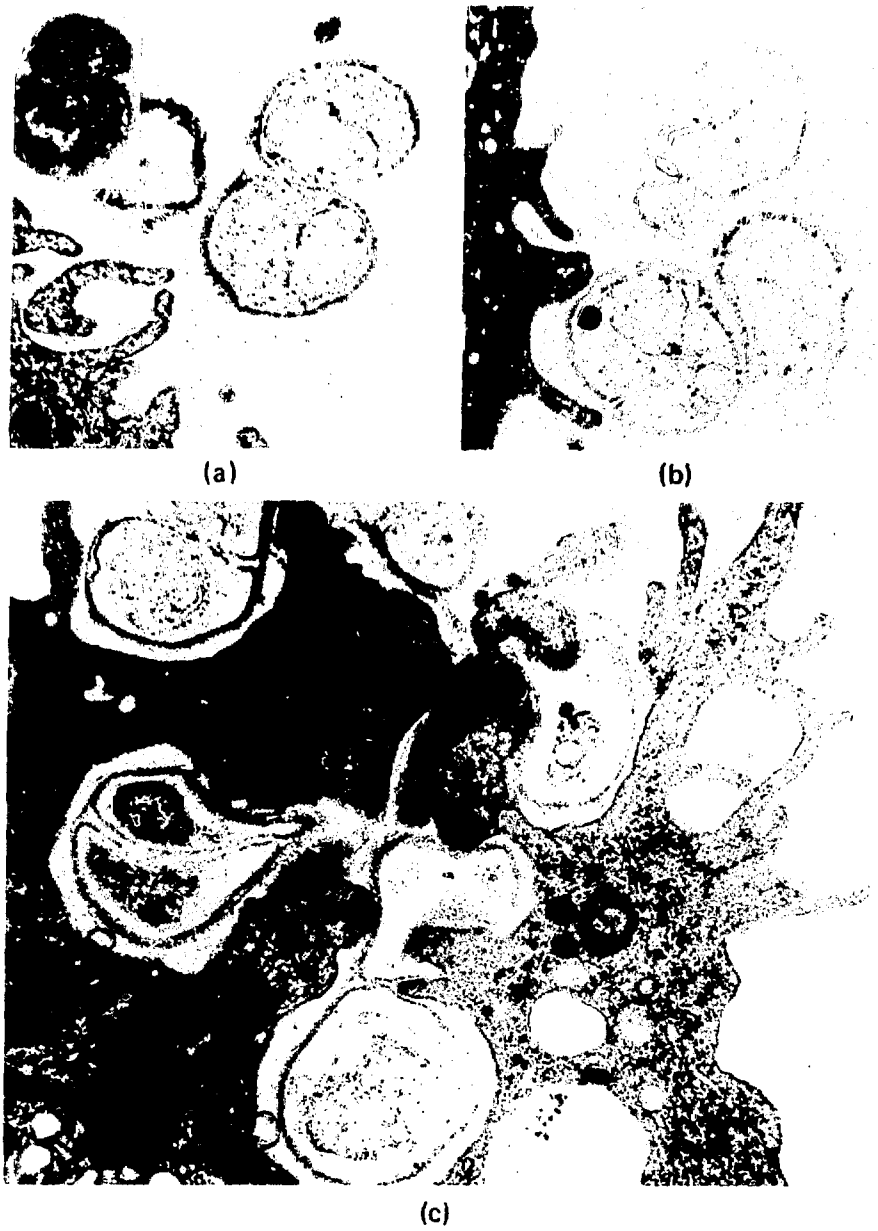

Fig. 8 Alveolar macrophages incubated with *Micrococcus lysodeiktieus* and observed by electron microscopy after different time intervals.

(a) 10-min incubation showing bacteria close to the cell surface being degraded. Inset: Section through typical viable bacteria. (Magnification, 21,750 X.)

(b) 20-min incubation showing sequential degradation of the bacteria extracellularly. (Magnification, 21,750 X.)

(c) 25 min showing phagocytosis of bacteria. Degraded bacteria are ingested by phagocytosis after 20 to 30 min incubation. Ingestion of intact bacteria was not observed, the bacteria being degraded extracellularly. (Magnification, 12,750 X.)

SUMMARY

We have postulated that oxidative-dependent bactericidal mechanisms are not of primary importance for rat alveolar macrophages as they appear to be for blood neutrophils. Perhaps nonoxidative-dependent bactericidal mechanisms may be important for these cells. Lysozyme, either alone or in collaboration with other intracellular and/or extracellular products, may be one such pathway that the alveolar macrophage can use to contribute to pulmonary defense.

ACKNOWLEDGMENTS

We acknowledge the excellent technical assistance of Kam-Yin Wong, Judy Chao, and Sue Omar.

This work was supported by the Medical Research Council of Canada (MA 5726 and MA 4858) and the Ontario Thoracic Society. W. Douglas Biggar and Jennifer M. Sturgess are Medical Research Council Scholars.

REFERENCES

1. M. L. Karnovsky, Chronic Granulomatous Disease—Pieces of a Cellular and Molecular Puzzle, *Fed. Proc.*, 32: 1527-1533 (1973).
2. A. J. Sbarra and M. L. Karnovsky, The Biochemical Basis of Phagocytosis. I. Metabolic Changes During the Ingestion of Particles by Polymorphonuclear Leukocytes, *J. Biol. Chem.*, 234: 1355-1362 (1960).
3. H. Stahelin, M. L. Karnovsky, A. E. Farnham, and E. Suter, Studies on the Interaction Between Phagocytes and Tubercle Bacilli. III. Some Metabolic Events in Guinea Pigs Associated with Infection with Tubercle Bacilli, *J. Exp. Med.*, 105: 265-277 (1957).
4. G. Y. N. Iyer, D. M. F. Islam, and J. H. Quastel, Biochemical Aspects of Phagocytosis, *Nature*, 192: 535-541 (1961).
5. S. J. Klebanoff, Antimicrobial Mechanisms in Neutrophilic Polymorphonuclear Leukocytes, *Seminars Haematol.*, 12(2): 117-142 (1975).
6. R. R. Strauss, B. B. Paul, A. A. Jacobs, and A. J. Sbarra, Role of The Phagocyte in Host—Parasite Interactions. XXVII. Myeloperoxidase—H_2O_2—Mediated Aldehyde Formation and Its Relationship to Anti-Microbial Activity, *Infect. Immunity*, 3: 595-602 (1971).
7. B. Holmes, A. R. Page, and R. A. Good, Studies of the Metabolic Activity of Leukocytes from Patients with a Genetic Abnormality of Phagocytic Function, *J. Clin. Invest.*, 46: 1422-1432 (1967).
8. S. J. Klebanoff and S. H. Pincus, Hydrogen Peroxide Utilization in Myeloperoxidase-Deficient Leukocytes: A Possible Microbicidal Control Mechanism, *J. Clin. Invest.*, 50: 2226-2229 (1971).

9. D. Romeo, R. Cramer, T. Marzi, M. R. Soranzo, G. Zabucchi, and F. Rossi, Peroxidase Activity of Alveolar and Peritoneal Macrophages, *J. Reticuloendothel. Soc.*, 13: 399-409 (1973).
10. R. S. Graham, Jr., and M. J. Karnovsky, The Early Stages of Absorption of Injected Horseradish Peroxidase in the Proximal Tubules of Mouse Kidney: Ultrastructure Biochemistry by a New Technique, *J. Histochem. Cytochem.*, 14: 291-298 (1966).
11. W. D. Biggar and J. M. Sturgess, Peroxidase Activity in Alveolar Macrophages, *Lab. Invest.*, 34: 31-42 (1976).
12. S. H. Pincus and S. J. Klebanoff, Quantitative Leukocyte Iodination, *New Engl. J. Med.*, 284: 744-750 (1971).
13. W. D. Biggar, S. Buron, and B. Holmes, Bactericidal Killing by Alveolar Macrophages: Evidence Against Myeloperoxidase and Hydrogen Peroxide Mediated Mechanisms, *Infect. Immunity*, 14: 6-10 (1976).
14. D. G. Nathan, R. L. Baehner, and D. R. Weaver, Failure of Nitroblue Tetrazolium Reduction in the Phagocytic Vacuoles of Leukocytes in Chronic Granulomatous Disease, *J. Clin. Invest.*, 48: 1895-1904 (1969).
15. R. L. Baehner and D. G. Nathan, Quantitative Nitroblue Tetrazolium Test in Chronic Granulomatous Disease, *New Engl. J. Med.*, 278: 971-976 (1968).
16. Richard T. Briggs, David B. Drath, M. L. Karnovsky, and M. J. Karnovsky, Localization of NADH Oxidase on the Surface of Human Polymorphonuclear Leukocytes by a New Cytochemical Method, *J. Cell Biol.*, 67: 566-586 (1975).
17. S. A. Omar, J. M. Sturgess, and W. D. Biggar, Cytochemical Demonstration of Hydrogen Peroxide Release by Rat Alveolar Macrophages and Blood Neutrophils, *Proc. Micros. Soc. Can.*, 3: 88-89 (1976).
18. E. Ouchi, R. J. Selvaraj, and A. J. Sbarra, The Biochemical Activities of Rabbit Alveolar Macrophages During Phagocytosis, *Exp. Cell Res.*, 40: 456-468 (1965).
19. T. P. Stossel, R. J. Mason, T. D. Pollard, and M. Vaughan, Isolation and Properties of Phagocytic Vesicles. 11. Alveolar Macrophages, *J. Clin. Invest.*, 51: 604-614 (1972).
20. S. Gordon, J. Todd, and Z. A. Cohn, In Vitro Synthesis and Secretion of Lysozyme by Mononuclear Phagocytes, *J. Exp. Med.*, 139: 1228-1248 (1974).
21. D. B. L. McClelland and R. Van Furth, In Vitro Synthesis of Lysozyme by Human and Mouse Tissues and Leukocytes, *Immunology*, 28: 1099-1114 (1975).
22. W. D. Biggar and J. W. Sturgess, Role of Lysosome in the Microbicidal Activity of Rat Alveolar Macrophages, *Infect. Immunity* (in press).

Effect of Cigarette Smoke on Macrophage Phagocytosis

R. K. HAROZ and L. MATTENBERGER-KREBER
Battelle, Geneva Research Center, Carouge, Switzerland

ABSTRACT

This paper describes a reproducible method that was developed for and permits the assessment of the effects of different smoking products on the basis of macrophage phagocytosis. The method routinely uses mouse peritoneal macrophages but yields similar findings when pulmonary macrophages from guinea pigs are used. The test uses the uptake of ^{51}Cr-labeled opsonized sheep red blood cells as a quantitative measure of macrophage phagocytosis. At low concentrations of aqueous extracts of cigarette smoke, a dose-response curve for red-cell ingestion can be obtained. The test is sensitive to different cigarettes and filter types. The testing of cigarettes equipped with different filters suggested a role for vapor-phase components in the toxic process but not exclusive of particulate matter. The depressant activity in smoke is moderated in the presence of thiols, such as glutathione or cysteine, which suggests a possible role for oxidants or free radicals in the smoke as responsible agents for the inhibitory effect on macrophage phagocytosis.

The addition of a nontobacco substitute material to a tobacco cigarette decreased the depressant activity of 100% tobacco smoke. A statistically significant difference was demonstrable between a 100% tobacco cigarette and cigarettes containing either 25 or 50% substitute. A further difference of similar magnitude existed between the two sample blends and the cigarette containing 100% substitute material. On a per cigarette basis, the nontobacco material was approximately fourfold to fivefold less toxic than tobacco. The comparison of the smoke chemistry of all cigarettes examined did not implicate a single class of compounds as the responsible toxic agent.

In our studies designed to evaluate the relative biological effects of different cigarette types, we have used both smoke-inhalation models and condensate application to mouse skin as means to assess relative toxic and tumorigenic effects. We have also established a battery of short-term tests designed to yield information on the relative toxicity

of different smoking materials either following in vivo or in vitro smoke exposure. One of these approaches has been the development of a reproducible test of phagocytosis by macrophages.

Because the alveolar macrophage plays an important role in the pulmonary defense process, inhalation of materials that interfere with macrophage clearance mechanisms may be an important contributory factor toward the development of chronic bronchitis and other lung diseases.[1] It has previously been demonstrated that cigarette smoke has a depressant effect on the ability of macrophages to function in in vitro systems.[2]

Since we were particularly interested in assessing phagocytosis, it was necessary to work at extremely low smoke concentrations. We have observed gross cellular damage by electron microscopy and loss of viability at higher smoke concentrations (unpublished results). Bacteria killing could have been used to assess phagocytosis, but it has been reported that at low smoke concentrations bacterial growth may interfere with the assay.[2] We therefore took a different approach using readily labeled sheep red blood cells as substrate. This method, as well as its use to discriminate between many different cigarette products designed to deliver smoke of reduced toxicity, is described in this paper. The attempt to achieve a less hazardous cigarette might be possible by (1) the use of different filters, (2) modification of the physical dimensions of the cigarette, or (3) replacement of tobacco by a less toxic substitute material. In this paper we describe the results of the inclusion of nontobacco materials into a cigarette and the subsequent effect on phagocytosis by macrophages. Substitute A is CYTREL, a registered trademark of the Celanese Corp. of America, and Substitute B is NSM, a trademark of New Smoking Materials Ltd.

MATERIALS AND METHODS

Isolation of Cells

Female mice were injected intraperitoneally with 1.5 ml of a 10% solution of proteose–peptone in sterile distilled water.[3] Three days later the animals were killed by neck dislocation. Four milliliters of heparinized Hanks' solution was injected into the peritoneal cavity, and the peritoneal fluid was then collected asceptically with a Pasteur pipette. The cells were centrifuged for 10 min at 250 x *g* at 4°C. For the lysing of contaminating red cells, the cell pellet was resuspended and agitated in approximately 5 volumes of 0.87% NH_4Cl, centrifuged, and washed three times with Hanks' buffer before preparation of the monolayers.[4]

Preparation of Monolayers

Monolayers were prepared in circular (35 mm diameter) plastic tissue-culture dishes with approximately 5×10^6 cells per dish. The culture medium consisted of Eagle's basal medium with Earle's salts supplemented with 0.66% *N*-2-hydroxyethylpiperazine-*N'*-2-ethanesulfonic acid (HEPES) buffer, 20% fetal-calf serum, 2m*M*/ml glutamine, 100 units/ml penicillin, and 50 μg/ml streptomycin. The percentage viability was determined by the dye-exclusion test with trypan blue.[5] Cells were counted with a hemocytometer, and monolayers were stained with May-Grünwald—Giemsa stain. Cell cultures were kept at 37°C and 100% humidity. For phagocytosis tests, cultures of 48 or 72 hr were used.

Preparation of Labeled Red Cells

Sheep red blood cells (SRBC's) were obtained in Alsever's solution. Three to five milliliters of a 10% suspension of SRBC's in phosphate-buffered saline (PBS) was incubated with 125 to 250 μCi of sodium ^{51}Cr for 1 hr at 37°C (Ref. 3). The cells were washed three times with large volumes of PBS before being submitted to opsonization.

Opsonization of SRBC's

Mouse antiserum to SRBC's was obtained following two immunizations intraperitoneally with SRBC's (first with 2×10^8 cells followed by 2×10^6 cells after 20 days). The mice were bled 10 days after the second immunization. The individual sera were pooled, and the globulin fraction was purified for use by ammonium sulfate precipitation.[3] Rabbit antiserum to SRBC's (Ambozeptor) was obtained from Germany. To a 10% suspension of ^{51}Cr-labeled red cells was added an equal volume of antiglobulin diluted 1 : 30 (mouse antisera) or 1 : 75 (rabbit antisera) with PBS. After incubation for 1 hr at 37°C, the cells were adjusted to 10% v/v and stored at 4°C. Cells were washed just before use to eliminate any lysed SRBC's and contaminating radioactivity, and only cells less than 4 days old were used.

Calibration Curve of SRBC's

Calibration curves were prepared for the number of red cells vs. protein content and, for each batch of red cells, for the protein content of red cells vs. counts per minute.

Macrophage Enumeration by Protein Analysis

After the monolayers had been washed three times with NaCl to eliminate all medium components and any cells that had not adhered to the Petri dish, they were digested in 1 ml of 1*N* NaOH and the protein was estimated by the Lowry method.[6] The protein content of the particular cell population was determined by relation to a calibration standard curve of bovine serum albumin vs. optical density.

Phagocytosis Test

A macrophage monolayer of 48 to 72 hr was used and the supernatant aspirated. A minimum of three and as many as five dishes were used for each experimental point. Aqueous extracts of smoke were prepared by collecting the middle puff (35-ml puff volume) of four cigarettes in 10 ml of culture medium. The solution was shaken for 15 min at room temperature to ensure complete smoke absorption. For the controls 2 ml of culture medium was added to the culture after aspiration of the supernatant, whereas for the test cultures 2 ml of appropriately diluted smoke-containing culture medium was used. After a preincubation of 10 min at 37°C, approximately 50×10^6 (0.1 ml of 2.5% cell suspension) opsonized ^{51}Cr-labeled SRBC's were added with gentle agitation to obtain an even distribution. Phagocytosis was allowed to proceed for 30 min at 37°C. The supernatant containing most of the nonphagocytized SRBC's was aspirated and discarded. The monolayer was gently rinsed with 1 ml of culture medium minus calf serum. So that the remaining nonendocytized SRBC's could be lysed, 1 ml of culture medium containing 50 μl of a mixture of mouse or rabbit anti-SRBC globulin and guinea pig serum (10 μl of anti-SRBC and 40 μl guinea pig serum) was added and allowed to incubate until complete lysis of red cells in the supernatant was achieved (usually about 20 min). The supernatant was then aspirated, and the monolayer was washed three times with physiological saline and allowed to air dry. One milliliter of 1*N* NaOH was then added, and the dishes were left at room temperature overnight. The digest was then aspirated, and the radioactivity was determined in an automatic sample changer gamma-ray spectrometer. Two samples of 0.2 ml each were then removed for the determination of total protein. Since the protein count should be proportional to the number of macrophages, it was first necessary to subtract the value of protein due to the ingested SRBC's. This was done by reference to the curve of counts per minute of SRBC's vs. protein content. The phagocytic index (K) is given as counts per

minute of SRBC's ingested per microgram of macrophage protein. The control value of K was taken to be 100% phagocytosis, and the percent phagocytosis of macrophages exposed to smoke was expressed as a percentage of this value. At the conclusion of many experiments, phagocytosis was measured by determining microscopically the percentage of macrophages with engulfed SRBC's.

RESULTS

Sheep red blood cell phagocytosis by mouse peritoneal macrophages occurred in a reproducible fashion in this monolayer culture system. Trials with freshly harvested cells had been carried out previously, but it was found that the phagocytic activity of peritoneal macrophages was much greater following a period of time in culture and therefore much more suitable for toxicity tests. Preliminary experiments established that the maximum rates of phagocytosis were obtained after 48 and 72 hr in culture.

The time course of particle uptake was studied to determine the optimum experimental conditions for the assessment of phagocytosis. Figure 1 is a typical example for two different cigarettes where extensive phagocytosis occurs during the first 20 min, and by 30 min the quantity of SRBC's endocytized has reached a plateau.

In addition, the effect of SRBC concentration was studied. Figure 2 shows that the phagocytic index (K) increases with the number of SRBC's and then remains constant, which suggests a saturation phenomenon. The curve in the presence of smoke is still linear since saturation is never reached owing to the drastically reduced level of phagocytosis. From this and similar experiments, the number of SRBC's to be used per dish was chosen to be 50×10^6, which gives a ratio of red cells/macrophages of 10 : 1. So that the contribution of protein from the two cell types could be determined, it was necessary to construct curves relating protein content to cell number. These are shown in Figs. 3 and 4. Depending on the macrophage protein content at the time of the phagocytosis experiment, the red cells, whose protein estimate was repeated for every new labeling and opsonization, were adjusted to give a final protein ratio of 2.75.

Effect of Cell Concentration on Macrophage Enumeration

Although the initial number of cells incubated per dish was adjusted to 5×10^6 cells, the percentage of macrophages adhering to the Petri dish was not absolutely the same from one batch to another

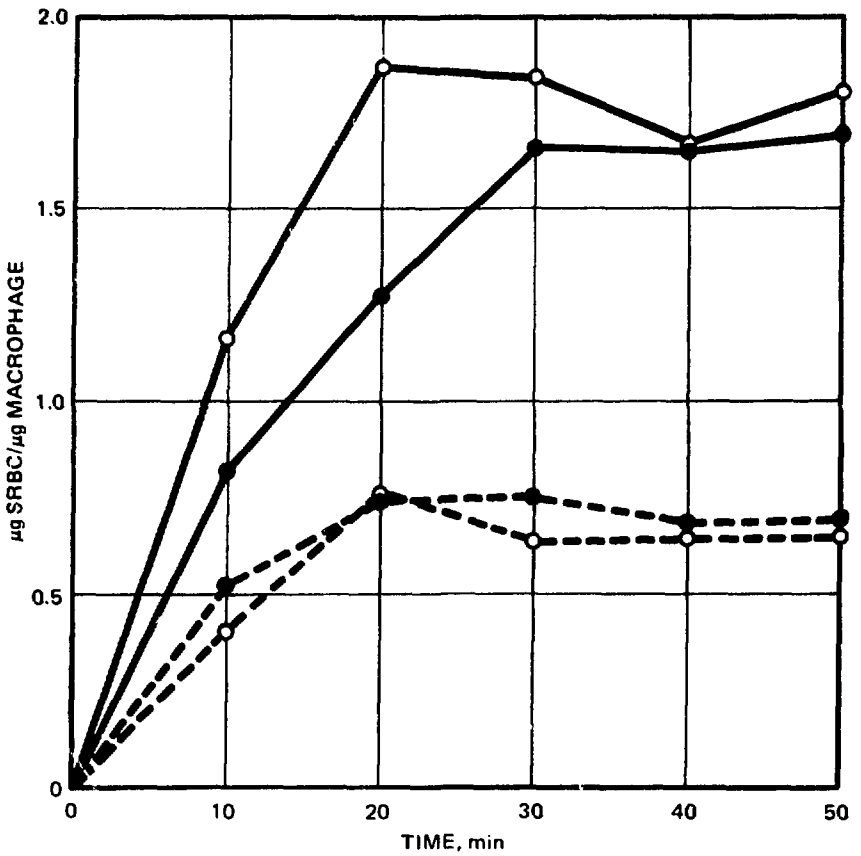

Fig. 1 Time course of phagocytosis of sheep red blood cells by mouse peritoneal macrophages. Particulate uptake is expressed as micrograms of SRBC protein per microgram of macrophage protein. Examples of two experiments: controls, ○—○ and ●—●; aqueous extracts of smoke from two different cigarettes, ○- - -○ and ●- - -●.

following 48 or 72 hr incubation. Since the main requirement for obtaining comparable results in testing the effect of smoke on phagocytosis was a constant ratio of both smoke and red cells to macrophages, it was necessary to determine before each phagocytosis experiment the macrophage monolayer protein content. Assays showed that 30 to 45 min exposure to 1*N* NaOH were sufficient to digest the monolayer, a sample of which was assayed by the Lowry method.

Effect of Serum

It was observed that the presence of serum in the medium into which smoke was collected resulted in increased inhibition of

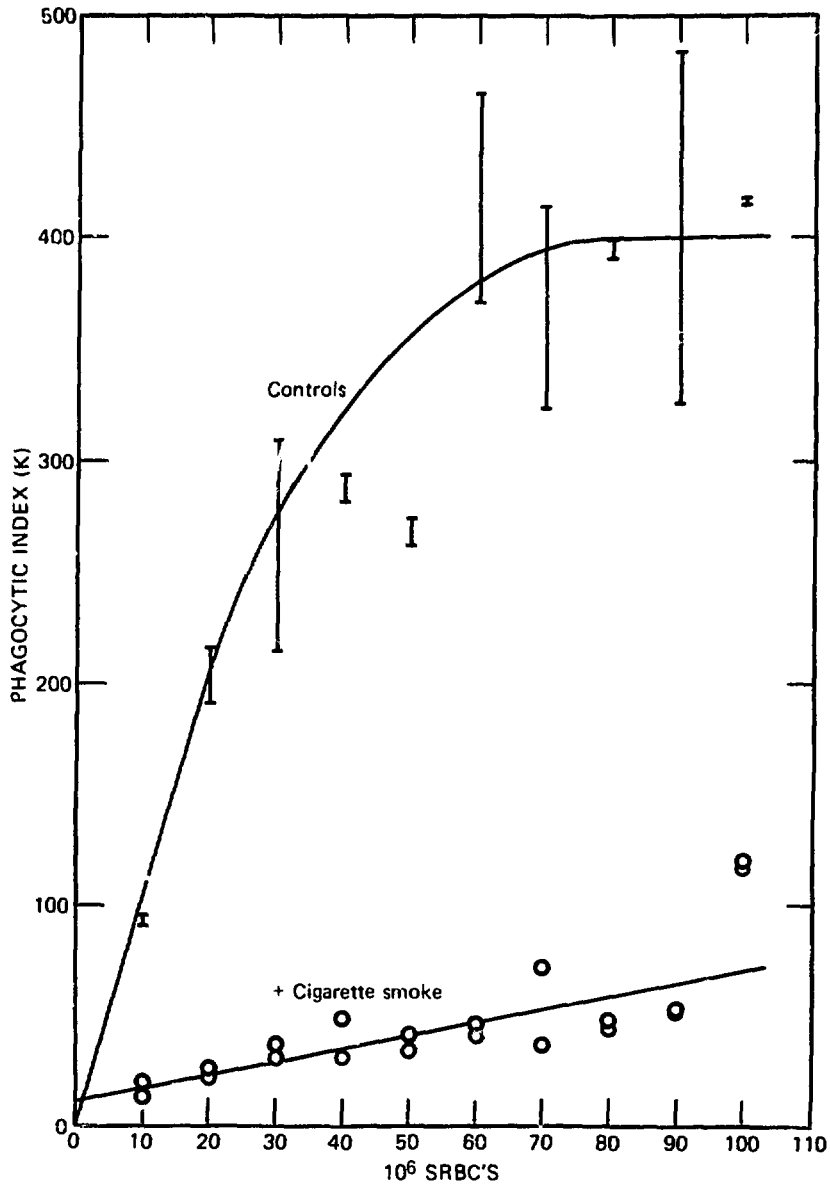

Fig. 2 Effect of sheep red blood cell concentration on particle ingestion in the absence or presence of cigarette smoke. Incubations were carried out for 30 min at 37°C. Phagocytic index is expressed as counts per minute of ^{51}Cr-labeled SRBC's ingested per microgram of macrophage protein.

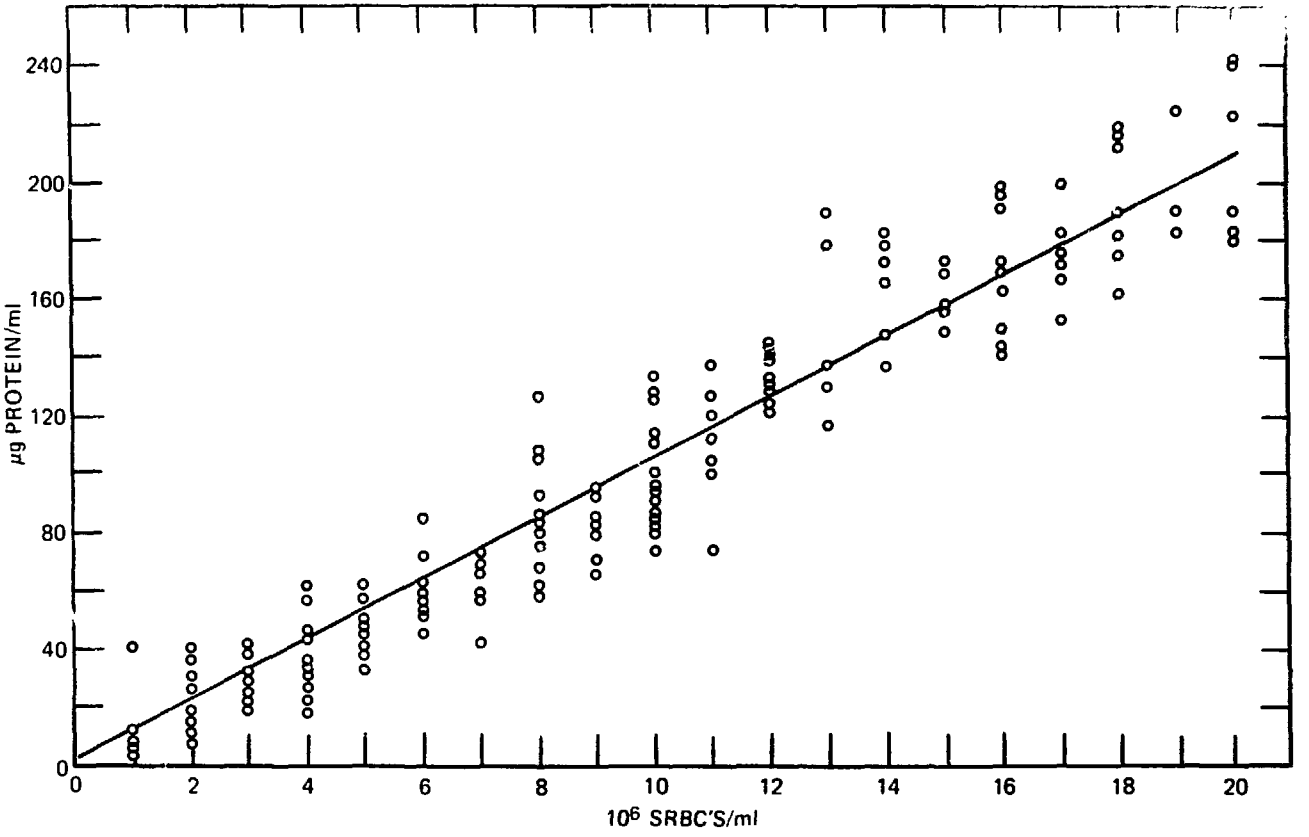

Fig. 3 Calibration curve of sheep red blood cell protein content vs. number of sheep red blood cells. From a 10% volume/volume SRBC suspension equivalent to 200×10^7 SRBC's per milliliter, appropriate dilutions were made to obtain a range of 10 to 100×10^6 cells. Sheep red blood cell protein content was determined following alkaline hydrolysis of the cells with NaOH. The results plotted are the average values of four experiments.

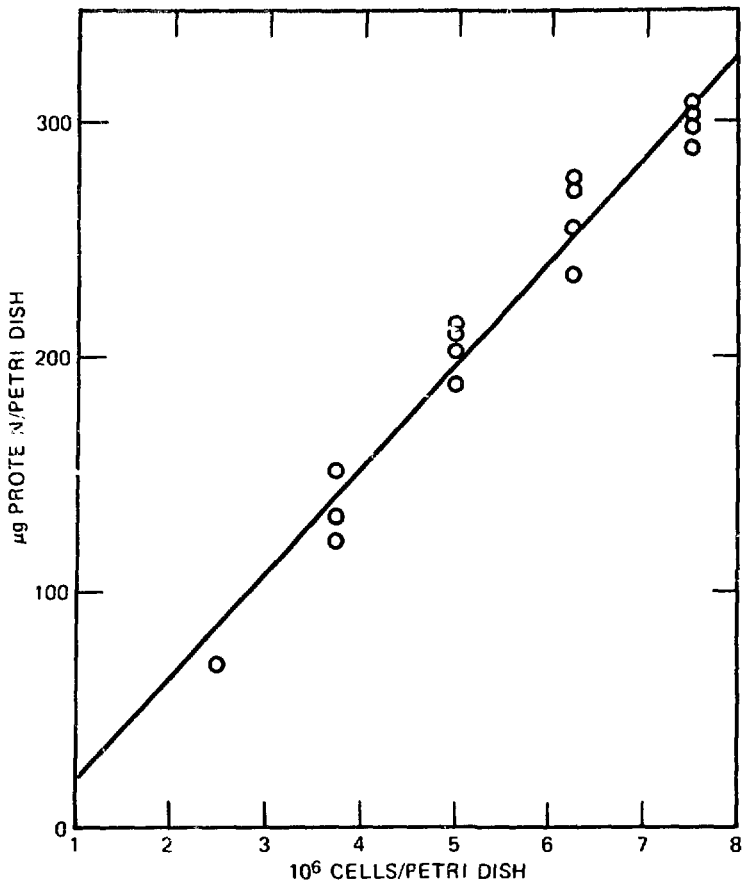

Fig. 4 Calibration curve of macrophage protein vs. number of macrophages. Dilutions of a solution containing a known number of macrophages were plated and the protein content was measured following alkaline hydrolysis after 48 or 72 hr in culture.

phagocytosis. This is perhaps related to the fact that some components of smoke may adhere to serum proteins. This observation has been made in other laboratories.[7,8] All experiments reported here were conducted in the presence of a standard quantity of serum.

Effect of Lysis of Nonendocytized SRBC's

Unphagocytized SRBC's had to be removed as gently as possible since smoke tended to render macrophages fragile, and therefore any mechanical movement for the removal of nonendocytized particles might detach a certain number of macrophages. Anti-SRBC sera mixed with guinea pig complement avoided strong agitation and was very efficient for lysis of extracellular SRBC's without damaging the

peritoneal macrophages or the engulfed SRBC's as observed microscopically.

Effect of Smoke Concentration

Cigarette smoke had a marked depressant effect on the phagocytic activity of peritoneal macrophages. Figure 5 depicts the effect of increasing concentrations of smoke on the phagocytosis of SRBC's. It can be seen that the inhibitory effect is a function of the smoke dose. However, at higher concentrations of smoke, a dose-response curve is not obtained. From electron-microscopy studies, we know that there is gross cellular damage at these concentrations. There is also cell death at higher concentrations. Therefore, to assure that we were assessing the ability to ingest target cells by a population of viable cells, we selected smoke concentrations that resulted in greater than 97% viable cells as determined by dye exclusion. Smoke has always been dissolved in medium before it is applied to macrophages, and the concentration to be tested has been adapted to the macrophage protein content to maintain the same ratio of smoke to macrophage number.

Effect of Glutathione

As reported previously,[7,9] thiols can afford protection against the effects of cigarette smoke, particularly vapor-phase components. We have examined this with several types of cigarettes and do see a partial protective effect. This is illustrated in Fig. 6. At low smoke concentrations and with less toxic cigarettes (3 and 4 for example), total protection is observed. However, at more toxic smoke concentrations, only partial protection is afforded even when the concentration of glutathione is increased.

Effect of Smoke Filtration

Smoke toxicity may be modified in several ways, including the addition of a filter capable of removing certain smoke components. By filtration it is relatively easy to remove broad classes of smoke components, and today almost all cigarettes are equipped with a filter that removes either a portion of the particulate matter or vapor-phase components or both.

Figure 7 illustrates the effect of filter ventilation on several products. In every case and at all doses tested, ventilation produced a less toxic smoke, at least by the criterion of this test. These two filter types, one nonventilated and the other ventilated, have a similar

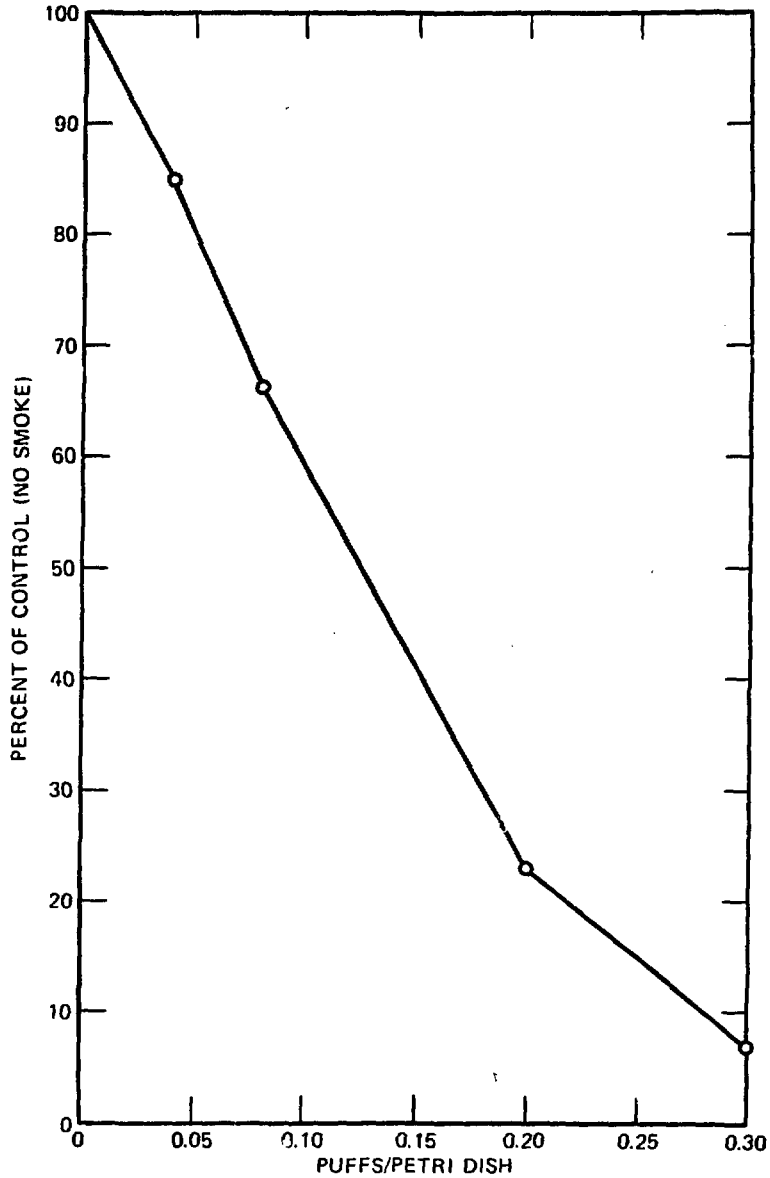

Fig. 5 Effect of increasing smoke concentrations on phagocytosis. Phagocytosis calculated from the specific activity counts per minute due to ingestion of SRBC/micrograms of macrophage protein content is expressed as percentage of controls, i.e., monolayers that have been treated in the same manner as the sample tested but in the absence of smoke. Smoke concentrations were obtained by dilution of a stock solution.

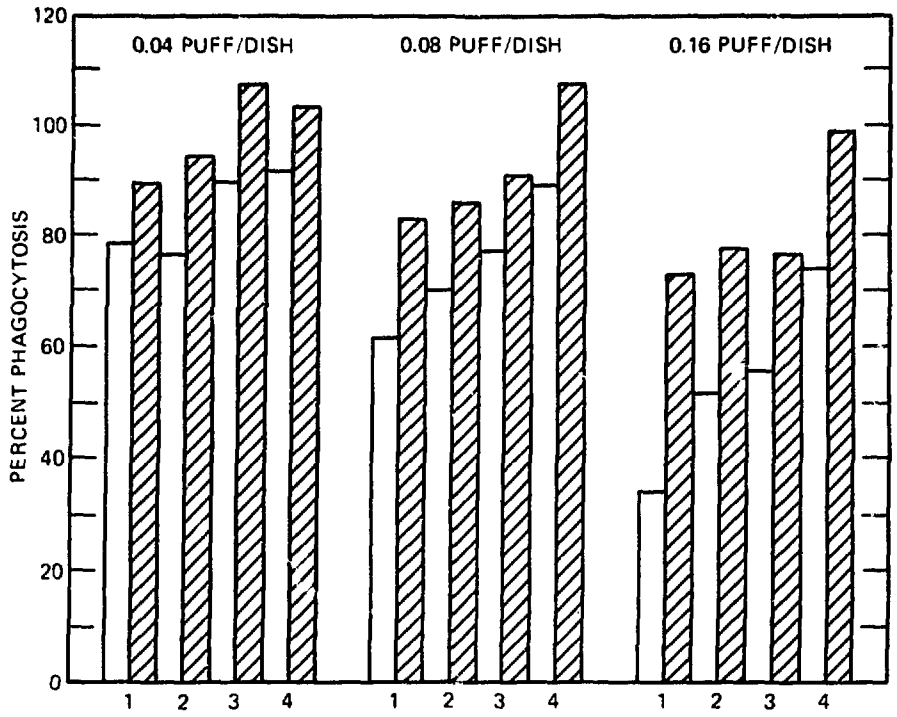

Fig. 6 Protection from the toxic effects of smoke afforded by glutathione. Comparison of the percent phagocytosis obtained in the absence (▭) and presence (▨) of 2m*M* glutathione at three dose levels. 1 refers to 100% tobacco; 2 refers to 75% tobacco, 25% substitute A; 3 refers to 50% tobacco, 50% substitute A; and 4 refers to 100% substitute A.

efficiency for the removal of particulate matter but differ slightly in their selective modification of vapor-phase components.

Whether or not the toxic components are in the vapor phase or particulate phase might be determined by different filter types. Comparison of cigarettes equipped with an activated-charcoal filter with those with a single cellulose acetate filter has revealed that a carbon filter reduces more toxicity than a cellulose acetate filter. This indicated that some, but certainly not all, of the toxic components are removed by the carbon filter. Since the charcoal filter also reduces particulate matter delivery, it is not possible to equate the reduced toxic effect solely to the vapor phase (see Table 1).

Effect of Nontobacco Supplements

In recent years there has been an effort to arrive at a less hazardous cigarette by the substitution of a less toxic material for

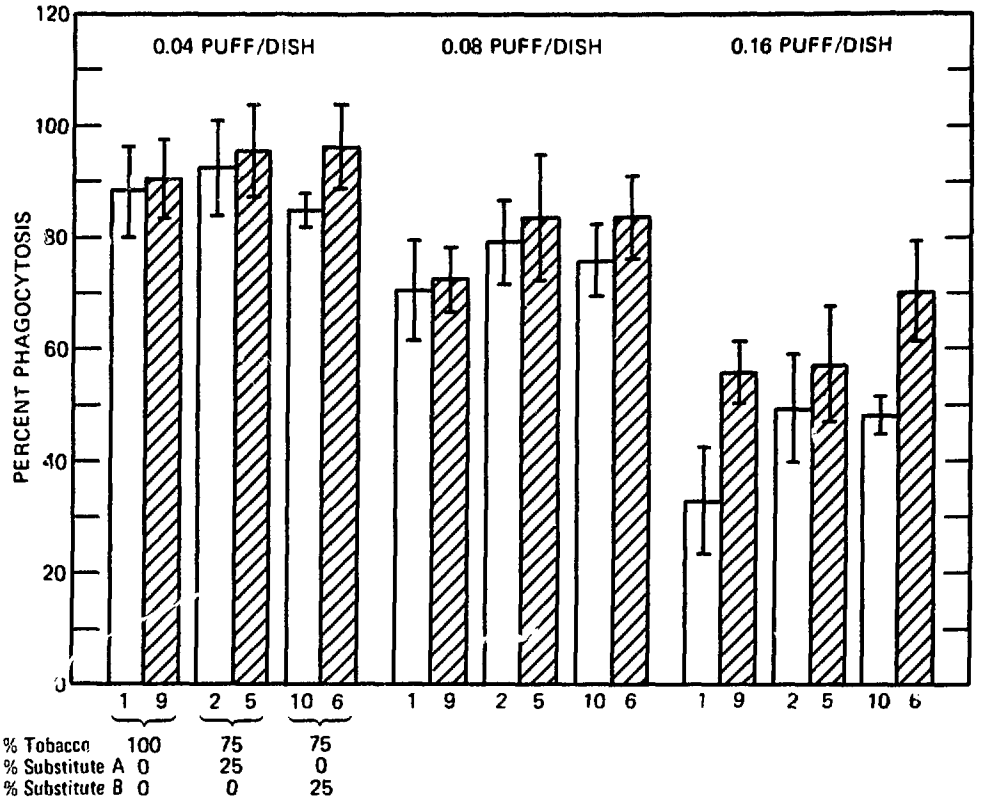

Fig. 7 Effect of filter ventilation on phagocytosis of sheep red blood cells. Comparison between nonventilated (▭) and ventilated (▨) filters at three dose levels. Mean of two experiments. The bars indicate the standard deviation.

tobacco. Such a substitute smoking material would perhaps have a much simpler smoke chemistry and might be fabricated to minimize or exclude known toxic agents. The following results show the effect of the addition of two different materials that are being proposed as tobacco supplements or substitutes.

Figure 8 shows the dose dependence of four different cigarettes containing increasing quantities of substitute material. As the amount of substitute material is augmented, the depressant effect of the cigarette smoke is diminished. This is demonstrated clearly in Fig. 9 at the three smoke concentrations tested. If one translates these per puff values into per cigarette values, the 100% substitute material cigarette would appear to be four to five times less toxic than the 100% tobacco cigarette. A similar pattern is found for substitute material B, as depicted in Fig. 10. Comparison of the two

TABLE 1

EFFECT OF VAPOR PHASE OR PARTICULATE PHASE ON PHAGOCYTOSIS

	0.04 Puff/dish		0.08 Puff/dish		0.16 Puff/dish	
	X*	Y*	X	Y	X	Y
Cigarette + cellulose acetate filter (vapor-phase effect)	84.0	75.2	57.3	70.2	28.3	38.1
	77.0	82.1	64.3	69.3	27.4	35.9
	87.9	83.1	65.8	67.7	29.4	36.3
	x† = 81.6 ± 4.6 ± 1.9		x = 65.8 ± 4.7 ± 1.9		x = 32.6 ± 4.7 ± 1.9	
Cigarette + carbon filter (particulate-phase effect)	88.9	82.6	81.3	83.0	59.0	49.0
	94.7	84.9	80.3	76.1	58.3	53.6
	89.4	82.5	72.2	74.2	67.0	49.7
	x† = 87.2 ± 4.7 ± 1.9		x = 77.9 ± 4.3 ± 1.8		x = 56.1 ± 6.8 ± 2.8	

*X and Y refer to experiments conducted with two separate batches of macrophages.
†x is the mean ± standard deviation ± standard error of the mean.

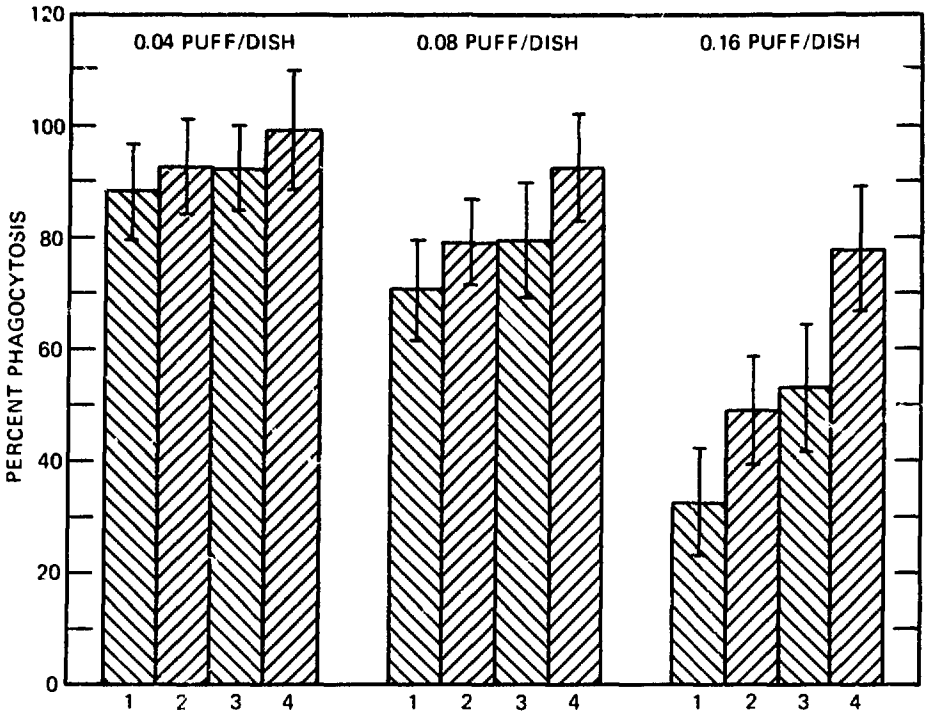

Fig. 8 Effect on phagocytosis of the addition of a nontobacco material to a 100% tobacco cigarette. Testing of substitute A at three dose levels. The numbers on the abscissa code cigarettes containing different quantities of substitute and tobacco. Standard deviations are indicated. Each point is the mean value of 40 to 50 Petri dishes. 1 refers to 100% tobacco; 2 refers to 75% tobacco, 25% substitute A; 3 refers to 50% tobacco, 50% substitute A; and 4 refers to 100% substitute A.

substitute materials shows that, per cigarette, substitute A was consistently less toxic than substitute B either when blended with tobacco or as the pure substitute material. Figure 11 demonstrates the relative toxicity per cigarette with the use of the results obtained at the 0.08 and 0.16 puff dose levels.

Relationship of Smoke Chemistry to Toxic Effect

Modification of a standard cigarette by either different means of filtration or the addition of tobacco supplements altered the toxic effect of aqueous smoke extracts on phagocytosis. In an effort to identify the responsible agents for this effect, individual cigarette-smoke chemistry was examined. An attempt was then made to

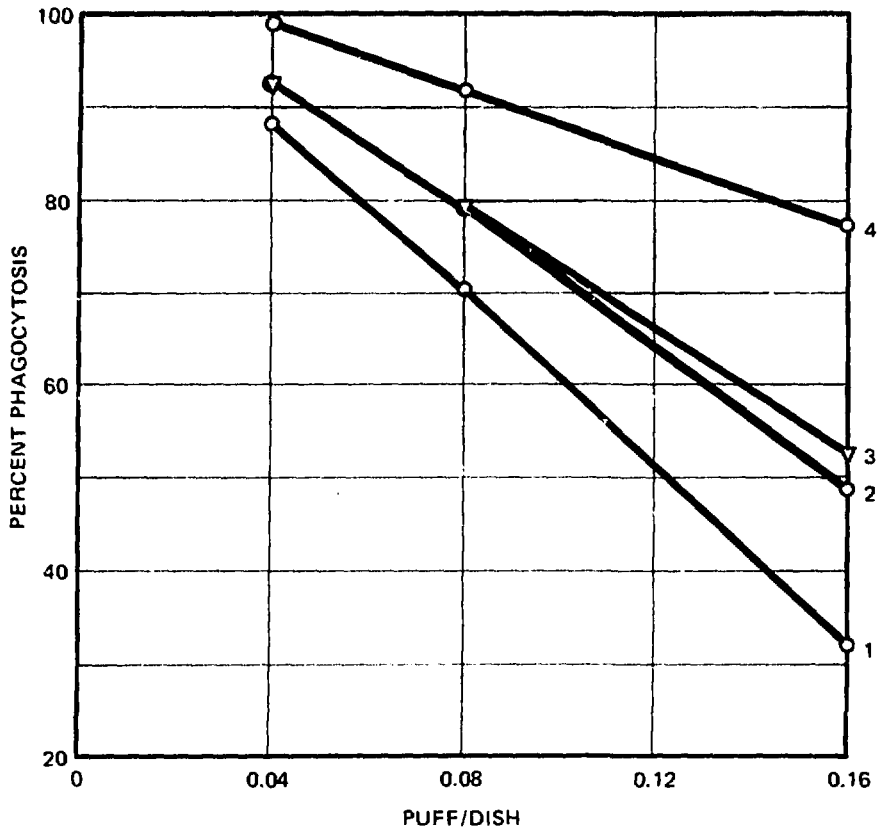

Fig. 9 Relation between quantity of smoke and degree of inhibition. The numbers beside each curve refer to the different cigarettes of substitute and tobacco as in Fig. 8.

correlate the relative toxicity of the different products to a chemical property of the smoke.

Table 2 is an attempt to rank the cigarettes on the basis of their toxic effects in this test system. The cigarette producing the greatest effect at a dose of 0.16 puff/dish was given a value of 1.00, and all other cigarettes were compared to this value. The comparison is on a per cigarette basis.

In general, samples delivering reduced quantities of almost all measured smoke components were less toxic. Further testing of individual chemicals or classes of chemicals found in the smoke would give an idea of the relative toxic effects of these components acting singly but would still not identify any synergistic effects produced by the thousands of components identified in the smoke of cigarettes.

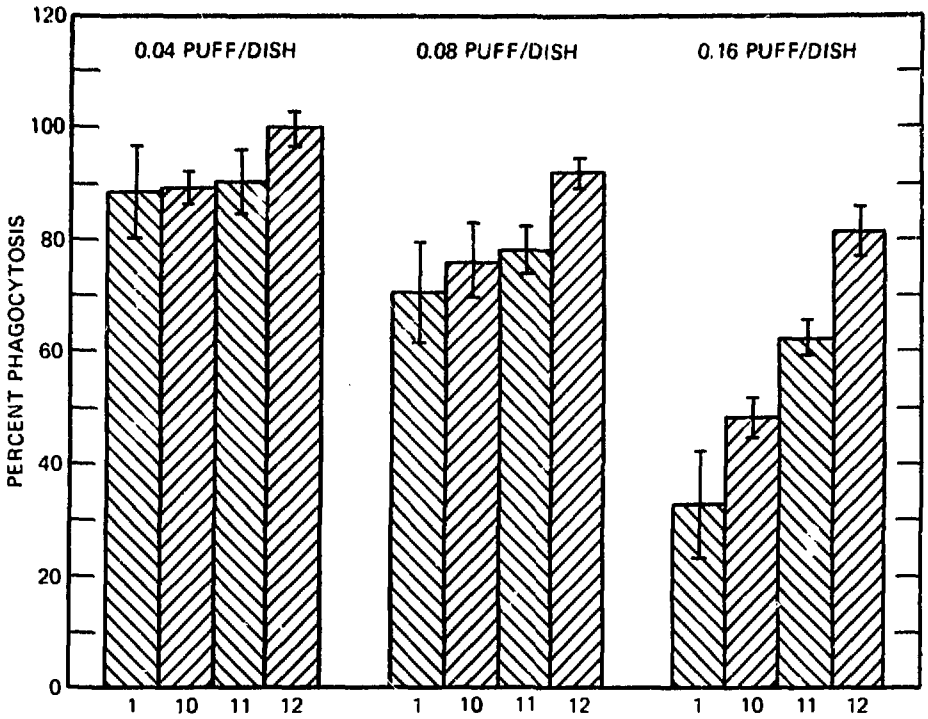

Fig. 10 Effect on phagocytosis of the addition of a nontobacco material to a 100% tobacco cigarette. Testing of substitute B at three dose levels. The numbers on the abscissa code different mixtures of substitute and tobacco. Standard deviations are indicated. 1 refers to 100% tobacco; 10 refers to 75% tobacco, 25% substitute B; 11 refers to 50% tobacco, 50% substitute B; and 12 refers to 100% substitute B.

DISCUSSION

The method developed for assessing phagocytosis, i.e., quantitating the ingestion of ^{51}Cr-labeled red cells by peritoneal macrophages maintained in culture, is a reproducible test for measuring the inhibitory effect of aqueous extracts of cigarette smoke. Reproducibility is achieved within an experiment and also between different batches of macrophages by adjusting the smoke and red-cell concentrations exactly to the macrophage cell concentration. The test gives similar findings with pulmonary macrophages of the guinea pig, but the advantage of using peritoneal macrophages rather than alveolar macrophages is that the cells can be collected in large amounts in a high state of purity and can be easily cultured. The use of monolayers offers the advantage that phagocytosis can be observed and followed under the microscope.

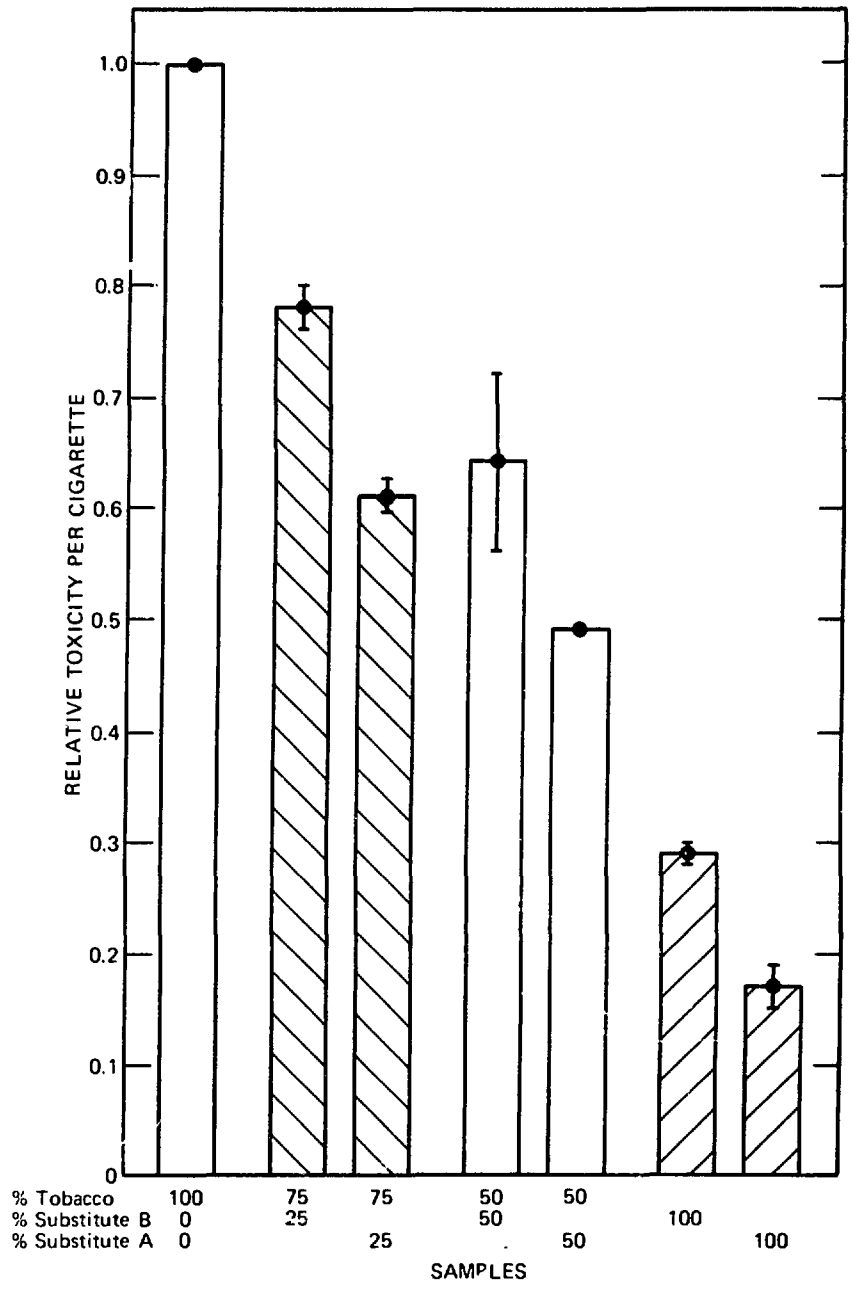

Fig. 11 Relative toxicity per cigarette of cigarettes containing substitute. The effect due to sample No. 1 (100% tobacco) was the most pronounced, and all substitute/tobacco blends and pure substitute cigarettes were compared to this. The bar graph indicates the mean value calculated using the value for phagocytosis inhibition obtained at two dose levels, 0.08 and 0.16 puff/dish.

TABLE 2

RELATIONSHIP OF PHAGOCYTOSIS INHIBITORY EFFECT WITH CIGARETTE-SMOKE CHEMISTRY*

Sample	Composition	Relative toxicity per cigarette	SH index†	PM	Nicotine	HCN	Phenols	Alde-hydes	Acro-lein	CO	NO_x	H_2S	NH_3	pH
1	100% T‡	1.00	1.00	19.8	1.42	272	87	2.3	112	17.5	94	51	24	6.0
10	25% B	0.76	0.95	16.5	1.04	250	60	2.1	104	17.0	80	33	25	5.9
9	100% T_v	0.67	0.88	10.2	0.89	160	48	1.2	49	11.2	71	48	15	6.6
2	25% A	0.62	0.79	15.3	0.94	223	52	2.2	99	15.9	61	32	24	6.3
11	50% B	0.56	0.89	12.7	0.56	186	40	1.7	135	15.8	71	34	23	6.1
5	25% A_v	0.53	0.48	7.7	0.52	102	30	0.9	40	8.8	50	36	14	7.1
3	50% A	0.49	0.65	10.9	0.51	118	28	1.4	93	12.5	50	27	21	6.7
6	25% B_v	0.45	0.73	9.6	0.54	124	30	1.1	67	10.9	75	39	13	6.8
12	100% B	0.29	0.69	5.6	0.01	56	6	1.2	224	11.4	54	13	14	6.4
4	100% A	0.19	0.29	4.1	0.02	5	7	0.5	56	5.4	34	6	113	7.3

*PM (particulate matter), nicotine, aldehydes, and carbon monoxide (CO) in milligrams per cigarette; others in micrograms per cigarette.

†Amount of cysteine destroyed (courtesy of Dr. R. R. Boxall).

‡T, tobacco; A, supplement A; B, supplement B; v, ventilated filter. All samples are equipped with an acetate-type filter, which removes a portion of the PM. The ventilated filters have a similar efficiency for PM but do remove some vapor-phase components selectively.

Sheep red blood cells as particles are suitable for the measurement of phagocytosis since the cells can be readily labeled and opsonized. The ^{51}Cr label is not lost from the cells, and red-cell integrity is not affected by the smoke concentrations used. The unphagocytized SRBC's are gently but efficiently eliminated by use of an anti-SRBC complement mixture. The lysis avoids mechanical movement that could damage the macrophages and affect their adherence to the Petri dish.

This test is sensitive to low concentrations of smoke from cigarettes with different filter types and with different combustion materials. Ventilated filters appear to produce smoke that has a less pronounced effect on the assay. This was seen when comparing cigarettes containing only tobacco with cigarettes supplemented with a nontobacco material.

The cigarette equipped with an activated-charcoal filter was less effective in inhibiting phagocytosis than a similar cigarette equipped with a cellulose acetate filter. The charcoal filter preferentially removes vapor-phase components but also retains some of the particulate phase. Therefore caution is necessary in implicating solely vapor-phase components without examining carefully the properties of the charcoal filter. However, results from other laboratories have suggested primarily vapor-phase components[2] as the responsible agents. Because glutathione affords protection to the phagocytosis process for both tobacco and substitute cigarettes, oxidation of sulfhydryl (SH) groups plays a role in the phagocytic competence of the macrophages. Powell and Green[9] have made this observation previously for tobacco cigarettes and have proposed a connection between impairment of macrophage phagocytic competence and inhibition of glyceraldehyde 3-phosphate dehydrogenase, an SH requiring enzyme. The identification of a particular compound or class of chemicals as the responsible agents for inhibition would be a requirement for subsequent elimination of these toxic agents. This does not prove to be simple because of the chemical complexity of smoke.

Several laboratories have reported inhibition of alveolar macrophage functions by various chemicals found in smoke,[2] by nicotine,[10,11] and by smoke extract.[12] In many cases the loss of competence was accompanied by cell death. Rylander[13] attempted to correlate smoke components of different cigarettes with free lung-cell response and found a relationship with acetaldehyde, tar, nicotine, hydrogen cyanide (HCN), and acrolein. We have performed a similar examination and found a general correlation between the delivery of several components and the effect of aqueous extract of

smoke from different cigarettes. However, acrolein would not appear to be one of the smoke components implicated.

Contrary to earlier findings[1-4] that cigarette smoke from tobacco substitutes is indistinguishable from pure tobacco in its in vitro cytotoxic effects on alveolar macrophage bactericidal activity, the present test shows that the inclusion of nontobacco substitute material diminishes the inhibitory effect of tobacco on phagocytosis. With increasing amounts of either of two tobacco supplements, the inhibitory effect on macrophage phagocytosis was diminished. Cigarettes with blends of 25% and 50% supplement were distinguishable from a 100% tobacco cigarette, and the cigarette of 100% substitute material was four to five times less inhibitory.

ACKNOWLEDGMENTS

The contributions of Drs. David Wilkins and Margherita Strolin Benedetti to the early phases of this research are acknowledged. We thank Martine Neumann for assistance in the preparation of the manuscript.

REFERENCES

1. R. Rylander, Lung Clearance of Particles and Bacteria Effects of Cigarette Smoke Exposure, *Arch. Environ. Health*, 23: 321-326 (1971).
2. G. M. Green and D. Carolin, The Depressant Effect of Cigarette Smoke on the In Vitro Antibacterial Activity of Alveolar Macrophages, *New Engl. J. Med.*, 276(8): 421-427 (1967).
3. A. Cruchaud and E. R. Unanue, Fate and Immunogenicity of Antigens Endocytosed by Macrophages, *Advan. Exp. Med. Biol.*, 12: 187-195 (1971).
4. R. B. Johnston et al., The Enhancement of Bacterial Phagocytosis by Serum, *J. Exp. Med.*, 129(2): 1275-1290 (1969).
5. H. Stähelin et al., Studies on the Interaction Between Phagocytes and Tubercle Bacilli, *J. Exp. Med.*, 104: 121-136 (1956).
6. O. H. Lowry et al., Protein Measurement with the Folin Phenol Reagent, *J. Biol. Cnem.*, 193: 265-275 (1951).
7. G. M. Green, Cigarette Smoke: Protection of Alveolar Macrophages by Glutathione and Cysteine, *Science*, 162: 810-811 (1968).
8. E. Nordenfelt, A Method for Studying Phagocytosis with ^{51}Cr-Labelled Yeast Cells, *Acta Pathol. Microbiol. Scand., Sect. B*, 78: 247-252 (1970).
9. G. M. Powell and G. M. Green, Cigarette Smoke—A Proposed Metabolic Lesion in Alveolar Macrophages, *Biochem. Pharmacol.*, 21: 1785-1998 (1972).
10. D. H. Meyer et al., Nicotine Effects on Alveolar Macrophage Respiration and Adenosine Triphosphatase Activity, *Arch. Environ. Health*, 22: 362-365 (1971).

11. S. L. Schwartz and J. E. Lundin, Observations on the Vacuologenic Activity of Nicotine in Macrophages, *J. Pharmacol. Exp. Ther.*, 189(2): 293-302 (1973).
12. G. K. York et al., Pulmonary Macrophage Respiration as Affected by Cigarette Smoke and Tobacco Extract, *Arch. Environ. Health*, 27: 96-98 (1973).
13. R. Rylander, Toxicity of Cigarette Smoke Components: Free Lung Cell Response in Acute Exposures, *Amer. Rev. Respirat. Dis.*, 108(5): 1279-1282 (1973).
14. M. Cutting et al., Impairment of Alveolar Macrophage Bactericidal Activity by Synthetic Tobacco Substitutes, *Amer. Rev. Respirat. Dis.*, 109: 12 (1974).

Cytotoxicity to Alveolar Macrophages of Metal Oxides Adsorbed on Fly Ash

CATHERINE ARANYI,* SANDRA ANDRES,* RICHARD EHRLICH,* JAMES D. FENTERS,* DONALD E. GARDNER,† and MICHAEL D. WATERS†

*IIT Research Institute, Life Sciences Research Division, Chicago, Illinois, and †Environmental Protection Agency, National Environmental Research Center, Research Triangle Park, North Carolina

ABSTRACT

Fly-ash particles fractionated into three size ranges (<2, 2 to 5, and 5 to 8 μm) and coated with various metal oxides were used to determine whether particle size and surface area are contributing factors to the in vitro toxicity of trace metals for alveolar macrophages (AM). When uncoated fly-ash particles and those coated with PbO, NiO, and MnO_2 in concentrations ranging from 50 to 1500 μg particles/ml were incubated with 10^6 AM/ml, reduced viability was observed on increase in concentration irrespective of type or size range of the particles. Within a given particle type and exposure concentration, decrease in particle size resulted in decreased viability and increased phagocytosis. The toxic effect was not due to the solubilization of the test elements into the incubating medium. The percentage of lead, nickel, or manganese adsorbed on the fly-ash particles varied within a relatively narrow range and was not affected by the particle size. Since the AM were exposed to the particles on a weight—dose per cell basis, their effective exposure load to the test elements was constant irrespective of the particle size. Thus the greater toxicity of the small particles appears to be due to surface interaction between particles and AM, and toxic effect is surface-area as well as dose related. These observations are further supported by decreases measured in total cellular protein levels and specific activity of lactate dehydrogenase.

The objective of this study was to examine the in vitro toxicity for alveolar macrophages (AM) of various sizes of particles coated with selected metal oxides. Fly-ash particles in three size ranges with oxides of lead, nickel, or manganese adsorbed onto their surface were

included in the studies. The parameters of toxicity were changes in viability, cell lysis, and activity of selected cellular enzymes.

METHODS

The fly-ash particles were fractionated by air classification into three size ranges, i.e., <2, 2 to 5, and 5 to 8 μm. The metals in the form of their hydroxides were then precipitated on the surface of the particles that were dispersed in an aqueous phase. After the particles had been filtrated and washed, they were heated to 675°C to convert the metal hydroxides to the respective oxides.

Alveolar macrophages were obtained from male albino New Zealand rabbits by tracheobronchial lavage.[1,2] The rabbits were killed by the injection of sodium pentobarbital into the marginal ear vein, and the lungs were lavaged in situ with warm (37°C) sterile saline through a catheter that was inserted into an incision in the trachea. The AM were centrifuged at 365 × g for 10 min and washed in Hanks' salt solution. Total cell counts were made in a hemocytometer, and viability was determined by the trypan-blue dye-exclusion technique.[3] Smears of air-dried cells were fixed in methanol and stained with Wright's stain for differential counts.

Medium 199 in Hanks' salt solution supplemented with *n*-2-hydroxyethylpiperazine-*n'*-2-ethanesulfonic acid (HEPES) buffer, gentamicin, and 10% heat-inactivated fetal-calf serum was used for incubation. Separate AM and particle suspensions were prepared in the medium at twice the projected exposure concentrations, and equal volumes of the two suspensions were mixed. The final AM concentration in the test suspensions was maintained constant at 10^6 AM/ml; the concentrations of the particles were varied to provide an exposure concentration ranging from 50 to 1500 μg particles 10^{-6} AM ml^{-1} medium.

The test suspensions were incubated in wells of disposable plastic cluster dishes that were placed on a rocker platform for agitation. After 21 hr of incubation at 37°C in a humidified 4% CO_2 atmosphere, the suspensions were transferred into siliconized test tubes. The AM attached to the cluster dishes were removed with rubber policemen and combined with the corresponding suspensions in the test tubes. Viability was determined by microscopic counting of 400 to 500 AM, and, from the same slides, the percentage of AM that had phagocytized was determined.

For determination of enzyme activity, the cells were first mixed with the particles in siliconized Erlenmeyer flasks, and then 10 ml of the test suspension containing 10^7 AM was distributed in four wells

of a disposable plastic cluster dish. This sample volume was used so that we would have sufficient numbers of AM required for the assays. After 21 hr of incubation, all cells were transferred into siliconized tubes, centrifuged at 365 x *g*, and washed in Hanks' salt solution three times. The cell pellet was resuspended in distilled water for osmotic shock, the volume adjusted to 2 ml, and the suspension placed in ice and sonicated with the microtip of an ultrasonic generator. The cell suspension was divided into two portions: one portion was used for enzyme assays after centrifugation at 63 x *g* to remove the metal particles, and the other portion was treated with sodium deoxycholate, the resulting lysate centrifuged at 10,000 x *g*, and the supernatant used for protein assay.

Enzyme activity was determined in triplicate with commercial assay kits. Acid phosphatase activity was determined by using the enzyme to hydrolyze *p*-nitrophenylphosphate at 37°C and measuring the liberated *p*-nitrophenol colorimetrically at 405 mμm. Beta-glucuronidase activity was measured by using phenolphthalein—glucuronic acid as a substrate and measuring the liberated phenolphthalein colorimetrically at 550 mμm. Lactate dehydrogenase (LDH) activity was analyzed by measuring the rate of oxidation of reduced nicotinamide adenine dinucleotide (NADH) at 366 mμm. This oxidation is proportional to the conversion by the enzyme of pyruvate to lactate. Total protein content was analyzed by the Lowry method[4] with the use of bovine serum albumin standard. Enzyme activities were calculated in milliunits per milligram of cellular protein. Changes in enzyme activity and in total cellular protein content were expressed as percentage of the corresponding controls. Since viability of the control AM was not affected by the 21-hr incubation, the viability values were reported directly as a percentage.

RESULTS

Viability of the macrophages was studied to establish the relative toxicity of the coated fly ash in all three particle size ranges. A close dose-response relationship between the concentration of the particles and viability was observed. Within each particle size viability of AM decreased when concentration of the particles was increased. This response appeared to be linear, providing a significant correlation coefficient ($r = 0.906$ to 0.975) on linear regression analysis of the data.

The viability values fitted by the least-square lines for the various size particles as well as the means of the actual percent viability are shown in Fig. 1. The data indicate that at a given concentration AM

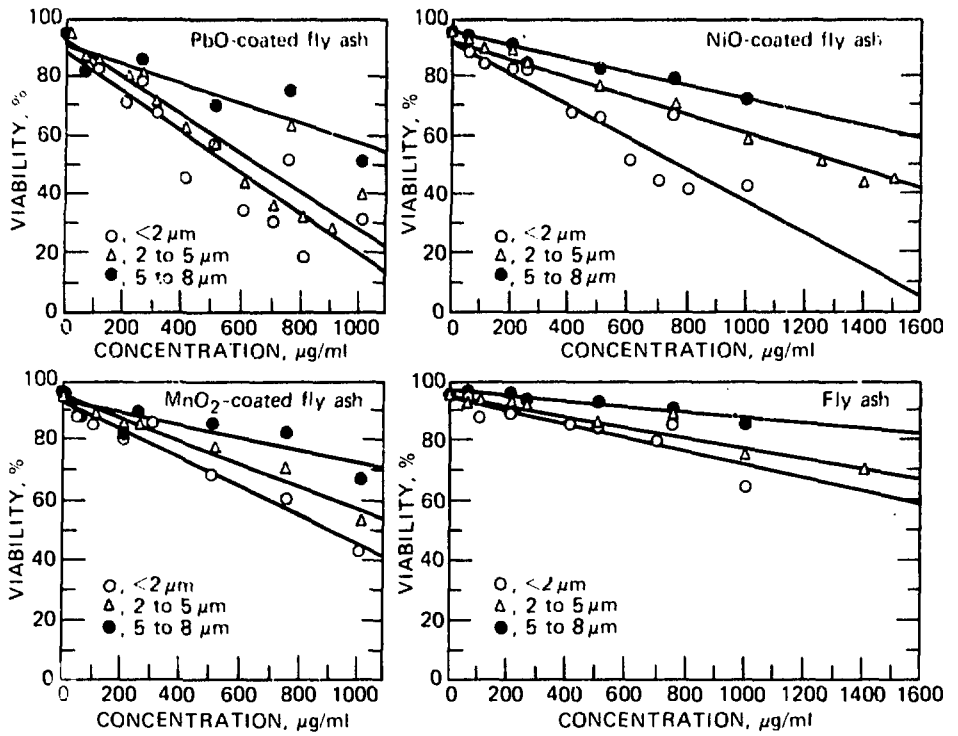

Fig. 1 Effect of concentration and size of fly-ash particles on viability of alveolar macrophages. Each point represents the mean of multiple cultures.

viability decreased with decrease in particle size of fly ash. Although uncoated fly-ash particles reduced AM viability to a much lesser extent, the size effect remained clearly evident.

Table 1 shows the estimated lethal concentrations (LC_{75}) of the various particles which reduce viability to 75% during a 21-hr exposure period. The results indicate that, irrespective of the particle size, PbO-coated fly ash was the most toxic, whereas the toxicity of NiO- and MnO_2-coated fly-ash particles was similar but lower than that of the PbO-coated fly ash. The uncoated fly-ash particles reduced viability at markedly higher concentrations than the coated particles.

The amounts of the test element deposited on the various fly-ash particles were analyzed by atomic absorption spectrophotometry. The data shown in Table 2 indicate that the percentage of adsorbed test metal varies within a relatively narrow range for all particles, and the variability within each particle type is even smaller. Therefore, on a weight-per-cell basis, the macrophages were exposed to fairly constant concentrations of the test metals irrespective of particle size. The fact that an increase in toxicity was observed with decreasing

TABLE 1

ESTIMATED CONCENTRATION OF PARTICLES REQUIRED TO REDUCE MACROPHAGE VIABILITY TO 75% DURING A 21-hr EXPOSURE

Fly ash	Particle concentration, $\mu g\ 10^{-6}$ AM ml^{-1}		
	Size range, <2 μm	Size range, 2 to 5 μm	Size range, 5 to 8 μm
Coated with			
PbO	180	270	470
NiO	320	550	870
MnO_2	375	510	860
Uncoated	870	1160	*

*Above the tested concentration range.

TABLE 2

PERCENT OF THE TEST ELEMENTS ADSORBED ON THE VARIOUS FLY-ASH CARRIER PARTICLES

Fly ash	Size range,* μm	Percent of test element
Coated with		
PbO	0 to 2	3.85
	2 to 5	3.84
	5 to 8	3.15
NiO	0 to 2	2.63
	2 to 5	2.91
	5 to 8	2.77
MnO_2	0 to 2	3.22
	2 to 5	3.67
	5 to 8	2.91
Uncoated	0 to 2	†
	2 to 5	†
	5 to 8	†

*Aerodynamic equivalent diameter.

†<0.03% lead and nickel and <0.01% manganese were in the uncoated fly ash.

particle size suggests that the toxic effect is due to concentration and to surface interaction between particles and alveolar macrophages. This is in agreement with the observations that within a given concentration the percentage of phagocytizing macrophages and the

apparent number of particles engulfed by the AM increase with decreasing particle size. Thus, since smaller particles can be phagocytized easier in larger numbers, they can provide more surface area for interaction with the lysosomal membrane or release of cytotoxic components within the phagolysosomes. Large particles do not affect AM viability as readily because they cannot be engulfed in similar numbers and because after engulfment less surface area is available to the particles to be acted on by the lysosomal hydrolases.

The highest exposure concentrations of the particles were incubated under conditions identical to those used in the dose-response experiments to assure that the cytotoxic effects were not due to solubilization of the test compounds in the culture medium. After incubation the particles were removed from the media by centrifugation and filtration through a 0.22-μm Millipore filter. After the particles had been incubated in the filtered medium for 21 hr, the viabilities of the AM did not differ from the controls, which indicates that the toxicity was not the result of solubilization of the test compounds in the extracellular medium.

Activity of acid phosphatase, LDH, and β-glucuronidase and the levels of total cellular protein in AM after 21 hr of incubation with the particles were studied to determine if a correlation with viability could be demonstrated or if a more sensitive indicator of cell dysfunction could be developed. The PbO- and NiO-coated <2-μm and 2- to 5-μm fly-ash particles were used at five concentrations for each particle type, which resulted in 30 to 80% viabilities. The results shown in Fig. 2 for <2-μm PbO-coated particles demonstrate that the decrease in viability was generally paralleled by the decreases in cellular protein levels (representing cell lysis), in specific activity of LDH, and, to a much lesser extent, in acid phosphatase. There appeared to be no change in the activity of β-glucuronidase. The decreases in viability, LDH activity, and protein levels showed significant linear dose-response relationships ($r = 0.990$, 0.980, and 0.933), and the estimated concentrations of the particles that reduced these experimental parameters to 50% were 450, 570, and 640 $\mu g\ 10^{-6}$ AM ml^{-1}, respectively.

Similar trends were found for the other particles examined. Although the doses of the compounds that resulted in 50% reduction of the enzymatic activities or cellular protein levels generally confirmed the toxic ranking determined during the viability experiments, the concentrations appeared to be higher than those affecting viability.

The PbO- and NiO-coated <2-μm and 2- to 5-μm fly-ash particles at concentrations that resulted in 50% reduction of viability were

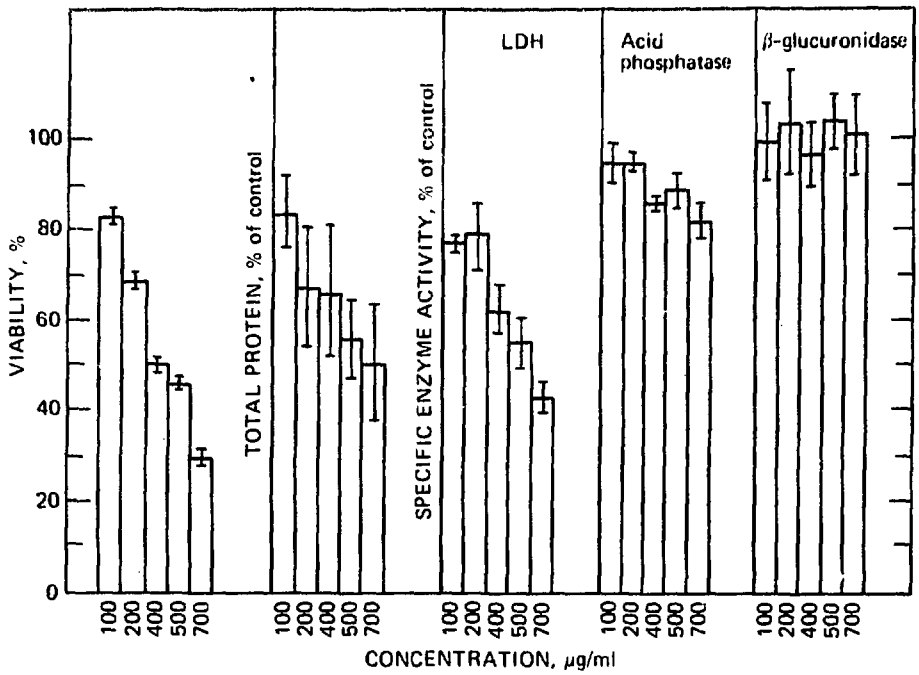

Fig. 2 Effect of exposure to PbO-coated fly-ash particles of $< 2\ \mu m$ on alveolar macrophage viability, total cellular protein content, and specific activity of LDH, acid phosphatase, and β-glucuronidase. Means ± standard error of three experiments are shown.

compared with uncoated fly-ash particles in the same size ranges and concentrations. Although the fly-ash particles per se affected all the experimental parameters used to evaluate toxicity, the decreases in these parameters were significantly smaller than they were after exposure to coated particles.

In summary, for a given test metal and a given particle concentration, toxic effects increased with decreasing particle size as determined by cell viability, total cellular protein levels, and specific activity of LDH. The toxic effect was not due to the solubilization of the metal compounds into the incubating medium. Since the percentage of lead, nickel, or manganese on the fly-ash particles was approximately the same for all particle sizes, the concentration of the test metals to which the AM were exposed was not affected by the particle size. Therefore the greater toxicity of smaller particles appeared to be due to the larger surface area. Thus the particle itself affects the toxicity of the compounds it transports into the intracellular milieu. Finally, the stability of the specific activity of the lysosomal hydrolases (acid phosphatase and β-glucuronidase) as compared to that of a soluble enzyme in the cytosol (LDH) suggests that the

release of hydrolytic enzymes in the cell may be a secondary event in the cytotoxic response. The determination of the sequence of events and mechanism of cell death will require further investigation.

ACKNOWLEDGMENTS

This investigation was supported by the U. S. Environmental Protection Agency, Contract No. 68-02-0761.

The authors gratefully acknowledge the contribution of Hubert Ashley of the Fine Particles Section of IITRI for preparation of the metal oxide-coated particles.

REFERENCES

1. O. N. Myrvik, E. S. Leake, and B. Fariss, Studies on Pulmonary Alveolar Macrophages from the Normal Rabbit: A Technique to Procure Them in a High State of Purity, *J. Immunol.*, 86: 128-132 (1961).
2. D. L. Coffin, D. E. Gardner, R. S. Holzman, and F. J. Wolock, Influence of Ozone on Pulmonary Cells, *Arch. Environ. Health*, 16: 633-636 (1968).
3. L. Weissbecker, R. D. Carpenter, P. C. Luchsinger, and T. S. Osdene, In Vitro Alveolar Macrophage Viability, *Arch. Environ. Health*, 18: 756-759 (1969).
4. O. H. Lowry, N. J. Rosebrough, A. L. Farr, and R. J. Randall, Protein Measurement with Folin Phenol Reagent, *J. Biol. Chem.*, 193: 265-275 (1951).

Enhanced Binding of Autologous Red Cells to the Macrophage Plasma Membrane as a Sensitive Indicator of Pollutant Damage

J. G. HADLEY,*‡ D. E. GARDNER,‡ D. L. COFFIN,‡ and D. B. MENZEL*†
Departments of *Physiology and Pharmacology and of †Medicine, Duke University Medical Center, Durham, North Carolina, and ‡Biomedical Research Branch, Environmental Protection Agency, Research Triangle Park, North Carolina

ABSTRACT

The alveolar macrophage (AM) represents the primary line of defense in host protection against inhaled infectious organisms. Following exposure to oxidant gases, the ability of the host to resist airborne bacterial infection is severely impaired, and damage to the AM defense system may be an important factor in increased susceptibility. Oxidant exposure could diminish the phagocytic capability of the macrophage system by either altering the phagocytic process per se (i.e., engulfment and digestion) or acting on cell surface structures responsible for the recognition and binding of material to the phagocyte. So that possible damage by oxidant exposure on the AM recognition mechanisms could be investigated, macrophages were isolated from rabbits and treated with a commercial preparation of wheat germ lipase. This treatment induced the binding of both heterologous (sheep) and autologous (rabbit) red blood cells to AM. The 50% effective concentration (EC_{50}) for rosette formation with the crude commercial preparation was 30 μg/ml for heterologous cells and 300 μg/ml for autologous cells. Macrophages isolated from rabbits exposed to 0.981 mg O_3/m^3 (0.5 ppm) for 3 hr or 3.167 mg NO_2/m^3 (7.0 ppm) for 24 hr exhibited increased binding of autologous cells. In the presence of 100 μg/ml of lipase, control cells formed 7.2 ± 1.4% rosettes compared to 66.0 ± 13.7% for cells treated with ozone and 51.7 ± 21.1% for cells treated with nitrogen dioxide. So that the oxidant alteration of the macrophage membrane could be further characterized, a highly purified, radiolabeled preparation of wheat germ agglutinin (WGA) was used as a probe of membrane structure. Preliminary evidence suggests that the oxidants increase the binding of WGA to the macrophage surface. This enhanced binding could be due either to the revelation of cryptic binding sites or the rearrangement of preexisting sites. Both of these alternatives could impair the recognition capability of the AM and therefore diminish the protective activity of the AM.

The alveolar macrophage (AM) represents the most important, most extensively studied, and least understood component of the pulmonary immune defense system. Phagocytosis, thought the prime function of macrophages, can be inhibited by a wide variety of environmental contaminants, including oxidant gases[1,2] and various metals.[3] The increased susceptibility of an organism to infection by airborne pathogens following oxidant exposure has also been attributed to a functional defect of the AM. The pollutant-induced alteration of the AM defense system may involve a more subtle and insidious lesion than can be detected by studies designed to measure viability,[1,2] phagocytic index,[3] or total hydrolytic enzyme content.[4] The rapidly growing knowledge[5] of the numerous functions regarding cell recognition, hormonal action, and other sensory stimuli, which are mediated via the plasma membrane of cells, gives added emphasis to the hypothesis that the cell membrane of the AM may indeed be the target site of pollutant damage.

In this study oxidant-induced alterations of the plasma membrane of AM were examined by measuring the ability of AM to form rosettes with autologous cells after treatment with a preparation of wheat germ lipase, which contains as an impurity the plant lectin, wheat germ agglutinin (WGA). Both O_3 and NO_2 were found to enhance rosette formation. So that oxidant alteration of cell surface structure could be characterized further, the binding of radioactively labeled WGA to the AM was studied. Preliminary results from these investigations indicate that oxidants alter plasma membrane receptor structures by increasing the apparent affinity of the receptors in a fashion analogous to the receptor alterations observed in cells following neoplastic transformation.

MATERIALS AND METHODS

Animals

Male New Zealand white rabbits weighing 1.5 to 2.5 kg were used as a source of AM. Purina Rabbit Chow and water were available ad libitum. No antibiotics or other drugs were administered the animals for at least 2 weeks prior to or during experimental use.

Isolation and Collection of AM

The procedure of Coffin et al.[1] was used to obtain AM. Briefly, animals were sacrificed by the intravenous injection of 150 mg of sodium pentobarbital (Nembutal, 50 mg/ml). A tracheostomy was performed, and a glass cannula was inserted into the trachea. Thirty

milliliters of isotonic saline was instilled and allowed to remain for 15 min. The saline was withdrawn with a 30-ml syringe. The instillation and withdrawal procedure was repeated four additional times without delay. The lavaged fluid containing the macrophages was filtered through gauze and centrifuged at 365 x *g* for 15 min at 4°C. The resulting cell pellet contained a relatively pure (>95%) macrophage population, as determined by differential counting of Giemsa-stained smears, and had a viability greater than 95%, as determined by the exclusion of 0.4% trypan blue.

Rosette Formation

Following isolation the AM was washed three times with medium 199 and resuspended to a concentration of 1×10^6 cells/ml in medium 199. Monolayers were formed by adding 0.5 ml of the macrophage suspension to each of four wells in tissue-culture chamber slides. The cells were incubated at 37°C for 30 min. Following incubation, nonadherent cells were removed by washing three times with phosphate-buffered saline (PBS), and 0.5 ml of PBS containing the appropriate concentration of lipase was added to the monolayers. The slides were allowed to stand undisturbed for 30 min at room temperature.

At the end of the 30-min incubation, the monolayers were washed three times with PBS, and 1 ml of a 1% v/v suspension of either sheep red blood cells (SRBC's) or autologous rabbit red blood cells (RRBC's) was added to the monolayers and allowed to remain for 30 min at room temperature. Unattached red cells were removed by washing the monolayers with PBS, and the remaining cells were fixed by the addition of 1 ml of 1% gluteraldehyde in PBS. Following a 1-hr fixation, the slides were stained for 10 sec with Camco Quik Stain and rinsed with tap water. The slides were examined for rosettes under oil immersion. A positive rosette was scored for those macrophages with four or more bound RBC's.

Preparation of ^{125}I-Labeled Wheat Germ Agglutinin

Wheat germ agglutinin was radiolabeled as described by Cuatrecasas.[6] Briefly, iodoWGA was prepared with carrier-free ^{125}I with the use of chloramine T. The resulting [^{125}I]WGA was purified by affinity chromatography on a ovomucoid—Sepharose 4B column. Greater than 93% of the WGA was retained on the column. The [^{125}I]WGA was eluted from the column by 0.2*M* acetic acid and had a specific activity of 1 to 2 μCi/μg.

Macrophage Binding of ^{125}I-Labeled Wheat Germ Agglutinin

For studies of the binding of the [^{125}I]WGA to the macrophage membrane, macrophages were suspended in PBS containing 0.2% bovine serum albumin (BSA) to a concentration of 2.5 to 5.5×10^5 cells per milliliter. Aliquots (100 μl) of this cell suspension were added to 1-ml disposable conical test tubes. Iodine-125-labeled WGA (100 μl) was added to give the indicated concentrations (10 ng to 200 μg/ml). For the determination of nonspecific binding, 200m*M* *N*-acetyl-D-glucosamine was added. Following incubation 0.8 ml of ice-cold PBS containing 0.1% BSA was added to each tube, and the tubes were centrifuged at 5000 x *g* for 45 sec. The supernatant was removed, and the AM was resuspended in 1 ml of PBS–BSA. The cells were centrifuged again, the supernatant removed, and the cell pellets counted in a well-type gamma counter. Data are expressed as the nanograms of WGA bound per 10^4 macrophages and are corrected for nonspecific binding. All data are mean ± standard error of at least three observations.

Oxidant Exposure

Rabbits placed in individual stainless-steel open-wire cages were exposed to oxidants in Hinners-type chambers.[7] The gas flow was set at one air change per minute. Ozone (O_3) was generated from 100% O_2 with the use of a neon-tube silent arc generator. Concentrations were continuously monitored by chemiluminescence and periodically assayed with the use of Saltzman[8] techniques. For the nitrogen dioxide (NO_2) exposures, 1% NO_2 in N_2 was diluted with filtered room air to obtain the desired concentration. Nitrogen dioxide levels were continuously monitored by chemiluminescence and periodically tested with the Saltzman[8] method.

RESULTS

Wheat Germ Lipase Mediated Rosette Formation

Wheat germ lipase treatment of AM induced the binding of both SRBC's and RRBC's to the macrophage in a dose-dependent manner. A representative log dose-response curve comparing the concentration of lipase used to treat the macrophages with the resulting percent rosette formation is depicted in Fig. 1. The EC_{50} for rosette formation was 30 μg/ml of lipase when SRBC's were used for the rosette assay and 300 μg/ml when autologous RRBC's were used. The difference in potency between SRBC's and RRBC's does not

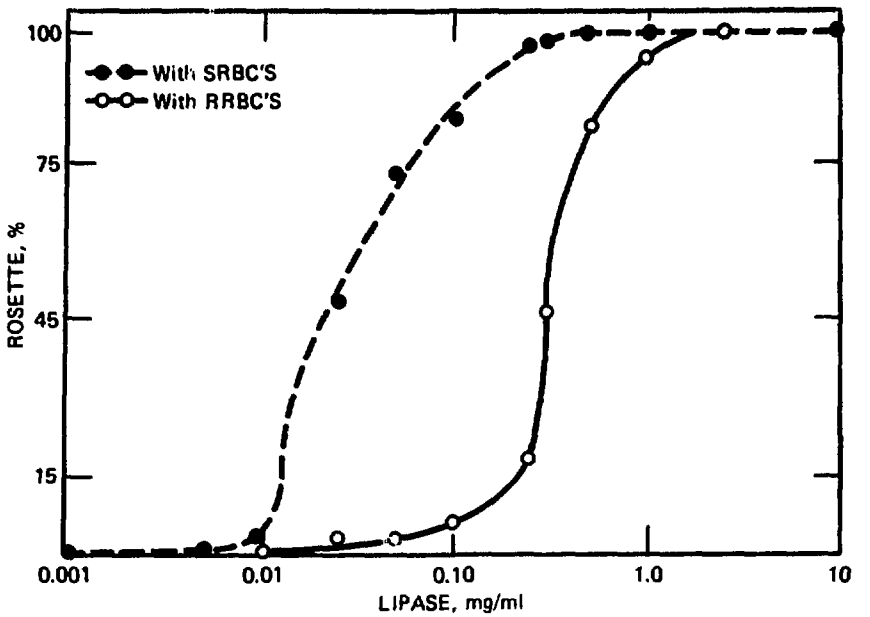

Fig. 1 Relation between lipase concentration and percent rosette formation by rabbit AM.

appear related to the agglutination of the red blood cells by lipase since RRBC's are agglutinated with lower concentrations of lipase than SRBC's (45 μg/ml lipase agglutinated RRBC's vs. 400 μg/ml agglutinated SRBC's) (J. Hadley, unpublished observations).

The rosette formation following wheat germ lipase treatment of AM is dependent on both the concentration of lipase used to treat the AM and the time of AM exposure to lipase. Divalent cations are not required for rosette formation, and the ability of macrophages to form rosettes following lipase treatment decreases in a time- and temperature-dependent manner (unpublished).

Effect of Oxidant Exposure on Lipase-Induced Rosette Formation

Rabbits were exposed to 0.985 mg O_3/m^3 (0.5 ppm) for 3 hr or 13.167 mg NO_2/m^3 (7 ppm) for 24 hr prior to isolation of their pulmonary macrophages. Following lipase treatment the macrophages were examined for rosette formation (Table 1). Control macrophages were obtained from rabbits that had been exposed to air only. Oxidant exposure significantly ($p < 0.05$) enhanced rosette formation by macrophages from both O_3- and NO_2-exposed animals. For example, NO_2 and O_3 exposure increased rosette formation with 0.1 mg/ml of lipase and autologous red blood cells by almost 10-fold.

TABLE 1

EFFECT OF OXIDANT EXPOSURE ON LIPASE-INDUCED ROSETTE FORMATION

Concentration of lipase used to induce rosette formation, mg/ml	Rosette formation, %		
	Control	O_3*	NO_2†
0.1	7.2 ± 1.4(5)‡	66.0 ± 13.7(7)	51.7 ± 21.0(3)
0.025	4.0 ± 2.4(4)	37.2 ± 14.6(6)	14.0 ± 2.9(3)

*Animals exposed 3 hr to 0.50 ppm O_3 prior to isolation of macrophages.

†Animals exposed 24 hr to 7 ppm NO_2 prior to isolation of macrophages.

‡Number in parentheses is the number of animals exposed.

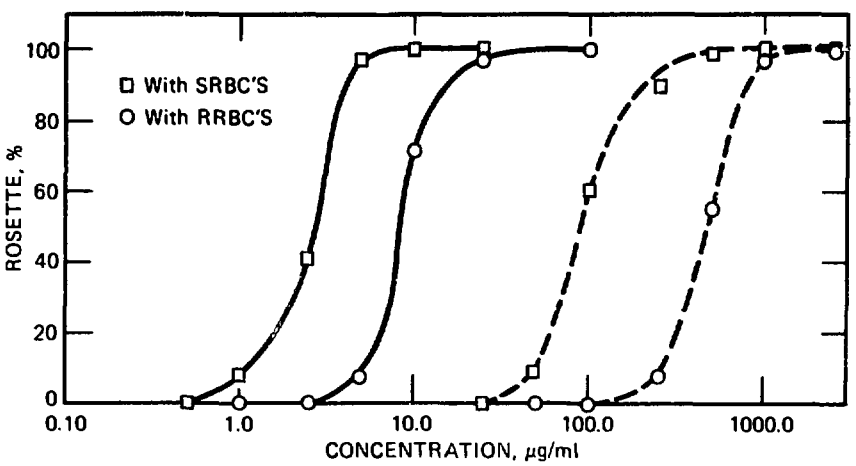

Fig. 2 Effect of concentration of lipase (- - -) or WGA (—) on rosette formation by AM.

Iodine-125-Labeled Wheat Germ Agglutinin Binding to Alveolar Macrophages

For a more accurate definition of the oxidant-induced alteration of macrophage membranes observed in the above studies, purified WGA, a known contaminant of wheat germ lipase, was examined for its ability to induce rosette formation in the test system. Figure 2 illustrates the relationship between the rosette formation and various concentrations of lipase or WGA. The WGA was more active than the crude wheat germ lipase preparation with both SRBC's and RRBC's in the formation of rosettes by treated AM. The WGA content of the

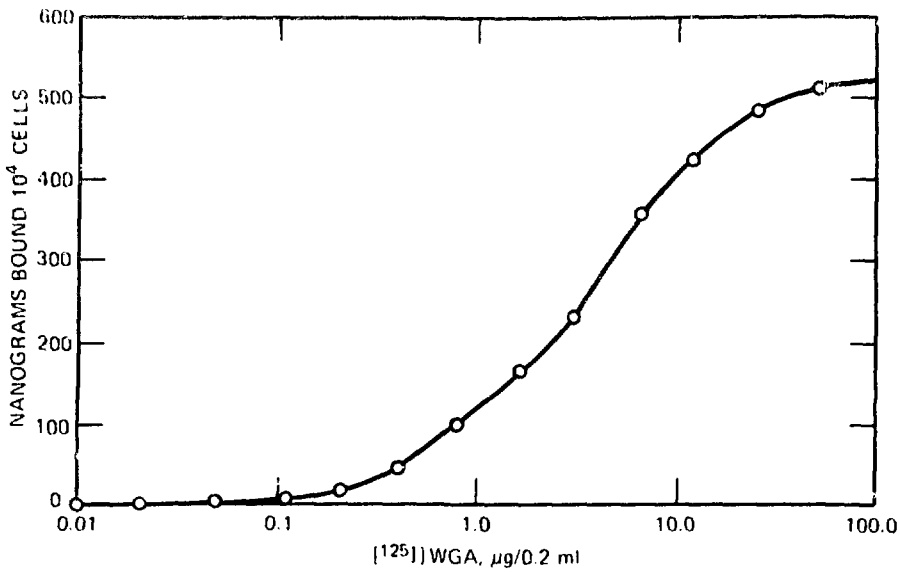

Fig. 3 Specific binding of [^{125}I]WGA to AM.

wheat germ lipase could well account for the majority of rosette-forming activity.

A complete characterization of [^{125}I]WGA binding to AM will be described elsewhere. Some of these findings will be reviewed here (unpublished). Figure 3 illustrates the specific binding of the [^{125}I]WGA to the AM. The binding appears to be a saturable process, although data at high [^{125}I]WGA concentrations vary considerably owing to agglutination of the AM. Examination of the binding of [^{125}I]WGA to AM at low concentrations of the iodolectin reveals that the amount of WGA bound to the AM is directly proportional to the concentration of the iodolectin (Fig. 4). Analysis of the data from Figs. 3 and 4 according to the scheme of Scatchard[9] gives the results shown in Fig. 5.

Oxidant-Induced Alterations in ^{125}I-Labeled Wheat Germ Agglutinin Alveolar Macrophage

Following exposure to O_3 (0.981 mg/m^3 for 3 hr), rabbits were sacrificed and their pulmonary macrophages isolated and examined for specific binding of WGA. Results from these experiments are shown in Table 2. At both concentrations of the WGA tested, AM from O_3-exposed animals bound a significantly greater amount ($p < 0.01$) of the labeled lectin than did AM from air-exposed animals.

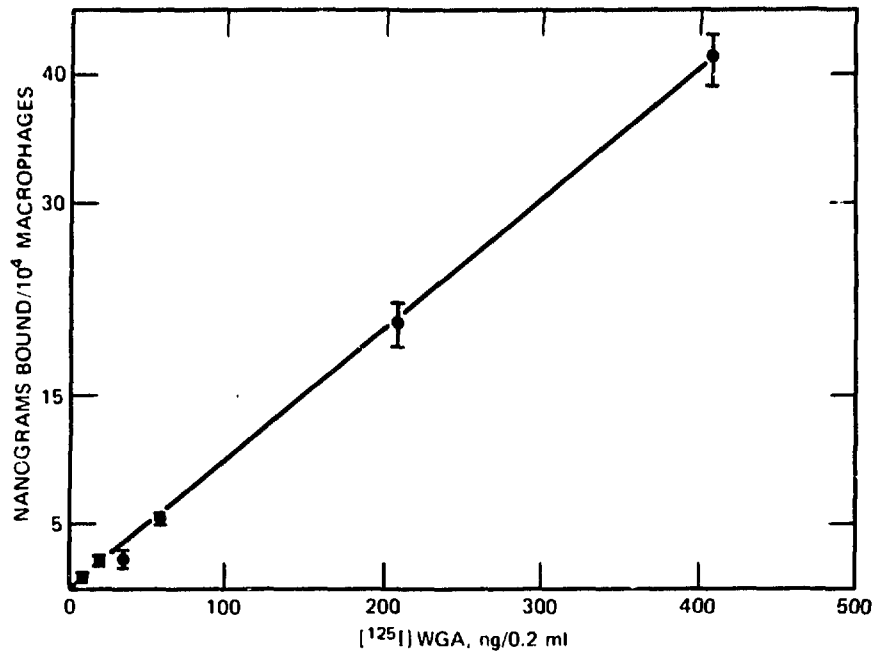

Fig. 4 Specific binding of [^{125}I]WGA to AM.

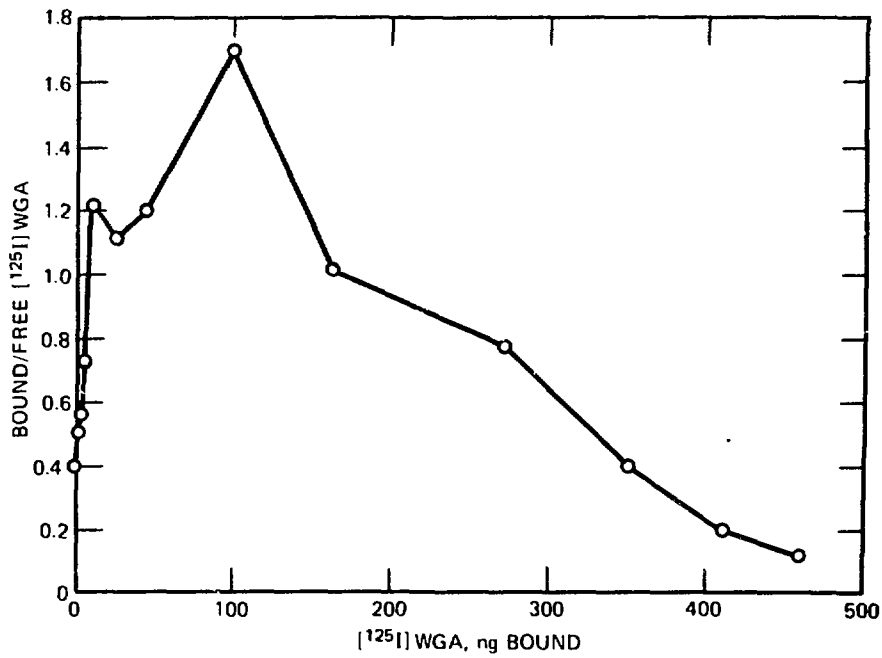

Fig. 5 Scatchard plot of [^{125}I]WGA binding to AM.

TABLE 2

EFFECT OF O_3 EXPOSURE ON [^{125}I]WGA BINDING BY ALVEOLAR MACROPHAGES

Concentration of WGA, ng/0.2 ml	Nanograms of [^{125}I]WGA bound per 10^4 macrophages		
	Air	O_3	Percent of control
208	20.5 ± 1.3(6)†	34.2 ± 2.8(9)	167*
406	42.5 ± 1.5(6)	59.9 ± 5.8(9)	141*

*$p < 0.01$.
†Number in parentheses is the number of experiments.

DISCUSSION

The vital role of the AM in host defense warrants intensive investigation into the mechanisms responsible for macrophage function. The AM, in its unique intrapulmonary environment, must be able to recognize and respond to a large number of external stimuli, including inert inhaled particles, antibody, or complement coated microbes, a variety of peptide hormones, and a host of chemotactic agents. Most, if not all, of these stimuli exert their influence by combining with distinct areas of the plasma membrane of the AM. These combining sites or receptors are believed to be complex proteins composed of both hydrophilic and lipophilic regions and are oriented in the membrane so as to present their glycosyl prosthetic groups to the external environment of the cell. These receptors may respond to occupancy individually or in a concomeric manner to promote their action. Response to occupancy may consist of membrane-associated enzyme activation (i.e., adenylate cyclase) and/or the translocation of the receptors within the plane of the membrane.[10]

The increasing knowledge of the role of the plasma membrane in translating extracellular stimuli into intracellular responses has been brought about in part by the use of various carbohydrate-binding proteins, collectively known as lectins.[11] These proteins demonstrate a marked affinity for various simple carbohydrates, many of which are present on the surface of mammalian cells. Some lectins have the ability to differentiate between normal and transformed or neoplastic cells.[12] Transformed cells are agglutinated at lower lectin concentrations than their nontransformed counterparts. Increased

lectin agglutinability can also be accomplished by mild proteolytic digestion of normal cells.[13] Whether the increase in agglutination observed in altered cells is due to an increase in the number or the affinity of binding sites, an alteration in the topographic distribution of the receptors in the membrane, or all those factors is not established.[13]

In the current study a crude preparation of lipase extracted from wheat germ was found to induce rosette formation between AM and both SRBC's and RRBC's. The binding was concentration and time dependent and was reversible. Rosette formation in these studies is akin to an agglutination reaction with only a portion of the cells involved exposed to the free lectin. The red blood cells added to the washed AM monolayers can only bind to lectin, which is available on the macrophage plasma membrane. A highly purified fraction from the lipase preparations, WGA, agglutinates many cell types[12] and induced rosette formation in our test system. In this sense the observed increase in rosette formation following oxidant exposure is not unlike the increased agglutinability by WGA observed in transformed or protease-treated cells.[13] In an attempt to elucidate the alterations observed in rosette formation following oxidant exposure, the binding of a radiolabeled preparation of WGA to AM was examined.

The binding of [^{125}I]WGA to AM was found to be a saturable process, with a maximum of approximately 500 ng bound per 10^4 cells. Assuming a macrophage diameter of approximately 35 μm, each macrophage can bind about 12×10^8 molecules of the lectin. This value is in good agreement with that reported by Cuatrecasas,[6] who, using these same assumptions, calculated that rat adipocytes bind 4×10^8 WGA molecules per cell. Evaluation of the binding data by Scatchard analysis yielded the complex profile illustrated in Fig. 4. Although such a relationship cannot be interpreted readily at the present time, the presence of receptor sites of markedly different affinities and the probable occurrence of interactions between binding sites are suggested. It is also of interest that this analysis bears a striking similarity to the Scatchard plot derived by Cuatrecasas[6] for ^{125}I binding to rat fat cells.

The AM from rabbits exposed to O_3 exhibited a marked increase in the amount of WGA bound. Although the cause of the increased binding is not apparent from these experiments, increased binding was observed at low lectin concentrations far removed from saturating concentrations (Fig. 3). Binding in this low concentration range may represent interaction with receptors having the highest affinity for the lectin. Indeed one can calculate that, at this low

lectin concentration, macrophages from control animals bound almost 50% of available lectin,* whereas macrophages from O_3-exposed animals bound nearly 75% of available lectin. Whether this increase is due to an alteration in the total number of binding sites or to a change in the affinity of preexisting sites is currently under investigation, and preliminary evidence suggests the latter possibility.

In this study WGA was used as a probe of AM membrane structure. Oxidant exposure enhanced WGA binding to the AM, and this enhancement could be observed in either a modified agglutination reaction (rosette formation) or in the binding of the radiolabeled lectin to the macrophage. These findings suggest that the use of membrane probes may prove to be a powerful tool by which pollutant effects can be accurately and sensitively monitored. Hopefully such information will lead to a better understanding of the mechanisms by which the AM serves its role in pulmonary defense.

REFERENCES

1. D. L. Coffin, D. E. Gardner, R. S. Holzman, and F. J. Wolock, Influence of Ozone on Pulmonary Cells, *Arch. Environ. Health*, 16: 633-639(1968).
2. D. E. Gardner, R. S. Holzman, and D. L. Coffin, Effects of Nitrogen Dioxide on Pulmonary Cell Population, *J. Bacteriol.*, 98(3): 1041-1043(1969).
3. J. A. Graham, D. E. Gardner, M. D. Waters, and D. L. Coffin, Effect of Trace Metals on Phagocytosis by Alveolar Macrophages, *Infect. Immunity*, 11(6): 1279-1283(1975).
4. D. J. Hurst, D. E. Gardner, and D. L. Coffin, Effects of Ozone on Acid Hydrolases of the Pulmonary Alveolar Macrophage, *J. Reticuloendothel. Soc.*, 8: 288-300(1970).
5. G. L. Nicolson, Transmembrane Control of the Receptors on Normal and Tumor Cells. I., *Biochim. Biophys. Acta*, 457: 57-108(1973).
6. P. Cuatrecasas, Interaction of Wheat Germ Agglutin and Concanavalin A on Isolated Fat Cells, *Biochemistry*, 12(7): 1312-1323(1973).
7. R. G. Hinners, J. K. Burkart, and C. L. Punte, Animal Inhalation Exposure Chambers, *Arch. Environ. Health*, 16: 194-206(1968).
8. B. E. Saltzman, Selected Methods for the Measurement of Air Pollutants, U.S. Department of Health, Education, and Welfare, Publication No. 99-AP-11.
9. G. Scatchard, The Attractions of Proteins for Small Molecules and Ions, *Ann. N.Y. Acad. Sci.*, 51: 660-673(1949).
10. J. M. Oliver and R. D. Berlin, *Immunobiology of the Macrophage*, Academic Press, Inc., New York, 1976.

*For example, Fig. 4 illustrates that, with 400 ng of [^{125}I]WGA available, 10^4 macrophages bind approximately 40 ng. Since the total number of macrophages in this experiment was 5.1×10^4, the macrophages bound 204 ng, or 50%, of the total available lectin.

11. N. Sharon and H. Lis, Lectins: Cell-Agglutinating and Sugar Specific Proteins, *Science*, 177(4053): 949-959(1972).
12. M. M. Burger and A. R. Goldberg, Identification of a Tumor Specific Determinant on Neoplastic Cell Surfaces, *Proc. Nat. Acad. Sci. U.S.A.*, 57: 359-366(1967).
13. M. M. Burger, Surface Changes in Transformed Cells Detected by Lectins, *Fed. Proc.*, 32(1): 91-101(1973).

Alveolar Macrophages: Phagocytosis-Induced Release of Neutrophil Chemotactic Activity

B. ROOS, H. U. KELLER, M. W. HESS, and H. COTTIER
Institute of Pathology, University of Bern, Switzerland

ABSTRACT

Rabbit alveolar macrophages induced with bacillus Calmette-Guérin release little if any measurable chemotactic activity in vitro. Neutrophil cytotaxins or rapidly activatable precursors or both can be demonstrated in lysates of such cells. Neutrophil chemotactic activity is released from alveolar macrophages following the ingestion of zymosan or immune complexes.

The accumulation of leucocytes and the release of macromolecules, particularly of neutral proteases and acid hydrolases, from these cells are of considerable importance in the pathogenesis of many forms of inflammation. It has been suggested that leucocytes that have arrived at the site of injury influence the course of cell accumulation by releasing cytotaxins, cytotaxigens,[1-5] and neutrophil immobilizing factors.[6,7] Neutrophils from peritoneal exudates release cytotaxins,[2] and this process is significantly stimulated following phagocytosis of immune complexes.[3] In contrast to peritoneal exudate neutrophils, alveolar macrophages showed no measurable spontaneous cytotaxin release.[3] Lysates of mononuclear cells exhibited either no[4] or little to moderate[2] chemotactic activity for neutrophil granulocytes. The possibility that phagocytosis might induce the release of neutrophil cytotaxins has, however, not been evaluated.

Recent studies have shown that phagocytosis stimulates macrophages to secrete a variety of enzymes and other mediators of inflammation (for review, see Ref. 8). We have therefore decided to investigate whether alveolar macrophages can be stimulated to

secrete neutrophil cytotaxins following phagocytosis. We hoped that such studies would contribute to the understanding of the pathogenesis of inflammatory reactions to inhaled particles or antigens.

MATERIALS AND METHODS

Animals

Adult rabbits of both sexes and of mixed stock weighing 3000 to 4000 g were used.

Harvesting of Neutrophilic Granulocytes

Neutrophils for chemotaxis tests were obtained by heart puncture of rabbits anesthetized with Nembutal. Phagocytosis and release of macromolecules were studied in peritoneal exudate neutrophils harvested 3 hr after intraperitoneal injection of 40 ml of 3.5% sterile sodium caseinate.

Harvesting of Alveolar Macrophages

Cells were obtained from rabbits by the method of *Myrvik et al.*[9] 4 weeks after two intravenous injections of bacillus Calmette-Guérin (BCG) on two consecutive days.

Agents

Immune complexes (ovalbumin—rabbit antiovalbumin) were formed at equivalence and washed.[10] Zymosan was treated as described by Weissmann, Dukor, and Zurier.[11] In contrast to other zymosan samples, the preparation used in the present experiments exhibited no spontaneous chemotactic activity. Asbestos (chrysotile A) was kindly provided by Dr. A. C. Allison, Clinical Research Center, Harrow, England.

Incubation Procedures and Measurement of Release of N-Acetyl-β-Glucosaminidase and Neutrophil Chemotactic Activity

Alveolar macrophages were cultured in tissue-culture dishes (60 by 15 mm) with flying cover slips in an atmosphere containing 5% CO_2 at 37°C. Each dish received 15×10^6 cells in a final volume of 3 ml of medium 199 containing penicillin (200 units/ml) and streptomycin (100 μg/ml). The cells were washed three times before the addition of particles, and the washing fluid was also evaluated for

enzymatic and chemotactic activity. Particles were added to a final concentration of 0.7 mg zymosan/ml, 50 μg asbestos/ml, or 4 mg immune complexes/ml. No serum or plasma was present in the culture fluid. Cells were then incubated with or without particles, and the supernatants of the cultures were harvested at the time intervals indicated. They were immediately centrifuged at 2600 x *g* for 10 min at 4°C. Cell counts were performed on the pellet, whereas the supernatant was analyzed spectrophotometrically for *N*-acetyl-β-glucosaminidase at pH 4.5 (Ref. 12). Phagocytosis and cell density were analyzed morphologically on Giemsa-stained flying cover slips. The remaining supernatants were immediately frozen and kept at −60°C and tested for neutrophil chemotactic activity the next day. Similar determinations were performed on cell lysates obtained by sonication. Nigrosin test and cell counts showed that the percentage of dead cells was small and revealed no difference between zymosan-treated cells and controls.

Random and directional locomotion was tested by counting the number of rabbit neutrophils that had moved through the entire thickness of the filter and expressed as percent neutrophils that had moved through the filter.[10]

RESULTS

A first series of experiments confirmed that peritoneal exudate neutrophils exhibited spontaneous release of small amounts of cytotaxins and that this process was stimulated by exposure to immune complexes. Alveolar macrophages showed no significant cytotaxin release under similar test conditions, i.e., an exposure time of 2 hr (Fig. 1a). From these experiments it was not clear whether neutrophils and alveolar macrophages differ in their capacity to phagocytose immune complexes and to become activated or in their capacity to synthesize and release cytotaxins and/or neutrophil immobilizing factors. Different types of particles and longer exposure times were therefore used to evaluate cytotaxin release from alveolar macrophages.

Uptake of zymosan by macrophages can easily be verified and quantitated morphologically, and it is known to cause secretion of various macromolecules. We found that stimulation with zymosan results in efficient release of both *N*-acetyl-β-glucosaminidase and neutrophil cytotaxins from alveolar macrophages (Fig. 1b). Chemotactic activity could also be detected in 1:10 diluted supernatants of zymosan-exposed alveolar macrophages after 3 and 5 hr of culture.

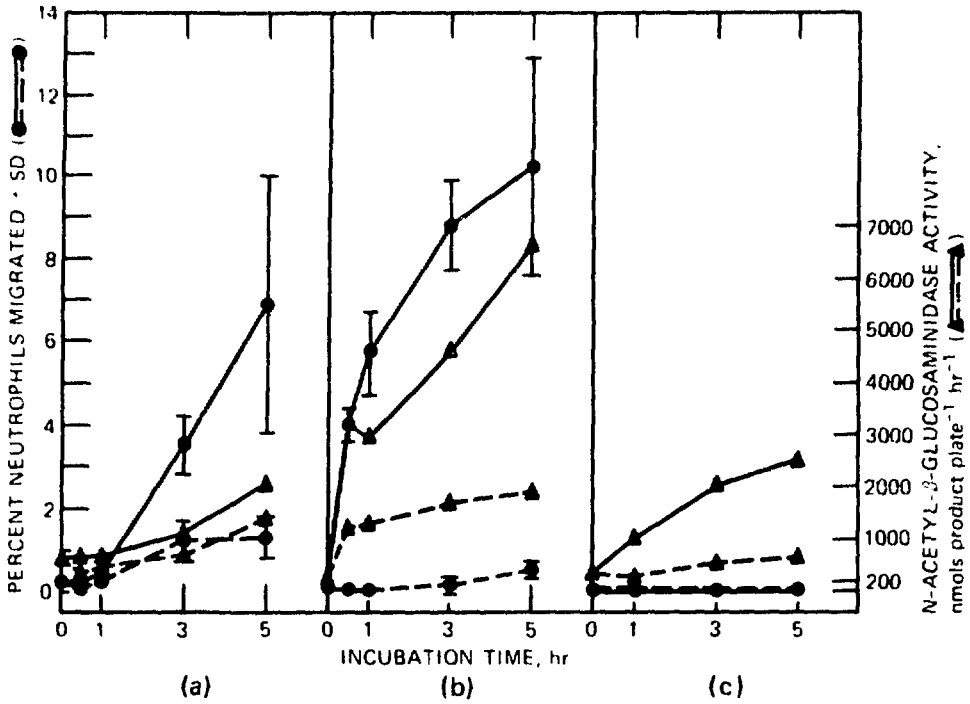

Fig. 1 Effect of immune complexes, zymosan, or asbestos on the release of neutrophil chemotactic activity and *N*-acetyl-β-glucosaminidase from alveolar macrophages. Release of chemotactic activity (●———●) and *N*-acetyl-β-glucosaminidase (▲———▲) in control cultures, as compared to release of chemotactic activity (●———●) and *N*-acetyl-β-glucosaminidase (▲———▲) from cells exposed to a final concentration of either 4 mg immune complexes/ml (a), 0.7 mg zymosan/ml (b), or 50 μg asbestos/ml (c).

Exposure to immune complexes produced only a small increase in *N*-acetyl-β-glucosaminidase activity in the supernatant as compared to controls, whereas significant chemotactic activity was detectable at 5 hr of incubation (Fig. 1a). Exposure of alveolar macrophages to asbestos resulted in a significantly increased secretion of *N*-acetyl-β-glucosaminidase but no (Fig. 1c) or little (Table 1) release of chemotactic activity.

Finally, we have evaluated whether chemotactic factors can be demonstrated in alveolar macrophages that have not yet been stimulated by phagocytosis in vitro. Substantial neutrophil chemotactic activity can be demonstrated in cell lysates obtained by sonication. On a cell-to-cell basis, however, the activity in lysates is somewhat lower than that demonstrated in the supernatants of zymosan-stimulated cells (Table 1).

TABLE 1

INTRACELLULAR AND EXTRACELLULAR NEUTROPHIL CHEMOTACTIC ACTIVITY IN BCG-INDUCED RABBIT ALVEOLAR MACROPHAGES

Test material	Percent neutrophils migrated ± SD
Medium control	9 ± 2
Supernatant of macrophages*	5 ± 1
Supernatant of macrophages + zymosan*	48 ± 5
Supernatant of macrophages + asbestos*	17 ± 3
Lysate of macrophages	36 ± 3

*Incubation time, 5 hr.

DISCUSSION

The essential new fact emerging from the present study is that substantial neutrophil chemotactic activity can be released by alveolar macrophages following appropriate stimulation. In the absence of stimulation in vitro, alveolar macrophages showed very little if any spontaneous cytotaxin release, but significant chemotactic activity can be demonstrated in lysates of such cells. This indicates that cytotaxins and/or rapidly activatable precursors are stored in alveolar macrophages. The activity has been located in the 15,000 x *g* supernatant of alveolar but not of oil-induced peritoneal macrophages, whereas the lysosomal fraction had little if any chemotactic activity.[2] The nature of these factors remains to be evaluated. It may be of interest in this context that appropriately stimulated peritoneal exudate macrophages secrete plasminogen activator.[13] Since at least the plasminogen activator isolated from human serum exhibits chemotactic properties,[14] possible links between these findings have to be evaluated. Even though substantial chemotactic activity has been demonstrated in cells that have not ingested particles in vitro, it is not excluded that some chemotactic activity could also be generated when macrophages degrade ingested materials. Although no relevant data are available with respect to zymosan, immunoglobulin split products were reported to exhibit neutrophil chemotactic activity.[15]

A number of limitations, inevitable at this preliminary stage, have to be pointed out. It has been demonstrated that blood monocytes following phagocytosis release neutrophil immobilizing factors.[6,7]

Blood monocytes can develop into alveolar macrophages, and it may well be that they retain this capacity. Such neutrophil immobilizing factors would interfere with cytotaxin quantitation. Consequently the chemotactic activity measured is not necessarily representative for the total amount of cytotaxins released. Furthermore, each particle was tested at one concentration only, and the incubation time was limited to 5 hr. Therefore it cannot be excluded that alveolar macrophages exposed to asbestos release marked chemotactic activity under other test conditions.

The secretion of cytotaxins from activated macrophages may be instrumental in attracting neutrophil granulocytes in vivo and thereby play a significant role in the development of pulmonary lesions. Borel[3] presented evidence to show that neutrophils that arrive at the site of injury release cytotaxins following phagocytosis. These mediators are believed to be instrumental in attracting more neutrophils and also macrophages. The result of the present study indicates that this process may also run the reverse course: Macrophages forming the first line of defense may be instrumental in attracting neutrophils.

ACKNOWLEDGMENTS

We thank Dr. A. C. Allison, Clinical Research Center, Harrow, England, for providing a sample of chrysotile A, Dr. M. Baggiolini, Wander AG, Bern, Switzerland, for valuable advice, and Miss B. Zanolari and Mrs. R. Graf for technical assistance.

REFERENCES

1. H. U. Keller and E. Sorkin, Chemotaxis von Leukocyten induziert durch Leukocyten In Vitro, *Helv. Phys. Acta*, 25: CR 199-CR 200 (1967).
2. J. F. Borel, H. U. Keller, and E. Sorkin, Studies on Chemotaxis. XI. Effect on Neutrophils of Lysosomal and Other Subcellular Fractions from Leukocytes, *Int. Arch. Allergy Appl. Immunol.*, 35: 194-205 (1969).
3. J. F. Borel, Studies on Chemotaxis, *Int. Arch. Allergy Appl. Immunol.*, 39: 247-271 (1970).
4. P. A. Ward, Chemotaxis of Mononuclear Cells, *J. Exp. Med.*, 128: 1201-1221 (1968).
5. S. H. Zigmond and J. G. Hirsch, Leukocyte Locomotion and Chemotaxis, *J. Exp. Med.*, 137: 387-410 (1973).
6. E. J. Goetzl and K. F. Austen, A Neutrophil Immobilizing Factor Derived from Human Leukocytes. I. Generation and Partial Characterization, *J. Exp. Med.*, 136: 1564-1580 (1972).

7. E. J. Goetzl and K. F. Austen, *Antibiotics and Chemotherapy*, Vol. 19, pp. 218-232, Karger, Basel, 1974.
8. P. Davies and A. C. Allison, The Macrophage as a Secretory Cell in Chronic Inflammation, *Agents Actions*, 6: 60-74 (1976).
9. Q. N. Myrvik, E. S. Leake, and B. Fariss, Studies on Pulmonary Alveolar Macrophages from the Normal Rabbit: A Technique to Produce them in a High State of Purity, *J. Immunol.*, 86: 128-132 (1961).
10. H. U. Keller, H. Gerber, M. W. Hess, and H. Cottier, Studies on the Neutrophil Chemotactic Response Using a Rapid and Reliable Method for Measuring Random Migration and Chemotaxis of Neutrophil Granulocytes, *Agents Actions*, 6: 326-339 (1976).
11. G. Weissmann, P. Dukor, and R. B. Zurier, Effect of Cyclic AMP on Release of Lysosomal Enzymes from Phagocytes, *Nature (London) New Biol.*, 231: 131-135 (1971).
12. W. E. Bowers, J. T. Finkenstaedt, and Chr. de Duve, Lysosomes in Lymphoid Tissue. I. The Measurement of Hydrolytic Activities in Whole Homogenates, *J. Cell. Biol.*, 32: 325-337 (1967).
13. S. Gordon, J. C. Unkeless, and C. A. Cohn, Induction of Macrophage Plasminogen Activator by Endotoxin Stimulation and Phagocytosis, *J. Exp. Med.*, 140: 995-1010 (1974).
14. A. P. Kaplan, E. J. Goetzl, and F. Austen, The Fibrinolytic Pathway of Human Plasma, *J. Clin. Invest.*, 52: 2591-2595 (1973).
15. H. Hayashi, M. Yoshinaga, and S. Yamamoto, The Nature of a Mediator of Leucocyte Chemotaxis in Inflammation, in *Antibiotics and Chemotherapy*, Vol. 19, pp. 296-332, Karger, Basel, 1974.

Effect of Particle Size on Regurgitative Exocytosis by Rabbit Alveolar Macrophages

CHAD B. SANDUSKY, MARK W. COWDEN, and SORELL L. SCHWARTZ
Department of Pharmacology, Georgetown University Schools of Medicine and Dentistry, Washington, D. C.

ABSTRACT

Current hypotheses on the etiology of environment-induced chronic obstructive pulmonary disease include the role of exocytosis of proteolytic enzymes by alveolar cells. One possible means of release of such enzymes is "regurgitative exocytosis," which has been described for a variety of types of leukocytes. Regurgitative exocytosis refers to the coalescence of lysosomal organelles with incompletely formed phagosomes, which results in the release of lysosomal enzymes to the cell exterior. The release of acid phosphatase (*p*-nitrophenyl-phosphate as the substrate) and elastase (*t*-butyloxycarbonyl-L-alanine *p*-nitrophenyl ester as the substrate) by rabbit alveolar macrophages over a 2-hr period during phagocytosis of latex beads (1.1 or 5.7 μm in diameter) or zymosan particles (3 to 5 μm in diameter) was evaluated.

Phagocytosis occurred with all particles studied, as indicated by light and scanning and transmission electron microscopy. Release of both enzymes during exposure to 5.7-μm-diameter latex beads showed a linear relationship to the number of particles per cell. On the other hand, no enzyme release occurred during phagocytosis of 1.1-μm-diameter latex beads even when given in equivalent surface area or volume to the 5.7-μm-diameter beads. The amount of enzyme release during exposure to zymosan fell between that for 5 and 10 particles per cell for the larger latex beads. The data imply that the size of the particle is a primarily important determinant of regurgitative exocytosis and that total surface and volume of particles presented to the cell is of secondary importance. This is not necessarily what would be expected on the basis of thermodynamic prediction and could indicate differences in membrane fluidity, based on particle size, which may occur during phagocytosis.

Following the observation of Laurell and Eriksson[1] in 1963 that patients deficient in the circulating enzyme inhibitor α_1-antitrypsin had increased incidence of precocious panlobular emphysema, there

developed in the literature the hypothesis that various proteolytic enzymes might be involved in the etiology of the disease. This hypothesis was supported by numerous subsequent reports that intratracheal administration of the relatively nonspecific enzyme papain[2,3] or more specific enzymes, such as elastase or collagenase,[4,5] produced lesions in the lungs of various species resembling chronic obstructive pulmonary disease (COPD). Later it was shown that enzymes with the greatest elastolytic activity had the greatest activity in producing morphological changes in lungs resembling COPD (Ref. 6). Indeed it has since been well documented that purified pancreatic elastase produces lesions in animal lungs similar to those in emphysema.[7,8]

Parallel to the development of the concept that cellular proteolytic enzymes, especially elastase, may play a contributing role in the development of COPD was the search for a possible source of such enzymes in vivo. Two cell types have received particular attention. Polymorphonuclear (PMN) leukocytes not only contain neutral proteases with elastolytic activity[9-12] but may also secrete some of their lysosomal enzymes during phagocytosis of numerous types of particles.[13-17] Macrophages of various species, although much less studied than PMN leukocytes, also contain elastase-like enzymes and may also release some lysosomal enzymes (including elastase)[18-20] either when stimulated[21,22] or following phagocytosis.[23] Thus it appears that elastase from both PMN leukocytes and macrophages could contribute to the etiology of COPD.

In this regard alveolar macrophages, strangely enough, have received much less attention than PMN leukocytes. We have studied rabbit alveolar macrophages in vitro to evaluate their elastase-like enzyme content. In addition, we studied enzyme release (both elastase and acid phosphatase) following phagocytosis of latex beads and zymosan particles. Included is a discussion of the possible effect of particle size on enzyme release as well as an evaluation of the importance of physical and chemical properties of latex particles when used in the study of phagocytosis or enzyme release or both. We have also proposed a mechanism for regurgitative exocytosis from rabbit alveolar macrophages (RAM).

MATERIALS AND METHODS

Harvesting of Rabbit Alveolar Macrophages

from rabbit lungs contained greater than 90% alveolar macrophages that had viability exceeding 90%.

Incubation Procedures

Rabbit alveolar macrophages were incubated in Hanks' balanced salt solution at 37°C. They were exposed in suspension to latex beads (1.1 or 5.7 μm in diameter), zymosan particles (3 to 5 μm in diameter), or medium alone for up to 120 min. At various times samples were removed, and cells and supernatants were separated by centrifugation. All cell and supernatant fractions were evaluated for enzyme and protein content, viability (trypan blue exclusion test), and total cell content (counting in a hemocytometer).

Enzyme Assays

Elastase-like enzyme activity was assayed according to a modification of the method of Visser and Blout[25] using the synthetic substrate *t*-butyloxycarbonyl-L-alanine *p*-nitrophenylphosphate (TBOC). Enzyme activity is expressed as nanomoles of TBOC hydrolyzed per minute per milligram of cell protein. Acid phosphatase activity was assayed with the use of *p*-nitrophenylphosphate (PNPP) as the substrate. Enzyme activity is expressed as nanomoles of PNPP hydrolyzed per minute per milligram of cell protein. Total cellular enzymes were assayed in suspensions of cells that were disrupted by freeze and thaw.

Chemical Assay

Protein content of the various cell fractions was measured by a modification of Lowry et al.[26]

Electron Microscopy (EM)

Transmission Electron Microscopy (TEM)

After incubation with latex beads, zymosan particles, or medium alone, rabbit alveolar macrophages were fixed in suspension with Ito—Karnovsky[27] fixative. After the pellets had been washed, dehydrated, and fixed in Epon,[28] thick sections were cut, stained with toluidine blue,[29] and examined with light microscopy for

Scanning Electron Microscopy (SEM)

Alveolar macrophages were allowed to attach to glass cover slips in Leighton tubes and then incubated with latex beads, zymosan particles, or medium alone for 60 min. The attached cells were then washed and fixed.[27] After the cells had been washed, they were dehydrated with ethanol with the use of the Critical Point Drying System and coated by gold–palladium ions in a Hummer apparatus. Samples were examined with an ETEC Autoscan B-1 scanning electron microscope.

RESULTS

Characteristics of RAM Suspensions

We studied our suspensions of RAM over a 2-hr period with respect to a number of parameters. The percent viability and enzyme levels (elastase and acid phosphatase) remained constant during the period of incubations. On the basis of these considerations, we judged that, under the conditions of our incubations, the suspensions of RAM would prove suitable in the study of the effect of phagocytosis on enzyme release (regurgitative exocytosis) from these cells.

Verification of Phagocytosis of Latex Beads (1.1 and 5.7 μm) and Zymosan Particles (3 to 5 μm): Electron Microscopy

Rabbit alveolar macrophages, which had been incubated with media alone, latex beads (1.1 or 5.7 μm in diameter), or zymosan particles (3 to 5 μm in diameter), were examined by both TEM and SEM to determine if the latex beads and zymosan particles were actually inside the cells. Light microscopy alone did not prove adequate to demonstrate that phagocytosis of these particles by RAM had actually occurred.

Figure 1a shows a representative low-power-transmission electron-microscope micrograph of RAM that had not been exposed to any latex beads or zymosan particles. There are few, if any, large vacuoles or particles present. In Fig. 1b the presence of zymosan (Z) particles can be noted intracellularly, which indicates that, when RAM are exposed to zymosan particles, phagocytosis of these particles occurred. Figures 1c and 1d show similar electron micrographs of RAM that have been incubated with latex beads (P) that were 1.1 and 5.7 μm in diameter, respectively. Although the propylene oxide used in the embedding procedure probably dissolved

the 1.1-μm-diameter polystyrene latex beads to a certain degree,[33] it can be clearly seen that phagocytosis of both sizes of beads did occur. This is indicated either by the presence of numerous vesicles in cells incubated with the 1.1-μm-diameter polystyrene latex (P) beads (Fig. 1c) or by the presence of the 5.7-μm-diameter polystyrene divinylbenzene (P) beads (Fig. 1d) themselves (which were not dissolved by the propylene oxide). From these studies, therefore, it appears that both sizes of latex beads (1.1 and 5.7 μm) and zymosan particles (3 to 5 μm) served as phagocytic stimuli for RAM in suspension.

One additional observation was made from these micrographs. All particles (both latex and zymosan) appeared to be contained in separate vesicles. Only rarely were more than one of the smaller latex beads or zymosan particles observed to be sequestered in the same vesicle. In no instance was more than one of the larger latex beads (5.7 μm) noted to be contained in the same vesicle.

When RAM from similar experiments were observed by SEM, similar results were obtained. Figure 2a shows a low-power SEM micrograph of RAM attached to a glass cover slip. These cells have the appearance of normal RAM, which had not been exposed to latex or zymosan. When RAM were incubated with either latex beads (1.1 or 5.7 μm) or zymosan particles (3 to 5 μm) for 60 min at 37°C, phagocytosis occurred, which was evidenced by the intracellular presence of all three sizes of particles. Figures 2b, c, and d show that phagocytosis occurred when RAM were incubated with either zymosan particles (3 to 5 μm) or latex beads (1.1 or 5.7 μm), respectively.

Enzyme Release in Response to Phagocytosis

Table 1 shows the results of experiments in which release of elastase (E) and acid phosphatase (AP) from RAM was evaluated following phagocytosis of 1.1- or 5.7-μm-diameter latex beads or 3- to 5-μm-diameter zymosan particles. Release of both E (10.2 ± 1.1%) and AP (12.5 ± 1.0%) occurred after incubation with zymosan particles (10 per cell) for 2 hr. Similarly, release of E (11.3 ± 0.9%) and AP (11.2 ± 0.7%) occurred after 2 hr of incubation with 5.7-μm-diameter latex beads (10 per cell). Lesser amounts of enzyme release occurred at 2 hr when RAM were incubated with 5.7-μm-diameter latex beads, 5 per cell (E, 9.2 ± 1.1%; AP, 8.3 ± 0.3%) or 1 per cell (E, 7.2 ± 2.1%; AP, 6.1 ± 1.2%). When 1.1-μm-diameter latex beads were incubated with RAM (100 per cell), there was no release after 2 hr when compared with control release. When the number of the smaller latex beads was increased to correspond to the volume (970

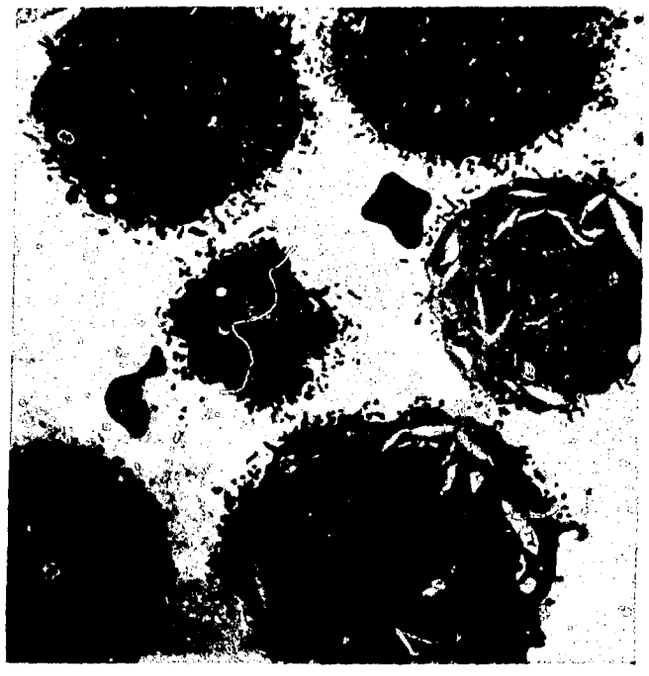

(a)

(b)

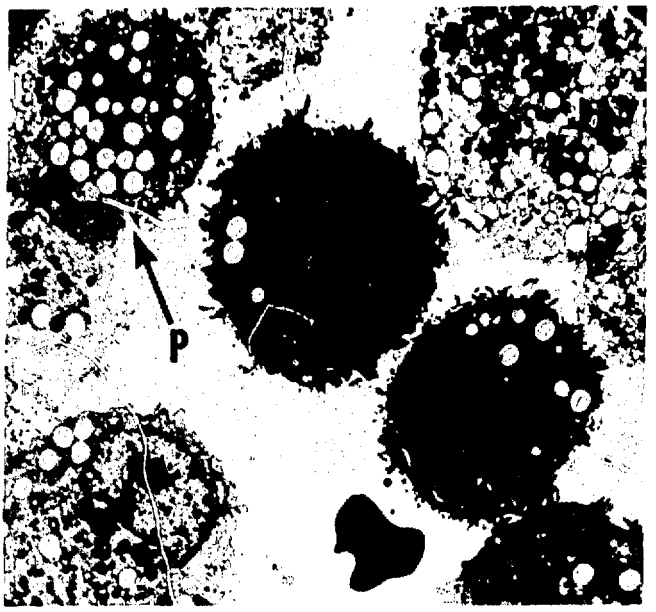

(c)

(d)

Fig. 1—Transmission electron microscopy of RAM after incubation in suspension at 37°C for 60 min with (a) media alone (control); (b) zymosan (Z) particles, 3 to 5 μm in diameter, 10 per cell; (c) polystyrene latex (P) beads, 1.1 μm in diameter, 100 per cell; or (d) polystyrene divinylbenzene (P) beads, 5.7 μm in diameter, 10 per cell. All particles were phagocytized by RAM under conditions of these incubations. Magnification, ~2600 X.

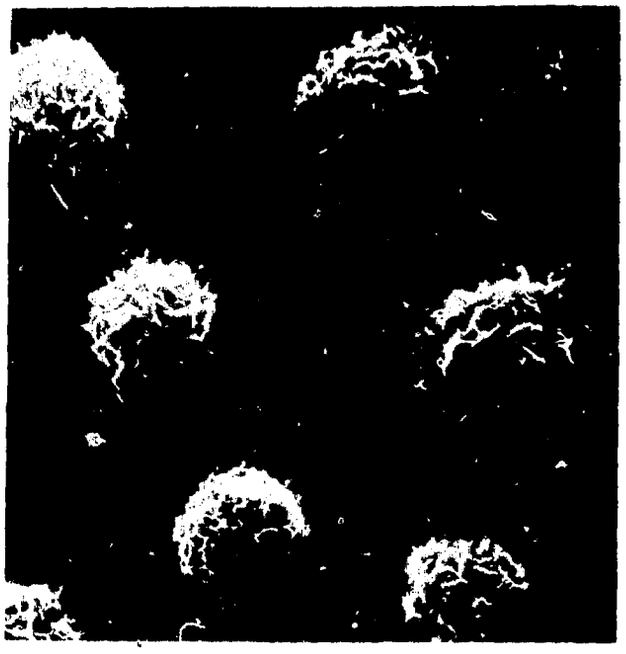

(a)

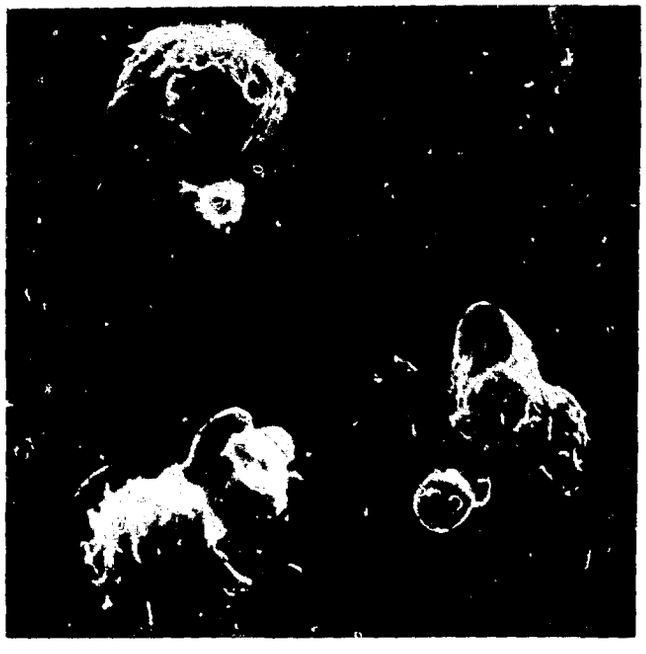

(b)

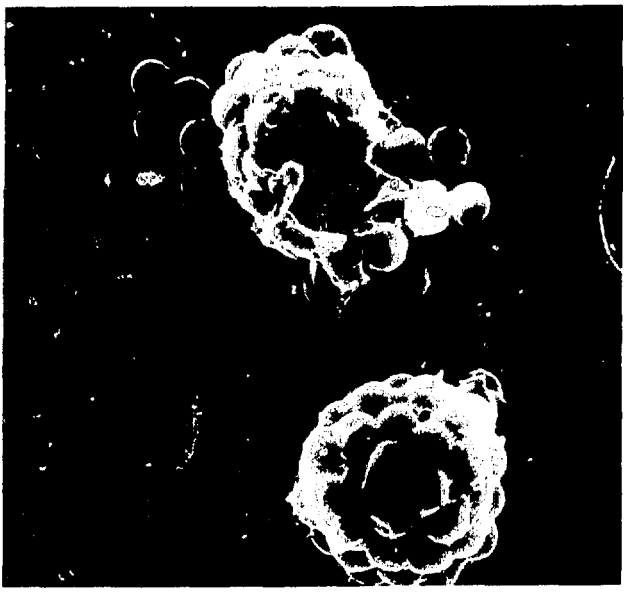

(c)

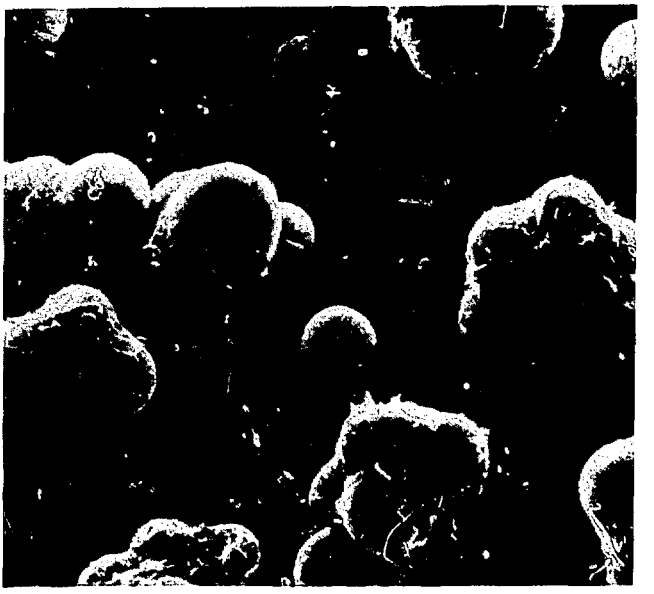

(d)

Fig. 2—Scanning electron microscopy of RAM attached to glass cover slips after incubation at 37°C for 60 min with (a) media alone (magnification, 2100 X); (b) zymosan particles (magnification, 2100 X), 3 to 5 μm in diameter, 10 per cell; (c) polystyrene latex beads (magnification, 2500 X), 1.1 μm in diameter, 100 per cell; or (d) polystyrene divinylbenzene beads (magnification, 2500 X), 5.7 μm in diameter, 10 per cell. All particles were phagocytized under the conditions of these incubations.

TABLE 1

PERCENT RELEASE OF ELASTASE (E) AND ACID PHOSPHATASE (AP)

Particle	No.	Number per cell	Surface area, μm^2	Volume, μm^3	0 min		60 min		120 min	
					E	AP	E	AP	E	AP
Zymosan (3 to 5 μm in diameter)	10	10	283 to 786	141 to 654	1.7 ± 0.5	2.9 ± 1.0	4.0 ± 0.9	7.3 ± 1.4	10.2 ± 1.1	12.5 ± 1.0
PDB* latex	4	10	1021	970	1.4 ± 0.7	1.6 ± 0.9	5.4 ± 1.3	6.8 ± 0.7	11.3 ± 0.9	11.2 ± 0.7
(5.7 μm	5	5	510	485	0.5 ± 0.5	1.7 ± 0.6	4.2 ± 0.3	6.9 ± 0.5	9.2 ± 1.1	8.3 ± 0.3
in diameter)	5	1	102	97	0.5 ± 0.5	2.1 ± 0.6	3.7 ± 0.7	4.7 ± 0.9	7.2 ± 2.1	6.1 ± 1.2
PSL†	3	100	380	70	4.3 ± 1.3	5.9 ± 2.4	3.8 ± 1.4	5.6 ± 2.0	6.8 ± 2.6	5.9 ± 2.2
(1.1 μm	4	269	1022	188	0	2.0 ± 0.8	1.1 ± 0.5	6.0 ± 0.9	2.1 ± 0.8	6.1 ± 1.4
in diameter)	4	1385	5263	970	0	2.3 ± 0.8	0.6 ± 0.3	4.8 ± 0.5	3.4 ± 1.4	6.2 ± 0.9

*PDB, polystyrene divinylbenzene latex (95/5).
†PSL, polystyrene latex.

μm^3) or surface area (1021 μm^2) of 5.7-μm-diameter beads (10 per cell) (where release over background was observed), there appeared to be some augmented release of E (2.1 to 3.4%) and AP (6.1 to 6.2%) at 2 hr of incubation. However, although not shown in Table 1, it was noted that there was an increase in the uptake of trypan blue by these cells. Between 11 and 15% of the cells stained with the dye, which indicates that perhaps this enzyme release corresponded to an increase in cell mortality. We cannot explain this increase in trypan blue uptake. In all other incubations, less than 10% of the cells took up the dye, which indicates that release of E and AP in response to phagocytosis of zymosan particles or 5.7-μm-diameter latex beads was not a result of cell death. Apparently, therefore, the size of the particle was more important than the total volume or surface area in stimulating selective exocytosis of E and AP from RAM during phagocytosis.

DISCUSSION

Over the past several years, the fact that polymorphonuclear (PMN) leukocytes contain lysosomal enzymes that can cause acute inflammatory reactions and irreversible tissue damage has become well established. Included among these enzymes is an elastase-like enzyme, first described by Janoff and Scherer,[9] which has been shown to be capable of degrading lung[34] and arterial wall elastin in vitro.[9] The presence of elastase-like enzyme activity has since been confirmed not only in the PMN leukocytes[10,35] but also in pulmonary alveolar macrophages.[18,20,36] A number of mechanisms have been proposed whereby PMN leukocytes will secrete various lysosomal enzymes. These mechanisms include regurgitative exocytosis, which is observed during phagocytosis of zymosan or immune complexes,[13-16] or a "reverse endocytosis," which is observed when cells are exposed to nonphagocytosable surfaces coated with immune complexes.[16,17] Macrophages, too, will secrete various lysosomal enzymes either in response to stimulation by thioglycollate[21,22] or during phagocytosis of zymosan.[23,37] The presence of elastase-like enzymes in macrophages led us to examine the possible role of elastase release from rabbit pulmonary alveolar macrophages during phagocytosis as a partial explanation of elastin changes observed in COPD.

Not only did we confirm the presence of elastase-like activity in rabbit alveolar macrophages but also we were able to demonstrate significant release of both elastase and acid phosphatase from these cells in response to phagocytosis of zymosan particles (3 to 5 μm)

and polystyrene divinylbenzene beads (5.7 μm). Very little, if any, release was observed with phagocytosis of polystyrene latex beads (1.1 μm), even when the total surface area or volume presented to the cells was equal to that of the larger latex beads. Indeed, what little release was observed with the smaller beads (269 or 1385 per cell) was associated with an augmented uptake of trypan blue, which suggests that the small percent release observed may have been correlated with a loss of cell viability. There was no such increase in trypan blue uptake associated with phagocytosis of either zymosan particles or the larger latex beads, which suggests that this was a selective lysosomal enzyme release via similar mechanisms proposed for the PMN leukocyte by Weisman et al.[13,14] and Henson.[16,17] The smaller amount of release observed with phagocytosis of the smaller latex beads (even at equivalent surface area and volume as the larger beads) suggested to us that the actual size of the particle may be an important determinant of regurgitative exocytosis and that the total surface and volume of particles presented to the cell is of secondary importance. It is worthy to note, however, according to our transmission and scanning electron micrographs, that both size particles were phagocytosed by alveolar macrophages and both might be expected to initiate regurgitative exocytosis.

Size effects on enzyme release following phagocytosis have been reported by others for the PMN leukocytes. Henson[16] and Baehner, Karnovsky, and Karnovsky[38] reported greater enzyme release from PMN leukocytes following phagocytosis of larger latex particles.

In the study of regurgitative exocytosis, experimenters have challenged PMN leukocytes with various particles, such as aggregated immune complexes, various types of opsonized and unopsonized latex particles with different polymer composition, and zymosan particles. On the basis of studies with enzymes usually associated with PMN leukocytes, light microscopy, and electron microscopy, several mechanisms to explain the release of hydrolytic lysosomal enzymes concomitant with phagocytosis have been proposed. Weissman et al.[13,14] and Henson[15-17] proposed that lysosomal organelles fuse with incompletely formed phagosomes, which results in the release of enzymes into the extracellular milieu—thus the term "regurgitative exocytosis." This mechanism is supported by the observation that greater release of β-glucuronidase occurs when PMN leukocytes phagocytize larger γG-Immunoglobulin (IgG) coated latex particles.[16,17] Henson postulated that larger particles cause the phagosome to remain open for a longer period of time and that this results in a greater release of enzymes. He has also suggested several additional mechanisms to explain the association of this enzyme

release with phagocytosis. One mechanism suggests that this enzyme release is a two-step process: A particle is phagocytosed and fused with a lysosome (forming a phagolysosome) and this phagolysosome is then fused with a newly forming phagosome. Henson[17] supports this idea by finding phagolysosomes containing more than a single particle and by drawing from previous work, where it was observed that the released alkaline phosphatase was not detected but could be found bound to the membrane surface of phagolysosomes.[39]

The mechanisms described above are attractive both for logic and simplicity, but they do tend to be rather descriptive and do not consider the process from a molecular or physical standpoint. They do not take into account whether or not fusion of the lysosomal organelle with the incompletely formed phagosome is thermodynamically the most preferable or, for that matter, possible. Here we would take a seemingly myopic view of current facts and concepts about cellular dynamics to ask questions, present some of our ideas, and propose, primarily for purposes of provocation, another model for regurgitative exocytosis.

The four primary questions that we would like to address are:

1. What is the role, if any, of the physical and chemical modification of the cell surface in facilitating regurgitative exocytosis?
2. How might membrane changes and cytoskeleton changes interact and affect regurgitative exocytosis?
3. Why is it that some particles induce regurgitative exocytosis and some do not? Is this difference due to the physical and chemical differences in the nature of the particle?
4. How might the surface of the particle be modified such that it alters (increases or decreases) regurgitative exocytosis?

Consider first the role that physical and chemical modification of the cell surface might take in regurgitative exocytosis. From a theoretical standpoint, following the approach and contact of a particle during phagocytosis, the particle surface would be expected to cause a marked perturbation in the associating membrane. In light of the current modification of the Singer—Nicolson concept of a fluid mosaic membrane, where more-solid lipid-protein domains are floating in a more-fluid lipoprotein sea,[40-42] the contact of the particle surface to the cell and subsequent vesiculation would tend to sort out the more-solid regions from the more-fluid regions owing to a surface stabilizing effect of the particle-membrane contact; i.e., the solid (more-frozen) domains would have a greater tendency to adhere to the particle surface whereas the more-fluid domains would tend to exclude themselves owing to their higher energy. This process would

cause a dynamic sorting of membrane at the growing tip of the cell's engulfing pseudopod and thus create a more-solid membrane adjacent to the cell-particle contact and a more-fluid membrane on the portion of the pseudopod not in contact with the particle. Thus the engulfing pseudopod membrane not associated with the particle surface would become more fluid whereas the prephagosomal membrane would become less fluid. A logical extension of this view of events would be that lysosomal fusion associated with exocytosis would occur in the more-fluid membrane portion of the extending pseudopod, i.e., the membrane not in direct contact with the particle. The more-solid portion of the membrane, that in contact with the particle, would compose a major portion of the phagosomal membrane.

There are several lines of evidence to support these views. The cell-membrane surface associated with phagocytizing particles is in close contact with the cell membrane. Indeed, protein bridges between the particle and the membrane have been seen.[43] This possibly shows some similarity between membrane-particle contact and tight junctions between cells. It has been observed[44,45] that phagosomal and phagolysosomal membranes contain more cholesterol and saturated fatty acid components (or domains) than do comparatively more-fluid membranes. Cells pretreated with cytochalasin B (3 to 10 μg/ml) are unable to engulf zymosan particles. However, particles seem to aggregate onto the cell surface and cause the cells to extrude lysosomal hydrolases directly from organelles. This discharge appears to occur at the seemingly fluid membrane surface adjacent to seemingly less-fluid membrane adhering to the zymosan particle.[46,47]

One cannot discuss physical and chemical changes in the plasma membrane associated with vesiculation and exocytosis without also considering associated changes in cytoskeletal elements. There is some evidence for the association of particular membrane sites with microtubules. Tsan and Berlin[48] studied the incorporation of 2.2-μm-diameter polyvinyltoluene (PVT) particles by PMN leukocytes and determined that, after the internalization of as much as 50% or more of the cell's plasma membrane, there was no loss of nonionic (lysine) transport sites. Their experiments also demonstrated that this was not a result of increased carrier synthesis. Why were these sites not incorporated within the cell during phagocytosis? Tsan and Berlin[48] suggested possible mechanisms, which include (1) the carriers cluster into groups, (2) the membrane involved in phagocytosis arises intracellularly, or (3) during phagocytosis carriers are pushed in the liquid membrane away from the part of the membrane to be internalized.

Ukena and Berlin[49] then were able to show that, when PMN leukocytes were treated with colchicine, the nonionic transport sites were internalized during phagocytosis. Since colchicine is known to depolymerize microtubules, it appears that nonionic transport sites might be associated with microtubular membrane sites and that these sites appear to be sorted out during phagocytosis. This sorting out could occur at the tip of the pseudopod or in the fluid membrane environment of pseudopod membrane not in contact with the particle. It would be quite interesting to know how a microtubular-connected component could be sorted out in the membrane. It is of interest that the microtubules appear to radiate from a centriolar growth or organization center with microtubular rays terminating in the membrane.[50] Freed and Lebowitz[51] documented this to be the region of highest density of acid phosphatase-rich particles capable of undergoing discrete, long, saltatory movements that are thought to play an important part in exocytosis.

For fusion to take place, it would also seem that the microfilament proteins below the membrane would have to be removed and that this event would occur in the region where there is a dynamic membrane alteration of the pseudopod not in contact with the particle. As mentioned earlier, cytochalasin B prevents polymerization of microfilaments. It also inhibits phagocytosis at high concentrations (5 μg/ml). However, it stimulates phagocytosis and chemotaxis at low concentrations.[14] This biphasic effect is of interest when considering the biphasic effect of cytochalasin B on microtubular structure. After treatment of the cells with cytochalasin B, lysosomes have been observed to lose their pericentriolar orientation and occupy a greater portion of the cytoplasmic volume. These facts suggest a marked interaction between microtubules and microfilaments.

A diagrammatic summary of our view of the physical and chemical factors involved in regurgitative exocytosis is shown and explained in Fig. 3. We realize, of course, that there are cellular energetics, cyclic nucleotides, ion requirements, etc., which are all an integral part of this process. Some of the factors are primarily concerned with the phagocytic process, some with the polymerization and depolymerization of microtubules, and some with activation (or inactivation) of enzyme systems. Our failure to mention them is not a reflection of our estimate of their importance. The model we present is intended to deal with additional factors in areas where much more experimentation is required. The obvious statement that is made with this model is that there is a possibility that the term "regurgitative exocytosis" could be a misnomer; i.e., there appears to be a reasonable possibility that the lysosomal organelles containing

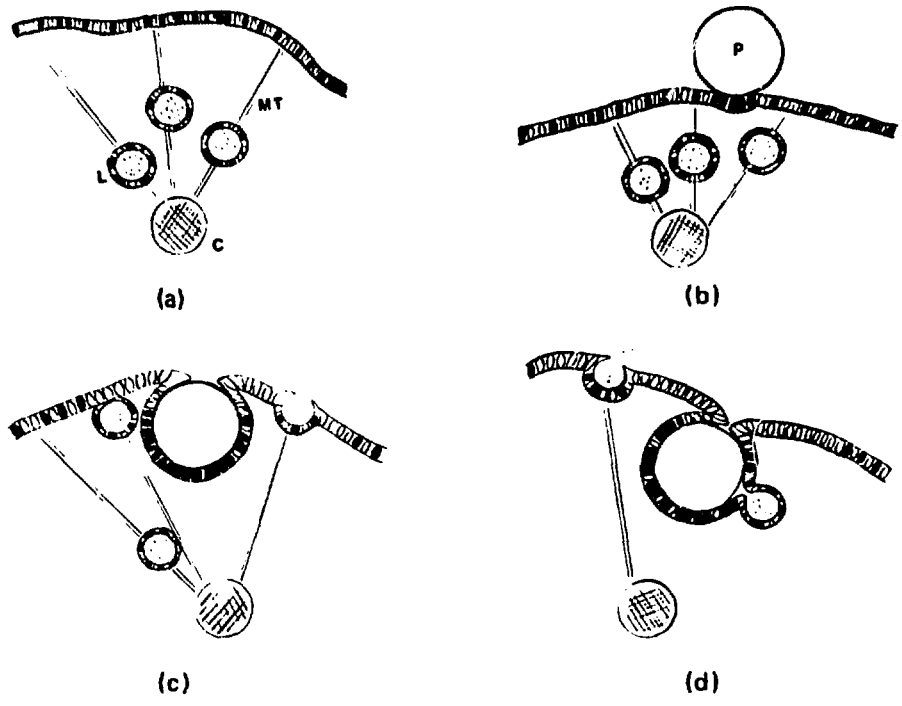

Fig. 3—Diagrammatic representation of model for regurgitative exocytosis. P, particle; L, lysosomal organelle; MT, microtubule; C, centriole; black areas of membrane, solid domains; white areas of membrane, fluid domains.

(a) Before phagocytosis membrane contains evenly distributed solid and fluid lipid domains as well as microtubule attachment sites.

(b) On contact with the membrane, the particle associates more tenaciously with solid membrane domains. The membrane adjacent to the attachment point would be expected to be more fluid.

(c) Microfilaments below the membrane in the attachment region would be expected to depolymerize and repolymerize, which would be necessary for pseudopodal growth. This would free the microtubular attachment sites, i.e., nonionic transport sites which partition into the more-fluid regions. Here, depending on the nature of the particle, size, charge density, and anionic character of the particle, microtubule polymerization and depolymerization result, which could initiate pseudopodal formation. As a result of this, the centriole microtubual organizer is stimulated, making either new microtubules or extending old ones. This results in the saltatory movement of lysosomes to the region of dynamic membrane flux, i.e., the membrane region adjacent to the particle contact at the apex or near the apex of the extending pseudopod. Here, where the membrane becomes more exposed or accessible, fusion results and enzymes are released. At the same time, continued vesiculation results in further concentration of solid domains around the particle.

(d) Continued vesiculation might eventually "draw" fluid portions of pseudopodal apex, with fusing lysosomal organelles, into the forming phagosome.

the enzymes destined for release do not fuse with the incompletely formed phagosome.

The model proposed is also consistent with differences in size effects on exocytosis occurring during phagocytosis; i.e., the larger particle would result in a larger area of advancing pseudopod and, by necessity, of fluid membrane available for fusion. It would also explain why almost no exocytosis was seen with the smaller particles even when total surface area and volume adjustments were made. The fact that no exocytosis occurred with the smaller particle originally caused us some concern. Following simple bubble theory, a small phagosome would be expected to have a higher surface free energy than a larger one. Thus it would be expected that thermodynamic drive for fusion would be greater for the smaller vesicle. This obviously is not verified by the experimental data. The data are consistent, however, with the hypothesis that the forming phagosomal membrane is transiently less fusible, i.e., during a period of dynamic concentration of solid domains in the vesicle membrane.

Finally, we also have to consider that the size differences observed may have been due to other factors. In developing our model we considered theoretical approaches that would compare the particles with respect to size, surface charge, surface charge density, radius of curvature, etc. During this evaluation we had to seriously consider chemical differences in the particles. The 1.1-μm-diameter particles were polystyrene, whereas the 5.7-μm-diameter particles were polystyrene/divinylbenzene (95/5). We found that we could not get polystyrene latex particles in the size range of 2 to 10 μm and substituted a polystyrene particle containing a 5% divinylbenzene copolymer. We made the assumption that the two particles were similar. If one considers how these particles are made, it becomes quite clear that there can be marked physicochemical differences among 100% polystyrene particles alone. Thus concluding that size alone is the sole contributing factor in determining the degree of regurgitative exocytosis could be misleading. Polystyrene particles of uniform size are made by the process of emulsion polymerization. One method is to initiate polymerization of the styrene monomers in an aqueous medium with persulfate ion. The growing polymer partitions into a detergent emulsion where additional monomers can add at the aqueous surface. This leaves a terminal sulfate group exposed at the surface in addition to the emulsifier.[52-54] During the process of making different size beads, the emulsifier, pH, reaction pressure, temperature, etc., might be changed, which would result in slightly different physical and chemical properties for the particles. For a size correlation to be made with respect to regurgitative

exocytosis, it would be necessary to remove the emulsifier (which would probably be different). The polystyrene particles that we used were stabilized with a sulfonate detergent, whereas the polystyrene divinylbenzene particles were stabilized with colloidal silica. To completely remove most emulsifiers, we would have had to use ion-exchange resins,[53-55] something we did not do. Most investigators dialyze or extensively wash beads before use. What this type of treatment accomplishes should be questioned. In general, it has been found that, even after the removal of the emulsifier, the charge density increases with increasing particle size, i.e., with increasing mass-to-surface ratio.[53] From the above consideration alone, it becomes evident that any conclusions regarding size effects in regurgitative exocytosis should also include an appreciation of important physical and chemical differences between various particles. Considering not only exocytic mechanisms but also the numerous investigations that have revealed physical, chemical, and immunological influences on endocytosis, more attention must certainly be paid to the chemical nature of test particles used.

ACKNOWLEDGMENTS

The authors gratefully acknowledge the assistance of Mary C. Williams, Inga Green, and Dorothy Minor in designing and executing experiments involving transmission and scanning electron microscopy.

Important advice and technical information was also provided by Dr. Leigh B. Bangs, Dow Chemical U.S.A., Midland, Mich.

This investigation was supported by U.S. Public Health Service grants ES 00754 and HL 16748.

REFERENCES

1. C. B. Laurell and S. Eriksson, The Electrophoretic α_1-Globulin Pattern of Serum in α_1-Antitrypsin Deficiency, *Scand. J. Clin. Lab. Invest.*, 15: 132-140 (1963).
2. V. Marco, D. R. Meranze, L. G. Bentivoglio, and P. Kimbel, Papain Induced Experimental Emphysema in the Dog, *Fed. Proc.*, 28: 526 (1969).
3. P. M. Gross, M. A. Babyok, E. Folker, and M. Kasehak, Enzymatically Induced Pulmonary Emphysema, *J. Occup. Med.*, 6: 481-487 (1964).
4. S. Park, S. I. P. Goldring, C. S. Shim, and M. H. Williams, Jr., Mechanical Properties of the Lung in Experimental Pulmonary Emphysema, *J. Appl. Physiol.*, 26: 738-744 (1969).
5. W. G. Johanson and A. K. J. Pierce, Effects of Elastase, Collagenase, and Papain on Structure and Function of Rat Lungs In Vitro, *J. Clin. Invest.*, 51: 288-293 (1972).

6. C. E. Blackwood, Y. Hosannoh, E. Perman, S. Keller, and I. Mandel, Experimental Emphysema in Rats: Elastolytic Titer of Inducing Enzyme as Determinant of the Response, *Proc. Soc. Exp. Biol. Med.*, 144: 450-454 (1973).
7. P. D. Kaplan, C. Kuhn, and J. A. Pierce, The Induction of Emphysema with Elastase. I. The Evolution of the Lesion and the Influence of Serum, *J. Lab. Clin. Med.*, 82: 349-356 (1973).
8. J. A. Hayes, A. Karthy, and G. L. Snider, The Pathology of Elastase-Induced Panacinar Emphysema in Hamsters, *J. Pathol.*, 117: 1-12 (1975).
9. A. Janoff and J. Sherer, Mediators of Inflammation in Leucocyte Lysosomes. IX. Elastinolytic Activity in Granules of Human Polymorphonuclear Leucocytes, *J. Exp. Med.*, 128: 1137-1151 (1968).
10. A. Janoff and R. S. Basch, Further Studies on Elastase-Like Esterases in Human Leucocyte Granulocytes, *Proc. Soc. Exp. Biol. Med.*, 136: 1045-1049 (1971).
11. A. Janoff, Human Granulocyte Elastase, *Am. J. Pathol.*, 68: 579-591 (1972).
12. G. Feinstein, C. J. Malemud, and A. Janoff, The Inhibition of Human Leucocyte Elastase and Chymotrypsin-Like Protease by Elastatinal and Chymostatin, *Biochem. et Biophys. Acta*, 429: 925-932 (1976).
13. G. Weisman, R. B. Zurier, P. J. Spieler, and I. M. Goldstein, Mechanisms of Lysosomal Enzyme Release from Leucocytes Exposed to Immune Complexes and Other Particles, *J. Exp. Med.*, 134: 149s-165s (1971).
14. G. Weisman, R. B. Zurier, and S. Hoffstein, Leucocytic Proteases and the Immunologic Release of Lysosomal Enzymes, *Am. J. Pathol.*, 68: 539-559 (1972).
15. P. M. Henson, The Immunologic Release of Constituents from Neutrophil Leucocytes. I. The Role of Antibody and Complement on Nonphagocytosable Surfaces or Phagocytosable Particles, *J. Immunol.*, 107: 1535-1546 (1971).
16. P. M. Henson, The Immunologic Release of Constituents from Neutrophil Leucocytes. II. Mechanisms of Release During Phagocytosis and Adherence to Nonphagocytosable Surfaces, *J. Immunol.*, 107: 1547-1557 (1971).
17. P. M. Henson, Interaction of Cells with Immune Complexes: Adherence, Release of Constituents, and Tissue Injury, *J. Exp. Med.*, 134: 114s-135s (1971).
18. A. Janoff, R. Rosenberg, and M. Gladstone, Elastase-Like, Estero-Protease Activity in Human and Rabbit Alveolar Macrophage Granules, *Proc. Soc. Exp. Biol. Med.*, 136: 1054-1058 (1971).
19. R. Rosenberg, R. Sandhaus, and A. Janoff, Further Studies of Human Alveolar Macrophage Alanine-p-Nitrophenyl Esterase, *Am. Rev. Respir. Dis.*, 106: 114-115 (1972).
20. J. O. Harris, G. N. Olsen, J. R. Castle, and A. S. Maloney, Comparison of Proteolytic Enzyme Activity in Pulmonary Alveolar Macrophages and Blood Leucocytes in Smokers and Nonsmokers, *Am. Rev. Respir. Dis.*, 111: 579-586 (1975).
21. Z. Werb and S. Gordon, Secretion of a Specific Collagenase by Stimulated Macrophages, *J. Exp. Med.*, 142: 346-360 (1975).
22. Z. Werb and S. Gordon, Elastase Secretion by Stimulated Macrophages, *J. Exp. Med.*, 142: 361-377 (1975).
23. N. R. Ackerman and J. R. Beebe, Release of Lysomal Enzymes by Alveolar Mononuclear Cells, *Nature*, 247: 475-477 (1974).

24. Q. Myrvik, E. S. Leake, and B. Faviss, Studies on Pulmonary Macrophages from the Normal Rabbit: A Technique to Procure Them in a High State of Purity, *J. Immunol.*, 86: 128-132 (1961).
25. L. Visser and E. R. Blout, Elastase Substrates and Inhibitors, *Fed. Proc.*, 28: 407 (1969).
26. O. H. Lowry, N. J. Rosenbrough, A. L. Farr, and R. J. Randall, Protein Measurement with Folin Phenol Reagent, *J. Biol. Chem.*, 193: 265-271 (1951).
27. S. Ito and M. J. Karnovsky, Formaldehyde-Glutaraldehyde Fixatives Containing Trinitro Compounds, *J. Cell. Biol.*, 39: 168a-169a (1968).
28. J. H. Luft, Improvements in Epoxy Resin Embedding Methods, *J. Biophys. Biochem. Cy ol.*, 9: 409-414 (1961).
29. A. G. Pearse, *Histochemistry*, pp. 665-678, Little, Brown and Company, Boston, 1968.
30. M. L. Watson, Staining of Tissue Sections for Electron Microscopy with Heavy Metals, *J. Biophys. Biochem. Cytol.*, 4: 475-478 (1958).
31. E. S. Reynolds, The Use of Lead Citrate at High pH as an Electron-Opaque Stain in Electron Microscopy, *J. Cell Biol.*, 17: 208-212 (1963).
32. J. H. Venable and R. Coageshall, A Simplified Lead Citrate Stain for Use in Electron Microscopy, *J. Cell Biol.*, 25: 407-408 (1965).
33. M. G. Wetzel and E. D. Korn, Phagocytosis of Latex Beads by *Acanthamoebi Castellanii (Neff)*. III. Isolation of the Phagocytic Vesicles and Their Membranes, *J. Cell Biol.*, 43: 90-104 (1969).
34. A. Janoff, R. A. Sandhaus, U. D. Hospelborn, and R. Rosenberg, Digestion of Lung Proteins by Human Leucocyte Granules In Vitro, *Proc. Soc. Exp. Biol. Med.*, 140: 516-519 (1972).
35. M. Gladstone, N. Klein, and E. Rothstein, Human Granulocyte Lysosomal Elastase Activity Using t-butyloxycarbonyl-L-alanine p-nitrophenyl ester and Elastin—Rhodamine as Substrates, *Am. Rev. Resp. Dis.*, 112: 629-632 (1975).
36. E. A. Levine, R. M. Senior, J. V. Bettler, The Elastase Activity of Alveolar Macrophages: Measurements Using Synthetic Substrates and Elastin, *Am. Rev. Resp. Dis.*, 113:25-30 (1976).
37. P. S. Ringose, M. A. Parr, and M. McLaren, Effects of Antiinflammatory and Other Compounds on the Release of Lysosomal Enzymes from Macrophages, *Biochem. Pharmacol.*, 24: 607-614 (1975).
38. R. I. Baehner, M. J. Karnovsky, and M. L. Karnovsky, Degranulation of Leucocytes in Chronic Granulomatous Disease, *J. Clin. Invest.*, 48: 187-192 (1969).
39. D. F. Bainton, Sequential Discharge of Polymorphonuclear Leucocyte Granules During Phagocytosis of Micro-Organisms, *J. Cell Biol.*, 47: 2 Pt. 2, 11a (1970).
40. S. J. Singer and G. L. Nicolson, The Fluid Mosaic Model of the Structure of Cell Membranes, *Science*, 175: 720-731 (1972).
41. D. Papabadjopoulos, K. Jacobson, S. Niv, and T. Isaac, Phase Transitions in Phospholipid Vesicles: Fluorescence Polarization and Permeability Measurements Concerning the Effect of Temperature and Cholesterol, *Biochem. Biophys. Acta*, 311: 330-348 (1973).
42. J. K. Blasie, Chairman, Workshop on Membrane Bioenergetics, *Biophys. J.*, 15: 921-952 (1975).
43. F. M. Griffen, Jr., J. A. Griffen, J. E. Leider, and S. C. Silverstein, Studies on the Mechanism of Phagocytosis. I. Requirements for Circumferential Attach-

ment of Particle-Bound Ligands to Specific Receptors on the Macrophage Plasma Membrane, *J. Exp. Med.*, 142: 1263-1282 (1975).
44. R. J. Mason, T. P. Stossel, and M. Vaughn, Lipids of Alveolar Macrophages, Polymorphonuclear Leucocytes, and Their Phagocytic Vesicles, *J. Clin. Invest.*, 51: 2399-2407 (1972).
45. J. E. Smolen and S. B. Shobet, Remodeling of Granulocyte Membrane Fatty Acids During Phagocytosis, *J. Clin. Invest.*, 53: 726-734 (1974).
46. S. E. Davis, R. Estensen, and P. G. Quie, Cytochalasin B. III. Inhibition of Human Polymorphonuclear Leucocyte Phagocytosis, *Proc. Soc. Exp. Biol. Med.*, 137: 161-166 (1971).
47. S. E. Malawista, J. B. L. Gee, and K. G. Bensch, Cytochalasin B Reversibly Inhibits Phagocytosis: Functional, Metabolic and Ultrastructural Effects in Human Blood Leukocytes and Rabbit Alveolar Macrophages, *Yale J. Biol. Med.*, 44: 286-300 (1971).
48. M. F. Tsan and R. D. Berlin, Effect of Phagocytosis on Membrane Transport of Nonelectrolytes, *J. Exp. Med.*, 134: 1016-1035 (1971).
49. T. E. Ukena and R. O. Berlin, Effect of Colchicine and Vinblastine on the Topographical Separation of Membrane Functions, *J. Exp. Med.*, 136: 1-7 (1972).
50. F. R. Frankel, Organization and Energy-Dependent Growth of Microtubules in Cells, *Proc. Nat. Acad. Sci.*, 73: 2798-2802 (1976).
51. J. J. Freed and M. M. Lebowitz, The Association of a Class of Saltatory Movements with Microtubules in Cultured Cells, *J. Cell Biol.*, 45: 334-354 (1970).
52. S. H. Haig and E. J. Heiser, Latex Fundamentals and Their Role in Paper Coating, *Pulp Pap. Mag. Can.*, 70: 3-12 (1969).
53. H. G. Van den Hul and J. W. Vanderhoff, Influences on the Mechanism of Emulsion Polymerization of Styrene from Characterization of the Polymer End-Groups, *Br. Polym. J.*, 2: 121-127 (1970).
54. J. W. Vanderhoff, H. J. Van den Hul, R. J. M. Tausk, and J. TH. G. Overbeek, *Clean Surfaces: Their Preparation and Characterization for Interfacial Studies*, pp. 15-44, Marcel Dekker, Inc., New York, 1970.
55. H. J. Van den Hul and J. W. Vanderhoff, Well-Characterized Monodisperse Latexes, *J. Colloid Interface Sci.*, 28: 336-337 (1968).

Cytokinetic Study of Alveolar Macrophage Renewal in Rats

R. MASSE, P. FRITSCH, D. NOLIBE, J. LAFUMA, and J. CHRETIEN
Commissariat à l'Énergie Atomique, Montrouge Cedex, France

ABSTRACT

Pools of alveolar macrophages and monocytes were measured by combining morphometry and the extraction of cells by lavage. The turnover rate of macrophages was evaluated by measuring the clearance rate of $^{59}Fe_2O_3$ previously administered by aerosols. The labeling index and S phase duration of cells in alveoli and lung capillaries were determined by autoradiography after ^{3}H-labeled thymidine and 5-^{125}Iododeoxyuridine incorporation. The disappearance rate was determined after specific incorporation of ^{125}Iododeoxyuridine in deoxyribonuclease (DNA) of alveolar macrophages. Steady-state parameters are presented. Under healthy conditions there are almost no macrophages in the interstitium space. Lung capillaries must be considered as a maturation compartment for macrophages before the last dividing stage in the alveoli. This is consistent with the large enrichment of monocytes in the lung and the ability of some of these monocytes to divide inside the capillaries.

Pulmonary alveolar macrophages belong to the mononuclear phagocyte system[1] and are derived from bone-marrow precursors of monocytes.[2] Under normal conditions most of these cells are located in the alveoli and represent the only defense of the flattened respiratory epithelium.

Several attempts have been made to evaluate the number of alveolar macrophages involved in the process of dust sequestration.[3,4] This number was found to increase very rapidly when large amounts of particles reached the respiratory tract.[5] The increase could not be correlated with the cytotoxicity of the engulfed particles,[6] however, since alveolar macrophage death can be followed by input of new cells. Therefore relevant physiological

parameters of cell turnover must be measured. For cell loss from the alveolar compartment, these parameters are: excretion rate of cells via the upper airways, cell death rate, and cell passage into the interstitium. The important rates of input are entry of new cells and division of alveolar macrophages.[7] Steady state is a necessary condition for physiological homeostasis;[6] however, steady state may be achieved by means which are not normal but which are meaningful early indications of disorders.

EVALUATION OF TOTAL ALVEOLAR POPULATION

The methods for estimating the total alveolar macrophage population have been previously described.[4] Briefly, they involve determination of the yield of alveolar macrophages after pulmonary lavage. The cells are labeled by previous exposure of animals to an aerosol of neutron-activated hematite. One week after exposure to the dust, particle clearance rate can be fitted by a single exponential curve whose half-life is equal to 27 days.[4] This phenomenon lasts at least 2 months and occurs when particles other than hematite are used.[8,9]

Morphometric analysis showed that this clearance rate represents direct output of engulfed particles via the airways and not the interstitial space and also that elimination of macrophages was achieved at random.[10] Under these conditions, when estimated by the recovery of hematite, cell recovery was found to be 40.80 ± 0.43% (Ref. 4). Improvement in the technique of harvesting the cells now permits recovery of 80 to 90% of the hematite cells.[11] This improvement in recovery made the extracted cells more representative of the whole population. It did not affect, however, evaluation of the size of the alveolar macrophage population in the same strain of rats and under the same physiological conditions. In Sprague—Dawley pathogen-free rats weighing about 300 g, the average number of cells is 30×10^6 cells (Refs. 4, 10, and 11).

EXTRAALVEOLAR PHAGOCYTES

Since interstitial phagocytes have been described as a source for alveolar macrophages,[12] we performed quantitative electron microscopic analysis of the cell partition in the deep lung, including alveoli, alveolar ducts, respiratory bronchioles, and the ends of the ciliated bronchioles.[13] Surprisingly, less than 0.1% of the cells in the deep lung were phagocytes compared to 2.5% ($\sigma = 0.9$) in the

alveoli.[13] These phagocytes were seen either beneath epithelial cytoplasm of the type II pneumocyte, near the junction with the type I (or II) pneumocyte, or inside lymphatic vessels. Therefore we can conclude that under specific pathogen-free conditions interstitial space, in the strictest sense, does not constitute a reservoir of alveolar macrophages. The conclusion, however, is entirely different if capillaries are included in the interstitium.[14] As shown in Table 1, capillaries contain a large store of monocytes, i.e., almost twice the entire alveolar macrophage population.

TABLE 1

LUNG CELL POPULATION IN THE DEEP LUNG OF THE RAT

	Pneumocytes		Fibroblasts	Endoblasts	Macrophages	Capillaries		
	Type I	Type II				Polymorphonucleates	Lymphocytes	Monocytes
Percent	7	13.9	23	31.8	2.5	9.7	7.4	4.6
Standard deviation	1.4	3.2	1.1	3.2	0.9	3	2.6	1.4

Recognition of the monocytes was first obtained by morphologic and renewal rate criteria.[13] Further investigations showed that the intracapillary leukocytes could be washed out of the capillary bed but efficiency of the recovery did not exceed 15 to 20 x 10^6 cells (Ref. 14). These extracted cells are being more precisely characterized.[11] The cell population washed from lung capillaries was composed of 15 to 20% monocytes, 50 to 60% lymphocytes, and 20 to 27% polymorphonucleates.[14]

Monocytes are positive for nonspecific esterase activity and form rosettes with antibody-complement sensitized erythrocytes (EAC), and they rapidly phagocitize opsonized red blood cells. About 70% of the cells are positive for peroxidase after inhibition of catalase;[15] 30% of the monocytes in the capillaries have no detectable peroxidase reaction, a fact of interest since rat alveolar macrophages are negative for this reaction. Large phagocytic cells are also washed out; they are negative for peroxidase reagents and strongly positive for EAC rosettes. The origin of these large cells is not certain, and, although they may be a contamination, they were often seen in the lung capillaries by electron microscopy (Fig. 1), some of them during mitosis.

It is of interest that cells were observed which were negative for peroxidase reagents and nonadherent to glass in the presence of

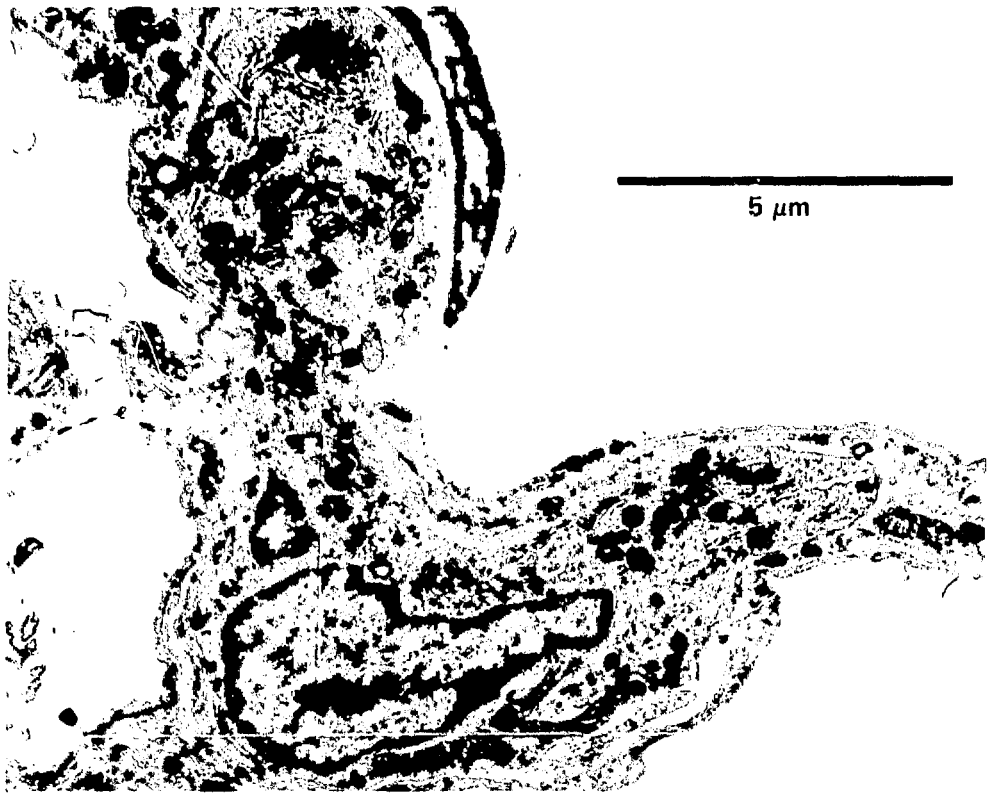

Fig. 1 Large intracapillary phagocyte. (Araldite embedding, Uranyl—lead stain.)

serum and which did not exhibit phagocytosis or form rosettes but gave a strong reaction for nonspecific esterase. These cells had round nuclei, were rich with azurophile granules in a scanty cytoplasm, and developed esterase activity within 10 min. These may represent some activated form of the T lymphocytes that have been described as esterase positive.[16]

ELIMINATION RATE OF ALVEOLAR MACROPHAGES

If we take into account the previously defined total population of alveolar macrophages, data in the literature suggest a very rapid turnover.[17] These data, based upon results from gastro-esophagal catheterization, did not clearly establish the alveolar origin of mononuclear excreted cells. Using the method wherein rats inhaled labeled iron oxide, we found only 0.5×10^6 to 0.75×10^6 cells excreted per day to be alveolar macrophages.[6] The elimination rate

can be directly deduced from the clearance rate of nontoxic particles during the elimination phase. This can be described by the single exponential curve

$$A = A_0 e^{-0.025 t}$$

In this case, the rate constant ($\lambda = 2.5\%$) represents the percentage of the population excreted per day, i.e., about 0.75×10^6 cells.

CELL DEATH RATE

The rate of cell death is the only parameter directly related to the toxicity of inhaled aerosols and as such must be evaluated as precisely as possible. DNA synthesis inside the alveoli[7] made estimation of death rate theoretically possible. To estimate the death rate, we used [5-^{125}I]iododeoxyuridine (IUdR) as a tracer[11] for DNA since it is poorly reutilized after cell death.[18] Administration of the label via intratracheal instillation prevents significant labeling of the blood monocyte source. As high as 0.2 to 0.4% of the injected dose of [^{125}I]IUdR was found incorporated in the alveolar macrophage DNA 2 hr after instillation. Present data indicate that half the total population died within 10 days.[11]

CELL RENEWAL

Proof that rat alveolar macrophages divide is provided by demonstration of DNA synthesis by labeled IUdR incorporation as well as by visual observation of mitosis. We have found that 0.06% ($\sigma = 0.08$) of cells were in mitosis in normal rats. These dividing cells can be seen only in lavage preparations of high yield and after using cytocentrifugation for preparing the smears (Fig. 2). The percentage of DNA-synthesizing cells was overestimated in our previous study.[10] Two factors seemed to contribute to this overestimation, i.e., poor recovery of cells and the use of animals pretreated with hematite. More recent data indicate that 2.5% ($\sigma = 0.5$) of the cells synthesize DNA. These data are based on more than 80% of the cell population[11] in specific pathogen-free rats. On the other hand, our evaluation of the duration of S phase was underestimated.[10] Although in agreement with other authors,[19] our estimate of 7.8 hr on the basis of the double labeling method no longer seems valid. This value was not confirmed by the method of observing the time course of labeled mitoses after intratracheal labeling. Results from

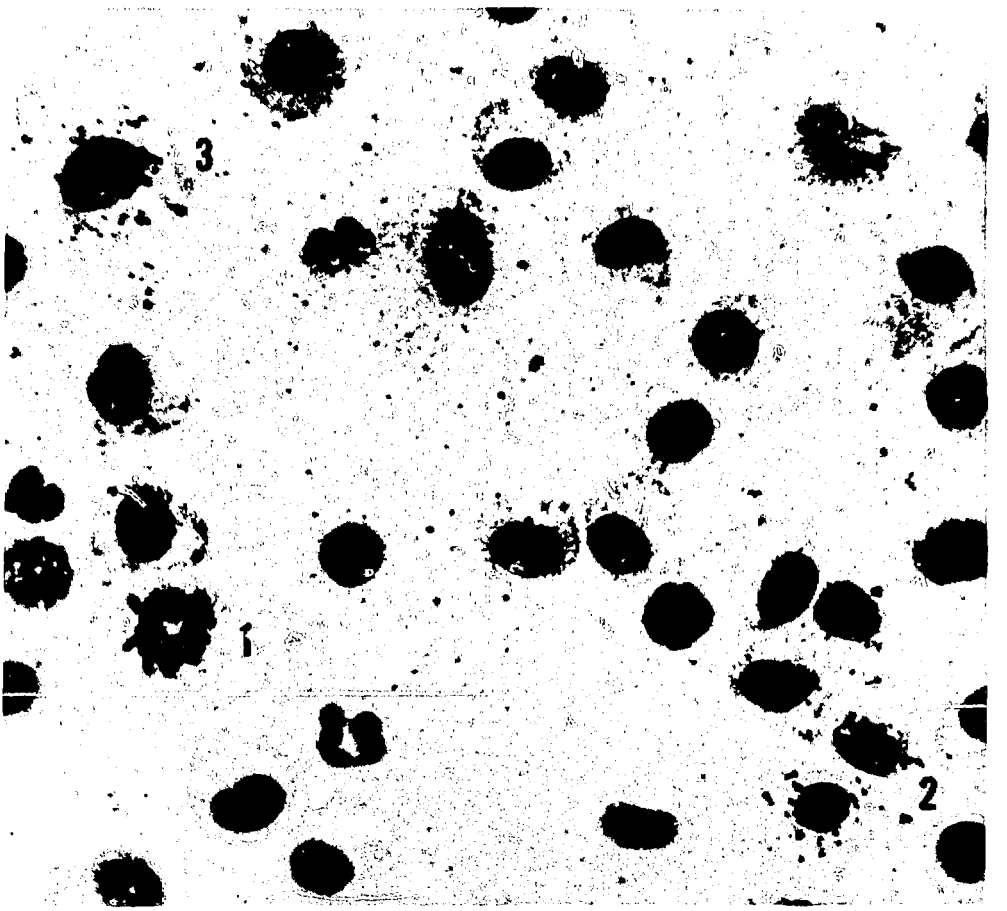

Fig. 2 Alveolar macrophages obtained by lavage after intratracheal injection of [^{125}I]IUdR. The activated ionographic method was used according to Rechenmann.[20] Unlabeled metaphase, 1. Labeled telophase, 2. Premitotic labeled cell, 3. (Giemsa stain; magnification, 1000 X.)

this method appear in Fig. 3; more than 1000 mitoses of alveolar macrophages were scored. Although the curve is not perfectly symmetrical, two facts are obvious: (1) S + G_2 + M lasts 22 hr, and (2) there is only one wave of mitosis. More than 600 mitoses were observed 24 hr after administration of the [^{125}I] IUdR, and none of these were found to be labeled. The origin of the discrepancy in the previous evaluation of the duration of the S phase is probably due to inhibition of the cell cycle caused by the use of doses of radioactive tracer which were too high. Such an effect appears very clearly in the renewal of lung cells[13] after thymidine injection (1 μCi/g). The labeled mitosis curve shown here was obtained after [^{125}I] IUdR

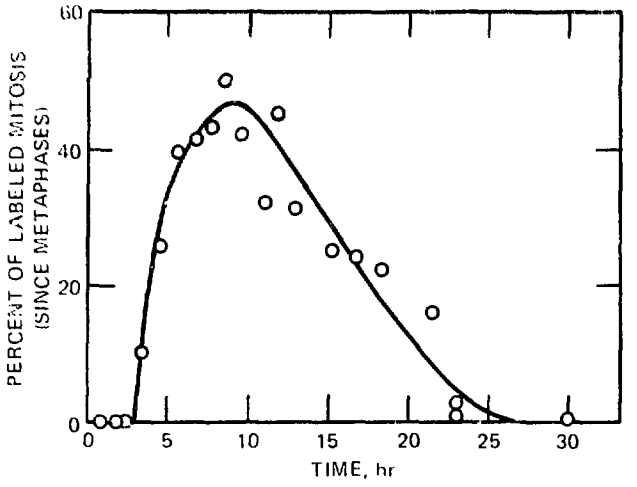

Fig. 3 Percentage of labeled mitosis, overall mitoses of alveolar macrophages, as a function of time after intratracheal injection of [^{125}I]IUdR.

injection (two disintegrations per cell per day). By using an activated ionographic method,[20] we could achieve a high autoradiographic efficiency.

CONCLUSIONS

Although there might exist some uncertainties, the steady-state kinetics of the normal alveolar macrophage population can be evaluated, and a schematic representation is shown in Fig. 4. Loss of cells is balanced by input due to cells that divide in the alveoli. The fact that lung capillaries contain a high population of monocytes which can divide into two macrophages in the alveoli explains how alveolar cells can rapidly increase under deleterious conditions.[5] Macrophage division is not required to increase the total number of phagocytes. This can be accomplished by direct passage of monocytes from the lung capillaries. Thus the division of alveolar macrophages should be regarded only as a maturation step during which the phagocyte acquires its specific (metabolic and immune) properties. Consequently, alveolar macrophage division must occur only in the young monocytes that have recently migrated from capillaries to alveoli. Observation of DNA synthesis[13] in capillary monocytes, mitosis of these monocytes inside the capillary, and variation in the enzymatic properties of the capillary monocytes indicate that maturation steps are initiated in the capillary prior to migration.

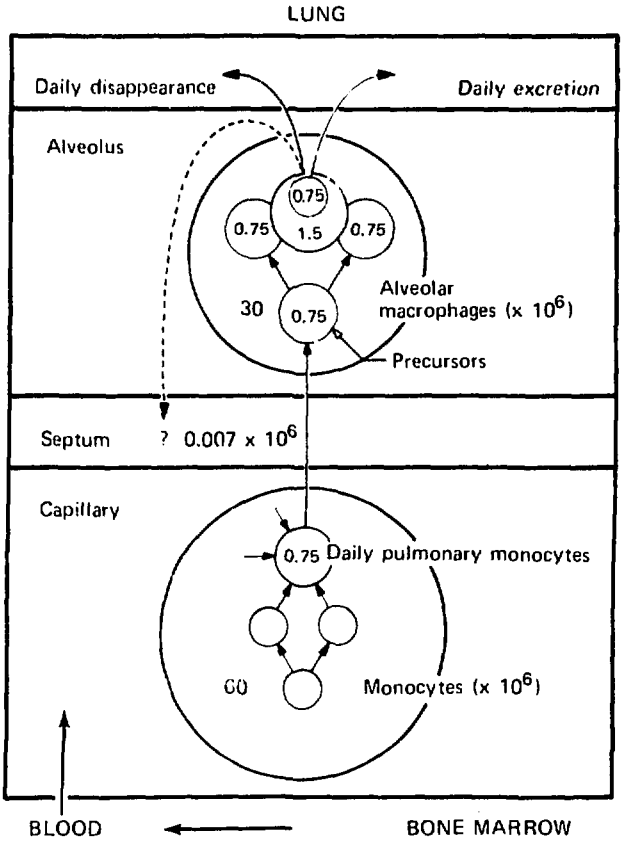

Fig. 4 Steady-state parameters of the alveolar macrophage population under healthy conditions.

REFERENCES

1. R. Van Furth, Z. A. Cohn, J. G. Hirsch, J. H. Humphrey, W. G. Spector, and H. L. Langevoort, The Mononuclear Phagocyte System. A New Classification of Macrophages, Monocytes, and Their Precursor Cells, *Bull. World Health Organ.*, 845-851 (1972).
2. M. O. Pinkett, C. R. Cowdrey, and P. C. Nowell, Mixed Hematopoietic and Pulmonary Origin of Alveolar Macrophages as Demonstrated by Chromosome Markers, *Amer. J. Pathol.*, 48: 859-867 (1966).
3. C. W. La Belle and H. Brieger, Patterns and Mechanisms in the Elimination of Dust from the Lung, in *Inhaled Particles and Vapours*, C. N. Davies (Ed.), Vol. 1, pp. 356-369, Pergamon Press, Inc., Elmsford, N. Y., 1961.
4. B. Sedaghat, R. Masse, J. C. Nenot, J. Lafuma, and J. C. Martin, Evaluation de la population totale des macrophages alvéolaires chez le rat, *Compt. Rend.*, Ser. D, 273: 229-232 (1971).
5. J. Brain, The Effects of Increased Particles on the Number of Alveolar Macrophages, in *Proceedings of the Third International Symposium on*

Inhaled Particles, London, Sept. 16—23, 1970, pp. 209-225, Unwin Brothers Limited, Surrey, England, 1971.

6. R. Masse, Etude cytologique comparée de l'influence du plutonium et de la silice inhalée sur le comportement du macrophage alvéolaire, in *Proceedings of the Third International Symposium on Inhaled Particles*, London, Sept. 16—23, 1970, pp. 247-259, Unwin Brothers Limited, Surrey, England, 1971.
7. R. Masse, J. C. Martin, A. Zagorcic, J. Lafuma, and L. Le Bouffant, Etude expérimentale de l'origine des macrophages alvéolaires du rat, *Compt. Rend.*, Ser. D, 270: 245-248 (1970).
8. J. C. Evans et al., Studies on the Deposition of Inhaled Fibrous Material in the Respiratory Tract of the Rat and Its Subsequent Clearance Using Radioactive Tracer Techniques, *Environ. Res.*, 6: 180-201 (1973).
9. C. L. Sanders, W. C. Cannon, G. J. Powers, R. R. Adee, and D. M. Meier, Toxicology of High Fired Beryllium Oxide Inhaled by Rodents. I. Metabolism and Early Effects, *Arch. Environ. Health*, 30: 546-551 (1975).
10. R. Masse, P. Fritsch, D. Nolibe, and B. Sedaghat, Evaluation quantitative et homeostasie de la population des macrophages alvéolaires, *Pathol.-Biol.*, 23: 464-469 (1975).
11. P. Fritsch, Thèse de Sciences, University of Paris, Paris, 1977.
12. D. H. Bowden and I. Y. R. Adamson, The Pulmonary Interstitial Cell as Immediate Precursor of the Alveolar Macrophage, *Amer. J. Pathol.*, 68: 521-537 (1972).
13. P. Fritsch, R. Masse, F. Lebas, J. Lafuma, and J. Chretien, Identification au microscope électronique des cellules incorporant la thymidine dans une population á faible taux de renouvellement. Application á l'étude des cellules du poumon profond, *Compt. Rend.*, Ser. D, 281: 1105-1108 (1975).
14. P. Fritsch, R. Masse, J. P. Levistre, J. Lafuma, and J. Chretien, Lung Capillaries as a Reserve for Monocytes, *J. Microsc. Biol. Cell.*, 25: 289-290 (1976).
15. T. Rytömaa, Identification and Counting of Granulocytes by Peroxidase Reaction, *Blood*, 19: 439-442 (1962).
16. J. Mueller, G. Brun del Re, H. Buerki, H. U. Keller, M. W. Hess, and H. Cottier, Nonspecific Acid Esterase Activity: A Criterion for Differentiation of T and B Lymphocytes in Mouse Lymph Nodes, *Eur. J. Immunol.*, 5: 270-274 (1975).
17. A. A. Spritzer and J. A. Watson, The Measurement of Ciliary Clearance in the Lungs of Rats, *Health Phys.*, 10: 1093-1097 (1964).
18. W. L. Hughes et al., Deoxyribonucleic Acid Metabolism In Vivo. I. Cell Proliferation and Death as Measured by Incorporation and Elimination of Iododeoxyuridine, *Fed. Proc. Chem. Med.*, 23: 640 (1964).
19. M. J. Evans, L. Cabral, R. Stephens, and G. Freeman, Cell Division of Alveolar Macrophages in Rat Lung Following Exposure to NO_2, *Amer. J. Pathol.*, 70: 199-207 (1973).
20. R. Rechenmann, Progress in Processing the Corpuscular Latent Image, Report EUR 4688e, European Atomic Energy Community, November 1971.

Specific Metabolic Activities of Pulmonary Endothelial Cells

UNA S. RYAN and JAMES W. RYAN
Papanicolaou Cancer Research Institute and Department of Medicine, University of Miami School of Medicine, Miami, Florida

ABSTRACT

The endothelial lining of the pulmonary vascular bed is far more than an inert barrier. Endothelial cells are metabolically active and are capable of processing a wide range of hormones and other excitatory substances, including biogenic amines, adenine nucleotides, and polypeptides. One enzyme of these cells is capable of inactivating bradykinin and of forming angiotensins II and III. These cells must also play at least a passive role in the processing of prostaglandins and related substances. In addition to their specific metabolic activities, pulmonary endothelial cells possess factors active in coagulation and fibrinolysis and may possess enzyme inhibitors, such as α_2-macroglobulin. Although endothelium of other vascular beds has similar or identical properties, the pulmonary endothelium is uniquely situated, between the central venous and systemic arterial circulations, to affect specific functions of the lungs as well as specific functions of distant organs. Thus kinins and some prostaglandins and biogenic amines do not survive passage through the lungs and do not enter systemic arterial blood. In contrast, the pulmonary endothelium is probably a major determinant of the quantities of angiotensins II and III which reach, via the systemic arterial circulation, peripheral organs and glands.

Since 1925 the lungs have been known to eliminate vasoactive substances and to do so in a highly efficient way.[1] The efficiency of metabolism might have suggested a role of the alveolar–capillary unit because it is at this level that circulating substances have their greatest exposure to lung cells. However, during the interval from 1925 to approximately 1968, most observations on the ability of the lungs to process circulating excitatory substances focused on the substances themselves rather than on the lungs. In 1968 Ryan,

Roblero, and Stewart[2] showed that bradykinin is rapidly and quantitatively metabolized during a single passage through the lungs. The metabolites were found to be released quantitatively and without delay into the pulmonary venous effluent. These observations led us to postulate that the enzymes responsible for the metabolism of bradykinin were likely to exist on or near the luminal surface of pulmonary endothelial cells. It is now evident that the lungs are capable of processing selectively a large number of substances of very different chemical types, including biogenic amines, adenine nucleotides, prostaglandins, polypeptides, drugs, and lipids. Furthermore, pulmonary endothelium may contain enzymes and other agents active in coagulation and anticoagulation reactions. For example, α_2-macroglobulin[3] and factor VIII (Ref. 4) are known to occur on endothelial cells of other tissues, and thromboplastin[5] is known to occur on pulmonary endothelial cells. The limits of the ability of the lungs to process lipids, hormones, hormone precursors, and drugs are not known. However, for the purposes of this brief overview, we plan to focus on interactions of the lungs with circulating substances processed actively by endothelial cells.

The pulmonary capillary bed is remarkable not only because of its position in the general circulation, dividing venous from arterial blood, but also because of its vastness, the large quantities of blood processed per unit time, and because of the delicate balance that must be maintained to provide the lungs with their hormonal and metabolic requirements while limiting the transport of salts and water into and out of the vascular space. In addition, one might suppose that the lungs, perhaps to a greater degree than other tissues, must allow some hormones and excitatory substances to pass unhindered from the venous to the systemic arterial circulation.

Low-power electron micrographs at the level of the alveolar capillary unit emphasize the extensiveness of the pulmonary alveolar—capillary unit and the thinness of the two primary cell types, the alveolar type I epithelial cells and the endothelial cells and their relative lack of intracellular organelles (Fig. 1). In man alveolar blood vessels (primarily capillaries) have been estimated to have a luminal surface area on the order of 70 m^2 (Ref. 6). However, the early calculations of surface area assumed a more or less regular ellipsoidal shape of capillaries having smooth luminal surfaces. It is now evident that the surfaces are not smooth but are covered with irregular complex projections.[7] The projections cannot fail to affect fluid dynamics at the cell body. Their size and the density of the meshwork is such that one can anticipate an eddy flow of cell-free plasma along the main body of the cell. This feature could well have

Fig. 1 Low-power electron micrograph of rat lung showing two capillaries. The alveolar—capillary unit is composed of type I epithelial cells (Ep) and endothelial cells (En). Except in the region of the nucleus (N), the endothelial cells are extremely thin (e.g., at asterisk) and contain few organelles. However, they contain large numbers of caveolae intracellulares, many of which open directly to the vascular lumen (arrows). Caveolae are shown at higher magnification in Fig. 4. (Magnification, 14,000 X.)

implications for the exchange of metabolites between endothelium and blood. Although the surface projections shown in Fig. 2 are of the main-stem pulmonary artery, there is ample evidence from examination of thin sections of endothelial cells of smaller vessels, including capillaries and venules, to indicate that surface projections are a common feature (Fig. 3). In addition to the surface projections, it is evident that pulmonary capillary endothelial cells contain enormous numbers of caveolae intracellulares (pinocytotic vesicles), a large proportion of which appear to communicate directly with the vascular lumen (Figs. 1 and 4).[8-10] Therefore apparently the true surface area of capillary endothelial cells is very much larger than previous estimates.

METABOLISM OF LIPIDS

Schoefl and French[11] and more recently Scow, Blanchette-Mackie, and Smith[12] have described morphological features of the processing of chylomicrons by endothelial cells of lactating mammary glands and of lungs. The endothelial cells of the lactating mammary glands are very much more active in this process, but it is notable that chylomicrons can be processed in the pulmonary circulation as well, possibly via lipoprotein lipase, which is suspected of occurring on or near the luminal surface.

BIOGENIC AMINES

Serotonin and norepinephrine are, to greater or lesser degrees, eliminated as they pass through the lungs, whereas epinephrine and histamine are allowed unhindered passage.[13] In addition, it is becoming clear that the pulmonary endothelium plays an active role in the removal of norepinephrine and serotonin from the circulation. Hughes, Gillis, and Bloom[14] have shown, by combined autoradiographic and biochemical techniques, that endothelial cells of isolated rat lungs actively take up [^{3}H] DL-norepinephrine. Nicholas et al.,[15] using [^{3}H] L-norepinephrine, have confirmed and extended these findings and have postulated that the uptake of norepinephrine is a sodium-dependent carrier-mediated transport. Both Hughes and collaborators and Nicholas et al. noted from their autoradiograph experiments that the distribution of silver grains was not uniform. Some capillary beds were heavily labeled, whereas others were not labeled at all, a point raising the possibility that the endothelial cells of the lungs are not a homogeneous population.

Fig. 2 Scanning electron micrograph of the luminal surface of the main stem pulmonary artery of the dog. The endothelial projections are approximately 250 to 350 nm in diameter and 300 to 3000 nm in length. They may take the form of knobs or longer arms, some of which branch or bud (black arrow). They are densest over the main body of the cell (*) but extend laterally to overlap adjacent cells (white arrows). (Magnification, 14,000 X.) [From U. Smith, J. W. Ryan, D. D. Michie, and D. S. Smith, Endothelial Projections: As Revealed by Scanning Electron Microscopy, *Science*, 1973: 925 (1971).]

Fig. 3 Part of an endothelial cell from a small pulmonary vein showing endothelial projections (P) (compare with Fig. 2). In addition to caveolae (arrows), this endothelial cell contains Weibel-Palade bodies (asterisks). (Magnification, 51,000 X.)

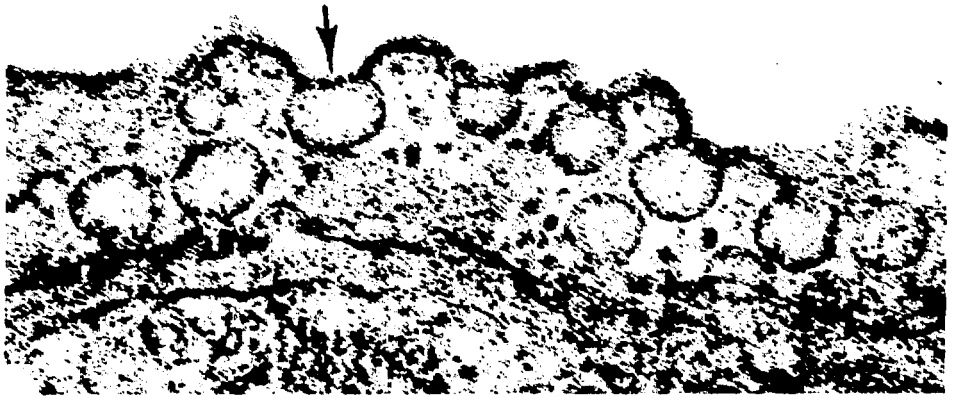

Fig. 4 Portion of capillary endothelial cell containing numerous caveolae. The luminal stoma is spanned by a delicate diaphragm, e.g., at arrow. (Magnification, 113,000 X.)

Strum and Junod[16] have described similar findings on the pulmonary processing of serotonin (5-hydroxytryptamine). The elimination of serotonin is more efficient than that of norepinephrine. Autoradiography has established that the endothelial cells accumulate radioactive material after exposure of the lungs to [^{3}H]serotonin (Ref. 17).

ADENINE NUCLEOTIDES

Adenosine 5′-triphosphate (ATP) does not survive passage from the pulmonary artery to the pulmonary vein.[18] We have reinvestigated the fate of ATP and its lower homolog adenosine 5′-monophosphate (AMP) using combined biochemical and cytochemical techniques.[8,9,20]

It is convenient to consider the metabolism of the adenine nucleotides together with the metabolism of the vasoactive polypeptides bradykinin and angiotensin I. Since although the nucleotides and peptides differ chemically, their kinetics of disappearance are similar, and it was studies of the fates of these substances during passage through the lungs that provided support for our hypothesis that the enzymes responsible for their metabolism were situated on the luminal surface of pulmonary endothelial cells.[8]

The metabolism of bradykinin, angiotensin I, and the adenine nucleotides by the lungs have the following features in common:

1. With the use of any one of the compounds labeled intrinsically with a radioisotope, it was found that all the radioactivity that enters the pulmonary circulation emerges without delay in the pulmonary venous effluent. None of the radioactivity is found in the form of the parent compound.

2. Blood enzymes are not required since the reactions are no less efficient in lungs perfused with artificial salt solutions.

3. Although radioactive ATP, AMP, bradykinin, and angiotensin I are extensively metabolized, the mean transit times and volumes of distribution of radioactivity are no greater than those of blue dextran (molecular weight, >2,000,000), a substance unlikely to leave the vascular space during a single passage through the pulmonary circulation.

All these data have been interpreted as indicating that the enzymes which hydrolyze bradykinin, angiotensin I, and the adenine nucleotides must be situated on or near the luminal surface of endothelial cells (Refs. 2, 8, 10, and 21 to 29). As implied by the preceding data, the metabolic reactions are extremely efficient. Thus we began a search for structural specializations that could account for the peculiar way in which these substances are processed. The very efficiency of processing of circulating substrates suggested that the relevant enzymes were apt to be prominent at the level of the microcirculation where solutes in blood would have their greatest exposure to a lung surface.

From the outset we were particularly interested in the endothelial caveolae since these structures appear to be admirably placed

for carrying out metabolic activities without requiring cellular uptake.[8] The great frequency with which these caveolae occur indicates that they vastly expand the surface area of endothelium (Figs. 1 and 4). However, in addition to their position and extensive surface area, caveolae became of even greater interest when we were able to show that they were responsible for the pulmonary processing of the adenine nucleotides.

The metabolism of adenine nucleotides by the lungs via phosphate esterase enzymes provides an excellent opportunity for examining the subcellular localization of the enzymes themselves. When intact lungs were perfused with 5′-AMP and $Pb(NO_3)_2$, the lead phosphate deposits were restricted to those caveolae and incipient caveolae open to the vascular lumen (Fig. 6).[20,26] These data suggest that, although a large number of cell types and organelles have phosphate esterase enzymes, it is only those enzymes facing the vascular lumen which are exposed to, and react with, circulating nucleotides. The apparent localization of adenosine triphosphatase (ATPase) and 5′-nucleotidase along the vascular lumen and associated caveolae very likely explains how the metabolic products of the adenine nucleotides are returned to the circulation with no apparent delay or uptake by tissue.

Cytochemical techniques are not applicable to studies of the enzymes that metabolize bradykinin and angiotensin I, but the apparent kinetics of metabolism of bradykinin and angiotensin I by intact lungs are virtually identical to those of the adenine nucleotides. Thus it seemed likely that the sites of enzymes that metabolize them might be similar.

MECHANISMS OF METABOLISM OF BRADYKININ AND ANGIOTENSIN I

Recently it has been possible to examine the pulmonary capillary bed directly. In 1972 Dorer et al.[30] succeeded in isolating angiotensin-converting enzyme (kininase II) in homogeneous form. They subsequently showed that the enzyme is also capable of degrading bradykinin[31] in a way analogous to that of an enzyme known previously as kininase II (Ref. 32). In fact, bradykinin appears to be the preferred substrate.[31] The enzyme converts angiotensin I to angiotensin II by removing the C-terminal dipeptide, His—Leu; a finding consistent with the observation that intact lungs metabolize [^{14}C]Leu^{10}—angiotensin I to yield radioactive His—Leu[23]. Bradykinin is inactivated by the enzyme in a similar manner but can be degraded in two steps: The C-terminal dipeptide,

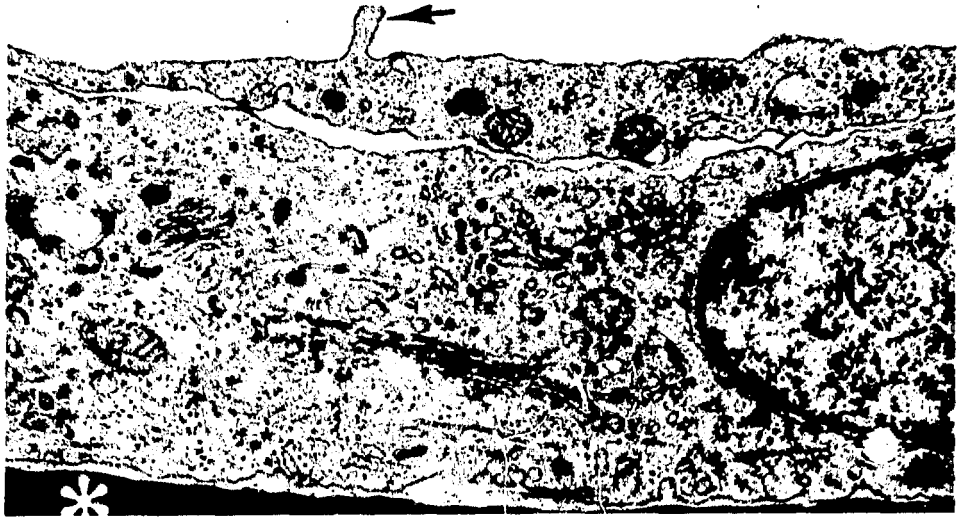

Fig. 5 Part of an endothelial cell from a confluent primary culture of pig lung endothelium. The cell has been prepared and sectioned without prior removal from the plastic culture flask. Part of the flask is seen at the bottom of the field (asterisk). The cytoplasm surrounding the nucleus (N) contains ultrastructural features characteristic of endothelial cells in situ, e.g., rough and smooth endoplasmic reticulum, caveolae, microfilaments, and microtubules. An endothelial projection is indicated by an arrow. (Magnification, 26,000 ×.)

Phe—Arg, is released and then the new C-terminal dipeptide, Ser—Pro, is removed. Again these findings are consistent with results of experiments using intact lungs: The venous effluent of lungs perfused with [^{3}H]Phe^8—bradykinin contains a single radioactive metabolite, namely, Phe—Arg[21,22].

In collaborative studies we prepared antibodies to hog lung angiotensin-converting enzyme.[33] The antiserum (goat) was purified by $(NH_4)_2SO_4$ precipitation and by chromatography on diethylaminoethyl (DEAE) cellulose. The final antibody fraction was coupled to microperoxidase (11-MP or 8-MP).[34,35] The antibody—microperoxidase conjugate was reacted with very small blocks of rat lung tissue which previously had been fixed with *p*-formaldehyde—picric acid and preincubated with nonimmune goat serum. Antibody localization was achieved by reacting the microperoxidase moiety with H_2O_2 and 3,3′-diaminobenzidine. Results are shown in Fig. 7. With the use of either conjugate, the luminal surface of the pulmonary endothelial cells reacted with the antibody—microperoxidase reagent as expected.[34,35] The reaction product, oxidized diaminobenzidine (DAB), was most abundant on the

Fig. 6 Endothelial cell of lungs perfused with 5′-AMP and lead nitrate. As AMP is hydrolyzed, free phosphate is deposited as a lead salt. Lead phosphate deposits are found in caveolae open to the vascular lumen (arrows). (Magnification, 95,000 ×.) [From U. Smith and J. W. Ryan, Pinocytotic Vesicles of the Pulmonary Endothelial Cell, *Chest*, 59: 13S (1971).]

Fig. 7 Unstained section of fixed rat lung which had been incubated with anti-angiotensin-converting enzyme conjugated to microperoxidase, 3,3′-diaminobenzidine and H_2O_2. The reaction product, indicating sites of angiotensin-converting enzyme, is localized along the luminal surface of the endothelial cells of small vessels (arrows). (Magnification, 74,000 ×.) [From U. S. Ryan, J. W. Ryan, C. Whitaker, and A. Chiu, Localization of Angiotensin Converting Enzyme (Kininase II). II. Immunocytochemistry and Immunofluorescence, *Tissue Cell*, 8: 130 (1976).]

surface of the endothelial cells of the microcirculation. On the latter, oxidized DAB can be seen along the surface of the numerous endothelial projections. Angiotensin-converting enzyme also occurs on the endothelial cells of much larger vessels, including pulmonary artery and aorta. However, because of the great efficiency with which bradykinin and angiotensin I are metabolized, it seems likely that the enzyme of the microcirculation accounts for the observed results.

Recently we have begun to examine independent methods of confirming the cellular and subcellular localization of angiotensin-converting enzyme. For these purposes we have used endothelial cells in culture. There are a number of ways in which these cells may be harvested. Two methods have given good results. In the first we collected vital Haütchen preparations by the method of Pugatch and Saunders.[36] Endothelial cells are collected as a pure monolayer on strips of cellulose acetate paper. Cells collected by this method were shown to be capable of converting angiotensin I to angiotensin II and of degrading bradykinin to form products like those produced by intact lungs.[27,37] Although the method of Pugatch and Saunders yields a pure monolayer, it is not ideal for large-scale culture. The second method was modified from methods developed for collecting endothelial cells from umbilical vein: Pulmonary arteries were incubated for brief intervals with 0.2% collagenase.

As is becoming more widely recognized, cells collected after enzymic digestion must be identified. Identification is a relatively small problem for cells with characteristic organelles (such as alveolar type II cells). However, endothelial cells are remarkable for their lack of characteristic organelles. Weibel-Palade bodies are useful where present but are not particularly prominent in pulmonary endothelial cells. Figure 5 shows the morphology of the monolayers obtained. In this particular instance the cells were obtained from lungs perfused with collagenase. This cell shows Golgi, filaments, projections, and caveolae—other fields show lipid droplets and Weibel-Palade bodies and rough endoplasmic reticulum.

After endothelial cells had been obtained in culture, it was necessary to show that they, like endothelial cells in situ, possessed angiotensin-converting enzyme. With the relatively small numbers of cells obtainable by culture, assay of a specific enzyme can be a technical challenge. Sensitivity of assay is critical, a point that we were able to address by the use of [^{125}I]Tyr^{8}—bradykinin. Using pure pig lung angiotensin-converting enzyme, we showed that the substrate is degraded to yield [^{125}I]Tyr—Arg. We then used the same substrate on incubation with the cells in culture and found

disappearance of substrate and formation of the expected reaction product.[37] The specificity of reaction was verified through the use of $BPP_{9\alpha}$, a specific inhibitor of angiotensin-converting enzyme. Cells preincubated with $BPP_{9\alpha}$ did not degrade [^{125}I]Tyr^{8}—bradykinin to yield [^{125}I]Tyr—Arg. Having shown that the enzyme persisted during culture, we then examined the cells immunocytochemically. As illustrated in Fig. 8, oxidized DAB occurs along the plasma membrane and associated caveolae.

It now appears feasible to establish the subcellular sites of angiotensin-converting enzyme even more precisely. Negatively stained preparations of pure angiotensin-converting enzyme indicate that the enzyme occurs in tetrameric or hexameric form. The diameter of the enzyme is approximately 60 Å. This may well be of interest in terms of results obtained previously. When one examines thin sections reacted with antibody—peroxidase conjugates, the deposition of oxidized DAB is particulate. Indeed it may correspond with globular particles seen in our freeze-fracture studies of endothelial cells.[38] A particulate deposition of reaction product had been observed previously in our studies of the subcellular localization of 5′-nucleotidase on endothelial cells using thin sections.[9] Globular particles can also be seen on unreacted sections. Freeze-fracture replicas show particles on both fracture faces. They are randomly distributed on undifferentiated portions of the endothelial plasma membrane but are grouped in rings or plaques in association with caveolae. These globular particles are of dimensions that could accommodate an enzyme, such as kininase II, with a molecular weight of 130,000 (Ref. 39) and are clearly well situated to process circulating substances, such as bradykinin and angiotensin I, and to release metabolic products back into the circulation.

Although much remains to be done to establish which, if any, of the particles are kininase II, useful conclusions can be made now: Pulmonary endothelial cells have on their plasma membrane an enzyme capable of inactivating bradykinin, a substance that lowers blood pressure, and of forming angiotensin II, a substance that raises blood pressure. The enzyme appears to have direct access to its substrates in circulating blood. The enzyme is not unique to pulmonary endothelial cells. We have shown that it occurs on endothelium of aorta,[27,35] and more recently Caldwell and colleagues[40] have published immunofluorescence data that were interpreted as showing that the enzyme occurs in endothelium of other tissues. Perhaps the unique feature of the pulmonary enzyme is that it occurs in an organ with an enormous microvascular bed which drains directly into the systemic arterial circulation. Thus products

Fig. 8 Pig lung endothelial cell in culture, fixed and incubated as described in Fig. 6, showing immunocytochemical localization of angiotensin-converting enzyme on plasma membrane and caveolae (arrows). (Magnification, 65,000 X.) [From U. S. Ryan, J. W. Ryan, and A. Chiu, Kininase II Angiotensin Converting Enzyme and Endothelial Cells in Culture, *Adv. Exp. Med. Biol.*, 70: 223 (1976).]

formed by the enzyme are likely to be distributed to all other organs. In the case of the metabolic product, angiotensin II, distribution via the systemic arterial circulation might be expected to have effects on specific activities and functions of distant target organs, such as the adrenal gland and kidney.

PROSTAGLANDINS

Degradation

It is well established that the lungs are capable of eliminating prostaglandins E_2 and $F_{2\alpha}$ arriving via the central venous circulation.[26,41-43] Piper and colleagues[44] have pointed out analogies between the elimination of kinins and prostaglandins and have postulated that the prostaglandins are probably degraded by enzymes situated on or near the luminal surface of pulmonary endothelial cells. Results of our previous studies do not support this disposition of enzyme.[26,43] Cellular uptake apparently precedes the formation of metabolites. Eling and Anderson[45] have evidence indicating that an active transport process is required. Our pilot studies using pulmonary endothelial cells in culture have shown that neither intact nor disrupted endothelial cells [with or without added nicotinamide adenine dinucleotide (NAD)] metabolize [^{3}H]$PGF_{1\alpha}$. Thus at present there is no clear evidence on which cells of the lungs are capable of degrading preformed prostaglandins.

Synthesis

Whether the lungs synthesize prostaglandins has come under renewed scrutiny. In 1965 Änggard and Samuelsson[46] reported that a low-speed supernatant of guinea pig lung homogenate is capable of metabolizing arachidonic acid to yield substances that co-chromatograph with PGE_2 and $PGF_{2\alpha}$. The structures were not proved. More recently Parkes and Eling[47] have shown that a microsomal fraction of guinea pig lungs is capable of metabolizing arachidonic acid to yield a substance that co-chromatographs with $PGF_{2\alpha}$. They also adduced evidence that a PGE_2-like compound was formed, but they emphasized that a major metabolite of arachidonic acid did not correspond with any of the classical prostaglandins. Recently Eling and Anderson[48] have gained evidence that the unidentified metabolite may be thromboxane-B_2.

Hamberg, Svensson, and Samuelsson[48] have reexamined the ability of guinea pig lungs and their microsomes to synthesize

prostaglandins and related substances. Isolated lungs perfused at a slow rate (2 ml/min) with an artificial salt solution containing arachidonic acid appear to produce primarily PGG_2, PGH_2, PHD (now known as thromboxane B_2), HHT, and hydroxy derivatives of arachidonic acid. Small quantities of PGE_2- and $PGF_{2\alpha}$-like substances were found, but their structures were not proved.

Other data bearing on the synthesis of prostaglandins and related compounds by the lungs are based on bioassay or radioimmunoassay results. For example, Piper and Vane[50] found that guinea pig lungs made anaphylactic or perfused with arachidonic acid or bradykinin release a PGE_2-like substance in large quantities along with a short-lived substance (half-life, 1 to 2 min) that they named RCS (rabbit aorta contracting substance). Through elegant chemical studies by Samuelsson and colleagues[51] using platelets incubated with arachidonic acid, it now appears that RCS is not a single substance but is a mixture of the endoperoxide precursors of the prostaglandins (PGG_2 and PGH_2; half-life, approximately 5 min) with a prostaglandin-related substance thromboxane-A_2 (half-life, approximately 30 sec).

All the foregoing data indicate that prostaglandin synthetase is a particulate enzyme that is especially prominent in microsomes. Microsomes can be defined in terms of a tissue homogenate but are less readily defined in terms of intact cells. Hence there are few data on the subcellular localization of prostaglandin synthetase. Recently we have begun to examine for the cellular and subcellular sites of prostaglandin synthetase with two different approaches. The first was patterned after that of Janszen and Nugteren,[52,53] who have argued that "oxygen-containing intermediates" of the prostaglandins might be capable of oxidizing 3,3′-diaminobenzidine to yield a precipitate detectable by light microscopy. We now understand their term, "oxygen-containing intermediates," to be prostaglandins G_2 and H_2, substances that are also precursors for the thromboxanes.

Using prefixed blocks of rat lung tissue in incubation with 3,3′-diaminobenzidine, we found light deposits of reaction product along the periphery of lipid droplets of pericytes or interstitial cells. When the blocks of lung tissue were pretreated with *p*-chloromercuribenzoate (*p*-CMB) ($10^{-4}M$), the deposition of reaction product became more prominent (Figs. 9 and 10).[54,55] The compound *p*-CMB was used in these studies as a substance known to cause the accumulation of prostaglandins G_2 and H_2, the peroxide precursors of prostaglandins and thromboxanes.[49]

Lipid droplets are not a prominent feature of pulmonary capillary endothelial cells but do occur in endothelial cells of large

Fig. 9 Portion of alveolar—capillary unit showing pericyte or interstitial cell (P) immediately adjacent to endothelial cell (En). The pericyte contains a large lipid droplet (L). (Magnification, 41,000 X.)

Fig. 10 Unstained section of glutaraldehyde-fixed rat lung that had been incubated with arachidonic acid in the presence of *p*-CMB and 3,3′-DAB. The reaction product is localized in lipid droplets of pericytes (asterisk). The endothelial cell is indicated (En). (Magnification, 50,000 X.)

blood vessels. We had available for these studies two lines of endothelial cells in culture, one derived from pulmonary artery and one from pulmonary vein. Both cell lines were found to be capable of metabolizing [^{3}H]- and [^{14}C]arachidonic acid to yield a variety of radioactive products, one of which was indistinguishable from thromboxane B_2. In addition, small amounts of prostaglandin E_2 were formed. Thromboxane B_2 and prostaglandin E_2 are not readily distinguished by thin-layer chromatography, but their derivatives are. Both substances are reduced to more-polar derivatives by borohydride, but only prostaglandin E_2 is converted to prostaglandin B_2 by treatment with base. As was expected the formation of thromboxane B_2 and prostaglandin E_2 was almost completely inhibited by pretreatment of the cells with indomethacin ($10^{-4}M$).

When we examined fixed and unfixed endothelial cells in culture for their reaction with diaminobenzidine, the deposits of reaction product again occurred on lipid droplets. However, the deposits were not clearly reduced in cells treated with indomethacin at dosage levels in excess of that needed to prevent the formation of thromboxane B_2 and prostaglandin E_2 (up to 1mM).

These results raised the possibility that other lipid peroxides, possibly those formed by lipoxygenase enzymes, might play a role in oxidation of DAB. In fact, aspirin and indomethacin indirectly cause the accumulation of hydroxy fatty acids formed by lipoxygenase enzymes. Thus we used 5,8,11,14-eicosatetraynoic acid (ETYA) (0.2 mg/ml), which inhibits both prostaglandin synthetase and lipoxygenase. However, cells pretreated with ETYA were still capable of accumulation of reaction product.

These results led to our second approach of using [^{3}H]aspirin labeled in the acetyl moiety. Roth and Majerus[5,6] have adduced evidence that aspirin acetylates specifically a protein component of platelets having the physicochemical characteristics of prostaglandin synthetase. Recently Rome et al.[5,7] have adduced evidence to indicate that [^{3}H]acetylsalicylate can be used to quantify active (vs. inactive) prostaglandin synthetase. Using our [^{3}H]aspirin, we have verified that acetylation of a protein is accomplished on incubation of the [^{3}H]aspirin with sheep lung microsomes. Approximately 0.5% of the total microsomal protein is acetylated.

We then incubated [^{3}H]aspirin with endothelial cells derived from bovine pulmonary artery. As indicated in Fig. 11, silver grains are localized over the cytoplasm of these cells and appear to have some relationship to rough endoplasmic reticulum.

Our results indicate that pulmonary endothelial cells in culture are capable of forming prostaglandins and prostaglandin-related

Fig. 11 Electron-microscope autoradiograph of cow pulmonary artery endothelial cell culture. The culture had been exposed to [^{3}H]aspirin and developed for 14 days. The silver grains, indicating sites of prostaglandin synthesis, appear to be localized in association with cisternae of the rough endoplasmic reticulum (arrows). (Magnification, 39,000 ×.)

substances, most notably thromboxane B_2 but also some prostaglandin E_2. The lipid droplets of these cells and the lipid droplets of pericytes of intact lung tissue show evidence of deposition of oxidized DAB. Cytoplasmic structures of the endothelial cells in culture are made radioactive after reaction with [^{3}H]acetylsalicylate, a potent irreversible inhibitor of prostaglandin synthetase. It is possible that we are observing two distinct phenomena. Although it is frequently argued that synthesis and release of prostaglandins are synonymous terms, it is a point not proved. Indeed, Lewis and Piper[58] have reported that glucocorticoids inhibit release but not synthesis. Although prostaglandins G_2 and H_2 and thromboxane A_2 have extremely short half-lives in aqueous media, it is now known that prostaglandins G_2 and H_2 are stable indefinitely in aprotic solvents. Lipid droplets may prove to be such a solvent system, a point raising the possibility that the deposition of oxidized DAB in lipid droplets may be indicative of a storage depot.

Work by Gerrard and colleagues[59] on thromboxane synthesis in platelets raises another possibility. They too observed the deposition of oxidized DAB that had not been modified by prior treatment of platelets with aspirin or indomethacin. They attribute the deposition of DAB on the dense tubular system as being due to the action of a peroxidase enzyme that acts in concert with prostaglandin synthetase to form prostaglandin G_2 and prostaglandin H_2. Biochemical evidence for the participation of such a peroxidase has been

presented by several groups, most recently by O'Brien and Rahimtula.[60] These data may help to explain how arachidonic acid can undergo several different chemical reactions (ring closure and the introduction of two peroxide groups), steps difficult to understand in terms of a single enzyme.

In these last terms our results might be interpreted as showing the sites of prostaglandin synthetase by acetylation with [^{3}H]aspirin and the sites of the related peroxidase or stored peroxides by the deposition of oxidized DAB.

Other Polypeptide Hormones

Rubenstein, Zwi, and Miller[61] have reported that insulin may be metabolized during circulation through the lungs. Recently an effort was begun to confirm these observations.[62] In a survey of insulin-like immunoreactivity in arterial and central venous blood (samples drawn simultaneously), no consistent evidence was found for the uptake or degradation of insulin by the lungs. Thus at present it is not clear whether insulin is metabolized by the lungs. If metabolism occurs, it probably does not proceed through degradation of the β-chain by angiotensin-converting enzyme.

STEROID AND THYROID HORMONES

The lungs, like other tissues, undoubtedly take up hormones for their own use. Glucocorticoids hasten the production of surfactant by fetal lungs (Rooney and Motoyama, this volume). Several investigators[63] have shown that homogenates of adult and fetal rat lung contain macromolecules, possibly receptors, capable of binding natural and synthetic glucocorticoids with high affinity and some specificity. Others (e.g., see Ref. 64) have shown that glucocorticoids accelerate the appearance of osmiophilic bodies of type II alveolar cells, the likely origin of the surfactant lining layer. Redding, Douglas, and Stein[65] have reported that the morphology of type II alveolar cells and the content of surface-active material in lungs lavage fluid of adult rats can be profoundly influenced by thyroid hormones: Thyroidectomy was associated with reduced surfactant, and the type II cells appeared to be immature. Thyroxine treatment had the opposite effects.

The disposition of metabolites following uptake of glucocorticoids and thyroxine has not been studied but may present a fruitful line of inquiry. Only part of the triiodothyronine (T-3) of serum

originates in the thyroid gland. Thus the T-3 that originates elsewhere has become a matter of concern, especially in view of so-called T-3 hyperthyroidism. Rabinowitz and Hercker[66] have reported that isolated rat hearts perfused with thyroxine may release up to 50% of the original thyroxine as T-3. We are unaware of studies on the amounts of thyroxine taken up by the lungs; but, in view of the large volume of blood processed by the lungs (especially during exercise, a condition in which T-3 use may be increased[67]), and their strategic position within the circulation, such studies may be indicated. Similarly, the disposition of the metabolites of glucocorticoids may be of interest since Giannopoulos[68] has shown that fetal lungs can convert cortisone to its more active analog, cortisol. Recently Nicholas and Kim[69] have shown that intact lungs convert [^{3}H]cortisone into [^{3}H]cortisol and that some of the cortisol thus formed is released into the pulmonary venous effluent. Subcellular fractions of rabbit, dog, and rat lungs metabolize testosterone.[70] However, the disposition of the metabolites is not known.

Thus, although the steroid and thyroid hormones are taken up by the lungs, no specific role of the endothelial cells has yet been shown in the metabolism of these substances.

CONCLUDING REMARKS

A priori, endothelial cells must play at least a passive role in all exchanges between blood and parenchymal cells. However, the foregoing discussion makes clear that pulmonary endothelial cells play much more than a passive role, especially in terms of the selective processing of blood-borne hormones, prohormones, and other excitatory agents. Questions arise as to whether any of the specific metabolic activities are unique to pulmonary endothelial cells. One cannot answer the question comprehensively on the basis of existing data. Angiotensin-converting enzyme is not unique to lung endothelium. Similarly, thromboplastin is widely distributed among virtually all organs and tissues, and one may presume that the biogenic amine transport systems are widely distributed. What does appear to be unique to pulmonary endothelium is its inability to degrade angiotensin II and angiotensin III (A. T. Chiu and J. W. Ryan, unpublished). Other unique features are due to the architecture of the lung and its strategic location within the circulatory system. The lung is the only organ to receive the entire cardiac output and is the only organ whose venous effluent drains directly into the systemic circulation. Hence the products (e.g., thromboxanes, angiotensin II, and possibly angiotensin III) formed within

the lungs and the pulmonary circulation can be expected to be delivered in bulk to all organs, including the lungs themselves, supplied by systemic arterial blood. Possibly over the next few years, we will begin to understand mechanisms by which the lungs (and pulmonary endothelial cells) can exert humoral influences over specific functions of distant organs.

ACKNOWLEDGMENTS

This work was supported by grants from the U. S. Public Health Service (HL 15691, HL 16407, HL 19764, and contract N01 HR3-3015) and the John A. Hartford Foundation, Inc., the Council for Tobacco Research—U. S. A., Inc., by an Established Investigatorship award to Dr. Una S. Ryan from the American Heart Association with funds contributed by the Heart Association of Palm Beach County, Fla.

REFERENCES

1. E. H. Starling and E. B. Verney, The Secretion of Urine as Studied on the Isolated Kidney, *Proc. Roy. Soc. (London), Ser. B.*, 97: 321-363 (1925).
2. J. W. Ryan, J. Roblero, and J. M. Stewart, Inactivation of Bradykinin in the Pulmonary Circulation, *Biochem. J.*, 110: 795-797 (1968).
3. C. G. Becker and P. C. Harpel, α_2-Macroglobulin on Human Vascular Endothelium, *J. Exp. Med.*, 144: 1-9 (1976).
4. E. A. Jaffe, L. W. Hoyer, and R. L. Nachman, Synthesis of Antihemophilic Factor Antigen by Cultured Human Endothelial Cells, *J. Clin. Invest.*, 52: 2757-2765 (1973).
5. S. M. Zeldis, Y. Nemerson, and F. A. Pitlick, Tissue Factor (Thromboplastin): Localization to Plasma Membranes by Peroxidase-Conjugated Antibodies, *Science*, 175: 766-768 (1972).
6. A. P. Fishman, Dynamics of the Pulmonary Circulation, *Handbook of Physiology*, Vol. 2, Circulation, W. F. Hamilton and P. Dow (Eds.), pp. 1167-1743, American Physiological Society, Washington, D. C., 1973.
7. U. Smith, J. W. Ryan, D. D. Michie, and D. S. Smith, Endothelial Projections: As Revealed by Scanning Electron Microscopy, *Science*, 173: 925-927 (1971).
8. U. Smith and J. W. Ryan, An Electron Microscopic Study of the Vascular Endothelium as a Site for Bradykinin and ATP Inactivation in Rat Lung, *Advances in Experimental Medicine and Biology*, Vol. 8, Bradykinin and Related Kinins, N. Back, F. Sicuteri, and M. Rocha e Silva (Eds.), pp. 249-252, Plenum Press, New York, 1970.
9. U. Smith and J. W. Ryan, Substructural Features of Pulmonary Endothelial Caveolae, *Tissue Cell*, 4: 49-54 (1972).
10. U. Smith and J. W. Ryan, Pulmonary Endothelial Cells and Metabolism of Adenine Nucleotides, Kinins and Angiotensin I, *Advances in Experimental*

Medicine and Biology, Vol. 21, Vasopeptides, N. Back and F. Sicuteri (Eds.), pp. 267-276, Plenum Press, New York, 1972.

11. G. I. Schoefl and J. E. French, Vascular Permeability to Particulate Fat: Morphological Observations on Vessels of Lactating Mammary Gland and of Lung, *Proc. Roy. Soc. (London), Ser. B.*, 169: 153-165 (1968).
12. R. O. Scow, E. J. Blanchette-Mackie, and L. C. Smith, Role of Capillary Endothelium in the Clearance of Chylomicrons, *Circ. Res.*, XXXIX: 149-162 (1976).
13. J. R. Vane, The Release and Fate of Vaso-Active Hormones in the Circulation, *Br. J. Pharmacol.*, 35: 209-242 (1969).
14. J. Hughes, C. N. Gillis, and F. E. Bloom, The Uptake and Disposition of DL-Norepinephrine in Perfused Rat Lung, *J. Pharmacol. Exp. Ther.*, 169: 237-248 (1969).
15. T. E. Nicholas, J. M. Strum, L. S. Angelo, and A. F. Junod, Site and Mechanism of Uptake of ^{3}H-l-Norepinephrine by Isolated Perfused Rat Lungs, *Circ. Res.*, XXXV: 670-680 (1974).
16. J. M. Strum and A. F. Junod, Radioautographic Demonstration of 5-Hydroxy-Tryptamine-^{3}H Uptake by Pulmonary Endothelial Cells, *J. Cell Biol.*, 54: 456-467 (1972).
17. A. F. Junod, Mechanism of Uptake of Biogenic Amines in the Pulmonary Circulation, in *Lung Metabolism*, A. F. Junod and R. de Haller (Eds.), pp. 387-398, Academic Press, Inc., New York, 1975.
18. L. Binet and M. Burstein, Poumon et Action Vasculaire de l'Adenosine-Triphosphate (A.T.P.), *Presse Med.*, 58: 1201-1203 (1950).
19. J. W. Ryan and U. Smith, A Rapid, Simple Method for Isolating Pinocytotic Vesicles and Plasma Membrane of Lung, *Biochem. Biophys. Acta*, 249: 177-180 (1971).
20. U. Smith and J. W. Ryan, Pinocytotic Vesicles of the Pulmonary Endothelial Cell, *Chest*, 59: 12S-15S (1971).
21. J. W. Ryan, J. Roblero, and J. M. Stewart, Inactivation of Bradykinin in Rat Lung, *Pharmacol. Res. Commun.*, 1: 192 (1969) (Abstract).
22. J. W. Ryan, J. Roblero, and J. M. Stewart, Inactivation of Bradykinin in Rat Lung, *Advances in Experimental Medicine and Biology*, Vol. 8, Bradykinin and Related Kinins, N. Back, F. Sicuteri, and M. Rocha e Silva (Eds.), pp. 263-272, Plenum Press, 1970.
23. J. W. Ryan, J. M. Stewart, W. P. Leary, and J. G. Ledingham, Metabolism of Angiotensin I in the Pulmonary Circulation, *Biochem. J.*, 120: 221-223 (1970).
24. J. W. Ryan, R. S. Niemeyer, D. W. Goodwin, U. Smith, and J. M. Stewart, Metabolism of (8-L-[^{14}C]Phenylalanine)-Angiotensin I in the Pulmonary Circulation, *Biochem. J.*, 125: 921-923 (1971).
25. J. W. Ryan, U. Smith, and R. S. Niemeyer, Angiotensin I: Metabolism by Plasma Membrane of Lung, *Science*, 176: 64-66 (1972).
26. J. W. Ryan and U. Smith, Metabolism of Adenosine-5′-Monophosphate During Circulation Through the Lungs, *Trans. Assoc. Amer. Physns.*, 84: 297-306 (1971).
27. J. W. Ryan and U. Smith, The Metabolism of Angiotensin I by Endothelial Cells, in *Protides of the Biological Fluids*, Vol. 20, H. Peeters (Ed.), pp. 379-384, Pergamon Press, Oxford, 1973.
28. U. Smith and J. W. Ryan, Electron Microscopy of Endothelial and Epithelial Components of the Lungs: Correlations of Structure and Function, *Fed. Proc.*, 32: 1957-1966 (1973).

29. J. W. Ryan and U. S. Ryan, Metabolic Activities of Plasma Membrane and Caveolae of Pulmonary Endothelial Cells, with a Note of Pulmonary Prostaglandin Synthetase, in *Lung Metabolism*, A. F. Junod and R. de Haller (Eds.), pp. 399-424, Academic Press, Inc., New York, 1975.
30. F. E. Dorer, J. R. Kahn, K. E. Lentz, M. Levine, and L. T. Skeggs, Purification and Properties of Angiotensin-Converting Enzyme from Hog Lung, *Circ. Res.*, XXXI: 356-366 (1972).
31. F. E. Dorer, J. W. Ryan, and J. M. Stewart, Hydrolysis of Bradykinin and Its Higher Homologues by Angiotensin-Converting Enzyme, *Biochem. J.*, 141: 915-917 (1974).
32. H. Y. T. Yang, E. G. Erdös, and Y. Levin, Characterization of a Dipeptide Hydrolase (Kininase II: Angiotensin I Converting Enzyme), *J. Pharmacol. Exp. Ther.*, 177: 291-300 (1971).
33. J. W. Ryan, U. S. Ryan, D. R. Schultz, C. Whitaker, A. Chung, and F. E. Dorer, Subcellular Localization of Pulmonary Angiotensin Converting Enzyme (Kininase II), *Biochem. J.*, 146: 497-499 (1975).
34. J. W. Ryan, A. R. Day, U. S. Ryan, A. Chung, D. I. Marlborough, and F. E. Dorer, Localization of Angiotensin Converting Enzyme (Kininase II). I. Preparation of Antibody-Heme-Octapeptide Conjugates, *Tissue Cell*, 8: 111-124 (1976).
35. U. S. Ryan, J. W. Ryan, C. Whitaker, and A. Chiu, Localization of Angiotensin Converting Enzyme (Kininase II). II. Immunocytochemistry and Immunofluorescence, *Tissue Cell*, 8: 125-146 (1976).
36. E. M. J. Pugatch and A. M. Saunders, A New Technique for Making Haütchen Preparations of Unfixed Aortic Endothelium, *J. Atheroscler. Res.*, 8: 735-738 (1968).
37. A. T. Chiu, J. W. Ryan, U. S. Ryan, and F. E. Dorer, A Sensitive Radiochemical Assay for Angiotensin Converting Enzyme (Kininase II), *Biochem. J.*, 149: 297-300 (1975).
38. U. Smith, J. W. Ryan, and D. S. Smith, Freeze-Etch Studies of the Plasma Membrane of Pulmonary Endothelial Cells, *J. Cell Biol.*, 56: 492-499 (1973).
39. M. Das and R. L. Soffer, Pulmonary Angiotensin-Converting Enzyme. Structural and Catalytic Properties, *J. Biol. Chem.*, 250: 6762-6768 (1975).
40. P. R. B. Caldwell, B. C. Seegal, K. C. Hsu, M. Das, and R. L. Soffer, Angiotensin-Converting Enzyme: Vascular Endothelial Localization, *Science*, 191: 1050-1051 (1976).
41. S. H. Ferreira and J. R. Vane, Prostaglandins: Their Disappearance and Release into the Circulation, *Nature (London)*, 216: 868-873 (1967).
42. P. J. Piper and J. R. Vane, Release of Additional Factors in Anaphylaxis and Its Antagonism by Anti-Inflammatory Drugs, *Nature (London)*, 223: 29-35 (1969).
43. J. W. Ryan, R. S. Niemeyer, and U. Ryan, Metabolism of Prostaglandin $F_{1\alpha}$ in the Pulmonary Circulation, *Prostaglandins*, 10: 101-108 (1975).
44. P. J. Piper, Importance and Nature of the Mechanism of Inactivation of Prostaglandins in the Lungs, in *Lung Metabolism*, A. F. Junod and R. de Haller (Eds.), pp. 325-335, Academic Press, Inc., New York, 1975.
45. T. E. Eling and M. W. Anderson, National Institute of Environmental Health Sciences, personal communication.
46. E. Änggard and B. Samuelsson, Biosynthesis of Prostaglandins from Arachidonic Acid in Guinea Pig Lung, *J. Biol. Chem.*, 240: 3518-3521 (1965).

47. D. G. Parkes and T. E. Eling, Characterization of Prostaglandin Synthetase in Guinea Pig Lung. Isolation of a New Prostaglandin Derivative from Arachidonic Acid, *Biochemistry*, 13: 2598-2604 (1974).
48. T. E. Eling and M. W. Anderson, National Institute of Environmental Health Sciences, personal communication.
49. M. Hamberg, J. Svensson, and B. Samuelsson, Prostaglandin Endoperoxides, a New Concept Concerning the Mode of Action and Release of Prostaglandins, *Proc. Nat. Acad. Sci. U. S. A*, 71: 3824-3828 (1974).
50. P. J. Piper and J. R. Vane, The Release of Prostaglandins from Lung and Other Tissues, *Ann. N. Y. Acad. Sci.*, 180: 363-385 (1971).
51. M. Hamberg, J. Svensson, and B. Samuelsson, Thromboxanes: A New Group of Biologically Active Compounds Derived from Prostaglandin Endoperoxides, *Proc. Nat. Acad. Sci. U. S. A.*, 72: 2994-2998 (1975).
52. F. H. A. Janszen and D. H. Nugteren, Histochemical Localization of Prostaglandin Synthetase, *Histochemie*, 27: 159-164 (1971).
53. F. H. A. Janszen and D. H. Nugteren, A Histochemical Study of the Prostaglandin Biosynthesis in the Urinary System of Rabbit, Guinea Pig, Gold Hamster, and Rat, in *Advances in the Biosciences*, Vol. 9, pp. 237-292, Pergamon Press, Oxford, 1973.
54. U. S. Ryan, J. W. Ryan, and A. T. Chiu, The Lungs and Prostaglandin Synthesis, *J. Cell Biol.*, 67: 376a (1975).
55. J. W. Ryan, U. S. Ryan, and A. T. Chiu, Synthesis of Thromboxanes by Lungs and Pulmonary Endothelial Cells, *J. Cell Biol.*, 70: 344a (1976).
56. G. J. Roth and P. W. Majerus, The Mechanism of the Effect of Aspirin on Human Platelets. I. Acetylation of a Particulate Fraction Protein, *J. Clin. Invest.*, 56: 624-632 (1975).
57. L. H. Rome, E. M. Lands, G. J. Roth, and P. W. Majerus, Aspirin as a Quantitative Acetylating Reagent for the Fatty Acid Oxygenase that Forms Prostaglandins, *Prostaglandins*, 11: 23-30 (1976).
58. G. P. Lewis and P. J. Piper, Inhibition of Release of Prostaglandins as an Explanation of Some of the Actions of Anti-Inflammatory Corticosteroids, *Nature (London)*, 254: 308-311 (1975).
59. J. M. Gerrard, J. G. White, G. H. R. Rao, and D. Townsend, Localization of Platelet Production in the Platelet Dense Tubular System, *Am. J. Pathol.*, 83: 283-298 (1976).
60. P. J. O'Brien and A. Rahimtula, The Possible Involvement of a Peroxidase in Prostaglandin Biosynthesis, *Biochem. Biophys. Res. Commun.*, 70: 832-838 (1976).
61. A. H. Rubenstein, S. Zwi, and K. Miller, Insulin and the Lung, *Diabetologia*, 4: 236-238 (1968).
62. F. E. Dorer, Veterans Hospital, Cleveland, Ohio, and J. W. Ryan, University of Miami, unpublished.
63. D. Toft and F. Chytil, Receptors for Glucocorticoids in Lung Tissue, *Arch. Biochem. Biophys.*, 157: 464-469 (1973).
64. N. S. Wang, R. V. Kotas, M. E. Avery, and W. M. Thurlbeck, Accelerated Appearance of Osmiophilic Bodies in Fetal Lungs Following Steroid Injection, *J. Appl. Physiol.*, 30: 362-365 (1971).
65. R. A. Redding, W. H. J. Douglas, and M. Stein, Thyroid Hormone Influence upon Lung Surfactant Metabolism, *Science*, 175: 994-996 (1972).
66. J. L. Rabinowitz and E. S. Hercker, Thyroxine: Conversion of Triiodothyronine by Isolated Perfused Rat Heart, *Science*, 173: 1242-1243 (1971).

67. L. B. Middlesworth, Metabolism and Excretion of Thyroid Hormone, *in Handbook of Physiology*, Vol. 3, Thyroid, M. A. Greer and D. H. Solomon (Eds.), pp. 215-231, American Physiological Society, Washington, D. C., 1974.
68. G. Giannopoulos, Uptake and Metabolism of Cortisone and Cortisol by the Fetal Rabbit Lung, *Steroids*, 23: 845-853 (1974).
69. T. E. Nicholas and P. A. Kim, The Metabolism of ^{3}H—Cortisone and ^{3}H—Cortisol by the Isolated Perfused Rat and Guinea Pig Lungs, *Steroids*, 25: 387-402 (1975).
70. J. Hartiala, Testosterone Metabolism in Rabbit Lung In Vitro, *Steroids Lipids Res.*, 5: 91-95 (1974).

Pulmonary Endothelial Cells: Kininase II and Other Peptide Hydrolase Enzymes

JAMES W. RYAN,* UNA S. RYAN,* and A. T. CHIU†
*Papanicolaou Cancer Research Institute and Department of Medicine, University of Miami School of Medicine, Miami, Florida, and †Medical College of Virginia, Richmond, Virginia

ABSTRACT

Angiotensin I and bradykinin disappear during a single passage through the pulmonary circulation. These polypeptide hormones are not taken up by the lungs but are hydrolyzed by enzymes on or near the luminal surface of the pulmonary endothelial cells. Kininase II (angiotensin-converting enzyme), a dipeptidyl carboxypeptidase with the capacity of inactivating bradykinin and of converting angiotensin I to its potent lower homolog, angiotensin II, is described in detail. In addition, the enzyme is capable of converting des-Asp^1—angiotensin I to angiotensin III, a compound even more active than angiotensin II in stimulating the secretion of aldosterone. With immunocytochemical techniques which used antibodies specific for kininase II, the enzyme was found to be situated along the luminal surface of pulmonary endothelial cells in situ and along the plasma membrane of endothelial cells in culture.

However, lungs contain other enzymes that are capable of inactivating bradykinin and of metabolizing angiotensin I to yield products other than angiotensin II. These enzymes also appear to be situated on the luminal surface of endothelial cells. Two of the enzymes are capable of removing the N-terminal amino acid residues of bradykinin and angiotensin I. For bradykinin, the removal of the N-terminal residue yields biologically inactive products. However, the removal of the aspartyl residue of angiotensin I yields a precursor of angiotensin III.

As described in the paper by Ryan and Ryan (this volume), bradykinin and angiotensin I are metabolized during a single passage through the pulmonary circulation.[1-6] Data available at present indicate that kininase II (angiotensin-converting enzyme) plays a central role in the processing of both polypeptides. The enzyme

converts angiotensin I to angiotensin II and is capable of degrading bradykinin in a two-step reaction.[7,8] Kininase II has been shown to be located along the luminal surface of endothelial cells of intact lungs and along the plasma membrane of pulmonary endothelial cells in culture.[9-13]

However, it has been known for several years that lungs contain other peptide hydrolase enzymes that are capable of degrading bradykinin and angiotensin I (Refs. 1 to 4). Furthermore, it seems likely that these peptide hydrolase enzymes occur on endothelial cells.[3] During the 3 to 5 sec required for blood to pass from the pulmonary artery to the left atrium of the heart, bradykinin is hydrolyzed in no fewer than five of its eight peptide bonds. Similarly, angiotensin I is hydrolyzed at several different sites. All the metabolic products of bradykinin are biologically inert. However, more than one of the metabolites of angiotensin I may possess biological activity. The venous effluent of lungs perfused with [^{14}C] Leu^{10}—angiotensin I contains a substance that we have not distinguished from des-Asp^{1}—angiotensin I (Refs. 4 and 5); a possible precursor of angiotensin III (des-Asp^{1}—angiotensin II).[14,15] Recently attention has been focused on angiotensin III as a potent aldosterone secretogogue having relatively little potency on vascular smooth muscle.[16]

The present study was begun to focus attention on the fact that kininase II is not the only peptide hydrolase enzyme involved in the processing of circulating bradykinin and angiotensin I by intact lungs. In addition, attention is directed to the fact that kininase II is a much more selective enzyme than previously thought and is capable of forming more than one biologically active metabolite. Both of these points must be taken into account in efforts to gain improved understanding of the hormonal mechanisms by which intact lungs may influence specific activities of organs and tissues at a distance and to evaluate effects of pharmacological blockade of kininase II in patients with renin-related hypertension.

ALTERNATIVE FATES OF BRADYKININ

Our early studies[1-3] showed that bradykinin (Arg—Pro—Pro—Gly—Phe—Ser—Pro—Phe—Arg) is hydrolyzed at several different peptide bonds during passage through the lungs. So far only one of the sites of hydrolysis can be attributed to kininase II. Using [^{14}C] Pro^{2}-bradykinin in perfusions of isolated lungs, we found two radioactive metabolites, Pro—Pro and Arg—Pro—Pro—Gly. These products indicate that hydrolysis occurs at three peptide bonds,

Arg^1—Pro^2, Pro^3—Gly^4, and Gly^4—Phe^5. Apparently all three of these hydrolytic reactions can be inhibited by 2-mercaptoethanol since the venous effluent of lungs perfused with [^{14}C]Pro^2—bradykinin and 2-mercaptoethanol contains a single radioactive metabolite, Arg—Pro—Pro—Gly—Phe—Ser. This metabolite indicates that lungs also contain an enzyme capable of hydrolyzing the Ser^6—Pro^7 bond.

The venous effluent of lungs perfused with [^{3}H]Phe^8—bradykinin contains a single radioactive metabolite, Phe—Arg, the radioactive metabolite expected from the action of kininase II. However, under conditions in which kininase II is inhibited, the radioactive metabolite is Pro—Phe—Arg. On incubation of bradykinin with pure pig lung angiotensin-converting enzyme in vitro, one obtains two dipeptides, Phe—Arg and Ser—Pro. It is not known at present whether both dipeptides are released by intact lung perfused with bradykinin.

ALTERNATIVE FATES OF ANGIOTENSIN I

The venous effluent of lungs perfused with [^{14}C]Leu^{10}—angiotensin I (H—Asp—Arg—Val—Tyr—Ile—His—Pro—Phe—His—Leu—OH) contains a number of radioactive metabolites, the most prominent of which is His—Leu, the product expected of kininase II (Ref. 4). However, it appears that the amount of His—Leu formed exceeds the amount of angiotensin II formed. This result could mean that some of the angiotensin II is degraded in subsequent metabolic steps. However, two other observations argue against this interpretation. First, intact lungs do not degrade, to any great extent, angiotensin II perfused via the pulmonary artery.[17-19] Second, it is now known that C-terminal lower homologs of angiotensin I are substrates for kininase II and yield His—Leu on hydrolysis.[14]

Other radioactive metabolites of [^{14}C]Leu^{10}—angiotensin I include a substance that we have not been able to distinguish from des-Asp^1—angiotensin I. The venous effluent of lungs perfused with [^{14}C]Phe^8—angiotensin I does, in fact, contain radioactive angiotensin II. However, over 80% of the radioactivity occurs in the form of C-terminal lower homologs of both angiotensin I and angiotensin II (Ref. 5).

Although at present one cannot readily assess the physiological importance of the lung peptide hydrolase enzymes other than kininase II (angiotensin-converting enzyme), our data indicate that, under conditions in which kininase II is inhibited, there remains a sufficient reserve of other enzymes such that bradykinin and

angiotensin I will not accumulate to any great extent. In fact, patients treated with the kininase II inhibitor $BPP_{9\alpha}$ (also known as SQ 20,881) do not appear to have blood concentrations of angiotensin I that are significantly higher than those of controls.[20]

SELECTIVITY OF ACTION OF KININASE II

Kininase II (angiotensin-converting enzyme) acts as a dipeptidyl carboxypeptidase. Early experiments using pure or highly purified enzyme showed that the enzyme is not specific (e.g., see Ref. 21). The ability of the enzyme to hydrolyze polypeptides as diverse in structure as bradykinin and angiotensin I suggested that the enzyme is not even very selective. In addition, data have been adduced to indicate that the enzyme will hydrolyze a wide range of acylated tripeptides, notably hippuryl—His—Leu, hippuryl—Gly—Gly, dansyl—Gly—Gly—Gly, and Boc—(NO_2)Phe—Phe—Gly. One report indicates that the enzyme will degrade the beta chain of insulin.[22]

However, recent data indicate that the lack of selectivity of kininase II is more apparent than real. Since 1969 bradykinin has been known to be inactivated during passage through the lungs at a rate clearly faster than those of its N-terminal higher homologs (e.g., Lys—bradykinin, Met—Lys—bradykinin, Gly—Arg—Met—Lys—bradykinin, and Polistes kinin).[3,23] Indeed, the rates of hydrolysis of the kinins appear to vary as an inverse function of size and charge. Recently Dorer, Ryan, and Stewart[24] have adduced evidence to indicate that much of the selectivity of hydrolysis of kinins by intact lungs can be explained in terms of the selectivity of action of kininase II (Table 1).

As indicated in the paper by Ryan and Ryan (this volume), bradykinin is a preferred substrate of kininase II (see also Refs. 8 and 14). In in vitro experiments bradykinin is a strong competitive inhibitor of the conversion of angiotensin I to angiotensin II by kininase II: In an incubation mixture in which bradykinin is at 5μM and angiotensin I is at 25μM, the conversion of angiotensin I to angiotensin II is inhibited by more than 90% (Table 2). However, angiotensin I as a substrate is strongly preferred over an acylated tripeptide such as hippuryl—His—Leu (Table 3). Similarly, the affinity of angiotensin I for the enzyme is, with one exception, greater than those of any of the C-terminal lower homologs of angiotensin I (Table 3). The one exception may be of physiological significance: Des-Asp^1—angiotensin I, a possible precursor of angiotensin III (des-Asp^1—angiotensin II), has a greater affinity for the enzyme than does angiotensin I. Thus in systems in which kininase II

TABLE 1

REACTION RATES FOR THE HYDROLYSIS OF BRADYKININ AND ITS HIGHER HOMOLOGS BY INTACT RAT LUNGS AND BY PURE PIG LUNG KININASE II
(Values are expressed in terms of percent)*

Kinin	Intact lungs	Kininase II
Bradykinin	100	100
Lys—bradykinin	96	65
Met—Lys—bradykinin	80	55
Lys—Lys—bradykinin	0	12
Gly—Arg—Met—Lys—bradykinin	<10	5
Polistes kinin	0	2

*For further details, see Refs. 3, 22, and 23.

TABLE 2

INHIBITION OF THE CONVERSION OF ANGIOTENSIN I TO ANGIOTENSIN II BY ANGIOTENSINS, KININS, AND RELATED COMPOUNDS

Inhibitor	Concentration of inhibitor	Inhibition, %
$BPP_{9\alpha}$ (SQ 20,881)	5n*M*	36.5
$BPP_{5\alpha}$	50n*M*	70.0
Bradykinin	5μ*M*	90.9
Angiotensin II	50μ*M*	34.1
Angiotensin III	25μ*M*	70.4
[Sar^1,Ala^8]angiotensin II	25μ*M*	54.2
Angiotensin II (3-8)-hexapeptide	50μ*M*	0

*Reaction mixtures contained angiotensin I at 25μ*M* and kininase II at 770p*M* in 50m*M* sodium phosphate buffer, pH 7.5, plus 100m*M* NaCl. For further details, see Ref. 14.

is limiting and in which angiotensin I and des-Asp^1—angiotensin I occur in similar molar concentrations, the formation of angiotensin III will be favored over that of angiotensin II. Although the significance is difficult to evaluate at the moment, it may be important to note that angiotensin III is a strong inhibitor of kininase II whereas angiotensin II is a weak inhibitor (Table 2).

TABLE 3

RELATIVE AFFINITIES OF ANGIOTENSIN I, ITS C-TERMINAL LOWER HOMOLOGS AND RELATED COMPOUNDS FOR KININASE II (ANGIOTENSIN-CONVERTING ENZYME)*

Compound	K_m, μM
Asp—Arg—Val—Tyr—Ile—His—Pro—Phe—His—Leu	33
Arg—Val—Tyr—Ile—His—Pro—Phe—His—Leu	11
Val—Tyr—Ile—His—Pro—Phe—His—Leu	170
Tyr—Ile—His—Pro—Phe—His—Leu	100
Ile—His—Pro—Phe—His—Leu	1000
hippuryl—His—Leu	3000
hippuryl—Gly—Gly	2000

*For further details, see Ref. 14.

CONCLUDING REMARKS

At present little is known of the physiological significance of the peptide hydrolase enzymes other than kininase II. However, there are clinical and pathophysiological circumstances under which these enzymes may become of primary importance. The polypeptide $BPP_{9\alpha}$ (SQ 20,881) is an exquisitely potent inhibitor of kininase II and has been used clinically in the treatment of renin-related hypertension.[25] Similarly, antagonists of angiotensin II, e.g., Sar^1, Ala^8—angiotensin II, are now known to be strong inhibitors of angiotensin-converting enzyme (e.g., see Ref. 14). These compounds are also being used clinically.[26] Thus it would appear to be timely further to examine alternative fates of angiotensin I and bradykinin during passage through the lungs.

In addition to consideration of alternative fates of these polypeptides, it would appear to be timely to reassess the selectivity of action of kininase II. The enzyme acts as a dipeptidyl carboxypeptidase, and it can, in fact, hydrolyze a wide variety of polypeptide substrates. However, the relative affinity of the enzyme for different substrates varies enormously, a point suggesting that the selectivity of action of the enzyme may be of physiological importance.

ACKNOWLEDGMENTS

This work was supported by grants from U.S. Public Health Service (HL 15691, HL 16407, HL 19764, HL 18415, and Contract

N01 HR3-3015) and from the John A. Hartford Foundation, Inc., the Council for Tobacco Research—U.S.A., Inc., by an Established Investigatorship award to Dr. Una S. Ryan from the American Heart Association, and by funds contributed by the Heart Association of Palm Beach County, Fla.

REFERENCES

1. J. W. Ryan, J. Roblero, and J. M. Stewart, Inactivation of Bradykinin in the Pulmonary Circulation, *Biochem. J.*, 110: 795-797 (1968).
2. J. W. Ryan, J. Roblero, and J. M. Stewart, Inactivation of Bradykinin in Rat Lung, *Pharmacol. Res. Commun.*, 1 : 192 (1969) (Abstract).
3. J. W. Ryan, J. Roblero, and J. M. Stewart, Inactivation of Bradykinin in Rat Lung, in *Advances in Experimental Medicine and Biology*, Vol. 8, Bradykinin and Related Kinins, N. Back, F. Sicuteri, and M. Rocha e Silva (Eds.), pp. 263-272, Plenum Press, New York, 1970.
4. J. W. Ryan, J. M. Stewart, W. P. Leary, and J. G. Ledingham, Metabolism of Angiotensin I in the Pulmonary Circulation, *Biochem. J.*, 120: 221-223 (1970).
5. J. W. Ryan, R. S. Niemeyer, D. W. Goodwin, U. Smith, and J. M. Stewart, Metabolism of (8-L-[^{14}C]Phenylalanine-Angiotensin I in the Pulmonary Circulation, *Biochem. J.*, 125: 921-923 (1971).
6. J. W. Ryan, U. Smith, and R. S. Niemeyer, Angiotensin I: Metabolism by Plasma Membrane of Lung, *Science*, 176: 64-66 (1972).
7. F. E. Dorer, J. R. Kahn, K. E. Lentz, M. Levine, and L. T. Skeggs, Purification and Properties of Angiotensin-Converting Enzyme from Hog Lung, *Circ. Res.*, XXXI: 356-366 (1972).
8. F. E. Dorer, J. R. Kahn, K. E. Lentz, M. Levine, and L. T. Skeggs, Hydrolysis of Bradykinin by Angiotensin-Converting Enzyme, *Circ. Res.*, XXXIV: 824-827 (1974).
9. J. W. Ryan and U. Smith, The Metabolism of Angiotensin I by Endothelial Cells, in *Protides of the Biological Fluids*, Vol. 20, H. Peeters (Ed.), pp. 379-384, Pergamon Press, Oxford, 1973.
10. A. T. Chiu, J. W. Ryan, U. S. Ryan, and F. E. Dorer, A Sensitive Radiochemical Assay for Angiotensin-Converting Enzyme (Kininase II), *Biochem. J.*, 149: 297-300 (1975).
11. J. W. Ryan, U. S. Ryan, D. R. Schultz, C. Whitaker, A. Chung, and F. E. Dorer, Subcellular Localization of Pulmonary Angiotensin Converting Enzyme (Kininase II), *Biochem. J.*, 146: 497-499 (1975).
12. J. W. Ryan, A. R. Day, U. S. Ryan, A. Chung, D. I. Marlborough, and F. E. Dorer, Localization of Angiotensin Converting Enzyme (Kininase II). I. Preparation of Antibody—Heme—Octapeptide Conjugates, *Tissue Cell*, 8: 111-124 (1976).
13. U. S. Ryan, J. W. Ryan, C. Whitaker, and A. Chiu, Localization of Angiotensin Converting Enzyme (Kininase II). II. Immunocytochemistry and Immunofluorescence, *Tissue Cell*, 8: 125-146 (1976).
14. A. T. Chiu, J. W. Ryan, J. M. Stewart, and F. E. Dorer, Formation of Angiotensin III by Angiotensin-Converting Enzyme, *Biochem. J.*, 155: 189-192 (1976).

15. B. S. Tsai, M. J. Peach, M. C. Khosla, and F. M. Bumpus, Synthesis and Evaluation of [Des-Asp^1]Angiotensin I as a Precursor for [Des-Asp^1]Angiotensin II ("Angiotensin III"), *J. Med. Chem.*, 18: 1180-1183 (1975).
16. E. L. Bravo, M. C. Khosla, and F. M. Bumpus, Action of [1-Des(Aspartic Acid), 8-Isoleucine]Angiotensin II upon the Pressor and Steroidogenic Activity of Angiotensin II, *J. Clin. Endocrinol. Metab.*, 40: 530-533 (1975).
17. J. A. Goffinet and P. J. Mulrow, Estimation of Angiotensin Clearance by an In Vivo Assay, *Clin. Res.*, 11: 408 (1963).
18. R. L. Hodge, K. K. F. Ng, and J. R. Vane, Disappearance of Angiotensin from the Circulation of the Dog, *Nature*, 215: 138-141 (1967).
19. W. P. Leary, University of Natal, and J. W. Ryan, University of Miami School of Medicine, unpublished.
20. J. H. Laragh, Cornell University Medical College, personal communication.
21. Y. S. Bakhle, Converting Enzyme, In Vitro Measurement and Properties, in *Handbook of Experimental Pharmacology*, Vol. 37, I. H. Page and F. M. Bumpus (Eds.), pp. 41-80, Springer-Verlag, Berlin, 1974.
22. R. Igic, E. G. Erdös, H. S. J. Yeh, K. Sorrells, and T. Nakajima, Angiotensin I Converting Enzyme of the Lung, *Circ. Res.*, Suppl. II, XXX and XXXI: II-51 (1972).
23. J. Roblero, J. W. Ryan, and J. M. Stewart, Assay of Kinins by their Effects on Blood Pressure, *Res. Commun. Chem. Pathol. Pharmacol.*, 6: 207-212 (1973).
24. F. E. Dorer, J. W. Ryan, and J. M. Stewart, Hydrolysis of Bradykinin and Its Higher Homologues by Angiotensin-Converting Enzyme, *Biochem. J.*, 141: 915-917 (1974).
25. H. Gavras, H. R. Brunner, J. H. Laragh, J. E. Sealey, I. Gavras, and R. A. Vukovich, An Angiotensin Converting-Enzyme Inhibitor to Identify and Treat Vasoconstrictor and Volume Factors in Hypertensive Patients, *New Engl. J. Med.*, 291: 817-821 (1974).
26. A. W. Pettinger, K. Keeton, and K. Tanaka, Radioimmunoassay and Pharmacokinetics of Saralasin in the Rat and Hypertensive Patients, *Clin. Pharmacol. Therap.*, 17: 146-158 (1975).

Structural Organization of Mucus in the Lung

JENNIFER M. STURGESS
Research Institute, The Hospital for Sick Children, Toronto, Ontario, Canada

ABSTRACT

Mucus is important to pulmonary defense because it acts as a protective barrier that separates epithelial cells from potentially harmful materials and as a vehicle for clearance of particulate and cellular material from the lung. The ultrastructure of mucus has been studied by scanning electron microscopy, and it has been shown that mucus forms a continuous lining over the airway epithelium of the rabbit and human lung. In structural arrangement, mucus forms series of overlapping plaques which vary in appearance from networks of branching and anastomosing fibers to smooth sheets. Newly secreted mucus and mucus adjacent to the epithelium have an open network structure, whereas upper layers of mucus show more tightly bound networks and smoother sheets. The dimensions of the fibrils and the size of the interfibril spaces vary considerably in different regions of the normal lung.

A smoother, more continuous layer of mucus with few fine networks is observed in the trachea, whereas more-expanded fibrous networks are observed in the main and lobar bronchi. In chronic obstructive lung disease, the mucus lining is significantly changed, with thicker, more closely bound plaques of condensed mucus, interrupted by channels leading to the pulmonary epithelium. The intricate structural organization of mucus reflects its complex physicochemical properties and its functional ability in clearing particulate material from the lung.

Mucus forms a protective barrier and isolates the pulmonary epithelium from harmful particulate matter, including irritants, which may be in solid, liquid, or gaseous phases, as well as infectious agents and cellular debris. The ability of mucus to act as a coupling agent for particulate matter and to clear it against the action of

gravity reflects its unique physicochemical properties. Glycoproteins that are responsible for the basic structure of mucus form a gel which is flexible but has pronounced viscous, elastic, and cohesive properties that promote the movement of particles out of the lung.

The chief components of mammalian mucus are glycoprotein macromolecules, containing more than 60% by weight of the carbohydrates galactose, *n*-acetyl glucosamine, fucose, and sialic acid. Mucus glycoproteins have been shown to form long thread-like molecules that intertwine and form gels even at low concentration in solution.[1] Cross-linkage between the carbohydrate residues of the long coiled glycoprotein molecules and protein and ions is responsible for the unique physicochemical properties of mucus.

Mucociliary clearance is dependent on mucus composition.[2] Structural changes in mucus may be of pathological significance since alterations in the mucus layer may fail to protect the underlying epithelial surfaces, thus resulting in mucus hypersecretion, retarding clearance of particulate matter, and leading to pulmonary infection.

Mucus possesses antimicrobial activity due to the presence of bound antibodies and to nonspecific microbicidal factors, including cationic proteins such as lysozyme.[3] Immunoglobulins, particularly IgA, produced in the lamina propria of the mucous membranes[4] are associated with mucus and contribute to local immune responses[5] and to opsonization of bacteria for phagocytosis.[6] Components of mucinous glycoproteins also may provide the basis for bacterial trapping, or aggregation[7] impeding bacterial interaction with epithelial cells and their colonization, e.g., blood group substance reactivity that may competitively inhibit bacteria.[8] Different molecular species of glycoproteins appear to have specificity for different bacterial species and strains, a property that may augment the cleansing function of mucus secretions. In contrast, early reports demonstrated that mucus, in common with other viscid materials, exhibits virulence-enhancing properties for bacteria, and it has been suggested that mucus interferes with the phagocytosis of bacteria.[9] For these reasons we have studied the organization of the mucus blanket in the lung to characterize its structural arrangement to better understand its behavior in pulmonary defense mechanisms.

MUCOCILIARY CLEARANCE

Several working hypotheses have been proposed to explain the mechanism for mucociliary clearance.[10-12] The one most widely accepted is that the airways of the lung are covered by a biphasic fluid layer with a lower serous component (also termed the

hypophase or sol layer) of low viscosity and an upper mucus component (the epiphase or gel layer) of high viscosity.

The upper mucus layer appears to be derived from mucus glycoproteins, whereas the lower layer may be of a different composition or it may be derived from the upper layer but is degraded by the shear stress exerted by cilia. Transport of mucus depends mainly on the propulsive force provided by cilia, and it is influenced by forces of gravity and of airflow. Cilia beat in the lower layer, and movement is transmitted to the mucus layer where inhaled particles are trapped. The rate of mucociliary transport varies, reaching as much as 12 mm/min in normal human trachea,[13] but it may be significantly retarded in lung disease.[14,15] The function of this transport system depends on a number of factors. Of particular importance are the nature and the amount of serous and mucus components in the fluid layer. Alterations in their balance would disturb the normal clearance mechanism and might contribute to pathogenesis of lung disease. Much of the understanding of the mucociliary clearance mechanism is derived from theoretical models of the lung, and further understanding of these mechanisms requires more detailed investigation of the nature of the mucus blanket and its physicochemical properties.

MICROSCOPIC OBSERVATIONS ON THE MUCUS BLANKET

Evidence for the existence of a continuous mucus blanket in the lung is based largely on light microscopic studies[11,16] and the examination of frozen sections (Fig. 1). These studies have demonstrated the mucus blanket to be approximately 5 μm thick in the major airways. In a recent brief report, the thickness of respiratory tract mucus has been assessed to be up to 5 μm in the major bronchi of the rabbit lung, reducing to 1 to 4 μm in bronchioles and to less than 0.1 μm in terminal bronchioles.[17] The biphasic nature of the mucus blanket has been illustrated in the extracellular lining of the frog palate where an upper layer which stains for glycoproteins is separated from the epithelial surface by a lower layer which contains little or no glycoprotein.[11]

Scanning electron microscopic studies have provided valuable information on the topography of cells in the lung.[18-20] This approach has been extended in our laboratory to study mucus secretion[21] and to study the mucus blanket in the lung.[22] Careful preparative techniques with gentle fixation, dehydration, and critical-point drying are essential to retain mucus in situ and to preserve

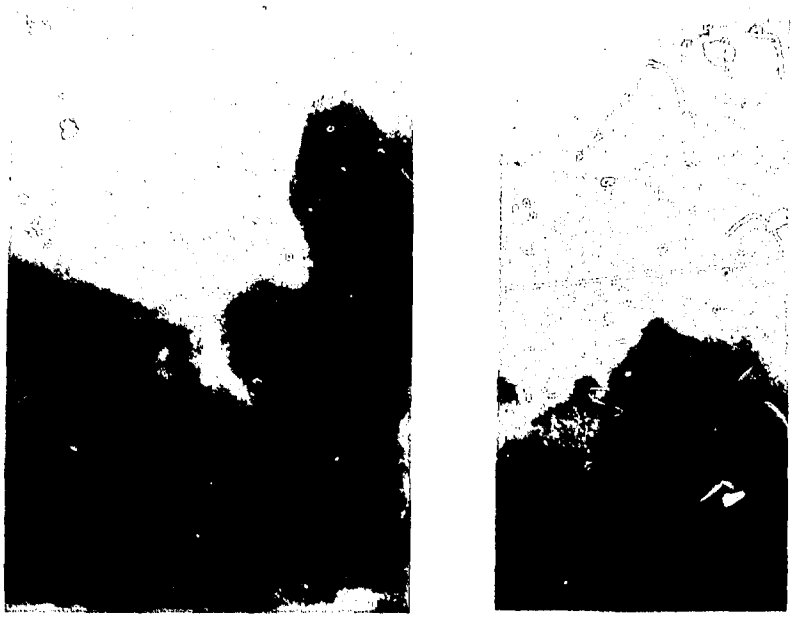

(a) (b)

Fig. 1 (a) Photomicrograph of frozen section of rabbit bronchus stained with haematoxylin and eosin. Patches of mucus are present overlying the epithelium. (Magnification, 700 X.) (b) Detail of epithelial surface, showing the lightly stained mucus layer, approximately 5 μm thick. (Magnification, 2400 X.)

the structural relationship between the tissue and extracellular material. Despite the hydrated state of mucus, the appearance of the mucus layer and the structural arrangement of the fibers is reproducible both in the rabbit and the human lung. However, Van As and Webster[23] have been unable to preserve more than small plaques or aggregates of mucus in the rat trachea for scanning electron microscopic studies. It seems likely that their observation reflects inadequate preservation of the mucus layer which is readily detached and dissociated. An alternative approach to demonstration of the extracellular lining has been described in bronchioles following fixation of the airways by vascular perfusion,[24,25] which prevents dissociation of surface material.

SCANNING ELECTRON MICROSCOPY OF THE MUCUS BLANKET

In situ studies of the mucus blanket have been carried out on tissue samples of the trachea and major bronchi of the rabbit lung, which were resected immediately after sacrifice. Samples of human

Fig. 2 Scanning electron micrograph of the mucus blanket overlying the rabbit trachea. The mucus forms a cohesive layer overlying the cilia. Spaces in the mucus blanket reveal cilia projecting from the epithelium. Small particles are observed on the mucus surface. (Magnification, 4000 X.)

trachea, major bronchi, and smaller airways have been obtained following surgical resection and from autopsy conducted within 1 hr after death. All samples were rinsed gently with saline and fixed with 1% glutaraldehyde in 0.1*M* sodium phosphate buffer. Samples, covered with lens paper to minimize the displacement of the mucus layer by convection currents during processing, were dehydrated in graded acetone solutions and dried from carbon dioxide by the critical-point method. The specimens were mounted on aluminum stubs with colloidal silver; they were then gold coated by the sputter coating technique and examined at 13 kV in a JEOL JSM-35U scanning electron microscope.

In both the rabbit and the human lung, the mucus blanket is continuous over large areas of the trachea and major bronchi (Fig. 2). It exhibits a complex surface structure varying from smooth sheets to intricate three-dimensional networks of fibrils. The mucus blanket closely follows the contours of the cell surfaces; this is particularly noticeable in the lower airway generations where the mucus layer appears to be thinner. The topography of ciliated and nonciliated mucus-secreting cells is observed through holes or discontinuities, caused during specimen preparation, in the mucus blanket. Removal of the mucus blanket by gentle aspiration with saline leaves ciliated and other cell surfaces cleared of mucus (Fig. 3). These indicate good preservation of the epithelial structure with cell-surface topography

Fig. 3 Scanning electron micrograph of the rabbit trachea showing ciliated epithelial cells observed under the mucus blanket illustrated in Fig. 1. The trachea is lined predominantly by ciliated epithelial cells interspersed with goblet cells and other nonciliated mucus-secreting cells. (Magnification, 7200 ×.)

similar to that reported in detail previously.[18-20] In the trachea, mucus forms a smooth cohesive layer that is continuous over large areas of the epithelium (Fig. 2). In some areas, overlapping layers of smooth sheets or plaques are observed (Fig. 4). These plaques may be smooth, perforated by holes, or comprised of fibrous networks. The mucus layer is situated over the tips of the cilia and is apparently separated from the area in which the cilia beat. There is little evidence of the content of the lower layer, except for a few residual fibrils which traverse between adjacent cilia and for residues of proteinaceous-like material which are occasionally observed on nonciliated cell surfaces. These findings suggest that the lower layer contains little macromolecular material and that it is distinct in nature from the upper mucus layer.

In the main and lobar bronchi, the mucus blanket has a more complex three-dimensional arrangement with more intricate networks of fibrils (Figs. 5 and 6). Characteristically the mucus blanket appears to be made up of series of plaque-like structures which overlap and are superimposed and interconnected. The structure of individual plaques varies from smooth sheets to perforated sheets to open networks of fibrils. The plaques show fewer smooth sheets, and the networks show a finer fibril diameter and more-expanded interfibril space progressively from the trachea down to the lobar bronchi.

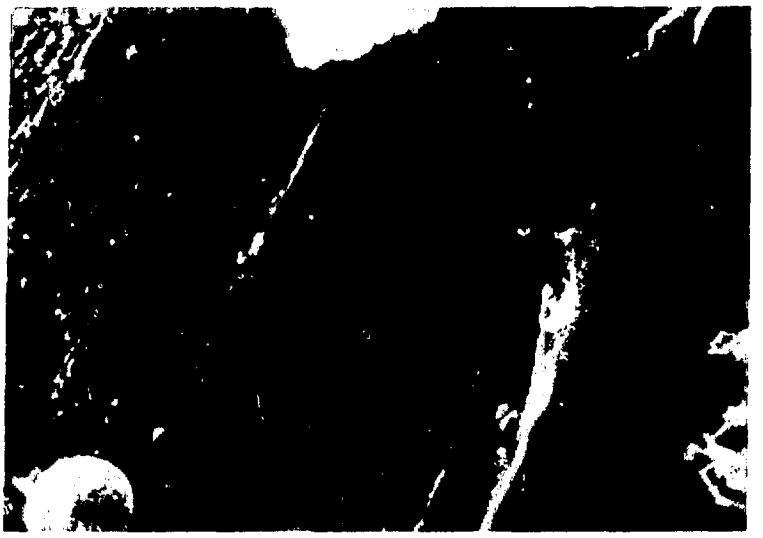

Fig. 4 Scanning electron micrograph of the mucus blanket overlying the human trachea. Overlapping layers of mucus are observed, each with a closely packed network of fibers. The interfiber spaces are small so that the mucus forms almost smooth sheets. Small particles, cells, and other particulate material are observed on the mucus surface. At the lower left corner are ciliated epithelial cells with the mucus blanket present over the tips of the cilia. (Magnification, 10,800 X.)

Examination of stereomicrographs with the scanning electron microscope indicates that, close to the cell surface, mucus plaques tend to be in more-open networks, whereas those toward the airway lumen are more cohesive and smooth. Newly secreted mucus in the lung also is characterized by open, expanded networks of fibrils.[21] These findings suggest that glycoproteins secreted from goblet cells and from the mucus-secreting cells form an open, fibrous network. Interaction between different glycoproteins and between glycoproteins and other components of the respiratory tract, such as proteins and ions, may lead to the alterations in structure, with shorter, thicker fibrils, more closely bound fibrous networks, and eventually to a cohesive sheet-like structure. These changes are observed within the layers of the mucus blanket at each airway generation and also as mucus is transported from lower airways to the trachea.

THE MUCUS BLANKET IN LUNG DISEASE

In chronic lung disease, the structural organization of the mucus blanket varies from that observed in the normal human lung. In asthma, mucus forms a very thick layer in the major bronchi. The

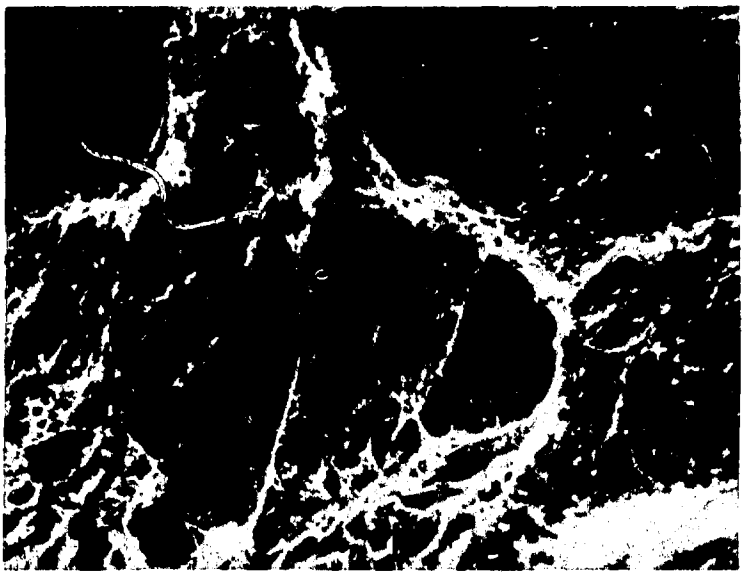

Fig. 5 Scanning electron micrograph of rabbit main bronchus to show the mucus blanket. Series of plaque-like structures show smoother sheet-like form and open fibrous networks. The overall structure has a complex three-dimensional arrangement. Particulate and cellular material are entangled among the mucus fibrils. (Magnification, 1800 X.)

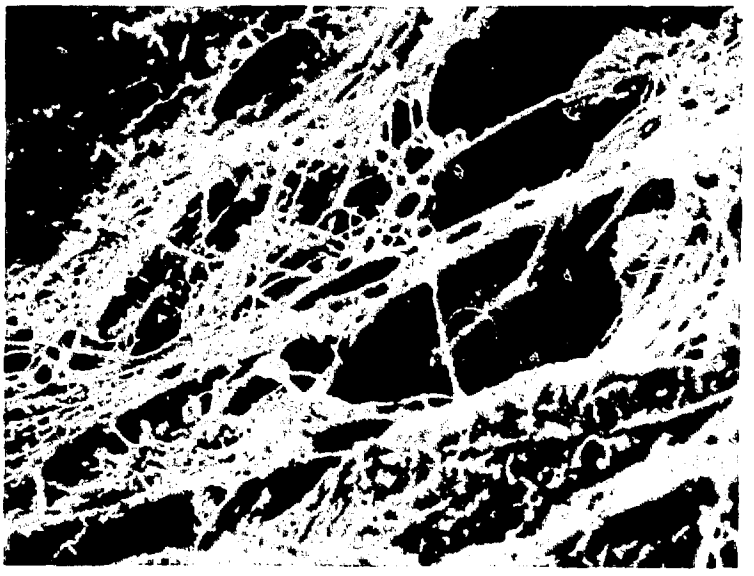

Fig. 6 Scanning electron micrograph of rabbit lobar bronchus to show the more-open fibrous networks that overlap the epithelial surface. Details of ciliated cells can be distinguished under the mucus layer. (Magnification, 3500 X.)

structural layer consists of very fine networks of fibrils and narrow interfibril spaces covering large areas of the epithelial surface. There are fewer smooth mucus plaques and fewer open three-dimensional networks.

In childhood bronchiectasis, the basic plaque-like structure of mucus is seen. The plaques appear to be more cohesive with numerous smooth sheets superimposed so that the mucus layer is very thick in all levels of major bronchi. The mucus blanket is perforated by numerous holes, a structural organization that may represent degradation by bacteria (Fig. 7).

FUNCTIONAL ASPECTS OF THE MUCUS BLANKET

This study demonstrates that the mucus blanket, both in the rabbit and in the human lung, forms a continous layer and that this layer is situated at the tips of the cilia. The mucus blanket appears to be more cross-linked and more cohesive in the trachea, compared with the main or lobar bronchi where it forms a much more expanded open structure. It would be of interest to observe some of the more-peripheral airways in a similar manner. At the present time studies on the extracellular lining of the bronchioles indicate that the layer is smooth and continuous but has no fibrous structure,[24] owing to the content of a proteinaceous material rather than glycoprotein. The nature and the behavior of these layers appear to be quite distinct.

On the surface of the mucus blanket, particulate matter is often observed ranging in size from 1 to 20 μm in diameter and including bacteria, spores, cellular debris, and other amorphous particles (Fig. 8). In many areas these particles become enclosed within the mucus blanket and embedded within the layers or fibers of the mucus (Fig. 5). The complex networks of mucus in the major airways may facilitate the trapping and coupling of particulate matter of mucus. It would seem that particles not trapped in the trachea would be effectively enmeshed in the more-expanded networks of mucus fibrils in the major bronchi.

The variation in composition of the mucus blanket in different airway generations may reflect a compositional change in the secretions. This may depend on the contribution of different secretory cells[26] in the different generations of the tracheobronchial tree, on the nature of the glycoprotein,[27] and on the presence of other proteins and fluids,[28,29] in the respiratory tract as well as the possible resorption of secretions in the larger airways.[30] From the

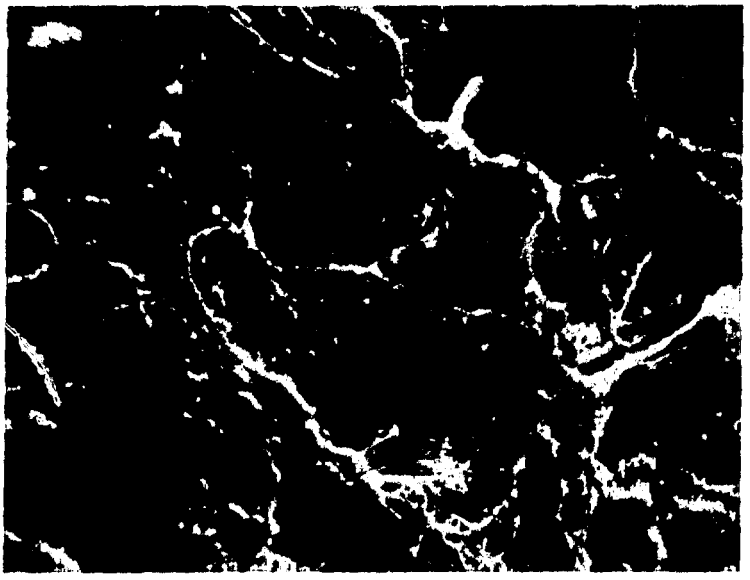

Fig. 7 Scanning electron micrograph of the mucus blanket from a patient with bronchiectasis. Smooth plaque-like structures and some fibrous networks are observed. Particles are trapped on the mucus surface. The mucus blanket is thick but is permeated by numerous holes. (Magnification, 4800 X.)

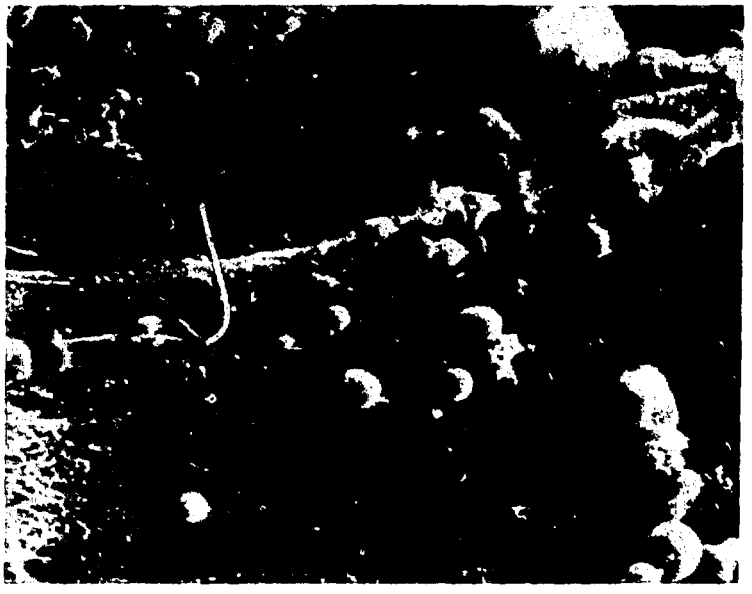

Fig. 8 Details of the mucus blanket overlying the human trachea to show the trapping of particulate material on the mucus blanket. This includes small particles such as bacteria, larger particles that may include macrophages, and shed epithelial cells. (Magnification, 5500 X.)

difference in organization, it seems likely that the efficiency of mucus in clearance of particulate matter may vary in different airway generations. The alignment of fibrils, the condensation of the fibrous networks, and the appearance of the smooth cohesive sheets of mucus would be expected to result in altered rheological properties of the secretions[31,32] and may influence the rates of mucociliary clearance among the airways.

Under normal conditions most particulate matter is trapped in the upper respiratory tract.[33] The nature of the mucus, its continuity, and its structural relationship with the epithelium determine both its ability to complete these functions and its influence on the function and behavior of cells in the peripheral airways.

Further study of the nature of mucus and its variation in different levels of the respiratory tract is extremely important in understanding the basis of pulmonary defense mechanisms.

ACKNOWLEDGMENTS

I wish to acknowledge the excellent technical assistance of E. Czegledy-Nagy and M. Starr. This work was supported by the Canadian Cystic Fibrosis Foundation and the Medical Research Council of Canada. J. Sturgess is an MRC Scholar.

REFERENCES

1. R. A. Gibbons, Physiochemical Methods for the Determination of the Purity, Molecular Size, and Shape of Glycoproteins, in *Glycoproteins, Their Composition, Structure and Function*, A. Gottschalk (Ed)., p. 29, American Elsevier Publishing Co., Inc., New York, 1972.
2. M. King, A. Gilboa, F. Meyer, and A. Silverberg, On the Transport of Mucus and Its Rheologic Simulants in Ciliated Systems, *Amer. Rev. Respirat. Dis.*, 110: 740 (1974).
3. J. Brownlie and K. G. Hibbitt, Antimicrobial Proteins Isolated from Bovine Cervical Mucus, *J. Reprod. Fertil.*, 29: 377 (1972).
4. F. J. Martinez-Tello, D. G. Braun, and W. A. Blanc, Immunoglobulin Production in Bronchial Mucosa and Bronchial Lymph Nodes, Particularly in Cystic Fibrosis of the Pancreas, *J. Immunol.*, 101: 989 (1968).
5. J. Bienenstock and D. Y. E. Perey, Immune Mechanisms of Mucosal Resistance, *Med. Clin. N. Amer.*, 56: 391 (1972).
6. M. Rabinovitch, Phagocytosis: The Engulfment Stage, *Seminars Hematol.*, 5: 134 (1968).
7. S. Kashket and C. G. Donaldson, Saliva-Induced Aggregation of Oral Streptococci, *J. Bacteriol.*, 112: 1127 (1972).

8. R. C. Williams and R. J. Gibbons, Inhibition of Streptococcal Attachment to Receptors on Human Buccal Epithelial Cells by Antigenically Similar Salivary Glycoproteins, *Infec. Immunity*, 11: 711 (1975).
9. W. J. Nungester, L. F. Jolirdonais, and A. A. Wolf, The Effect of Mucin on Infections by Bacteria, *J. Infect. Dis.*, 59: 11 (1936).
10. K. H. Kilburn, A Hypothesis for Pulmonary Clearance and Its Implications, *Amer. Rev. Respirat. Dis.*, 98: 449 (1968).
11. J. Sadé, N. Eliezier, A. Silberberg, and A. C. Nevo, The Role of Mucus in Transport by Cilia, *Amer. Rev. Respirat. Dis.*, 102: 48 (1970).
12. J. Blake, On the Movement of Mucus in the Lung, *J. Biomech.*, 8: 179 (1975).
13. D. B. Yeates, N. Aspin, H. Levison, and A. C. Bryan, Measurements of Mucociliary Transport Rates in Man, *Fed. Proc.*, 33: 365 (1974).
14. J. Sanchis, M. Dolovich, C. Rossman, W. Wilson, and M. Newhouse, Pulmonary Mucociliary Clearance in Cystic Fibrosis, *New Engl. J. Med.*, 288: 651 (1973).
15. D. B. Yeates, J. M. Sturgess, S. R. Kahn, H. Levison, and N. Aspin, Mucociliary Transport in Trachea of Patients with Cystic Fibrosis, *Arch. Dis. Childhood*, 51: 28 (1976).
16. T. Dalhamn, A Method for Determination In Vitro of the Rate of Ciliary Beat and Mucus Flow in the Trachea, *Acta. Physiol. Scand.*, 33: 1 (1955).
17. D. L. Luchtel, Ultrastructural Observations on the Mucous Layer in Pulmonary Airways, *J. Cell Biol.*, 70: 350a (1976).
18. J. A. Nowell and W. S. Tyler, Scanning Electron Microscopy of the Surface Morphology of Mammalian Lungs, *Amer. Rev. Respirat. Dis.*, 103: 313 (1971).
19. M. F. Greenwood and P. Holland, The Mammalian Respiratory Tract Surface. A Scanning Electron Microscopic Study, *Lab. Invest.*, 27: 296 (1972).
20. B. Holma, Scanning Electron Microscopic Observations of Particles Deposited in the Lung, *Arch. Environ. Health*, 18: 330 (1969).
21. E. Czegledy-Nagy and J. M. Sturgess, The Effect of Cystic Fibrosis Serum on Mucus Secretion, *Lab. Invest.*, 35: 588 (1976).
22. J. M. Sturgess, The Mucous Lining of Major Bronchi in the Rabbit Lung, *Amer. Rev. Respirat. Dis.*, (in press).
23. A. Van As and I. Webster, The Morphology of Mucus in Mammalian Airways, *Environ. Res.*, 7: 1 (1974).
24. R. V. Ebert and M. J. Terracio, Observations on the Secretions of the Bronchioles with the Scanning Electron Microscope, *Amer. Rev. Respirat. Dis.*, 112: 491 (1975).
25. J. Gil and E. R. Weibel, Extracellular Lining of Bronchioles After Perfusion Fixation of Rat Lungs for Electron Microscopy, *Anat. Rec.*, 196: 185 (1971).
26. L. Reid, Bronchial Mucus Production in Health and Disease, in *The Lung*, A. A. Liebow and D. E. Smith (Eds.), p. 87, International Academy of Pathology Monograph, The Williams & Wilkins Company, Baltimore, Md., 1968.
27. D. Lamb and L. Reid, Histochemical Types of Acid Glycoproteins Produced by the Mucous Cells of the Tracheobronchial Glands in Man, *J. Pathol.*, 98: 213 (1969).

28. R. Havez, P. Roussel, P. Degand, and G. Biserte, Etude des structures fibrillaires de la secretion bronchique humaine, *Clin. Chim. Acta*, 17: 281 (1967).
29. J. F. Forstner, G. G. Forstner, and J. M. Sturgess, Physical Changes Induced in Mucin by Calcium: Implications for the Obstructive Complications in Cystic Fibrosis, in Proceedings of the Seventh World Congress on Cystic Fibrosis, June 1—3, 1976, Paris, in press.
30. T. Asmundsson and K. H. Kilburn, Mucociliary Clearance Rates at Various Levels of Dog Lungs, *Amer. Rev. Respirat. Dis.*, 102: 388 (1970).
31. J. M. Sturgess, A. J. Palfrey, and L. Reid, The Viscosity of Bronchial Secretion, *Clin. Sci.*, 38: 145 (1970).
32. M. Litt, Flow Behavior of Mucus, *Ann. Otol., Rhinol., Laryngol.*, 80: 330 (1970).
33. A. W. Wright, Structure and Function of the Respiratory Tract in Relation to Infection, *Bacteriol. Rev.*, 25: 219 (1961).

Biochemical Studies on Normal and Hormone-Accelerated Development of Pulmonary Surfactant

SEAMUS A. ROONEY and ETSURO K. MOTOYAMA
Yale University Lung Research Center and Departments of Pediatrics and Anesthesiology, Yale University School of Medicine, New Haven, Connecticut

ABSTRACT

To elucidate the biochemical events relating to surfactant during fetal and early postnatal development, we examined the phospholipid content and composition of rabbit lung lavage and tissue during the period 27 days' gestation (full-term, 31 days) to 2 days after birth. We also examined the activities of enzymes involved in the synthesis of pulmonary phosphatidylcholine and phosphatidylglycerol—the major surface-active components of surfactant—from 19 days' gestation. In addition, since corticosteroids and thyroxine are known to accelerate fetal lung maturation, we examined the effect of cortisol and thyroxine administration to the fetuses at 24 to 25 days on pulmonary phospholipid content, composition, and biosynthesis at 27 days.

There was a four-fold increase in the amount of total phospholipid in lung lavage during the period 27 to 31 days. There was a further 10-fold increase to adult levels 1 day after birth. During the same period phosphatidylcholine increased from 29% of the total phospholipid at 27 days to 68% at 31 days and 80% after birth, whereas sphingomyelin decreased from 38% of the total at 27 days to 7% at 31 days and 2 to 3% after birth.

During fetal development the activity of pulmonary choline kinase changed little, that of cholinephosphate cytidylyltransferase, cholinephosphotransferase, and glycerophosphate phosphatidyltransferase decreased, whereas that of 1-acylglycerophosphate and lysolecithin acyltransferases increased. There was a postnatal increase in the activities of cholinephosphate cytidylyltransferase, cholinephosphotransferase, and both acyltransferases.

Lung lavage from cortisol-treated fetuses contained almost twice as much phospholipid, the composition of which resembled that of a more-mature fetus, as did saline-injected littermates. Thyroxine produced similar changes but to a lesser extent. Cortisol treatment also stimulated the activities of pulmonary cholinephosphate cytidylyltransferase and lysolecithin acyltransferase to a small (22% and 33%, respectively) but significant ($p < 0.02$) extent. These studies suggest that cortisol accelerates normal maturation of the lung.

Pulmonary surfactant is the material that lowers surface tension at the air–liquid interface in the lung and prevents alveolar collapse on expiration. Surfactant is largely phospholipid, the major component of which is phosphatidylcholine.[1] Disaturated species of phosphatidylcholine, particularly dipalmitoylglycerophosphocholine, appear to be the major surface-active components of surfactant.[1] A second surface-active component is phosphatidylglycerol.[2,3]

During the latter part of gestation, the fetal lung matures and begins to produce significant amounts of surfactant. This process can be accelerated by hormones, such as corticosteroids[4] and thyroxine.[5] Idiopathic respiratory distress syndrome (RDS) of the newborn, the major cause of morbidity and mortality among premature infants, is associated with inadequate amounts of surfactant and may be prevented by such hormones.[4,6] Thus, in the prevention and treatment of RDS, a knowledge of surfactant production and its control is essential. Toward this end we have carried out studies on pulmonary phospholipid content, composition, and biosynthesis during fetal-rabbit development.

MATERIALS AND METHODS

Albino New Zealand rabbits, whose time of conception was known to within 2 hr, were used. When hormone was to be administered to the fetuses, a laparotomy was performed on the doe, at either 24 or 25 days' gestation, under halothane–nitrous oxide anesthesia. One milligram of cortisol (hydrocortisone sodium succinate) or 1 μg of thyroxine (sodium-L-thyroxine) was injected into each fetus in one uterine horn and a similar amount into its amniotic sac. The fetuses in the opposite uterine horn were similarly injected with 0.9% NaCl and served as littermate controls. In some experiments all fetuses in other does were injected with saline and served as nonlittermate controls.

All fetuses were delivered by cesarean section, following the administration of sodium pentobarbital to the doe, and were prevented from breathing by placing a ligature around their necks while they were still in the amniotic sac. Newborn rabbits were sacrificed 1 to 2 days after normal delivery (during which period they remained with the mother) with intraperitoneal sodium pentobarbital. The lungs were either immediately excised and processed for enzyme assays or lavaged with 0.9% NaCl, following which lipid extractions were performed on both the saline lavage and the washed lungs, as previously described.[7]

Lipids were extracted, identified, and quantitated by phosphorus assay as described previously.[3,7] The amount of phospholipid in lung tissue and lavage is expressed per unit lung dry weight (obtained on lyophilization).

Choline kinase (EC 2.7.1.32), cholinephosphotransferase (EC 2.7.8.2), and glycerophosphate phosphatidyltransferase (EC 2.7.8.5) were assayed in the homogenate, cholinephosphate cytidylyltransferase (EC 2.7.7.15) in the 100,000 x *g* supernate, and 1-acylglycerophosphate acyltransferase (EC 2.3.1.51) and lysolecithin acyltransferase (EC 2.3.1.23) in the microsomal fraction as described previously.[7,8] All enzyme activities are expressed per unit protein, which was determined by the procedure of Lowry et. al.[9]

RESULTS

Normal Developmental Profile for Phospholipids

The phospholipid content of lung lavage, representing surfactant, and lung tissue from fetal, newborn, and adult rabbits is shown in Table 1. There was a fourfold increase in the amount of total phospholipid in lung lavage during 27 to 31 (full-term) days' gestation. During the same period the amount of phosphatidylcholine increased almost 10-fold. There was a further approximately 10-fold increase in the amounts of both total phospholipid and phosphatidylcholine to adult levels 24 hr after birth. There was little developmental change in the amount of total phospholipid in lung tissue, but the amount of phosphatidylcholine essentially doubled during the period 27 days' gestation to 1 to 2 days after birth.

These findings are also shown in Table 2. At 27 days' gestation only 0.2 to 0.3% of the total lung phospholipid was recovered in the lavage. This had increased to about 1% at 31 days but increased dramatically after birth to 6 to 8% (total phospholipid) and 10 to 13% (phosphatidylcholine).

The phospholipid compositions of lavage and tissue are shown in Tables 3 and 4, respectively. There were striking developmental changes in the composition of the lavage phospholipid (Table 3). Phosphatidylcholine increased from 29% of the total at 27 days to almost 70% at 31 days and to about 80%, the adult level,[3] after birth. At the same time sphingomyelin decreased from almost 40% of the total at 27 days to 7% at 31 days and to 2 to 3%, the adult level,[3] after birth. This change resulted in a dramatic increase in the phosphatidylcholine/sphingomyelin ratio from less than 1 at 27 days to 10 at 31 days and 30 to 40 after birth. In the tissue (Table 4)

TABLE 1

PHOSPHOLIPID CONTENT OF LUNG LAVAGE AND TISSUE FROM FETAL, NEWBORN, AND ADULT RABBITS*

Gestational age, days	Number of litters†	Lung lavage		Lung tissue	
		Total phospholipid	Phosphatidylcholine	Total phospholipid	Phosphatidylcholine
		Phospholipid phosphorus/g lung dry weight (± SE)			
		μg		mg	
27	6	9.2 ± 2.1	2.6 ± 0.7	3.5 ± 0.3	1.3 ± 0.1
28	4	13.4 ± 1.6	5.4 ± 0.1	4.1 ± 0.3	1.7 ± 0.0
29	3	13.4 ± 3.2	7.4 ± 2.4	3.9 ± 0.4	1.7 ± 0.2
30	5	16.2 ± 2.6	8.4 ± 1.6	4.1 ± 0.1	1.8 ± 0.1
31	4	37.6 ± 8.0	25.4 ± 5.1	4.3 ± 0.3	2.2 ± 0.2
+1	‡	346 ± 8	274 ± 3	4.6 ± 0.1	2.4 ± 0.1
+2	‡	477 ± 11	389 ± 14	5.2 ± 0.2	2.7 ± 0.1
Adult	§	306 ± 46	264¶	4.6 ± 0.2	2.5¶

*From S. A. Rooney, T. S. Wai-Lee, L. Gobran, and E. K. Motoyama, Phospholipid Content, Composition and Biosynthesis During Fetal Lung Development in the Rabbit, *Biochim. Biophys. Acta*, 431: 451-452 (1976).

†Lung wash and tissue from all fetuses in each litter were pooled. Materials from each litter were analyzed separately (except for phosphatidylcholine) from lung wash when two groups of three, two, and one to two litters were analyzed at 27, 28, and 29 days, respectively.

‡Two groups of three and two newborn rabbits were analyzed at 1 and 2 days postnatal, respectively.

§The adult data are from five rabbits.

¶Calculated from the total phospholipid value and the data in Ref. 3.

phosphatidylcholine, as a percentage of the total, also increased but to a much lesser extent than in the lavage. In the tissue sphingomyelin increased in amount, in marked contrast to the lavage.

There was little developmental change in the relative amount of phosphatidylglycerol, the other surface-active component of surfactant, in either the lavage or lung tissue, although, of course, in absolute amount it increased with development in the lavage.

Effects of Hormones on Phospholipids

The effect of the administration of cortisol and thyroxine to fetal rabbits at 25 days' gestation on the phospholipid content and composition of lung lavage 2 days later is shown in Tables 5 and 6, respectively. There was 70% more total phospholipid and 130% more

phosphatidylcholine in the lung lavage from the cortisol-treated fetuses than in that from their control littermates (Table 5).[10] Cortisol also changed the phospholipid composition of the lavage. Lavage from the cortisol-treated fetuses contained relatively more phosphatidylcholine and less sphingomyelin, and thus a higher phosphatidylcholine/sphingomyelin ratio, than did that from the controls. When compared with the data in Tables 1 and 3, it is seen that these changes are in the direction of increased pulmonary maturation.

TABLE 2

PERCENTAGE OF TOTAL LUNG PHOSPHOLIPID IN THE LAVAGE DURING DEVELOPMENT

Gestational age, days	Total phospholipid	Phosphatidylcholine
27	0.3	0.2
28	0.3	0.3
29	0.3	0.4
30	0.4	0.5
31	0.9	1.1
+1	7.0	10.3
+2	8.4	12.6
Adult	6.2	12.7

Thyroxine also caused changes in the direction of increased maturation and in the content and composition of fetal-rabbit lung-lavage phospholipid (Table 6), but these changes were less marked than those produced by cortisol. There was no change in the amount of total phospholipid in the lavage, but the amount of phosphatidylcholine was 30% greater in the lavage from the thyroxine-treated fetuses than in that from their control littermates. There was a small (20%), but statistically significant, increase in the amount of phosphatidylcholine as a percentage of the total phospholipid following thyroxine administration. There was little change in the amount of sphingomyelin, whereas the phosphatidylcholine/sphingomyelin ratio increased by 30%, although this was not statistically significant.

Neither cortisol nor thyroxine had any effect on the content or composition of lung-tissue phospholipid.

TABLE 3

PHOSPHOLIPID COMPOSITION OF LUNG LAVAGE FROM FETAL AND NEWBORN RABBITS*†

Gestational age, days	Number of experiments	% phospholipid phosphorus ± SE						
		PC	PE	Sph	PI + PS	PG	LBPA	PC/Sph
27	2	28.6 ± 1.8	8.8 ± 1.3	37.6 ± 3.6	13.4 ± 0.5	5.8 ± 0.8	5.9 ± 1.8	0.8
28	2	39.4 ± 0.9	8.3 ± 1.8	20.8 ± 0.5	19.3 ± 3.8	4.8 ± 1.2	7.6 ± 3.1	1.9
29	2	49.7 ± 0.1	9.2 ± 0.9	11.1 ± 3.8	15.4 ± 0.5	6.9 ± 1.8	8.0 ± 1.8	5.1
30	5	52.7 ± 3.4	8.0 ± 0.8	12.9 ± 1.3	16.0 ± 2.3	5.2 ± 0.9	5.1 ± 0.2	4.3
31	4	68.1 ± 1.3	5.9 ± 0.1	7.0 ± 0.5	11.8 ± 0.2	3.6 ± 0.6	3.7 ± 0.5	9.9
+1	2	79.3 ± 0.6	4.3 ± 0.1	2.6 ± 0.1	7.3 ± 0.3	3.7 ± 0.1	3.0 ± 0.1	31.1
+2	2	81.5 ± 1.1	4.2 ± 0.5	2.1 ± 0.2	6.3 ± 0.2	3.5 ± 0.4	2.6 ± 0.8	39.2

*From S. A. Rooney, T. S. Wai-Lee, L. Gobran, and E. K. Motoyama, Phospholipid Content, Composition and Biosynthesis During Fetal Lung Development in the Rabbit, *Biochim. Biophys. Acta*, 431: 451 (1976).

†In each experiment lung washes from all fetuses in three liters were pooled at 27 days' gestation, two to three at 28 days, one to two at 29 and 30 days, and one at 31 days. Lung washes from three and two newborn rabbits were pooled per experiment at 1 and 2 days postnatal, respectively. PC, phosphatidylcholine; PE, phosphatidylethanolamine; Sph, sphingomyelin; PS, phosphatidylserine; PI, phosphatidylinositol; PG, phosphatidylglycerol; LBPA, lyso-bis-phosphatidic acid.

TABLE 4

PHOSPHOLIPID COMPOSITION OF LUNG TISSUE FROM FETAL AND NEWBORN RABBITS*†

Gestational age, days	Number of experiments	% phospholipid phosphorus ± SE					
		PC	PE	Sph	PI + PS	PG	LBPA
27	6	37.9 ± 2.8	25.6 ± 1.4	9.6 ± 0.4	18.4 ± 1.4	4.2 ± 1.1	4.2 ± 1.8
28	4	38.6 ± 1.4	18.7 ± 0.6	15.4 ± 0.5	16.2 ± 1.0	7.0 ± 0.2	4.1 ± 0.1
29	4	42.9 ± 2.2	18.4 ± 1.6	13.2 ± 1.4	17.1 ± 1.1	4.8 ± 0.7	3.6 ± 0.4
30	6	44.7 ± 1.4	21.2 ± 1.2	11.9 ± 0.7	17.1 ± 0.8	3.0 ± 0.6	2.0 ± 0.6
31	4	50.4 ± 1.1	19.3 ± 0.5	13.5 ± 1.2	11.0 ± 1.6	3.5 ± 0.6	2.3 ± 0.2
+1	2	51.8 ± 0.5	19.4 ± 0.5	15.2 ± 0.0	7.9 ± 0.1	2.8 ± 0.1	2.9 ± 0.1
+2	2	51.4 ± 1.6	13.6 ± 0.5	20.4 ± 0.5	7.3 ± 0.8	3.5 ± 0.1	3.8 ± 0.3

*From S. A. Rooney, T. S. Wai-Lee, L. Gobran, and E. K. Motoyama, Phospholipid Content, Composition and Biosynthesis During Fetal Lung Development in the Rabbit, *Biochim. Biophys. Acta*, 431: 452 (1976).

†In each experiment the lungs from all fetuses in each litter were pooled. Two groups of three and two rabbits were used at 1 and 2 days postnatal, respectively. Abbreviations are as in Table 3.

TABLE 5

EFFECT OF CORTISOL ON PHOSPHOLIPID CONTENT AND COMPOSITION OF FETAL-RABBIT LUNG LAVAGE*†

	Control	Cortisol treated	Treated/ control	P
	μg phospholipid phosphorus/ g lung dry weight			
Total phospholipid	15.6 ± 1.7	25.5 ± 2.5	1.7	<0.02
Phosphatidylcholine	5.5 ± 0.9	12.0 ± 1.3	2.3	<0.05
	% phospholipid phosphorus			
Phosphatidylcholine	34.6 ± 2.1	47.0 ± 1.9	1.4	<0.005
Phosphatidylethanolamine	9.0 ± 0.7	7.2 ± 0.5	0.8	NS
Sphingomyelin	30.0 ± 1.1	22.4 ± 0.9	0.7	<0.005
Phosphatidylinositol + phosphatidylserine	10.7 ± 1.0	10.5 ± 1.4	1.0	NS
Phosphatidylglycerol	2.7 ± 0.2	1.9 ± 0.1	0.7	<0.005
Lyso-bis-phosphatidic acid	3.4 ± 0.7	2.8 ± 0.5	0.8	<0.05
Lysophosphatidylcholine	9.7 ± 0.3	8.2 ± 0.3	0.8	<0.001
Phosphatidylcholine/ sphingomyelin ratio	1.2 ± 0.1	2.1 ± 0.1	1.8	<0.005

*From S. A. Rooney, L. Gobran, I. Gross, T. S. Wai-Lee, L. L. Nardone, and E. K. Motoyama, Studies on Pulmonary Surfactant. Effects of Cortisol Administration to Fetal Rabbits on Lung Phospholipid Content, Composition and Biosynthesis, *Biochim. Biophys. Acta*, 450: 126 (1976).

†The fetuses were injected with cortisol or 0.9% NaCl at 25 days' gestation and delivered at 27 days as described in Materials and Methods. The data are the means (± SE) from four experiments, in each of which fetuses from five litters were pooled. Statistical analysis was by paired *t* test. NS, not significant.

Normal Developmental Profile for Enzymes

Phosphatidylcholine is synthesized de novo in the lung by transfer of choline from CDPcholine to a diacylglycerol in a reaction catalyzed by cholinephosphotransferase. CDPcholine is formed from cytidine triphosphate (CTP) and phosphorylcholine by the action of cholinephosphate cytidylyltransferase. Phosphorylcholine is formed from choline and adenosine triphosphate (ATP) by the action of choline kinase. The activities of these three enzymes in developing fetal and neonatal rabbit lung are shown in Figs. 1 to 3. Choline kinase activity (Fig. 1) decreased a little during development, whereas the activities of cholinephosphate cytidylyltransferase

TABLE 6

EFFECT OF THYROXINE ON PHOSPHOLIPID CONTENT AND COMPOSITION OF FETAL-RABBIT LUNG LAVAGE*

	Control	Thyroxine treated	Treated/ control	p
	μg phospholipid phosphorus/ g lung dry weight			
Total phospholipid	18.2 ± 1.8	20.3 ± 1.4	1.1	NS
Phosphatidylcholine	6.4 ± 1.0	8.4 ± 1.3	1.3	<0.05
	% phospholipid phosphorus			
Phosphatidylcholine	34.6 ± 3.1	40.7 ± 3.8	1.2	<0.01
Phosphatidylethanolamine	9.2 ± 0.6	8.0 ± 0.6	0.9	<0.01
Sphingomyelin	26.6 ± 1.7	24.2 ± 2.4	0.9	NS
Phosphatidylinositol + phosphatidylserine	11.5 ± 0.6	10.8 ± 0.6	0.9	NS
Phosphatidylglycerol	3.4 ± 1.2	3.0 ± 0.8	1.0	NS
Lyso-bis-phosphatidic acid	4.8 ± 1.6	4.2 ± 1.1	1.0	NS
Lysophosphatidylcholine	9.9 ± 1.1	9.0 ± 0.9	0.9	NS
Phosphatidylcholine/ sphingomyelin ratio	1.3 ± 0.2	1.8 ± 0.3	1.3	NS

*The fetuses were injected with thyroxine or 0.9% NaCl at 25 days' gestation and delivered at 27 days as described in Materials and Methods. The data are the means (± SE) from five experiments, in each of which fetuses from four to five litters were pooled. Statistical analysis was by paired *t* test. NS, not significant.

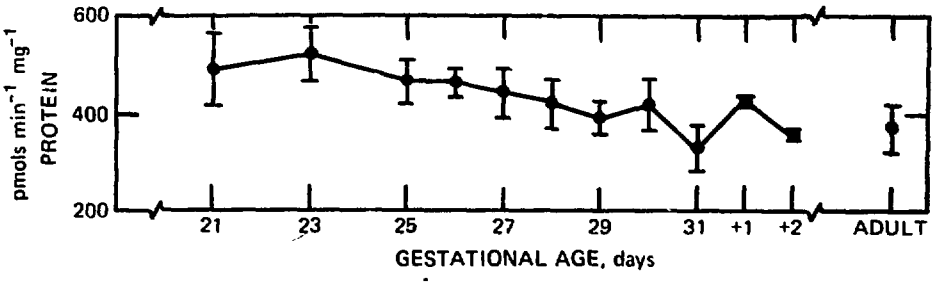

Fig. 1 Developmental profile of rabbit-lung choline kinase activity. Each point is the mean of duplicate determinations on two to four samples, each of which consisted of the lungs from all fetuses in one to two litters. The bar represents ± SE. (Figure based on data from Ref. 7.)

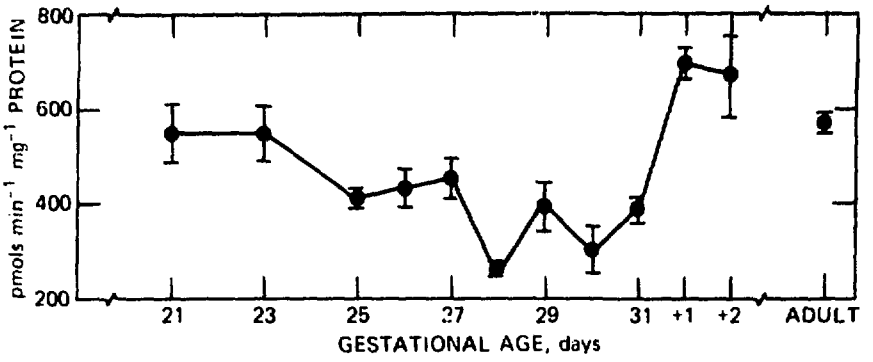

Fig. 2 Developmental profile of rabbit-lung cholinephosphate cytidylyltransferase activity. Experimental details as in Fig. 1.

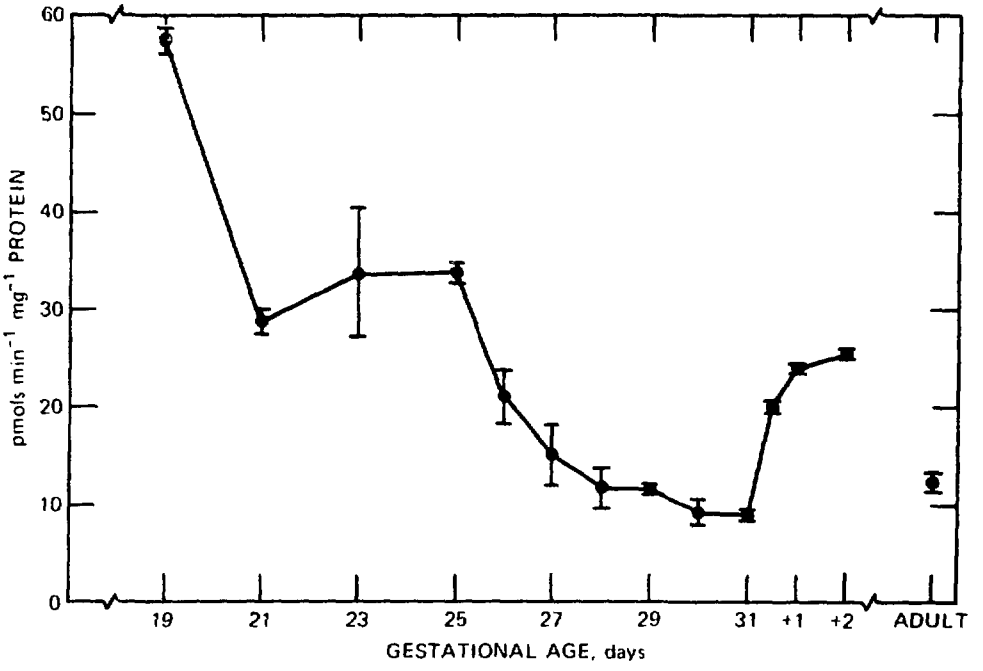

Fig. 3 Developmental profile of rabbit-lung cholinephosphotransferase activity. Experimental details as in Fig. 1.

(Fig. 2) and cholinephosphotransferase (Fig. 3) decreased during fetal development but increased sharply after birth.

Since desatured species of phosphatidylcholine are the major surface-active components of pulmonary surfactant, the activities of two enzymes possibly involved in the synthesis of these lipids were measured. These were 1-acylglycerophosphate acyltransferase, which

may be involved in the insertion of a second saturated acyl group into 1-satured-2-lysophosphatidic acid during the de novo synthesis of phosphatidylcholine, and lysolecithin acyltransferase, which may be similarly involved in the acylation of 1-satured-2-lysophosphatidylcholine. The activities of these enzymes are shown in Fig. 4. Both enzyme activities generally increased during development, although there was a decrease at 28 and 31 days.

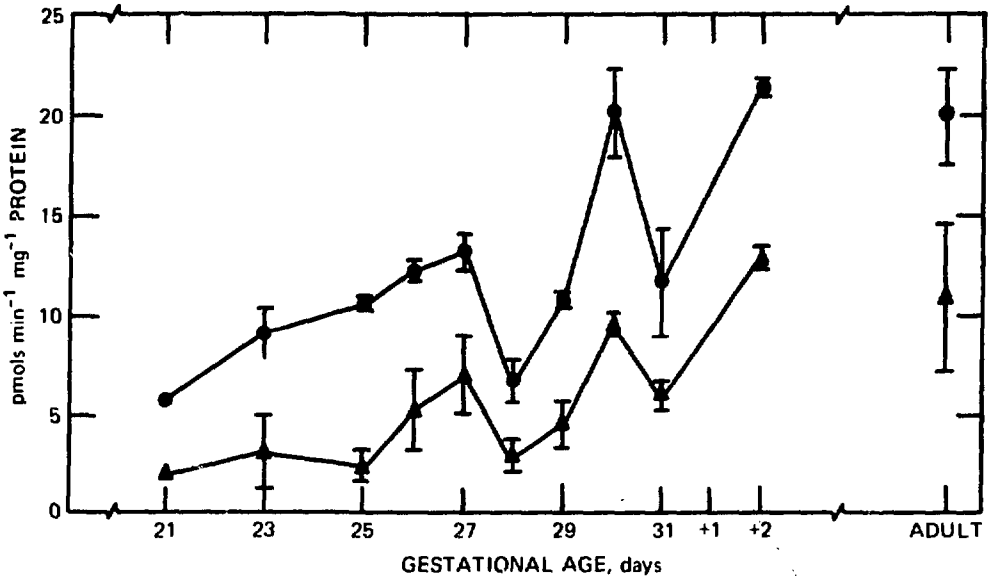

Fig. 4 Developmental profile of rabbit-lung 1-acylglycerophosphate acyltransferase (●) and lysolecithin acyltransferase (▲) activities. Experimental details as in Fig. 1.

There was a general decrease in the activity of glycerophosphate phosphatidyltransferase, an enzyme involved in the synthesis of phosphatidylglycerol, during the developmental period studied (Fig. 5).

Gross and Warshaw[11] have previously demonstrated that there is little developmental change in the activities of the enzymes of de novo fatty acid synthesis in the fetal-rabbit lung.

Effects of Hormones on Enzymes

The effect of cortisol administration to fetal rabbits at 25 and 24 days' gestation on the activities of a number of enzymes of pulmonary phospholipid and fatty-acid synthesis is shown in Tables 7 and 8, respectively. Two days after the administration of cortisol, there was a small, but statistically significant, increase in the

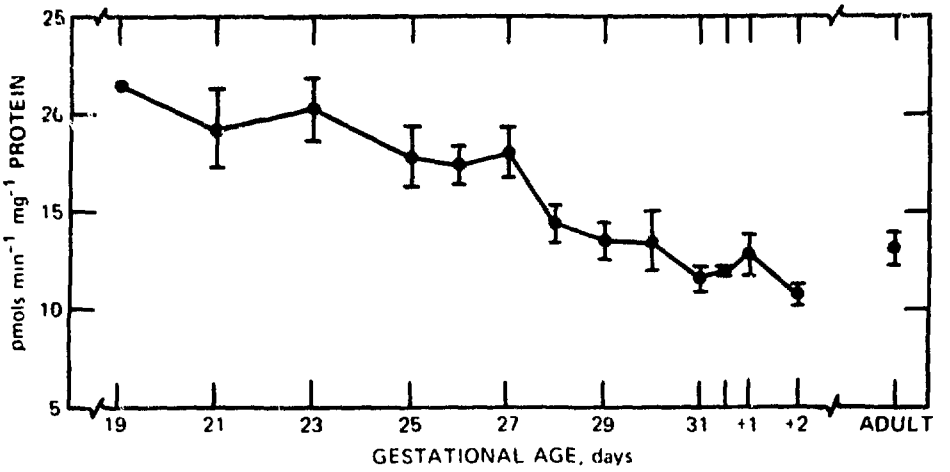

Fig. 5 Developmental profile of rabbit-lung glycerophosphate phosphatidyltransferase activity. Experimental details as in Fig. 1.

TABLE 7

EFFECT OF CORTISOL ON ENZYMES OF PHOSPHOLIPID SYNTHESIS IN FETAL-RABBIT LUNG*†

Enzyme	No.	Control	Cortisol treated	Treated/ control	p
		pmols min^{-1} mg^{-1} of protein			
Choline kinase	8	330 ± 13	330 ± 23	1.00	NS
Cholinephosphate cytidyltransferase	13	299 ± 32	351 ± 37	1.22	<0.02
Cholinephosphotransferase	14	52.7 ± 4.3	53.9 ± 4.0	1.09	NS
Glycerophosphate phosphatidyltransferase	8	16.3 ± 2.1	15.4 ± 1.5	0.97	
		nmols min^{-1} mg^{-1} of protein			
1-Acylglycerophosphate acyltransferase	14	20.1 ± 1.9	22.2 ± 1.9	1.14	NS
Lysolecithin acyltransferase	12	3.? ± 0.3	4.1 ± 0.3	1.33	<0.02

*From S. A. Rooney, L. Gobran, I. Gross, T. S. Wai-Lee, L. L. Nardone, and E. K. Motoyama, Studies on Pulmonary Surfactant. Effects of Cortisol Administration to Fetal Rabbits on Lung Phospholipid Content, Composition and Biosynthesis, *Biochim. Biophys. Acta*, 450: 125 (1976).

†The fetuses were injected with cortisol or 0.9% NaCl at 25 days' gestation and delivered at 27 days. The data are the means (± SE) from the number of experiments indicated. In each experiment fetuses from three to four litters were pooled. Statistical analysis was by paired *t* test. NS, not significant.

activities of cholinephosphate cytidylyltransferase and lysolecithin acyltransferase (Table 7), whereas the activities of choline kinase, cholinephosphotransferase, glycerophosphate phosphatidyltransferase, and 1-acylglycerophosphate acyltransferase were not changed.

TABLE 8

EFFECT OF CORTISOL ON ENZYMES OF PHOSPHOLIPID AND FATTY-ACID SYNTHESIS IN FETAL-RABBIT LUNG*†

Enzyme or enzyme system	No.	Control	Thyroxine treated	Treated/ control	p
		pmols min^{-1} mg^{-1} of protein			
Glycerophosphate phosphatidyltransferase	8	16.9 ± 1.6	25.9 ± 3.2	1.53	<0.005
Cholinephosphotransferase	8	36.2 ± 3.9	37.9 ± 4.1	1.08	NS
CDPdiacylglycerol-inositol phosphatidyltransferase	4	719 ± 41	673 ± 62	0.94	NS
Acetyl-CoA carboxylase	6	1430 ± 110	1170 ± 110	0.82	<0.01
Fatty-acid synthetase	6	1798 ± 151	1470 ± 303	0.77	NS
Microsomal fatty-acid elongation system	4	21.3 ± 2.7	22.0 ± 2.7	1.05	NS
		cpm min^{-1} mg^{-1} of protein			
De novo fatty-acid synthesis	4	1188 ± 222	673 ± 108	0.58	<0.025
		nmols min^{-1} mg^{-1} of protein			
1-Acylglycerophosphate acyltransferase	7	6.4 ± 1.1	7.1 ± 1.1	1.22	NS
Lysolecithin acyltransferase	5	1.5 ± 0.3	1.7 ± 0.7	1.10	NS

*Data from Refs. 8 and 12.

†The fetuses were injected with cortisol or 0.9% NaCl at 24 days' gestation and delivered at 27 days. The data are the means (± SE) from the number of experiments indicated. In each experiment fetuses from four litters were pooled. Statistical analysis was by paired *t* test. NS, not significant.

Three days after the administration of cortisol, the stimulation of lysolecithin acyltransferase was not apparent, but there was a 53% stimulation of glycerophosphate phosphatidyltransferase (Table 8), an effect that was not apparent after 2 days (Table 7). In addition, after 3 days de novo fatty-acid synthesis as well as the activities of acetyl-CoA carboxylase and fatty synthetase was inhibited.

There was no difference between control and thyroxine-treated fetuses in the activities of any of the enzymes of phospholipid and fatty-acid synthesis listed in Table 8 at 27 days' gestation following the administration of thyroxine at 24 days.

Choice of Controls for Study of Hormone Effects

The experimental model used in this study, i.e., littermate control model, in which the fetuses in one uterine horn are injected with the hormone and those in the opposite horn are injected with saline and are used as controls, has been extensively and successfully used in a number of morphological, physiological, and biochemical studies from this laboratory (Refs. 5, 8, 10, and 12–14). It has the advantage that the control and hormone-treated fetuses are of identical gestational age, and maternal biological and environmental as well as experimental differences are eliminated. There are, however, two potential disadvantages to this model. It is possible, although unlikely,[15] that some hormone may be transferred, via the maternal circulation, from the hormone-injected uterine horn to the opposite, control, horn. If this were true we would expect differences, especially in the phospholipid content and composition of lung lavage, between littermate controls and nonlittermate controls. There were, however, no such differences either in these parameters or in the activities of the enzymes of pulmonary phospholipid synthesis.

A second disadvantage with this model, as well as with the nonlittermate control model, is that the effect of the stress of the surgery and associated manipulations is not taken into consideration. Thus, so that this effect could be examined, littermate controls and nonoperated fetuses at the same gestational age (27 days) were examined with respect to lung-lavage phospholipid content and composition as well as the activities of enzymes of pulmonary phospholipid synthesis. The results are shown in Table 9. Saline injection alone produced a number of maturational effects. It increased the amount of total phospholipid and phosphatidylcholine in lung lavage, increased the relative amount of phosphatidylcholine, and decreased the relative amount of sphingomyelin, which resulted in an increase in the phosphatidylcholine/sphingomyelin ratio, and it decreased the activities of choline kinase and cholinephosphate cytidylyltransferase. All these changes are in the direction of increased maturation. However, saline injection caused a huge increase in the activity of cholinephosphotransferase, which normally decreased during fetal development and did not increase in activity until after birth (Fig. 3).

DISCUSSION

Maturation of the fetal lung and its acceleration by corticosteroids and thyroxine have been studied in a number of laboratories

TABLE 9

EFFECT OF THE SURGICAL PROCEDURE ON THE PHOSPHOLIPID CONTENT AND COMPOSITION OF LUNG LAVAGE AND ON THE ACTIVITIES OF ENZYMES OF PULMONARY PHOSPHOLIPID SYNTHESIS*†

	Saline injected	Uninjected	Saline injected/ uninjected	p
	μg phospholipid phosphorus/ g lung dry weight			
Phospholipid content of lung lavage				
Total phospholipid	20.1 ± 1.7 (18)	9.2 ± 2.1 (6)	2.18	<0.005
Phosphatidylcholine	7.0 ± 0.6 (16)	2.6 ± 0.7 (2)	2.69	<0.05
	% phospholipid phosphorus			
Phospholipid composition of lung lavage				
Phosphatidylcholine	35.2 ± 1.3 (17)	28.6 ± 1.8 (2)	1.23	‡
Sphingomyelin	30.4 ± 1.2 (17)	37.6 ± 3.6 (2)	0.81	‡
Phosphatidylcholine/ sphingomyelin ratio	1.2 ± 0.1 (17)	0.8 ± 0.1	1.57	‡
	pmols min^{-1} mg^{-1} of protein			
Enzymes				
Choline kinase	342 ± 15 (11)	445 ± 54 (4)	0.77	<0.025
Cholinephosphate cytidyltransferase	342 ± 15 (16)	452 ± 39 (4)	0.76	<0.02
Cholinephosphotransferase	53.4 ± 3.8 (17)	15.1 ± 3.0 (4)	3.54	<0.001
Glycerophosphate phosphatidyltransferase	16.7 ± 1.5 (11)	18.0 ± 1.3 (4)	0.93	NS

*From S. A. Rooney, L. Gobran, I. Gross, T. S. Wai-Lee, L. L. Nardone and E. K. Motoyama, Studies on Pulmonary Surfactant. Effects of Cortisol Administration to Fetal Rabbits on Lung Phospholipid Content, Composition and Biosynthesis, *Biochim. Biophys. Acta*, 450: 124, 126 (1976).

†Fetuses injected with 0.9% NaCl at 25 days' gestation and those not injected were delivered at 27 days. The data are the means (± SE) from the number of experiments (in parentheses). Statistical analysis was by the *t* test for independent variables. NS, not significant.

‡Insufficient data for statistical analysis.

by morphological, physiological, and surface—physical criteria (Refs. 4—6, 13, 14, and 16). A number of biochemical studies[16-19] have also been carried out, but there have been no previous studies in which the phospholipid content and composition of lung lavage (representative of surfactant) and lung tissue as well as the activities of pulmonary phospholipid biosynthesis during normal fetal develop-

ment have been correlated with those during hormone-accelerated maturation.

The results in this paper show that there was a substantial increase in the amount of phospholipid, principally phosphatidylcholine (the major surface-active component of surfactant), in lung lavage during the period 27 days' gestation to full term at 31 days. During the same period there was also a smaller increase in the amount of phosphatidylcholine in lung tissue. However, enzyme activities during this period did not correlate well with the changes in lipid content. The activities of three enzymes of de novo phosphatidylcholine synthesis—choline kinase, cholinephosphate cytidylyltransferase, and cholinephosphotransferase—decreased during fetal development. Following birth there was a huge increase in the amount of phospholipid (almost 80% phosphatidylcholine at this stage) in lung lavage. At the same time the activities of cholinephosphate cytidylyltransferase and cholinephosphotransferase also increased.

The administration of cortisol clearly accelerated fetal-lung maturation as shown by the increase in the amount of total phospholipid and phosphatidylcholine in lung lavage following the administration of the hormone. The phospholipid composition of the lavage from the steroid-treated fetuses resembled that of an untreated fetus at a later gestational age. Cortisol also had effects on certain enzymes. The activities of cholinephosphate cytidylyltransferase and lysolecithin acyltransferase were stimulated in the hormone-treated fetuses. The stimulation of cholinephosphate cytidylyltransferase is of interest since this enzyme increases in activity just after birth when there is a tremendous increase in the amount of lavage phospholipid. In addition, there is evidence from other systems[20] that the cytidylyltransferase reactions may be rate limiting in the synthesis of phosphatidylethanolamine and phosphatidylcholine. The stimulation of lysolecithin acyltransferase is also interesting since this enzyme may be involved in the synthesis of the surface-active species of phosphatidylcholine via a deacylation and reacylation mechanism. This enzyme, together with 1-acylglycerophosphate acyltransferase, increases in activity during normal development.

These effects, therefore, suggest that cortisol stimulates the production of pulmonary surfactant by accelerating normal lung development rather than by a nonphysiological pharmacological mechanism. Cortisol may, however, have some nonphysiological effects on the lung too. Three days after the administration of cortisol at 24 days' gestation, there was a 53% increase in the activity

of pulmonary glycerophosphate phosphatidyltransferase. Concomitantly there was an increase in the relative amount of phosphatidylglycerol in lavage.[10] These effects, which were not apparent after treatment with cortisol for 2 days, may be unrelated to normal development since the activity of glycerophosphate phosphatidyltransferase decreases during normal development, whereas there is no developmental increase in either the total amount of phosphatidylglycerol in lung tissue or in its relative amount in lavage. The inhibition of the enzymes of fatty-acid synthesis 3 days after the administration of cortisol may also be a nonphysiological effect of the hormone. It is difficult to reconcile a decrease in fatty-acid synthesis with an increase in phospholipid synthesis unless de novo fatty-acid synthesis is of little quantitative importance.

Some of the changes produced by the administration of cortisol are also produced, to a lesser extent, by saline injection alone. This is probably due to release of endogenous corticosteroids or other hormones in response to stress. For cholinephosphotransferase it is possible that the more than threefold increase seen on saline injection alone represents maximal induction of this enzyme. Thus no further increase in activity is possible on the administration of exogenous steroids. This may explain the difference between the present findings and those of Farrell and Zachman[17] that corticosteroids stimulated the activity of cholinephosphotransferase in fetal-rabbit lung. Other workers[16,21] have also reported that other parameters of lung maturation are accelerated by saline injection alone. So that the effect of endogenous hormones, released in response to stress, in the investigation of the mechanism of cortisol action can be eliminated, studies in which the hormone is administered to the doe are currently under way in our laboratory. Preliminary results indicate that the effects on phospholipid content and composition of lung lavage described in this paper are also evident in that model.

ACKNOWLEDGMENTS

This work was supported by a grant (SCOR HL-14179) from the National Institutes of Health.

The expert technical assistance of Patricia M. Canavan, Laurice Gobran, Ying Huang, Theresa S. Wai-Lee, and Charlene Zigas as well as the collaborative efforts of Ian Gross and Linda L. Nardone are gratefully acknowledged.

REFERENCES

1. J. Goerke, Lung Surfactant, *Biochim. Biophys. Acta*, 344: 241-261 (1974).
2. R. F. Henderson and R. C. Pfleger, Surface Tension Studies of Phosphatidyl Glycerol Isolated from the Lungs of Beagle Dogs, *Lipids*, 7: 492-494 (1972).
3. S. A. Rooney, P. M. Canavan, and E. K. Motoyama, The Identification of Phosphatidylglycerol in the Rat, Rabbit, Monkey and Human Lung, *Biochim. Biophys. Acta*, 360: 56-67 (1974).
4. P. M. Farrell and M. E. Avery, Hyaline Membrane Disease, *Am. Rev. Respir. Dis.*, 111: 657-688 (1975).
5. B. Wu, Y. Kikkawa, M. M. Orzalesi, E. K. Motoyama, M. Kaibara, C. J. Zigas, and C. D. Cook, The Effect of Thyroxine on the Maturation of Fetal Rabbit Lungs, *Biol Neonate*, 22: 161-168 (1973).
6. M. E. Avery and B. D. Fletcher, *The Lung and Its Disorders in the Newborn Infant*, W. B. Saunders Company, Philadelphia, 1974.
7. S. A. Rooney, T. S. Wai-Lee, L. Gobran, and E. K. Motoyama, Phospholipid Content, Composition and Biosynthesis During Fetal Lung Development in the Rabbit, *Biochim. Biophys. Acta*, 431: 447-458 (1976).
8. S. A. Rooney, I. Gross, L. N. Gassenheimer, and E. K. Motoyama, Stimulation of Glycerolphosphate Phosphatidyltransferase Activity in Fetal Rabbit Lung by Cortisol Administration, *Biochim. Biophys. Acta*, 398: 433-441 (1975).
9. O. H. Lowry, N. J. Rosebrough, A. L. Farr, and R. J. Randall, Protein Measurement with the Folin Pheonol Reagent, *J. Biol. Chem.*, 193: 265-275 (1951).
10. S. A. Rooney, L. Gobran, I. Gross, T. S. Wai-Lee, L. L. Nardone, and E. K. Motoyama, Studies on Pulmonary Surfactant. Effects of Cortisol Administration to Fetal Rabbits on Lung Phospholipid Content, Composition and Biosynthesis, *Biochim. Biophys. Acta*, 450: 121-130 (1976).
11. I. Gross and J. B. Warshaw, Enzyme Activities Related to Fatty Acid Synthesis in Developing Mammalian Lung, *Pediatr. Res.*, 8: 193-199 (1974).
12. I. Gross, S. A. Rooney, and J. B. Warshaw, The Influence of Cortisol on the Enzymes of Fatty Acid Synthesis in Developing Mammalian Lung ar ` Brain, *Pediat. Res.*, 9: 752-755 (1975).
13. E. K. Motoyama, M. M. Orzalesi, Y. Kikkawa, M. Kaibara, B. Wu, C. J. Zigas, and C. D. Cook, Effect of Cortisol on the Maturation of Fetal Rabbit Lungs, *Pediatrics*, 48: 547-555 (1971).
14. Y. Kikkawa, M. Kaibara, E. K. Motoyama, M. M. Orzalesi, and C. D. Cook, Morphologic Development of Fetal Rabbit Lung and Its Acceleration with Cortisol, *Am. J. Pathol.*, 64: 423-442 (1971).
15. R. V. Kotas, B. D. Fletcher, J. Torday, and M. E. Avery, Evidence for Independent Regulators of Organ Maturation in Fetal Rabbits, *Pediatrics*, 47: 57-64 (1971).
16. B. J. Russell, L. Nugent, and V. Chernick, Effects of Steroids on the Enzymatic Pathways of Lecithin Production in Fetal Rabbits, *Biol. Neonate*, 24: 306-314 (1974).
17. P. M. Farrell and R. D. Zachman, Induction of Cholinephosphotransferase and Lecithin Synthesis in the Fetal Lung by Corticosteroids, *Science*, 179: 297-298 (1973).
18. A. C. G. Platzker, J. A. Kitterman, E. J. Mescher, J. A. Clements, and W. H. Tooley, Surfactant in the Lung and Tracheal Fluid of the Fetal Lamb and

Acceleration of Its Appearance by Dexamethasone, *Pediatrics*, 56: 554-561 (1975).

19. E. J. Mescher, A. C. G. Platzker, P. L. Ballard, J. A. Kitterman, J. A. Clements, and W. H. Tooley, Ontogeny of Tracheal Fluid, Pulmonary Surfactant, and Plasma Corticoids in the Fetal Lamb, *J. Appl. Physiol.*, 39: 1017-1021 (1975).
20. R. Sundler and B. Akesson, Regulation of Phospholipid Biosynthesis in Isolated Rat Hepatocytes. Effect of Different Substrates, *J. Biol. Chem.*, 250: 3359-3367 (1975).
21. M. F. Robert, A. T. Bator, and H. W. Taeusch, Pulmonary Pressure-Volume Relationships After Corticotropin (ACTH) and Saline Injections in Fetal Rabbits, *Pediatr. Res.*, 9: 760-762 (1975).

Respiratory Epithelium in the Dolphin Lung

J. C. FANNING
Department of Pathology, The University of Adelaide,
Adelaide, South Australia

ABSTRACT

The respiratory zone of the dolphin lung consists of respiratory bronchi, alveolar ducts and sacs, and alveoli. The respiratory bronchus is generally less than 1 mm in diameter, has cartilage plates in its wall, myo-elastic bundles that form sphincters, and a capillary plexus immediately beneath the epithelium which is composed of cuboidal and squamous cells. The cuboidal cells are found in the gaps in the capillary plexus. They are somewhat flattened, measure up to 10 μm in diameter, and have many short microvilli 0.5 × 0.1 μm on their surface. They contain no inclusions or secretory granules. The capillaries are covered by squamous cells with thin lateral cytoplasmic processes which are only 100 nm thick in some areas. These cells are very similar to the type I cells of the alveoli.

The alveoli have a thick connective tissue core with a separate capillary plexus on each surface. The epithelium consists of type I and II cells. The type I cells have very attenuated lateral processes which in some areas are only 30 to 40 nm thick and contain only occasional pinocytotic vesicles in these areas. The type II cells occur in groups of two or three in the intercapillary niches and in the junctional regions of the septum. They contain cytosomes with osmiophilic lamellae up to 2 μm, microvilli 0.4 × 0.1 μm on their surface, and much folding of the lateral and basal plasma membrane. It is suggested that the respiratory bronchus has evolved as a means of increasing the respiratory surface area during prolonged shallow dives. The blood—air barrier in the alveoli has been reduced to 120 to 200 nm to compensate for the thickness of the septum and for the exposure of the capillaries to only one alveolus.

The dolphin is a mammal ideally adapted to the marine environment in which it lives. It is capable of diving to depths of several hundred meters and staying submerged for prolonged periods without developing the bends.

Details of the capture, transportation, and general characteristics of the animals, and the methods of fixation of the lung specimens used in this study, have been described.[1,2] Briefly, the lung specimens were fixed by intratracheal instillation of 1% glutaraldehyde–1% paraformaldehyde; they were then either (a) embedded in epoxy resin after suitable post fixation for transmission electron microscopy (TEM) or (b) dried to the critical point and coated with gold–palladium for scanning electron microscopy (SEM).

RESULTS

The airways contain cartilage plates in their walls to their termination in the alveolar ducts. Circular bundles of smooth muscle are found in bronchi 2 mm or less in diameter. Smooth muscle is not found proximal to this level. The lining of this terminal portion of the bronchi changes gradually from ciliated columnar epithelium with goblet cells to ciliated cuboidal epithelium with secreting cells resembling Clara cells.[2]

In bronchi 0.5 to 1 mm in diameter, the circular muscle bundles become sphincters situated between the cartilage plates, at bifurcations, and around the opening of the alveolar ducts (Fig. 1). The epithelium in this segment of the bronchial tree consists of two cell types: (a) cuboidal cells with microvilli and (b) squamous cells. There is a prominent capillary plexus immediately beneath the epithelium in this sphincteric segment (Figs. 2 and 3).

The cuboidal cells are somewhat flattened, measuring up to 10 μm in diameter and 6 to 8 μm high. They are found singly or in groups in the gaps between the capillaries. The cells have microvilli 0.5 x 0.1 μm on their apical surface, a convoluted nucleus, ovoid mitochondria, many free ribosomes, and many small vesicles (Figs. 3 and 4). Secretory granules and inclusions are found only in the cells near the termination of the airway. In this region some of the cells may contain lamellar inclusions similar to those of the type II alveolar cells. The capillaries are covered by squamous cells that are very similar to the type I cells in the alveoli. Their nucleus and the scant cytoplasmic components are found between the capillaries. The blood–air barrier in this segment ranges from 200 to 350 nm thick; this segment has been called the respiratory bronchus.[2] The airways terminate by dividing into alveolar ducts which give rise to alveolar sacs and alveoli (Fig. 1). Occasionally alveoli arise directly from the terminal portion of the airway. Alveoli are polygonal in shape and range in size from 0.1 to 0.25 mm in diameter. The alveolar septum

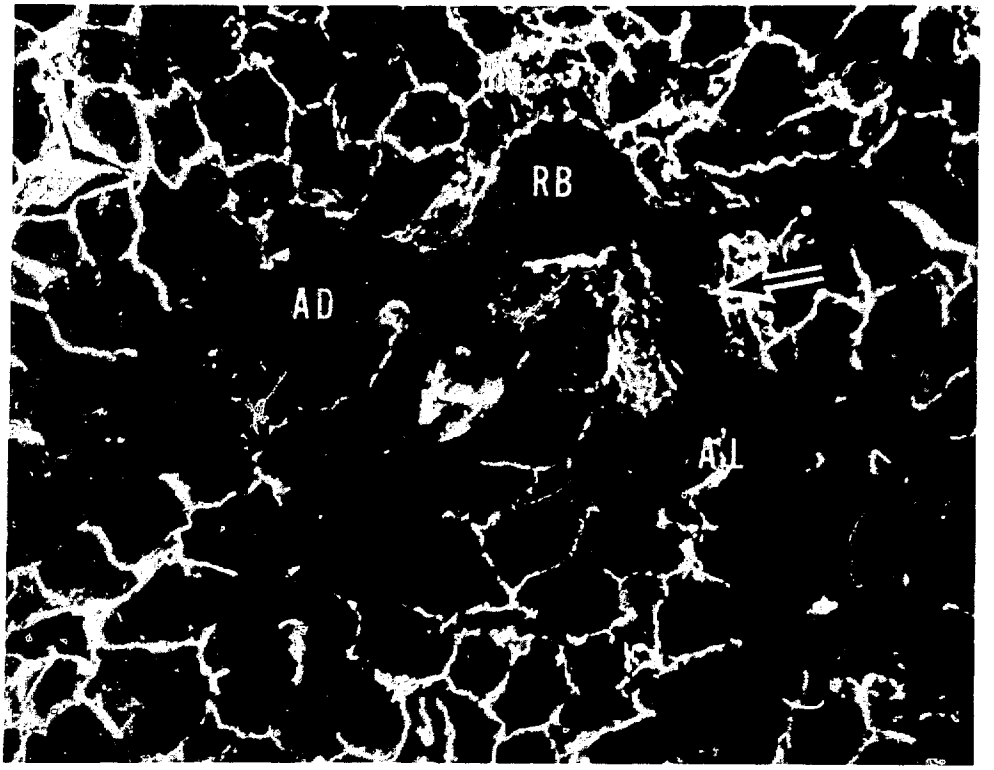

Fig. 1 Scanning electron micrograph of division of a respiratory bronchus (RB), alveolar ducts (AD), and alveoli (AL). Note the sphincters (indicated by arrow) and the absence of pores of Kohn. (Magnification, 370 ×.)

consists of a connective-tissue core 3 to 10 μm thick with a network of capillaries on each surface (Figs. 5 and 6).

Epithelial cells have been identified as type I and type II cells. The type I cells have very attenuated lateral processes which in some areas are only 30 to 40 nm thick, containing occasional small pinocytotic vesicles. In most areas the processes are 50 to 100 nm thick and contain many pinocytotic vesicles 5 to 25 nm (Fig. 7). The nucleus and cytoplasmic organelles are found in the gaps between the capillaries.

The type II cells occur in groups of two or three in the intercapillary niches or in the junctional regions of the septum (Figs. 6 and 8). They are cuboidal cells 10 to 20 μm in size and contain characteristic membrane-bound osmiophilic multilamellar bodies up to 2 μm in diameter, multivesicular bodies, and a prominent Golgi complex (Fig. 9). The free surface has microvilli 0.4 × 0.1 μm, and

the lateral surfaces have prominent infoldings and interdigitating processes. Occasional unmyelinated nerve fibers are found in relationship to the basal membrane of the cells.

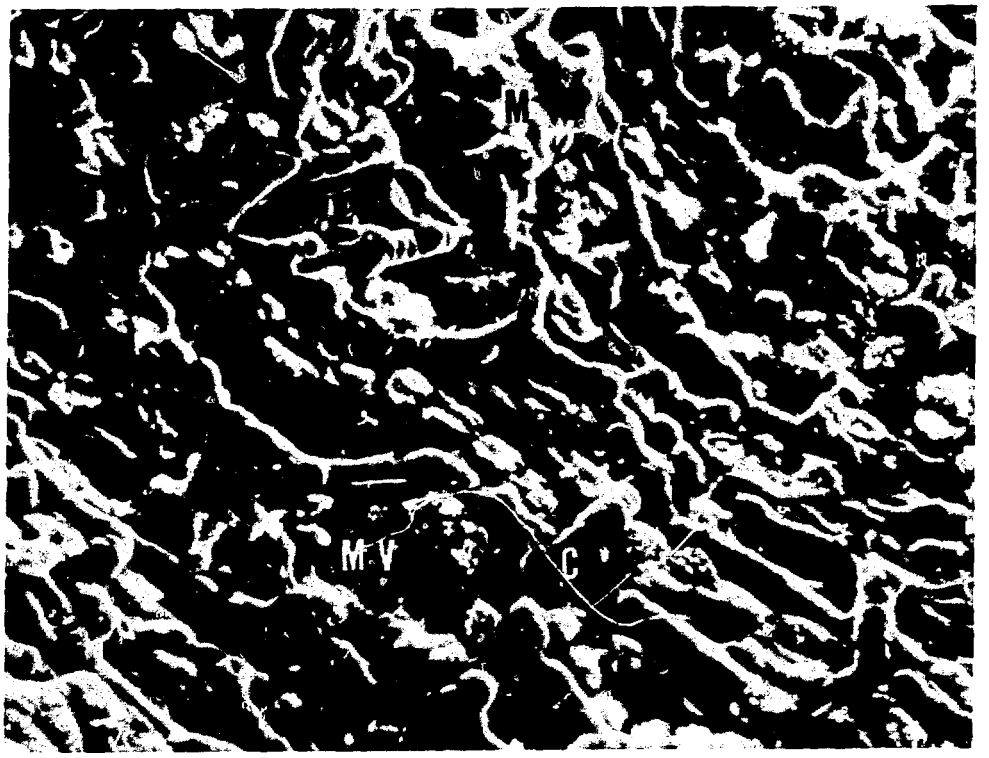

Fig. 2 Scanning electron micrograph of lining of respiratory bronchus showing capillary plexus engorged with red cells (C) covered by squamous epithelium macrophages (M), microvillous cells (MV). (Magnification, 700 ×.)

The capillary plexuses on each surface are not completely independent, because occasional transseptal anastomoses are found away from the septal junctions. The plexuses appear to be arranged in many areas so that gaps on one surface correspond to vessels on the complementary surface (Fig. 5).

The blood—air barrier is 150 to 200 nm thick in most areas, decreasing to 120 nm in some areas (Fig. 7). Macrophages are frequently seen in the alveoli and respiratory bronchi. Myelin figures, presumably surfactant, are also seen in the subpleural alveoli.

Fig. 3 High-power micrograph of similar area as in Fig. 2 showing lining of respiratory bronchus with microvillous cells in the gaps in capillary plexus. (Magnification, 1500 X.)

DISCUSSION

The possibility that gas exchange could occur in the terminal bronchi of the dolphin was first discussed by Wislocki.[3] He described the change in the epithelium from the bronchial pattern to the squamous type and noted the presence of the capillary plexus. Both transmission and scanning electron microscopy have confirmed the

Fig. 4 Transmission electron micrograph of microvillous cell between capillaries. (Magnification, 8750 X.)

presence of a capillary plexus covered by a thin squamous epithelium which is morphologically capable of gas exchange.[2,4] In addition a second cell type not previously described in mammalian lungs has been found. Initial observations suggest that this cell is not a secretory cell, but further investigation is required.

The structure of the cetacean lung with its double capillary network was first described in the common dolphin by Fiebiger.[5] Since then numerous observers have reported similar findings in other cetaceans.[2]

It has been shown[6] that in deep dives about 85% of the inspired oxygen is utilized, whereas in shallow dives up to 95% is utilized. It is

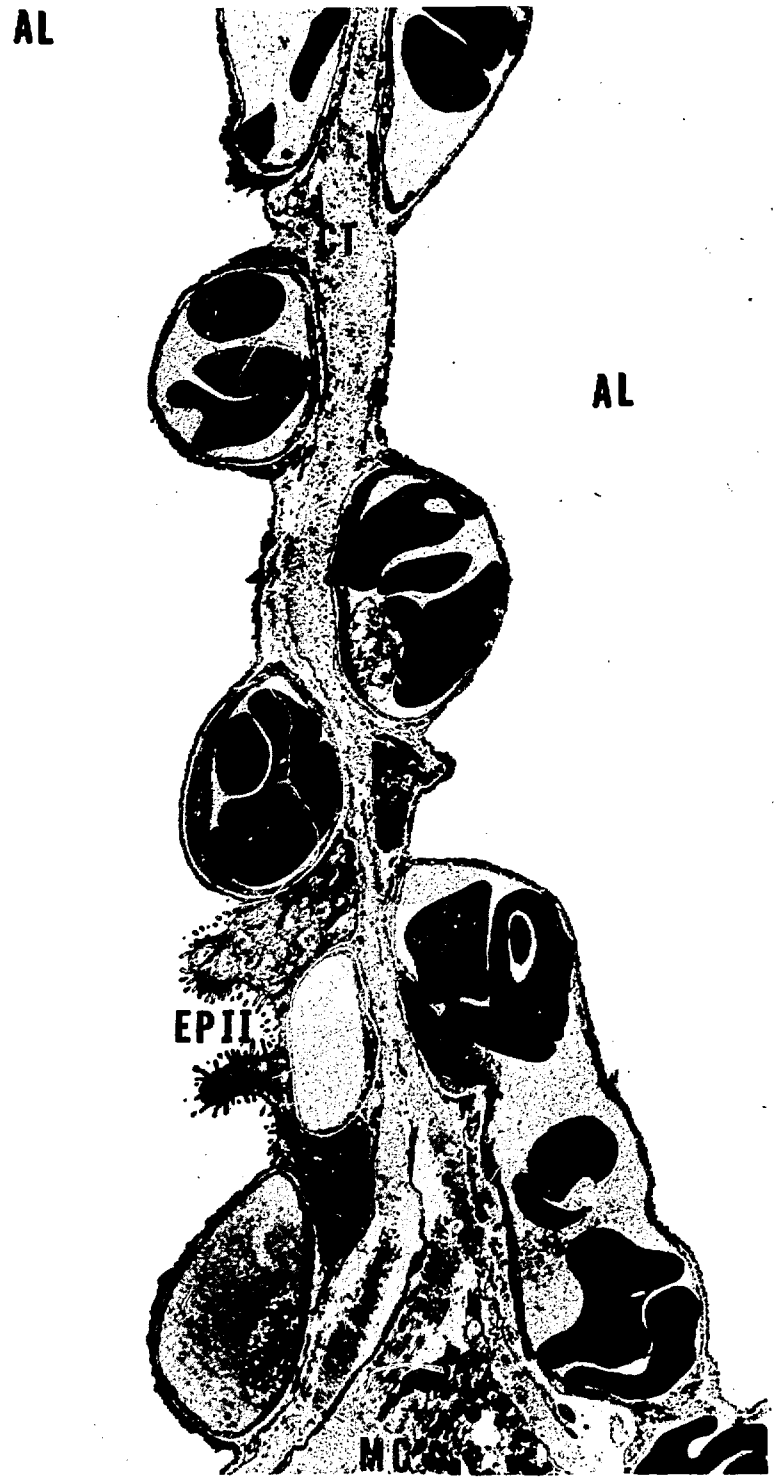

Fig. 5 Low-power transmission electron micrograph of alveolar septum. Note the arrangement of the capillary plexuses on each surface, the connective-tissue core (CT), two type II cells (EP II), and a mast cell (MC) in the septal junction. No type I cell nuclei can be seen. (Magnification, 4000 X.)

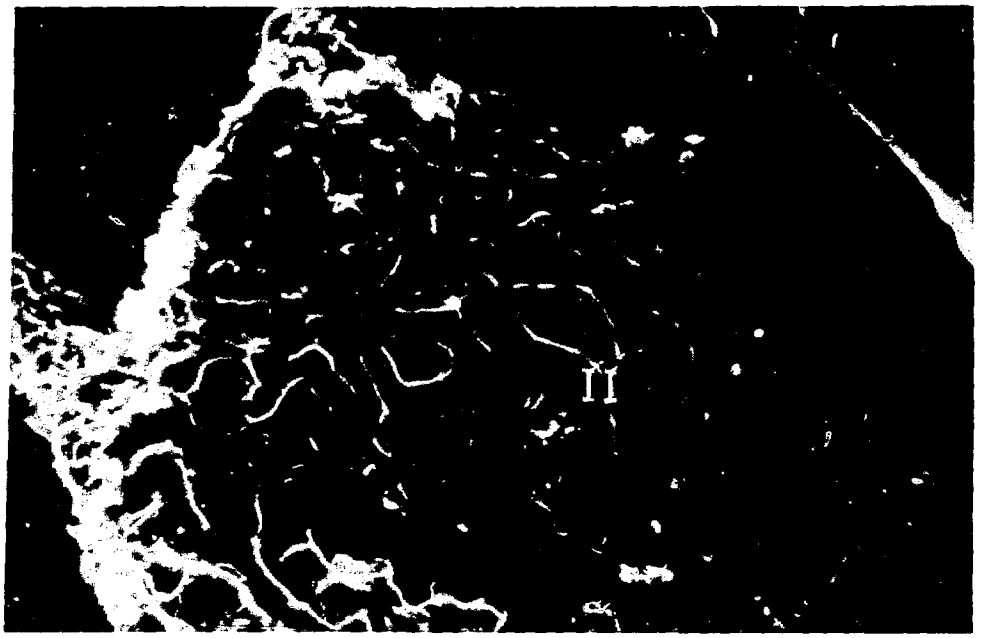

Fig. 6 Scanning electron micrograph of an alveolus showing the capillary plexus and several groups of type II cells. (Magnification, 700 X.)

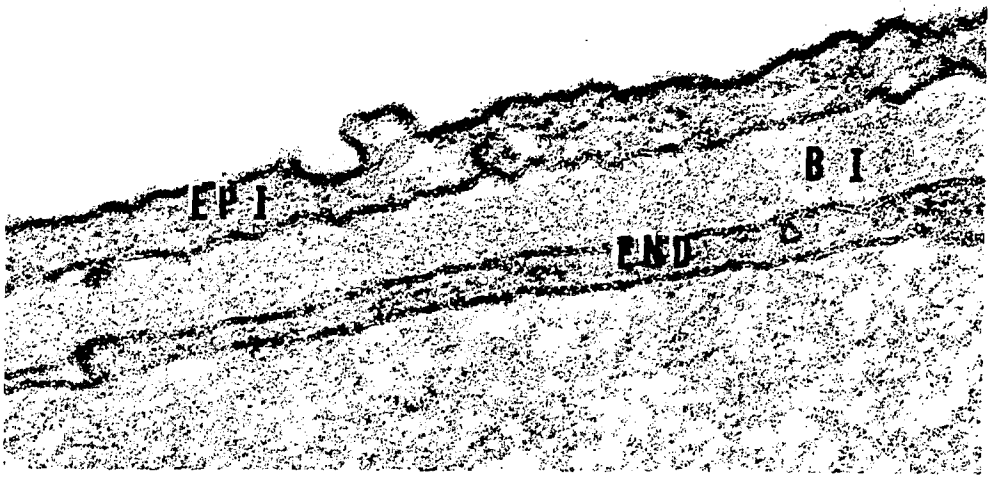

Fig. 7 Transmission electron micrograph of blood—air barrier showing type I cells (EP I), fused basal laminae (B I), and capillary endothelial cell (END). (Magnification, 50,000 X.)

Fig. 8 Scanning electron micrograph of type II alveolar cells. (Magnification, 2300 X.)

suggested that during deep diving the alveoli collapse, forcing air out from the larger bronchi and trachea, but that during shallow dives the air is trapped in the alveoli and respiratory bronchi, enabling further gas exchange to occur.

Ridgway[7] has stated that in dolphins alveolar collapse commences at a depth of 10 meters. It may be that the thick alveolar septum and the double capillary network facilitates folding of the alveolar septum without reducing the available surface area for gas absorption.

Although there is a relative increase in connective tissue, both cartilage and fibers, the general pattern of the respiratory zone agrees with the characteristic mammalian pattern.[4,8]

Fig. 9 Transmission electron micrograph of type II alveolar cells showing characteristic multilamellar bodies (ML). (Magnification, 25,000 X.)

ACKNOWLEDGMENT

This work was supported in part by a grant-in-aid from the National Health and Medical Research Council of Australia.

REFERENCES

1. R. J. Harrison and J. C. Fanning, Anatomical Observations on the South Australian Bottle-Nosed Dolphin (*Tursiops truncatus*), in *Investigation on Cetacea*, Vol. 5, G. Pilleri (Ed.), pp. 203-217, Berne, Switzerland, 1974.

2. J. C. Fanning and R. J. Harrison, The Structure of the Trachea and Lungs of the South Australian Bottle-Nosed Dolphin, in *Functional Anatomy of Marine Mammals*, Vol. 2, R. J. Harrison (Ed.), pp. 231-252, Academic Press, Inc., New York, 1974.
3. G. B. Wislocki, On the Structure of the Lungs of the Porpoise, *Amer. J. Anat.*, 44: 47-77 (1929).
4. E. R. Weibel, Morphological Basis of Alveolar-Capillary Gas Exchange, *Physiol. Rev.*, 53: 419-495 (1973).
5. J. Fiebiger, Uber. Eigentum lichkeiter im Aufbau der Delphinlunge und ihre physiologische. Bedeutung, *Anat. Anz.*, 48: 540-546 (1916).
6. S. H. Ridgway, B. C. Sconce, and J. Kanwisher, Respiration and Deep Diving in the Bottle-Nosed Dolphin, *Science*, 166: 1651-1654 (1969).
7. S. H. Ridgway, in *Mammals of the Sea: Biology and Medicine*, S. H. Ridgway (Ed.), pp. 590-747, Charles C Thomas, Publisher, Springfield, Illinois, 1972.
8. V. E. Krahl, Anatomy of the Mammalian Lung, in *Handbook of Physiology, Section 3*, Vol. I, pp. 213-284, American Physiological Society, Washington, D. C., 1964.

Fine Structural Observations on the Origin and Development of Lamellar Bodies in Alveolar Type II Pneumocytes

GERALD CALLAS and W. J. deGROOT
Department of Anatomy, Department of Internal Medicine,
The University of Texas, Medical Branch, Galveston, Texas

ABSTRACT

Many investigators believe that osmophilic inclusion bodies in type II pneumocytes arise from multivesicular bodies. However, their origin from mitochondria has been suggested by others. From our investigation with euthyroid, hypothyroid, and hyperthyroid animals, we present strong morphologic evidence that lamellar bodies arise from both mitochondria and multivesicular bodies. Transformation figures in mitochondria and multivesicular bodies were observed in all groups of animals but were more numerous and better defined in the hypothyroid animals. In mitochondria, single lamellar structures that are associated with the inner lamina of the mitochondrial membrane appear. In the area of the developing lamellar body, the matrix becomes less dense, and some of the mitochondrial cristae appear to be incorporated into the lamellar inclusion. The lamellar structure then becomes more complex, whereas the cristae disappear.

The structural precursors of the osmophilic inclusion bodies of the type II pneumocyte are not known, although different groups of investigators have suggested both mitochondria[1-5] and the multivesicular bodies[6-9] as possible or probable precursors. Meban[10] demonstrated phosphatidic acid phosphatase activity in the granular pneumocyte localized in the lining membrane of the lamellar body. He also reported enzymatic activity in the multivesicular bodies situated adjacent to inclusion bodies and suggested that the stained multivesicular bodies may communicate with the inclusion vesicles as advocated by Sorokin.[6] Flaks and Flaks[11] have suggested that both multivesicular bodies and mitochondria may be precursors of the lamellar bodies.

Varying thyroid function has a marked effect on the type II alveolar cells. Redding, Douglas, and Stein[12] reported that increased amounts of thyroid hormone resulted in a distinct stepwise enlargement of the alveolar type II cells combined with an increase in size and numbers of their lamellar inclusion bodies. A reverse effect is seen with decreased thyroid activity.

This paper is concerned with the use of varying states of thyroid function to study lamellar body formation.

MATERIALS AND METHODS

Sprague—Dawley adult male rats weighing 250 to 300 g at the start of the experiment were used. Twenty animals were radiothyroidectomized by the intraperitoneal injection of 800 μCi of $Na^{131}I$. Hyperthyroidism was produced in 10 radiothyroidectomized rats by feeding a diet containing 0.3 to 0.4% desiccated thyroid for 4 weeks. The remaining 10 rats were allowed to become hypothyroid. Ten untreated rats were used as controls. Twenty-four hours prior to sacrifice, oxygen consumption was determined for each animal as an index of thyroid function.

Under nembutal anesthesia, a tracheostomy was performed on all animals, and the lungs were inflated to a transpulmonary pressure of 15 cm of H_2O prior to perfusion. The animals were prepared by perfusion through the right ventricle with the use of a standard hospital intravenous infusion set. The perfusion pressure was approximately 25 cm of H_2O. A normal saline prewash (0.5% procaine hydrochloride in normal saline with 1 cm^3 of sodium heparin per 100 ml) was used to flush and vasodilate the animal's circulatory system until a clear return was obtained from the left atrium. Without allowing the flow to stop, this was immediately followed by 3% glutaraldehyde in 0.1*M* phosphate buffer at a pH of 7.4 and an osmolarity of 500 to 550 milliosmols. After the animals had been perfused, the lungs were removed, cut into 1-mm blocks, and placed in cold fixative for an additional 2 hr. Following postfixation in 1% OsO_4 in 0.1*M* phosphate buffer for 2 hr, the tissue was dehydrated through a graded series of cold ethyl alcohol and embedded in low-viscosity embedding media. Sections were cut with a diamond knife on an ultramicrotome and picked up on copper grids. The tissue was stained with lead citrate and uranyl acetate and was viewed and photographed in an electron microscope.

RESULTS

Oxygen consumption was 18 to 23 $cm^3\ kg^{-1}\ min^{-1}$ for controls, 36 to 53 $cm^3\ kg^{-1}\ min^{-1}$ for hyperthyroid animals, and 10 to 13 $cm^3\ kg^{-1}\ min^{-1}$ for hypothyroid animals. The observations reported here occur in all groups of animals; therefore the forms that best illustrate the sequence for the proposed development of the lamellar body will be described with the use of examples from all three groups of animals.

The first indication of lamellar body formation in mitochondria is the appearance of one or two lamellae that appear to arise from the inner mitochondrial membrane (Figs. 1 and 2). The lamellae have a spacing of 70 to 80Å. The developing lamellar body then becomes larger and more complex by the formation of additional lamellae (Figs. 3 to 9) until a mature lamellar body is formed (Fig. 10).

Dense lamellae were also observed within the multivesicular bodies (Figs. 11 to 16). These structures ranged from multivesicular bodies that contained a few membranous lamellae to lamellar inclusion bodies that occupied almost the entire multivesicular body. Occasionally multivesicular bodies were observed in close approximation to mature lamellar bodies.

DISCUSSION

From the present morphologic study, there appears to be two possible routes for the development of the osmophilic inclusion bodies in the type II pneumocytes. The first route consists of the progressive development of lamellae within the mitochondria until the entire mitochondrion is transformed into a mature lamellar body. Other investigators also have suggested that mitochondria were the source of lamellar bodies.[1-5] Some support of lamellar transformation of mitochondria was provided by the findings of the lamellar bodies in the mitochondrial fraction of lung tissue.[3] This idea has not been accepted by many others because the number of intermediates between the mitochondria and lamellar bodies have been considered as insufficient to support this concept. The present study has demonstrated that there is a stepwise sequence of events in the development of the lamellar body from mitochondria. All groups of animals exhibited these changes, but they were more numerous in the hypothyroid group. Flaks and Flaks[11] have suggested that mitochondria may undergo lamellar transformation only after fusion with nonlamellated inclusion bodies. In our study nonlamellated

(Text continues on page 201.)

Fig. 1 Electron micrograph of an early stage in the development of an osmophilic body (arrow) within a mitochondrion (M) from a control rat alveolar type II pneumocyte. The inclusion consists of a clear zone containing some amorphous material surrounded by a single lamella. (Magnification, 47,250 X.)

Fig. 2 Developing lamellar bodies (arrows) are observed in two mitochondria (M) from control rat type II pneumocytes. The inclusion body appears to originate from the inner mitochondrial membrane (arrow heads). The lamellae have a spacing of 70 to 80Å. (Magnification, 96,250 X.)

Figure 3

Figure 4

Figs. 3 and 4 Further stages in the development of lamellar inclusion bodies (arrows) within control type II pneumocyte mitochondria (M). (Figure 3 magnification, 73,500 X; Fig. 4 magnification, 46,250 X.)

Figure 5

Figure 6

Figs. 5 and 6 Developing lamellar bodies (arrows) at one pole of the mitochondria (M). The mitochondria from control type II pneumocytes show a decrease in density or absence of matrix in the area of the developing osmophilic inclusion bodies. (Magnification, 73,500 X.)

Figure 8

Figure 7

Figure 9

Figs. 7, 8, and 9 In hypothyroid rats, as more lamellae form the inclusion bodies increase in size within the mitochondria (M) of type II pneumocytes and become more complex. At this stage of development, the mitochondria begin to lose some of their characteristic features. (Figure 7 magnification, 180,000 X; Fig. 8 magnification, 180,000 X; Fig. 9 magnification, 121,500 X.)

Figure 8

Figure 7

Figure 9

Figs. 7, 8, and 9 In hypothyroid rats, as more lamellae form the inclusion bodies increase in size within the mitochondria (M) of type II pneumocytes and become more complex. At this stage of development, the mitochondria begin to lose some of their characteristic features. (Figure 7 magnification, 180,000 X; Fig. 8 magnification, 180,000 X; Fig. 9 magnification, 121,500 X.)

Fig. 10 Mature lamellar body from a hyperthyroid rat type II pneumocyte. (Magnification, 45,000 X.)

Fig. 11 Early stage of lamellar development (arrow) in a multivesicular body from a hypothyroid rat lung type II alveolar cell. (Magnification, 99,000 X.)

dense bodies were also observed in all groups of animals, but no fusion with mitochondria was observed.

The other route involves a similar sequence within the multivesicular bodies. The observations in this study confirm the findings of Sorokin.[6] He suggested that the osmophilic inclusion bodies of type II pneumocytes were special lysosomes derived from multivesicular bodies. The vesicles of the multivesicular bodies were thought to be derived from Golgi vesicles, the contents of which would, in part, originate in the granular endoplasmic reticulum.

From the observations in this study, it would appear that there is a relationship between mitochondria and multivesicular bodies in the formation of the osmophilic inclusion bodies in type II pneumocytes. Since the changes observed in transformed mitochondria and multivesicular bodies appeared to be similar in magnitude, both organelles may be an important pathway in the formation of lamellar bodies.

ACKNOWLEDGMENT

Supported by National Institutes of Health grant DHEW HL 16942-01.

REFERENCES

1. R. E. Pattle, C. Schock, P. Dirnhuber, and J. M. Creasey, Lamellar Transformation of Lung Under Conditions of Stress, *Nature*, 240: 468-469 (1972).
2. T. Caulet, J. J. Adnet, C. Hopfner, and G. Legeay, Les Cellules a Inclusions Lipidiques de la Bordure de L'alvéole Pulmonaire—Etude Histochimique et Ultrastructurale, *Pathol.-Biol.*, 17: 165-173 (1969).
3. M. H. Klaus, O. K. Reiss, W. H. Tooley, C. Piel, and J. A. Clements, Alveolar Epithelial Cell Mitochondria as Source of the Surface-Active Lung Lining, *Science*, 137: 750-751 (1962).
4. G. L. Woodside and A. J. Dalton, The Ultrastructure of Lung Tissue from Newborn and Embryo Mice, *J. Ultrastruct. Res.*, 2: 28-54 (1958).
5. H. Schulz, Elektronen Optische Untersuchungen der Normalen Lunge und der Lunge bei Mitralstenose, *Virchows Arch.*, 328: 528-604 (1956).
6. S. P. Sorokin, A Morphologic and Cytochemical Study of the Great Alveolar Cell, *J. Histochem. Cytochem.*, 14: 884-897 (1967).
7. A. H. Niden, Bronchiolar and Large Alveolar Cells in Pulmonary Phospholipid Metabolism, *Science*, 158: 1323-1324 (1967).
8. M. A. Campiche, A. Gautier, E. I. Hernandez, and A. Reymond, An Electron Microscope Study of the Fetal Development of Human Lung, *Pediatrics*, 32: 976-994 (1963).
9. H. E. Karrer, The Ultrastructure of the Mouse Lung: General Architecture of Capillary and Alveolar Walls, *J. Biophys. Biochem. Cytol.*, 2: 241-252 (1956).

(References continue on page 204.)

Figure 12

Figure 13

Figure 14

Figure 15

Figs. 12, 13, 14, and 15 Varying stages in the development of osmophilic inclusion bodies (arrows) from multivesicular bodies from control rat lung pneumocytes. (Figure 12 magnification, 126,000 X; Fig. 13 magnification, 99,000 X; Fig. 14 magnification, 12,000 X; Fig. 15 magnification, 165,000 X.)

Fig. 16 Electron micrograph showing a multivesicular body attached to a mature lamellar body (LB). (Magnification, 52,500 X.)

10. C. Meban, Localization of Phosphatidic Acid Phosphatase Activity in Granular Pneumocytes, *J. Cell Biol.*, 53: 249-252 (1972).
11. B. Flaks and A. Flaks, Electron-Microscope Observations on the Formation of the Cytoplasmic Lamellar Inclusion Bodies in Murine Pulmonary Tumours Induced In Vitro, *J. Pathol.*, 108: 211-217 (1972).
12. R. A. Redding, W. H. J. Douglas, and M. Stein, Thyroid Hormone Influence upon Lung Surfactant Metabolism, *Science*, 175: 994-996 (1971).

Electron Microscopic Observations of Intracisternal A Type Particles in a Transplantable Murine Alveolar Cell Carcinoma with Remarks on the Cellular Origin of This Tumor

AARON J. LADMAN* and JOHN M. YUHAS†
*Department of Anatomy, School of Medicine, and †Cancer Research and Treatment Center, The University of New Mexico, Albuquerque, New Mexico

ABSTRACT

Transmission electron microscopic observations on an alveolar cell carcinoma after in vivo and in vitro transplantation reveal the presence of intracisternal A type (ICA) particles in the endoplasmic reticulum and nuclear envelope. These ICA particles are described, and a sequence of events is reconstructed which considers the origin, growth, and eventual autophagy of these particles by the carcinoma cells. Additional data suggest that the tumor retains structural characteristics of type I and type II epithelial cells as well as the alveolar macrophage. Measurement of surfactant content of the tumor with a Wilhelmi balance supports the morphologic analyses that the tumor produces little or no surfactant as compared to normal lung.

A spontaneously occurring lung tumor in a BALB/C mouse, identified as an alveolar cell carcinoma by light microscopy at Oak Ridge National Laboratory, has been carried in our laboratory for over 50 in vivo transplant generations by Yuhas.[1] Unpublished chemical analysis of an earlier transplant generation suggested that this tumor might produce surfactant. To establish morphologic correlates for this possibility, we studied this tumor by transmission electron microscopy at several time intervals after in vivo and in vitro transplantation. Our results revealed the presence of intracisternal A (ICA) particles and other features of these cells which suggest that their probable origin is a differentiation from either type I or type II cells or their epithelial progenitors. Lamellated bodies characteristic of surfactant-producing cells in normal lung have not been found in our material.

MATERIALS AND METHODS

In vivo tumors were harvested from BALB/C mice 7, 10, 12, and 16 days after subcutaneous intrascapular inoculation of 5×10^7 cells derived from single cell suspensions.[2] These tumors were diced into 1- to 2-mm cubes and were fixed in 2.5% glutaraldehyde buffered to pH 7.3 with 0.075*M* cacodylate–HCl buffer for 1 to 2 hr at room temperature. In vitro tissue cultures were decanted of medium[3] after 1, 4, and 8 days of culture and flooded with glutaraldehyde. Cells were dislodged from the floor of the flask with a rubber policeman and collected into centrifuge tubes. After 30 min to 1 hr of fixation, the cells were formed into a pellet by spinning them at about 2000 X for 1 to 2 min. Both the solid tumors and the pellets were postfixed in 1% osmium tetroxide in the same buffer for 1 hr at room temperature; they were then washed and stained en bloc with 1% magnesium uranyl acetate in 0.05*M* maleate buffer at pH 6 for 1 to 2 hr in the dark or, on occasion, overnight in the refrigerator. All material was dehydrated in ethanol and embedded in Epon 812.[4] Sections 1 to 2 μm thick were cut with glass and diamond knives and stained with toluidine blue.[5] Thin sections of suitable blocks were cut with diamond knives, picked up on 75 x 300 mesh grids without supporting films, stained with lead citrate[6] and uranyl acetate,[7] and viewed in a Hitachi HU-11C electron microscope at 75 kV.

The supernatant fluid from homogenates of the tumor derived from a recent in vivo passage and normal lung were examined for surface activity on a Wilhelmi balance. Under the conditions of this test, approximately 35 mg of tissue (at a concentration of 100 mg/ml of normal saline) was floated onto the surface of the trough (approximately 100 cm^2 in area) and the area was compressed and expanded at 2 min and at 30 min after application. An x–y rectilinear recorder transduced the surface activity into curves displaying hysteresis as a function of the approximate amount of surfactant activity.

RESULTS

Inspection of 1.5-μm plastic sections of the solid tumors revealed an epithelial conglomerate of considerable morphologic variability in terms of cell size and shape, nuclear configuration and stainability, and nucleolar size and disposition (Fig. 1). These characteristics were less pleomorphic and more uniform in the tissue cultures. In virtually all cells a juxtanuclear region of variable size is identified by light microscopy (Figs. 2 and 3). This region corresponds to the Golgi

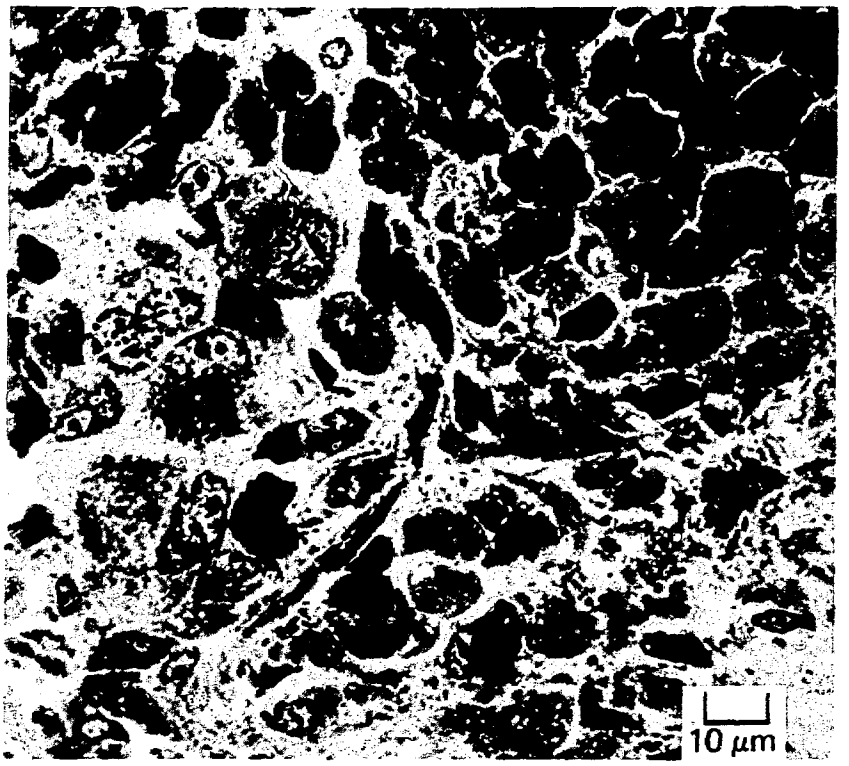

Fig. 1 A 1.5-μm section of tumor transplanted subcutaneously 16 days earlier. The tumor cells differ in size and shape and are relatively pleomorphic. The cells feature large nuclei with prominent nucleoli. The larger cells on the left have conspicuous juxtanuclear material.

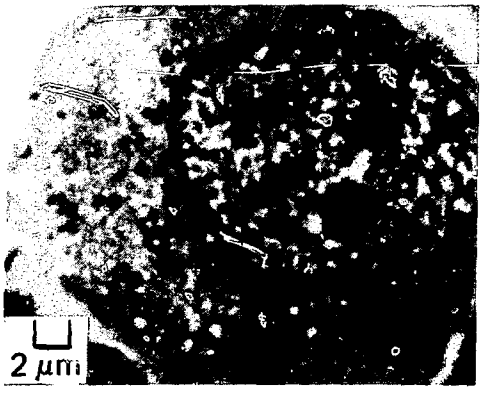

Fig. 2 Higher magnification of a larger cell from a 14-day tumor transplant. Vacuoles can be identified in the juxtanuclear area with the light microscope.

Fig. 3 Higher magnification of a tumor cell obtained from a 1-day tissue culture. The juxtanuclear material indents the nucleus at its upper pole.

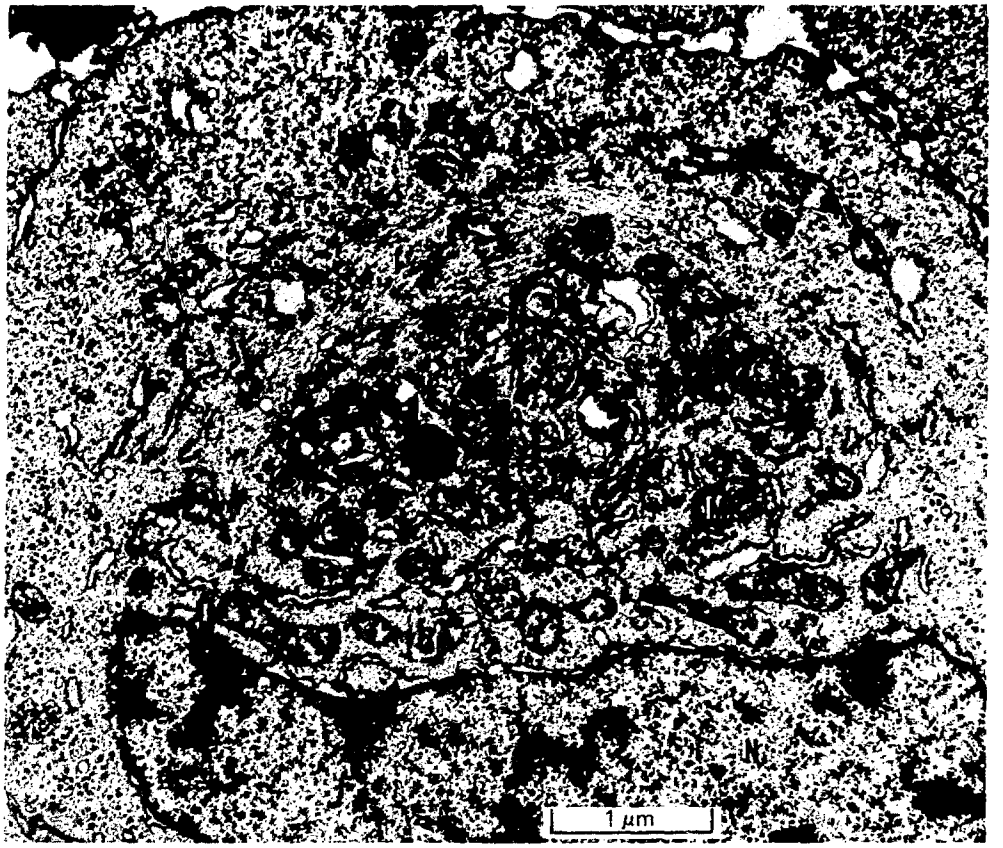

Fig. 4 A region comparable to that shown in Figs. 2 and 3 seen in a low-power field of a 12-day transplanted tumor. Within the juxtanuclear area are contained mitochondria (M), elements of endoplasmic reticulum, and some dense bodies (presumably of lysosomal origin). Encircling these organelles are bundles of filaments (f) delimiting this area from an ectoplasm less rich in organelles. Within the cisternae of the endoplasmic reticulum are dark bodies, the intracisternal A type (ICA) particles. At the periphery of the cell are large accumulations of polysomes and free ribosomes indicative of a cell active in protein synthesis. Some microvilli can be seen at the periphery of the cell in section

zone and its related membranes of endoplasmic reticulum (ER), mitochondria, and lysosomal dense bodies by electron microscopy (Fig. 4). The ER contains numerous intracisternal A type (ICA) particles in various stages of development. These ICA particles are approximately 90 to 120 nm in their smallest diameter, and they possess a lucent core surrounded by a 30-nm dense rim (Figs. 5 to 13). A 6-nm membrane derived from the ER encloses the particle and separates it from the cisternal contents (Figs. 7 to 12). In

Fig. 5 The cytoplasm of a 3-day culture of tumor cells illustrating the intracisternal A type (ICA) particles, surrounding mitochondria, and parts of a Golgi complex. Depending upon the plane of section, there may be more or fewer of the ICA particles localized within a particular cell. Microvilli (mv) are easily seen at the cell's surface.

favorable sections a sequence can be constructed which appears to represent the formation of ICA particles. The cytoplasmic leaflet of the ER membrane (erm in Figs. 7 to 12) becomes more dense by apposition of a band of material on its cytoplasmic side. This band apparently extends laterally and may incorporate the ribosomes attached to the ER membrane. Such densified half membranes protrude into the cisternal space preceded by the ER membrane. This invagination of the wall of the cisterna defines a rounded body (which may vary in shape, depending upon the plane of section), the ICA particle, with a hemispheric rim at the periphery of which is the continuity of ER membrane and at whose core is a stalk of cytoplasm which in many planes of section appears detached or free within the cisterna (Figs. 6 to 12). Frequently, particles are observed budding from the cytoplasmic membrane of the nuclear envelope (Fig. 13). Occasionally, C type particles are found in the extracellular environment in the vicinity of the microvilli of the cells (Fig. 14). They have not been found budding from the cytoplasm.

In some cisternae, morphological evidence of lysosomal activity is found, which may be related to the degradation products of ICA particles. These consist of membrane-bounded large vacuoles containing membranous whorls, clear or dense vesicles with or without solid

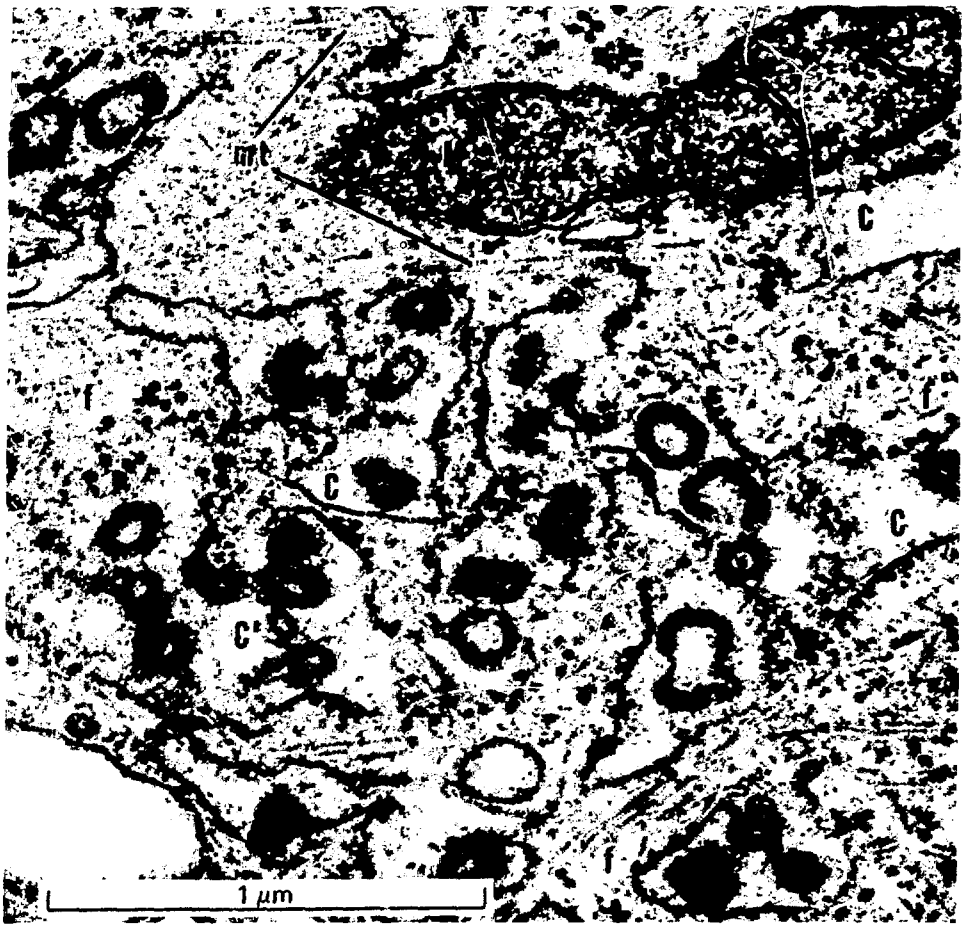

Fig. 6 Intracisternal A type (ICA) particles shown in relation to the cisternal space (C) of the endoplasmic reticulum. Those ICA particles within the cisternal space are surrounded by a unit membrane derived from the endoplasmic reticulum (ER). The dense outer shell of the particle is immediately subjacent to the membrane. A lucent core is usually apparent within a particle, depending upon the plane of section. In some instances the particle is attached to the membrane of the endoplasmic reticulum by a stalk-like process. Microfilaments (f) and microtubules (mt) can be seen coursing through the background cytoplasm.

cores, and a heterogeneity of densities from light flocculent distributions to heavy particulate material suggestive of lipofuscins (Figs. 15, 16, 18, and 19). Large multivesicular bodies (mvb's) (Figs. 15, 17, and 19) are frequently seen in these cells. Evidence from numerous other studies indicates that mvb's are regarded as a form of secondary lysosomes and appear to be functioning in that role here. The earliest association of ICA particles with lysosomes

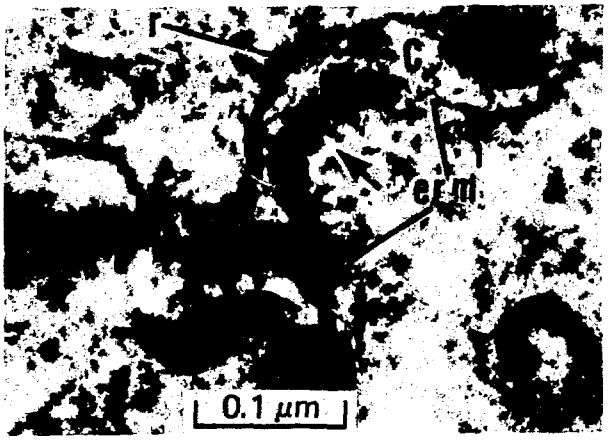

Fig. 7

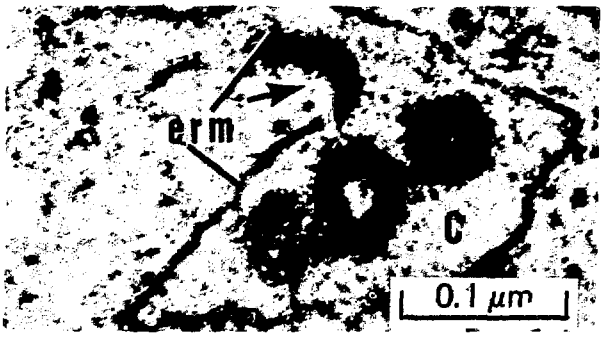

Fig. 8

Figs. 7 to 13 A series of photomicrographs taken from various preparations of tumor cells containing ICA particles which have been arranged in sequence that interprets the mode of formation of the particle within the cisternae. In Figs. 7 and 8, the endoplasmic reticulum membrane (erm), either with or without ribosomes, becomes more electron dense (arrows). In Figs. 9 and 10, the density appears to invaginate the cisternal cavity and remains delimited by a unit membrane (erm) derived from and continuous with the endoplasmic reticulum membrane. Such invaginations form a stalk-like arrangement (s) of the endoplasmic reticular membrane around the base of the particle. In Fig. 10 there is further prolongation of the stalk of this ICA particle as it projects into the substance of the cisterna. Occasionally one sees a scalloped margin of the cytoplasmic face of an invaginating endoplasmic ret cular membrane (erm) that has become electron opaque (Fig. 11), suggestive of the formation of multiple ICA particles which invaginate concurrently. Several of these are seen isolated, or nearly so, in Fig. 12 within the cisterna. In Fig. 13, the cytoplasmic component of the nuclear envelope contains an ICA particle attached by a stalk (s) to the cytoplasmic area subjacent to this region of the membrane. The nucleus (N) is seen above, and the density of the flocculent material within the nuclear envelope (ne) suggests active protein secretion.

(Figures continue on following pages.)

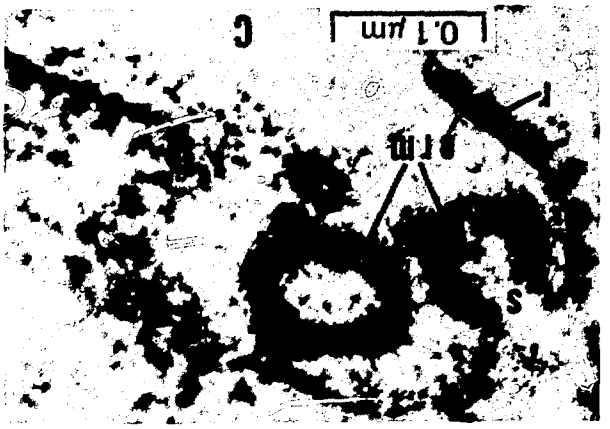

Fig. 9 See preceding page for legend.

Fig. 10 See preceding page for legend.

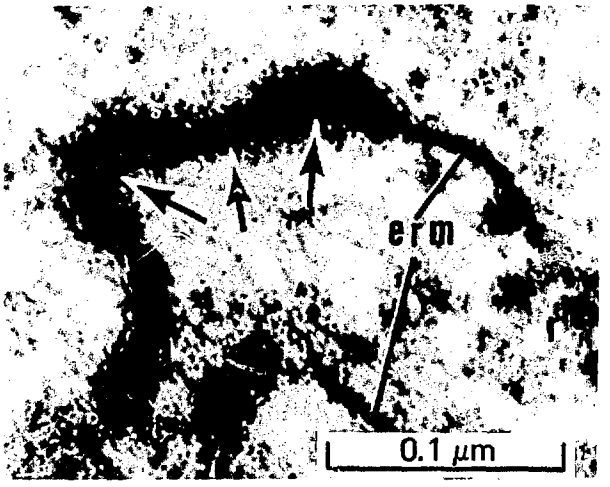

Fig. 11 See preceding page for legend.

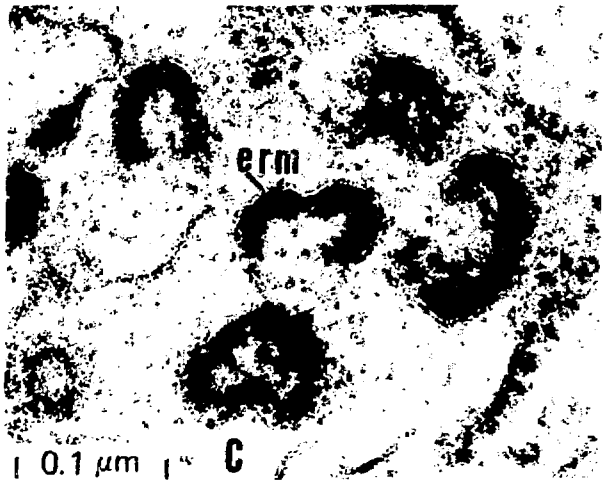

Fig. 12 See page 211 for legend.

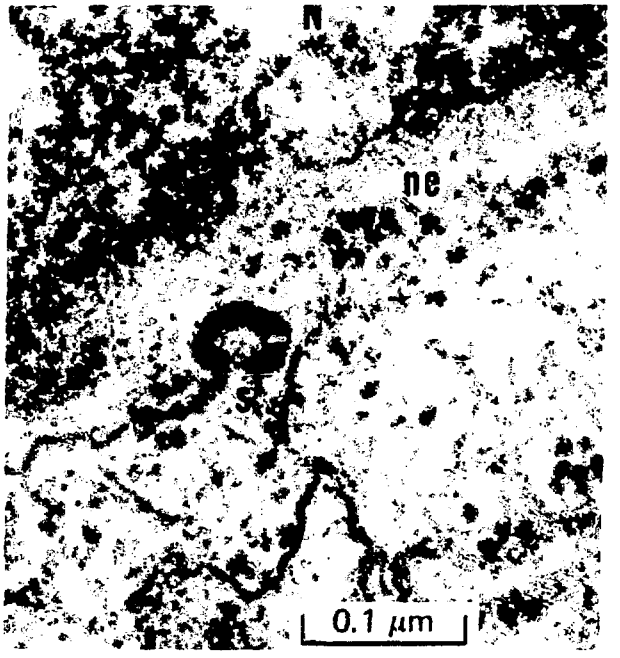

Fig. 13 See page 211 for legend.

produces a variety of membrane-bounded densities as seen in Fig. 15 (1 to 6). These consist of stages in the autodigestion of the contained ICA particles. Particulate densities of variable size suggest the disruption of ICA particles; the presence of condensed membranes of high electron density indicates a selective precipitation of oriented

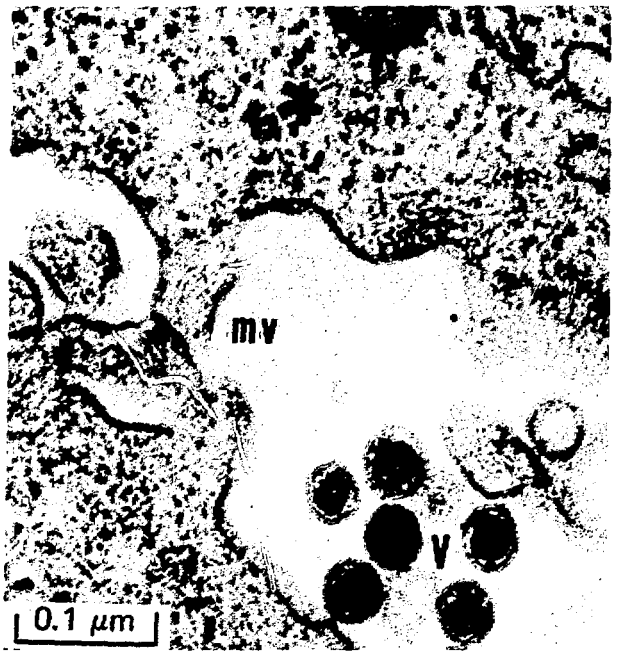

Fig. 14 C-type virus (V) particles in the extracellular environment, found in the vicinity of profiles of microvilli (mv). No evidence of budding of those particles is found.

products to form membranous whorls (residual bodies). See Fig. 16, Fig. 18 (1 and 2), and Fig. 19 (1 to 3).

The tumor cells, whether in vivo or in vitro, possess sparse, small microvilli on their surfaces (Figs. 4 and 5, respectively; also Figs. 14, 17, and 19). In the samples examined no evidence of adhesive specializations, i.e., tight junctions or desmosomes between cells, was encountered. Yet, in the preparations of tissue-culture cells of 4 to 8 days, the cells were relatively tightly packed and adjacent plasma membranes were closely adherent. If desmosomes or other junctional complexes were present, they were extremely small and relatively restricted in their localization and therefore not readily observed. Basal laminae are notably lacking from these cells (Figs. 4, 5, 14, and 17 to 19). The peripheral ectoplasm is filled with free ribosomes or polyribosomes (Figs 4 and 17), a characteristic of many undifferentiated cells. Cytoplasmic glycogen, a feature of developing type II cells,[8] was not observed in these tumor cells. Cells of this tumor possess 5-nm-wide microfilaments of indeterminate length and 20- to 24-nm-wide microtubules (Figs. 4, 5, 16, and 17). Such organized depositions of microfilaments are normally present in squamous cells like endothelia as well as in macrophages. Microtubules are ubiqui-

Fig. 15 Within the cisternae of cells from a 4-day tissue culture, elements of the intracisternal A type (ICA) particles undergo various stages of autophagy, here numbered 1 to 6. The formation of membranous lamellae (3 and 4) as well as coacervates of dense material (1, 2, 5, and 6), having either light or dark matrices, can be seen in areas that were formerly occupied by endoplasmic reticulum. These autophagosomes have resulted from fusion with lysosomes to bring about the heterogeneous-appearing, membrane-bounded elements. An enlarged multivesicular body (mvb) and mitochondrion (M) are identified.

tous among a great variety of cells, irrespective of their tissue of origin. An additional feature of some of these cells is the size of their mitochondria. In Figs. 18 and 20, a tumor cell with enlarged mitochondria is compared with a portion of the cytoplasm of a type II cell taken from a normal mouse lung. It is evident that mitochondrial size in both cells is approximately equal. In addition to a similarity in mitochondrial size, membranous whorls of much lighter density and less compactness, which we regard as lysosomal products (the numbered items in Figs. 18 and 19) should be compared with the lamellated bodies of normal lung in Fig. 20 (1 to 3). These membranous bodies within the tumor cells may represent

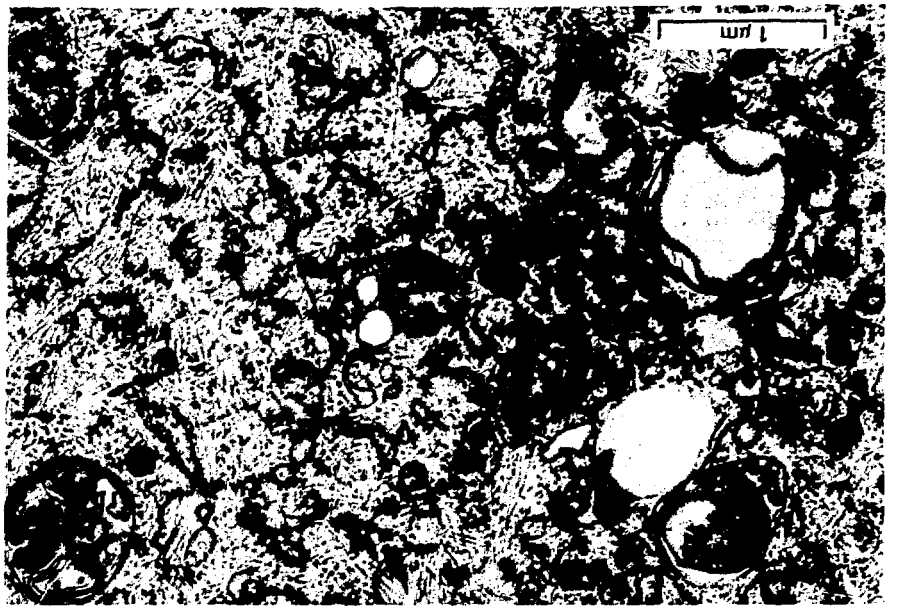

Fig. 16 A very fine, filamentous, cytoplasmic matrix is found in many of the cells. This 4-day tissue culture illustrates a residual body (rb), a stage in autophagy, as well as intracisternal A type (ICA) particles within the cisternae.

abortive efforts at intracellular surfactant production. Thus the tumor presents features of type I squamous cells and alveolar macrophages (microfilaments) and of type II cells (large mitochondria and abortive lamellated bodies).

To determine if the tumor contained surfactant activity in greater concentration than normal lung (e.g., a type II cell tumor might be expected to have a greater concentration of surfactant activity per milligram of tissue), we examined aliquots of the tumor and normal lung with a Wilhelmi balance. Hysteresis curves were described for normal lung after 2 min and 30 min, with the net change after 30 min of a reduction in surface tension from 45 to 12 dynes/cm. The tumor described a hysteresis curve between 52 and 28 dynes/cm after 30 min. Thus, although the tumor possessed some surface activity, it was not equal to nor did it exceed normal lung under our experimental conditions. It should be noted that non-lung tissue such as liver will produce hysteresis curves similar to that of the tumor. This nascent surface activity may be related to the sphingomyelin composition of the contained membranes. If this tumor had its origin in a type II cell or its progenitor, it no longer retains the differentiated state to produce surfactant as in normal lung.

Fig. 17 A portion of the cytoplasm of a 14-day tumor cell clearly shows cytoplasmic structure suggestive of other types of alveolar cells. Noteworthy is the presence of a peripheral filamentous (f) ectoplasm subjacent to the plasma membrane that possesses some microvilli. Next to the nucleus are groups of cellular microfilaments (f) not unlike those one might encounter in alveolar macrophages. Microtubules (mt) are also present. Two vesicular bodies bearing multiple small vesicles (1 and 2) are identified as multivesicular bodies (mvb's). These mvb's are a class of lysosomes. A perinuclear space of the nuclear envelope (ne) is conspicuous, as is the somewhat dilated cisterna (C) of the endoplasmic reticulum (ER) and associated ribosomal particles.

Fig. 18 A view of the periphery of a cell from an 8-day tissue culture showing large mitochondria (M). Also, two vacuoles containing membranous whorls are numbered 1 and 2. These vacuoles are probably autophagosomes, but they may represent an attempt at synthesis of surfactant precursor. They are usually found beneath the cell surface.

DISCUSSION

ICA Particles

Intracisternal A type particles are present in a wide variety of normal and neoplastic mouse tissues.[9-13] Our morphological observations of their occurrence and disposition in this alveolar cell carcinoma compare favorably with earlier reports. Many regard ICA particles as a biologic curiosity since they possess many of the properties of oncornaviruses except functional activity.[14] Unfor-

Fig. 19 Another cell from an 8-day tissue culture which shows microvilli (mv), examples of autophagosomes (1 to 3), and a multivesicular body (4). When compared to the lamellated bodies of a type II cell as seen in Fig. 20, these membranous whorls are less dense and are poorly compacted. If these autophagosomes are considered as a stage in an abortive attempt to manufacture surfactant, the cellular control of that process is no longer active in these tumor cells.

tunately, our studies do not provide the kind of data which would clarify the metabolic role of ICA particles in the genesis of oncornaviruses.

Our observations can be of interest to virologists, however, concerning the manner in which the ribonucleic acid (RNA) of the ICA particles is formed and recycled. The densification of the cytoplasmic leaflet of the endoplasmic reticulum membranes which involve the attached ribosomal particles as the first stage in the

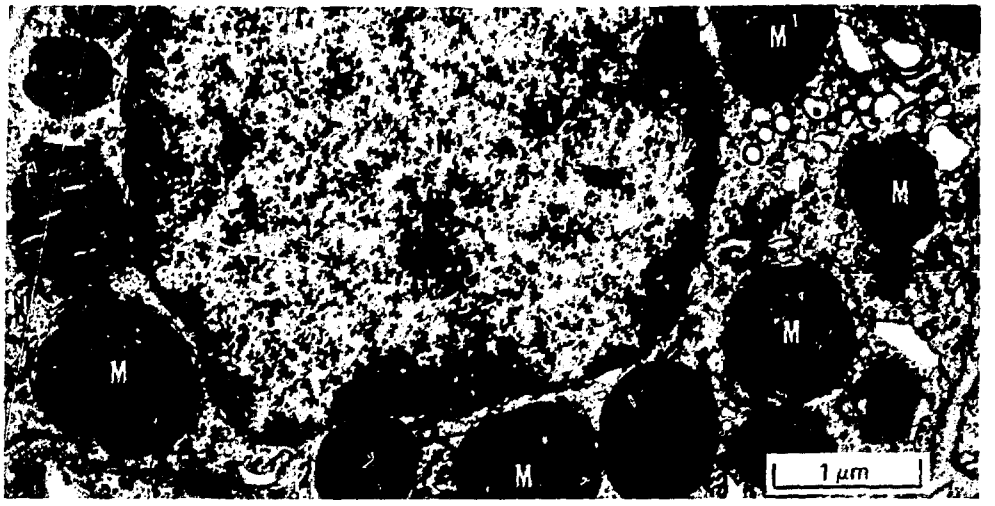

Fig. 20 A view of the cytoplasm of an alveolar type II cell from normal mouse lung illustrating the presence of large mitochondria (M) and lamellated bodies (1 to 3). The lamellated bodies consist of dense osmiophilic membranes, which are packed very closely and enclosed by a limiting membrane. Whereas large mitochondria similar to those seen in type II cells are also found in this tumor, dense bodies like these have not been observed in the tumors examined.

formation of ICA particles appears to represent a mechanism which incorporates the cells' own RNA into the shell of the ICA particle. When the densified wall of the endoplasmic reticulum (ER) invaginates into the cisterna, a stalk with cytoplasmic matrix is found enclosed in these membranes. This matrix area, which may be composed of soluble enzymes and other nonprecipitable substances, is destined to become the core of the ICA particle. Since the ICA particle is not usually found extracellularly, it appears to be retained intracisternally by a continuity with the ER membrane.[15] When lysosomal elements fuse with the cisternal contents and surround the ICA particles with soluble acid hydrolases, autophagy commences.[16] The initial steps consist of the formation of residual bodies in which membranous elements persist in membrane-bounded vesicles, and the more soluble substances consisting of amino acid fragments and other shorter chain proteins are returned to the cytoplasmic pool to be recycled. It is presumed that the structural proteins and RNA's associated with the nonmembranous fractions of the ICA particles are the substances recycled under the conditions of lysosomal autophagy.

Cellular Origin of Tumor

Evidence is presented that the tumor is a relatively undifferentiated carcinoma which contains some structures that can be associated with type I and type II epithelial cells and with alveolar macrophages. The tumor cells possess microfilaments which are found in squamous-type cells and macrophages, although the presence of microfilaments has been described in a wide variety of other nonepithelial cells. Of greater significance, however, is the fact that they do not possess junctional specializations and are lacking in basal laminae. Although sparse microvilli are present both in vivo and in vitro, these are not so regular in size or organization as those found in normal lung. A comparison of the size of mitochondria in some of the tumor cells with their counterparts in type II cells of normal lung suggests that this similarity may reflect a closer association in terms of the differentiation of the former from the latter.[17] In contrast to this suggestion are the data on the measurement of surface activity with the Wilhelmi balance. These data showed reduced hysteresis curves when compared with those of normal lung. Whereas the tumor may have been derived from either a type I or a type II cell, it retains only limited morphological semblance to either of these cell types. On the basis of its morphology and surfactant content, the tumor does not produce surfactant as found in normal lungs, and thus if the type II epithelial cell was the tumor's progenitor, the present tumor has lost its capacity to synthesize and release surfactant.

ACKNOWLEDGMENTS

The authors are grateful to Dr. Rogene Henderson of the Inhalation Toxicology Research Institute of the Lovelace Foundation in Albuquerque for her assistance in the use of her Wilhelmi balance; to Judi DeLongo for her excellent technical assistance; and to the National Cancer Institute, Division of Cancer Research Resources and Centers, for support under grants CA-14052 and CA-16127.

REFERENCES

1. J. M. Yuhas, N. H. Pazmino, J. O. Proctor, and R. E. Toya, A Direct Relationship Between Immune Competence and the Subcutaneous Growth Rate of a Malignant Murine Lung Tumor, *Cancer Res.*, 34: 722-728 (1974).

2. J. M. Yuhas, N. H. Pazmino, and E. Wagner, Development of Concomitant Immunity in Mice Bearing the Weakly Immunogenic Line 1 Lung Carcinoma, *Cancer Res.*, 35: 237-241 (1974).
3. J. M. Yuhas, R. E. Toya, and N. H. Pazmino, Neuraminidase and Cell Viability: Failure to Detect Cytotoxic Effects with Dye-Exclusion Techniques, *J. Nat. Cancer Inst.*, 53: 465-468 (1974).
4. J. H. Luft, Improvements in Epoxy Resin Embedding Methods, *J. Biophys. Biochem. Cytol.*, 9: 409-414 (1961).
5. B. F. Trump, E. A. Smuckler, and E. P. Benditt, A Method for Staining Epoxy Sections for Light Microscopy, *J. Ultrastruct. Res.*, 5: 343-348 (1961).
6. J. H. Venable and R. Coggeshall, A Simplified Lead Citrate Stain for Use in Electron Microscopy, *J. Cell Biol.*, 25: 407-408 (1965).
7. M. L. Watson, Staining of Tissue Sections for Electron Microscopy with Heavy Metals, *J. Biophys. Biochem. Cytol.*, 4: 475-478 (1958).
8. K. H. O'Hare and M. N. Sheridan, Electron Microscopic Observations on the Morphogenesis of the Albino Rat Lung, with Special Reference to Pulmonary Epithelial Cells, *Amer. J. Anat.*, 127: 181-206 (1970).
9. P. C. Calarco and D. Szollosi, Intracisternal A-Particles in Ova and Preimplantation Stages of the Mouse, *Nature (London) New Biol.*, 243: 91-93 (1973).
10. M. Potter, Immunoglobulin-Producing Tumors and Myeloma Proteins of Mice, *Physiol. Rev.*, 52: 631-719 (1973).
11. N. A. Wivel and G. A. Smith, Distribution of Intracisternal A-Particles in a Variety of Normal and Neoplastic Mouse Tissues, *Int. J. Cancer*, 7: 167-175 (1971).
12. R. Peach and W. E. Koch, A Cytoplasmic Inclusion in Mouse Trigeminal Neurons, *Amer. J. Anat.*, 140: 439-444 (1974).
13. W. Biczysko, D. Solter, C. Graham, and H. Koprowski, Synthesis of Endogenous Type A Particles in Parthenogenetically Stimulated Mouse Eggs, *J. Nat. Cancer Inst.*, 52: 483-489 (1974).
14. R. G. Krueger, Intracisternal A Particles from FLOPC-1 BALB/C Myeloma: Presence of High-Molecular-Weight RNA and RNA-Dependent DNA Polymerase, *J. Virol.*, 18: 745-756 (1976).
15. K. Perk and J. E. Dahlberg, Murine Intracisternal A Type Particles Fail to Separate from the Membrane of the Endoplasmic Reticulum, *J. Virol.*, 14: 1304-1306 (1974).
16. W. Bloom and D. W. Fawcett, *A Textbook of Histology*, 10th ed., pp. 48-52, W. B. Saunders Company, Philadelphia, 1975.
17. I. Y. R. Adamson and D. H. Bowden, Derivation of Type I Epithelium from Type 2 Cells in the Developing Rat Lung, *Lab. Invest.*, 32: 736-745 (1975).

Cytochemical Study of Glucose-6-Phosphate Dehydrogenase in Prenatal and Postnatal Rat Lungs

D. S. NEGI, K. D. LUNAN, and R. J. STEPHENS
Stanford Research Institute, Menlo Park, California

ABSTRACT

Glucose-6-phosphate dehydrogenase (G6PDH) was localized in rat lungs at different stages of gestation, on the day of birth, and in the adult animal. The first indication of the enzyme activity was observed in the epithelial cells of the elongating lung buds at about 14 days of gestation. This activity was restricted to the apical portion of the cells lining the developing airways. Between 16 and 18 days of gestation, the intensity of the reaction gradually increased in the epithelial cells of the bronchioles, and enzyme activity also appeared in alveolar type II cells. By the day of birth, the G6PDH activity had intensified considerably, but its distribution pattern remained unchanged. Adult lungs had achieved maximum intensity prior to 40 days of age.

Histochemical studies of organs and tissues are useful in the partitioning of chemical activities among the component tissues and cells. This demarcation of chemical boundaries to specific cells and tissues cannot be achieved by the fractionation and extraction methods of biochemistry.

In recent years there has been a growing interest in the developmental studies of the mammalian lung. However, most of these studies are purely morphometric in nature and generally deal with the postnatal lung growth.[1,2] Histochemical work on lung development is scant,[3] and little is known about the differentiation and cellular distribution of glucose-6-phosphate dehydrogenase (G6PDH) during the prenatal and postnatal development of the lung.

Glucose-6-phosphate dehydrogenase is a widely distributed enzyme in the animal and plant kingdoms, including bacteria.[4]

Together with phosphoglucoisomerase it plays a significant role in the metabolism of glucose, or glycogen, via the pentose phosphate shunt. The importance of the latter pathway in the generation of pentoses for the nucleotides, present not only in ribonucleic acid (RNA) and deoxyribonucleic acid (DNA) but also in coenzymes, such as nicotinamide adenine dinucleotide (NAD) and coenzyme A (CoA), is well known. The pentose phosphate pathway is also by far the most important source of $NADPH_2$ generation, which acts as a reducing agent in many synthetic reactions. Thus, by influencing the activity of the pentose phosphate shunt, G6PDH can control the production of its intermediary metabolites by altering the proportion of glucose that is metabolized via the Embden—Meyerhoff pathway and Krebs cycle as against the pentose shunt pathway.

Biochemical studies on the effect of NO_2 and O_3 on maturing rat lungs (35 to 40 days old) have consistently shown an increase of approximately 100% in G6PDH activity when the animals were exposed to NO_2 at 15 ppm for 72 hr as compared with a 50% increase when exposed to 0.9 ppm O_3 for the same length of time (see paper by Lunan et al., this volume). The above levels of the two toxic gases cause a remarkably similar amount of injury and repair in animals of this age.[5,6] Similar studies on nursing mothers and their infants, however, have shown a striking difference in the response of the two. Nursing mothers are hypersensitive, whereas postnatal animals (between 1 and 20 days of age) are extraordinarily resistant to injury from either NO_2 or O_3, although a mild cellular response has been observed in the epithelium of the terminal airways of animals exposed to NO_2 between 10 and 20 days of age.[7] After weaning at 20 days of age, there is an increasing tissue response in both the conducting airways and the proximal parenchymal tissue which reaches a plateau shortly after 30 days of age.

Biochemical response of G6PDH activity in the postnatal animals appears to parallel the observed sequence of structural injury and repair. Therefore we became interested in the cytochemical distribution of the enzyme during both prenatal and postnatal development.

MATERIALS AND METHODS

Timed pregnant Sprague—Dawley rats were obtained from Hilltop Laboratory Animals (Pittsburgh, Pa.). At daily intervals starting with the 10th day of gestation, one pregnant female was killed by an overdose of sodium pentobarbital. Since the lung buds prior to about the 16th day of gestation were too small for proper handling, the tissue was obtained as an approximately 2-mm-thick

slice through the entire peripulmonary thoracic region. Lungs from the fetuses of 17-day gestation and older as well as from the newborn and young adults were isolated and quickly divided into 2-mm^3 blocks. The tissues were quenched by dropping them in liquid nitrogen directly or in basket-type containers with a string attached for easy retrieval.

For sectioning, a tissue block was frozen to the cryostat chuck inside the chamber with a drop of distilled water or OCT (Tissue-Tek Products) compound, and the chuck, with the tissue attached, was placed on the "quick-freeze" block of the cryostat for 3 min. The tissue was then allowed to equilibrate with the temperature in the cryostat chamber (−20°C). Ten-micron-thick cryostat sections were cut and mounted close together, two to three sections per slide, shortly after the incubation medium had been prepared. The sections were allowed to dry thoroughly at room temperature with the use of a small hand-held fan.

Incubation Medium

The incubation medium contained the following ingredients. The amounts listed are for 20 ml of the complete medium. The control medium contains all the components of the complete medium except G-6-P (substrate). Details on the preparation of the incubation medium are given elsewhere.[8]

Polyvinyl alcohol (PVA) solution, 22% in Tris-maleate buffer (0.2*M*, pH 7.2), ml	20
Nitro blue tetrazolium chloride (NBT), mg	10
Nicotinamide adenine dinucleotide phosphate (NADP), mg	10
D-glucose-6-phosphate (G-6-P), sodium salt, mg	60

The fresh-frozen sections were incubated in the complete or control medium for 30 min at 37°C. Small incubation wells, made by cutting about 2-mm-deep sections from a 15- to 18-mm-wide glass tube were used around the sections to contain the medium and prevent runoff. After the sections had been incubated, the medium was washed off with distilled water, and the sections were mounted in glycerine jelly. The preparations were examined and photographed. The results are based on the observation of lungs from two animals at each developmental stage.

RESULTS

No perceptible amount of G6PDH could be demonstrated cytochemically in the foregut or developing primary and secondary

bronchi prior to the 14th day of gestation. On the 14th day, however, the apical cytoplasm of the columnar cells lining the expanding airways gave a positive response when deposits of NBT formazan were detectable, although the response was minimal (Fig. 1). At this time the conducting airways continue to lengthen and divide. However, the parenchymal elements are still undifferentiated, and mesenchymatous tissue surrounds the branching airways.

The lung undergoes considerable morphological differentiation during the next 3 to 4 days, and by the 18th day the alveolar spaces have started to form, and the lumens of the bronchioles become greatly enlarged. The G6PDH activity in the bronchioles is still

Fig. 1 Cryostat sections (7 μm thick) of lung from a 14-day-old fetus that had been incubated 20 min at 37°C for G6PDH localization. Maturing (upper) and a newly differentiated (lower) bronchiole with surrounding undifferentiated parenchyma are shown. Note the earliest inception of G6PDH (arrow) on the apical or lumen (L) side of the bronchiolar epithelium (BE). The newly differentiated secondary bronchiole (SB) shows no reaction at this early stage. (Magnification, 125 X.)

largely confined to the apical margins of the epithelial cells. In addition, G6PDH activity now appears elsewhere in the lung. These extrabronchiolar regions of activity generally appear as isolated spherical areas scattered throughout the differentiating parenchyma (Fig. 2). Examination of a mature lung for G6PDH distribution indicates that these sites of activity correspond in their general size and distribution to the location of maturing alveolar type II cells.

Between the 19th and 20th day of gestation, the activity of G6PDH in the bronchiolar epithelium, as well as in the extrabronchiolar sites, appears more intense (Fig. 3). The latter are not clearly distinguishable as type II cells until after birth (21 days). One day after birth the enzyme shows a further increase in activity, and,

Fig. 2 Cryostat sections (7 μm thick) of lung from an 18-day-old fetus that had been incubated 20 min at 37°C for G6PDH localization. Note the expanding lumen (L) and enzyme-active bronchiolar epithelium (BE). Extrabronchiolar sites of activity (arrows) represent the presumptive alveolar type II cells. The mesenchymal (M) tissue and the blood vessel (BV) are enzyme negative. (Magnification, 125 X.)

Fig. 3 Cryostat sections (7 μm thick) of lung from a 20-day-old fetus that had been incubated 20 min at 37°C for G6PDH localization. The enzyme-active bronchiolar epithelium (BE) and type II (T2) cells are shown. (Magnification, 275 X.)

although its distribution pattern remains unchanged, it is now clear that both ciliated and nonciliated cells of the conducting airways and the type II cells in the parenchyma contain substantial amounts of the enzyme (Fig. 4).

The activity and distribution of G6PDH in a 40-day-old young adult lung are shown in Figs. 5 and 6. In a normal animal maximum levels of the enzyme are present by this stage. Note the clear demonstration of the activity in the alveolar type II cells (Fig. 6). In contrast, the type I epithelial cells, together with the blood vessels, connective tissue, and smooth muscle surrounding the airways and larger blood vessels, are negative in their response to the cytochemical procedure.

Control experiments were carried out for each of the experimental stages shown in the figures. The control sections were treated

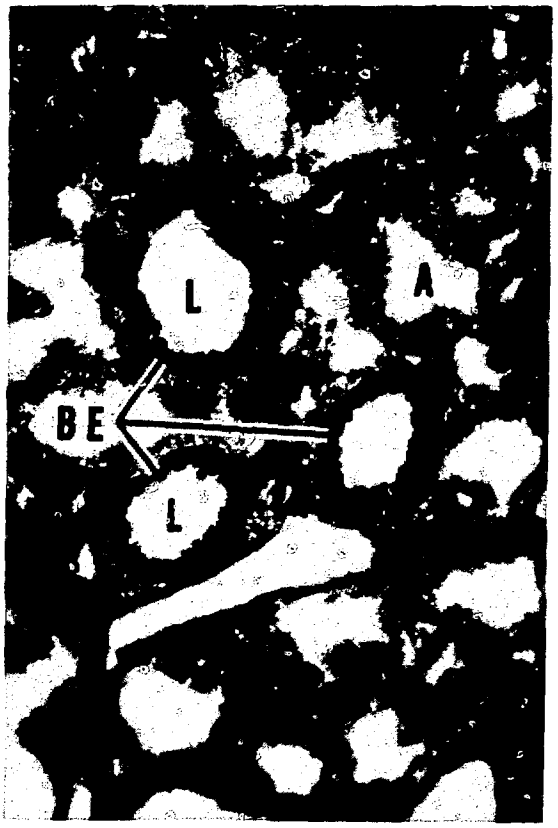

Fig. 4 G6PDH localization in a 1-day-old postnatal lung showing a visible increase in the enzyme activity at the bronchiolar epithelium (BE) as well as the extrabronchiolar sites. Lumen (L); alveolus (A). (Magnification, 125 X.)

identically to the section for the enzyme reaction except for the exclusion of the enzyme substrate (G-6-P) from the incubation medium. None of the control sections showed the characteristic NBT formazan deposition at the enzyme sites. One control, from a 40-day-old rat (Fig. 7), is included here as an example. We are currently exploring avenues to quantitate the cytochemical response most accurately with the hope that we will be able to demonstrate location of the increased enzyme activity.

DISCUSSION

Although mainly qualitative in nature, the results demonstrate a systematic and cell specific evolution of G6PDH activity in the

Fig. 5 G6PHD distribution in the bronchiolar epithelium (BE) and type II cells (T2) of a 40-day-old rat. Note the absence of the enzyme from the blood vessel (BV) and mesenchymal (M) tissue. (Magnification, 125 X.)

Fig. 6 Type II cells (T2) are the only extrabronchiolar sites of G6PDH activity in an adult (40 days) lung. The cells of the alveolar septa (AS) are devoid of enzyme reaction. (Magnification, 550 X.)

Fig. 7 Control section from a 40-day-old rat lung. Note the general absence of the NBT formazan from both active sites in Fig. 5. (Magnification, 125 X.)

prenatal rat lung. The enzyme was first detectable histochemically about the 14th day of gestation. At this stage the enzyme distribution was primarily along the lumen side of the bronchiolar epithelium. No reaction was obtained elsewhere in the lung bud at this stage of development.

Table 1 summarizes the results of the biochemical assay of G6PDH in the prenatal lung on the 14th, 18th, and 20th day of gestation and in the 1-day-old and 40-day-old postnatal lung.

It is evident from the table that there is a 44% increase in the biochemical activity of the enzyme between the 14th and 18th day. The differentiating type II cells, which become enzymatically active during this period, apparently account for a substantial part of this 44% increase. The increase was less pronounced (19%) between the 18th and the 20th day of gestation. The greatest increase (53.8% in 2 days), however, was observed in the 1-day-old postnatal lung. During the subsequent nursing period, there is a slow and histochemically undetectable increase in G6PDH activity that becomes stabilized within a week after weaning.

The study thus shows that the inception of G6PDH activity in the developing lung buds takes place in the bronchiolar epithelium on or about the 14th day of gestation. Type II cells, which constituted the only other enzyme-active components of the mature

TABLE 1

G6PDH IN PRENATAL AND POSTNATAL RAT LUNGS

Age,* days	G6PDH,† IU/g of wet tissue	Increase, %
−14	0.68 ± 0.01‡	
−18	0.98 ± 0.08	44.1
−20	1.17 ± 0.04	19.4
1	1.80 ± 0.06	53.8
40	2.83 ± 0.53	57.2

*Minus sign (−) before the age indicates gestation age.

†Biochemical changes in glucose-6-phosphate dehydrogenase activity in the prenatal and postnatal rat lung corresponding to the days of tissue collection for histochemical study.

‡This assay was performed using the entire peripulmonary thorax segment of the fetus.

lung, became active between the 14th and 18th day of gestation. One day after birth the lungs show a marked increment in G6PDH activity that becomes stabilized after weaning when the young adults have been on a carbohydrate-rich laboratory rat chow for about a week.

The significance of the inception of, and increase in, G6PDH activity at the observed stages of pulmonary development are highly conjectural. The relative abundance of the enzymes of the Krebs cycle[9,10] and glycolytic[11] and pentose shunt pathways[10,12] in the lungs indicates that it is a metabolically active organ. Since G6PDH is a key enzyme for the pentose shunt pathway, its inception and increase in activity can be taken as an indicator of the overall rate of the pentose shunt pathway at a given time. In addition to the biosynthesis of pentose sugars for nucleic acids, etc., the pentose phosphate shunt is generally regarded as by far the most efficient pathway for reduced nicotinamide adenine dinucleotide phosphate (NADPH) generation, which in turn is important for fatty acid synthesis.[13]

Sorokin[1,3] has indicated that, in the early stages of lung bud induction, the energy needs for cell division and synthesis of new protoplasm are met by the large accumulations of glycogen in the

advancing segments of the developing lung. It appears, therefore, that, in the maturing portions of the lung where the glycogen content occurs in diminishing amounts, the energy for cell maturation and differentiation is met by increasing reliance on the activity of the oxidative pathways and enzymes, such as G6PDH. It is of interest to note that there is some correspondence with respect to the time of glycogen decrease, as reported by Sorokin, and G6PDH induction, as observed in the present study (about the 14th day of gestation).

In another role G6PDH may be related to the production of phospholipids and pulmonary surfactants. As has already been pointed out, the pentose phosphate shunt is by far the most efficient source of NADPH generation, and the importance of the latter as a reducing agent in the biosynthesis of fatty acids from simple precursors is well recognized. Although the chemical nature of pulmonary surfactant is not fully understood, there is increasing evidence that its production is related to the accumulation of fatty acids and phospholipids in the lung.[14-16] Thus Gluck, Scribney, and Kulovich[14] reported a rise in the concentration of lipids before term in rabbit fetus, with the phospholipids constituting the major fraction. Azzopardi and Thurlbeck,[16] in their work on the histochemistry of the bronchiolar epithelium, concluded that the nonciliated (Clara) cells, which are rich in phospholipids, may be an important source of surfactant production. Similarly, Niden,[15] working with mouse lung, proposed that the nonciliated bronchiolar cell is the major site of pulmonary phospholipid production, which he presumed to be surfactant. The present study shows no distinction between ciliated and nonciliated cells of the bronchiolar epithelium with regard to G6PDH activity. Although Niden considers the alveolar type II cells to be phagocytotic and responsible for the clearance of lipids as well as other materials from the alveolar area, Sorokin[17] regards them as secretory along with the bronchiolar epithelium. Dermer[18] also believes that type II cells are the sites of synthesis and storage of the surfactant phospholipids. Thus there appears to be sufficient evidence to support the existence of a direct relationship between the G6PDH-positive pulmonary cells and the production of surfactant. However, the exact mechanism of the relationship and whether or not it is solely through NADPH and fatty acid synthesis is unclear.

Ayers, Tierney, and Herzog,[19] among others, have ascribed a protective function to the enzymes of the pentose pathway. It is now generally believed[19,20] that NADPH produced during the pentose pathway reduces glutathione, which in turn reduces some oxidants,

thereby affording protection to the lungs against oxidant injury. Since G6PDH is a key enzyme for the pentose pathway, a marked postnatal increase in its activity could be in response to the rather sudden exposure of the lungs to an alien oxidative environment of the newly born pups. The latter notion gains support from the fact that fetal development normally occurs under low oxygen tension,[1] and, as shown by organ culture experiments, even advanced stages of lung development can take place under entirely anaerobic conditions.[2,3]

ACKNOWLEDGMENTS

We wish to thank Donald Groth, Marlene Sloan, and May McKoon for their competent technical assistance.

This work was supported by Public Health Service grant ES00842-04.

REFERENCES

1. S. Sorokin, Recent Work on Developing Lungs, in *Organogenesis*, pp. 467-491, Holt, Rinehart & Winston, Inc., New York, 1965.
2. P. H. Burri, Postnatal Growth of the Rat Lung. III. Morphology, *Anat. Rec.*, 180: 77-98 (1974).
3. S. Sorokin, H. A. Padykula, and E. Herman, Comparative Histochemical Patterns in Developing Mammalian Lungs, *Dev. Biol.*, 1: 125-151 (1959).
4. M. Florkin and H. S. Mason (Eds.), *Comparative Biochemistry*, Vol. III, p. 433, Academic Press, Inc., New York, 1962.
5. R. J. Stephens, G. Freeman, and M. J. Evans, Early Response of Lungs to Low Levels of Nitrogen Dioxide: Light and Electron Microscopy, *Arch. Environ. Health*, 24: 160-179 (1972).
6. R. J. Stephens, M. F. Sloan, M. J. Evans, and G. Freeman, Early Response of Lungs to Low Levels of Ozone, *Am. J. Pathol.*, 74: 31-57 (1974).
7. R. J. Stephens, D. S. Negi, K. D. Lunan, D. G. Groth, and M. F. Sloan, Stanford Research Institute, unpublished, 1976.
8. D. S. Negi and R. J. Stephens, An Improved Method for the Histochemical Localization of Glucose-6-Phosphate Dehydrogenase in Animal and Plant Tissues, *J. Histochem. Cytochem.*, 25: 149-154 (1977).
9. A. G. E. Pearse, Extension of the Limits of Cellular Pathology: The Role of Enzyme Histochemistry, *J. Clin. Pathol.*, 11: 520-534 (1958).
10. D. G. Walker, A Survey of Dehydrogenases in Various Epithelial Cells in the Rat, *J. Cell Biol.*, 17: 255-277 (1963).
11. R. O. Oren et al., Metabolic Patterns in Three Types of Phagocytizing Cells, *J. Cell Biol.*, 17: 487-501 (1963).
12. S. Salisbury-Murphy, D. Rubenstein, and J. C. Beck, Lipid Metabolism in Lung Slices, *Am. J. Physiol.*, 211: 988-992 (1966).
13. J. Katz, B. R. Laudau, and G. E. Bartsch, The Pentose Cycle, Triose Phosphate Isomerization, and Lipogenesis in Rat Adipose Tissue, *J. Biol. Chem.*, 241: 727-740 (1966).

14. L. Gluck, M. Scribney, and M. V. Kulovich, The Biochemical Development of Surface Activity in Mammalian Lung, *Pediat. Res.*, 1: 247-265 (1967).
15. A. H. Niden, Bronchiolar and Large Alveolar Cell in Pulmonary Phospholipid Metabolism, *Science*, 158: 1323-1324 (1967).
16. A. Azzopardi and W. M. Thurlbeck, The Histochemistry of the Nonciliated Bronchiolar Epithelial Cells, *Am. Rev. Respir. Dis.*, 99: 516-525 (1969).
17. S. Sorokin, Activities of the Great Alveolar Cell, in *Conference on Neonatal Respiratory Adaptation*, T. Oliver (Ed.), Washington, D. C., National Institute of Child Health and Human Developments, 1965.
18. G. B. Dermer, A Method for the Visualization of Pulmonary Surfactant in the Light Microscope, *Arch. Int. Med. Symp.*, 9: 31-36 (1971).
19. L. N. Ayers, D. F. Tierney, and S. A. Herzog, Production of NADPH by the Pentose Pathway, a Possible Mechanism to Protect Lung from Oxygen, *Fed. Proc.*, 31: 355 (Abstract) (1972).
20. C. K. Chow and A. L. Tappel, An Enzymatic Protective Mechanism Against Lipid Peroxidation Damage to Lungs of Ozone-Exposed Rats, *Lipids*, 7: 518-524 (1972).
21. S. Sorokin, A Study of Development in Organ Cultures of Mammalian Lungs, *Develop. Biol.*, 3: 60-83 (1961).

Glucose-6-Phosphate Dehydrogenase Response of Postnatal Lungs to NO_2 and O_3

KENNETH D. LUNAN, PATRICIA SHORT, DALBIR NEGI, and ROBERT J. STEPHENS
Life Sciences Division, Stanford Research Institute, Menlo Park, California

ABSTRACT

The glucose-6-phosphate dehydrogenase (G6PDH) content of rat lungs does not increase until after 15 days of age following 3 days of exposure to 14 ppm NO_2 and until after 20 days of age with the similar exposure to 0.9 ppm O_3. The enzyme response to either gas increases linearly with age. With NO_2 it plateaus at 40 to 50 days, but with O_3 it peaks at 35 days of age and then drops sharply. In the linear regions the NO_2 response is always about 50% greater than the O_3 response. Continuous exposure to O_3 beginning at 10, 20, or 25 days produces about the same enzyme response by 33 days as a 3-day exposure beginning at 30 days. With 30- to 45-day-old rats, continuous NO_2 exposure produces a maximal G6PDH response at between 3 and 7 days, which then drops by 20% by 14 days of exposure. In contrast, animals allowed to recover in air after 3 days of exposure, the G6PDH returns to normal by 14 days. The capacity for G6PDH response begins at about the time of weaning. Dietary factors have not been implicated in this response to oxidant gases.

Studies in other laboratories have shown that, among the numerous metabolic and cellular responses of rat lungs to oxidant-gas exposure,[1] the increase in the content of G6PDH is prominent.[2-4] The present view is that, in addition to supplying metabolites for nucleotide, fatty acid, and steroid biosyntheses, the increased G6PDH also supplies reduced nicotinamide adenine dinucleotide phosphate (NADPH), which is needed to reduce lipid peroxides formed in cell membranes as a consequence of the oxidant-gas exposure.[2-4] We have investigated the comparative ability of NO_2 and O_3 to evoke this enzyme response in lungs of rats varying in age from 10 to 50 days.

The data presented here support the view that the two oxidant gases, NO_2 and O_3, act by different mechanisms[2,5-6] and demonstrate that early postnatal animals are resistant to cell damage by oxidant-gas exposure.

METHODS AND MATERIALS

The concentrations of the gases used, 14 ppm NO_2 and 0.9 ppm O_3, were chosen because they produced approximately the same morphological responses in the lungs of weanling rats.[7-10] In one experiment 20 ppm NO_2 was used. The exposure chambers and gas-monitoring equipment have been described previously.[11] Young Sprague—Dawley rats were bred at Stanford Research Institute from pregnant females supplied by Hilltop Laboratory Animals. So that sufficient animals could be obtained for experimental and control groups, several litters were divided with each group containing the same number of pups from each litter.

Ten- to 50-day-old rats were exposed to NO_2 or O_3 for periods varying from 1 day to 8 months. The rats were killed by an intraperitoneal injection of an overdose of sodium pentobarbital. The lungs were removed, homogenized in 5 volumes of 0.9% saline containing 0.5 m*M* ethylenediaminetetraacetic acid (EDTA), and centrifuged at 27,000 x *g* for 25 min at 4°C. The supernatant was assayed for G6PDH with the G6PDH STAT-PACK (Calbiochem). In early experiments the lungs were either perfused with saline or the values were corrected for the G6PDH content of the blood occluded in the lung. However, because the corrections had negligible effect on the results, the procedure was discontinued.

The inositol content of laboratory chow was determined with a Hewlett—Packard gas chromatograph. An aqueous extract of chow was lyophilized, dissolved in formamide, and silylated with Tri-Sil "Z" and bis(trimethylsilyl)-trifluoroacetamide (BSTFA) (Pierce Chemical Co.). The sample was injected onto a 6-ft by 1.3-mm-ID glass column packed with a 50—50 mixture of 3% SE-30 plus 3% OV-17 on gas chromatograph Q. The oven was temperature programmed at 150°C to 210°C at 4° per minute with a carrier flow rate of 20 ml of N_2 per minute.

The simulated rat milk diet was formulated by Teklad Test Diets (Table 1). The deoxyribonucleic acid (DNA) was assayed by the method of Burton.[12]

TABLE 1

SIMULATED RAT MILK DIET TD 75408*

	g/kg of diet
Casein, vitamin-free test	350.36
Lactose	130.43
Corn oil	380.43
Nonnutritive fiber (cellulose)	93.78
Mineral mix, *Williams—Briggs* modified (Teklad # 170911)	35.00†
Vitamin mix (Teklad # 40060)	10.00‡

*Teklad test diets.

†Supplies the following elements in milligrams per kilogram of diet: calcium, 6232; chlorine, 3472; copper, 5.2; iodine, 0.59; iron, 25.2; magnesium, 465; manganese, 50.1; phosphorus, 3993; potassium, 3828; sodium, 2109; sulfur, 642; zinc, 11.8.

‡Supplies the following nutrients in milligrams per kilogram of diet: *p*-aminobenzoic acid, 110; ascorbic acid, 1016; biotin, 0.441; vitamin B_{12}, 29.7; calcium pantothenate, 66.1; choline, 1434; folic acid, 1.98; inositol, 110; menadione (vitamin K_3), 49.6; niacin, 99.1; pyridoxine, 22.0; riboflavin, 22.0; thiamine HCl, 22.0; vitamin A palmitate, 39.6; vitamin D_2, 4.40; vitamin E acetate, 242; cornstarch, 4667.

RESULTS

Earlier experiments indicated that a 3-day exposure produced a maximum G6PDH increase in weanling rats. When the enzyme level after a 3-day exposure to NO_2 and O_3 was measured in lungs of younger rats, the surprising result was obtained (Fig. 1) that rats exposed to 10 days of age to either gas do not respond with an enzyme elevation, and at 15 days only NO_2 evokes an enzyme response. After this time the magnitude of the enzyme response increases linearly and at about the same rate for both gases up to age 40 days. Generally, NO_2 causes a doubling of the enzyme level at age 30 to 40 days, whereas O_3 exposure results in a 50% increase.

When these data are plotted as percentage of control values (Fig. 2), a further difference in the response to NO_2 and O_3 is obtained. The NO_2 response tends to level off after age 30 days at about 110%, whereas the O_3 response drops markedly after age 35 days.

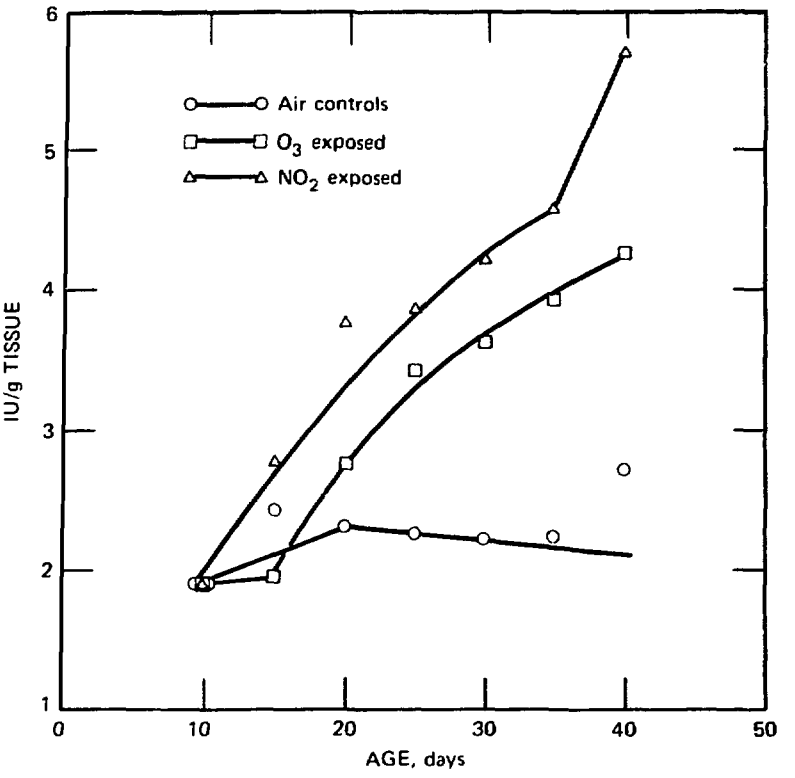

Fig. 1 Glucose-6-phosphate dehydrogenase in rat lungs exposed to oxidant gases.

When animals are continuously exposed to O_3, another interesting pattern emerges (Fig. 3). Animals of various ages, the earliest at 10 days, were exposed continuously to O_3, and the enzyme levels were determined periodically up to age 31 or 32 days. When exposure began at 10 days, no enzyme increase occurred until after age 20 days, which is consistent with Figs. 1 and 2. Then the enzyme level rose slowly, and at 31 days it was 50% above the control value. When exposure began at 20 days of age, the enzyme increase began after 3 days of exposure, rose at about the same rate, and again reached a level about 50% above the controls. When the exposure began at 25 days, the enzyme increased at a faster rate but again reached the same final level. Thus the data suggest that, regardless of when O_3 exposure begins, the same final level is reached at about age 32 days, and with O_3 no increase is possible prior to 20 days of age.

Comparable data for continuous NO_2 exposure are not yet available. However, Fig. 4 shows the results of an experiment in which 30-day-old rats were exposed continuously to 20 ppm NO_2

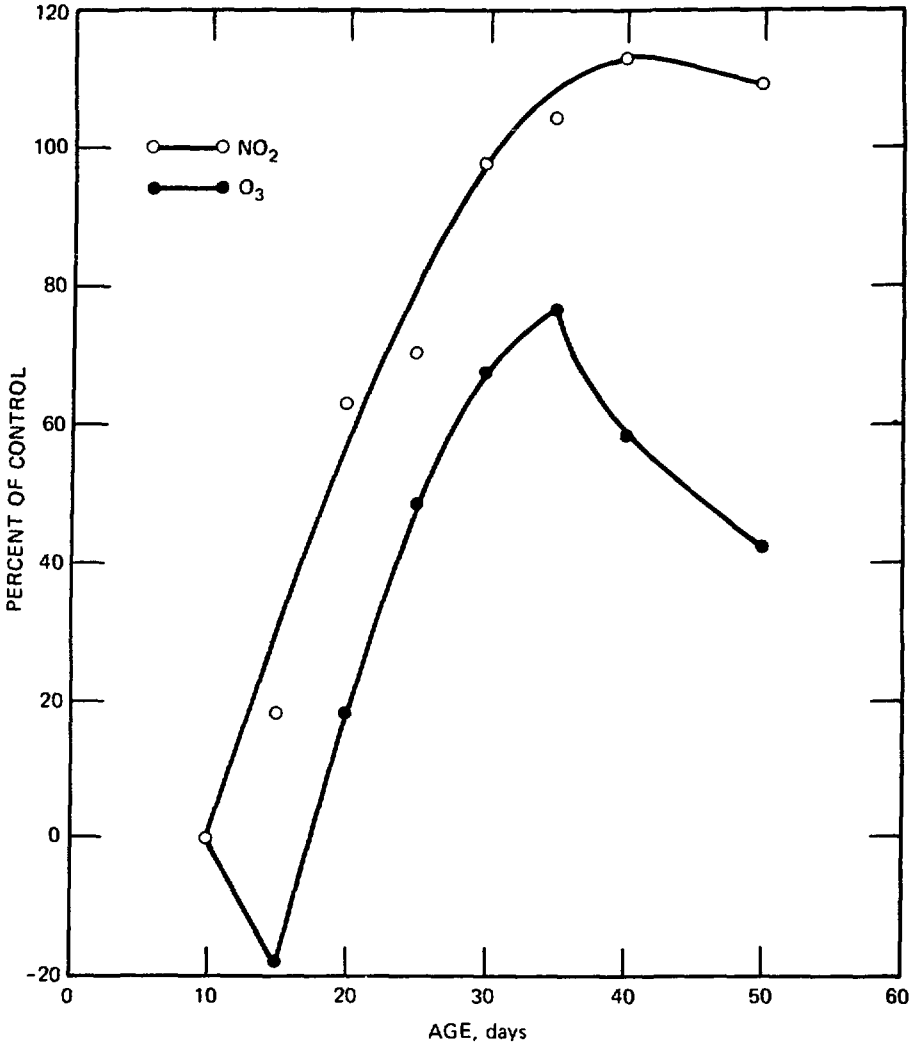

Fig. 2 Percent increase in lung G6PDH activity after oxidant-gas exposure.

for 2 weeks. The G6PDH activity peaked at 3 days and declined slightly by the end of 2 weeks of exposure. When animals were removed from the NO_2 after 3 days of exposure and allowed to recover in air, the enzyme level decreased to control values at the end of 2 weeks.

Returning to the O_3 exposures, we have considered the possibility that the inability of rats to respond to O_3 until after age 20 days may reflect the abrupt change in diet occurring at that time when they are weaned to laboratory chow. Rat milk is known to have a high content of both inositol[13] and fat,[14] whereas chow is low in fat and high in carbohydrate. At the time of this work, no data were

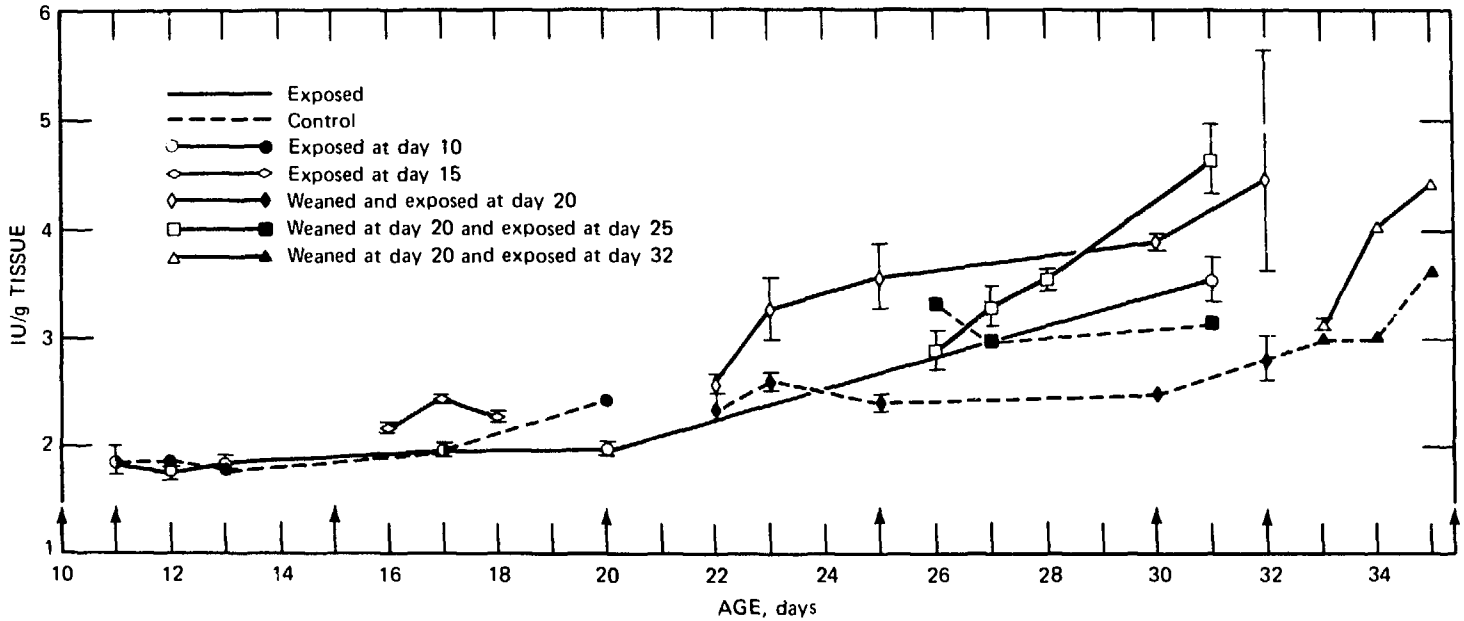

Fig. 3 Glucose-6-phosphate dehydrogenase in rat lungs exposed continuously to 0.9 ppm O_3.

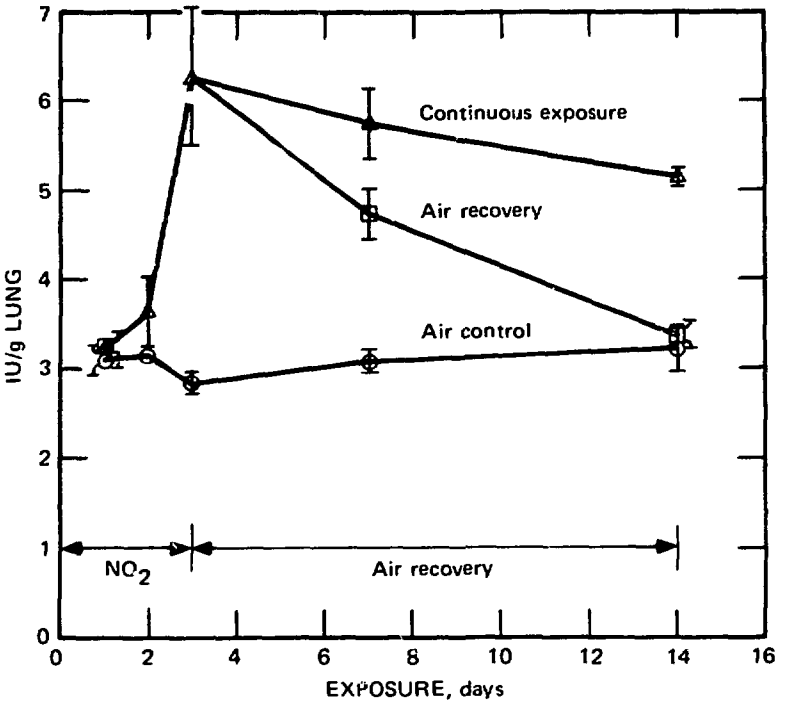

Fig. 4 Glucose-6-phosphate dehydrogenase in rat lungs after continuous exposure to 20 ppm NO_2 and air recovery.

available on the inositol content of chow. Gas chromatographic analysis of the chow later showed a content of 0.4 mg of inositol per gram of chow. Estimations of the intake of chow or rat milk indicated that animals on chow in fact received twice the amount of inositol (4 mg/day) as rats on milk (approximately 1.6 mg/day).

Nevertheless, a group of animals weaned to chow at 20 days were supplemented with a 10-fold excess of inositol in their drinking water. These animals gained weight at the same rate as water-fed controls, which indicates that the inositol had no adverse effect on their growth. Another group of rats were maintained on mother's milk. However, these animals did not gain weight, which indicates that they were not receiving adequate food from the mother. This result was unexpected, and consequently pair-fed controls were not provided. At 30 days of age, both groups were exposed to 0.9 ppm O_3 or 14 ppm NO_2 for 3 days, and then the lungs were assayed for G6PDH activity.

Table 2 shows that lungs from milk-fed and inositol-supplemented rats had the same increase in G6PDH activity as the control rats. For all three dietary groups, the response evoked by NO_2 exceeded that due to O_3, as previously noted. These data

TABLE 2

EFFECT OF INOSITOL AND MOTHER'S MILK ON G6PDH LEVELS IN LUNGS OF RATS EXPOSED TO OXIDANT GAS

Exposure	Diet,* IU/g fresh weight		
	Chow	Inositol	Milk
Air			
Average	2.47	2.40	2.41
± SD	0.29	0.19	0.29
O_3			
Average	3.26	2.93	2.95
± SD	0.31	0.31	0.27
ν†	10	11	10
t†	4.545	3.621	3.296
p†	<0.005	<0.005	<0.01
NO_2			
Average	3.86	3.62	3.98
± SD	0.21	0.57	0.63
ν	10	11	10
t	9.447	5.003	5.514
p	<0.001	<0.001	<0.001

*For each gas no significant differences were evident among the dietary groups.

†Parameters of Student's *t*-test for independent variables: ν, number of degrees of freedom; t, t statistic; and p, probability of statistical significance.

suggest that inositol alone had no effect on suppressing the elevation of G6PDH following oxidant-gas exposure. However, because of the stress of lowered food intake imposed on the milk-fed animals, we cannot assess from this experiment the effect of whole milk on the enzyme increase.

Another approach was taken in which animals at age 20 days were weaned to an isocaloric synthetic diet having the same fat and carbohydrate content as rat milk at 15 to 20 days of lactation. At age 30 days they were exposed to 14 ppm NO_2 for 3 days, and the G6PDH activity in lungs was measured. The growth rates of both the high-fat and chow-fed control groups were identical.

The data in Table 3 show that the enzyme response in both dietary groups was identical. This indicates that the high-fat content supplied by the corn oil in this diet was unable to suppress the increase in enzyme activity due to NO_2 exposure.

TABLE 3

EFFECTS OF A SIMULATED MILK (HIGH-FAT) DIET ON G6PDH LEVELS IN THE LUNGS AND LIVER OF RATS EXPOSED TO NO_2

Experiment	Diet, IU/g fresh weight		*t*-test		
	Chow	High-fat	ν*	t*	p*
Lungs					
Air control					
Average	1.72	1.64	8	0.456	N.S.†
± SD	0.17	0.34			
NO_2-exposed					
Average	3.90	3.68	10	1.152	N.S.
± SD	0.17	0.43			
ν	8	10			
t	19.405	9.213			
p	<0.001	<0.001			
Liver					
Air control					
Average	2.93	1.07	10	10.213	<0.001
± SD	0.18	0.33			
NO_2-exposed					
Average	2.56	0.51	10	5.725	<0.001
± SD	0.75	0.45			
ν	8	10			
t	0.936	2.462			
p	N.S.	<0.05			

*Symbols are defined in Table 2.
†N.S., not significant.

The G6PDH activity in the liver of rats fed the high-fat diet is considerably lower than that in the chow-fed controls. This effect is well known,[15-16] which indicates that liver supplied with preformed fatty acids does not require the metabolic machinery, including G6PDH, to synthesize this material. The G6PDH activity in the livers from NO_2-exposed animals fed the high-fat diet is significantly lower than that in the air controls. The chow-fed animals do not show an NO_2 effect, and its explanation is unknown at this time.

DISCUSSION

Several observations demonstrate that NO_2 and O_3 attack rat lung by different mechanisms: NO_2 provokes an increase in G6PDH

activity only after age 15 days, whereas a similar response to O_3 does not occur until after 20 days of age. The enzyme increase induced by NO_2 exposure is always higher than that caused by O_3 at concentrations of the gases that produce similar morphological responses.[7-10] Finally, the maximum G6PDH activity induced by NO_2 exposure levels off at about twice the control level at about 30 to 40 days of age, whereas in O_3-exposed lungs the enzyme peaks at 35 days of age and drops sharply thereafter. These differences in the responses of lungs to the two gases are not surprising since they are known to have different reaction mechanisms.[5-6]

The most significant observation is that prior to 15 to 20 days of age neither gas induces an elevation of G6PDH in rat lungs, and no morphological damage occurs. The timing of the appearance of an enzymatic response for the two gases coincides closely with the appearance and severity of morphological damage as judged by light and electron microscopy.[17]

These observations indicate that the lungs of young rats 15 to 20 days of age are resistant to both NO_2 and O_3 and that this resistance is gradually lost as the animals age from 20 to 30—40 days. The loss of resistance begins at the time of weaning, at 20 days of age when the diet changes abruptly from high-fat milk to low-fat chow. However, when animals weaned to a synthetic high-fat diet resembling rat milk at 15 days of lactation were exposed to NO_2, G6PDH activity increased just as much as the chow-fed controls. This result suggests that a high concentration of dietary fat alone is not responsible for the resistance of neonatal lungs to oxidant gas. Rat milk is a rich source of myoinositol, but dietary supplementation with this substance did not inhibit the loss of resistance to NO_2 or O_3. Indeed, it was estimated that the daily intake of inositol from chow was similar to or more than that from milk.

The source(s) of resistance to oxidant-gas exposure in neonatal lungs raises many interesting questions worthy of further research. For example, it is likely that the unsaturated fatty acid composition of neonatal lungs is similar to that of older lungs (preliminary data from this laboratory suggest that this is the case). If this is true and lipid peroxidation occurs in young lungs exposed to oxidant gas, then the disposal of the toxic lipid peroxides must not involve G6PDH and the glutathione shuttle. Alternatively, it is reasonable to expect that membrane damage caused by lipid peroxidation would be reflected in morphological damage, both of which are observed in older lungs.[2,17] Since structural damage does not occur in neonatal lungs, then peroxidation may not occur either. However, if neonatal and older lungs have similar fatty acid compositions, then neonatal

lungs must have one or more unique defense mechanisms to prevent peroxidation of the unsaturated fatty acids. Dietary factors may be involved. Neonatal lung cells may have a higher content of materials, such as vitamin E or sulfhydryl-containing compounds, which can buffer against peroxidative damage. Also, the age of the lung cells themselves may be important. These and other questions will have to be considered before the mechanism of resistance to oxidant gases by neonatal lungs can be understood.

ACKNOWLEDGMENTS

We thank Dr. Gustave Freeman, Director, Medical Sciences Department of the Life Sciences Division, SRI, for helpful discussions and for making available the NO_2 and O_3 exposure chambers. Dr. R. J. Spanggord performed the inositol assay. K. Jean Koskela assisted in the early phase of the research. This work was supported by National Institutes of Health Program Project grant 00842.

REFERENCES

1. C. E. Cross, A. J. De Lucia, A. K. Reddy, M. Z. Hussain, C. K. Chow, and M. G. Mustafa, Ozone Interactions with Lung Tissue, *Am. J. Med.*, 60: 929-935 (1976).
2. C. K. Chow and A. L. Tappel, An Enzymatic Protective Mechanism Against Lipid Peroxidation Damage to Lungs of Ozone-Exposed Rats, *Lipids*, 7: 518-524 (1972).
3. C. K. Chow, C. J. Dillard, and A. L. Tappel, Glutathione Peroxidase System and Lysozyme in Rats Exposed to Ozone or Nitrogen Dioxide, *Environ. Res.*, 7: 311-319 (1974).
4. A. J. De Lucia, M. G. Mustafa, C. E. Cross, C. G. Plopper, D. L. Dungworth, and W. S. Tyler, Biochemical and Morphological Alterations in the Lung Following Ozone Exposure, *AIChE (Am. Inst. Chem. Eng.) Symp. Ser.*, 71(145): 93-100 (1975).
5. J. N. Roehm, J. G. Hadley, and D. B. Menzel, Oxidation of Unsaturated Fatty Acids by O_3 and NO_2, *Arch. Environ. Health*, 23: 142-148 (1971).
6. J. N. Roehm and D. B. Menzel, Antioxidants vs. Lung Disease, *Arch. Int. Med. Symp.*, 9: 228-233 (1971).
7. R. J. Stephens, G. Freeman, and M. J. Evans, Early Response of Lungs to Low Levels of Nitrogen Dioxide, *Arch. Environ. Health*, 24: 160-179 (1972).
8. R. J. Stephens, M. F. Sloan, M. J. Evans, and G. Freeman, Early Response of Lung to Low Levels of Ozone, *Am. J. Pathol.*, 74: 31-57 (1974).
9. M. J. Evans, L. V. Johnson, R. J. Stephens, and G. Freeman, Cell Renewal in the Lungs of Rats Exposed to Low Levels of O_3, *Exp. Mol. Pathol.*, 24: 70-83 (1976).

10. M. J. Evans, L. V. Johnson, R. J. Stephens, and G. Freeman, Renewal of the Terminal Bronchiolar Epithelium in the Rat Following Exposure to NO_2 or O_3, *Lab. Invest.*, 35: 246-257 (1976).
11. G. Freeman, L. T. Juhos, N. J. Furiosi, R. Mussenden, R. J. Stephens, and M. J. Evans, Pathology of Pulmonary Disease from Exposure to Interdependent Ambient Gases (NO_2 and O_3), *Arch. Environ. Health*, 29: 203-210 (1974).
12. K. Burton, Determination of DNA Concentration with Diphenylamine, *Methods Enzymol.*, 12(B): 163-166 (1968).
13. L. E. Burton and W. W. Wells, Studies on the Developmental Pattern of the Enzymes Converting Glucose-6-Phosphate to Myo-Inositol in the Rat, *Dev. Biol.*, 37: 35-42 (1974).
14. T. D. Luckey, T. J. Mende, and J. Pleasants, The Physical and Chemical Characterization of Rats Milk, *J. Nutr.*, 54: 345-359 (1954).
15. D. R. Romsos and G. A. Leveille, Effect of Diet on Activity of Enzymes Involved in Fatty Acid and Cholesterol Synthesis, *Adv. Lipid Res.*, 12: 97-146 (1974).
16. J. J. Volpe and P. R. Vagelos, Saturated Fatty Acid Biosynthesis and Its Regulation, *Ann. Rev. Biochem.*, 42: 21-60 (1973).
17. R. J. Stephens, D. S. Negi, K. D. Lunan, D. G. Groth, and M. F. Sloan, unpublished, 1976.

Isolation and Characterization of Type II Alveolar Epithelial Cells and Alveolar Macrophages

YUTAKA KIKKAWA and FRED SMITH
Department of Pathology, New York Medical College, Valhalla, New York

ABSTRACT

A method was described for the isolation of viable and highly homogeneous population of type II alveolar epithelial cells from rat and rabbit lungs. After almost 500 such experiments, it was found that the purity of the preparation was 91 ± 7.0% and the viability was 92 ± 3.0%. Changes in trypsin concentration to 0.5% from the original 1% did not alter the gross yield of cells or the viability of these cells. The number of type II cells harvested with this method was $14.3 \pm 3.0 \times 10^6$ cells from 3-kg white New Zealand rabbits. A new simplified method to stain type II cells is described.

With the cells thus obtained, chemical characterization of type II cells and alveolar macrophages was performed. Type II cells were found to have a special capability of synthesizing palmitic acid from fatty acid precursors. Another feature of the type II cell is its ability to modulate unsaturated lecithins to a disaturated lecithin class. These two features were significantly different from macrophages. It is suggested that these precursors may be used as biochemical markers for type II cells in culture. Choline incorporation into disaturated lecithin did not differentiate type II cells from alveolar macrophages.

As an example for demonstrating the usefulness of isolated type II cells in pathological conditions, the type II cells were isolated after bleomycin treatment. Type II cells after bleomycin treatment exhibited increased ability to synthesize disaturated lecithins, but the ability of macrophages to synthesize disaturated lecithins was markedly depressed after this experiment. These data indicate that bleomycin stimulates surfactant production of type II cells and that a reported increase of disaturated lecithins in alveolar wash after bleomycin treatment may be the result of hyperactive type II cells. The current state of the art in lung cell isolation and culture is also discussed.

We have described a method for isolating homogeneous populations of type II alveolar epithelial cells from rat lung.[1] This method was

modified for the isolation of rabbit type II cells.[2] Since the original description of this method, we have had almost 2 years of experience with this technique, and biochemical characterization of type II cells and alveolar macrophages has advanced since our last publication.[3,4] There has been some modification of this technique during the last 2 years. This paper describes our experience in the isolation technique and summarizes the results of our studies on chemistry of type II cells and macrophages.

The usefulness of this technique in pathological conditions will be described in this paper. Recently, light- and electron-microscopic studies were carried out in mice treated with bleomycin in this laboratory.[5] It has been shown that in mice there is a hypertrophy of type II cells along with an increase of intracytoplasmic lamellar inclusions within the first week of treatment. In these animals we have demonstrated a marked increase of disaturated phosphatidylcholine within the alveolar wash fluids. Some of the several alternatives for the interpretation of these data are destruction of type II cells, destruction of macrophages, impairment of surfactant clearance, hypersecretion of the surfactant from hyperactive and/or increased numbers of type II cells, or any combination of the above. To study the mechanism producing increased phosphatide concentration in the alveolar wash fluids, we examined the possibility of obtaining type II cells from bleomycin-treated rabbit lungs. This report describes the successful isolation of type II cells from experimental animals and the results of functional studies on these isolated cells.[6]

Furthermore, various techniques to isolate lung epithelial cells are reviewed and compared. As will become apparent, there exists a deep gap of knowledge between freshly isolated type II cells and "type II-like cells" grown in culture. It is hoped that this paper may aid in bridging this gap in the future.

MATERIALS AND METHODS

Isolation Procedure

Approximately 500 New Zealand white male rabbits (2 to 3 kg) were used for this study. Rabbits were anesthetized with an injection of 50 mg of sodium pentobarbital per kilogram of body weight into the ear veins. After midline incision, the thoracic and abdominal cavities were opened, and a 20-gage needle was inserted into the inferior vena cava just above the diaphragm and tied in place. Approximately 1 liter of physiological saline was allowed to flow

into the inferior vena cava at a 50 cm H_2O pressure. With the start of infusion, the abdominal aorta was transected and the animal exsanguinated. Immediately after the above procedure, the superior vena cava was tied, and the trachea was cannulated with Teflon tubing. Thereafter the lungs were ventilated with room air until the end of infusion of saline.

The tracheobronchial tree was irrigated three times with Joklik's tissue culture medium. The lavage solution was stored at 0°C and was used as the source of alveolar macrophages. The lung parenchyma was then roughly dissected away from tracheobronchial trees with forceps and was stored in a Petri dish placed on ice. The lung fragments were then chopped into small blocks (0.5 mm in greatest dimension) with a Sorvall TC-2 tissue sectioner and placed in cooled (4°C) 100 ml of Joklik's solution. Tissue blocks were then shaken for 2 min with a vortex test-tube shaker. Free cells were discarded by filtering the suspension through nylon bolting cloth (HC160, Tetko, Inc.). Tissue blocks were incubated 30 min in 200 ml of 1% or 0.5% trypsin (Difco, 1/250, Difco Laboratories) in Joklik's medium. Two milliliters of a suspension of $BaSO_4$ was added to this solution. The suspension was prepared by vigorously mixing 40 to 50 mg of colloidal $BaSO_4$, particle size 0.1 to 0.3 μm, with 10 ml of Joklik's solution on a vortex mixer. The suspension was allowed to sediment at unit gravity for 1 hr, and the 2-ml aliquot was pipetted from the lower 6 ml. The $BaSO_4$, purchased from the C. F. Fleet Company, was dialyzed 2 days against distilled water. After 30 min of trypsinization, 40 ml of fetal-calf serum was added, and stirring was continued for another 5 min. The suspension was cooled to 4°C, and the cells were harvested by filtering the suspension through nylon bolting cloth (HC41, HC15). The suspension was filtered by adding an additional 300 ml of Joklik's medium (4°C). The crude cell suspension was then pelleted by centrifugation (10 min at 3000 rpm) in a refrigerated centrifuge. Pelleted cells were resuspended in 100 ml of cold Joklik's solution by gentle agitation with a glass pipette precoated with silicone. The cells were washed twice by repeating this procedure, and the last pellet was suspended in 100 ml of solution. The cell yield was counted in a Coulter counter, which was gaged to count particles larger than 300 μm^3. The cells were diluted to different concentrations for experiments designed to determine optimal cell density for the final isopycnic centrifugation. For most of the experiments, however, 500×10^6 cells were diluted in 120 ml of Joklik's solution. The cells were then layered on Ficoll–Joklik solution with a density of 1.047 (measured at 4°C). Each 50-ml tube had 25 ml of Ficoll–Joklik solution and 15 ml of cell suspension.

Centrifugation was carried out for 1 hr at 2300 X *g* in a refrigerated centrifuge.

The cells on top of a 1.047 Ficoll—Joklik layer were collected and washed three times with cold Joklik's solution at 2000 rpm for 10 min each. Cell numbers were counted in a Coulter counter. Smears of the cells were made and were stained in the following manner. This method was substantially simpler than our original published method.

1. Air dried.
2. Stained for 30 sec in Harris' hematoxylin stain.
3. Washed 5 sec in tap water.
4. Dipped in lithium carbonate once.
5. Washed 5 sec in tap water.
6. Dehydrated through graded series of ethanol solutions.
7. Cleared with xylene.

This smear was used in counting the purity of the cells.

Cell viability was determined with the trypan-blue dye exclusion method as described previously.[1] Electron-microscopic examination was carried out as described previously.[1,2]

Collection of Alveolar Macrophages

Alveolar macrophages were obtained by alveolar lavage with Joklik's solution. Only those lavage fluids which contained macrophages in a concentration of 95% or more were used.

Quantitative and Qualitative Lipid Analysis

A pool of 1×10^8 type II cells and a macrophage pool of similar size were obtained from four to six animals for each experiment; three separate experiments were performed. The cells were stored as centrifuged pellets at −20°C prior to analysis. The details of the method have been previously described.[2]

Precursor Study

About 5×10^6 cells were suspended in 1 ml of Hanks' solution of pH 7.4 in an open test tube for each assay; assays were done at least in duplicate for each experiment. The cells were incubated at 37°C with constant shaking for 30 min before radiolabeled precursors were introduced, and incubation was continued for 1 hr thereafter. For each precursor study, type II cells and macrophages, each in duplicate, and a control without cells were run simultaneously. Three experiments were conducted for each precursor.

The following isotopically labeled compounds were obtained from New England Nuclear Corporation: [1,2-^{14}C]ethanolamine hydrochloride (2.0 mCi per millimole), [1,2-^{14}C]choline chloride (21 mCi per millimole), [U-^{14}C]glycerol (111.8 mCi per millimole), L-[*methyl*-^{14}C]methionine (45.7 mCi per millimole), [1-^{14}C]palmitic acid (55 mCi per millimole), [1-^{14}C]oleic acid (55 mCi per millimole), [1-^{14}C]linoleic acid (57 mCi per millimole), [1,2-^{14}C]-acetate (54 mCi per millimole), and [1-^{14}C]palmitoyl,2-lysolecithin (22.1 mCi per millimole). Precursors were added to each 1-ml assay in the following amounts: 10 nmols of [1,2-^{14}C]choline chloride; 10 nmols of methyl-labeled choline; 20 nmols of ethanolamine; 2.4 μmols of glycerol; 20 nmols of methyl-labeled methionine; 87 nmols of palmitic, oleic, and linoleic acid;[3] 18.5 nmols of acetate; and 70 nmols of lysolecithin.[4] The concentration of choline, glycerol, ethanolamine, methionine, and acetate had been previously found to be at saturation levels. After incubation the cell suspensions were spun at 2000 rpm for 5 min, and the supernatant was decanted. The cells were then osmotically lysed with 0.5 ml of distilled water. Lipid extraction, thin-layer chromatography, and lecithin adduction were carried out as described.[2,3] The radioactivity was determined by scraping the silica from the thin-layer plates into counting vials, mixing with 1 ml of water and 10 ml of Aquasol (New England Nuclear Corporation), and counting in a Packard Tri-Carb liquid scintillation counter.

Isolation of Bleomycin-Treated Type II Cells and Macrophages and Its Precursor Incorporation

Six rabbits received bleomycin (Blenoxane, Bristol Laboratories) at a dose of 5 mg per kilogram of body weight for 7 days. Six rabbits received a daily injection of saline as control. Three rabbits were sacrificed at day 7 and the other three at day 14. Three controls were also sacrificed at day 7 and three at day 14.

The lungs after alveolar wash were subjected to the procedures for the isolation of type II cells as previously described. In both experimental and control groups, yields were similar at 15×10^6 type II cells per rabbit. Purity was better than 93% in both groups.

Macrophages were obtained after the alveolar washing fluid was collected for chemical study. The pellet of the cells obtained after centrifugation was suspended in 40 ml of Joklik's solution and allowed to stand at 4°C for 2 hr. The sediment contained macrophages in high purity (better than 95%).

For this experiment, [*methyl*-^{14}C]choline chloride (specific activity, 30 mCi/mmol) at a concentration of 10 nmols/ml of

incubating medium was used. Type II cells (5×10^6) and macrophages were each suspended in 1 ml of phosphate-buffered Hanks' solution for 30 min at 37°C, at which time precursor choline was added in 50-μl volume. All assays were carried out at 37°C in a rotating water bath in unstoppered centrifuge tubes; 1 hr after the addition of substrates, the assay was terminated by centrifuging, aspirating and discarding the substrate solution, and lysing the cells in 0.5 ml of distilled water. From a given rabbit, two to four aliquots of 5×10^6 cell suspension of a given cell type were used. The lipids were extracted and separated, and the radioactivity was determined as described elsewhere.[5,6]

RESULTS

Table 1 shows the results of crude cell yields and purity and viability of type II cell yields after 112 experiments with 1% trypsin and 152 experiments with 0.5% trypsin. In essence, there are no appreciable

TABLE 1

TYPE II CELL YIELD, VIABILITY, AND PURITY

Trypsin concentration, %	Crude cell yield	Type II	Viability, %	Purity, %
1.0*	$482 \pm 36 \times 10^6$†	$14.2 \pm 2.5 \times 10^6$	92 ± 3.0	91 ± 7.0
0.5‡	$475 \pm 25 \times 10^6$	$13.8 \pm 1.8 \times 10^6$	93 ± 3.0	92 ± 8.0

*Total number of experiments, 112.
†Values are mean ± SEM.
‡Total number of experiments, 152.

changes between 1% and 0.5% trypsin in all the parameters we have studied. In both groups the yield of mixed cells after trypsinization was in the neighborhood of 500 million cells. Recovered type II cells were almost always 3% of the total cells layered on the gradient. Since about 30% of crude cell suspension is type II cells, as reported previously,[1] about 10% of the dissociated type II cells are recovered with this technique. These results have been obtained consistently except for exceptionally hot and humid days and the days when the isolation procedure took an exceptionally long time. On the average, the total time required for the completion of this procedure was 5 hr. As a rule, the shorter the period, the better the results in terms of purity and viability.

TABLE 2

EFFECT OF CELL DENSITY ON TYPE II CELL PURITY*

Concentration of crude cells/15 ml	Number of experiments	Type II cells	
		Purity, %	Viability, %
150×10^6	4	60 ± 12.0†	90 ± 4.0
120×10^6	4	65 ± 10.0	88 ± 5.0
100×10^6	4	85 ± 6.0	92 ± 2.0
80×10^6	4	93 ± 4.0	89 ± 6.0
60×10^6	4	93 ± 3.0	93 ± 5.0
40×10^6	4	92 ± 2.0	91 ± 2.0

*200 cells on smear were counted for each experiment.
†Values are mean ± SEM.

Table 2 indicates the effect of cell density on the purity of type II cells. In all experiments 25 ml of Ficoll—Joklik solution and 15 ml of cell suspension were used in a 50-ml tube. The gradients were centrifuged for 1 hr at 2300 × *g*. The results indicated that a cell density over 100×10^6 cells per 50-ml tube is detrimental in the recovery of purer type II cells. When the purity was poor, polymorphonuclear leukocytes, lymphocytes, and macrophages were the chief contaminants, whereas contaminants at a better purity were chiefly lymphocytes and macrophages. In Table 1 experiments done with over 100×10^6 cells per tube were eliminated from the figure. The results in Table 1 reflect experiments conducted with a cell density of almost always 80 million cells per tube. The viability had little correlation with purity.

We have previously published the results of a modified Papanicolaou procedure for light-microscopic staining of type II cells.[1] The staining of type II cells described here is easily and quickly done, and the result was similar to our original method.[1] After mounting, stains did not fade for as long as 2 years.

Figure 1 is an electron micrograph of a typical type II cell pellet. Endoplasmic reticulum was often dilated after the isolation procedure. Lamellar bodies appear normal as compared to in vivo lamellar bodies. It is to be noted that block staining enhances electron density of inclusions of rabbit cells both in vivo and in vitro and hence the appearance differs from that previously published.[2]

Figure 2 shows freeze-fractured lamellar bodies of isolated type II cells. Orderly lamellae as seen in this preparation are similar to those reported elsewhere.[7,8] Lamellae are uniform without

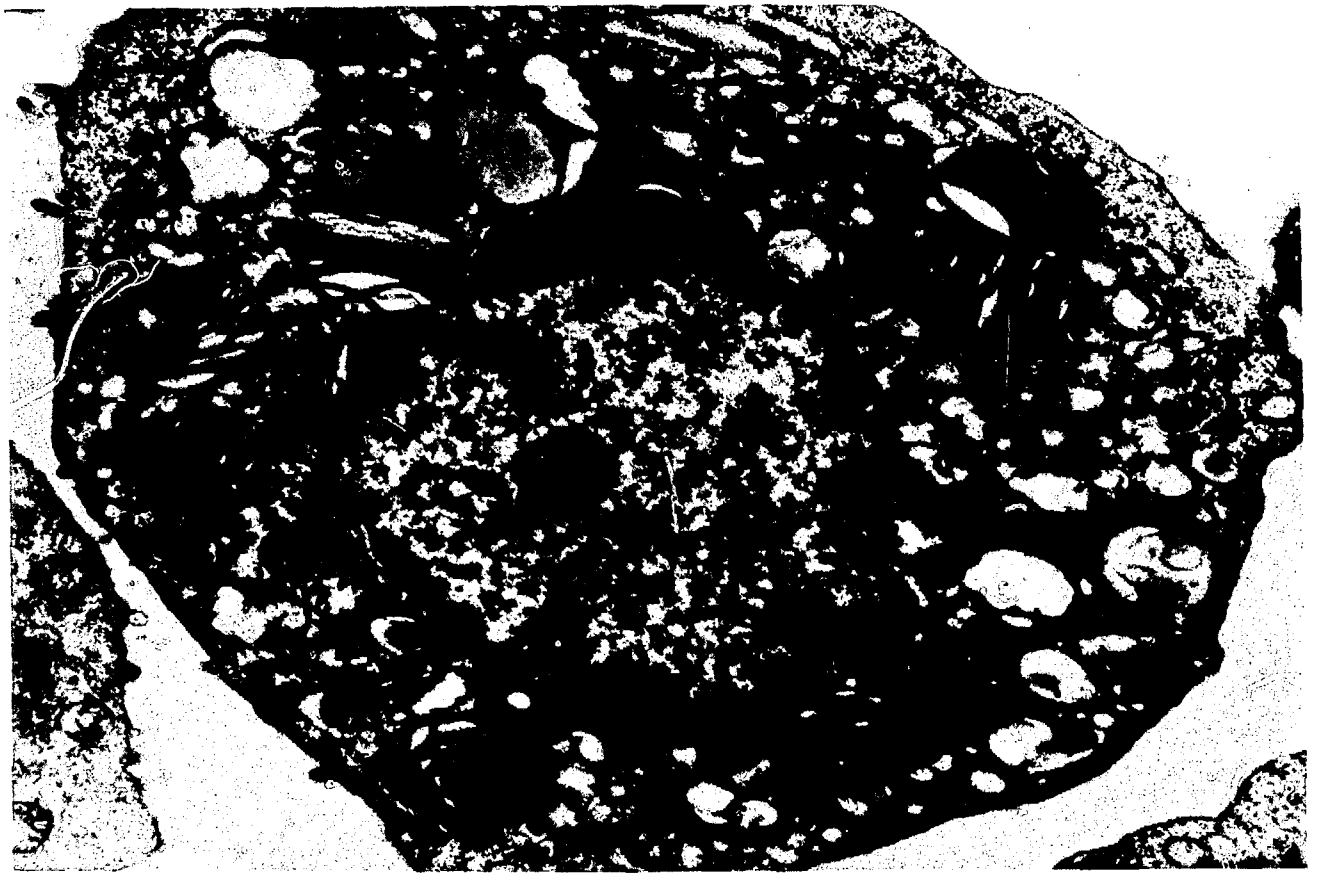

Fig. 1 Isolated type II cell retains microvilli. There is dilation of endoplasmic reticulum; lamellar inclusions appear normal. Rabbit type II cell, uranyl acetate and lead citrate stain. (Magnification, 15,000 X.)

Fig. 2 Lamellar body of isolated type II cell. Note stacks of lamellae without intermembranous particles. Freeze-fractured preparation, −145°C, platinum and carbon replica. (Magnification, 200,000 ×.)

TABLE 3

LIPID, PROTEIN COMPOSITION, TYPE II CELLS, AND MACROPHAGES

Cell type	Protein, mg	Total lipid, mg	Total lipid phosphorus, μg	Total disaturated lecithin,* %
Type II†	5.7 ± 2.1‡	4.5 ± 1.1	110.0 ± 17.0	23.8 ± 1.2
Macrophage†	13.6 ± 1.4	5.2 ± 1.0	155.0 ± 12.0	10.1 ± 0.8

*Percent of total phospholipid.
†Analysis of 100×10^6 cells.
‡Values are mean ± SEM.

intermembranous particles. There were no tubular myelin figures in our fractured samples.

Table 3 shows concentrations of disaturated lecithin (DSL) in type II cells and macrophages. As shown, type II cells contain twice as much DSL as macrophages.[2]

Table 4 demonstrates DSL concentrations of type II cells,[2] macrophages,[2] and various organs.[9] This comparison indicates that whole-lung homogenates fail to document high concentration of DSL in the lung. Isolated preparations of type II cells, however, clearly indicate that these cells contain exceptionally high concentration of surfactant lecithin.

Table 5 is a summary of rates of precursor incorporation into the disaturated lecithin fraction of type II cells abstracted from our previous publications.[2,3,4] These data indicate substantial differences in synthetic ability between type II cells and macrophages. With the use of cells suspended in Hanks' balanced salt solution, type II cells did not differ from macrophages in the ability to synthesize DSL when choline was used as a precursor, whereas other substrates, such as lysolecithin, palmitate, oleate, linoleate, and acetate, showed a clear difference.

TABLE 4

DISATURATED LECITHIN CONCENTRATION (μg/mg PROTEIN)

Type II cells	Macrophages	Lung	Brain	RBC	Liver
4.6*	1.1*				
	1.06†	1.34†	1.67†	0.01†	0.90†

*From Ref. 2.
†From Ref. 9.

TABLE 5

DISATURATED LECITHIN SYNTHESIS IN TYPE II CELLS AND MACROPHAGES*†

Substrate	Type II cells disaturated lecithin, pmols	Macrophages disaturated lecithin, pmols
Choline	369	498
Ethanolamine	0	0
Lysolecithin	451	60
Palmitate	4727	399
Oleate	390	99
Linoleate	231	54
Acetate	89	‡

*Summarized from Refs. 2 to 4.

†Values are for 10^7 cells incubated in Hanks' medium for 1 hr at substrate saturation level.

‡Negligible.

Table 6 summarizes the results of in vitro incorporation of labeled choline into the disaturated class of lecithin in type II cells and macrophages after bleomycin treatment.

After 1 hr of incubation with precursor choline, the type II cells synthesized 1.6 times as much total lecithin after bleomycin treatment (day 14). When lecithins were separated into DSL and other lecithins, DSL was shown to be increased roughly three to four times in the experimental group. This trend was seen also at day 7. Macrophages after bleomycin administration progressively lost their ability to incorporate choline into disaturated lecithin. At day 14 disaturated lecithin synthesis from precursor choline dropped to 25% of the control value.[5]

DISCUSSION

The lung is a difficult organ to study in many respects. For ultrastructural study, one is required to examine many more sections than with solid organs because a large volume is occupied by air. Furthermore, the lung contains many different cell types. It is stated that the lung contains 40 different cell types.[10] For practical purposes, there is a smaller number of important cells that require intense studies. These are the ciliated and goblet cells of the airways,

TABLE 6

IN VITRO INCORPORATION OF [*METHYL*-^{14}C]CHOLINE INTO LECITHIN IN TYPE II CELLS AND MACROPHAGES AFTER BLEOMYCIN TREATMENT

	Control	Day 7	Day 14
Type II Cells			
Number of cells	5×10^6	5×10^6	5×10^6
Amount of lecithin synthesized, nmol*	0.83 ± 0.21	1.12 ± 0.24	1.35 ± 0.37
Composition of lecithin, %			
DSL†	35 ± 3	51 ± 3	70 ± 4
Others†	65 ± 3	49 ± 3	30 ± 4
Macrophages			
Number of cells	5×10^6	5×10^6	5×10^6
Amount of lecithin synthesized, nmol	0.72 ± 0.15	0.45 ± 0.13	0.18 ± 0.07
Composition of lecithin, %			
DSL	32 ± 3	30 ± 3	33 ± 4
Others	68 ± 3	70 ± 3	67 ± 4

*Values are mean ± SEM (3).
†DSL, disaturated lecithin; others, other lecithin.

types I and II alveolar epithelial cells, Clara cells, the vascular endothelial cells, and some mesenchymal cells, in addition to the free alveolar macrophages. Particularly important, as well as distressing, is the fact that no one type of lung cell predominates in number over the other cell types. Because of this heterogeneity, biochemical studies with whole lung will not necessarily give insight into the function of individual cell types. For example, dipalmitoyl phosphatidylcholine (DPL), a unique pulmonary surfactant lipid, is not a unique compound quantitatively or qualitatively if lung homogenate is used for this study.[9] Our studies with freshly isolated alveolar type II cells, however, for the first time demonstrated that the quantity of this DPL is uniquely higher in the type II cells.[2] Alveolar washing fluid gives another special compartment for study, and this compartment has been shown to contain an unusually high proportion of DPL among other phospholipids. Thus after almost 20 years of study on pulmonary surfactant, it has now become reasonable to relate the synthesis and the secretion of pulmonary surfactant to

type II cells. The above example shows how important it is to obtain pure population of cells to gain better knowledge of any biological system.

Our results on the synthetic capability of type II cells are obtained from type II cells of rabbits. The incubating medium was a simple balanced salt solution, and incubations were limited to a 1-hr interval. It is important to recognize that the results thus obtained may be significantly altered from those which may obtain in type II cells in vivo since these cells have gone through rather vigorous procedures. As our previous report indicates, trypsin treatment of macrophages results in marked reduction of their ability to incorporate [^{14}C]choline into lecithin.[2] The results obtained with macrophages may be considered close to those operative in in vivo macrophages. For a better insight into in vivo type II cell functions, it will be necessary to study the function of type II cells in short- and long-term culture in many different culture media. Even with certain reservations inherent to the type II cells thus isolated, certain important functional differences between type II cells and macrophages have become apparent. These differences exist in the handling of lysolecithin, fatty acids, such as palmitate, and fatty acid precursor, such as acetate, whereas the values for choline were similar in both cells.[4] The magnitude of difference could not be accounted for by a difference in permeability of precursors into the cells or the pool size of unlabeled compounds used as the precursors. These differences indicate that type II cells synthesize palmitate from precursors at a significantly greater rate than do macrophages and that DSL synthesis in type II cells seems dependent on deacylation of unsaturated lecithin and remodeling of this lysolecithin into disaturated lecithin either by reacylation or transacylation. Further, that in our system [^{14}C]choline was ineffective in differentiating these two cell types speaks for a hypothesis that [^{14}C]choline incorporation in lecithin reflects the synthesis of monounsaturated lecithin through the cytidine diphosphate—choline pathway.

Careful consideration is required to translate our results directly into cultured cell lines. For our results to be more applicable to cells in culture, biochemical studies, similar to those just reported with isolated cells, must be carried out with different enriched media. Chemical results obtained from freshly isolated type II cells in enriched media should then be followed for some period of time. Only then can some meaningful comparison be made between freshly isolated type II cells and other type II-like cell lines. Our results, however, clearly indicate that, in all cell lines available, incorporation of acetate, palmitate, lysolecithin, and choline should be carried out

to come to some understanding as to the origin and function of type II-like cell lines.

Three approaches in obtaining pure populations of type II cells are (1) isolation by enzymatic dispersion and gradient centrifugation, as we have done; (2) cloning of cells in primary culture; and (3) reconstruction of type II cell lined alveoli in culture after dissociation of mixed cells by enzyme.

Our laboratory has been involved in the first approach for the last 3 years. Our experience in this separation technique has involved mostly Sprague—Dawley rats and New Zealand white rabbits. We have, however, had successful experiences with human lungs obtained at operating rooms. It is to be noted that any departure from the basic methods can be a disaster in terms of purity or viability of these cells. For example, number and speed of washing of cells after trypsin digestion and gradient centrifugation affect [^{14}C]choline incorporation profoundly. Longer than usual hours spent in cell separation, such as with newly hired technicians, also have similar effects. The number of cells layered on a given gradient affects purity rather drastically (Table 2). Therefore the number of cells obtained after trypsinization should be recorded and the number of gradients adjusted for each experiment. The counting of the number of crude cells is also important because the effect of trypsin varies according to the lot number of trypsin that was commercially obtained (Difco Laboratories). When we exclude these unfortunate experiments, we have had rather consistent results in our cell-separation experience, as indicated in Table 1. These results have been obtained from several different persons engaged in this project. Hence the purity tends to be lower than the initial value reported.[1]

Another approach to the separation of type II cells has used principles similar to those we have described.[11] Further purification of the yield was accomplished by differential adhesion in primary culture of these cells. The details of this study are published in this symposium (see R. Mason, this volume). It is important to note that these type II cells have now been shown to secrete DPL into culture medium under certain specified conditions. The biochemical characterization of these cells, however, is not yet available.

As mentioned earlier, there are several clones of cells that might be type II cells (we have collectively termed these type II-like cell lines). Kniazeff and his associates[12] reported several clones of epithelial cells from fetal-cat lung which they believed represented type II cells. The clones A, C, and D were diploid. These had doubling times of about 20 hr. Published electron micrographs, however, showed so-called "lamellar bodies" at low power without

orderly lamellae, as shown in Fig. 2. These clones may well be type II cell clones. They require further morphological and biochemical studies to be considered as a useful model.

Lieber and his associates[13] have described a cell line (A549) that has been growing for the last 4 years. These cells are presumably derived from a human alveolar cell carcinoma. These are transformed cells. Published micrographs of these cells, however, demonstrate all the criteria for type II cells. They have shown that 50% of lecithin radioactivity is in DSL after 6 hr of labeling with choline. This may be an indication that synthesis of DSL is quite normal in these cells. It should be noted, however, that further chemical studies are needed to establish this as a useful model of type II cells in culture.

Stoner and his associates[14] also reported a type II-like cell line from mice. Clones of epithelial-like cells were established from urethane-induced mouse lung adenoma. Electron microscopy of one clone showed that the cells contained lamellar inclusion bodies similar in appearance to those seen in the adenoma precursor, the type II alveolar pneumocyte. The clones exhibited characteristics associated with both "transformed" and "normal" cells in culture; i.e., although aneuploid, the cells grew at a slower rate than most transformed cells, did not form colonies in soft agar, and, after prolonged subculture, were not tumorigenic when transplanted subcutaneously into appropriate hosts. Hydrocortisone treatment of the cloned cells led to growth stimulation and the eventual acquisition of neoplastic potential. The cells are producing a C-type ribonucleic acid virus into the culture medium. Again in this clone there has been no chemical characterization.

Douglas and Kaighn[15] reported diploid clones from normal rat lung. Four out of many clones were considered epithelial in morphology. On the basis of electron microscopic morphology, two of the epithelial clones (L-2 and L-3) were considered to be type II cell derived. Published micrographs do not allow the observer to conclude the nature of these cells. There is no biochemical study of these clones as yet.

Douglas and Teel[16] described an in vitro model system in which monodisperse fetal-rat lung cells reorganize to form alveolar-like structures when cultured on a gelatin sponge matrix. The alveolar-like structures are composed of cells that have morphologic characteristics like those of the type II alveolar pneumonocytes of intact lung. The presence of osmiophilic lamellar bodies and tubular myelin in the lumen of the alveolar-like structures suggest that the cells in these structures are producing pulmonary surfactant. The formation and long-term maintenance of these alveolar-like struc-

tures may provide a unique in vitro model system for studies of the synthesis, storage, and secretion of pulmonary surfactant. This system also requires further biochemical characterization.

REFERENCES

1. Y. Kikkawa and K. Yoneda, The Type II Epithelial Cell of the Lung. I. Method of Isolation, *Lab. Invest.*, 30: 76-84 (1974).
2. Y. Kikkawa, F. Smith, K. Yoneda, B. Packard, and F. Suzuki, The Type II Epithelial Cell of the Lung. II. Chemical Composition and Phospholipid Synthesis, *Lab. Invest.*, 32: 295-302 (1975).
3. F. Smith, B. Packard, and Y. Kikkawa, Lecithin Synthesis in Alveolar Type II Cells and Pulmonary Macrophages, *Am. Div. Resp. Dis.*, 121: 904 (1975).
4. F. Smith and Y. Kikkawa, Disaturated Lecithin Synthesis in Type II Cells and Macrophages, unpublished.
5. Y. Aso, K. Yoneda, and Y. Kikkawa, Morphological and Biochemical Study of Pulmonary Changes Induced by Bleomycin in Mice, *Lab. Invest.* (in press).
6. Y. Aso, K. Yoneda, and Y. Kikkawa, Bleomycin-Induced Pulmonary Fibrosis, Morphologic and Biochemical Study, *Am. Rev. Resp. Dis.*, 111: 914 (1975).
7. U. Smith, D. S. Smith, and J. W. Ryan, Tubular Myelin Assembly in Type II Alveolar Cells: Freeze Fracture Studies, *Anat. Rec.*, 176: 125-127 (1973).
8. J. Lauweryns and M. Gombeer-Desmecht, L'Ultrastructure De LaCloison, Interalveolaire Du Poumon Apres Cryodescapage, *J. Microscopie*, 10: 139-148 (1971).
9. R. Mason, Disaturated Lecithin Concentration of Rabbit Tissue, *Am. Rev. Resp. Dis.*, 107: 678 (1973).
10. S. P. Sorokin, The Cells of the Lungs, in *Morphology of Experimental Respiratory Carcinogenesis*, AEC Symposium Series, Gatlinburg, Tenn., May 13—16, 1970, P. Nettesheim, M. G. Hanna, Jr., and J. W. Deatherage (Eds.), pp. 3-44, CONF-700501, NTIS, 1970.
11. R. Mason, M. Williams, and J. Clements, Isolation and Identification of Type II Alveolar Epithelial Cells, *Chest*, 67: 2 (1975).
12. A. J. Kniazeff, G. D. Stoner, L. Terry, R. Wagner, and R. P. Hoppenstand, Characteristics of Epithelial Cells Cultured from Feline Lung, *Lab. Invest.*, 34: 495-500 (1976).
13. M. Lieber, B. Smith, A. Szakal, W. Nelson-Rees, and G. Todaro, A Continuous Tumor Cell Line from a Human Lung Carcinoma with Properties of Type II Alveolar Epithelial Cells, *Int. J. Cancer*, 17: 62-70 (1976).
14. G. D. Stoner, Y. Kikkawa, A. J. Kniazeff, K. Miyai, and R. Wagner, Clonal Isolation of Epithelial Cells from Mouse Lung Adenoma, *Cancer Research*, 35: 2177-2185 (1975).
15. W. H. J. Douglas and M. E. Kaighn, Clonal Isolation of Differentiated Rat Lung Cells, *In Vitro*, 10: 230-237 (1974).
16. W. H. J. Douglas and R. W. Teel, An Organotypic In Vitro Model System for Studying Pulmonary Surfactant Production by Type II Alveolar Pneumocytes, *Am. Rev. Resp. Dis.*, 113: 17-23 (1976).

CONF-760927--1

Flow-System Analysis of Exfoliated Pulmonary Cells: Results of Initial Characterization Studies in Hamsters

J. A. STEINKAMP, K. M. HANSEN, J. S. WILSON, and G. C. SALZMAN
Biophysics and Instrumentation Group and Mammalian Biology Group,
Los Alamos Scientific Laboratory, University of California,
Los Alamos, New Mexico

ABSTRACT

This paper summarizes results of preliminary experiments to develop cytological and biochemical indicators for estimating damage to respiratory cells in test animals exposed by inhalation to toxic agents associated with nonnuclear energy production, the specific goal being the application of advanced multiparameter flow-system technologies to the detection of early atypical cellular changes in lung epithelium. Samples of normal Syrian hamster lung cells, composed of leukocytes, macrophages, ciliated columnar cells, and basal undifferentiated cells, were stained with fluorescent dyes specific for different biochemical parameters and were analyzed in liquid suspension as they flowed through a chamber intersecting a laser beam of exciting light. Multiple sensors measured the total or two-color fluorescence and light scatter on a cell-by-cell basis. Cellular parameters proportional to optical measurements (i.e., cell size, deoxyribonucleic acid content, total protein, nonspecific esterase activity, and nuclear and cytoplasmic diameters) were displayed as frequency-distribution histograms. Samples of lung cells were also separated according to various cytological parameters and were identified microscopically. The basic operating features of the methodology are discussed briefly, along with specific examples of preliminary results illustrating the initial characterization of exfoliated pulmonary cells from normal hamsters. As the flow technology is adapted further to the analysis of respiratory cells, measurements of changes in physical and biochemical properties as a function of exposure to toxic agents will be performed.

The application of advanced flow-system technologies to the measurement of physical and biochemical properties in respiratory cells provides a new approach for assessing early damage to the lung epithelium of mammals exposed by inhalation to toxic by-products from nonnuclear energy production. Specifically, our efforts are

directed toward developing automated cytological and biochemical methods for estimating early atypical cellular changes in exfoliated lung cells,[1,2] the end objective being the examination of human sputum samples from occupationally exposed populations. So that analytical techniques for quantitative assessment of damage can be developed, automated cell analysis and sorting instrumentation[3] designed and constructed at the Los Alamos Scientific Laboratory (LASL) is being applied presently to characterize respiratory cells from normal Syrian hamsters.

The initial goals are to adapt cell preparation and staining techniques developed for flow-analysis systems[4] to the characterization of lung cells with the use of the multiparameter cell separator[5] and multiangle light-scatter[6] systems. Steps include acquisition of adequate numbers of exfoliated cells for flow analysis by lavaging the lungs with saline, adaptation of cytological techniques designed for dispersal of human gynecological specimens to hamster lung epithelium to obtain single-cell suspensions, adaptation of existing staining techniques for measurement of cellular biochemical parameters [e.g., deoxyribonucleic acid (DNA) content and total protein], and initial characterization of lung cells with the use of flow-analysis instrumentation. Presented here is a brief description of the cell analysis and sorting techniques used to determine simultaneous fluorescence and light-scatter properties of respiratory cells, with examples of results from preliminary studies involving characterization based on cell size, DNA content, total protein, nonspecific esterase activity, nuclear and cytoplasmic diameters, and multiangle light-scatter properties. As the flow-system technology is adapted further for the analysis of exfoliated lung-cell samples from normal hamsters and subsequent characterization studies are completed, measurements of early changes in the various physical and biochemical cellular properties as a function of exposure to toxic agents associated with energy production will be attempted.

MATERIALS AND METHODS

Cell-Sample Acquisition and Staining

Syrian hamsters were sacrificed by administering 15 mg of sodium pentobarbital intraperitoneally. The trachea was surgically exposed and intubated with a 19-gage blunted stainless-steel needle bent 45° at the midpoint and attached to a syringe containing 3 cm^3 of phosphate-buffered saline. The trachea was secured around the needle by tying it with chromic gut, and the lungs were lavaged[7] to

obtain exfoliated respiratory cells that were fixed in 35% ethanol. Clumps and sheets of epithelial cells were disaggregated into single cells by forcing through a 25-gage needle. Samples were evaluated by staining with the routine Papanicolaou method and were examined microscopically to determine the cell types present. Differential counts (summarized in Table 1) indicate that washings are composed of macrophages, leukocytes, ciliated columnar cells, and basal undifferentiated cells plus a considerable amount of small debris.

TABLE 1

DIFFERENTIAL CELL COUNTS OF NORMAL HAMSTER LUNG-CELL SAMPLES OBTAINED BY LAVAGING THE LUNGS WITH NORMAL SALINE*

Hamster number	Macrophages, %	Leukocytes, %	Basal undifferentiated cells, %	Ciliated columnar cells, %
1	74	18	7	1
2	79	14	6	1
3	74	17	7	2
4	44	43	12	1

*Determined microscopically from Papanicolaou-stained samples.

So that cell viability could be demonstrated, unfixed samples (2.5 ml) were stained with fluorescein diacetate [FDA (10 μl of 0.5 g FDA/100 ml of acetone)] at 0°C for 30 min with the use of the "fluorochromasia" procedure[8] and were then analyzed for fluorescence. Live cells accumulate fluorescein intracellularly since FDA readily enters the cell to be hydrolyzed by esterases but cannot then pass out through the intact cell membrane. Fixed lung cells were stained for DNA with mithramycin[9,10] and then analyzed for total DNA content and cell size by measuring fluorescence and light scatter, respectively. Nuclear and cytoplasmic diameter distributions were determined similarly from analog signal time durations, as described below. Both FDA- and mithramycin-stained samples remained in the stain solution during analysis. Two-color fluorescence analysis of DNA content and total protein in respiratory cells was accomplished by staining the fixed samples with propidium iodide (PI) and fluorescein isothiocyanate (FITC), which fluoresce red and green, respectively.[10,11] These samples were rinsed and then

suspended in phosphate-buffered saline for two-color fluorescence analysis. Nuclear and cytoplasmic diameters were measured from analog red (nucleus) and green (cytoplasm) fluorescence signal time durations, respectively, as described below.

Instrumentation

The principle of measurement is as follows. Lung cells stained in liquid suspension, as described above, are introduced into a flow chamber at approximately 10^3/sec (Fig. 1) where they flow across a fluid-filled viewing region (constant velocity) and intersect a narrow, elliptically shaped, argon–ion laser beam.[5] As the cells cross the narrow wall of laser illumination, bound dyes are excited to fluoresce, and the cells scatter light, the laser wavelength settings being 457 and 488 nm for excitation of mithramycin and FDA/PI–FITC, respectively. Fluorescence provides quantitative information on constituents to which the dyes are bound (e.g., DNA content and total protein), whereas light scatter yields data on size[12] and internal structure.[13,14] Both are electrooptically measured, the fluorescence sensor being a dual photomultiplier-tube array that determines total or two-color fluorescence of selectable color regions. Small-angle light scatter (whole-cell size) is measured by focusing the forward light scattered onto a photodiode detector with a collection angle of 0.7 to 2.0° (Ref. 15).

Nuclear and cytoplasmic diameters also can be measured by determining the time required for the cell nucleus and cytoplasm to pass across the "thin wall" of laser excitation. This technique, as reported originally,[16] is similar in concept to the "slit-scan" principle[17,18] but relies on quantitative two-color fluorescence staining of the nucleus and cytoplasm with PI and FITC. As doubly stained cells cross the laser beam, analog red (nucleus) and green (cytoplasm) fluorescence signal time durations are converted electronically into signals, the amplitude of which is proportional to the respective diameters.[16] In a more-recent development, nuclear and cytoplasmic diameter measurements are based on staining the cell nucleus alone with mithramycin and determining the respective diameters from nuclear fluorescence and light scatter signal time durations.[19]

After optical measurement, the stream carrying the cells emerges into air as a liquid jet from the flow-chamber-exit nozzle (Fig. 1). A piezoelectric transducer mechanically coupled to the chamber and electrically driven at about 40 kHz produces uniform liquid droplets (40,000/sec) by regularly disturbing the emerging jet (vibrational

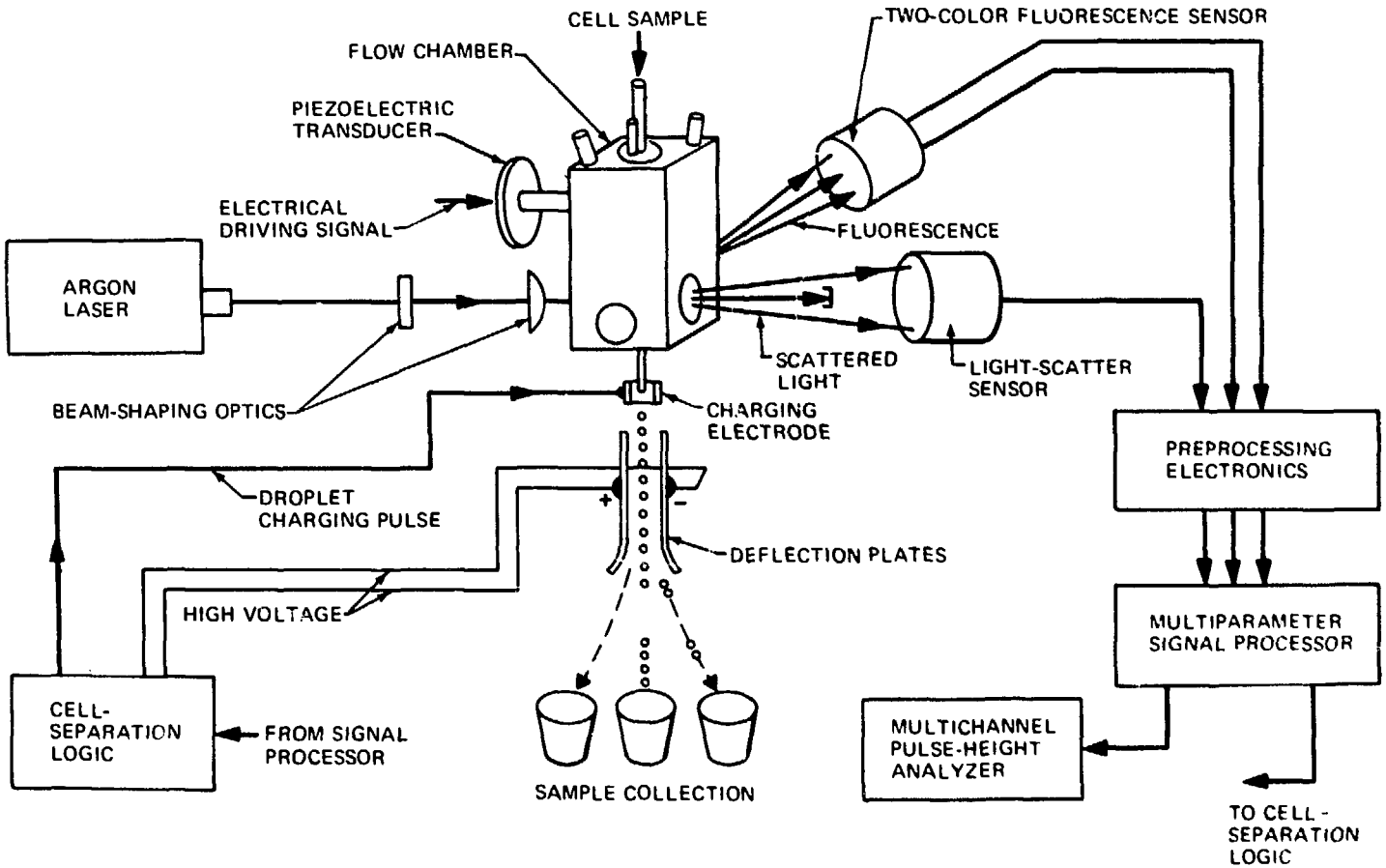

Fig. 1 Diagram of the multiparameter cell-separator system, illustrating laser excitation, flow chamber, fluorescence and light-scatter sensors, signal-processing and cell-separation electronics, and droplet charging and deflection scheme.

energy), thus causing the cells to be isolated into droplets[20] with approximately 2% containing a single cell.

Optical signals proportional to the measured cellular parameters are processed electronically on a cell-by-cell basis as single parameters, ratios, and gated single parameters with a hard-wire signal-processing unit (Fig. 1). A multichannel pulse-height analyzer accumulates and displays the processed signals as pulse-amplitude frequency-distribution histograms. Single-parameter analysis is performed by selecting a cellular parameter and displaying its distribution. Ratios of parameters are computed on a single-cell basis and are displayed as histograms. Gated single-parameter analysis permits the examination of particular subclasses of cells within selectable ranges on different cellular parameter values. For example, the distribution of protein content for G_1-phase cells can be obtained by analyzing only those protein signals from cells having G_1 DNA content.[11] Gated analysis techniques permit similar distributions to be determined from weakly fluorescing cells by requiring coincidence with light-scatter[21] or surface-area signals.[22]

When experiments require that cells be separated, processed signals activate sorting by comparing their amplitude with preselected ranges of a single-channel pulse-height analyzer (SCA) located within the cell-separation logic block (Fig. 1). The SCA range is chosen to correspond to a distribution region in which cells to be separated are located. If the signal amplitude then falls within the selected SCA range, an electronic time delay is activated which, after an appropriate time period between optical sensing and droplet formation (about 1000 μsec), triggers a charging pulse as the cell arrives at the droplet formation point. This causes a group of droplets, one of which contains the cell, to be charged and deflected electrostatically into a collection vessel.[20] Cells not meeting the preset criteria do not trigger the above sequence of events and pass undeflected into a different vessel. In a typical experiment, lung cells were sorted at rates of a few hundred per second. The sorted suspension was then deposited onto a microscope slide with the use of centrifugal cytological methods (Shandon Scientific) for counterstaining and microscopic examination.

In addition to measuring small-angle light scatter, a new flow instrument capable of determining light scatter at 32 angles simultaneously[6] has also been used to analyze respiratory cells. As the cells pass through a flow chamber and are illuminated with a helium–neon laser, scattered light is detected with a circular photodiode array, is stored in a computer, and is then processed as a scatter diagram of light-scatter intensity vs. angle. The scatter

diagram is converted into a cluster diagram, which permits individual light-scatter patterns from each cell to be grouped according to a mathematical clustering algorithm.[2,3]

RESULTS AND DISCUSSION

Figure 2 shows a fluorescence distribution recorded on a hamster lung washing after treatment with FDA. The distribution, which is a measure of intracellular enzymatic activity (nonspecific esterases) and integrity of the cell membrane (i.e., cell viability), shows three distinct regions of cells consisting of peaks 1, 2, and 3. Lung cells corresponding to combined peaks 1 and 2 (channels 10 to 50) have been identified initially by sorting and microscopic examination as being composed principally of leukocytes. Respiratory cells corresponding to peak 3 have been identified similarly as primarily macrophages. Data from other hamsters also indicate that the total number of cells within the different regions (peaks) varies considerably from animal to animal. Further tests are planned to determine where epithelial cells are located and to correlate FDA

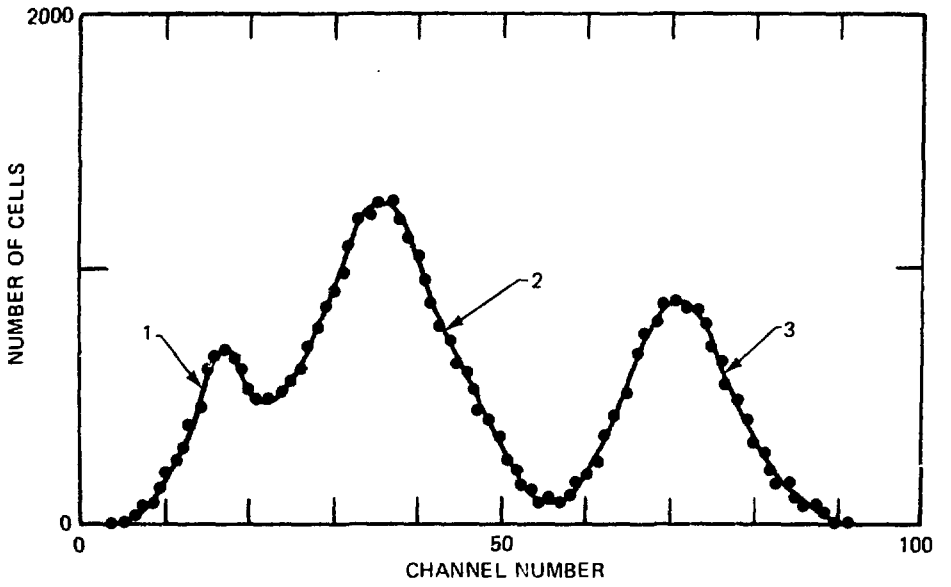

Fig. 2 Frequency-distribution histogram for a normal hamster lung washing stained with fluorescein diacetate and analyzed for fluorescence. The horizontal axis is proportional to the logarithm of intracellular fluorescence signal amplitude and covers a three-decade range.

activity with cell size with the gated analysis techniques described above. Quantitative analysis of other cell enzyme activities with the use of different fluorogenic substrates will be attempted also.

The measurement of DNA content and cell size is illustrated in Fig. 3 for a lung-cell sample stained with mithramycin. Figure 3a shows the DNA distribution that is unimodal, which indicates cells having 2C diploid DNA content. The cell-size (small-angle light scatter) distribution (Fig. 3b) shows a heterogeneous population of cells differing considerably in size with much overlap. Gated single-parameter analysis methods, coupled with cell sorting, were used to identify partially the individual size distributions for nucleated and nonnucleated cells in the following manner. The size distribution of nonnucleated cells (Fig. 3c) was determined by recording the light-scatter signals from only those cells (including debris) which scattered light but which did not fluoresce. Preliminary results, based on gated analysis and subsequent separation (channels 5 to 80 of Fig. 3c), indicate that the distribution is made up of erythrocytes and small debris. The size distribution of nucleated respiratory cells is shown in Fig. 3d and indicates much larger sized cells. This distribution was obtained by recording light-scatter signals from only those cells which both fluoresced and scattered light. These cells were also separated (channels 30 to 100 of Fig. 3d) and identified microscopically as consisting of leukocytes, macrophages, etc. Therefore, by requiring or not requiring coincidence of light scatter with nuclear fluorescence signals, size can be measured from a heterogeneous mixture of nucleated and nonnucleated cells. The individual size distributions (Figs. 3c and 3d) also demonstrate the regions to which they correspond in the total cell-size distribution (see Fig. 3b).

Flow-analysis methods can be used also to characterize cells according to nuclear and cytoplasmic diameters based on quantitative fluorescence staining of either the nucleus alone or in combination with the cytoplasm. For example, Fig. 4 shows the nuclear and cytoplasmic diameter distributions for a lung washing stained with mithramycin. The nuclear diameter distribtuion (Fig. 4a), obtained by measuring the fluorescence signal time durations, is unimodal and indicates cells of similar-sized nuclei. However, the cytoplasmic diameter distribution (Fig. 4b), determined from light-scatter signal time durations, shows that diameters vary over a considerable range. Gated analysis techniques again were used to find what portion of the cytoplasmic diameter distribution consisted of nucleated and nonnucleated cells. The cytoplasmic diameter distribution of nonnu-

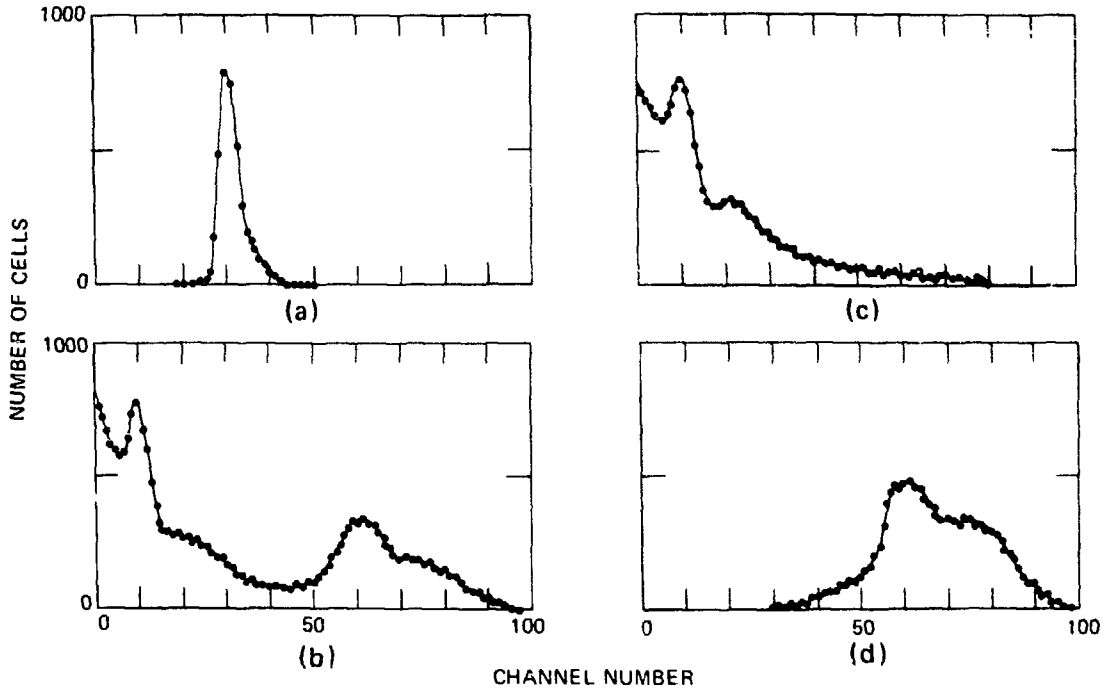

Fig. 3 Frequency-distribution histograms of DNA content and cell size for a normal hamster lung washing stained with mithramycin and analyzed for fluorescence and small-angle light scatter, respectively. (a) DNA content distribution. (b) Cell-size distribution. (c) Cell-size distribution of nonnucleated cells and debris obtained by recording only light-scatter signals from nonfluorescing cells and debris. (d) Cell-size distribution of nucleated cells obtained by recording only light-scatter signals from fluorescing cells. The horizontal axes of the three cell-size distributions are proportional to the logarithm of light-scatter signal amplitude and cover a three-decade range.

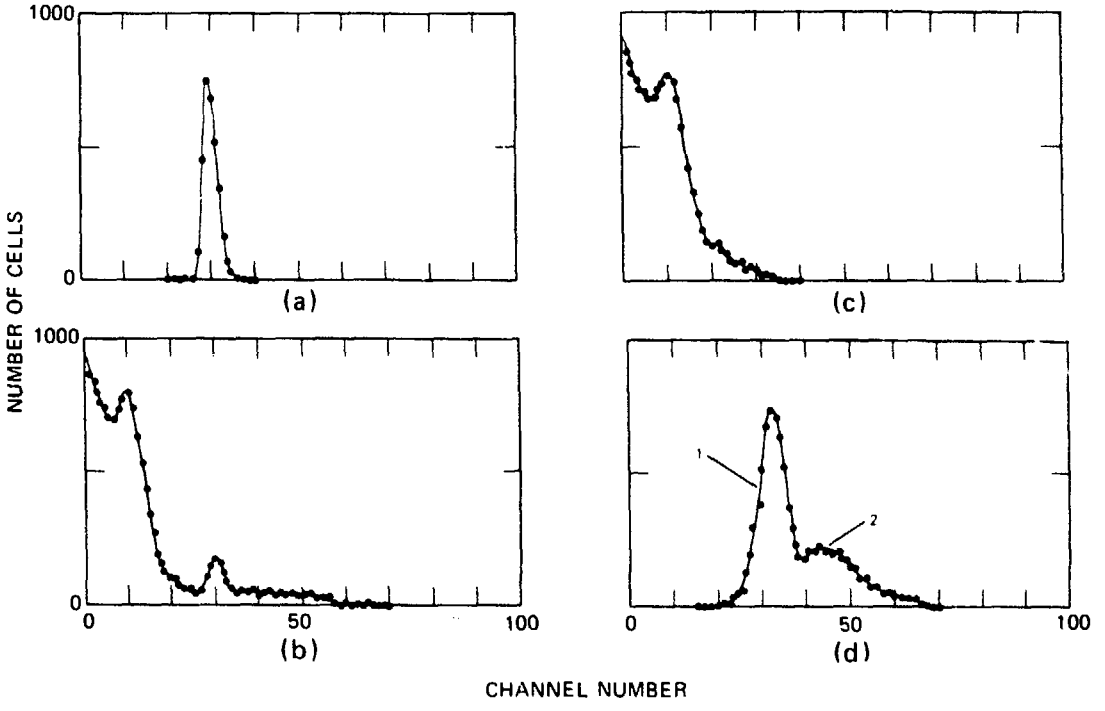

Fig. 4 Frequency-distribution histograms of nuclear and cytoplasmic diameters from a normal hamster lung washing stained with mithramycin and analyzed for fluorescence and small-angle, light-scatter, and signal time durations, respectively. (a) Nuclear diameter distribution. (b) Cytoplasmic diameter distribution. (c) Cytoplasmic diameter distribution of nonnucleated cells, including debris, obtained by recording only cytoplasm diameter signals from nonfluorescing material. (d) Cytoplasmic diameter distribution of nucleated cells obtained by recording only cytoplasm diameter signals from fluorescing cells.

cleated cells (Fig. 4c), obtained by recording the diameter of only those cells (including debris) which did not fluoresce but which scattered light, is composed primarily of small debris and erythrocytes. The cytoplasmic diameter distribution of nucleated cells (Fig. 4d) was determined by recording diameter signals from only those which fluoresced and scattered light in coincidence. This distribution indicates a minimum of two populations differing in diameter by about 1.3. Similar data recorded on another lung washing indicated three distinct cell types. Experiments are under way to verify what cells correspond to the different peaks in the diameter distributions and to improve instrumentally the resolution of the diameter measurements.

Two-color fluorescence analysis of DNA content, total protein, and nuclear and cytoplasmic diameters in respiratory cells stained with PI—FITC is shown in Fig. 5. The DNA-content distribution (Fig. 5a) is unimodal and similar to that recorded with the use of mithramycin (Fig. 3a). The total protein distribution (Fig. 5b), which was obtained by recording only those green fluorescence (protein) signals coincident with red fluorescence (DNA-content) signals, is broad and indicates a wide range of cellular protein values consisting of major (peak 1) and minor (peak 2) regions. The nuclear diameter distribution (Fig. 5c), which was determined from measurements of red fluorescence signal time duration, is unimodal (uniformly sized nucleus) and similar to the distribution recorded in Fig. 4a with the use of mithramycin as a nuclear stain. However, the cytoplasmic diameter distribution (Fig. 5d), as derived from green fluorescence signal time durations in coincidence with DNA-content signals, is bimodal and shows a minimum of two cell populations differing in diameter by a factor of about 2. Future experiments will involve separating cells on the basis of cytoplasmic diameter with this technique.

The two-color PI—FITC method permits the determination of DNA content, total protein, and nuclear and cytoplasmic diameters in lung-cell samples. Except for analysis of total protein, the newer and simpler mithramycin staining procedure allows the measurement of all the above cell parameters. It is also possible to combine these parameters into ratios on a cell-by-cell basis and to display them as frequency-distribution histograms. Nuclear-to-cytoplasmic ratios have been shown previously to be an important parameter in automated analysis of abnormal gynecological specimens.[17] Future experimentation will include measurement of nuclear-to-cytoplasmic size relationships combined with DNA, protein, and cell-size mea-

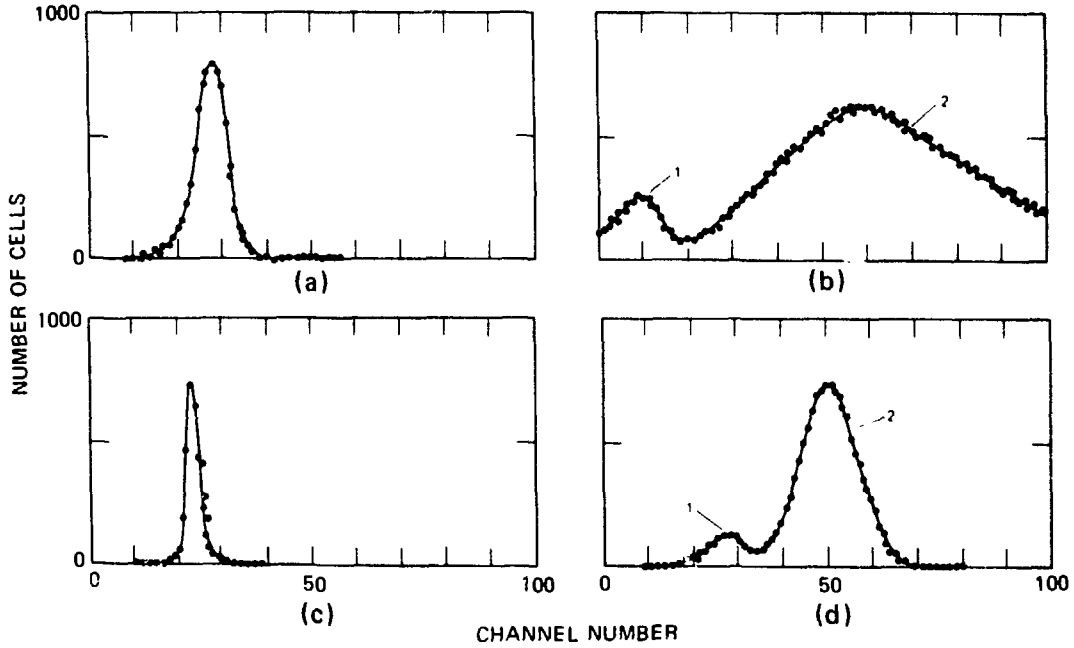

Fig. 5 Frequency-distribution histograms of DNA content, total protein, and nuclear and cytoplasmic diameters from a normal hamster lung washing stained with PI and FITC and analyzed for two-color fluorescence properties. (a) DNA content distribution (red fluorescence). (b) Total protein distribution obtained by recording only green fluorescence signals from nucleated cells. (c) Nuclear diameter distribution obtained from red fluorescence signal time durations. (d) Cytoplasmic diameter distribution obtained by recording only green fluorescence signal time durations from nucleated cells.

surements and sorting to correlate cell types with instrumental analysis.

In preliminary studies designed to measure subtle differences in lung-cell morphology, flow multiangle light-scatter techniques have been used to classify exfoliated hamster respiratory cells on the basis of differences in scatter patterns. Figure 6 shows an example of a cluster light-scatter diagram measured on an unfixed and unstained lung washing in which at least three groups can be distinguished on the basis of differences in angular light-scatter intensity. Recent data indicate that possibly four to five cell types can be detected. Future experiments will involve separating cells differing in light-scatter patterns and identifying what types correspond to the various regions of the cluster diagrams. These experiments will depend on the addition of a cell-sorting capability to the multiangle light-scatter flow system.[6]

CONCLUSIONS

These preliminary results demonstrate the potential capability of applying advanced multiparameter flow-system technology to analyze and separate exfoliated respiratory cells, the specific goal being the development of cytological and biochemical indicators for future use in estimating early damage to the lung epithelium of mammals exposed by inhalation of toxic agents associated with nonnuclear energy production. Lung cells from normal hamsters will continue to be analyzed with the various flow-analysis methods for initial characterization purposes. These will include DNA content, total protein, esterase activity, whole-cell size, nuclear and cytoplasmic size relationships, and multiangle light-scatter properties. Emphasis will continue to be placed on new methods that may be potential indicators of early atypical cellular changes. For example, quantitation of specific cell enzyme activities with the use of fluorogenic substrates for possible determination of alkaline and acid phosphatase, lipase, peroxidase, esterase, and others, such as antigenic properties, may provide methods for assessing early damage. Not only will lung cells be characterized further on the basis of the above parameters but also they will be separated routinely and examined microscopically. This will permit a correlation of measured parameters with morphological observations. As experimentation proceeds, it may be necessary to modify the present cell-preparation and -staining procedures and instrumental analysis methods developed in the initial characterization studies.

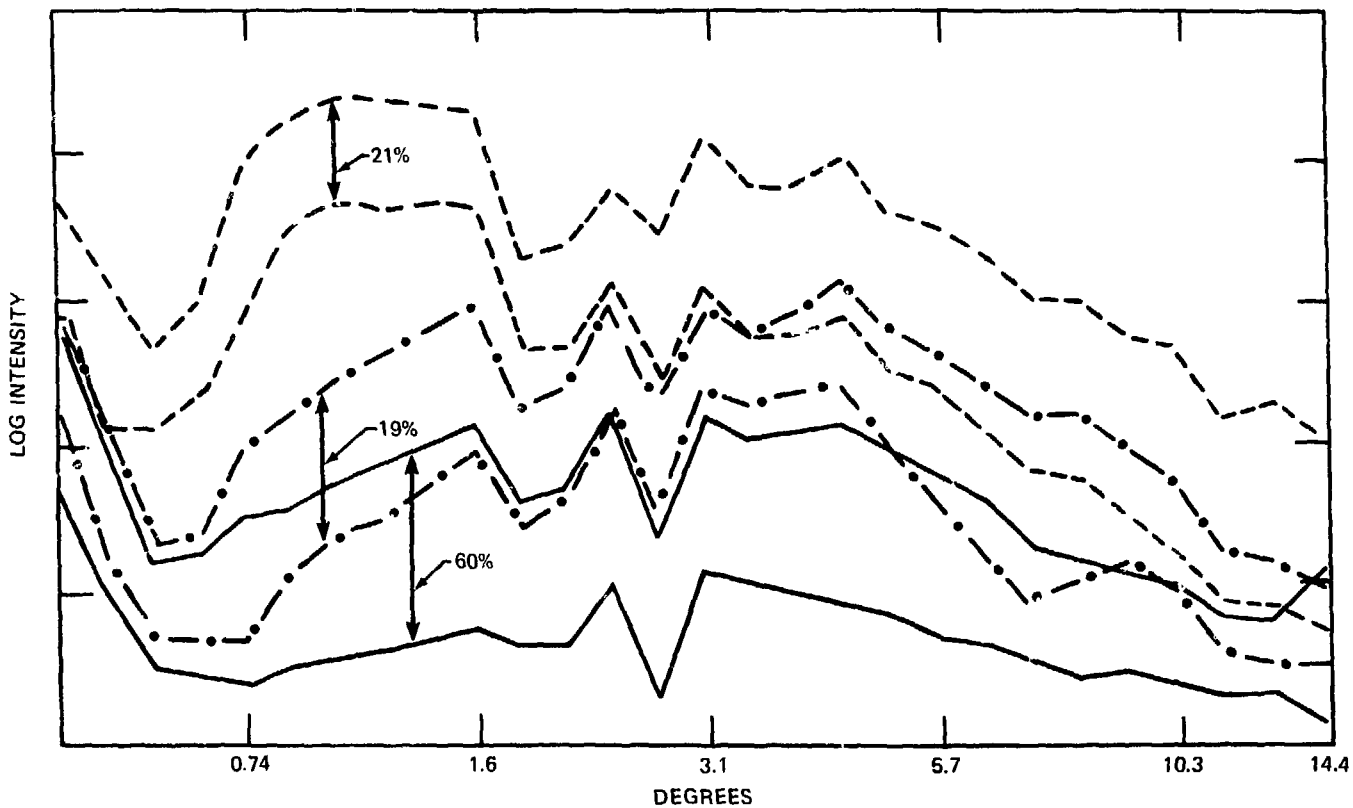

Fig. 6 Cluster diagram derived from the multiangle light-scatter pattern (three-decade log intensity vs. angle) recorded on a normal hamster lung-cell sample. Each cluster, which represents a cell-size grouping, is enclosed by a broken or solid line and shows an excursion of one standard deviation from the mean. The percentages represent the approximate number in each size class (cluster).

ACKNOWLEDGMENTS

This work was performed under the auspices of the Energy Research and Development Administration with joint support from the U. S. Environmental Protection Agency (agreement EPA-IAG-D5-E681). We thank M. Ingram (advice concerning acquisition of lung cells), D. M. Smith (consultations), J. Grilly (photography), and C. E. Oldenborg and E. M. Sullivan (manuscript preparation).

REFERENCES

1. J. A. Steinkamp, M. Ingram, K. M. Hansen, and J. S. Wilson, Detection of Early Changes in Lung Cell Cytology by Flow-Systems Analysis Techniques, ERDA Report LA-6267-PR, Los Alamos Scientific Laboratory, NTIS, 1976.
2. J. A. Steinkamp, K. M. Hansen, J. S. Wilson, and G. C. Salzman, Detection of Early Changes in Lung-Cell Cytology by Flow-Systems Analysis Techniques, ERDA Report LA-6478-PR, Los Alamos Scientific Laboratory, NTIS, 1976.
3. P. F. Mullaney, J. A. Steinkamp, H. A. Crissman, L. S. Cram, and D. M. Holm, Laser Flow Microphotometers for Rapid Analysis and Sorting of Individual Mammalian Cells, in *Laser Applications in Medicine and Biology*, Vol. 2, pp. 151-204, M. L. Wolbarsht (Ed.), Plenum Press, New York—London, 1974.
4. H. A. Crissman, P. F. Mullaney, and J. A. Steinkamp, Methods and Applications of Flow Systems for Analysis and Sorting of Mammalian Cells, in *Methods in Cell Biology*, Vol. 9, pp. 179-246, D. M. Prescott (Ed.), Academic Press, Inc., New York, 1975.
5. J. A. Steinkamp, M. J. Fulwyler, J. R. Coulter, R. D. Hiebert, J. L. Horney, and P. F. Mullaney, A New Multiparameter Separator for Microscopic Particles and Biological Cells, *Rev. Sci. Instrum.*, 44: 1301-1310 (1973).
6. G. C. Salzman, J. M. Crowell, C. A. Goad, K. M. Hansen, R. D. Hiebert, P. M. LaBauve, J. C. Martin, and P. F. Mullaney, A Flow-System Multiangle Light-Scattering Instrument for Cell Characterization, *Clin. Chem.*, 21: 1297-1304 (1975).
7. H. Schreiber and P. Nettesheim, A New Method for Pulmonary Cytology in Rats and Hamsters, *Cancer Res.*, 32: 737-745 (1972).
8. B. Rotman and B. W. Papermaster, Membrane Properties of Living Mammalian Cells as Studied by Enzymatic Hydrolysis of Fluorogenic Esters, *Proc. Natl. Acad. Sci. U.S.A.*, 55: 134-141 (1966).
9. H. A. Crissman and R. A. Tobey, Cell Cycle Analysis in Twenty Minutes, *Science*, 184: 1297-1298 (1974).
10. H. A. Crissman, M. S. Oka, and J. A. Steinkamp, Rapid Staining Methods for Analysis of DNA and Protein in Mammalian Cells, *J. Histochem. Cytochem.*, 24: 64-71 (1976).
11. H. A. Crissman and J. A. Steinkamp, Rapid, Simultaneous Measurement of DNA, Protein, and Cell Volume in Single Cells from Large Mammalian Cell Populations, *J. Cell Biol.*, 59: 766-771 (1973).
12. P. F. Mullaney and P. N. Dean, The Small Angle Light Scattering of Biological Cells, *Biophys. J.*, 10: 764-772 (1970).

13. A. Brunsting and P. F. Mullaney, Differential Light Scattering from Spherical Mammalian Cells, *Biophys. J.*, 14: 439-453 (1974).
14. A. Brunsting and P. F. Mullaney, Differential Light Scattering: A Possible Method of Mammalian Cell Identification, *J. Colloid Interface Sci.*, 39: 492-496 (1972).
15. P. F. Mullaney, M. A. Van Dilla, J. R. Coulter, and P. N. Dean, Cell Sizing: A Light Scattering Photometer for Rapid Volume Determination, *Rev. Sci. Instrum.*, 40: 1029-1032 (1969).
16. J. A. Steinkamp and H. A. Crissman, Automated Analysis of DNA, Protein and Nuclear to Cytoplasmic Relationships in Tumor Cells and Gynecologic Specimens, *J. Histochem. Cytochem.*, 22: 616-621 (1974).
17. L. L. Wheeless and S. F. Patten, Slit-Scan Cytofluorometry, *Acta Cytol.*, 17: 333-339 (1973).
18. L. L. Wheeless, J. A. Hardy, and J. Balasubramanian, Slit-Scan Flow System for Automated Cytopathology, *Acta Cytol.*, 19: 45-52 (1975).
19. J. A. Steinkamp, K. M. Hansen, and H. A. Crissman, Flow Microfluorometric and Light Scatter Measurement of Nuclear and Cytoplasmic Size in Mammalian Cells, *J. Histochem. Cytochem.*, 24: 291-297 (1976).
20. M. J. Fulwyler, Electronic Separation of Biological Cells by Volume, *Science*, 150: 910-911 (1965).
21. P. F. Mullaney and W. T. West, A Dual-Parameter Flow Microfluorometer for Rapid Cell Analysis, *Brit. J. Phys.*, E6: 1006-1008 (1973).
22. J. A. Steinkamp and P. M. Kraemer, Flow Microfluorometric Studies of Lectin Binding to Mammalian Cells. II. Estimation of the Surface Density of Receptor Sites by Multiparameter Analysis, *J. Cell. Physiol.*, 84: 197-204 (1974).
23. C. A. Goad, MUMPS Code-Building Package for Data-Base Management, ERDA Report LA-6065-MS, Los Alamos Scientific Laboratory, NTIS, 1975.

Secretion of Disaturated Phosphatidylcholine by Primary Cultures of Type II Alveolar Cells

ROBERT J. MASON, MARY C. WILLIAMS, and LELAND G. DOBBS
Cardiovascular Research Institute, Departments of Medicine and Anatomy, University of California School of Medicine, San Francisco, California

ABSTRACT

Type II alveolar cells make and secrete pulmonary surface-active material. Factors that control secretion are not well understood but are potentially important in the management of respiratory distress syndromes. We have developed a primary culture method for isolating type II alveolar cells. A partially purified population is obtained by enzymatic digestion of lung with trypsin and bouyant density centrifugation. The population is further purified by differential adherence. The cultured cells are 89% type II cells and represent 65% of the type II cells originally plated. To study secretion, we incubate the cells with [^{14}C]choline for 20 hr, wash away the medium and nonadherent cells, add fresh medium, incubate for 30 min for reequilibration, and then incubate for a subsequent 60 min with or without pharmacologic agents. The medium is analyzed for radioactive disaturated phosphatidylcholine (DSPC). Basal secretion is 5.7% of total cellular DSPC in 90 min. Secretion is stimulated to 15.5% with phorbol myristate acetate ($2 \times 10^{-8} M$) and to 10.4% of cellular DSPC with the calcium ionophore A23187 ($5 \times 10^{-6} M$). Although we do not know the physiologic importance of the effect of phorbol myristate acetate, this compound does not appear to be cytotoxic in that it does not affect the ultrastructural appearance of type II cells or reduce the exclusion of the vital dye, erythrosin B.

Primary cultures of type II cells are potentially valuable for studying many different metabolic processes.

Pulmonary surface-active material lowers the surface tension at the air—liquid interface in the small air spaces in the lung and thereby prevents alveolar instability and atelectasis.[1] The type II alveolar cell is acknowledged to be the source of surface-active material, which is

stored in the lamellar inclusion bodies.[1-3] It is, however, uncertain what factors control the secretion from type II cells and the subsequent absorption of surface-active material to the air—liquid interface. Studies with intact lungs or lung slices have indicated that secretion may be altered by both physical and chemical means: Secretion is stimulated by hyperventilation[4-7] and by treatment with cholinergic compounds,[7-10] adrenergic compounds,[8] and thyroxine;[11] secretion is inhibited by treatment with colchicine.[12,13] With intact lung it is difficult to differentiate primary effects (events that affect type II cells directly) from secondary effects (events that affect type II cells indirectly). Primary effects on secretion might be more readily studied with isolated type II cells.

In this report we describe the purification of type II cells from rat lung by differential adherence in primary culture and the effects of certain chemical compounds on the secretion of disaturated phosphatidylcholine (DSPC), a major component of purified surface-active material.[14] A preliminary report of these studies has been published.[15]

METHODS

Primary Culture

Solutions Used in the Cell-Isolation Procedure

Solution A contains NaCl, 128m*M*; KCl, 5m*M*; sodium phosphate buffer, 2.5m*M*; HEPES buffer (N-2-hydroxyethyl piperazine N-2-ethanesulfonic acid), 17m*M*; glucose, 5.5m*M*; gentamicin, 10 μg/ml; $CaCl_2$, 1.9m*M*; and $MgSO_4$, 1.2m*M*. The pH of this solution is adjusted to 7.4 at 22°C; the osmolality is 290 mOsm. *Solution B* is the same as solution A but does not contain $CaCl_2$ or $MgSO_4$. The *albumin-fluorocarbon emulsion* is made by adding 12 ml of a 10 mg/ml solution of defatted bovine serum albumin (Sigma Chemical Company) in solution A to 4 ml of fluorocarbon FC-75 (Minnesota Mining Company). This mixture is sonicated and then diluted with an additional 44 ml of the albumin solution before use. The *trypsin—deoxyribonuclease (DNase) solution* contains recrystallized trypsin from bovine pancreas (Sigma Chemical Company) (0.1 mg/ml) and DNase (Sigma Chemical Company or P. L. Biochemicals Inc.) (30 μg/ml) dissolved in solution A. The *trypsin inhibitor—DNAase solution* contains soybean trypsin inhibitor (Sigma Chemical Company) (1 mg/ml) and DNase (30 μg/ml) in solution A.

Cell Isolation and Primary Culture

Adult male Sprague—Dawley specific pathogen-free rats (180 to 250 g) are obtained from Hilltop Laboratory Animals, shipped in a filtered cage, and housed in a laminar flow hood until they are sacrificed. Type II cells are prepared as previously described but with a reduced concentration of trypsin (0.1 mg/ml).[16] In brief, for each experiment, four rats are anesthetized and given an intraperitoneal injection of sodium heparin (250 units/100 g of body weight) to prevent coagulation and pentobarbital (5 mg/100 g of body weight). Fifteen minutes later the abdominal aorta is transected, a tracheostomy is performed, and the lungs are ventilated three times with 7 ml of air. The chest is then opened and the lungs are briefly perfused via the pulmonary artery with solution B.

The lungs are then removed from the thorax and instilled via the trachea with solution B (five times with 10 ml/lavage). The lungs are then instilled with 10 ml of the albumin—fluorocarbon emulsion and immersed in 0.15*M* NaCl for 20 min at 37°C to allow the remaining macrophages to ingest the heavy emulsion. The lungs are removed from the saline bath and instilled five times with solution B and once with the trypsin—DNase solution. After the lungs drain, 10 ml of the trypsin—DNase solution is instilled, and the lungs are placed in saline at 37°C for a total of 20 min. After 10 min, additional trypsin—DNase solution is instilled as necessary to keep the lungs expanded.

The lungs are removed from the saline and filled with the trypsin inhibitor—DNase solution. The mediastinal structures and any remaining nonpulmonary tissue are removed. Each lung is minced with scissors for 45 sec, the minced lung tissue and mincing solution are brought to 20 ml with additional trypsin inhibitor—DNase solution, and the 20 ml is poured into a siliconized 250-ml glass Erlenmeyer flask. The four flasks are shaken in a reciprocating water bath at 100 cycles/min for 10 min. The minced lung tissue and cellular suspension is then passed through a series of increasingly fine filters: cotton gauze, 100-μm nylon mesh and finally 20-μm nylon mesh (Tobler, Ernst, and Trubler, Inc.).

The filtered suspension of cells is then layered onto a discontinuous sterile albumin gradient. The albumin is prepared by diluting Pathocyte 4 (Miles Labs) with 0.15*M* NaCl to densities of 1.080 and 1.040 and then passing the albumin solutions through 0.45-μm filters (Millipore Corp.). Each gradient is prepared with a sterile technique in a sterile 50-ml plastic centrifuge tube. Ten milliliters of the 1.080 albumin solution is placed in the bottom of the tube, 10 ml of the 1.040 albumin solution is layered on top of this, and 20 ml of cell

suspension is layered on top of the 1.040 albumin solution. The gradient is centrifuged at 315 x *g* (1200 rpm) for 20 min at 4°C.

All subsequent handling of the cells is done with sterile pipets and centrifuge tubes. All solutions are passed through 0.45-μm filters. The band between the densities of 1.040 and 1.080 is aspirated. The cells are washed twice with the trypsin inhibitor—DNase solution, and the cells from the four animals are pooled and resuspended in Dulbecco's modified Eagle's medium supplemented with 10% fetal-calf serum and 10 μg/ml gentamicin. The final cell concentration is approximately 5×10^5/ml. The tissue-culture media and fetal-calf sera are supplied by the Cell Culture Facility of the University of California Medical Center.

The cells are gassed with 10% CO_2 in air and allowed to settle and attach in a 75-cm^2 culture flask (Falcon) for 3 hr at 37°C. During this time most of the macrophages adhere. The nonadherent cells are removed and plated in 60-mm or 35-mm Petri dishes (Corning Glass Works). During the next 20 hr of culture, most of the type II cells adhere. The nonadherent cells are aspirated, the adherent cells are washed three times, and fresh media is added.

Evaluation of Cells in Culture

Purity is determined by differential counts of smears stained with the modified Papanicolaou stain.[17] Cells are removed from the Petri dishes in 4 min at 37°C with 0.05% trypsin and 0.02% ethylenediaminetetraacetic acid (EDTA) in Puck's saline A (Ref. 18), which is supplied by the Cell Culture Facility. Plating efficiency is calculated by comparing measurements of deoxyribonucleic acid (DNA) in the initial cell suspension to the adherent cells in culture. The DNA is measured by the method of Burton[19] with calf thymus DNA (Type V, Sigma Chemical Co.) as the standard; increased sensitivity is achieved by reducing volumes of reagents.

Cells prepared for transmission electron microscopy are placed in primary culture for 20 hr, incubated with Dulbecco's modified Eagle's medium with 3 mg/ml bovine serum albumin for 1 hr (see below for protocol for secretion), washed, and removed from the Petri dish with trypsin. The cells are fixed with 2% glutaraldehyde and 1% paraformaldehyde in phosphate buffer. They are then postfixed with 1.5% osmium tetroxide in veronal acetate buffer, stained en bloc with 1.5% uranyl acetate, dehydrated in acetone, embedded in Epon, sectioned, stained with uranyl acetate and lead citrate, and examined in a Zeiss EM-10 transmission electron microscope.

SECRETION OF DISATURATED PHOSPHATIDYLCHOLINE

For each experiment approximately 2 μCi of [*Methyl*-^{14}C] choline (40 mCi/m*M*) (New England Nuclear Corp.) is added to the cell suspension after the initial 3-hr period of adherence and before the suspension is plated in individual Petri dishes. After 20 hr the nonadherent cells and media are aspirated, and the cells adherent to the plates are washed three times with solution A. Either 1.6 ml (per 35-mm Petri dish) or 2.5 ml (per 60-mm Petri dish) of Dulbecco's modified Eagle's medium containing 3 mg/ml of fraction V bovine serum albumin (Miles Labs.) is added to each Petri dish. The Petri dishes are incubated at 37° for 30 min, removed to room temperature while 20 μl of the appropriate control or test solutions is added to each plate, and are then returned to the incubator for 60 min. Test solutions of phorbol myristate acetate (PMA) (12-0-tetradecanoyl phorbol-13-acetate) (Consolidated Midland Corporation) are made by diluting a stock solution of PMA, 2 mg/ml in dimethyl sulfoxide (DMSO) (J.T. Baker) 1 : 20 in double distilled water and subsequently diluting this solution in 0.15*M* NaCl to the desired concentrations. Test solutions of the calcium ionophore A23187 (a gift of Robert L. Hamill, Ph.D., of Lilly Research Laboratories) are made by diluting a stock solution of A23187 (5 mg/ml in DMSO) 1 : 40 in double distilled water and then in 0.15*M* NaCl to the desired concentration. At the end of the hour, the medium from each Petri dish is aspirated, centrifuged at 500 rpm (150 x *g*) for 5 min to remove any cells, and an aliquot is taken for lipid extraction.[20,21] Cells from control incubations are scraped off the bottom of the dishes in methanol and processed for lipid extraction. One milligram of lung lipid is added as carrier and for calculating recoveries on the basis of a measured DSPC content. The DSPC is isolated by alumina column chromatography after reaction with osmium tetroxide in carbon tetrachloride.[21] Aliquots are taken to determine lipid phosphorus for calculating recoveries for measurement of radioactivity for quantitating secretion.[22]

RESULTS

Primary Culture

During the initial 3 hr of incubation, many of the macrophages and a few of the type II cells adhere to the tissue-culture flask. The cells that adhere during the next 20 hr are mostly type II cells. Lymphocytes, a major contaminating cell, do not adhere in the

presence of serum. At 20 hr the purity of the adherent cells is 89.2 ± 4.6% (N = 17, mean ± standard deviation) The plating efficiency, based on measurement of DNA, is 44 ± 8% for all cells and 65 ± 8% (N = 5) for type II cells.

Figures 1 and 2 are photomicrographs of type II cells that have been in culture for 2 days. So that the cells can be photographed, they are cultured in special plastic chambers mounted on a glass microscope slide (Lab-Tek Products, Miles Laboratories Inc.). The cells are incubated for a few minutes at room temperature with the fluorescent dye, phosphine 3R (1 μg/ml), to cause the lamellar bodies to fluoresce.[22] The cells tend to form aggregates, a phenomenon that is common in primary cultures of other cells.[23] Figure 3 is a transmission electron micrograph of type II cells on the first day of culture. The lamellar bodies in these cells are very large, and some of them appear to be formed by the fusion of smaller lamellar bodies. Some tight junctions remain between attached cells; these junctions were apparently not disrupted when the cells were removed from the Petri dish with trypsin. The cytoplasm of many of the type II cells contains slit-like structures. We believe that these structures may be alterations in the endoplasmic reticulum rather than cholesterol clefts because they are bordered by limiting membranes and some contain electron dense filamentous material. Similar structures have been shown previously in type II cells[24,25] and in macrophages.[26] Ultrastructural examinations of the cells have not been performed after the first day in culture.

The importance of serum to achieve selective differential adherence and a high plating efficiency is shown in Fig. 4. In the absence of serum, most cells adhere at 3 hr; the media is therefore not removed in experiments performed with serumless media. At 24 hr only 20% of the cells are still adherent, and only 44% of these are type II cells. In this experiment about 2×10^6 cells (11.4 μg of DNA) were added in a volume of 5 ml to each 60-mm culture dish.

After the initial 20 hr, the cells in culture flatten out to form a monolayer of epithelial cells. Lamellar inclusion bodies (as visualized with phosphine 3R or the Papanicolaou stain) remain large for the first 3 days of culture. After 5 days in culture, some cells contain very small inclusion bodies and other cells appear to have no lamellar bodies; differential counts of the Papanicolaou-stained smears are difficult to perform because of the small size of the inclusion bodies. In cultures maintained from 1 to 3 weeks, no large inclusion bodies are seen with phosphine 3R or the Papanicolaou stain.

Figure 5 shows the change in percent of type II cells and DNA content in replicate cultures maintained for up to 5 days. After the

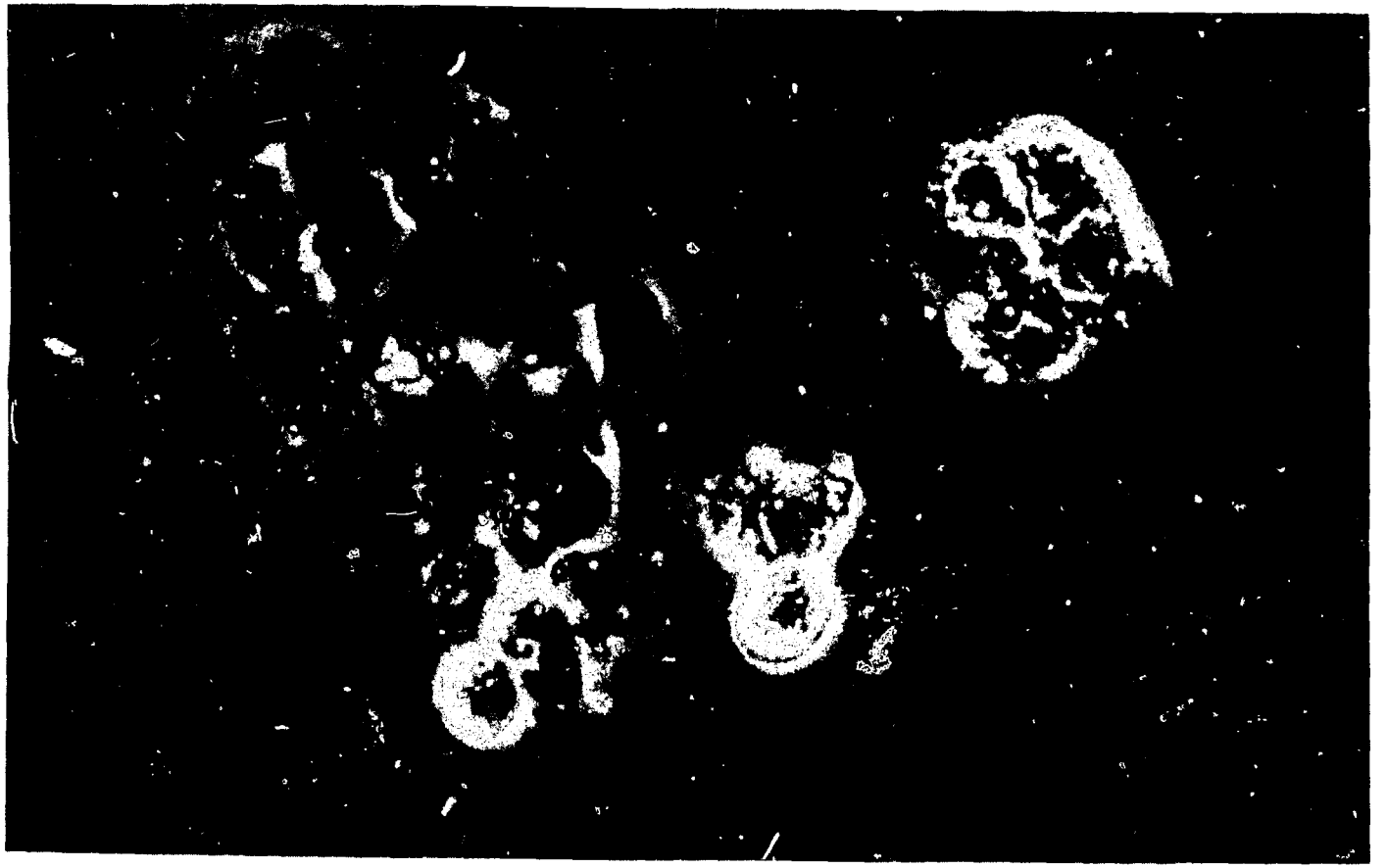

Fig. 1 Photomicrograph of type II cells cultured for 2 days as described in the methods. The cells are visualized by phase microscopy. (Magnification, 1100 ×.)

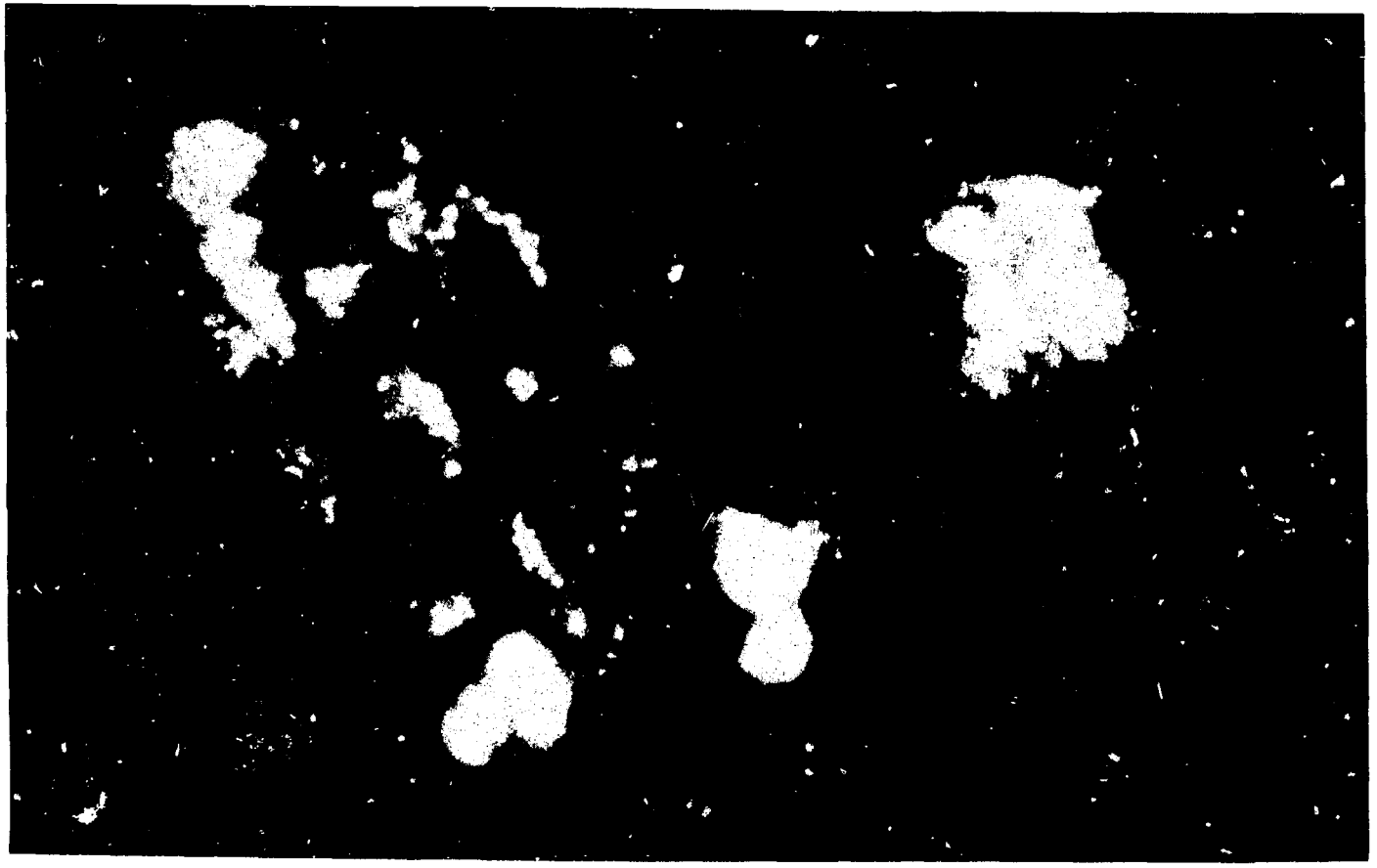

Fig. 2 Photomicrograph of type II cells cultured for 2 days as described in the methods. The cells are visualized with fluorescent microscopy. (Magnification, 1100 X.)

Fig. 3 Transmission electron micrograph of type II cells on the first day of culture. The cells are cultured for 1 day, washed, incubated for an additional hour to simulate a control culture for a release experiment, removed from the Petri dish with trypsin, and processed for electron microscopy. Note the very large lamellar inclusion bodies.

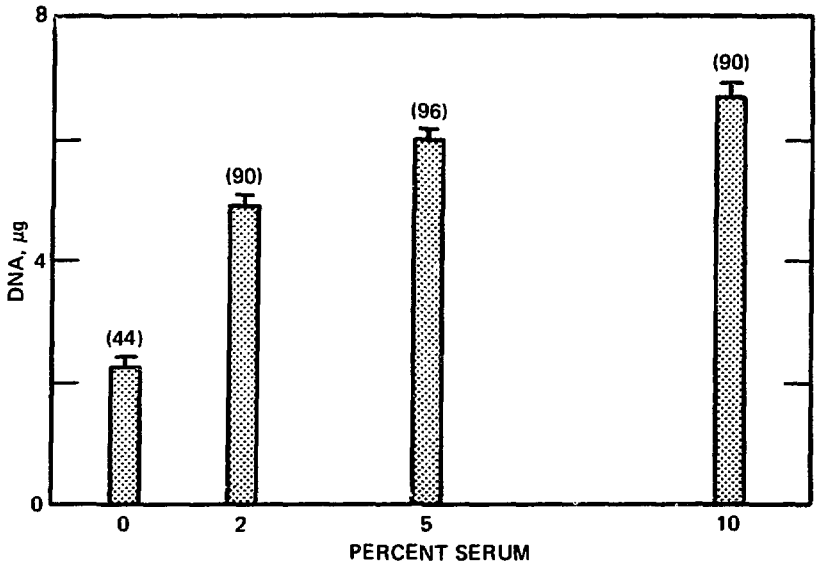

Fig. 4 Importance of serum for primary culture of type II cells. Serum is required for differential adherence and for a high plating efficiency of type II cells after 20 hr in culture. The numbers in parentheses are percent type II cells.

initial 3-hr adherence, 49% of the nonadherent cells are type II cells; at 20 hr in culture, 91% of the adherent cells are type II cells. In this and other experiments, the percent of cells judged to be type II cells decreases with time after the first day. There is also a slight decrease in DNA content. After the first day the cells also appear to be larger, but precise determinations of cell size have not been made.

Secretion

During the 90-min incubation period (30-min equilibration time after the addition of fresh media and 60-min incubation with control solutions), cells release 5.7 ± 1.8% (N = 10) of the total cellular [^{14}C]DSPC into the medium. From the data in Fig. 6, there is a slow release of this labeled compound in control cultures (3.3% per hour). The addition of DMSO in concentrations of 0.2 to 0.002% did not cause release over control values. These concentrations are the same as the final concentration of DMSO in the experiments with the calcium ionophore A23187 ($5 \times 10^{-6} M$) and with PMA ($2 \times 10^{-8} M$).

Phorbol myristate acetate is an active ingredient of croton oil[27] which causes secretion of lysosomal enzymes in polymorphonuclear leukocytes[28-30] and release of granules from platelets.[31] The PMA ($2 \times 10^{-8} M$) causes the release of 15.5 ± 3.0% (P = 0.001, N = 10) of

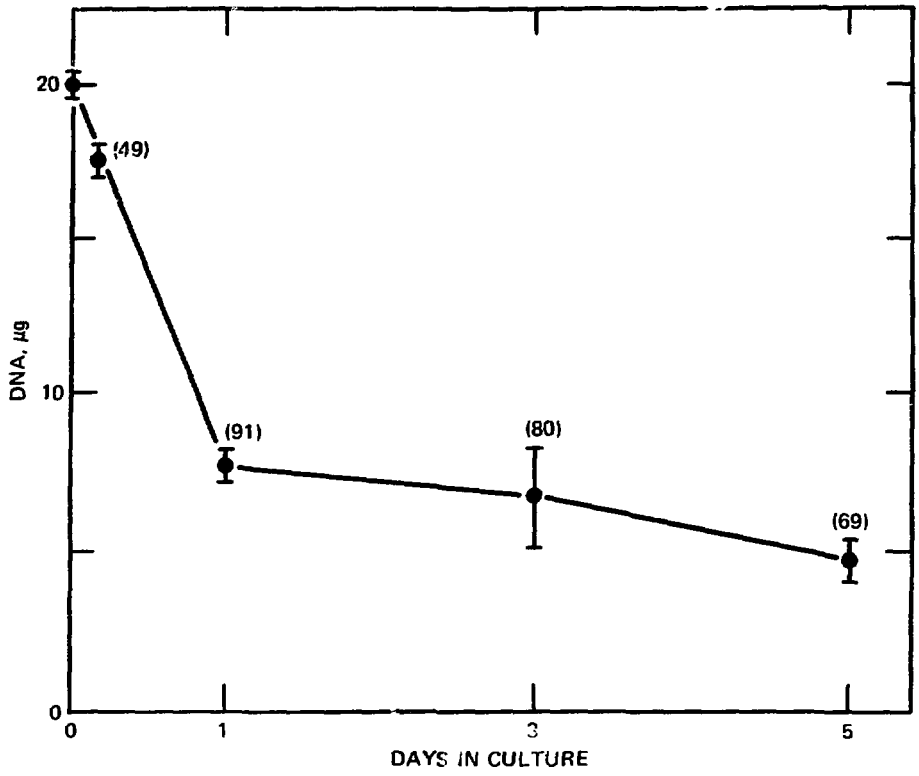

Fig. 5 Deoxyribonucleic acid content and percent type II cells (in parentheses) in replicate cultures maintained for up to 5 days.

total cellular [^{14}C]DSPC. The amount of labeled lipid in the medium in all these experiments includes that released during the 30-min equilibration period as well as the 60 min of incubation with the drug. The time course of release with PMA is shown in Fig. 6. Note that in this experiment 2.3% is released during the 30-min equilibration period before PMA is added and that there is a time lag of 15 min following the addition of PMA before a more rapid linear rate is achieved.

A dose–response curve for PMA is shown in Fig. 7. In this experiment the control release is high; there is no effect of PMA with a concentration less than $10^{-8}M$, and there is minimal stimulation with a concentration greater than $10^{-7}M$. In other experiments we have observed some stimulation of secretion by concentrations as low as $2 \times 10^{-9}M$ and additional stimulation at concentrations greater than $10^{-6}M$. We have not studied these variations in response to differing concentrations, but one explanation involves the low solubility of PMA in water (approximately $10^{-6}M$) (Ref. 32). When dilutions were made with higher concentrations of DMSO in water

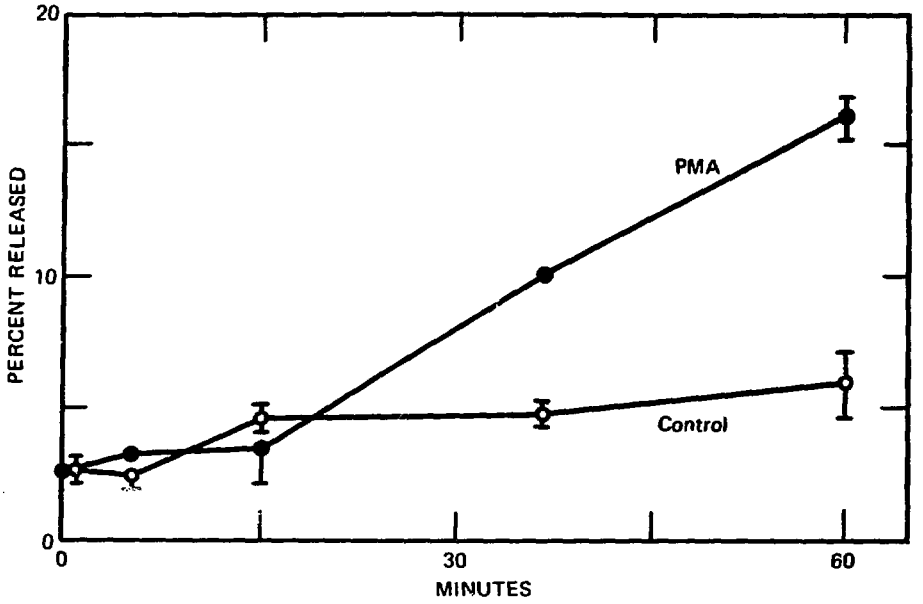

Fig. 6 Time course of secretion with phorbol myristate acetate.

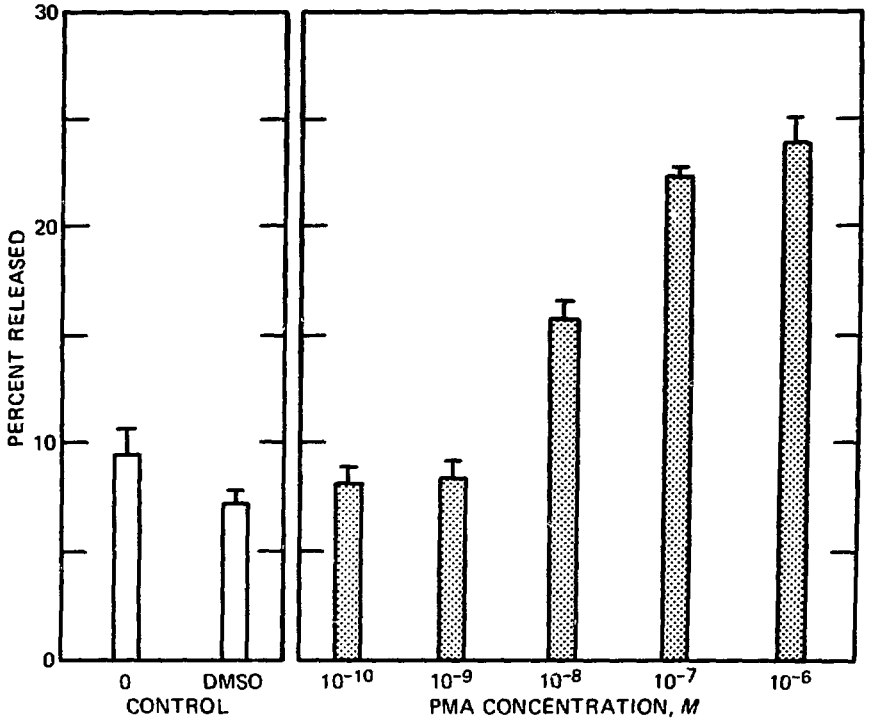

Fig. 7 Dose—response of secretion with phorbol myristate acetate. The concentration of DMSO in the column labeled DMSO is 0.4%; the same concentration is present with 10^{-6} *M* PMA. Other concentrations of PMA have proportionately less DMSO.

(0.8%), stimulation of secretion was observed at higher PMA concentrations.

We believe that the increased release of [^{14}C]DSPC in cultures treated with PMA is due to increased secretion and not to cytotoxicity. Transmission electron micrographs of cells treated with $2 \times 10^{-8} M$ PMA for 1 hr do not exhibit morphologic changes of toxicity. At this concentration of PMA, there is no change in exclusion of the vital dye erythrosin B (88 to 94% of cells exclude the dye).[33] The PMA ($2 \times 10^{-8} M$) increases the conversion of [1-^{14}C]glucose to $^{14}CO_2$ [an increase of 69 ± 35% (mean ± SD), N = 4, P = 0.03], as has been reported with polymorphonuclear leukocytes.[29] However, plating efficiency for all cells is diminished slightly in the presence of $2 \times 10^{-8} M$ PMA (from 44% to 39%); this may be related to the effect of PMA on surface glycoproteins.[34]

The calcium ionophore A23187 ($5 \times 10^{-6} M$) also increases secretion. Release of [^{14}C]DSPC in five experiments is 10.4 ± 2.3%, which has a P value of 0.003 in a paired *t*-test and is a mean increase of 118% over control release. The calcium ionophore is also effective at $1 \times 10^{-6} M$. We have not done studies to show that the release is totally calcium dependent. There is no change in vital dye exclusion of cells treated with the ionophore. The amount of DMSO used as a vehicle for the water-insoluble ionophore did not cause release. There is no effect of the calcium ionophore on oxidation of [1-^{14}C]glucose. Future studies will be needed to prove calcium dependency and exclude any toxicity.

DISCUSSION

Type II alveolar cells isolated by the initial published method[16] vary considerably in purity from preparation to preparation. The main contaminating cells are macrophages and lymphocytes. Although preparations that have a low percentage of type II cells can be further purified by procedures based on cell size,[35] the yield of cells after such procedures is not adequate for most biochemical experiments. The use of differential adherence in primary culture to purify type II cells has several appealing features: it is based on a property inherent to the cells involved (i.e., macrophages adhere more than type II cells and type II cells adhere more than lymphocytes); it is consistent in yielding preparations of nearly pure type II cells; and it allows the cells time to recover from the isolation procedure, a fact that may be of considerable importance when considering the acute loss and subsequent regeneration of cell surface receptors.[36]

The disadvantage of the method lies in the introduction of variables associated with cell culture. The basic concern is whether cells in culture behave in a similar fashion to cells in vivo. A major concern with type II cells in culture involves the lamellar inclusion bodies. Why do cells in culture initially develop very large inclusion bodies? Does the presence of large lamellar bodies imply a failure of secretion (perhaps secondary to the absence of the normal physiologic stimuli to secretion) or does it imply cell damage? Why do cells in culture lose their lamellar bodies after 5 days in culture? Is this loss an indication of a failure to manifest a differentiated function of type II cells, of the development of type II cells into the squamous type I cells,[37] or of the loss of type II cells and an overgrowth of fibroblasts? We do not currently know the answers to these questions, and, although some of the answers will be forthcoming, other answers may not be. Since the cells in culture flatten and appear to increase in size and since there is no net increase in DNA (cells plus media) over the time period that the cells are in culture, it seems unlikely that the observed changes in cell morphology represent merely an overgrowth of fibroblasts and death of type II cells. There is, however, no certain way at the present time of deciding whether a cell, in culture and without lamellar bodies, is a type I cell or a type II cell that has lost its lamellar bodies. The distinction between type I and type II cells is currently based on ultrastructural characteristics of cells in the intact lung and not on biochemical or functional characteristics that can be tested in vitro. Perhaps in the near future surface antigens or receptors will be found which permit differentiation of type I and type II cells in culture, and we will not have to rely completely on the presence of lamellar bodies to identify type II cells.

The secretion of pulmonary surface-active material is a known physiologic function of type II alveolar cells. We have chosen DSPC as a marker for surface-active material because it exists in high concentration in purified surface-active material and it is relatively, but not absolutely, specific for surfactant.[1,14,38,39] The assay developed in this laboratory for DSPC is adaptable to the analysis of multiple samples.[21] Although our experiments to date have not demonstrated large or consistent stimulation of secretion of DSPC with various neurotransmitters, prostaglandins, and derivatives of cyclic nucleotides, we have been able to demonstrate a stimulation of secretion with both PMA and the calcium ionophore A23187. These two compounds have been shown to cause the secretion of lysosomal enzymes in phagocytic cells,[28,40,41] and it therefore seems likely that they might also cause secretion of lamellar inclusion bodies since

lamellar bodies can be considered to be specialized lysosomes in that they arise from multivesicular bodies, contain acid hydrolases, and are surrounded by a limiting membrane.

Although the mechanism whereby PMA induces secretion is not known, it is likely that it involves an interaction between PMA and the plasma membrane. In chick fibroblasts, PMA causes a loss of the LETS or Z glycoprotein, a 220,000 dalton surface glycoprotein.[34,42] The mechanism of secretion, however, may also be related to intracellular processes. The PMA has many effects on cell ultrastructure and metabolism. In lymphocytes PMA increases blastogenesis.[43] In platelets PMA induces aggregation and causes a release of serotonin and adenine nucleotides.[31] In polymorphonuclear leukocytes, PMA causes an increase in the number of microtubules; this increase is followed by the disappearance of specific granules and the appearance of cytoplasmic vacuoles.[28,30] These morphologic changes are accompanied by the secretion of lysozyme and β-glucuronidase.[28] In addition, PMA causes an increase in oxygen consumption and hexose monophosphate shunt activity and a decrease in the uptake of 2-deoxyglucose and in the incorporation of amino acids into protein.[29,44]

The calcium ionophore A23187 has been used in many cell types to show that calcium movement is involved in the secretory process.[40,41,45] It is not clear if there needs to be a net flux of calcium into cells or just a redistribution of intracellular calcium to stimulate secretion. Our studies with the calcium ionophore suggest that calcium is involved in the secretory process by type II cells, but we have not shown that the secretory process is absolutely dependent on calcium. Because there is a relatively narrow range between physiologic effects and toxic effects with this compound, further conclusions will have to await additional experiments.

ACKNOWLEDGMENTS

The authors are deeply appreciative of the technical assistance of Sarah Jones and Jean Nellenbogen and the advice and encouragement of Drs. John A. Clements and Robert Greenleaf. Robert Mason is an Established Investigator of the American Heart Association. Mary C. Williams is the recipient of a Research Career Investigator Award (HL-00221) from the National Heart, Lung and Blood Institute (NHLBI). Leland Dobbs is the recipient of a Young Investigator Pulmonary Research Grant HL-19518 from the NHLBI. This work was supported by Program Project Grant HL-06285 and Specialized

Center of Research in Pulmonary Diseases HL-14201 from the NHLBI.

REFERENCES

1. J. Goerke, Lung Surfactant, *Biochim. Biophys. Acta*, 344: 241-261 (1974).
2. Y. Kikkawa, K. Yoneda, F. Smith, B. Packard, and K. Suzuki, The Type II Epithelial Cells of the Lung. II. Chemical Composition and Phospholipid Synthesis, *Lab. Invest.*, 32: 295-302 (1975).
3. J. Gil and O. K. Reiss, Isolation and Characterization of Lamellar Bodies and Tubular Myelin from Rat Lung Homogenates, *J. Cell Biol.*, 58: 152-171 (1973).
4. E. E. Faridy, S. Permutt, and R. L. Riley, Effect of Ventilation on Surface Forces in Excised Dogs' Lungs, *J. Appl. Physiol.*, 21: 1453-1462 (1966).
5. I. Wyszodgrodski, K. Keyi-Aboagye, H. W. Tausch, Jr., and M. E. Avery, Surfactant Inactivation by Hyperinflation: Conservation by End-Expiratory Pressure, *J. Appl. Physiol.*, 38: 461-466 (1975).
6. J. B. McClenahan and A. Urtnowski, Effect of Ventilation on Surfactant, and Its Turnover Rate, *J. Appl. Physiol.*, 23: 215-220 (1967).
7. M. J. Oyarzún and J. A. Clements, The Effect of Increased Ventilation, Cholinergic Stimulation and Blockade Upon Phospholipid Content (PL) of Rabbit Lung Lavage Fluid, *Physiologist*, 18: 342 (1975).
8. D. B. Olsen, Neurohumeral—Hormonal Secretory Stimulation of Pulmonary Surfactant in the Rat, *Physiologist*, 15: 230 (1972).
9. V. E. Godenberg, S. Buchingham, and S. C. Sommers, Pilocarpine Stimulation of Granular Pneumocyte Secretion, *Lab. Invest.*, 20: 147-158 (1969).
10. T. E. Morgan and B. C. Morgan, Surfactant Synthesis, Storage and Release by Alveolar Cells, in *Respiratory Distress Syndrome*, pp. 117-125, C. A. Villee, D. B. Villee, and J. Zucherman (Eds.), Academic Press, Inc., New York, 1973.
11. R. A. Redding, W. H. J. Douglas, and M. Stein, Thyroid Hormone Influence Upon Lung Surfactant Metabolism, *Science*, 175: 994-996 (1972).
12. D. Massaro, In Vivo Protein Secretion by Lung. Evidence for Active Secretion and Interspecies Differences, *J. Clin. Invest.*, 56: 263-271 (1975).
13. T. J. Delahunty and J. M. Johnston, The Active Effect of Colchicine and Vinblastine on the Release of Pulmonary Surface Active Material, *J. Lipid Res.*, 17: 112-116 (1976).
14. R. J. King, The Surfactant System of the Lung, *Fed. Proc.*, 33: 2238-2247 (1974).
15. R. J. Mason, Secretion of Disaturated Phosphatidylcholine by Primary Cultures of Type II Alveolar Cells, *J. Cell Biol.*, 70: 208a (1976).
16. R. J. Mason, M. Williams, and J. A. Clements, Identification and Isolation of Type II Alveolar Epithelial Cells, *Chest*, 67: 36S-37S (1975) Supplement.
17. Y. Kikkawa and K. Yoneda, The Type II Epithelial Cell of the Lung. I. Method of Isolation, *Lab. Invest.*, 30: 76-84 (1974).
18. T. T. Puck, S. J. Cieciura, and H. W. Fisher, Clonal Growth in Vitro of Human Cells with Fibroblastic Morphology, *J. Exp. Med.*, 106: 145-158 (1957).
19. K. Burton, Determination of DNA Concentration with Diphenylamine, in *Methods in Enzymology*, Vol. XII, Nucleic Acids, Part B, pp. 163-166, L. Grossman and K. Moldave (Eds.), Academic Press, Inc., New York, 1968.

20. R. J. Mason, G. Huber, and M. Vaughan, Synthesis of Dipalmitoyl Lecithin by Alveolar Macrophages, *J. Clin. Invest.*, 51: 68-73 (1972).
21. R. J. Mason, J. Nellenbogen, and J. A. Clements, Isolation of Disaturated Phosphatidylcholine with Osmium Tetroxide, *J. Lipid Res.*, 17: 281-284 (1976).
22. R. J. Mason and M. C. Williams, Identification of Type II Alveolar Cells with Phosphine 3R, *Am. Rev. Respir. Dis.*, 113: 47 (1976) Supplement.
23. B. A. Laishes and G. M. Williams, Conditions Affecting Primary Cell Cultures of Functional Adult Rat Hepatocytes. I. The Effect of Insulin, *In Vitro*, 12: 521-532 (1976).
24. R. A. Redding, T. Arai, W. H. J. Douglas, H. Tsurutani, and J. Overs, Early Changes in Lungs of Rats Exposed to 70% O_2, *J. Appl. Physiol.*, 38: 136-142 (1975).
25. D. J. Svoboda, Ultrastructure of Pulmonary Adenomas in Mice, *Cancer Res.*, 22: 1197-1201 (1962).
26. J. O. Harris, D. Bice, and J. G. Salvaggio, Cellular and Humoral Bronchopulmonary Immune Response of Rabbits Immunized with Actinomyces Antigens, *Am. Rev. Respir. Dis.*, 114: 29-43 (1976).
27. G. Weismann, W. Troll, B. L. van Duuren, and G. Sessa, Studies on Lysosomes. X. Effects of Tumor-Promoting Agents Upon Biological and Artificial Membrane Systems, *Biochem. Pharmacol.*, 17: 2421-2434 (1968).
28. I. M. Goldstein, S. T. Hoffstein, and G. Weissmann, Mechanisms of Lysosomal Enzyme Release from Human Polymorphonuclear Leukocytes, *J. Cell Biol.*, 66: 647-652 (1975).
29. J. E. Repine, J. G. White, C. C. Clawson, and B. M. Holmes, The Influence of Phorbol Myristate Acetate on Oxygen Consumption by Polymorphonuclear Leukocytes, *J. Lab. Clin. Med.*, 83: 911-920 (1974).
30. J. G. White and R. D. Estensen, Selective Labilization of Specific Granules in Polymorphonuclear Leukocytes by Phorbol Myristate Acetate, *Am. J. Pathol.*, 75: 45-60 (1974).
31. J. G. White, G. H. R. Rao, and R. D. Estensen, Investigation of the Release Reaction in Platelets Exposed to Phorbol Myristate Acetate, *Am. J. Pathol.*, 75: 301-314 (1974).
32. K. Jacobson, C. E. Wenner, G. Kemp, and D. Papahadjopoulos, Surface Properties of Phorbol Esters and Their Interaction with Lipid Monolayers and Bilayers, *Cancer Res.*, 35: 2991-2995 (1975).
33. H. J. Phillips, Dye Exclusion Tests for Cell Viability, in *Tissue Culture Methods and Applications*, pp. 406-408, P. F. Kruse, Jr., and M. K. Patterson (Eds.), Academic Press, Inc., New York, 1973.
34. P. M. Blumberg, P. E. Driedger, and P. W. Rossow, Effects of Phorbol Myristate Acetate on Chicken Embryo Fibroblasts, *J. Cell Biol.*, 70: 414a (1976).
35. R. J. Mason, M. C. Williams, and R. D. Greenleaf, Isolation of Lung Cells, in *Lung Cells in Disease*, A. Bouhuys (Ed.), pp. 39-52, American Elsevier Publishing Company, New York, 1976.
36. T. Kono, Destruction and Restoration of the Insulin Effector System of Isolated Fat Cells, *J. Biol. Chem.*, 244: 5777-5784 (1969).
37. I. Y. R. Adamson and D. H. Bowden, Derivation of Type I Epithelium from Type 2 Cells in the Developing Rat Lung, *Lab. Invest.*, 32: 736-745 (1975).
38. R. J. Mason, T. P. Stossel, and M. Vaughan, Tissue Concentration of Disaturated Lecithins, *Am. Rev. Respir. Dis.*, 107: 678-679 (1973).

39. S. L. Young and D. F. Tierney, Dipalmitoyl Lecithin Secretion and Metabolism in the Rat Lung, *Am. J. Physiol.*, 222: 1539-1544 (1972).
40. R. J. Smith and L. J. Ignaro, Bioregulation of Lysosomal Enzyme Secretion from Human Neutrophils: Roles of Guanosine 3′:5′-Monophosphate and Calcium in Stimulus-Secretion Coupling, *Proc. Natl. Acad. Sci. U.S.A.*, 72: 108-112 (1975).
41. R. D. Estensen, M. E. Reusch, M. L. Epstein, and H. R. Hill, Role of Ca^{2+} and Mg^{2+} in Some Human Neutrophil Functions as Indicated by Ionophore A23187, *Infect. Immun.*, 13: 146-151 (1976).
42. R. O. Hynes, Cell Surface Proteins and Malignant Transformation, *Biochim. Biophys. Acta*, 458: 73-107 (1976).
43. J. L. Wang, D. A. McClain, and G. M. Edelman, Modulation of Lymphocyte Mitogenesis, *Proc. Nat. Acad. Sci. U.S.A.*, 72: 1917-1921 (1975).
44. L. R. DeChatelet, P. S. Shirley, and R. B. Johnston, Jr., Effect of Phorbol Myristate Acetate on the Oxidative Metabolism of Human Polymorphonuclear Leukocytes, *Blood*, 47: 545-554 (1976).
45. S. Kondo and I. Schulz, Calcium Ion Uptake in Isolated Pancreas Cells Induced by Secretagogues, *Biochim. Biophys. Acta*, 419: 76-92 (1976).

Ultrastructural Characteristics of Pulmonary Alveolar Macrophages Induced to Multiply In Vitro

DANIEL L. LUCHTEL* and YVONNE NAUM†
*Department of Environmental Health, University of Washington, Seattle, Washington, and †Virginia Mason Research Center, Seattle, Washington, and Department of Medicine, University of Washington, Seattle, Washington

ABSTRACT

Correlative scanning and transmission-electron-microscopy studies on the in vitro growth of pulmonary alveolar macrophages (PAMs) are described. Pulmonary alveolar macrophages, obtained by lavage of C57Bl/6J mouse lungs, were grown in liquid culture. Control cultures were fed Ham's F12 with 15% fetal-calf serum (F12*), and experimental cultures were fed F12* : conditioned medium (1 : 1) (CM). The viable cells of the lavage suspension consisted of 98% PAMs and 2% lymphocytes. Newly attached cells in culture (0-day cultures) were a morphologically homogeneous population of PAMs. The number of PAMs in CM may increase up to 10 times in 10 days, whereas their number stays the same or decreases in F12*. In both media considerable polymorphism developed, but, in general, cells were either rounded or flattened on the substrate. With scanning electron microscopy no marked surface differences were apparent between proliferating and nonproliferating populations, although cells in CM showed more surface activity in terms of blebs and lamellipodia. Transmission electron microscopy revealed numerous lysosomes, residual bodies, and vacuoles in the cytoplasm of PAMs. In nonproliferative cultures, apparently viable macrophages maintained a similar morphology from 0 through 10 days of culture. In 10-day CM cultures, the most striking features of the cells were the presence of large, apparently macroendocytotic, vacuoles in the cytoplasm and more-pronounced polymorphism. This PAM culture system can be used in further study of the role of macrophages in immune response and in the pathogenesis of lung diseases.

We have previously reported that pulmonary alveolar macrophages (PAMs) obtained by lung lavage of C57Bl/6J mice proliferate extensively in response to factor(s) in media conditioned by lung-cell lines.[1,2] Smears of cells in the lung lavage of healthy animals reveal a

high degree of morphological homogeneity.[1,3] More than 97% of these cells are apparently macrophages. Our studies of the proliferative responses and morphological changes in this population are facilitated by the characteristic ability of PAMs to attach to surfaces.[4,5]

Their subsequent growth, including replication, has been studied in a liquid-culture system.[1,2] After an initial lag period of 3 days, PAMs from young adult mice can multiply 10-fold during the subsequent 7-day period. Growing PAMs in culture have been maintained for up to 15 weeks. Such growth has remained dependent on inclusion of factor(s) present in conditioned media. Thus far our knowledge of the factor(s) is that it is nondialyzable, of less than 50,000 daltons molecular weight, and resistant to freezing and thawing and to inactivation by proteases. During in vitro sojourn the PAM population becomes morphologically heterogeneous, with a greater range of heterogeneity being expressed in proliferating populations compared with nonproliferating populations. We report here ultrastructural observations of the cells obtained in lung lavage and the cells in proliferating and nonproliferating cultures. These studies confirm our previous reports of the proliferative capacity of lung-lavage cells and the identity of these cells as macrophages.

MATERIALS AND METHODS

The methodology relating to procurement of PAMs and their in vitro treatment is essentially as described previously.[2]

Animals

Male C57Bl mice (6 weeks old) obtained from Simonson Laboratories were used as the source of PAMs in these experiments. At the Virginia Mason Research Center, animals were housed in plastic cages (up to 6 animals per cage) and supplied water and feed ad libitum until used (0.5 to 6 weeks).

Collection of Lung-Free Cells

Mice were anesthetized with pentobarbital. The trachea was exposed aseptically, and a sterile polyethylene cannula was attached. Cell suspensions were obtained by lavage with isotonic saline. Only suspensions essentially free of blood cells were used. The cell pellet obtained after centrifugation at 200 × *g* for 10 min was resuspended in F12. Differential counts of Giemsa-stained smears indicated that the cell suspensions thus obtained were quite homogeneous: 96% to

97% of the cells were macrophages and ±3% were lymphocytes. More than 97% were judged viable on the basis of dye exclusion.

Cell-Culture Conditions

All cultures were incubated at 37°C in a humidified atmosphere at 5% CO_2 in air. The basic medium used in these experiments was Ham's F12 (Ref. 6), supplemented with 15% fetal-calf serum and penicillin–streptomycin at final concentrations of 500 and 50 μg/ml, respectively (Microbiological Associates). Conditioned medium was prepared from F12 medium exposed to confluent cultures of the mouse lung cell line 43074 (Ref. 7) at an early (4th) passage level. The collected media (all determined to be PPLO negative in the laboratory of Dr. G. E. Kenny, Department of Pathobiology, University of Washington) were passed through a Nucleopore (General Electric Company) membrane filter of 0.45-μm pore size; nutrients depleted in used medium were supplied by the addition of an equal volume of fresh F12 + 10% (final volume) FBS to the filtered conditioned medium.

Experimental Design

This protocol was designed to provide maximal cell material for morphologic studies. A single drop of cell suspension (approximately 10 μl) was delivered to each of a number of glass cover slips placed in tissue-culture dishes (for scanning electron microscopy) or directly onto the plastic surface (for transmission electron microscopy). An incubation period of 1.5 hr at 37°C, allowing for attachment of macrophages, was followed by aspiration of the suspending medium, rinse, and replacement with either control or conditioned medium. Cultures were processed for electron microscopy at 0 day (immediately after the 1.5-hr incubation described above), at 2 or 3 days, and at 10 days.

Electron-Microscopic Methods

Cells from lung lavages were fixed in 2% glutaraldehyde in 0.1*M* cacodylate buffer (pH 7.4), centrifuged, and resuspended in 1% OsO_4 in 0.1*M* cacodylate buffer. The cells were then centrifuged in BEEM capsules (bottleneck embedding capsules, size 00) at 1300 × *g* for 10 min. After centrifugation, the cells from the lung lavage of one mouse formed a thin relatively flat layer at the bottom of the capsule. The pellet was then dehydrated by successive gentle changes of ethanol and propylene oxide and embedded in Epon. After polymerization, the pellet was reembedded in fresh Epon to facilitate

the cutting of cross sections through the entire depth of the pellet. This method of preparing a pellet of cells was used so that sections of the pellet could be used as representative samples of the total cell population.

Cell cultures were fixed by adding 2% glutaraldehyde in 0.2*M* cacodylate (pH 7.4) to an equal volume of culture medium covering the cells or by adding 2% glutaraldehyde to the culture medium to a final concentration of 1% glutaraldehyde (the culture medium maintained a pH of 7.2 in a final concentration of 1% glutaraldehyde). The cultures were then postfixed in 1% OsO_4 in 0.1*M* cacodylate. For transmission electron microscopy, cultures grown in plastic Petri dishes were dehydrated in ethanol and processed through several changes of Epon without intermediate changes in propylene oxide. After polymerization, the plastic dishes were cracked away from the thin discs of Epon. Portions of the cultures were sawed out and mounted on aluminum slugs. "Face-on" sections of the cultures were cut; i.e., the cuts were parallel to the surface of the cultures. Thin sections were stained with uranyl acetate and lead citrate. For scanning electron microscopy, cultures grown on glass cover slips were dehydrated in ethanol, processed through amyl acetate, and critical-point dried. They were then coated with a layer of gold and palladium.

RESULTS

So that the cell types making up the cell population of the lung lavage could be determined, 300 cells from two different areas of a pellet from one animal were counted consecutively. Top and bottom halves of the pellet were sampled equally. Low-magnification pictures (700 X) were taken of sections on 200-mesh grids. One section from each block was photographed to avoid duplication of cell counts. Only cells showing some portion of the nucleus were counted.

Approximately 80% of the cells in a lung lavage were apparently viable alveolar macrophages (see Table 1 and Fig. 1). Although all features are not displayed by all cells, the macrophages are characterized by numerous surface folds, various and numerous inclusions and vacuoles, and eccentric nuclei (often of convoluted shape). In Fig. 1 all the viable cells showing some portion of their nuclei appear to be macrophages. Approximately 20% of the cells in a lavage appeared moribund (pycnotic nuclei and fragmented cytoplasm). Examples of such cells are shown in Fig. 1. Lymphocytes made up approximately 2% of the lavage cells. It should be

TABLE 1

CELLULAR COMPOSITION OF LUNG LAVAGE (300 CELLS COUNTED)

Cell type	No. of cells	Percentage
Alveolar macrophages	237	79
Moribund alveolar macrophages	28	9
Moribund ciliated cells	10	3
Unidentifiable moribund cells	20	7
Lymphocytes	5	2

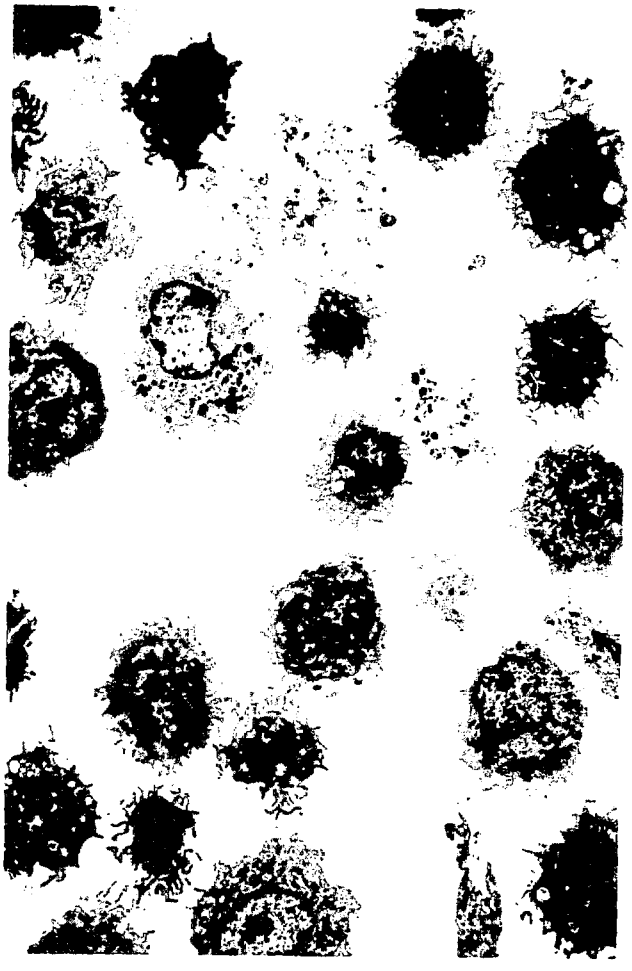

Fig. 1 Low-magnification electron micrograph showing a survey view of the lung-lavage pellet. Except for the moribund-appearing cells (which are difficult to identify), the cells are alveolar macrophages. (Magnification, 1500 ×.)

noted that, of the viable-appearing cells, 98% were alveolar macrophages.

Figures 2 to 4 show the range of appearances for the macrophages from a lavage Heterogeneous cytoplasmic inclusions (residual bodies and primary and secondary lysosomes) are typical of the macrophages. Short segments of rough endoplasmic reticulum, Golgi membranes, and mitochondria were also present. The cell surface was usually quite folded. Although not resolved at the magnifications shown, dense arrays of microfilaments were present at the cell periphery, and some microfilaments were present throughout deeper regions of the cytoplasm. Some macrophages (Fig. 4) contained many electron lucent vacuoles.

Scanning electron microscopy proved to be an excellent method of surveying cell density and vitality of the cultures. Figure 5 is a micrograph showing the approximate center of a culture fixed 1.5 hr after initiation of the culture. Except for a few moribund cells, the adhering cells were alveolar macrophages (as confirmed by transmission electron microscopy; Figs. 8 to 12). Except for some cell flattening and spreading on the substrate, cultures of cells maintained for 10 days in control medium were similar in appearance to the 0-day cultures (Fig. 6). Cells grown for 10 days in conditioned medium showed a dramatic increase in cell density (Fig. 7).

Transmission electron microscopy confirms that the attached viable cells in control or conditioned medium at 0 day, 2 or 3 days, and 10 days were alveolar macrophages (Figs. 8 to 12). At 0 day the viable-appearing cells (Fig. 8) were quite similar in appearance to lavage macrophages (Figs. 2 to 4). The only striking difference was the peculiar increase in electron density of the mitochondrial matrix. This was not seen in cells at later times. Perhaps this was a response of the mitochondria to the lavage conditions and initiation of the cultures. Moribund ciliated cells (readily identified by the presence of cilia) were also regularly seen at day 0. Many of these were in the process of being phagocytized by macrophages. After 2 days in culture, the macrophages had essentially the same appearance (Figs. 9 and 10). After 10 days in culture in control medium, moribund macrophages were regularly seen. Even in viable-appearing cells, many of the mitochondria were fragmented, and the residual bodies were very electron dense (Fig. 11). After 10 days in conditioned medium, many of the macrophages had large vacuoles (Figs. 12 and 13). All the cells appeared to be macrophages, and occasionally sections of cells in mitosis were seen.

Figure 14 shows an attached alveolar macrophage fixed at 0 day (1.5 hr after initiation of culture). Although some of the attached

(Text continues on page 311.)

Figure 2

Figs. 2 to 4 Morphological variations of the alveolar macrophages in the lavage pellet. Those in Fig. 2 are probably the most numerous, although macrophages with the morphology of those in Fig. 3 are also quite typical (note the moribund ciliated cell in Fig. 3). Macrophages with numerous large vacuoles are also occasionally seen (Fig. 4). (Figure 2 magnification, 6000 X. Figure 3 magnification, 4500 X. Figure 4 magnification, 8000 X.)

Figure 3

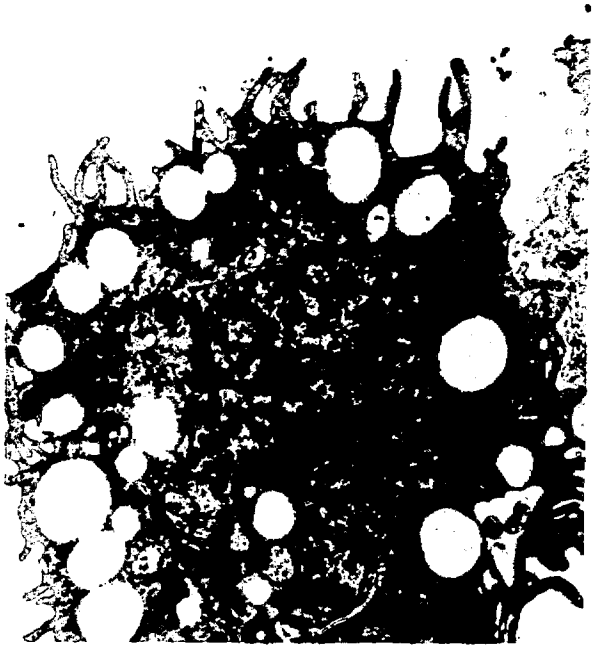

Figure 4

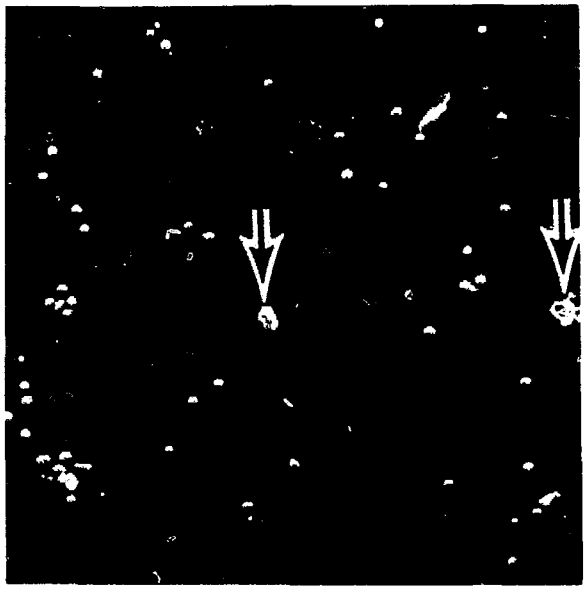

Figure 5

Fig. 5 Scanning electron micrograph showing an alveolar macrophage culture fixed at 0 day (1.5 hr after initiation of culture). The attached macrophages are either rounded or somewhat spread or flattened. A few moribund cells or cell fragments are also present (arrows). Some of these moribund cells can be identified as ciliated cells (not resolved at this magnification). All the viable attached cells appear to be alveolar macrophages (as also confirmed by transmission electron microscopy). (Magnification, 150 X.)

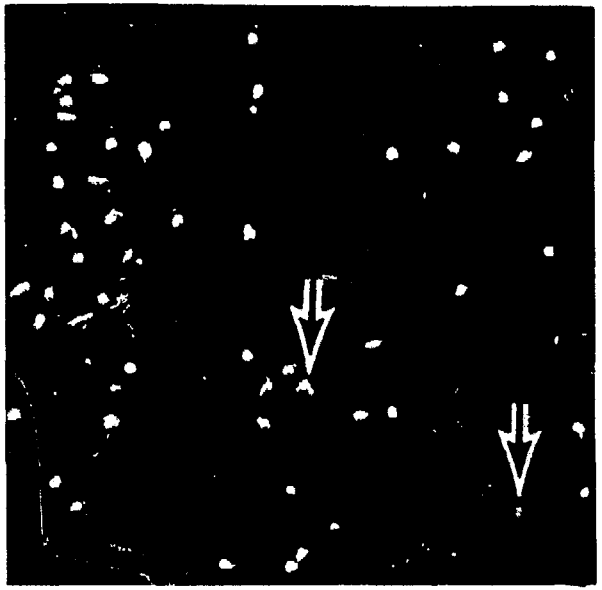

Figure 6

Fig. 6 Alveolar macrophage culture fixed at 10 days, control medium. Compared to 0-day cultures, the flattened cells are generally more spread on the substrate. Several cells appear to be moribund or are fragments of moribund cells (arrows). (Magnification, 150 X.)

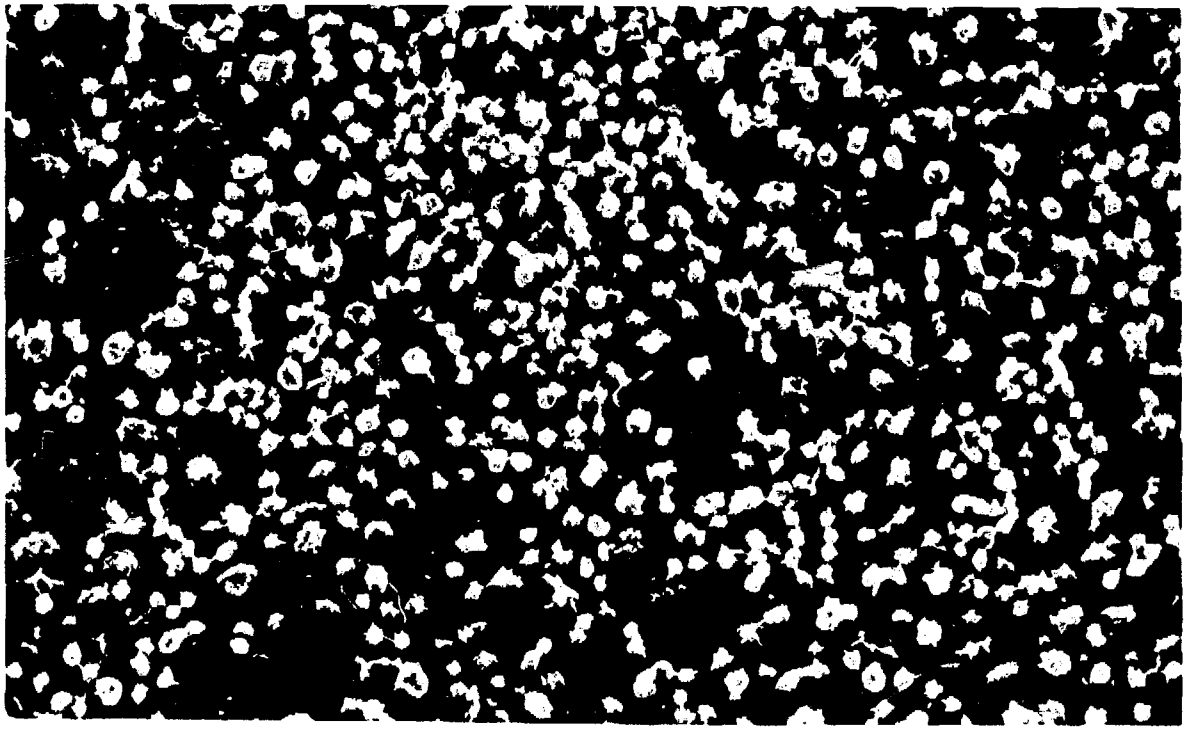

Fig. 7 Alveolar macrophage culture fixed at 10 days, conditioned medium. The macrophages shown in Figs. 5, 6 and 7 are all at approximately the center of the cultures. The increase in cell number in the conditioned medium culture compared to the control can be easily appreciated. The macrophages in the conditioned medium culture can vary in appearance from highly flattened and spread to a more rounded appearance. (Magnification, 250 X.)

Fig. 8 Alveolar macrophage fixed at 0 day. Numerous lysosomes are distributed throughout the cytoplasm. The mitochondrial matrix is quite electron dense (particularly in comparison with later cultures). Other organelles in the cytoplasm are endoplasmic reticulum, bundles of microfilaments, coated vesicles, and large vacuoles. Some of the vacuoles at the cell periphery are probably not true intracellular vacuoles but are indentations of the plasma membrane which, at the level of the section, appear as vacuoles (compared with the transmission electron micrograph of Fig. 13). (Magnification, 6000 X.)

Fig. 9 Alveolar macrophage fixed at 2 days, control medium. Compared to 0-day cultures, the cellular appearance is quite similar except for an apparent increase in the membranes of the Golgi apparatus. (Magnification, 4800 X.)

Fig. 10 Alveolar macrophage fixed at 2 days, conditioned medium. The Golgi membranes and lysosomes are typically a major component of the cytoplasm. Large vacuoles are also more evident. The surface folds are more numerous and have a thinner profile than cells of the control cultures. (Magnification, 3200 X.)

Fig. 11 Alveolar macrophage fixed at 10 days, control medium. The most striking features of these cells are the light staining (and apparently abnormal) mitochondria and the very densely staining residual bodies (arrows). (Magnification, 4800 X.)

Fig. 12 Alveolar macrophage fixed at 10 days, conditioned medium. The cytoplasmic appearance of these cells is not definably different from 2- or 3-day cultures in conditioned medium except for the presence of very large vacuoles. Extensive networks of branching, thin surface folds, extend from the cell periphery. (Magnification, 4000 X.)

Figure 9

Figure 10

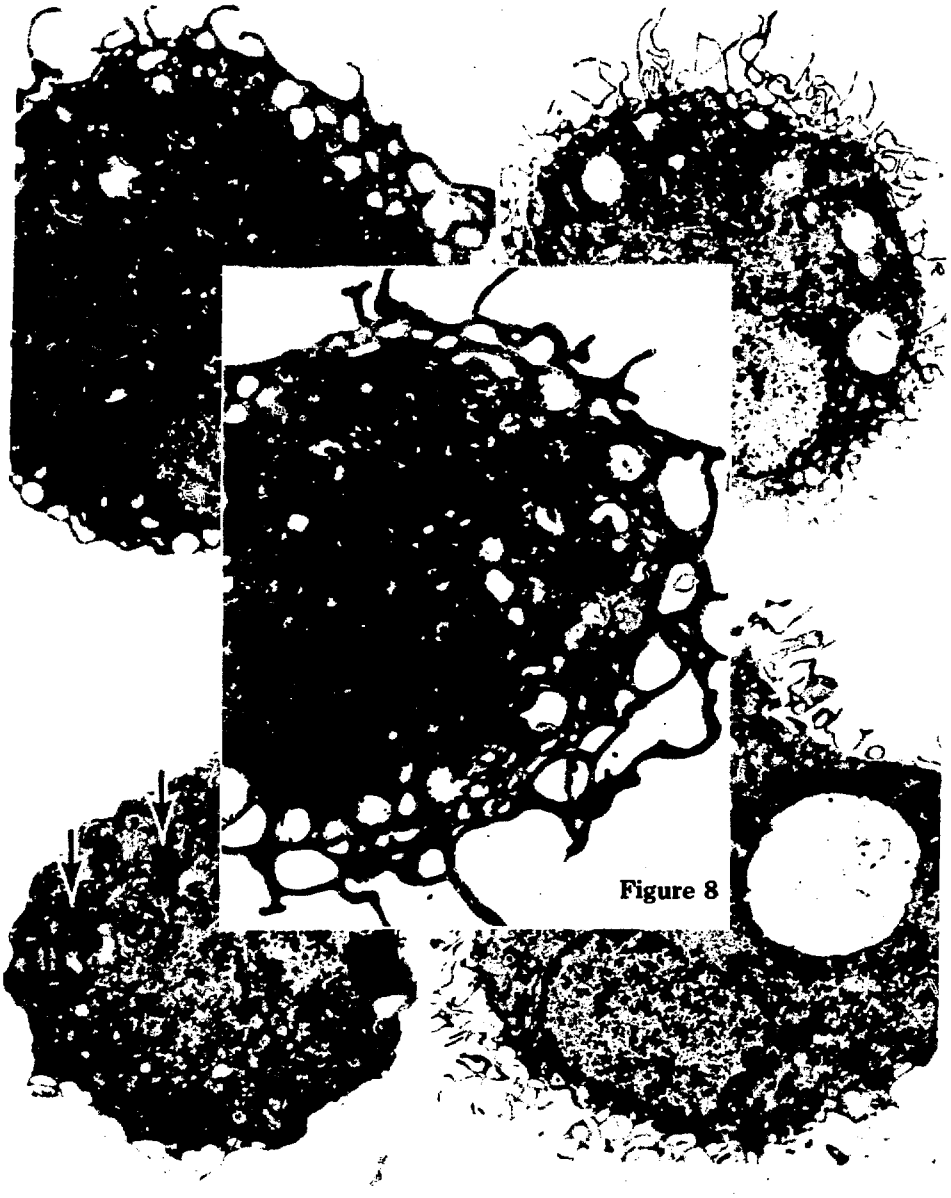

Figure 8

Figure 11

Figure 12

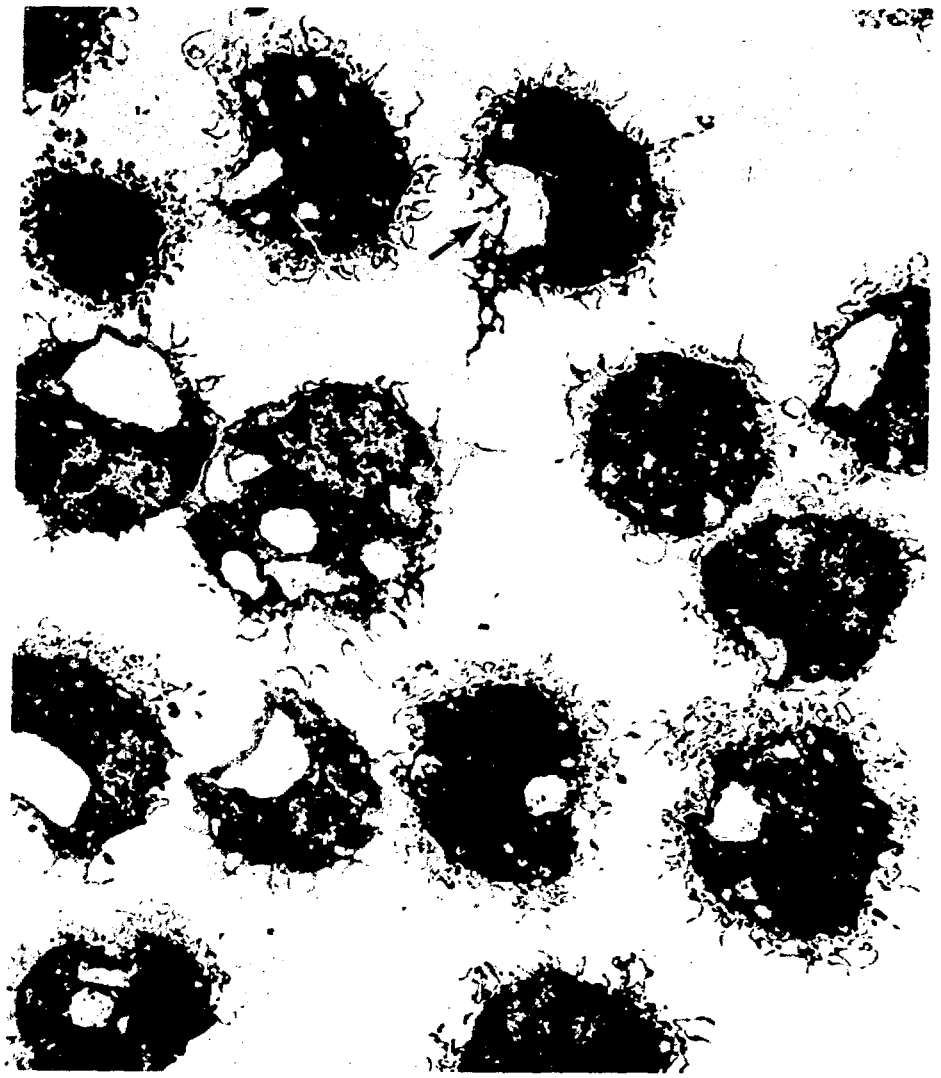

Fig. 13 Alveolar macrophages fixed at 10 days, conditioned medium. A survey view to show the ubiquity of the large vacuoles within these cells. These vacuoles are apparently endocytotic; occasionally a section showing an opening to the outside is found (arrow). (Magnification, 2400 X.)

Fig. 14 Alveolar macrophage fixed at 0 day. The cell surface shows many surface folds or ridges. (Magnification, 8000 ×.)

cells are more rounded, this cell is typical in showing a dome-shaped central region surrounded by a more flattened "skirt" of cytoplasm. After 3 days in culture, both control and conditioned medium cultures showed rounded cells and flattened cells (Figs. 15 and 16). The cells in conditioned medium showed more convoluted cell surfaces consisting of blebs, lamellipodia, and pseudopodia (Fig. 16).

At 10 days control medium and conditioned medium cultures were similar in that both rounded and flattened cells were present in both cultures (Figs. 17 and 18). In the center of the conditioned medium cultures, the rounded cell was much more numerous than the flattened cell (Figs. 7 and 18). At the periphery of these cultures, however, the flattened cell was more numerous (Fig. 19). The cells may display unusual polymorphism (Figs. 19 and 20).

Figure 15

Figure 16

Fig. 15 Alveolar macrophages fixed at 3 days, control medium. The cells may be rounded or flattened on the substrate. In both cases, however, there tends to be a dome-shaped central region surrounded by a somewhat smoother surface "skirt" of cytoplasm. The skirt may be scalloped, and long pseudopodia may extend from it. (Magnification, 2975 X.)

Fig. 16 Alveolar macrophages fixed at 3 days, conditioned medium. The cells are similar to cells in control medium, although surface blebs and lamellipodia are more distinct, both on the rounded and flattened cells. (Magnification, 1700 X.)

Figure 17

Figure 18

Fig. 17 Alveolar macrophages fixed at 10 days, control medium. (Magnification, 1275 X.)

Fig. 18 Alveolar macrophages fixed at 10 day conditioned medium. The surface features of individual cells grown in control medium (Fig. 17) and conditioned medium are similar. (Magnification, 1275 X.)

Figure 19

Fig. 19 Alveolar macrophages fixed at 10 days, conditioned medium. This micrograph was obtained from the edge of the culture (Figs. 7 and 18 show the approximate center of the same culture). Near the edge of the culture, a higher proportion of the cells are flattened and spread on the substrate. Although most of these flattened cells are circular in outline, the cell periphery of others is highly scalloped or indented, being stellate in outline. The arrow denotes a cell shown at higher magnification in Fig. 20. (Magnification, 125 X.)

Figure 20

Fig. 20 Alveolar macrophage fixed at 10 days, conditioned medium. The cell surface is relatively smooth except for the tips of the "arms" where surface ridges or lamellipodia are present. (Magnification, 1275 X.)

DISCUSSION

The present description of PAMs in lung lavage is in general agreement with previous observations.[8] The cells have a single eccentrically placed nucleus, a variety of inclusions and vacuoles, and extensive membrane ruffling. Without cytochemical evidence it is difficult to identify the nature of the vacuoles that accumulate in the growing macrophages. It is not likely that these vacuoles are secondary lysosomes because of their electron lucency. They may be an accumulated metabolic product or, more likely, a type of endocytotic vacuole. Although such large vacuoles are an unusual cellular feature, macrophages of the lung lavage may also show a striking accumulation of vacuoles (Fig. 4). It should also be noted that these vacuoles probably do not represent a pathological response since cultures derived from lavage cells have been passaged and maintained for more than 3 months.[1] Both in vivo studies and in vitro studies with nongrowing PAMs have suggested that the alveolar macrophage is different from macrophages in other parts of the body.[9]

In our previous work we determined that increase in cell number does not occur before 3 days in this system[2] and that this quiescent period is followed by a logarithmic growth phase for at least the next 7 days. Thus, for this study, sampling times of cultured material correspond to initiation of cultures (0 day), premitotic cells (2 or 3 days), and log phase cells (10 days).

The observed morphological heterogeneity of PAMs in culture is at least in part due to the static nature of the evidence presented here. The heterogeneity may represent transitory morphologies related to stage in the cell cycle or be of some functional or metabolic significance. Preliminary evidence, obtained by observing cultures with phase microscopy and photographing marked areas, demonstrates transitory morphologies of PAMs in vitro.[10] Pulmonary alveolar macrophages in CM seem to migrate and change shape more than cells in control medium. Additionally, the phenotypic range of PAMs could reflect a functional heterogeneity of the cells in lung wash analogous to functional heterogeneity of peritoneal macrophages.[11] We have previously observed that macrophage derivatives of various morphologies (round, stellate, elongated, and polygonal) can all phagocytize zymosan particles.[1]

A number of recent studies attest to the proliferative capacity of PAMs in vivo,[12,13] with the ultimate precursor of PAMs residing in the bone marrow.[14-17] Although results of most in vitro studies

with PAMs have supported the interpretation of this cell as an "end of the line cell,"[18,19] Lin, Kuhn, and Kuo[20] have demonstrated a fraction of free alveolar cells from hamsters, rats, and mice that are capable of colony formation in both soft agar and liquid cultures. These cells also required conditioned medium factor(s) for their growth, and only mononuclear phagocytes were found in the colonies. This study confirms and extends our previous reports[1,2,21] demonstrating proliferation of PAMs in response to factor(s) released by other lung cells. Such factor(s) could be made available to PAMs in instances of tissue injury, e.g., result of exposure to NO_2 (Refs. 12 and 22), high O_2 (Ref. 23), or inflammation.[24] We suggest that it may be possible that the increased number of macrophages in the alveoli after these environmental insults may be due to macrophage proliferation as well as to increased migration from the interstitium. It is not necessary to suggest that the macrophages are particularly resistant to the insults. After the environmental stress, newly arrived macrophages may further augment their numbers by active proliferation.

Some interesting questions raised by these studies are: (1) What is the identity of the mitogen and its source and mechanism of action? (2) Are all PAMs in the lung lavage equally responsive to the mitogen, and does this vary with age or physiological state of the animal? and (3) Is multiplication of PAMs required to express a functional heterogeneity inherent in the population? We suggest that answers to these questions are relevant to greater understanding of the role of PAMs in healthy and diseased lungs as well as to defining more precisely the role of the macrophage in immune defense.

ACKNOWLEDGMENTS

We thank Jack Boykin for his technical assistance. This work was supported by NHLI SCOR HL14152.

REFERENCES

1. S. C. Soderland and Y. Naum, Growth of Pulmonary Alveolar Macrophages In Vitro, *Nature*, 245: 150-152 (1973).
2. Y. Naum, Growth of Pulmonary Alveolar Macrophages In Vitro: Responses to Media Conditioned by Lung Cell Lines, *Cytobios*, 14: 211-220 (1975).
3. Q. N. Myrvik, E. S. Leake, and B. Fariss, Studies on Pulmonary Alveolar Macrophages from the Normal Rabbit: a Technique to Procure Them in a High State of Purity, *J. Immunol.*, 86: 28-132 (1961).
4. R. Oren, A. E. Farnham, K. Saito, E. Milofsky, and M. L. Karnovsky, Metabolic Patterns in Three Types of Phagocytizing Cells, *J. Cell Biol.*, 17: 487-501 (1963).

5. C. Voisin, J. Guillaume, C. Aerts, C. van Morleghem, and C. Gernez-Rieux, Culture In Vitro de Macrophages Alvéolaires de Cobaye, *C. R. Hebd. Séances Acad. Sci.*, 256: 3504-3506 (1963).
6. R. G. Ham, Clonal Growth of Mammalian Cells in a Chemically Defined, Synthetic Medium, *Proc. Natl. Acad. Sci. U. S. A.*, 53: 288-293 (1965).
7. Y. Naum, S. Palmer, and T. E. Morgan, Morphologic and Metabolic Characteristics of Cell Lines Derived from Lung Tissue of C57Bl Adult Mice, unpublished.
8. M. Fedorko and J. G. Hirsch, Structure of Monocytes and Macrophages, *Semin. Hematol.*, 7: 109-124 (1970).
9. A. B. Cohen and W. M. Gold, Defense Mechanisms of the Lungs, *Annu. Rev. Physiol.*, 37: 325-350 (1975).
10. Y. Naum, Virginia Mason Research Center, unpublished observations.
11. W. S. Walker, Functional Heterogeneity of Macrophages: Subclasses of Peritoneal Macrophages with Different Antigen-Binding Activities and Immune Complex Receptors, *Immunology*, 26: 1025-1037 (1974).
12. M. J. Evans, L. J. Cabral, R. J. Stephens, and G. Freeman, Cell Division of Alveolar Macrophages in Rat Lung Following Exposure to NO_2, *Amer. J. Pathol.*, 70: 199-207 (1973).
13. D. W. Golde, T. N. Finley, and M. J. Cline, The Pulmonary Macrophage in Acute Leukemia, *New Engl. J. Med.*, 290: 875-878 (1974).
14. E. D. Thomas, R. E. Ramber, G. E. Sale, R. S. Sparkes, and D. W. Golde, Direct Evidence for a Bone Marrow Origin of the Alveolar Macrophage in Man, *Science*, 192: 1016-1018 (1976).
15. J. J. Godleski and J. Brain, The Origin of Alveolar Macrophages in Mouse Radiation Chimeras, *J. Exp. Med.*, 136: 630-643 (1972).
16. M. O. Pinkett, C. R. Cowdry, and P. C. Nowell, Mixed Hematopoietic and Pulmonary Origin of "Alveolar Macrophages" as Demonstrated by Chromosome Markers, *Am. J. Pathol.*, 48: 859-867 (1966).
17. M. Virolainen, Hematopoietic Origin of Macrophages as Studied by Chromosome Markers in Mice, *J. Exp. Med.*, 136: 943-951 (1968).
18. D. H. Bowden and I. Y. R. Adamson, The Alveolar Macrophage Delivery System, *Am. J. Pathol.*, 83: 123-134 (1976).
19. D. H. Bowden, The Alveolar Macrophage, in *Current Topics in Pathology*, pp. 1-36, Springer, Berlin, 1971.
20. H. Lin, C. Kuhn, and T. Kuo, Clonal Growth of Hamster Free Alveolar Cells in Soft Agar, *J. Exp. Med.*, 142: 877-886 (1975).
21. Y. Naum, Identification of Alveolar Macrophages in Cultures of Lung Tissue, *J. Cell Biol.*, 63: 242a (1974).
22. G. Freeman, S. C. Crane, and N. J. Furiosi, Healing in Rat Lung After Subacute Exposure to Nitrogen Dioxide, *Am. Rev. Respir. Dis.*, 100: 662-676 (1969).
23. D. S. Bonikos, K. G. Bensch, and W. H. Northway, Progressive Irreversible Pulmonary Damage Caused by Chronic Exposure to 100% Oxygen, *Am. J. Pathol.*, 78: 9a (1975).
24. K. M. Wynne, W. G. Spector, and D. A. Willoughby, Macrophage Proliferation In Vitro Induced by Exudates, *Nature*, 253: 636-637 (1975).

Endocrine (APUD-Type) Cells in Dissociated Cell Suspensions of Rabbit Trachea

K. SONSTEGARD and E. CUTZ
Department of Pathology and the Research Institute, The Hospital for Sick Children, Toronto, Ontario, Canada

ABSTRACT

Argyrophilic amine-storing and neurosecretory granule-containing cells, referred to as Kultschitzky cells (K. cells) have recently been identified in tracheobronchial mucosa of human and various mammals. Although the function of K. cells in lung has not yet been established, these cells appear identical to the cells of the polypeptide hormone-producing amine precursor uptake and decarboxylation endocrine system. The relationship of K. cells to the origin of lung carcinoid and oat-cell carcinomas has been previously demonstrated. Studies on K. cells in normal lungs are complicated by their scattered distribution and low numbers in a mixed population of tracheobronchial epithelial cells.

This study reports on a method for dissociation of tracheal epithelial cells with the recovery of K. cells in dispersed cell preparations. During our initial experiments various mechanical and/or enzymatic methods were applied to whole rabbit tracheae, and cell suspensions were evaluated for yield, viability, degree of single cell dissociation, morphology, ultrastructural preservation, and percentage of cells recovered. The presence of K. cells was monitored by silver staining, formaldehyde-induced fluorescence, and electron microscopy. Simple scraping and/or stripping of mucosa followed by enzymatic treatment did not provide satisfactory cell preparations. The following enzyme treatments at various concentrations and time intervals were used: trypsin, trypsin with collagenase or ethylenediaminetetraacetic acid, collagenase, and pronase. The most satisfactory results were obtained with 1% pronase in Joklik's modified minimal essential medium (37°C, 5% CO_2 in air). Single cell suspensions (yields up to 20×10^6 and 95% viability) were obtained after 60 min of treatment. The K. cells were identified in dispersed cell preparations and retained their characteristic features, e.g., amine precursor uptake, argyrophilia, and neurosecretory granules.

The complex anatomy of the lung and the heterogeneity of its cell population presents a major obstacle for studies on specific pulmonary cell types, particularly as they relate to their function, interrelationship, and responses to injury. One of the important recent developments in the study of lung epithelial cells has been the use of cell separation methods to obtain homogeneous preparations of single types of cells. However, most of these studies have focused on the isolation of alveolar type II cells,[1-3] but the separation of airway epithelial cells has not been previously reported.

The tracheobronchial (TB) mucosa is composed of a mixed population of specialized epithelial cells, the main types being the ciliated and nonciliated cells. The ciliated cells usually predominate in the upper respiratory tract and extend up to the terminal airways.[4] Among the nonciliated cells, the goblet cells, intermediate and basal cells are the most familiar cell types. In small bronchioles the goblet-cell population is replaced by dome-shaped Clara cells.[5] The occurrence within the TB mucosa of yet another type of distinctive cell with presumed endocrine function has only recently been appreciated. These cells are referred to as Kultschitzky cells (K. cells) by analogy with similar cells in the gastrointestinal tract.[6] The main features of K. cells include cytoplasmic argyrophilia, amine contents, and the presence of specific neurosecretory-type granules.[7,8] In this respect the lung K. cells appear identical to the cells constituting the amine precursor uptake and decarboxylation (APUD) endocrine system.[9]

Although the function of the major types of TB epithelial cells is generally well understood, information regarding the role of K. cells in normal or diseased lung is manifestly incomplete. The purpose of this study was to develop a cell dissociation procedure for the isolation of various types of TB epithelial cells, including the K. cells. One of the important requirements was to obtain single cell suspensions of viable epithelial cells suitable for separation into specific cell types. As a model rabbit tracheal mucosa was used since it is readily accessible and contains K. cells identical to those found in the intrapulmonary bronchi.[10]

MATERIALS AND METHODS

Adult male New Zealand white rabbits (6 to 7 lb) were sacrificed by Nembutal injection into the ear vein. The trachea and lungs were removed en bloc. The trachea was sectioned below the cricoid cartilage and at the bifurcation, which formed a segment that varied in length from 4 to 6 cm with an internal diameter of approximately 0.4 to 0.6 cm. The trachea was flushed three to four times with cold

(4°C) Joklik's modified minimal essential medium (MEM, Gibco) and kept in a volume of Joklik's medium until use.

Cell Dissociation Procedures

Mechanical Procedure

Cells were obtained by scraping the mucosal surface of the opened trachea with a metal spatula. The cells were collected in Hanks' balanced salt solution (HBSS, 4°C) and pelleted at 1200 rpm for 5 min. A mechanical stripping method with a fine-toothed forceps and #58 beaver blade removed large areas of the mucosal lining. The strips were pooled in cold HBSS and then minced.

Mechanical and Enzymatic Procedures

So that the cells obtained by the preceding method could be further dissociated, the cell preparations were incubated at 37°C for various time intervals (15 to 60 min) with different concentrations of trypsin, ethylenediaminetetraacetic acid (EDTA), collagenase, and pronase (Table 1).

Enzymatic Procedure

Experiments with enzymatic dissociation of the intact tracheal lining were carried out initially by tying securely one end of the trachea, filling the lumen with enzyme solution, and tying off the opposite end. After incubation at 37°C with the chosen enzyme solution (Table 1), the cells were removed by flushing the trachea three to four times with warmed Joklik's medium with the use of a 50-ml syringe.

The following modification of the above method provided the most reliable and satisfactory results. Each end of the trachea was securely fastened to 40 cm of Tygon tubing. One end of the tubing was clamped, and the tracheal lumen was filled to capacity with warmed (37°C) 1% pronase through the opposite tubing. The latter was clamped, and the trachea with attached tubings was placed in an Erlenmeyer flask containing warmed Joklik's medium and a 5% CO_2 in air atmosphere. The flask was agitated gently in a shaker water bath at 37°C for 30 min. One end of the tubing was then connected to a perfusion pump, and the tracheal lumen was perfused with warmed Joklik's. The perfusates containing dissociated cells were collected in 200 ml of Joklik's medium supplemented with 40% fetal-calf serum at room temperature. The trachea was then filled with enzyme solution and incubated as before for two additional 15-min periods, after which the cells were again collected by

TABLE 1

AVERAGE YIELDS AND VIABILITY OF DISSOCIATED TRACHEAL EPITHELIAL CELLS OBTAINED BY VARIOUS METHODS

Method	Enzyme treatment	Incubation time, min	Yield	Viability, %
Scraping only			Low, clumps	<50
Scraping + enzyme	Trypsin* (0.25%)	15	Low, clumps, few single cells	<50
	Trypsin (0.25%) + EDTA (0.02%)	30	Low, clumps, few single cells	<50
	Trypsin (0.1%) + collagenase† (0.01%)	30	Low, clumps, few single cells	<50
Stripping + enzyme	Trypsin (0.25%)	30	5.0×10^6	70
	Trypsin (0.25%) + EDTA (0.02%)	30 to 40	9.5×10^6	70
	Pronase‡ (1%)	45	11×10^6	99
	Pronase (1%)	60	11×10^6	96
Enzymatic	Trypsin (1%)	30	1.9×10^6	76
	Trypsin (1%)	75	11×10^6	60
	Collagenase (1%)	90	1.4×10^6	70
	Pronase (1%)	60	20×10^6	96

*Trypsin (Difco, 1 : 250).
†Collagenase (Worthington, type I).
‡Pronase (E. Merck, Pronase E).

perfusion. The final volume of the cell suspensions was adjusted to 400 ml with cold Joklik's medium to avoid reaggregation and further dilute the pronase. The cell suspension was filtered through a nylon bolting cloth, and the cells were recovered by 5 min of centrifugation at 1200 rpm. The pellets were resuspended in cold Joklik's medium for an additional wash and were carefully resuspended in a known volume for counting.

Methods for Evaluation of Dissociated Cells

Light Microscopy

For the assessment of yield and viability, the cells were counted in a hemocytometer chamber with the use of the trypan blue exclusion method.

The differential cell counts and qualitative assessment of dispersed cells were performed on cytocentrifuge-sedimented cells. The latter were fixed in Bouin's solution and stained with hematoxylin and eosin (H&E), periodic acid-Schiff (PAS), World Health Organization (WHO) keratin–mucin stain,[10] and Grimelius' silver nitrate stain for argyrophilic cells.[11]

The tracheal tissues were examined in paraffin-embedded and H&E-stained sections to assess the efficiency of removal of the mucosal lining by various dissociation procedures.

Formaldehyde-Induced Fluorescence (FIF)

For the detection of amine-containing cells by the FIF method, cytocentrifuged preparation of cells with and without prior incubation with L-dihydroxyphenylalanine (L-DOPA) was examined. The incubation with L-DOPA and the preparation of dissociated cells for FIF were identical to those previously described for tissue sections.[11] In control samples exposure to paraformaldehyde was omitted.

Electron Microscopy

For transmission electron microscopy (TEM), cell pellets were fixed in 2% glutaraldehyde in phosphate buffer (pH 7.4), postfixed in 1% osmic acid, and embedded in Epon. One-micron Epon sections were stained by toluidine blue and PAS methods. Ultrathin sections were stained with uranyl acetate and lead citrate.

For scanning electron microscopy (SEM), the cells were fixed in 2% glutaraldehyde and cytocentrifuged onto cover slips. The samples were then processed by the critical-point drying method with the use of liquid CO_2 and coated with gold–palladium.

Tissue Culture

So that the quality of the cells obtained by enzymatic dissociation could be further assessed, 5×10^5 to 10^6 cells per milliliter were seeded into Corning culture flasks in a modified MEM supplemented with 15% fetal-calf serum and incubated at 37°C in 5% CO_2 air atmosphere. The cultures were evaluated for cell attachment and growth after 12 to 24 hr.

RESULTS

The details of the results from various cell dissociation procedures are shown in Table 1. The cell preparations obtained by simple scraping were unsatisfactory in many respects. The majority of cells

remained in large clumps, and their viability was low. Further incubation of the scraped cells with proteolytic enzymes did not dissociate the cell clumps and resulted in extensive cellular damage.

The cell suspensions obtained by enzymatic treatment of the minced mucosal strips provided higher single cell yields and viability with better morphological preservation of the cells. However, the drawback of this method was significant contamination by connective tissue and blood cells. Furthermore, the incompleteness of cell removal by both the scraping and stripping methods was apparent in paraffin sections of the remaining tracheal tissue. Therefore the differential cell counts on these preparations were unreliable.

The method of enzymatic incubation of intact trachea proved the most satisfactory, although the cell yields, viability, and quality of cell preparations varied according to the type of enzyme used.

Incubation with either collagenase or trypsin provided lower yields of single cells compared to pronase. In the case of collagenase, nearly all cells remained in clumps and sheets. Following incubation with trypsin, a larger number of single cells was obtained, but many cells still remained in clumps. The increase in enzyme concentration or incubation time usually caused more extensive cell damage. In addition, the trypsin solutions had a tendency to change pH toward alkalinity, which caused the dissociated cells to become entangled in viscous mucous-like material.

The most consistent and satisfactory single cell suspensions were obtained with 1% pronase. The average yield of 20×10^6 cells with viability greater than 90% was obtained after 60 min of incubation. The collection of cells by perfusion at intervals during incubation improved the morphologic preservation of dissociated cells. Following the completion of enzyme treatment, the trachea showed complete denudation of the epithelial lining with an intact basement membrane and submucosa left behind. The majority of dissociated cells obtained by incubation with pronase were rounded and appeared in single cell suspension (Fig. 1). In comparison, a cell preparation obtained with 1% trypsin contained many cell clumps (Fig. 2). At higher magnification the excellent cytologic preservation of pronase-dissociated cells (Fig. 3) is in contrast with that obtained by trypsin, where cytoplasmic vacuolation, cell blebbing, and necrosis are evident (Fig. 4).

Morphology of Major Types of Dissociated Epithelial Cells

Since the quality of cell preparations obtained with pronase treatment was superior compared to other methods, only the former will be described in more detail.

Figure 1

Fig. 1 Low magnification of a cell pellet obtained by 60 min of incubation of intact trachea with 1% pronase and the cells collected by perfusion. The great majority of dissociated cells are distributed as single cells. 1-μm Epon section, toluidine blue stain. (Magnification, 200 X.)

Figure 2

Fig. 2 Low magnification of a cell pellet obtained from trachea after 75 min of incubation with 1% trypsin and cells removed by flushing. In this preparation clumps and sheets of cells predominate. 1-μm Epon section, toluidine blue stain. (Magnification, 200 X.)

Figure 3

Figure 4

Fig. 3 Cells dissociated with pronase show, at higher magnification, excellent cytological detail. In the mixture of various epithelial cells, well-preserved ciliated (Ci) and goblet (Go) cells are present. 1-μm Epon section, toluidine blue stain. (Magnification, 1000 ×.)

Fig. 4 Cells dissociated with trypsin show extensive cellular damage and cell clumps (arrow) (in contrast to Fig. 3). 1-μm Epon section, toluidine blue stain. (Magnification, 1000 ×.)

Among the differentiated cell types, the ciliated cells were the most frequent. The goblet cells were easily identified by the presence of mucous granules stained by PAS and WHO methods. The differential cell counts on cytocentrifuge cell preparations were as follows: 45.8 ± 3.4% ciliated cells, 14.3 ± 4.2% goblet cells, and 39.8 ± 5.8% intermediate and small basal cells. Contamination with connective-tissue cells was not observed, and only few blood cells were present.

The TEM of pronase-dissociated tracheal epithelial cells showed excellent overall ultrastructural preservation (Fig. 5). Although the cells appeared in various planes of sectioning, the differentiated cells could be usually identified by their cytoplasmic and nuclear morphology and cell size. The cilia of ciliated cells and mucc···

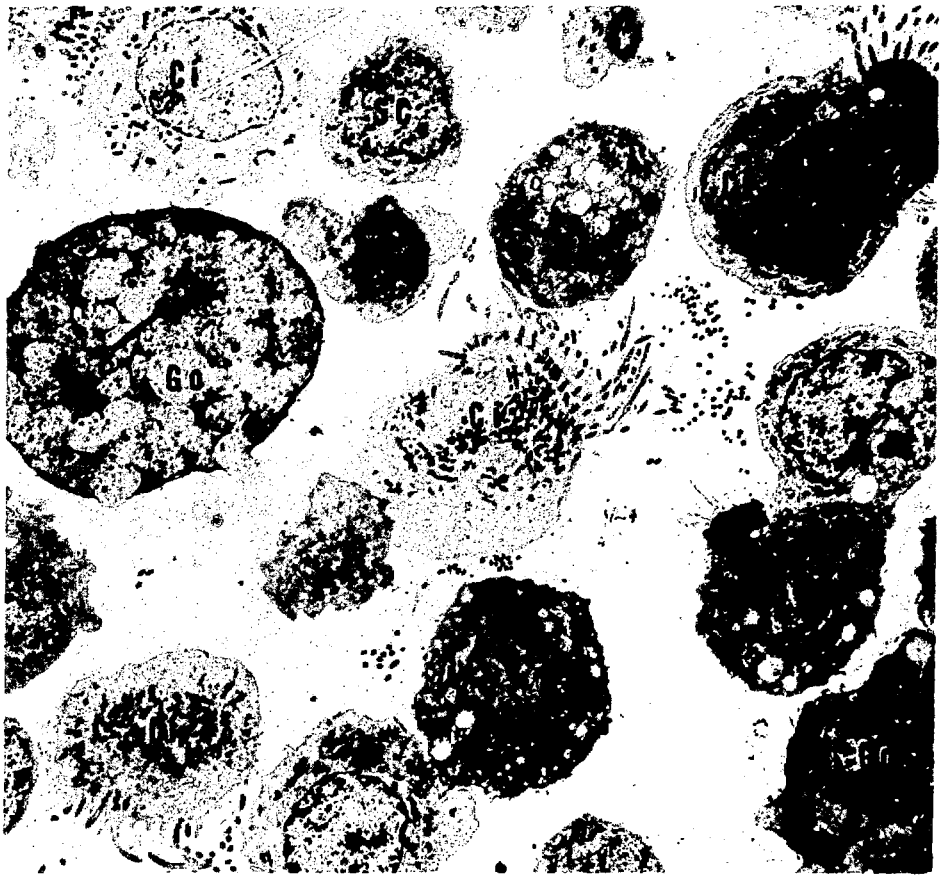

Fig. 5 Low-magnification transmission electron microscopy of cells shown in Figs. 1 and 3. The ultrastructure of ciliated (Ci) and goblet (Go) cells is well preserved. The small cells (SC) probably represent basal undifferentiated cells. (Magnification, 2400 X.)

granules in goblet cells appeared intact. A mild to moderate degree of ultrastructural alterations due to the enzyme effect on cells consisted of cytoplasmic blebbing, concentration of organelles in the perinuclear region, occasional cytoplasmic vacuoles, and increased density of mitochondrial matrix.

The SEM appearance of dissociated cells generally corresponded to that expected from both the light-microscopy and TEM studies. The majority of cells were spherical with irregular cell surfaces forming slender folds and short projections (Fig. 6). The hallmark of ciliated cells was the presence of well-preserved cilia on the apical surfaces. Although the nonciliated cells differed in size, they could not be further classified.

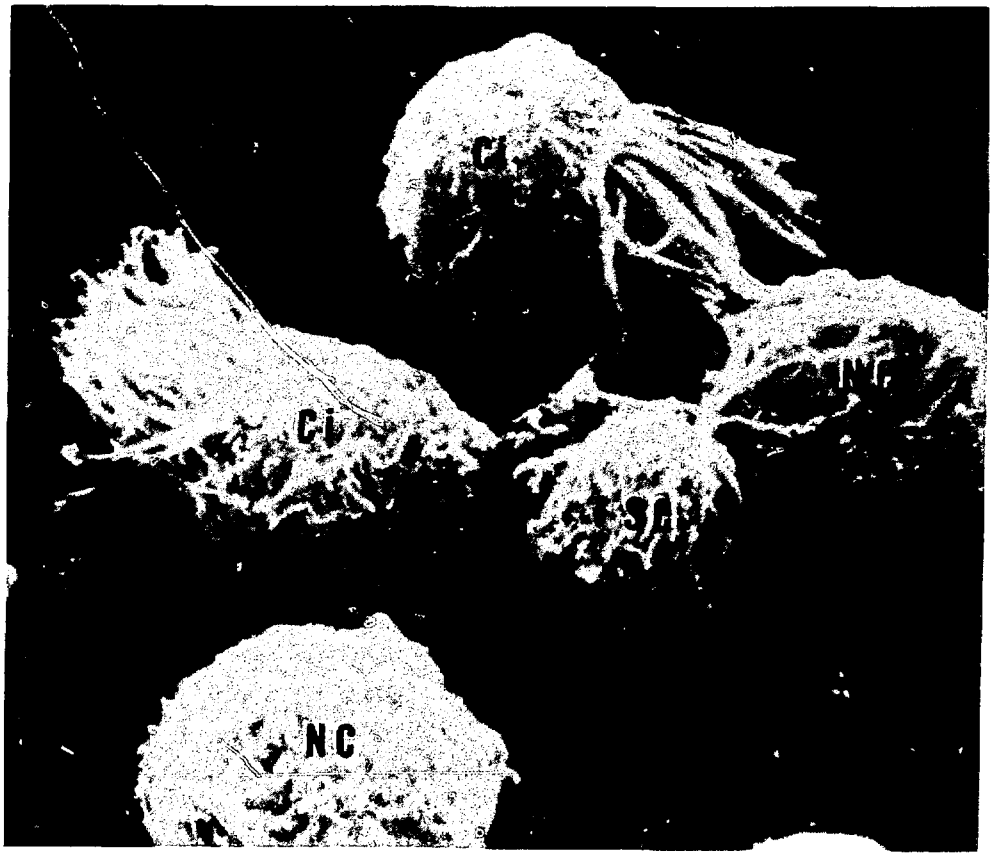

Fig. 6 Scanning electron microscopy of pronase-dissociated tracheal cells showing irregular cell surfaces of the isolated ciliated (Ci) and nonciliated (NC) cells. The larger NC cells may represent goblet cells, whereas the SC is probably a basal cell. (Magnification, 3300 X.)

Morphology of Dissociated Kultschitzky Cells (K. Cells)

Since the cytoplasmic argyrophilia is one of the main light-microscopic features of K cells, Grimelius' silver nitrate stain was used on cytocentrifuge cell preparations. By this method the cytoplasm of K. cells contained fine argyrophilic granules (Fig. 7). The K. cells were usually oval or round. In some slides one to two K. cells were seen per high-power field, but, owing to the small number of K. cells, precise quantitative data could not be obtained. We have estimated that the K. cells in rabbit trachea form less than 1% of the epithelial cells.

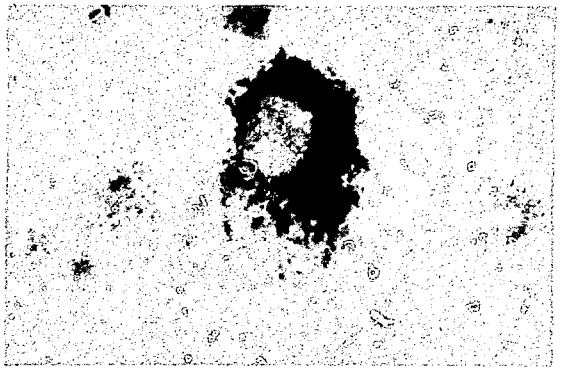

Fig. 7 Cytoplasm of an isolated K. cell showing fine black argyrophilic granules. The nucleus is unstained. Cytocentrifuge preparation, Grimelius' stain. (Magnification, 1000 ×.)

With the use of the FIF method, cells with intense yellow-green cytoplasmic fluorescence were identified only in samples previously incubated with L-DOPA (Fig. 8). In nonincubated samples the intensity of fluorescence was very weak.

By TEM several of the cell pellets examined contained cells with cytoplasmic dense core vesicles (DCV) characteristic of K. cells (Fig. 9). The size (1400 Å) and morphology of DCV in dissociated K. cells (Fig. 9 inset) were identical to those previously described in tissue sections of rabbit trachea.[10] The pronase effect on K. cells was minimal, and, except for mild dilatation of smooth endoplasmic reticulum, no other changes were found.

Tissue-Culture Characteristics of Dissociated Cells

The primary cultures of dissociated cells served as an additional means to evaluate the quality of the preparations obtained by the

Fig. 8 Two intensely fluorescent cells in a formaldehyde-induced fluorescence preparation of dissociated tracheal epithelial cells. In vitro incubation with L-DOPA, cytocentrifuge preparation. (Magnification, 800 X.)

pronase treatment. The ciliated cells retained their ciliary beat up to 8 hr after isolation, and the majority of cells attached within the first 12 to 24 hr in vitro. Confluent monolayers of epithelial cells were formed after 8 days in culture. Details of these studies will be reported elsewhere.

DISCUSSION

It is well recognized that the success of cell separation largely depends on the quality of the initial cell suspensions.[12] The methods used for cell dissociation must be geared toward the recovery of the particular cell type(s) to be investigated since some types of cells may be selectively destroyed during the dissociation procedure.[13] Therefore it is important to critically evaluate the morphologic and cytochemical preservation of dissociated cells. This report concentrates on cell dissociation methods applied to isolation of airway epithelial cells. Among the various cell dissociation methods and enzymes tested, incubation of intact trachea with 1% pronase followed by perfusion was found to be the most effective in dissociating the tracheal epithelial lining into individual viable cells. The method of cell collection was critical to the yield since higher yields were obtained only by perfusion. Although the use of pronase has been the subject of some controversy,[14] in this study high cell viability was obtained even with relatively high concentrations of pronase. This may reflect a low substrate specificity of pronase for tracheal epithelial cells. The excellent preservation of pronase-dissociated cells was confirmed not only by light microscopy and EM studies but also by tissue culture.

Fig. 9 Transmission electron microscopy of an isolated tracheal K. cell with well-preserved electron-dense cytoplasmic granules. Nucleus (Nu) and mitochondria (Mi) are also well preserved. (Magnification, 9000 X.) Insert: Higher magnification transmission electron microscopy of cytoplasmic granules shows well-preserved homogeneous core and a limiting membrane (arrowhead). (Magnification, 26,400 X.)

Of particular interest was the recovery and preservation of K. cells in dissociated cell preparations. It was possible to monitor these cells by histochemical methods similar to those used for their identification in tissue sections.[10] The FIF method demonstrated the amine handling properties of K. cells, which is one of the primary characteristics of APUD cells.[9] Because of the low endogenous amine content in tracheal K. cells,[10] prior incubation with amine precursor (L-DOPA) was required.[15] The demonstration of intracellular amine in dissociated tracheal K. cells after incubation with L-DOPA confirmed that the decarboxylating mechanism in isolated K. cells remained intact. Similarly, the cytoplasmic argyrophilia of K. cells was well preserved.

At the ultrastructural level the cytoplasm of isolated K. cells retained its characteristic cytoplasmic granules referred to as DCV. Since the DCV are considered the storage site of amines and polypeptide hormones,[15] it was important to examine DCV for possible changes induced by the dissociation technique. Although ultrastructural changes following pronase treatment have recently been reported to occur in DCV of pituitary APUD cells,[16] no such changes were found in the present study.

The K. cells in trachea and bronchi of human and various animal species have only recently been identified, and their function remains unknown. Although it has been suggested that these cells may have an endocrine function, and in addition to amines may produce polypeptide hormones,[7,8,15] thus far no direct evidence has been obtained. The potential importance of these cells in normal lung function and their possible role in various pulmonary diseases deserves further investigation. Availability of methods for dissociation and monitoring of tracheal K. cells may provide a new tool for in vitro studies on metabolic and secretory activity of these cells. The methodology described also provides well-preserved single cell suspensions of various tracheal epithelial cells, including K. cells, which are suitable for further separation into specific cell types.

ACKNOWLEDGMENT

This work was supported in part by a grant from the Ontario Thoracic Society.

REFERENCES

1. K. G. Gould, R. E. Clements, A. L. Jones, and J. M. Felts, Dispersal of Rabbit Lung into Individual Viable Cells: A New Model for the Study of Lung Metabolism, *Science*, 178: 1209-1210 (1972).

2. Y. Kikkawa and K. Yoneda, The Type II Epithelial Cell of the Lung. I. Method of Isolation, *Lab. Invest.*, 30: 76-84 (1974).
3. R. Mason, M. C. Williams, and J. A. Clements, Isolation and Identification of Type II Alveolar Epithelial Cells, *Chest*, 67: 365-375 (1975).
4. J. Rhodin and T. Dalhaman, Electron Microscopy of the Tracheal Ciliated Mucosa in Rat, *Z. Zellforsch.*, 44: 345-412 (1956).
5. E. Cutz and P. E. Conen, Ultrastructure and Cytochemistry of Clara Cells, *Am. J. Pathol.*, 62: 127-134 (1971).
6. K. G. Bensch, C. B. Gordon, and L. R. Miller, Studies on the Bronchial Counterpart of the Kultschitzky (Argentaffin) Cell and Innervation of Bronchial Glands, *J. Ultrastruct. Res.*, 12: 668 (1965).
7. J. M. Lauweryns and J. C. Peuskens, Argyrophil (Kinin and Amine Producing?) Cells in Human Infant Airway Epithelium, *Life Sciences*, 8: 577 (1969).
8. E. Hage, Amine Handling Properties of APUD-Cells in the Bronchial Epithelium of Human Fetuses and in the Epithelium of Main Bronchi of Human Adults, *Acta. Pathol. Microbiol. Scand. (Sect. A)*, 81: 64-70 (1973).
9. A. G. E. Pearse, The Cytochemistry and Ultrastructure of Polypeptide Hormone Producing Cells of the APUD Series and the Embryologic, Physiologic and Pathologic Implications of the Concept, *J. Histochem. Cytochem.*, 17: 303-313 (1969).
10. E. Cutz, W. Chan, V. Wong, and P. E. Conen, Ultrastructure and Fluorescence Histochemistry of Endocrine (APUD-Type) Cells in Tracheal Mucosa of Human and Various Animal Species, *Cell Tissue Res.*, 158: 425-437 (1975).
11. E. Cutz, W. Chan, V. Wong, and P. E. Conen, Endocrine Cells in Rat Fetal Lungs, Ultrastructural and Histochemical Study, *Lab. Invest.*, 30: 458-464 (1974).
12. T. G. Pretlow, E. E. Weir, and J. G. Zettergren, Problems Connected with the Separation of Different Kinds of Cells, *Int. Rev. Exp. Pathol.*, 14: 91 (1975).
13. K. Shortman, Physical Procedures for the Separation of Animal Cells, *Ann. Rev. Biophys. Bioeng.*, 1: 93-130 (1972).
14. G. Poste, Tissue Dissociation with Proteolytic Enzymes, *Exp. Cell Res.*, 65: 359-367 (1971).
15. Ch. Owman, R. Hakanson, and F. Sundler, Occurrence and Function of Amines in Endocrine Cells Producing Polypeptide Hormones, *Fed. Proc.*, 32: 1785-1791 (1973).
16. J. G. Schofield and L. Orci, Release of Growth Hormone from Ox Pituitary Slices After Pronase Treatment, *J. Cell. Biol.*, 65: 223-227 (1975).

Immune Properties of the Alveolar Macrophage

RONALD P. DANIELE, DAVID J. GORENBERG, and JAMES H. DAUBER
Cardiovascular—Pulmonary Division, Departments of Medicine and Pathology, University of Pennsylvania, Philadelphia, Pennsylvania

ABSTRACT

Since the lung potentially constitutes a large compartment for macrophage—lymphocyte interaction, three immune properties of guinea pig alveolar macrophages were studied: (1) the capacity to serve as accessory cells in lymphocyte responses to mitogens, (2) the degree of macrophage membrane activation, and (3) the response to chemotactic stimuli. Peritoneal macrophages were compared to alveolar macrophages with respect to each of these functions. The collaborative potential of alveolar and peritoneal macrophages was examined by determining their effect on mitogen- [phytohemagglutinin (PHA)] induced lymphocyte proliferation. Purified tracheobronchial lymph node cells were co-cultured with autologous macrophages, and the response to PHA was measured at 72 hr by the uptake of tritiated thymidine. Macrophages enhanced the response of lymphocytes to PHA, and alveolar macrophages appeared superior in this function. Macrophage activation was assessed by measuring the incorporation of [^{14}C]glucosamine into membrane associated macromolecules of lavaged lung and peritoneal macrophages. Alveolar macrophages were more active than peritoneal macrophages and capable of further stimulation by lymphocyte-derived factors. In contrast to peritoneal macrophages, alveolar macrophages responded poorly to chemotactic stimuli. These results suggest that alveolar macrophages are well-suited to serve in both the collaborative and effector phases of the immune response.

In the lung's defense against respirable particles that reach the distal airways, the alveolar macrophage assumes major importance.[1] Until recently, much attention has been directed toward metabolic and nonspecific phagocytic functions of the alveolar macrophage. It is becoming clear, however, that the alveolar macrophage is a component of the lung's immune system.[2] In other immune tissues the

macrophage functions in both the afferent and efferent limbs of the immune response.[3] Thus, in the immune defense against foreign substances, macrophages play at least two important roles: they collaborate with lymphocytes in antigen recognition and serve as effector cells in antigen disposal. Since the lung potentially constitutes a large compartment for macrophage–lymphocyte interaction, three immune properties of the guinea pig alveolar macrophage were studied: (1) the capacity to serve as accessory cells in lymphocyte responses to mitogens, (2) the degree of macrophage membrane activation, and (3) the response to chemotactic stimuli. Peritoneal macrophages were compared to alveolar macrophages with respect to each of these functions.

MATERIALS AND METHODS

Animals

Male and female Hartley guinea pigs weighing 350 to 450 g were used. Animals in apparent ill health or whose lungs did not appear normal on gross examination were excluded.

Preparation of Cells

Peritoneal cells were obtained by lavaging the peritoneal cavity with 200 to 350 ml of sterile Hanks' balanced salt solution (HBSS). The cells were washed three times, counted, and resuspended at the specified cell concentration in Eagle's minimal essential medium (MEM) supplemented with 10% fresh autologous normal guinea pig serum. Cell yields from unstimulated peritoneum averaged 10×10^6 cells.

Lung cells were obtained by methods previously described in detail.[4] In brief, the animals were anesthetized with an interperitoneal (0.05 mg/g weight) or a subcutaneous (0.3 mg/g weight) dose of sodium pentobarbital. The chest cavity was opened and the animal exsanguinated and sacrificed by cardiac puncture. The lungs were lavaged with cold HBSS that was free of calcium and magnesium; the lung cells were then washed and counted as described above.

After lung lavage, all visible tracheobronchial lymph nodes were dissected from surrounding tissues and placed in cold HBSS. The nodes were minced and teased apart with 21-gauge needles. A suspension of cells and node fragments was passed through a 250-μm stainless-steel mesh. The resulting cell suspension was freed of clumps by allowing them to settle for 5 min and removing the single-cell

suspension supernates. All cells were washed three times with HBSS, counted, and resuspended in Eagle's MEM supplemented with 10% guinea pig serum.

Viability of all cell suspensions was determined with trypan blue and was consistently greater than 95% for lung and peritoneal cells; viability for lymph node cells ranged between 75% and 90%.

For differential counting of lung and peritoneal cells, cell suspensions were first incubated with latex particles, as previously described.[2,4] Cytocentrifuge preparations were then made and stained with Wright—Giemsa reagent. Monocytes and macrophages were identified by size, the presence of large lipid vacuoles, or ingested latex particles.

Response of Lymphocytes to Mitogens

Lymph node cells (5×10^5 cells/ml) were inoculated into 0.9 ml of Eagle's MEM supplemented with glutamine (2.5 μg/ml), penicillin (200 IU/ml), streptomycin (200 μg/ml), and 10% v/v autologous guinea pig serum. An optimal dose (30 μg) of PHA was added to experimental cultures. Cultures were incubated at 37°C in 5% CO_2 and air. At 16 hr prior to termination of the experiment, 0.25 μCi of tritiated thymidine, [^{3}H]TdR (specific activity, 6.7 Ci/mmol), was added. The cells were then precipitated on glass filter paper using a cell harvester.[5] The filter disks were dried and placed in a scintillation cocktail, and the activity was measured in a liquid scintillation spectrometer.

Lymphocyte-Macrophage Interaction

Autologous lung or peritoneal cells were added to lymph node cell cultures at the outset of the experiment. The numbers of lung or peritoneal cells added were such that the ratio of macrophage to lymphocyte was 1 : 5. Mitogen responses were determined as described above. In additional experiments, lung or peritoneal cells were treated with mitomycin to eliminate proliferation of the few remaining lung or peritoneal lymphocytes. Mitomycin treatment of lung or peritoneal cells consisted of incubating the cells in 25 μg/ml of mitomycin for 45 min at 37°C; the cells were then washed twice in sterile HBSS. Control cultures consisted of mitomycin-treated lung or peritoneal cells cultured alone in the presence of PHA, with mitogen responses determined as described above. When mitomycin cells were used in the experimental protocol described above, the small contribution of proliferating lung or peritoneal lymphocytes did not alter the results obtained when cells, untreated with mitomycin, were used.

Macrophage Activation

Details of these methods have also been described.[6] Macrophage monolayers were prepared by adding 1 x 10^6 lung or peritoneal cells to flat-bottomed, glass vials (15 x 45 mm) containing 1 ml of Eagle's MEM supplemented with 10% guinea pig serum and antibiotics. The cell suspensions were incubated for 2 hr at 37°C in 5% CO_2 and air; nonadherent cells were then removed by gentle agitation and washing the macrophage monolayers with warm medium. The monolayers consisted of greater than 97% macrophages, and the viability was greater than 95%. The cultures were then incubated for 24, 48, or 72 hr at 37°C in 5% CO_2 and air. At 6 hr prior to termination of the experiment, 0.25 μC of [^{14}C]*d*-glucosamine was added to the cultures. The monolayers were then washed with HBSS and the macrophages detached from the glass surface by adding 0.1 ml of a 1% v/v solution of Triton X-100 to each culture. The vials were agitated in a vortex mixer, and the cells were counted in a particle counter. The cell suspensions were then harvested onto glass filters using a cell harvester, and scintillation counting was performed as described above. Counts were corrected for cell numbers and expressed as counts per minute per 10^6 cells.

In separate experiments, 0.5 ml of the culture medium was replaced at the outset of the experiment with supernates obtained from 72-hr PHA-stimulated tracheobronchial lymph node cell cultures. The supernates were centrifuged at 1500 g to remove cells and cell debris and were then frozen at −20°C until use. Controls consisted of adding 0.5 ml of supernates from lymph node cells cultured in the absence of PHA. PHA was added to the control supernates at the termination of the cultures at a concentration equivalent to test cultures.

For autoradiography, 1 x 10^6 alveolar macrophages were grown on glass cover slips for 72 hr at 37°C in 5% CO_2 and air. For the final 16 hr of cultures, 20 μCi of tritiated glucosamine was added. Autoradiographs were then prepared by standard dipping techniques used in this laboratory.[7] Slides were exposed for 3 and 7 days.

Chemotactic Assay

Guinea pig peritoneal or lung cells were suspended in Gey's balanced salt solution containing 2% bovine serum albumin and placed on top of 5-μm or 8-μm pore-size polycarbonate filters in 8-mm-diameter blind-well Lucite chemotactic chambers.[8] A standard concentration of activated complement was placed in the lower chamber. Complement was activated by incubating 1 part fresh

guinea pig serum with 1 part endotoxin (*Escherichia coli* : 0127 : B8 lipopolysaccharide, 3000 μg/ml) and 8 parts gelatin—veronal buffer. The wells were incubated at 37°C in humidified air. The filters were removed after various incubation periods, fixed, and stained. Chemotaxis was quantitated by counting the number of macrophages that migrated through the filter in 20 oil-immersion fields in triplicate samples.

RESULTS AND DISCUSSION

As shown in Table 1, macrophages equaled 70% of the cells recovered by lung lavage in the guinea pig; the remainder of cells were comprised of eosinophils and lymphocytes. It is noteworthy that the distribution of cells recovered from unstimulated peritoneal washings was similar to that from the lung, including the relatively large proportion of eosinophils, which ranged between 5 and 30% of the cells. This was not true, however, if the peritoneum was first stimulated with glycogen or mineral oil. The cells recovered 5 days after such stimulation consisted almost entirely of macrophages and lymphocytes. Although the distribution of cells recovered from unstimulated peritoneum and lung was similar, alveolar macrophages were significantly larger ($p < 0.001$) than peritoneal macrophages with mean (± standard deviation) diameters of 12 ± 2 μm and 10 ± 1 μm, respectively.

TABLE 1

CELLS IN GUINEA PIG LUNG LAVAGES*

	Mean ± standard deviation, %
Macrophages	70 ± 10
Lymphocytes	13 ± 5
Eosinophils	17 ± 8

*Number of animals = 14.

Lymphocyte–Macrophage Interaction

Figure 1 indicates the response to PHA of tracheobronchial lymph node cells cultured alone and in the presence of lung or peritoneal cells. Lymph node cells gave a peak response at 40 hr, which rapidly declined to the ordinate by 5 days. The addition of

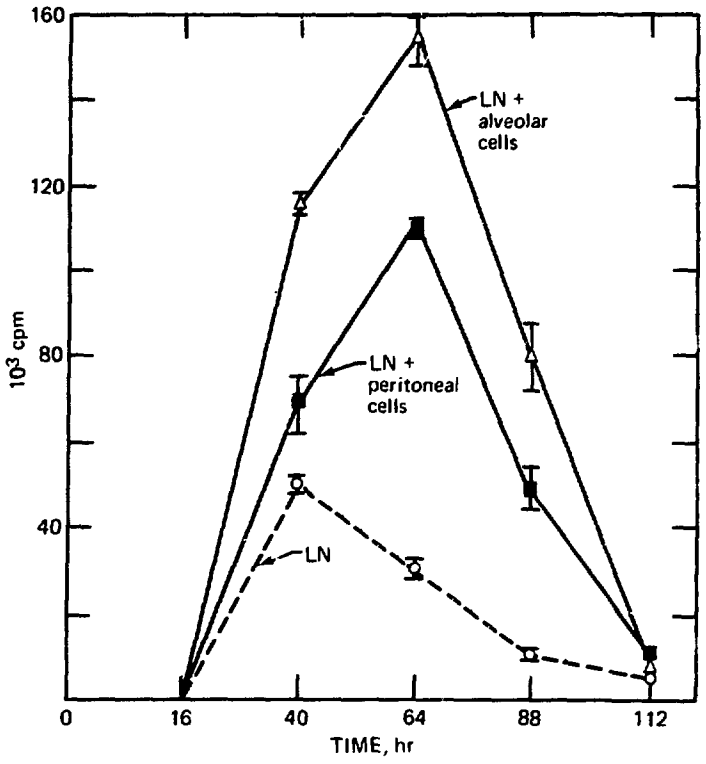

Fig. 1 Response of lymph node (LN) cells to PHA. Cells were cultured alone and in the presence of peritoneal (unstimulated) or lung cells; the ratio of LN cells to lung or peritoneal macrophages was 5 : 1.

autologous mitomycin-treated peritoneal cells more than doubled the peak response, which was displaced to 64 hr and declined to the base line by 5 days. In the presence of equal numbers of autologous lung cells, however, the peak proliferative response of lymph node cells was tripled by 64 hr; again, the response declined to the base line by 5 days. At 2, 3, and 4 days, the proliferative response of lymph node cells was consistently greater when cultured with lung cells than when cultured with peritoneal cells. Comparable results were obtained when glycogen-stimulated peritoneal cells were used. The cells responsible for the enhanced lymphocyte response appeared to be macrophages, since comparable results were obtained in subsequent experiments[9] in which highly purified (greater than 98%) alveolar or peritoneal macrophages were co-cultured with autologous lymph node cells. To obtain highly purified macrophages, we found it necessary to allow lung and peritoneal cells to adhere to glass Petri dishes overnight at 37°C. Thus the difference in the capacity of

alveolar and peritoneal macrophages to serve as accessory cells persisted after short-term culture.

The enhanced mitogen responsiveness of lymphocytes measured over a 5-day period suggests that a greater number of lymphocytes are responding to PHA in the presence of phagocytic cells and that alveolar macrophages are superior to peritoneal macrophages in this function. There is increasing evidence[10] that mitogen stimulation of lymphocytes is fundamentally similar to the process of antigen stimulation of lymphocytes. As a model of antigen stimulation, mitogen stimulation is thus a powerful tool for investigating the nature of membrane signals and cellular interactions in the immune response. With regard to the latter function, it is not yet clear whether the ability of the macrophage to serve as an accessory cell in mitogen or antigen stimulation is related to (1) optimal presentation of mitogen to the lymphocyte,[11] (2) their capacity to maintain cell viability,[12] or (3) to the production of substances that act as additional signals for lymphocyte proliferation.[13,14] In any case, recent evidence suggests that there is an absolute requirement for macrophages in lymphocyte response to mitogens[15] and that, for antigenic stimulation of T cells, cell surface contact between lymphocyte and macrophages is also required.[16]

Membrane Activation Studies

The requirement for lymphocyte–macrophage contact in lymphocyte responses to antigens suggested that mechanisms involved in accessory cell function might reside, at least in part, at the macrophage membrane level. For example, one possible explanation for the observed differences between alveolar and peritoneal macrophages to serve as accessory cells might be related to a fundamental difference in the state of membrane activation. One measure of macrophage membrane activation is the incorporation of glucosamine into membrane-associated macromolecules.[6]

Figure 2 compares the membrane activity of alveolar and peritoneal macrophages as measured by the cellular incorporation of radiolabeled glucosamine, [^{14}C]glucosamine. Alveolar macrophages were six times ($p < 0.01$) more active than peritoneal macrophages at 72 hr. Comparable results were also obtained at 24 and 48 hr of culture and when unstimulated and glycogen-stimulated peritoneal cells were used. Figure 2 also shows the macrophage responses to factors derived from supernates of tracheobronchial lymph nodes stimulated by PHA. Both alveolar and peritoneal macrophages increased their incorporation of [^{14}C]glucosamine when they were cultured with supernates from PHA-stimulated lymphocytes, but

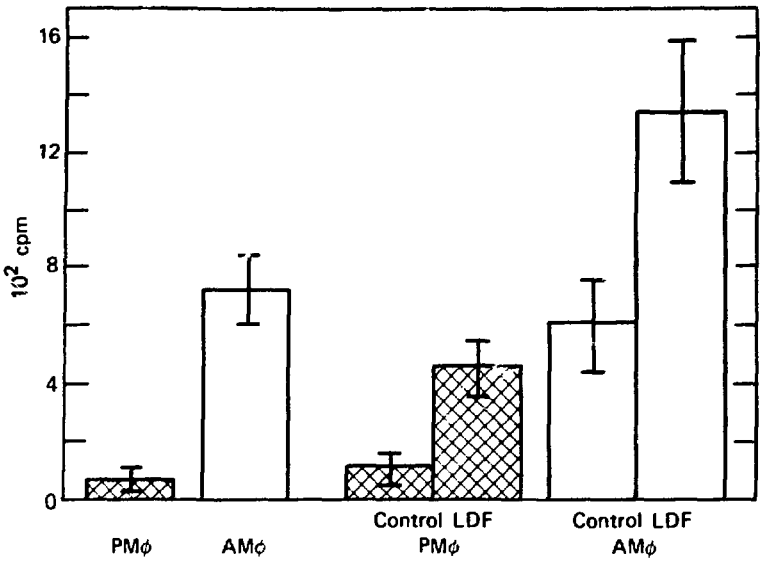

Fig. 2 The incorporation of [^{14}C] lucosamine into alveolar (AMϕ) and peritoneal (PMϕ) macrophages, measured in counts per minute per 10^6 cells. Also shown is the response of PMϕ and AMϕ to lymphocyte-derived factors derived from supernates of PHA-stimulated lymph node cells. Controls consisted in the addition of equivalent volumes of supernates from unstimulated lymph node cells but with a similar concentration of PHA as test supernates.

alveolar macrophages did so less than peritoneal macrophages. Alveolar and peritoneal macrophages increased their uptake of glucosamine by factors of 2 and 6, respectively.

Figure 3 is an autoradiograph of a monolayer of alveolar macrophages pulsed for a period of 12 hr with tritiated glucosamine. The grains appear to be localized to the cytoplasm and cell surface. Although Figure 3 does not differentiate between surface and cytoplasmic incorporation of [^{3}H]glucosamine, other experimenters[6] have observed, using ultrathin autoradiograph sections and cell fractionation procedures, that peritoneal macrophages preferentially incorporate glucosamine into the cell membrane.

Changes in membrane activation as measured by glucosamine incorporation have correlated well with other indices (e.g., response to the macrophage inhibition factor) of macrophage activation resulting from specific interaction between antigen and sensitized lymphocytes.[6,17] Similar phenomenon, including increased glucosamine uptake, has occurred when macrophages were cultured in the presence of lymphocytes stimulated by polyclonal mitogens for T cells[18] (e.g., PHA) and B cells (e.g., endotoxin).[19]

Fig. 3 An autoradiograph of a monolayer of alveolar macrophages pulsed for 18 hr with [^{3}H]glucosamine.

One possible explanation for the enhanced incorporation of glucosamine into alveolar macrophages might be related to their increased size. Using the measured diameters for alveolar and peritoneal macrophages and assuming a spherical shape for the cells, the calculated increase in surface area of alveolar macrophages would be no greater than 1.5 times that of peritoneal macrophages. Therefore it seems that the increase in size could theoretically account for only part of the increased glucosamine uptake by alveolar macrophages. Another explanation for the increased glucosamine uptake in alveolar macrophages is that the environment of the respiratory tract promotes activation of alveolar macrophages. This is hardly surprising in view of the important biologic function of activated macrophages in their enhanced capacity to ingest and

destroy bacteria. Thus the sterility of the lower respiratory tract depends on the sustained bactericidal activity of resident alveolar macrophages.

Chemotaxis

Another property of activated macrophages is an alteration in cell motility.[8] To make some assessment of macrophage motility, the authors tested and compared alveolar and peritoneal macrophages for their ability to migrate across nucleopore membranes in response to a standard concentration of activated components of complement (C5a). In contrast to peritoneal macrophages, alveolar macrophages measured over a 5-hr period responded poorly to C5a (Fig. 4). For alveolar macrophages, there was a negligible difference in cell migration in chambers containing C5a as compared to negative

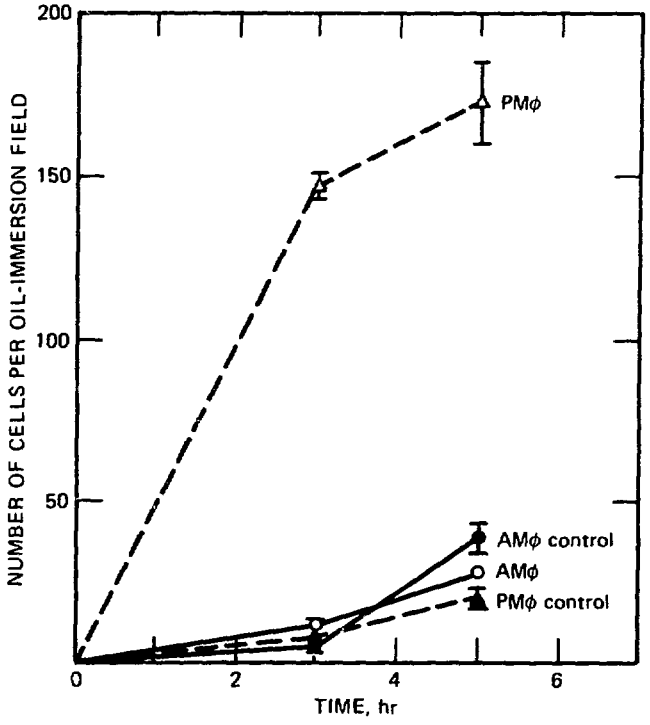

Fig. 4. The chemotactic response of alveolar (AMϕ) and peritoneal (PMϕ) macrophages to C5a. Chemotaxis is measured by the mean number of cells that migrated per 20 oil-immersion fields. Each point equals the mean ± standard error of triplicate samples. Controls consisted of chemotactic chambers containing endotoxin without serum.

controls. To exclude the possibility that the poor alveolar macrophage migration was related to increased cell size, we repeated additional studies with 8-μ pore-size filters, and similar results were obtained.

The relatively poor response to C5a observed in guinea pig alveolar macrophages confirms the results found in rabbit alveolar macrophages.[20] The reasons for this lack of chemoactivity are unclear. One possible explanation is that alveolar macrophages require a higher oxygen tension for optimal chemotaxis. Alveolar macrophages have different metabolic requirements than peritoneal macrophages and derive their energy primarily from oxidative metabolism rather than from glycolysis.[21] Another possible explanation is that alveolar macrophages or their precursors have already responded to chemotactic factors in the migration from blood or interstitial spaces into the bronchoalveolar air spaces and have thus become deactivated in the process. Deactivation, or diminished chemotactic responsiveness, occurs rapidly in eosinophils after interaction with eosinophilic chemotactic factor of anaphylaxis.[22]

SUMMARY

The results of these studies indicate that, despite the poor response to chemotactic stimuli, alveolar macrophages possess several properties that render them capable of collaborative and effector cell function. These include their enhanced capacity to serve as accessory cells in lymphocyte responses to mitogens and their relatively increased membrane activity as measured by the uptake of glucosamine. One hypothesis that may explain these apparently contradictory findings is that alveolar macrophages or their precursors (e.g., blood monocytes) have already responded to chemotactic signals originating within the respiratory tract. Thus, when alveolar macrophages take up residence in the bronchoalveolar air spaces, they are exposed to a number of activating stimuli and differentiate into fully "armed" effector cells. The morphologic and functional heterogeneity observed for alveolar macrophages[23] may reflect various stages in this differentiation process.

Note Added in Proof

Since the preparation of this paper, we have found that, despite poor chemotactic responses to complement and lymphocyte-derived factors, alveolar macrophages respond well to factors contained in bacterial filtrates and to the presumptive bacterial metabolites, *N*-formylmethionyl peptides.

ACKNOWLEDGMENTS

This work reported in this paper was supported in part by a Young Investigator Award (HL-17221) (Dr. Daniele) from the National Heart and Lung Institute, by a grant from the American Thoracic Society, and by a grant from SCOR (HL-15061). The authors wish to thank Dr. Alfred P. Fishman and Dr. David T. Rowlands, Jr., for their advice and review of the manuscript.

REFERENCES

1. G. M. Green, In Defense of the Lung, *Am. Rev. Respir. Dis.*, 102: 691-703 (1970).
2. R. P. Daniele, M. D. Altose, and D. T. Rowlands, Immunocompetent Cells from the Lower Respiratory Tract of Normal Human Lungs, *J. Clin. Invest.*, 56: 986-995 (1975).
3. E. R. Unanue, The Regulatory Role of Macrophages in Antigenic Stimulation, *Adv. Immunol.*, 15: 95-165 (1972).
4. D. J. Gorenberg and R. P. Daniele, Characterization of Immunocompetent Cells Recovered from the Respiratory Tract and Tracheobronchial Lymph Node of Normal Guinea Pigs, *Am. Rev. Respir. Dis.*, 114: 1099-1106 (1976).
5. R. J. Hartzman, M. L. Bach, F. H. Bach, G. B. Thurman, and K. W. Sell, Precipitation of Radioactively Labelled Samples: A Semi-Automatic Multiple Sample Processor, *Cell Immunol.*, 4: 182-186 (1972).
6. M. E. Hammond and H. F. Dvorak, Antigen-Induced Stimulation of Glucosamine Incorporation by Guinea Pig Peritoneal Macrophages in Delayed Hypersensitivity, *J. Exp. Med.*, 136: 1518-1532 (1972).
7. P. C. Nowell, R. P. Daniele, and L. A. Winger, Kinetics of Human Lymphocyte Proliferation: Proportion of Cells Responsive to Phytohemagglutinin and Correlation with E Rosette Formation, *J. Reticuloendothel. Soc.*, 17: 47-56 (1975).
8. S. M. Wahl, L. C. Altman, J. J. Oppenheim, and S. E. Mergenhagen, In Vitro Studies of a Chemotactic Lymphokine in the Guinea Pig, *Int. Arch. Allergy Appl. Immunol.*, 46: 768-784 (1974).
9. D. J. Gorenberg and R. P. Daniele, A Comparison of Alveolar and Peritoneal Macrophages as Accessory Cells in PHA-Induced Proliferation of Guinea Pig Lymphocytes, in Proceedings of the Eleventh Leukocyte Culture Conference, Tucson, Ariz., September 23—25, 1976 (in press).
10. M. Greaves and G. Janossy, Elicitation of Selective T and B Lymphocyte Responses by Cell Surface Binding Ligands, *Transplant. Rev.*, 11: 87-130 (1972).
11. H-P. Lohrmann, L. Novikovs, and R. G. Graw, Jr., Cellular Interactions in the Proliferative Response of Human T and B Lymphocytes to Phytomitogens and Allogeneic Lymphocytes, *J. Exp. Med.*, 139: 1553-1567 (1974).
12. C. Chen and J. G. Hirsch, The Effects of Mercaptoethanol and of Peritoneal Macrophages on the Antibody-Forming Capacity of Non-Adherent Mouse Spleen Cells In Vitro, *J. Exp. Med.*, 136: 604-617 (1972).

13. A. S. Rosenthal, J. T. Blake, J. J. Ellner, D. K. Greineder, and P. E. Lipsky, The Role of Macrophages in T Lymphocyte Antigen Recognition, in *Immune Recognition*, A. S. Rosenthal (Ed.), pp. 539-554, Academic Press Inc., New York, 1975.
14. J. Calderon and E. R. Unanue, Two Biological Activities Regulating Cell Proliferation Found in Cultures of Peritoneal Exudate Cells, *Nature (London)*, 253: 359-361 (1975).
15. D. L. Rosenstreich, J. J. Farrar, and S. Dougherty, Absolute Macrophage Dependency of T Lymphocyte Activation by Mitogens, *J. Immunol.*, 116: 131-139 (1976).
16. A. S. Rosenthal, J. T. Blake, and P. E. Lipsky, Inhibition of Macrophage—Lymphocyte Interaction by Cytochalasin B During Antigen Recognition by T Lymphocytes, *J. Immunol.*, 115: 1135-1139 (1975).
17. G. B. Mackaness, in *Infectious Agents and Host Reactions*, Stuart Mudd (Ed.), pp. 61-75, W. B. Saunders Co., Philadelphia, Pa., 1970.
18. M. E. Hammond, S. S. Selvaggio, and H. F. Dvorak, Antigen-Enhanced Glucosamine Incorporation by Peritoneal Macrophages in Cell-Mediated Hypersensitivity. I. Studies on Biology and Mechanism, *J. Immunol.*, 115: 914-921 (1975).
19. J. M. Wilton, D. L. Rosenstreich, and J. J. Oppenheim, Activation of Guinea Pig Macrophages by Bacterial Lipopolysaccharide Requires Bone Marrow-Derived Lymphocytes, *J. Immunol.*, 114: 388-393 (1975).
20. P. A. Ward, Chemotaxis of Mononuclear Cells, *J. Exp. Med.*, 128: 1201-1221 (1968).
21. M. L. Karnovsky, S. Simmons, E. A. Glass, A. W. Shafer, and P. D. Hart, in *Mononuclear Phagocytes*, R. von Furth (Ed.), pp. 110-117, Blackwell Oxford, England, 1970.
22. S. I. Wasserman, D. Whitmer, E. J. Goetzl, and K. F. Austen, Chemotactic Deactivation of Human Eosinophils by the Eosinophil Chemotactic Factor of Anaphylaxis, *Proc. Soc. Exp. Biol. Med.*, 148: 301-306 (1975).
23. W. S. Walker, Functional Heterogeneity of Macrophages, in *Immunobiology of the Macrophage*, D. S. Nelson (Ed.), pp. 91-110, Academic Press Inc., New York, 1976.

Evaluation of Trace-Element Interactions Using Cultured Alveolar Macrophages

JOELLEN L. HUISINGH,* JAMES A. CAMPBELL,† and MICHAEL D. WATERS*
*Environmental Protection Agency and †Northrop Services, Inc., Environmental Research Center, Research Triangle Park, North Carolina

ABSTRACT

It is important to consider the interactions of toxic trace elements in an evaluation of the toxicity of environmental pollutants. The in vitro toxicity screening system developed at the Environmental Research Center using the rabbit alveolar macrophage provides a particularly useful system for evaluating trace-element interactions since crude particulates containing multiple trace elements can be introduced into the system.

Mercury, cadmium, and vanadium are the three most toxic metals that have been tested in the macrophage system. When cells were exposed simultaneously to toxic concentrations of cadmium or mercury and nontoxic concentrations of sodium selenite, the macrophages had significantly higher viability, cell number, and adenosine triphosphate concentration than when they were exposed to the cadmium or mercury salts alone. In analogous experiments, zinc was found to protect against cadmium toxicity, and copper protected the macrophage against the lytic effects of vanadium.

The phagocytic rabbit alveolar macrophage is a particularly appropriate cell in which to evaluate the cellular toxicity of airborne environmental chemicals, including particulates. Previous studies from the Environmental Research Center[1,2] have reported the use of this cell type in a screening system to rank the cytotoxicity of a series of metallic chlorides.

A modification of this system has been used recently to compare the relative cytotoxicity of a series of size fractionated industrial particulates.[3] Spark-source mass spectrometry was used to determine the elemental concentration of approximately 70 elements in these

particulate samples. The toxicity of the particulates was then predicted on the basis of a mathematical summation of the toxicities of the individual elements present in the sample.[4] This method does not take into account interactions that may occur between elements. The predicted toxicity of one-third of these samples was nearly twice the toxicity that was actually observed when the particulates were tested with the screening system that uses the rabbit alveolar macrophage. This suggests that the cytotoxic response of the macrophages may reflect antagonistic trace-element interactions resulting from a combination of elements in the sample.

The trace-element interactions reported in whole animals are antagonistic rather than synergistic[5] and include interactions between: cadmium and zinc, cadmium and copper, cadmium and selenium, copper and zinc, mercury and selenium, lead and calcium, and copper and molybdenum.[6] Several of these interactions have been shown to occur in mammalian cells in culture.[7]

The results reported here are part of a study designed to assess trace-element interactions in the rabbit alveolar macrophage that is used as a cytotoxicity screening system. The parameters measured in these experiments were percent viability, viability index, and adenosine triphosphate (ATP) content, which M. D. Waters et al. (unpublished data) have shown to correlate highly with phagocytic activity following exposure to soluble metallic chlorides.

METHODS

The techniques used for the procurement and maintenance of rabbit alveolar macrophages are modified from the procedures described previously.[2] New Zealand white rabbits were killed by injection of sodium pentobarbital (150 mg) into the marginal ear vein. After a tracheostomy was performed, lung lavage in situ was carried out by instilling 30 ml of sterile saline in the lungs of each rabbit. The initial instillation was allowed to remain for 15 min. Five subsequent infusions of 30 ml each were withdrawn immediately. Lavage fluid that contained blood or mucous was discarded. The cellular yield consisted of an average of 30 to 40 million cells per rabbit; of these, 95 to 98% were macrophages, 1 to 3% were polymorphonuclear leukocytes, and 1 to 2% were lymphocytes.

The pooled cells were collected by centrifugation at 365 x *g* for 15 min at 5°C and were resuspended in 37°C medium 199 in Hanks' salt solution supplemented with 20% heat-inactivated fetal-calf serum, 100 units/ml penicillin, and 100 μg/ml kanamycin and streptomycin. The cell suspension was adjusted to 10^6 cells/ml, and

2 ml was added to 25-cm^2 tissue-culture flasks. The macrophages were allowed to attach for 3 hr at 37°C in a humidified atmosphere of 4% CO_2 and 96% air. At the end of this period, 2 ml of 2x concentrated test medium containing the dissolved metals was added to each flask and incubated for 20 hr. At the end of the 20-hr incubation period, the medium from each flask was poured off and retained. The attached cells were removed by trypsinization and added to the medium retained above.

Initial experiments (Table 1) were conducted as described previously[8] with only the cells that attached after 3 hr. The concentration responses were very similar when both attached and unattached cells were exposed as described above and all subsequent interaction experiments were performed as described here.

Simultaneous determinations of cell number per milliliter and cell viability by the trypan-blue dye exclusion technique were performed on a cell suspension using a Cytograf model 6301 (Biophysics Systems). Viability was expressed directly as a percentage of 1000 cells classified. The viability index was determined by multiplying (percent viability) x (number of cells in the experimental culture/number of cells in the control). The viability index is a parameter that defines the combined effect of a test compound on viability and cell number. Adenosine triphosphate was determined

TABLE 1

EC50 VALUES* FOR PERCENT VIABILITY AND VIABILITY INDEX† FOR METALLIC SULFATES IN RABBIT ALVEOLAR MACROPHAGES AFTER 20 HR

Compound	Percent viability (EC50), m*M*	Viability index (EC50), m*M*
$HgSO_4$	0.053 (0.040—0.071)	0.037 (0.024—0.051)
$CdSO_4$	0.079 (0.063—0.102)	0.051 (0.040—0.065)
VSO_4	0.171 (0.109—273)	0.048 (0.025—0.076)
$CuSO_4$	0.605 (0.526—0.702)	0.553 (0.469—0.647)
$Zn(NH_4)_2SO_4 \cdot 6H_2O$	0.673 (0.601—757)	0.493 (0.432—0.562)
$ZnSO_4$	0.812 (0.656—1.05)	0.519 (0.434—0.626)
$MnSO_4$	4.31 (2.54—9.94)	1.28 (0.868—2.20)
$NiSO_4$	5.91 (4.32—9.58)	3.00 (2.35—4.26)

*Effective concentration resulting in 50% response after 20 hr. 95% confidence intervals are shown in parentheses.

†Viability index = (percent viability) x (total intact cells in experimental culture/total intact cells in controls).

with a Du Pont model 760 Luminescence Biometer as described previously.[8] Adenosine triphosphate levels were adjusted per 10^6 cells and expressed as a percent of control.

The metals were prepared as 100m*M* stock solutions in deionized water, filtered through a 0.22-μm membrane, and stored frozen. Aliquots of these stocks were diluted in culture medium, minus serum, just prior to testing, and the pH was adjusted if necessary to between 6.2 and 7.4. Aliquots of each concentration of metal tested were frozen for atomic absorption spectrophotometry. Analysis of actual metal concentrations in the test media were determined on a Perkin—Elmer model 306 atomic absorption spectrophotometer equipped with a model HGA-2100 graphite furnace. Conditions used for atomic absorption spectrophotometry were those described in the Perkin—Elmer instrument manual.

A complete concentration-response curve was determined for each metal sulfate using a minimum of six concentrations run in triplicate to obtain the values reported. Each metal was tested with a minimum of four different pools of alveolar macrophages on different days. Experiments on trace-element interactions were performed at least twice, and each treatment concentration was examined in triplicate with the exception of the ATP levels, which were run in duplicate.

RESULTS AND DISCUSSION

The relative toxicity of a series of metallic sulfates tested in the rabbit alveolar macrophage over a 20-hr exposure period in vitro are shown in Table 1. The three most toxic metals of those tested are mercury, cadmium, and vanadium. Copper and zinc exhibited moderate toxicity, and the least toxic metals of those tested were manganese and nickel. The concentrations of these metallic sulfates, which caused a 50% decrease in cell viability and viability index (EC50 values), are similar to those published previously for the metallic chlorides.[1,2] When the same pool of macrophages was used in concentration-response experiments with $NiCl_2$ and $NiSO_4$, no significant differences were seen in the concentration response for percent viability, as shown in Fig. 1. In analogous experiments with zinc and cadmium, chlorides and sulfates exhibited the same concentration response with respect to viability and viability index.

Trace-element interactions that are most likely to affect the net toxicity of a crude sample are those which involve either metals in particularly high concentration in the sample or metals that are the more toxic. Of the more toxic metals (cadmium, mercury, and

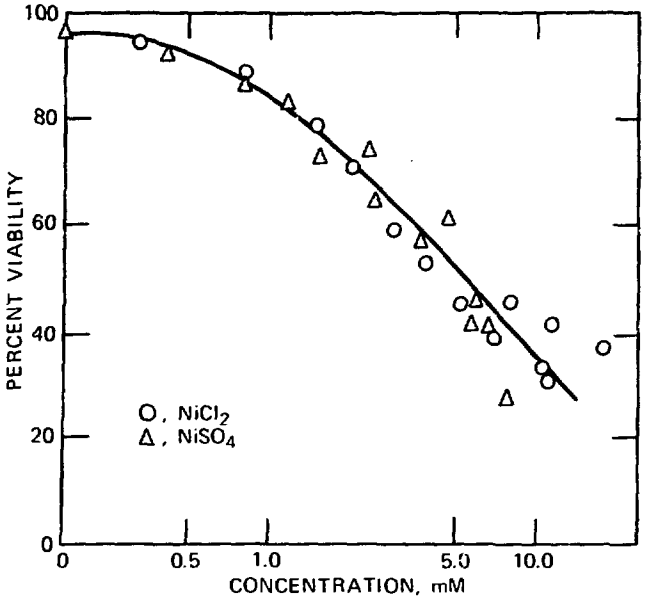

Fig. 1 Comparison of the effect of $NiCl_2$ and $NiSO_4$ on the percent viability of rabbit alveolar macrophages after 20 hr.

vanadium) examined with the alveolar macrophage, a number of interactions involving cadmium (e.g., with zinc, copper, and selenium) and mercury (with selenium) have been reported in whole animals.[6] A recent review of vanadium toxicology[9] suggests that vanadium may interact with copper.

The antagonistic interaction between cadmium and zinc is well-known. Initial studies with chicks[10] and later with mice and rats[11] showed that cadmium interfered with the metabolism of zinc, copper, and iron and that the toxic effects of cadmium could be largely overcome by administering additional zinc or copper. Exposure of rabbit alveolar macrophages to $CdSO_4$ (0.08m*M*), plus increasing concentrations of $ZnSO_4$ (from 0.08 to 0.16m*M*), showed increasing protection by zinc against cadmium toxicity, as shown in Fig. 2. All three parameters measured (percent viability, viability index, and ATP concentrations) increased up to 2-, 3-, and 4.4-fold, respectively, with increasing concentrations of $ZnSO_4$ up to 0.16m*M*. The lack of increased protection above 0.16m*M* $ZnSO_4$ is probably due to increasing toxicity of zinc, as indicated by the control cultures that contained $ZnSO_4$ alone.

Selenium in the form of selenite was first shown by Parizek et al.[12] to protect against the toxicity of both cadmium and mercury in whole animals. The effect of sodium selenite on the cytotoxic

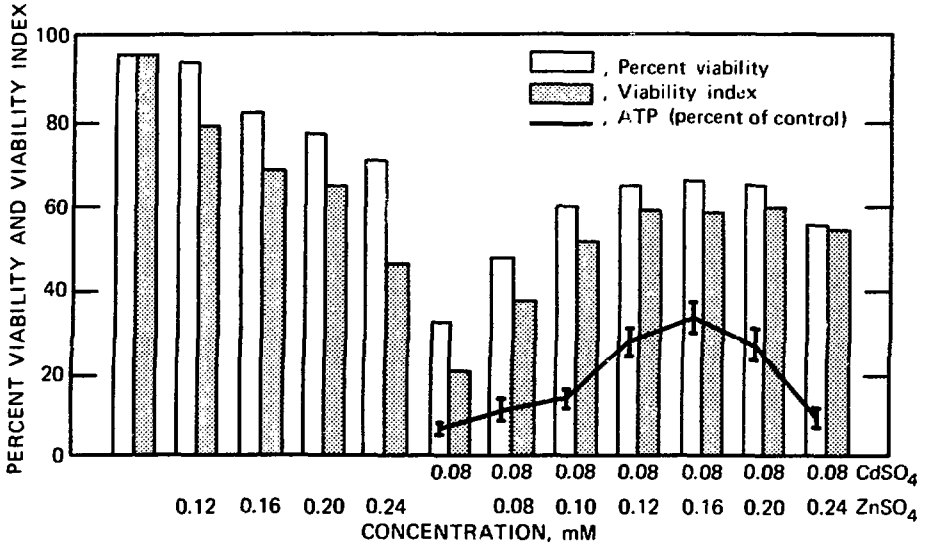

Fig. 2 Interaction of $CdSO_4$ and $ZnSO_4$ in rabbit alveolar macrophages after 20 hr. The standard errors per data point for percent viability and for viability index were less than 5% of the respective means. The standard errors per data point for ATP content are shown by vertical bars.

response observed in the alveolar macrophage due to cadmium and mercury salts is shown in Fig. 3 and 4. As little as 0.004m*M* of selenium in the presence of 0.08m*M* of cadmium or mercury (1 : 20 molar ratio) resulted in some protective effect on the alveolar macrophage in vitro. The protection observed in the cadmium—selenium experiment with 0.08m*M* of $CdCl_2$ and 0.016 to 0.032m*M* of Na_2SeO_3 resulted in increased percent viability, viability index, and ATP concentrations of 1.8-, 2.0-, and 2.1-fold, respectively. Parizek et al.[12] observed the protection of selenium against cadmium toxicity in the rat in the same range of selenium—cadmium molar ratios as observed in the macrophage.

The interaction between Na_2SeO_3 and $HgSO_4$ (Fig. 4) in the alveolar macrophage differs in two respects from that discussed above for selenium and cadmium. First, the protection is observed over a wider concentration range, with very little decrease in protection at the highest concentrations of selenium used. Second, the selenium protected to a greater extent against mercury toxicity, increasing all three parameters measured to nearly 100% of control values. This extensive protection by such low concentrations of selenium is particularly important since mercury is the most toxic element we have evaluated in this cytotoxicity screening system.

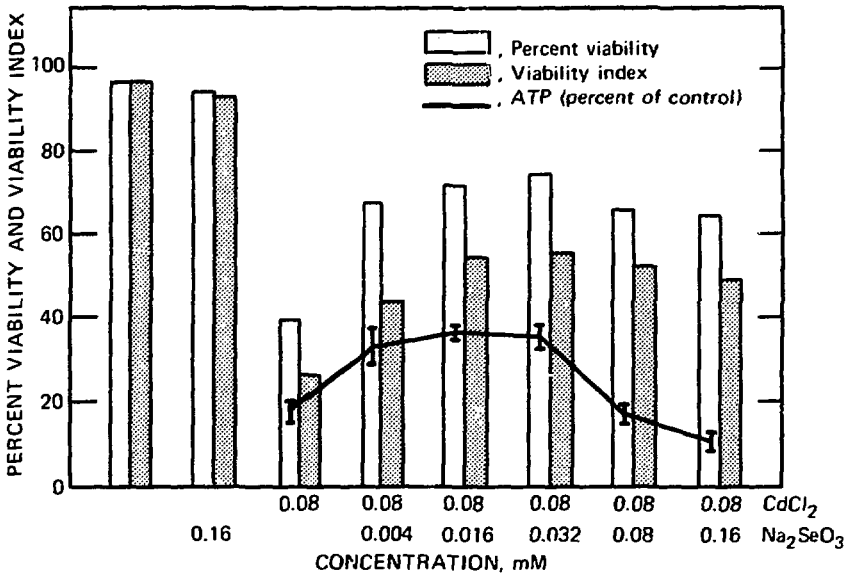

Fig. 3 Interaction of $CdCl_2$ and Na_2SeO_3 in rabbit alveolar macrophages after 20 hr. The standard errors per data point for percent viability and for viability index were less than 8% of the respective means. The standard errors per data point for ATP content are shown by vertical bars.

Both VSO_4 and NH_4VO_3 are highly toxic to alveolar macrophages in culture, ranking after mercury and cadmium in terms of percent viability. These two vanadium compounds and the vanadium oxides discussed in an earlier report[13] are the most cytolytic of the metals examined thus far. At the lowest concentrations of vanadium, where there was little effect on cellular viability, cell numbers were significantly decreased. As shown in Figs. 5 and 6, 0.1m*M* vanadium, which reduced the percent viability to 65 to 68%, decreased the viability index to 12%. The addition of increasing concentrations of either $CuCl_2$ or $CuSO_4$ resulted in increases in both the percent viability and the viability index. The increase in the viability index, however, was nearly four times the increase observed in the percent viability, indicating that copper protected against the lytic effect of vanadium. With the exception of the indirect evidence reviewed by Waters[9] which suggests that vanadium may interfere with copper metabolism, we know of no other experimental studies that have reported the protection of copper against vanadium toxicity.

When alveolar macrophages were exposed to increasing concentrations of divalent metal ions, the ATP content and phagocytic index of the macrophage decreased to a greater extent than viability

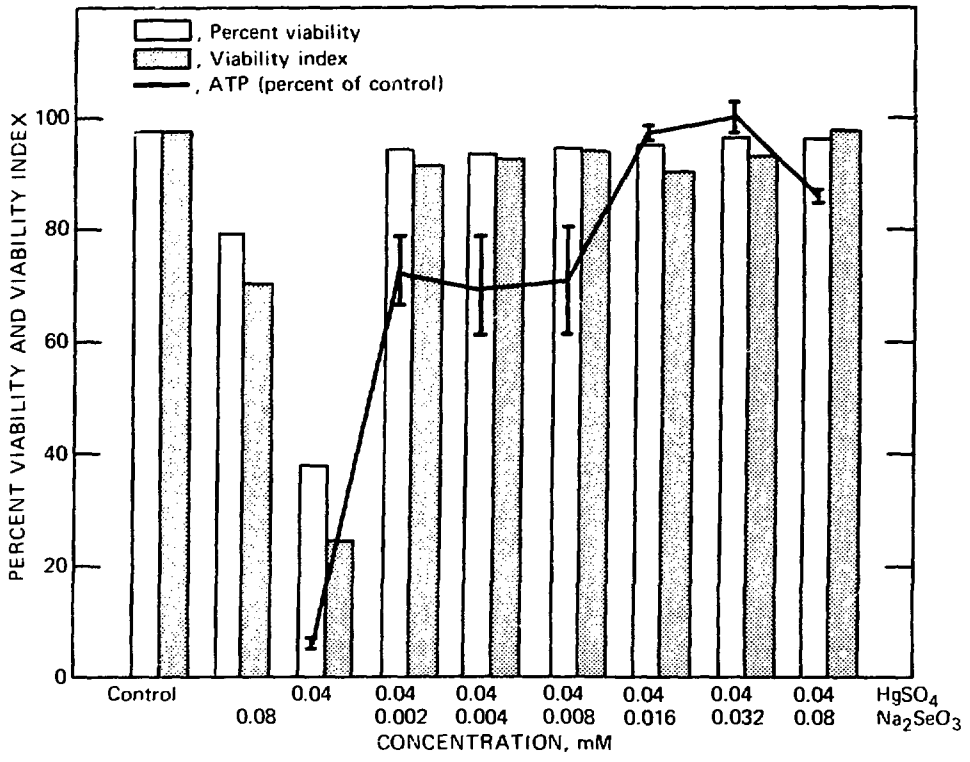

Fig. 4 Interaction of $HgSO_4$ and Na_2SeO_3 in rabbit alveolar macrophages after 20 hr. The standard errors per data point for percent viability and for viability index were less than 8% of the respective means. The standard errors per data point for ATP content are shown by vertical bars.

(M. D. Waters, personal communications). In the experiments reported here, the ATP content per 10^6 macrophages did initially increase with increasing viability as the concentration of antagonizing element increased. At the higher concentrations of the antagonizing element in every case except mercury and selenium, the ATP content decreased after reaching a maximum, but the percent viability remained higher. In these studies the ATP content of the antagonizing element alone was not measured, and ATP values per 10^6 macrophages are expressed as a percent of the control cultures. More extensive studies of the effect of these trace elements alone and in combination on the ATP content of the macrophage are now in progress, and the ATP values shown should be considered as relative values.

The supernatant fraction from a copper smelter particulate sample that was previously found to be highly toxic in the alveolar

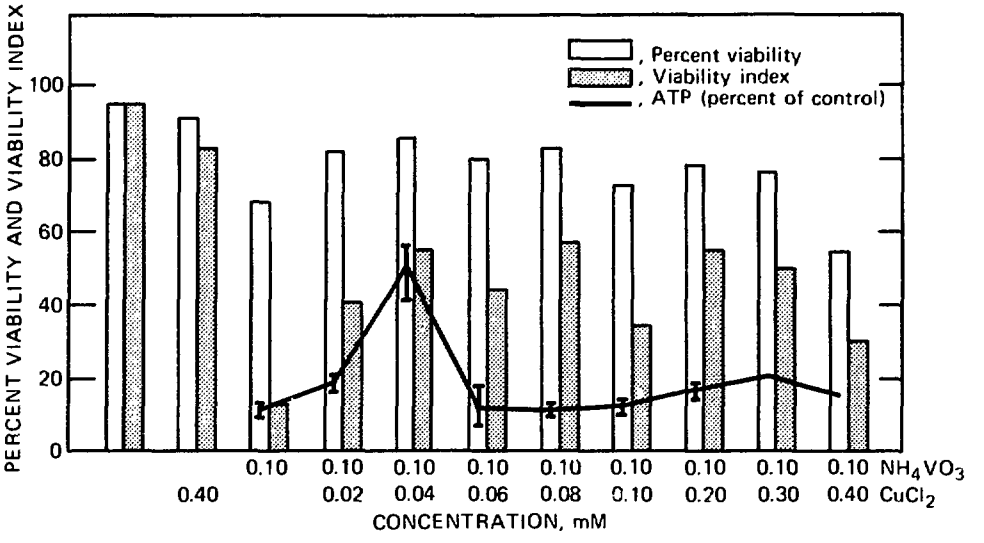

Fig. 5 Interaction of $CuCl_2$ and NH_4VO_3 in rabbit alveolar macrophages after 20 hr. The standard errors per data point for percent viability and for viability index were less than 10% of the respective means. The standard errors per data point for ATP content are shown by vertical bars.

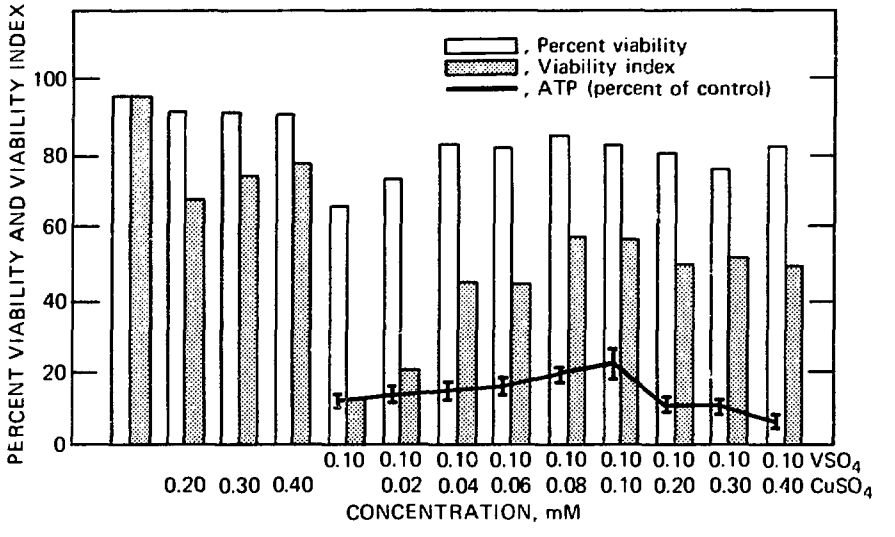

Fig. 6 Interaction of $CuSO_4$ and VSO_4 in rabbit alveolar macrophages after 20 hr. The standard errors per data point for percent viability were less than 5% and for viability index were less than 15% of the respective means. The standard errors per data point for ATP content are shown by vertical bars.

macrophage test system (EC50 for viability = 5 μg/ml)[3] had a predicted toxicity based on the elemental composition of nearly twice the actual toxicity.[4] The soluble supernatant fraction of the sample exhibited as much toxicity as the particulate itself. The sample contained the following elements: over 1% copper, arsenic, lead, antimony, and bismuth; and over 0.1% zinc, tin, selenium, silver, and cadmium. Elements in this sample which are known to interact antagonistically in whole animals include zinc and copper, selenium and arsenic, zinc and cadmium, and selenium and cadmium.

The supernatant fraction of this sample was incubated with alveolar macrophages alone and in the presence of nontoxic concentrations of cadmium, mercury, copper, zinc, and selenium (Fig. 7). In 0.15m*M* $ZnSO_4$, the percent viability and the viability index of the copper smelter sample increased 1.7- and 2-fold, respectively. Zinc is known to protect whole animals from both copper and cadmium toxicity, two elements that are present in this industrial particulate.

SUMMARY

In the evaluation of the rabbit alveolar macrophage as an in vitro test system for screening air and other crude particulate matter for

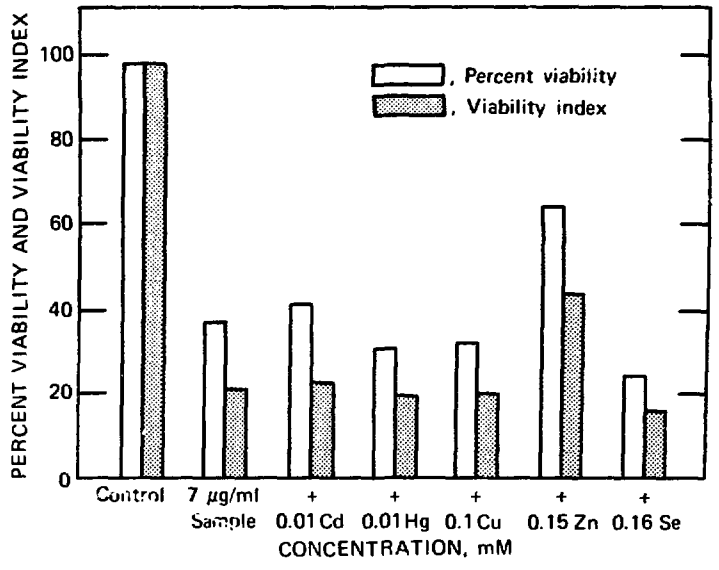

Fig. 7 Effect of cadmium, mercury, copper, zinc, and selenium on the toxicity of the supernatant fraction from a copper smelter sample (3 to 10 μm). The standard errors per data point for percent viability and for viability index were less than 10% of the respective means.

relative cytotoxicity, it is important that the alveolar macrophages in culture respond to trace-element interactions approximately as they would occur in a whole-animal or human-exposure situation.

Alveolar macrophages were shown to exhibit several trace-element interactions previously reported in whole animals. Zinc protected against cadmium toxicity in the macrophage, and selenium protected against both cadmium and mercury toxicity in a relative range previously reported for whole animals.

The alveolar macrophage may also provide a useful tool for screening metals and other elements for interactions, as suggested by the observation that copper protects the macrophages from the lytic effect of vanadium.

ACKNOWLEDGMENTS

The authors gratefully acknowledge the contributions of the following individuals: A. G. Stead for statistical analysis, T. A. Hinners for selenium analysis, C. C. Cox and B. G. Russell for metals analysis, and H. F. Stack and the staff of the Northrop Services Testing Unit for their technical support.

REFERENCES

1. M. D. Waters, T. O. Vaughn, J. A. Campbell, and D. L. Coffin, Screening Studies on Metallic Salts Using the Rabbit Alveolar Macrophage, *In Vitro*, 10: 342-343 (1974).
2. M. D. Waters, D. E. Gardner, C. Aranyi, and D. L. Coffin, Metal Toxicity for Rabbit Alveolar Macrophages In Vitro, *Environ. Res.*, 9: 32-47 (1975).
3. J. A. Campbell, B. G. Brown, B. F. Russell, and H. F. Stack, *Bioassay of Eighteen Particulate Samples Utilizing the Rabbit Alveolar Macrophage Test System*, Report TN-262-1547, Northrop Services, Inc., Research Triangle Park, N. C.
4. H. Mahar, *Evaluation of Selected Methods for Chemical and Biological Testing of Industrial Particulate Emissions*, Report 600/2-76-137, Industrial Environmental Research Laboratory, 1976.
5. G. Matrone, Chemical Parameters in Trace-Element Antagonisms, in *Trace Element Metabolism in Animals—2*, W. G. Hoekstra, J. W. Suttie, H. E. Ganther, and W. Mertz (Eds.), pp. 91-103, University Park Press, Baltimore, 1974.
6. D. Huisingh and J. Huisingh, Factors Influencing the Toxicity of Heavy Metals in Food, *Ecology of Food and Nutr.*, 3: 263-272 (1974).
7. J. Huisingh, S. Potter, R. Munoz, and G. Matrone, Trace Element Interactions in Mammalian Cell Culture, in *Environ. Health Perspect.*, 17: 288 (1977).
8. M. D. Waters, T. O. Vaughan, D. J. Abernethy, H. R. Garland, C. C. Cox, and D. L. Coffin, Toxicity of Platinum(IV) Salts for Cells of Pulmonary Origin, *Environ. Health Perspect.*, 12: 45-56 (1975).

9. M. D. Waters, Toxicology of Vanadium, in *Advances in Modern Toxicology*, R. A. Goyer and M. A. Mehlman (Eds.), Vol. 2, pp. 147-189, Halsted Press, John Wiley & Sons, Inc., New York, 1977.
10. C. H. Hill, G. Matrone, W. L. Payne, and C. W. Barber, In Vivo Interactions of Cadmium with Copper, Zinc and Iron, *J. Nutr.*, 80: 227-235 (1963).
11. C. R. Bunn and G. Matrone, In Vivo Interactions of Cadmium, Copper, Zinc and Iron in the Mouse and Rat, *J. Nutr.*, 90: 395-399 (1966).
12. J. Parizek, I. Ostadalova, J. Kalouskova, The Detoxifying Effects of Selenium, in *Interrelations Between Compounds of Selenium and Certain Metals, Newer Trace Elements in Nutrition*, W. Mertz and W. E. Cornatzer (Eds.), pp. 85-122, Marcel Dekker, New York, 1971.
13. M. D. Waters, D. E. Gardner, and D. L. Coffin, Cytotoxic Effects of Vanadium on Rabbit Alveolar Macrophages In Vitro, *Tox. Appl. Pharmacol.*, 28: 253-263 (1974).

Effect of Irritant Atmospheres on Macrophage Behavior

G. V. KATZ* and S. LASKIN
New York University Medical Center, Department of Environmental Medicine, New York, New York

ABSTRACT

Studies were developed in which rats were preexposed to irritant gases. Pulmonary alveolar macrophages (PAM) harvested from these rats by lung lavage were cultured and challenged with polystyrene latex spheres.

The phagocytic activity of the PAM for periods up to 7 days was measured by trypsinizing the viable adhering cells daily, releasing latex spheres, and then quantitating the resulting suspension by nephelometric analysis.

Adhesion of cells to the culture surface was found to be significantly greater in those studies where macrophages were harvested from rats preexposed to gaseous irritants when compared to unexposed controls. This stimulation was unaffected by the presence of latex.

Exposure of rats to 5, 10, and 20 ppm sulfur dioxide significantly stimulated phagocytic activity. Although some stimulation was seen with formaldehyde at 10 ppm, activity at 20 ppm was depressed. Studies with nitrogen dioxide show results paralleling controls at 10 ppm with a significant depression at 25 ppm.

Gaseous and particulate pollutants associated with major urban areas throughout the world are a source of serious health concern. When pollutants are inhaled, the pulmonary alveolar macrophage (PAM) functions as a primary defense against their retention. However, the efficiency of the PAM is dependent on the nature of the insult. Quantitative assessments of the effects of inhaled materials on the PAM in vivo are severely limited. It is convenient, therefore, to study the actions of particles and gases on cultures. Thus asbestos,[1]

*Present address: Eastman Kodak Company, Kodak Park, Rochester, N. Y. 14650.

quartz,[1] and cigarette smoke,[2] for example, have been demonstrated to exert a cytotoxic effect, reducing the mobility of macrophages. Quartz[3] also reduces their viability. In addition, other studies[4-8] have shown that such common irritant gases as ozone or nitrogen dioxide also affect macrophages by reducing their phagocytic efficiency. Despite the variety of studies performed, little is known quantitatively about the effects produced by gaseous irritants on phagocytic efficiency. Preliminary studies have been completed in our laboratory demonstrating that as a result of exposures of rats to irritant gases or vapors, such as nitrogen dioxide (NO_2), formaldehyde (CH_2O), or sulfur dioxide (SO_2), phagocytosis by the PAM in culture may be depressed or stimulated.[9] These studies, including additional results of recent investigations, are reviewed here.

METHODS AND MATERIALS

Groups of 10 male Sprague—Dawley rats (age 12 to 13 weeks) were exposed in 1.3 m^3 inhalation chambers to levels of 10 and 25 ppm NO_2, 10 and 20 ppm CH_2O, and 1, 5, 10, and 20 ppm SO_2, all for 24 hr. As a result of observations with SO_2, an additional study of a single 8-hr exposure at 10 ppm was also performed.

Cells from the various exposure groups were harvested and cultured in Leighton tubes (5×10^5 cells/ml) in the presence or absence of polystyrene latex spheres (0.8 μm) for periods up to 7 days. The phagocytic activity of the macrophages was measured by trypsinizing the viable adhering cells daily, releasing latex spheres, and then quantitating the resulting suspension by nephelometric analysis. The recovery, processing, and enumeration of cells from rat lungs, culture techniques, and polystyrene latex analysis have been previously described.[9]

Transmission electron microscopy (TEM) was performed according to the procedures outlined by Wolff and Konrad.[10]

Scanning electron microscopy (SEM) was performed on unexposed macrophages with or without latex challenge (2.0 μm) for periods up to 2 weeks using procedures similar to those outlined by Parakkal et al.[11]

RESULTS

Phagocytic Efficiency of the Pulmonary Alveolar Macrophage in Culture

The average latex uptake by cultured macrophages harvested from the lungs of unexposed rats is shown in Table 1. The

TABLE 1

POLYSTYRENE LATEX UPTAKE BY MACROPHAGES IN CULTURE HARVESTED FROM UNEXPOSED RATS

	Days in culture						
	1	2	3	4	5	6	7
Cumulative average number of latex spheres per macrophage	90	262	609	1037	1582	2051	1864
±2 standard errors	26	88	136	194	310	440	444

cumulative average number of spheres phagocytized increases daily, reaching approximately 2000 spheres by days 6 and 7. For a comparison, these control data are also plotted in Figs. 1 to 6 with standard errors.

The average uptake by cultured macrophages harvested from the lungs of 6- and 20-week-old rats is compared to control levels in Fig. 1. Although 12- to 13-week-old rats were used exclusively in these studies, variations in rat age (6 to 20 weeks) from which macrophages were harvested did not affect polystyrene latex uptake.

The average latex uptake by macrophages in culture harvested from rats exposed to NO_2, CH_2O, or SO_2 for 24 hr is shown in Figs. 2 to 5.

Exposure to 10 ppm NO_2 resulted in latex uptake paralleling control levels. However, 25 ppm NO_2 significantly ($p < 0.01$) depressed phagocytosis on days 4 to 6 (Fig. 2). On day 7 the depression was still apparent.

Similarly, exposure of rats to 20 ppm CH_2O significantly ($p < 0.01$) depressed uptake such that there was little difference between the values on days 3 and 7 (Fig. 3). In contrast, a stimulatory effect ($p < 0.01$) on phagocytosis was observed during the first 2 days in culture when macrophages were harvested from rats exposed to 10 ppm CH_2O.

Marked stimulation ($p < 0.01$) of phagocytosis beginning on the first day in culture was observed when rats were exposed to 10 and 20 ppm SO_2 (Fig. 4). By the second and third days in culture, macrophages from these groups had engulfed a cumulative average attained by controls only after 5 days. Although not as marked, significant stimulation was also observed between 2 and 4 days at the 5 ppm SO_2 level (Fig. 5). Exposures of 1 ppm SO_2 did not affect phagocytic activity of macrophages in culture, and levels paralleled controls for the entire 7-day period.

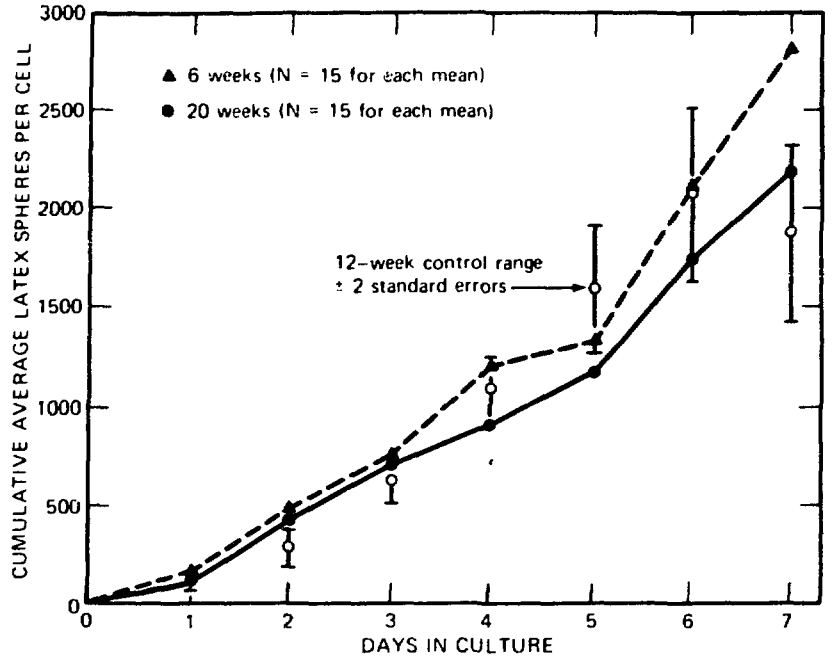

Fig. 1 Effect of age on average latex uptake by rat pulmonary alveolar macrophages.

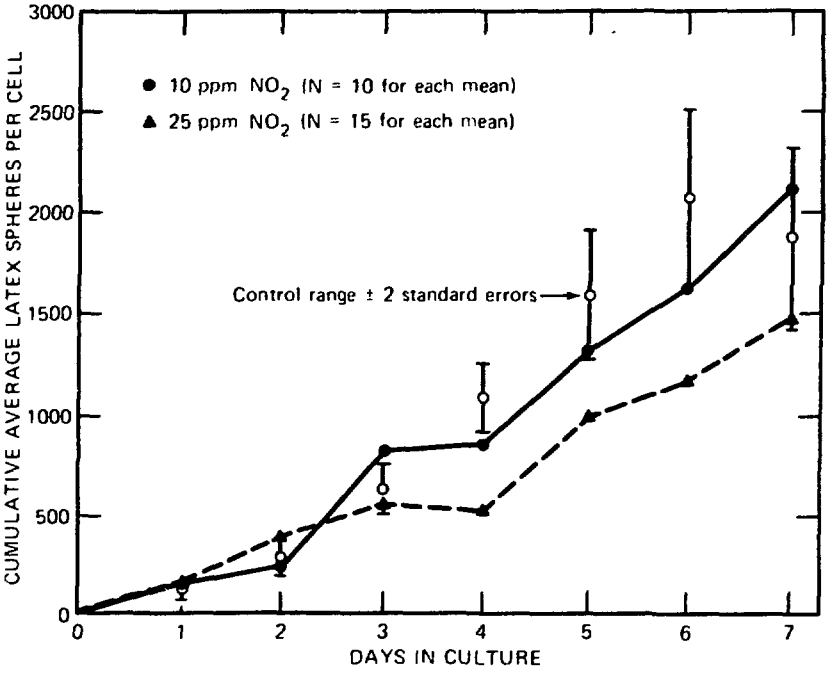

Fig. 2 Average latex uptake by pulmonary alveolar macrophages from rats preexposed to 10 and 25 ppm nitrogen dioxide for 24 hr.

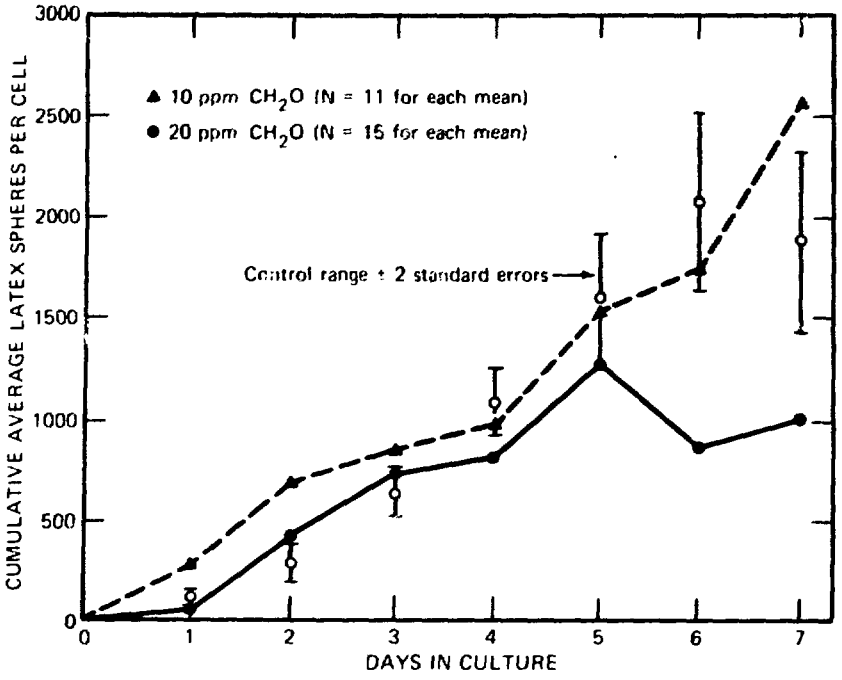

Fig. 3 Average latex uptake by pulmonary alveolar macrophages from rats preexposed to 10 and 20 ppm formaldehyde for 24 hr.

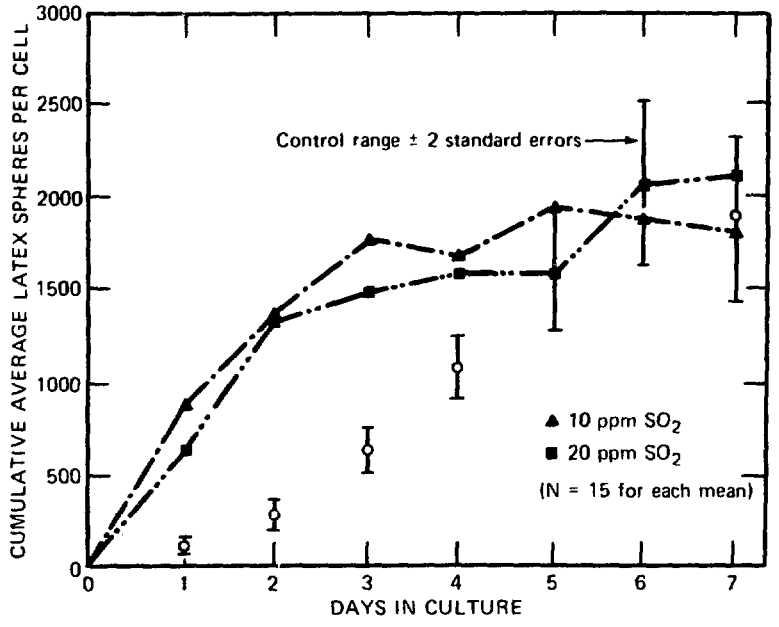

Fig. 4 Average latex uptake by pulmonary alveolar macrophages from rats preexposed to 10 and 20 ppm sulfur dioxide for 24 hr.

Latex uptake by macrophages in culture harvested from rats exposed to 10 ppm SO_2 for a single 8-hr exposure is compared to the 24-hr exposure in Fig. 6. Stimulation of phagocytosis is observed only on day 2. The marked effect following 24-hr exposures was not seen.

Effects of Irritant Exposure on Pulmonary Alveolar Macrophage Adhesion to Culture Surface

The eosin-y exclusion test[1,2] demonstrated that the macrophages adhering to the culture surface represented a viable population. Patterns of adhesion were shown when the results of the various experiments were grouped according to exposure.

Adhesion was significantly greater for at least 5 of the 7 days in cultures of macrophages harvested from irritant exposed rats when compared to those cultures of macrophages harvested from unexposed rats. This effect is shown in Table 2.

When irritant exposure was combined with polystyrene latex challenge, adhesion of cells to the culture surface still remained significantly greater than control groups that were similarly challenged with latex (Table 3).

Microscopic Observations

Microscopic observations on macrophages directly after harvest from rat lungs and in culture have been described.[9] These observations included the presence of densely staining toluidine-blue bodies in macrophages directly after exposure to 10 and 25 ppm NO_2 and 20 ppm CH_2O. In addition, cells exposed to 20 ppm CH_2O showed marked morphologic and cytoplasmic changes. Once in culture, all macrophages appeared morphologically similar.

When challenged with latex, phagocytosis begins immediately. After 4 days in culture, cells are so engorged with latex that cytological observations are difficult (Fig. 7). Latex uptake appeared microscopically similar for all treatments with the exception of the 10 and 20 ppm SO_2 groups, where the macrophage cytoplasm was already occluded with latex after 1 day's challenge. This finding was confirmed by TEM (Fig. 8).

Observations on macrophages in culture using SEM are shown in Figs. 9 to 11. To date, this study encompasses only preliminary observations on controls with or without latex for periods up to 2 weeks in culture.

After 24 hr in culture, some cells remain rounded while others project pseudopods (Fig. 9). Filopodia (fine cytoplasmic extensions) may be seen projecting great distances from the cell body.

(Text continues on page 370.)

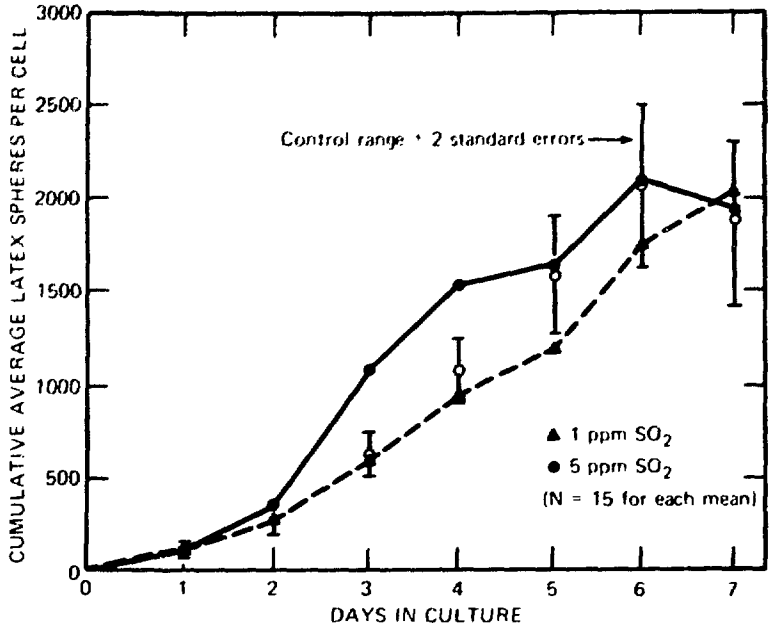

Fig. 5 Average latex uptake by pulmonary alveolar macrophages from rats preexposed to 1 and 5 ppm sulfur dioxide for 24 hr.

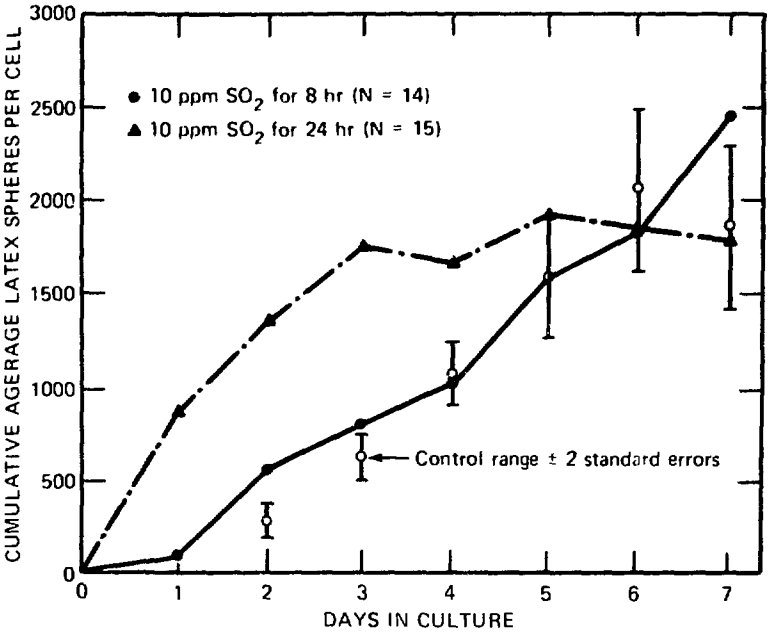

Fig. 6 Comparison of average latex uptake by pulmonary alveolar macrophages from rats preexposed to 10 ppm sulfur dioxide for 8 and 24 hr.

TABLE 2

MACROPHAGE ADHESION TO CULTURE SURFACE—EFFECT OF IRRITANT GAS

Time in culture, days	Number of viable adhering macrophages*			
	Unexposed controls	Nitrogen dioxide	Formaldehyde	Sulfur dioxide
1	1.92 ± 0.10	1.92 ± 0.26	4.08 ± 0.84†	1.98 ± 0.16
2	1.29 ± 0.04	2.10 ± 0.20†	2.40 ± 0.58†	1.57 ± 0.08†
3	1.01 ± 0.08	1.67 ± 0.22†	2.20 ± 0.22†	1.33 ± 0.14†
4	0.84 ± 0.08	1.91 ± 0.28†	2.71 ± 0.44†	1.24 ± 0.08†
5	0.79 ± 0.08	1.58 ± 0.10†	0.97 ± 0.28	1.21 ± 0.18†
6	0.69 ± 0.06	1.33 ± 0.26†	1.96 ± 0.34†	0.87 ± 0.14
7	0.43 ± 0.06	1.48 ± 0.08†	2.11 ± 0.72†	0.72 ± 0.14†

*Mean value X 10^5 plus or minus two standard errors for at least 10 determinations per treatment group per day. All cultures were initiated with 5 X 10^5 cells.

†Designates significant increase in adhesion ($p < 0.01$) by macrophages harvested from irritant exposed rats when compared to unexposed controls.

TABLE 3

MACROPHAGE ADHESION TO CULTURE SURFACE—EFFECT OF IRRITANT GAS PLUS LATEX CHALLENGE

Time in culture, days	Number of viable adhering macrophages*			
	Unexposed controls plus latex	Nitrogen dioxide plus latex	Formaldehyde plus latex	Sulfur dioxide plus latex
1	1.46 ± 0.12	2.03 ± 0.28†	4.17 ± 1.12†	1.59 ± 0.10
2	1.10 ± 0.10	2.11 ± 0.22†	1.82 ± 0.28†	1.33 ± 0.08†
3	0.73 ± 0.10	1.56 ± 0.16†	1.61 ± 0.14†	1.19 ± 0.08†
4	0.77 ± 0.08	1.60 ± 0.32†	1.81 ± 0.18†	1.01 ± 0.01†
5	0.59 ± 0.06	1.34 ± 0.18†	1.34 ± 0.32†	0.79 ± 0.06
6	0.44 ± 0.06	1.39 ± 0.50†	1.33 ± 0.20†	0.53 ± 0.04†
7	0.24 ± 0.04	0.70 ± 0.26†	0.63 ± 0.22†	0.52 ± 0.22†

*Mean value X 10^5 plus or minus two standard errors for at least 10 determinations per treatment group per day. All cultures were initiated with 5 X 10^5 cells.

†Designates significant increase in adhesion ($p < 0.01$) by macrophages harvested from irritant exposed rats when compared to unexposed controls.

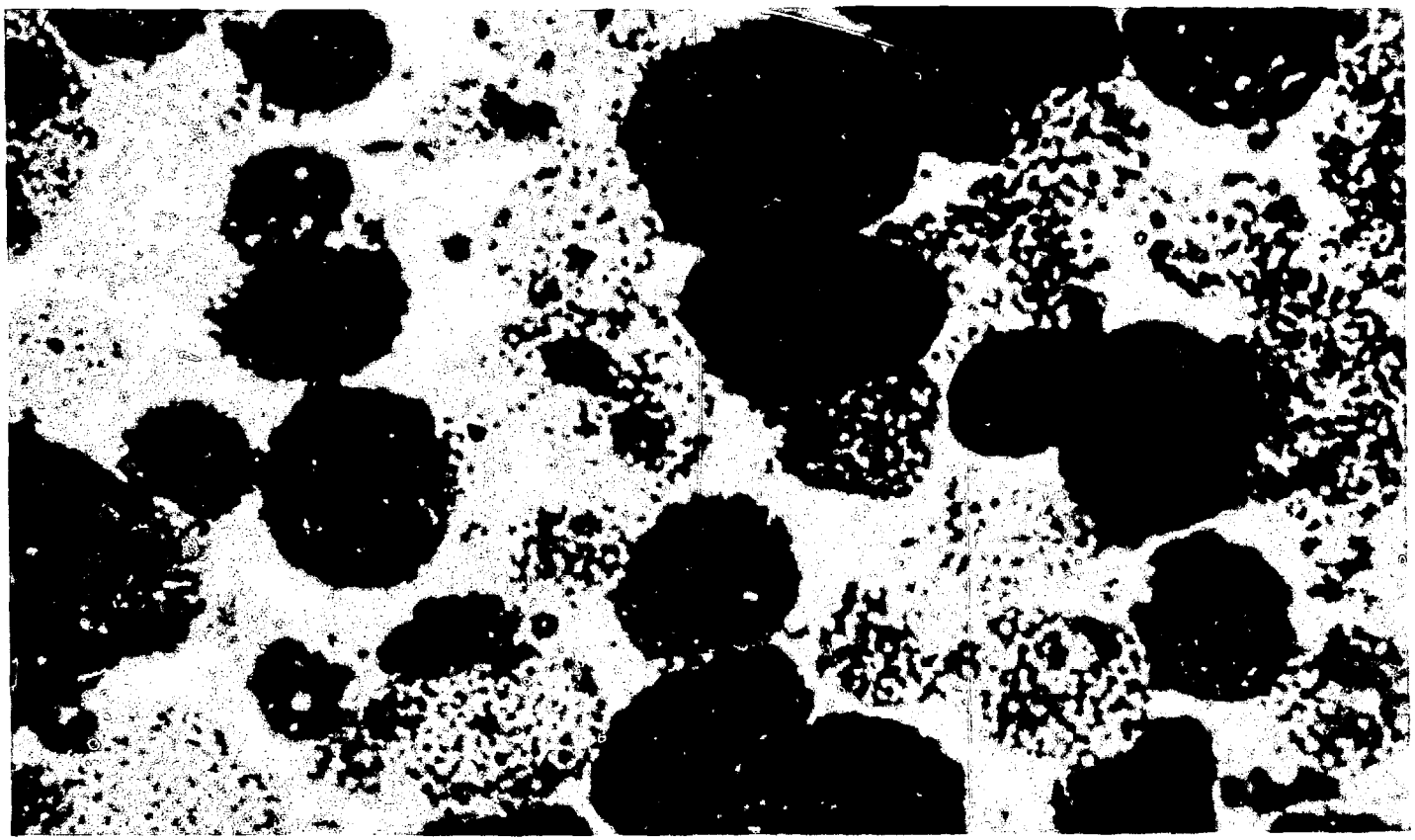

Fig. 7 Pulmonary alveolar macrophages harvested from unexposed rats, followed by culture, and challenged with latex. By 7 days in culture, cells are engorged with latex. Toluidine-blue, thick section of pellet prepared for electron microscopy. (Magnification, 1120X.)

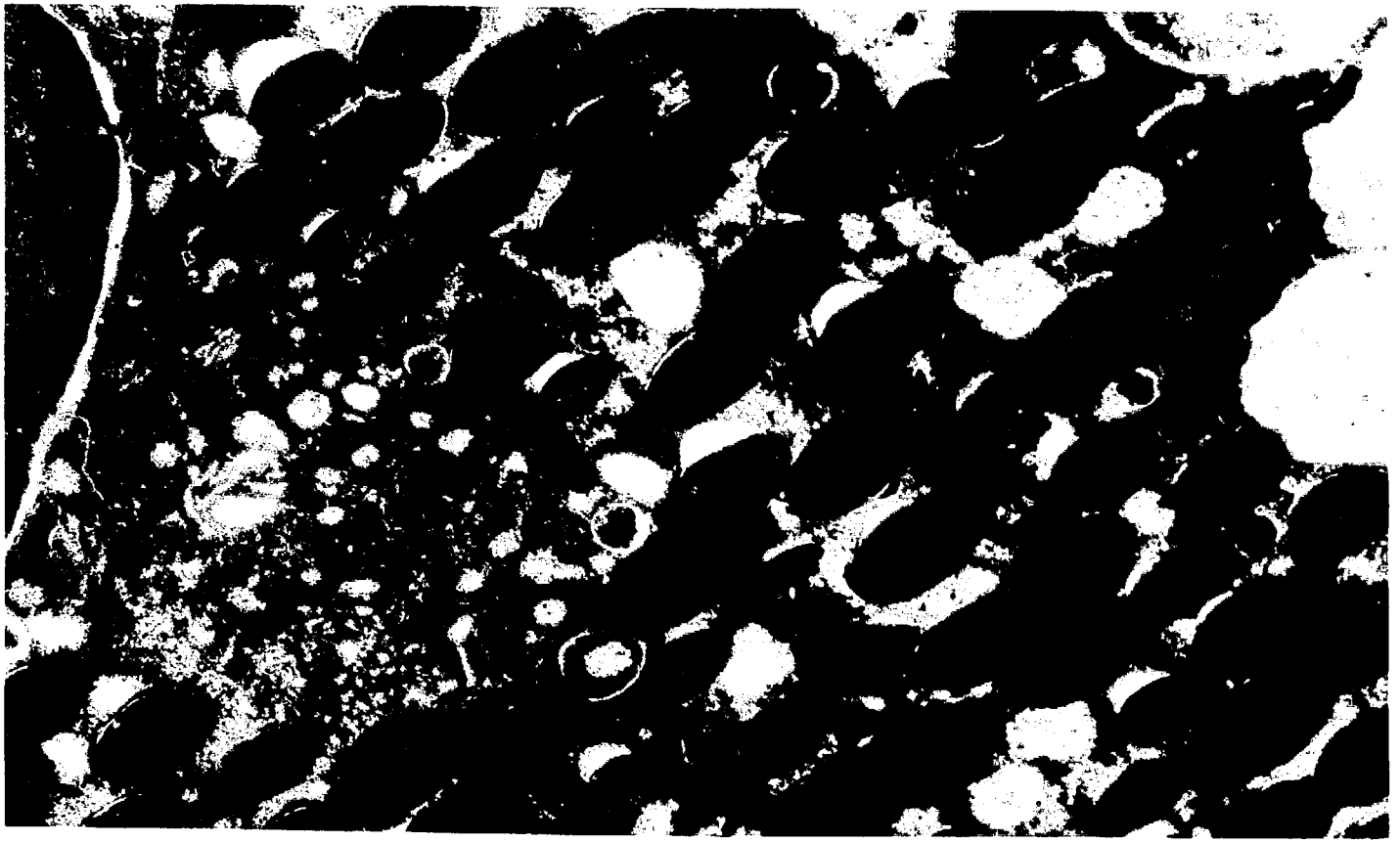

Fig. 8 Transmission electron micrograph of a pulmonary alveolar macrophage harvested from a rat preexposed to 20 ppm sulfur dioxide for 24 hr, followed by culture, and challenged with latex. Cell is laden with latex within 24 hr in culture. (Magnification, 28,000X.)

Fig. 9 Scanning electron micrograph of pulmonary alveolar macrophages in culture harvested from an unexposed control rat. Within 24 hr, macrophages adhere to culture surfaces and may project extensions such as filopodia or pseudopods. (Magnification, 3000X.)

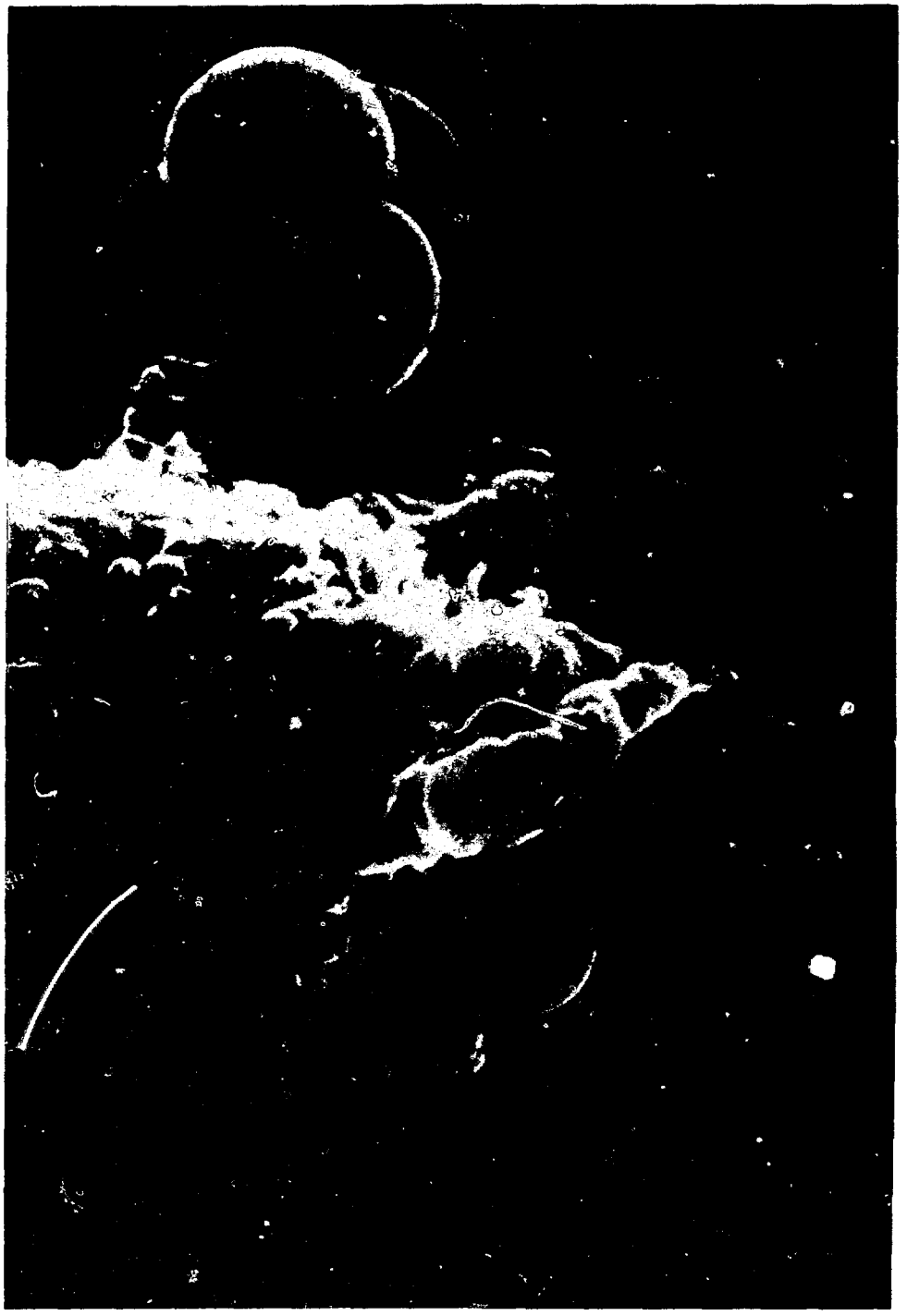

Fig. 10 Scanning electron micrograph of a pulmonary alveolar macrophage in culture harvested from an unexposed control rat. Attachment and ingestion of latex spheres (2.0 μm) begins within the first 24 hr in culture. (Magnification, 13,600X.)

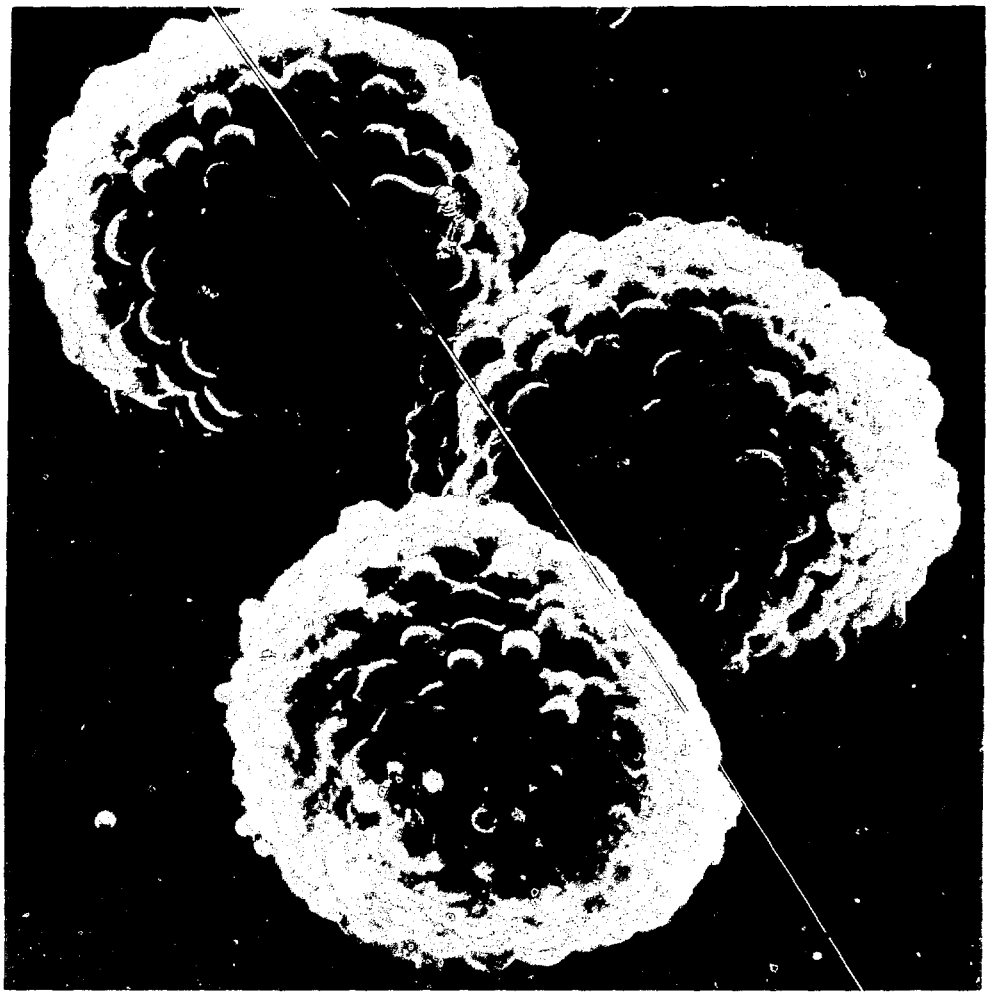

Fig. 11 Scanning electron micrograph of pulmonary alveolar macrophages in culture harvested from an unexposed control rat. Within 2 weeks in culture, cells are engorged with latex spheres (2.0 μm). Some spheres still remain attached externally to the membrane surface. (Magnification, 3200X.)

A macrophage in culture for 24 hr challenged with polystyrene latex spheres (2.0 μm) is shown in Fig. 10. Adhesion of the particles to the cell surface and extending pseudopods can be seen.

In preliminary studies after 2 weeks in culture, a number of cells have remained viable and show adhesive properties similar to controls. Although spheres can be seen attached to the cell surface, the macrophage is so engorged that numerous spheres are visible beneath the membrane (Fig. 11).

DISCUSSION

Macrophages engulf large quantities of polystyrene latex spheres. The extent of phagocytosis is, however, dependent on particle size. This has been demonstrated in short-term cultures with guinea pig peritoneal and human blood phagocytes.[13] In the present study, rat alveolar macrophages were capable of engulfing approximately 2000 spheres each. Variations in the age of the rat (6 to 20 weeks) did not affect the phagocytic efficiency of the macrophages in culture. Phagocytic efficiency was affected, however, when the macrophages were harvested from rats exposed to NO_2, CH_2O, or SO_2.

The impairment of phagocytic efficiency observed in macrophages harvested from rats exposed to 25 ppm NO_2 parallels the findings of Acton and Myrvik.[7] They demonstrated reduced phagocytosis of killed Bacillus Calmette—Guerin vaccine by macrophages from rats after exposure to 15 and 25 ppm NO_2. In our studies the additional findings of large numbers of densely staining toluidine-blue bodies,[9] seen directly after exposure to 10 and 25 ppm NO_2 and 20 ppm CH_2O, are suggestive of some biochemical alterations.

Although increased phagocytic activity was observed after a 24-hr exposure to 10 ppm CH_2O, marked stimulation was elicited by 24-hr exposures to 5, 10, and 20 ppm SO_2. The stimulation never significantly exceeded the average cumulative maximum uptake of latex spheres seen by the sixth and seventh days in unexposed control groups. However, in the 10 and 20 ppm studies, this level was reached much sooner. The shorter exposure period with SO_2 apparently did not provide sufficient dosage to elicit the response following 24-hr exposures.

The reason for the phagocytic stimulation by SO_2 exposures has not been determined. Changes in enzymatic activity,[14] tissue proteins,[15] and blood plasma[16-17] have been observed. These changes after SO_2 exposure may account for changes in phagocytic activity if SO_2 reacts with intrapulmonary or intravascular alveolar macrophage stem cells.

The significance of the increased adhesive properties of macrophages after gaseous exposure is uncertain. Congregation of guinea pig macrophages in culture after in vivo exposure to NO_2 has been observed.[18] Exposure to irritant gases may lead to alterations in basic properties of cell surfaces.

Preliminary results of SEM, limited to control studies with and without latex, suggest that phagocytosis occurs in culture for periods of up to 2 weeks. The large quantities of latex that a macrophage is capable of engulfing, which was demonstrated by

direct quantitative analysis and by light microscopy and TEM, have been also observed by SEM.

The common irritant gases (NO_2, CH_2O, and SO_2) result in marked qualitative and quantitative changes in the PAM. As a result, they may represent a serious potential hazard both industrially and environmentally. Future studies are needed to determine the mechanism of action.

ACKNOWLEDGMENTS

The author wishes to express his sincere appreciation to a great scientist, teacher, and friend, Professor Sidney Laskin. His death on Nov. 28, 1976, was a great loss. His expertise, guidance, and friendship will be missed.

Acknowledgment is also given to the following who participated in one or more phases of the work: Fredrick Blanchard, Reade Moulton, Laura Luchi, Dorothy Natalizio, and Roger Sparling.

This investigation is supported by Contract No. NO1 CP33260 from the National Cancer Institute and is part of a Center program supported by grant ES00260 from the National Institutes of Environmental Health Sciences and grant CA13343 from the National Cancer Institute.

REFERENCES

1. T. H. Belt, F. Friedman, and F. J. King, The Effect of Asbestos on Tissue Cultures. A Comparative Study with Quartz and Coal Dust, *J. Pathol. Bacteriol.*, 59: 159-164 (1947).
2. C. Leuchtenberger and R. Leuchtenberger, The Behavior of Macrophages in Lung Cultures After Exposure to Cigarette Smoke. Evidence for Selective Inhibition by Particulate Matter and Stimulation by the Gas Phase of Cell Metabolism of Alveolar Macrophages, *Adv. Exp. Med. Biol.*, 15: 347-360 (1971).
3. E. G. Beck, P. F. Holt, and E. T. Nasrailah, Effects of Chrysotile and Acid Treated Chrysotile on Macrophage Cultures, *Br. J. Ind. Med.*, 28: 179-185 (1971).
4. A. R. Dowell, K. H. Kilburn, and P. C. Pratt, Short Term Exposure to Nitrogen Dioxide, *Arch. Intern. Med.*, 9: 214-220 (1971).
5. D. E. Gardner, R. S. Holzman, and D. L. Coffin, Effects of Nitrogen Dioxide on Pulmonary Cell Populations, *J. Bacteriol.*, 98: 1041-1043 (1969).
6. R. Ehrlich, Effect of Air Pollutants on Respiratory Infection, *Arch. Environ. Health*, 6: 638-642 (1963).
7. J. Acton and Q. N. Myrvik, Nitrogen Dioxide Effects on Alveolar Macrophages, *Arch. Environ. Health*, 24: 48-52 (1972).

8. C. L. Vassallo, B. M. Domm, R. H. Poe, M. L. Duncombe, and B. L. Gee, NO_2 Gas and NO_2—Effects On Alveolar Macrophage Phagocytosis and Metabolism, *Arch. Environ. Health*, 26: 270-274 (1973).
9. G. V. Katz, and S. Laskin, Pulmonary Macrophage Response to Irritant Gases, in *Air Pollution and the Lung*, Symposium Proceedings, Ma'alot, Israel, Mar. 16-19, 1975, pp. 83-100, John Wiley & Sons, New York, 1976.
10. K. Wolff and K. Konrad, Phagocytosis of Latex Beads by Epidermal Keratinocytes In Vivo, *J. Ultrastruct. Res.*, 39: 262-280 (1971).
11. P. Parakkal, J. Pinto, and J. M. Hanifin, Surface Morphology of Human Mononuclear Phagocytes During Maturation and Phagocytosis, *J. Ultrastruct. Res.*, 48: 216-226 (1974).
12. J. H. Hanks and J. H. Wallace, Determination of Cell Viability, *Proc. Soc. Exp. Biol. Med.*, 98: 188-192 (1958).
13. J. Roberts and J. H. Quastel, Particle Uptake by Polymorphonuclear Leucocytes and Ehrlich Ascites Carcinoma Cells, *Biochem. J.*, 89: 150-156 (1963).
14. W. O. Negherbon, *Sulfur Dioxide, Sulfur Trioxide, Sulfuric Acid and Fly Ash: Their Nature and Their Role in Air Pollution*, Publication 66-900, Hazelton Laboratories, Edison Electric Institute, New York, 1966.
15. T. A. Bystrova, *Effects of Sulfur Dioxide Studies with the Aid of Labeled Atoms, U.S.S.R. Literature on Air Pollution and Related Occupational Diseases: A Survey*, U. S. Dept. of Commerce, Office of Translation Services, 1962.
16. A. F. Gunnison and A. W. Benton, Sulfur Dioxide: Sulfite: Interaction with Mammalian Serum and Plasma, *Arch. Environ. Health*, 22: 381-388 (1971).
17. E. V. Elfimova and N. N. Pushkina, Ascorbic Acid Excretion in the Urine as an Indicator of the Harmful Effects of Atmospheric Pollution, *Hyg. Sanit.*, 31: 255-257 (1966).
18. R. P. Sherwin, V. Richters, M. Brooks, and R. D. Buckley, The Phenomenon of Macrophage Congregation In Vitro and Its Relationship to In Vivo Exposure of Guinea Pigs, *Lab. Invest.*, 18: 269-277 (1968).

Visualization of Fly-Ash Particles in Macrophages Using Color X-Ray Mapping

JAMES PAWLEY* and GERALD FISHER†
*Donner Laboratory, Lawrence Berkeley Laboratory, Berkeley, California; †Radiobiology Laboratory, University of California, Davis, California

ABSTRACT

A new method is described for applying color X-ray mapping to the microanalysis of coal fly ash both before and after ingestion of the fly ash by mouse pulmonary alveolar macrophages. The system uses a scanning electron microscope with energy dispersive X-ray spectrometer and a color television monitor to produce simultaneous X-ray maps of three elements. Because higher average real-time count rates are possible when the sample is scanned at television rate, three element maps of fields containing 100 to 200 particles can be produced in 1 to 5 min, and thus the system is valuable as a screening tool. Particles having cross sections as small as 0.5% of the scanned area can be detected, provided that the element being mapped constitutes at least 10 to 20% of the mass of the particles. Particles inside critical point dried pulmonary alveolar macrophages, previously exposed to respirable polydisperse stack fly ash in vitro, have been mapped successfully.

As the energy industry increases its reliance on coal, there has been a renewed interest in the ultimate fate and possible biological effects of the by-products of coal production and combustion.[1-4]

In 1974, 6×10^8 tons of coal were mined in the United States and, after combustion, 11% of this was ash. In modern utility boilers fired with pulverized coal, 80% of the ash is converted to fly ash. Most of this is removed from the flue gas by electrostatic precipitators or other collection devices, but approximately 10^6 tons is probably released to the atmosphere. The material most likely to escape the precipitators is small [mass median diameter (MMD) < 5 μm] and this prolongs its residence time in the atmosphere and also

increases the probability that, once inhaled, the material will be deposited in the lung.[5] Furthermore, some of the trace elements that are known to be biologically harmful seem to be preferentially concentrated in or on smaller particles.[6]

The massive quantity of this material produced must not blind us to the fact that most biological effects will be produced at the cellular level by a small number of particles weighing a few picograms. Because these particles are too small for careful study in the light microscope, the study of fine particulates on a particle-by-particle basis requires such microtechniques as scanning and transmission electron microscopy and electron microprobe analysis. Obtaining information on elemental composition using the microprobe is complicated by the difficulty of obtaining data on a statistically significant number of particles either in their free state or after their interaction with biological targets, such as the pulmonary macrophage.

This paper describes an optimized method of color X-ray mapping which we hope can help alleviate this problem by permitting a large number of particles to be screened for the presence of up to three elements simultaneously. This method differs from previous methods of color X-ray mapping[7,8] because it is 10 to 30 times more rapid and requires minimal operator involvement.

METHODS

Since a preliminary version of this system has been described[9] and a more complete description containing examples of colored X-ray maps will soon be available,[10] only a brief outline of the operation of the system is included here.

The sample is scanned at television rate in a scanning electron microscope (SEM) using a current sufficient to produce the maximum possible average real-time count rate from an attached dispersive X-ray spectrometer detector (about 3000 cps for a detector with a linear amplifier time constant, t_C = 8 to 10 μsec). The output of the linear amplifier is applied to three single-channel analyzers [Fig. 1(a)] so arranged that a high logic signal is passed to one of three latches whenever the linear amplifier signal is in that window. A strobe pulse is produced by the linear amplifier at the instant that the linear output reaches a peak, which is exactly 44 μsec after the X ray is detected (t_0). This strobe pulse triggers the latches so that their outputs continue to mirror the state of their inputs at the instant that the strobe pulse arrives. The latch outputs are each fed to one input of an AND gate. The strobe pulse is also

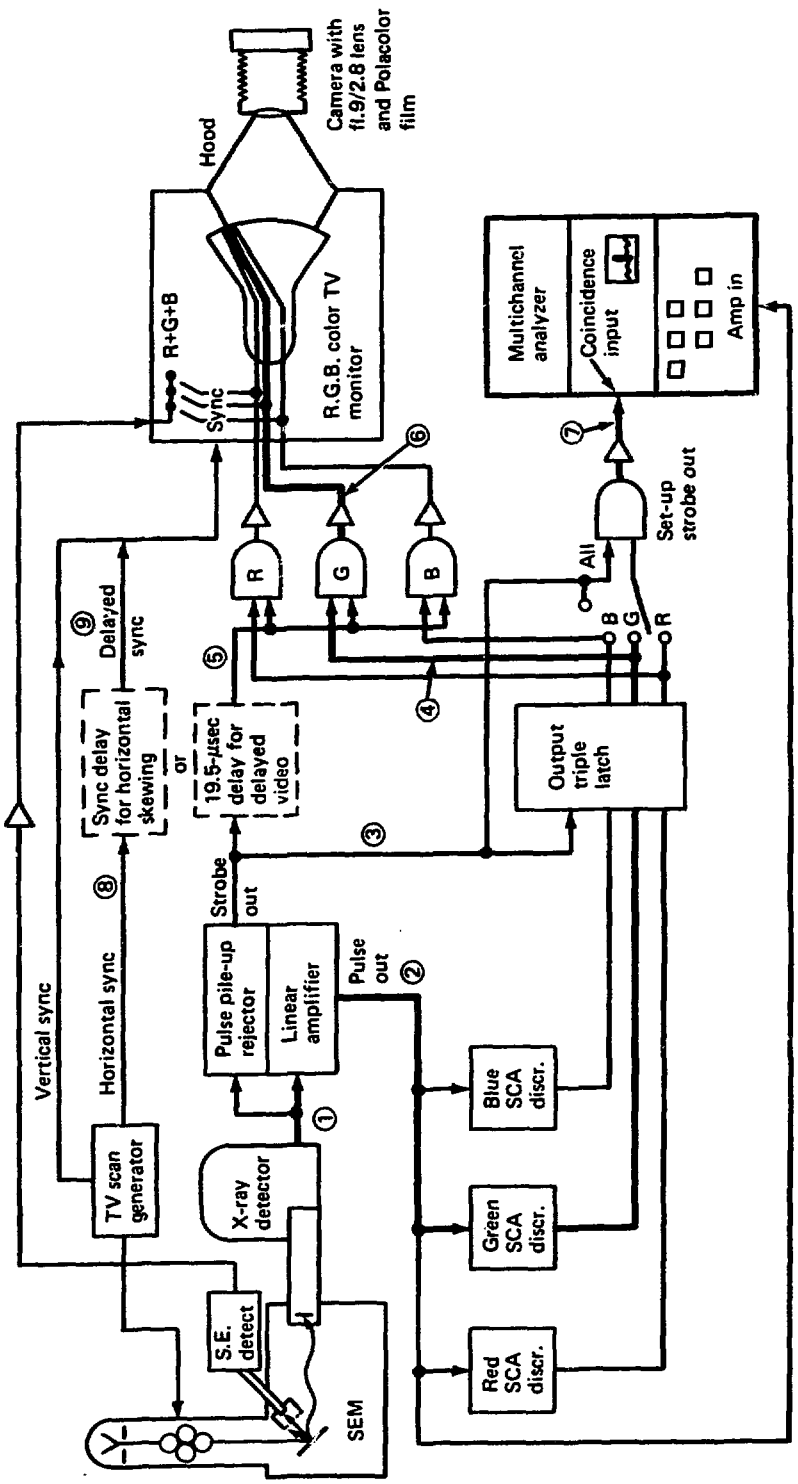
Camera with f1.9/2.8 lens and Polacolor film
Hood
R+G+B
Sync
R.G.B. color TV monitor
Multichannel analyzer
Coincidence input
Amp in
Set-up strobe out
All
B
G
R
Output triple latch
Vertical sync
Horizontal sync
TV scan generator
Sync delay for horizontal skewing
or
19.5-μsec delay for delayed video
Delayed sync
Strobe out
Pulse pile-up rejector
Linear amplifier
Pulse out
X-ray detector
S.E. detect
SEM
Blue SCA discr.
Green SCA discr.
Red SCA discr.
(a)

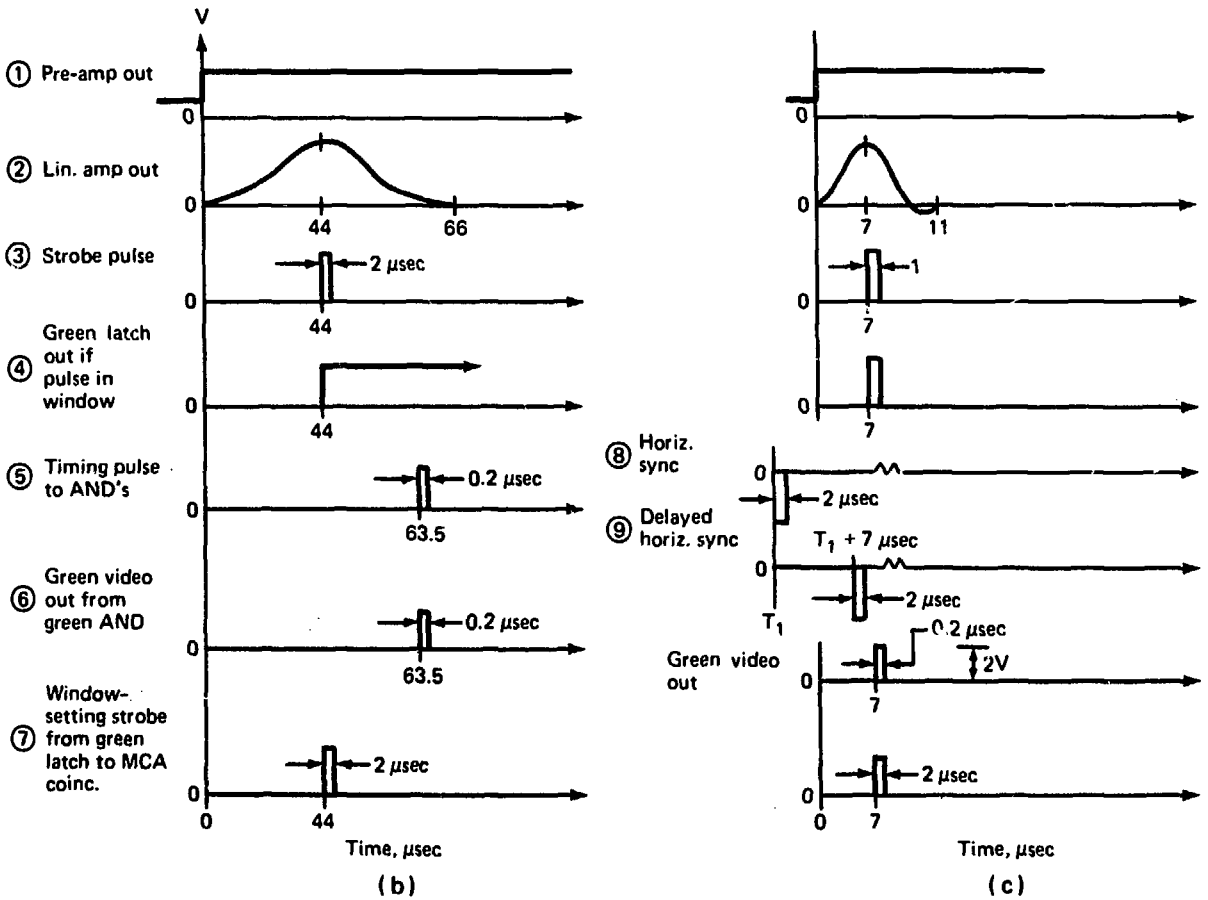

Fig. 1 Block diagram of simultaneous three-element color X-ray mapping system. Signals present in the system, when used in delayed video mode or horizontal scan skewing mode, are diagrammed in parts (b) and (c), respectively.

used to produce a delayed video pulse 0.2 μsec wide and delayed by exactly 19.5 μsec, which is applied to the second input of all three AND gates. These gates will therefore produce a 0.2-μsec pulse a total of 44 + 19.5 = 63.5 μsec after t_0 only if the linear-amplifier output pulse peak was in the appropriate window. After this pulse is buffered, it is passed to one input of a red—blue—green color television monitor, where it is displayed as a dot of a particular primary color. This dot is then recorded on instant process color film. The delay circuitry is necessary because the time between t_0 and the time that the linear amplifier output can be analyzed (44 μsec) is long compared to television horizontal sweep rate (63.5 μsec/line). The delay procedure has the effect of displaying an X-ray count exactly one line below the point from which it is detected and is called delayed video. The pulses referred to are shown in Fig. 1(b); the circled numbers indicate the parts of the schematic diagram where each pulse will be found.

Delayed video produces a display dead time of 63.5 μsec, which is comparable to the dead time of an amplifier having a $t_C = 8$ μsec. If a linear amplifier having $t_C < 8$ μsec is used to increase the maximum real-time count rate at some loss in energy resolution, a different system may be used to compensate for the delay between t_0 and the linear amplifier peak. This second method is called horizontal scan skewing, and the relevant pulses are shown in Fig. 1(c). The video pulses are not delayed but are passed on immediately after the strobe pulse arrives. Registration is preserved by delaying the horizontal sync pulses sent to the monitor so that the display beam lags the probing beam by the correct amount.

A signal composed of the output of a switch-selected latch ANDed with the strobe pulse is passed to an attached multichannel analyzer (MCA) used in the coincidence mode. This allows a spectrum composed of only the counts in a particular window to be generated on the MCA, and thus the window is easy to set.

The samples used to prepare the maps shown during the symposium, which are not included here because publishing considerations do not permit the reproduction of figures in color, consist of NBS No. SRM-1633* coal fly ash, size-classified stack fly ash, or mouse pulmonary alveolar macrophages exposed to the stack fly ash. The NBS fly ash was deposited onto smooth carbon SEM stubs and coated with carbon by vacuum evaporation. A fine fraction

*National Bureau of Standards, Standard Reference Material, No. 1633, *Trace Elements in Coal Fly Ash.*

(MMD = 2.2 μm) stack fly ash[11] was deposited on Formvar-coated copper EM grids to reduce the bremsstrahlung production in the substrate. The mouse pulmonary alveolar macrophages were obtained by lung lavage and exposed to stack fly ash of 2.2-μm MMD by a modification of the method detailed elsewhere in this volume.[12] After exposure, drops of cell suspension were placed on Formvar-coated EM grids that had first been dipped in 0.1% poly-lysine solution[13] and then blotted dry. The poly-lysine made the cells adhere to the Formvar while the grids were first fixed in cacodylate-buffered glutaraldehyde—formaldehyde and then dehydrated in ethanol before being critical point dried using amyl acetate and liquid CO_2. After the grids were dried, they were coated with evaporated carbon.

With a 25-kV beam voltage, we recorded maps and corresponding secondary electron images from the television monitor. Exposure times were 3 to 10 min, and 5 x 10^4 to 3 x 10^5 counts were recorded at magnifications of 2000 to 5000x (on the print). Elements mapped during the initial studies reported here included aluminum, sulfur, potassium, calcium, titanium, and iron, although future studies will map elements known to have deleterious biological effects, such as cadmium, selenium, arsenic, and lead.

RESULTS AND DISCUSSION

The results showed the method to be effective in producing images in 1 to 5 min which were sufficient to detect particles having high concentrations of a mapped element in fields containing up to 200 particles. The samples of NBS and fine stack fly ash proved to be very heterogeneous, and several maps showed that virtually all of a particular element in a field of over 100 particles was concentrated in a single particle. Conclusions based on such maps regarding the elemental composition of individual particles were verified by spot-mode analysis of the particles involved. Fine particles containing high concentrations of iron, calcium, or titanium which had been phagocytized by pulmonary alveolar macrophages could be clearly visualized, particularly if they were near the cell surface. One map included a part of a copper EM grid in the field of view, and, although this gave rise to a perceptible increase in the background level, this increased background level is in no way comparable to the intensities produced by the intracellular particles.

Our studies are just beginning, but we hope to use this tool to discover whether trace elements of biological interest, such as cadmium, selenium, arsenic, zinc, and lead, are distributed nonuni-

formly, as are the elements mapped in this study. This knowledge will permit a better estimation of the biological toxicity of such particles. It may also provide a test for one theoretical explanation for the predominance of such elements in smaller particles because, if small particles show the increased concentration simply because they provide a greater specific surface area on which volatile elements can condense as the flue gases cool,[6,14] then we would not expect large variations in concentration between particles of the same size. Finally, by correlating information on the elemental composition of particles within pulmonary alveolar macrophages with the morphological appearance of the cells after various periods of incubation, we hope to determine differential uptake rates and toxicity on a cell-by-cell basis.

ACKNOWLEDGMENTS

We are grateful to Dr. T. L. Hayes, Donner Laboratory, Lawrence Berkeley Laboratory, and to Dr. W. S. Tyler, California Primate Research Center, University of California, Davis, for their encouragement and support. We also thank Dr. C. Mosher, Nuclear Equipment Corp., San Carlos, Calif., for his aid in the technical design of the prototype. This project was supported, through the Donner Laboratory, by the Energy Research and Development Administration, Environmental Protection Agency Award D5-E681, and the National Heart and Lung Institute of the National Institutes of Health (Fellowship 1 F32 HL 02884-01); and, through the Radiobiology Laboratory, by the Energy Research and Development Administration.

REFERENCES

1. R. L. Davison, D. F. S. Natusch, J. R. Wallace, and C. A. Evans, Jr., Trace Elements in Fly Ash, *Environ. Sci. Tech.*, 8(13): 1107-1113 (1974).
2. W. L. Faith and A. A. Atkinsson, Jr., *Air Pollution*, 2nd ed., Wiley-Interscience, New York, 1972.
3. G. L. Fisher, D. P. Y. Chang, and M. Brummer, Fly Ash Collected from Electrostatic Precipitators: Microcrystalline Structures and the Mystery of the Spheres, *Science*, 192: 555-557 (1976).
4. J. M. Ondov, R. C. Ragaini, R. E. Heft, G. L. Fisher, D. Silberman, and B. A. Prentice, *Interlaboratory Comparison of Neutron Activation and Atomic Absorption Analyses of Size-Classified Stack Fly Ash*, Proceedings of the Eighth Methods and Standards for Environmental Measurement Materials Research Symposium, National Bureau of Standards, Gaithersburg, Maryland, 1976 (in press).

5. D. F. S. Natusch and J. R. Wallace, Urban Aerosol Toxicity: The Influence of Particle Size, *Science*, 186: 695-699 (1974).
6. D. F. S. Natusch, J. R. Wallace, and C. A. Evans, Toxic Trace Elements: Preferential Concentration in Respirable Particles, *Science*, 183: 202-204 (1974).
7. H. Yakowitz and K. F. T. Heinrich, Color Representation of Electron Microprobe: Area-Scan Images by a Color Separation Process, *J. Res. Natl. Bur. Stand., A*, 73: 113 (1969).
8. M. P. Jones, J. Gavrilovic, and C. H. M. Beaven, Colour Synthesis as an Aid to Electron Probe X-Ray Microanalysis, *Trans. Inst. Min. Met., B*, 75: B274 (1966).
9. J. B. Pawley, T. L. Hayes, and T. H. Falk, Simultaneous Three Element X-Ray Mapping Using Color TV, in *Proceedings of the 9th SEM Symposium*, Toronto, Canada, Om Johari (Ed.), pp. 187-195, Univ. Chicago Press, Chicago, 1976.
10. J. B. Pawley and G. L. Fisher, Rapid Elemental Characterization of Coal Combustion By-Products Using Simultaneous Three-Color X-Ray Mapping and Digital Scan-Stop, *J. Microsc.* (in press).
11. A. R. McFarland, G. L. Fisher, B. A. Prentice, and R. W. Bertch, A Fractionator for Size-Classification of Aerosolized Solid Particulate Matter, *Environ. Sci. Tech.* (in press).
12. F. F. Hahn, G. L. Newton, and L. Bryant, In Vitro Phagocytosis of Monodisperse Particles by Alveolar Macrophages (this volume).
13. D. Mazia, G. Schatten, and W. Sale, Adhesion of Cells to Surfaces Coated with Poly-Lysine: Applications to Electron Microscopy, *J. Cell Biol.*, 66: 198-200 (1975).
14. R. W. Linton, A. Loh, and D. F. S. Natusch, Surface Predominance of Trace Elements in Airborne Particles, *Science*, 191: 852-854 (1976).

The Influence of Environmental Toxicity on the Antibacterial Activity of the Alveolar Macrophage

ELLIOT GOLDSTEIN
Department of Internal Medicine, University of California at Davis,
Davis, California

ABSTRACT

Recognition of the association between exposure to airborne contaminants and the development of respiratory infection has resulted in many tests relating the effect which such exposures have on the antibacterial activity of the alveolar macrophage system. These tests measure the effect of exposure to the contaminant on one or more of the complex biophysical reactions (i.e., chemotaxis, ingestion, and inactivation) performed by the macrophage when eradicating invading bacteria. Experimental systems exist for studying these parameters in in vitro and in vivo systems. Many valuable data concerning the toxicity of ozone, nitrogen dioxide, sulfur dioxide, cigarette smoke, and, more recently, metallic contaminants have been obtained from these studies. Because the experiments, especially those in vivo, can be performed with any inhaled contaminant or with combinations of contaminants, these experimental models can be used to assess the potential of virtually any environmental vapor or particulate to enhance pulmonary susceptibility to bacterial infection. The validity of extrapolating such results in a qualitative fashion from the experimental models to human exposures is well substantiated. However, extreme caution is necessary before quantitative comparisons can be made between the experimental exposures and those naturally occurring for humans.

Toxicologic methods to evaluate health risks from the ever-increasing numbers of contaminants entering the atmosphere as by-products of otherwise beneficial industrial processes are of utmost importance to society. Ideally these tests should be performed in situ by using epidemiological techniques or in volunteers by using measurements of pathophysiologic parameters. Unfortunately the expense and the complexity of epidemiological investigations limit

these studies to selected contaminants that are either widely disseminated or suspected of causing human illness. In the design of volunteer studies, ethical as well as practical considerations often preclude toxicologic appraisal. As a result of these investigational limitations, much reliance must be placed on experiments conducted with animal or cell systems.

Recognition of the association between exposure to noxious gases (ozone,[1,2] nitrogen dioxide,[3-5] or sulfur dioxide,[1,6]) or to airborne particulates (sulfates,[6] silica,[7] or asbestos[8]) and the development of respiratory infection has resulted in the use of microbiological and immunological parameters to evaluate toxicity. It is implicit in these experiments that abnormalities found in the experimental model apply in the same manner to instances of contaminant-induced human infection. The validity of this extrapolation in qualitative terms is apparent. However, since mice aren't men, extreme caution is necessary when comparing these data with ambient exposures in humans.

Normally the lungs are maintained sterile by the combined antibacterial activity of the mucociliary, phagocytic, and immune systems. These systems, acting independently and in concert, cleanse the lungs of bacteria, regardless of site of deposition. Inhaled or aspirated bacteria that impact in upper regions of the lung are physically removed by mucociliary transport mechanisms.[9,10] Bacteria that descend beyond the mucociliary system to reach alveolar regions are captured and killed by alveolar macrophages. These ubiquitous pulmonary phagocytes are the principal means for inactivating intrapulmonary bacteria.[11,12] Antibodies expedite phagocytosis by attracting macrophages to invading bacteria and by rendering the microorganisms suitable for ingestion.[11,13,14]

The manner in which airborne contaminants interfere with mucociliary and immune function is beyond the scope of this symposium, and this review is therefore confined to the effect of these contaminants on the antibacterial function of alveolar macrophages.

The extraordinary ability of alveolar macrophages to seek out, ingest, and inactivate invading bacteria results from the integration of a number of complex biophysical reactions. Macrophages are attracted to bacteria by chemotactic factors which are elaborated by the bacteria themselves or which are formed from the interaction of bacteria and host tissues.[13-15] Culture filtrates of *Staphylococcus epidermidis* and *Escherichia coli* are chemotactic in the absence of serum.[16] More often, chemotactic factors result from the attachment of antibody to bacterial cell wall surfaces. The antigen—

antibody complex activates the complement system to form peptides (C3a and C5a) with chemotactic activity.[17] Some bacteria bypass this antigen—antibody step by elaborating proteases that cleave the parent C3 and C5 proteins directly.[13] Simultaneously with chemotaxis, serum opsonins attach to bacterial surfaces, rendering the microorganisms susceptible to phagocytosis. Figure 1, which comes from the work of Dr. Hotse Bartlema of the Medical Biological Laboratory in The Netherlands, illustrates the ability of macrophages to engulf microorganisms by means of bacteria-seeking pseudopodia. Once ingested, bacteria are isolated within phagosomes; microbicidal enzymes that were in inactive states (secondary lysosomes) are activated, and this lysosomal structure fuses with the phagosome to form the phagolysosome. In this manner activated enzymes interact with intracellular bacteria without injuring the cell itself.[13,19]

The complexity of the above physiologic events provides numerous potential sites for an environmental toxin to interfere with microbicidal function. Toxins may impair chemotaxis by inactivating chemotactic substances or by impeding cellular mobility; they may inhibit the ingestive process by damaging phagocytic membranes;

Fig. 1 A cell culture of alveolar macrophages demonstrating ingestion of *Listeria monocytogenes* by pseudopodia. (Gram stain; magnification, 800 X.) (Courtesy of H. Bartlema and R. Braunius, Medical Biological Laboratory, The Netherlands.)

they may prevent bacterial destruction by inactivating intracellular enzyme systems.

The effect of exposure to environmental agents on cell functions (chemotaxis, ingestion, and inactivation) can be studied in vitro or in vivo. Chemotaxis is measured in vitro by removing pulmonary macrophages and testing their rates of migration towards a chemotactic attractant in a Boyden-type chamber.[20,21] Although the results are affected by technical factors, e.g., the adhesiveness of macrophages to the filter membrane, the tortuosity and size of pore channels, and the loss or detachment of cells into the underlying medium, the tests are sufficiently standardized to assess qualitative differences in chemotactic function.[15,22,23] Technical improvements, such as the use of a second filter that is impermeable to cells,[24] or the measurement of cell fronts within the filter,[25] permit more precise quantitation of chemotactic rates.

Toxicologic studies performed with alveolar macrophages indicate (1) that macrophages from healthy cigarette smokers have normal mobility[26] and (2) that exposure to extracts of cotton capable of causing byssinosis does not result in altered chemotaxis.[27] Future tests of the effect of exposure of alveolar macrophages to gaseous and particulate contaminants should yield additional toxicologic information. Such experiments are best performed by exposing the intact animal to the toxicant before removing the macrophages since in vitro exposure of macrophages to toxicants introduces errors secondary to the artificial nature of the exposure. It is worth emphasizing that measurements of chemotaxis cannot as yet be performed in vivo.

Tests to measure rates of phagocytic ingestion are in a more advanced state than are those for chemotaxis. These tests can be divided into two categories. The first method exposes lavaged macrophages to the contaminant and test bacteria or microspheres.[28,29] Rates of ingestion are compared for treated and control cells. A second method, which is a combination of in vivo and in vitro techniques, consists of injecting bacteria intratracheally into animals and then exposing the animals to the contaminant.[30-32] The macrophages are removed by lavage and the number of intracellular bacteria are counted microscopically. Because exposure to the toxicant occurs in vivo, this latter method more closely approximates realistic conditions. In both methods time-related visual measurements of the number of ingested microorganisms, or the number of particles, or the radioactivity in instances in which the particles are radiolabeled, permit determination of rates of ingestion.

Studies of the effect of gaseous pollutants on the ingestive function of alveolar macrophages have shown that exposure to ozone,[29,30] nitrogen dioxide,[31-33] or cigarette smoke,[34-36] inhibits the rate at which bacteria are phagocytized by these cells. The effect of other airborne toxicants (hydrocarbons, sulfates, nitrates, metallic compounds, etc.) on bacterial ingestion by alveolar macrophages has received much less attention.[36]

Exposure to metallic contaminants on phagocytosis is usually studied by testing the ability of macrophages to ingest the contaminants themselves[37] or Teflon particles coated with the metal.[28] Because many interrelated variables such as the number of cells, the number of particles, the duration of exposure, the ionic concentrations of the media, and the electrostatic potential of the particle can affect phagocytosis, interpretation of these results is difficult.[37] Experiments in which attempts have been made to control these variables indicate that the rate of uptake of iron oxide particles by alveolar macrophages differs from that for chromium oxide particles.[37] Similarly, particles coated with silver are ingested at slower rates than particles coated with aluminum or chromium.[28] Although the toxicologic importance of these differences is unclear, the recent observation that metallic ions (Ni^{2+}, Mn^{2+}, Cr^{3+}) are cytotoxic for alveolar macrophages suggests that the uptake of these particles is not innocuous.[38] Because ingestion is important to phagocytic functions, it can be anticipated that the effect of airborne agents on this parameter will be evaluated more thoroughly in future toxicologic experiments.

The in vitro techniques for determining rates of bacterial ingestion by alveolar macrophages can also be used to measure rates of intracellular bacterial killing. Ingested bacteria are not counted; instead, the cell suspensions are lysed, and the number of viable bacteria are determined by pour-plate techniques.[39,40] These tests have shown that exposure to ozone,[29] nitrogen dioxide,[33] and nitrate ion,[33] at concentrations much above ambient, causes impairments in intracellular bacterial killing. The deleterious effects are believed to be due to interference with cellular enzymes responsible for bacterial killing.[29,30,33]

The pathophysiologic events that determine the fate of inhaled bacteria can be studied in vivo in rodent models.[12,41-45] Because these investigations are fundamental to understanding the interaction of bacteria with macrophages in the intact lung, the experimental methods merit description. The rodents (mice, rats, guinea pigs) are infected with high concentrations of finely dispersed aerosols of test bacteria. Animals are sacrificed immediately after infection and at

various times thereafter. Rates of bacterial killing are determined in excised lungs by comparing the number of viable bacteria at later time periods with the number present immediately after infection.[41] If the bacteria are radiolabeled with phosphorus-32 or sulfur-35, very precise measurements of pulmonary bacterial inactivation can be made because each animal serves as its own control, with the radioactivity providing an index of the number of inhaled bacteria.[42-44] The rate of bacterial ingestion by macrophages is measured by histologically determining the intra- or extracellular location of intrapulmonary bacteria at each time period.[12] Figure 2 shows the results of experiments in which phagocytic ingestion was demonstrated to be an exceedingly rapid process occurring within minutes after the deposition of inhaled bacteria. Also apparent is the

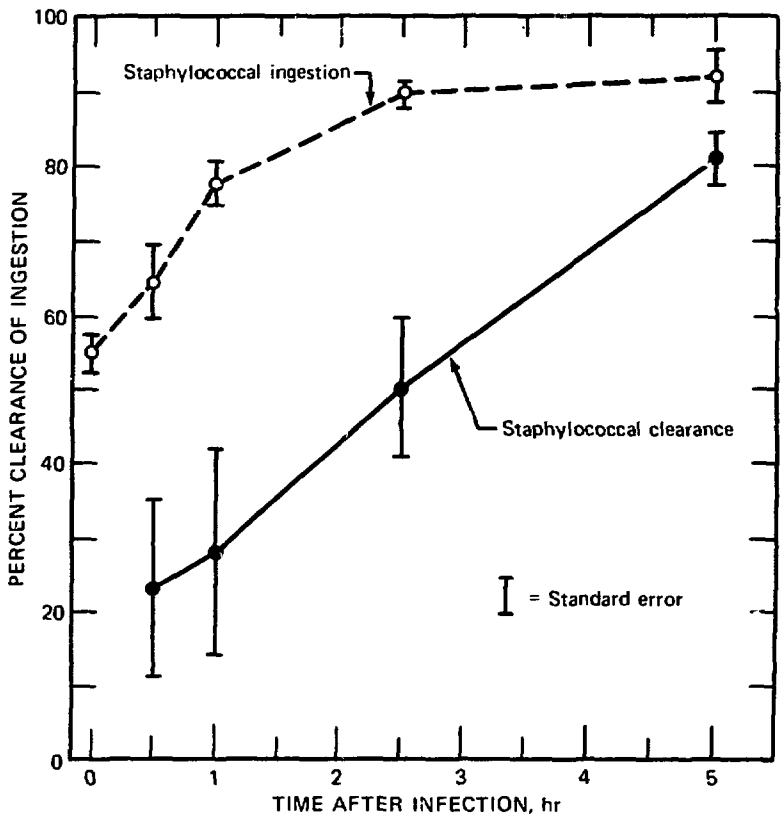

Fig. 2 Comparison of murine rates for staphylococcal ingestion (right lung) and staphylococcal clearance (left lung) at various times after exposure to bacterial aerosols. [From E. Goldstein, W. Lippert, and D. Warshauer, Pulmonary Alveolar Macrophage—Defender Against Bacterial Infection of the Lung, *Journal of Clinical Investigation*, 54: 519-528 (1974).]

fact that, in this experimental model, bacterial inactivation results almost exclusively from phagocytosis. These techniques further permit measurement of rates of bacterial degradation by macrophages.[4,5] The entire sequence of pathophysiologic events involving the interaction of *Staphylococcus aureus* with alveolar macrophages is illustrated in Fig. 3, which compares rates of staphylococcal ingestion, inactivation, and destruction in the lung. Comparison of these processes shows that most inhaled bacteria are ingested by macrophages within 2 hr of their entrance into the lung; the bacteria are killed by 4 hr, and 80% of them are partially destroyed by 8 hr. These results are in accord with in vitro evidence that macrophages

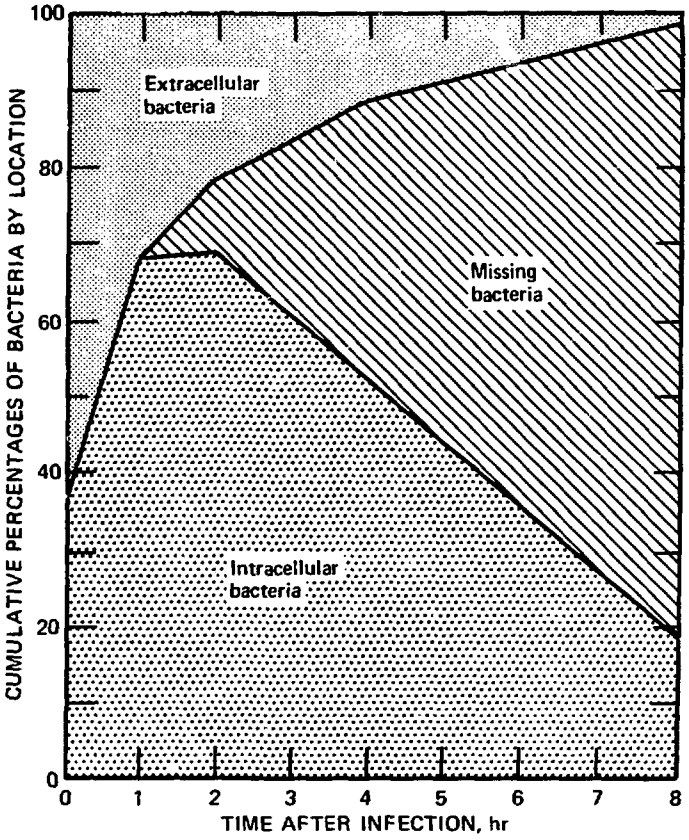

Fig. 3 Cumulative percentages of intracellular, extracellular, and partially digested (missing) *Staphylococcus aureus* in the lungs of mice at various times after infection with bacterial aerosols. [From M. Kim, E. Goldstein, J. P. Lewis, W. Lippert, and D. Warshauer, Murine Pulmonary Alveolar Macrophages: Rates of Bacterial Ingestion, Inactivation, and Destruction, *Journal of Infectious Diseases*, 133(3): 310-319 (1976), The University of Chicago Press.]

are attracted to, ingest, and inactivate staphylococci in 1 to 2 hr[35,46] and that cell wall components of gram-positive bacteria are destroyed 1 to 3 hr later.[47-49]

The effects of exposure to ozone,[12,50-53] nitrogen dioxide,[54-55] sulfur dioxide,[56,57] automobile exhaust,[58] cigarette smoke,[59] silica,[60] and high oxygen tensions[52,61] have been studied by these methods. Exposure to above-ambient levels of ozone, nitrogen dioxide, and sulfur dioxide depresses pulmonary antibacterial function.[50-57] These impairments are dose related and are attributable to pollutant-induced damage to the alveolar macrophage. Tests with ozone show that this noxious gas causes severe impairments in intracellular killing of ingested bacteria and lesser impairments in bacterial ingestion.[12] As a result of these abnormalities, intrapulmonary bacteria proliferate to cause pneumonia (Figs. 4 and 5). In addition to explaining the pathogenesis of contaminant-

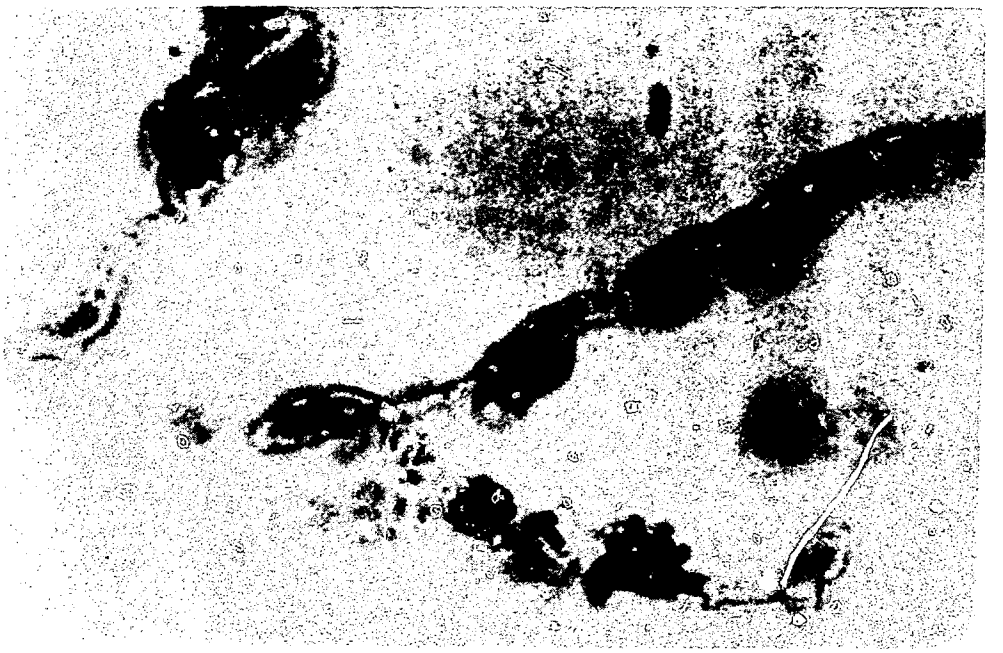

Fig. 4 Two large clumps of staphylococci which appear to be growing out from unidentified cells of the pulmonary alveolar region. The specimen is from a rat exposed to 2.5 ppm of ozone for 4 hr. Three other intracellularly located staphylococci are also present. (Brown and Brenn stain; magnification, 700 X.) [From E. Goldstein, W. Lippert, and D. Warshauer, Pulmonary Alveolar Macrophage—Defender Against Bacterial Infection of the Lung, *Journal of Clinical Investigation*, 54: 519-528 (1974).]

Fig. 5 Pneumonic infiltrate containing polymorphonuclear leukocytes and macrophages in a rat that was exposed to ozone following an aerosol infection with *Staphylococcus aureus*. (Hematoxylin and eosin stain; magnification, 400 X.)

induced respiratory infection, these laboratory models permit testing of mixtures of airborne toxicants.[62-64] Hamsters exposed for 2 hr to 28.2 mg/m^3 (15 ppm) of nitrogen dioxide and an additional hour's exposure to tobacco smoke exhibit diminished resistance to klebsiellal pneumonia.[62] In contrast, mice infected with *Staphylococcus aureus* and then exposed to various combinations of concentrations of nitrogen dioxide and ozone suffer reductions in antibacterial activity equivalent to that expected if each pollutant acted independently.[63] Also, the presence of silicosis did not enhance the antibacterial deficit produced by exposure to ozone.[64]

In conclusion, methods are available for testing the effect of exposure to airborne contaminants on each of the parameters involved in the killing of intrapulmonary bacteria by alveolar macrophages. Many valuable data concerning the toxicity of different air contaminants have already been obtained from experiments that relate exposure to airborne contaminants to one or more of these parameters of cellular function. Because these studies can be performed with any inhaled contaminant or with combinations of contaminants, the hazard of presently unstudied or minimally

studied agents, such as pesticides, metallic compounds, sulfate or nitrate anions, particulates, occupational vapors, and hydrocarbon-containing industrial effluents, is assessable by these methods. Furthermore, the development and use of animal models that mimic human disease states should significantly enhance our ability to assess the health risk of unusually susceptible individuals to man-made airborne contaminants.

ACKNOWLEDGMENTS

This work was supported by Public Health Service research grant ES00628 from the National Institute of Environmental Health, by Energy Research and Development Administration contract E(04-3) 472, and by grant A5-034-87 from the California Air Resources Board.

REFERENCES

1. J. R. Goldsmith, Effects of Air Pollution on Human Health, in *Air Pollution*, 2nd ed., A. S. Stern (Ed.), Chap. 14, pp. 547-615, Academic Press, Inc., New York, 1968.
2. D. V. Bates, Air Pollutants and the Human Lung, *Amer. Rev. Resp. Dis.*, 105: 1-13 (1972).
3. C. A. Lillington, Health Effects from Air Pollution, in *Environmental Problems in Medicine*, W. McKee (Ed.), Chap. 16, pp. 314-324, Charles C Thomas, Publisher, Springfield, 1974.
4. E. Goldstein, Reevaluation of the United States Air Quality Standard for Nitrogen Dioxide, *Rev. Environ. Health*, 2: 5-37 (1975).
5. J. Ramirez and A. R. Dowell, Silo-Filler's Disease: Nitrogen Dioxide Induced Lung Injury: Long Term Follow-Up and Review of the Literature, *Ann. Intern. Med.*, 74: 569-576 (1971).
6. J. G. French, G. Lowrimore, W. C. Nelson, J. F. Finklea, T. English, and M. Hertz, The Effect of Sulfur Dioxide and Suspended Sulfates on Acute Respiratory Disease, *Arch. Environ. Health*, 27: 129-133 (1973).
7. L. P. Tepper and E. P. Redford, Pulmonary Reactions Due to the Inhalation of Noxious Agents, in *Harrison's Principles of Internal Medicine*, 6th ed., Chap. 288, pp. 1322-1327, McGraw-Hill Book Company, New York, 1970.
8. I. J. Selikoff, W. J. Nicholson, and A. M. Langer, Asbestos Air Pollution, *Arch. Environ. Health*, 25: 1-13 (1972).
9. K. H. Kilburn, Cilia and Mucus Transport as Determinants of the Response of the Lung to Air Pollutants, *Arch. Environ. Health*, 14: 77-91 (1967).
10. G. M. Green, Pulmonary Clearance of Infectious Agents, *Annu. Rev. Med.*, 19: 315-336 (1968).
11. G. M. Green, The J. Burns Amberson Lecture—In Defense of the Lung, *Amer. Rev. Resp. Dis.*, 102: 691-703 (1970).
12. E. Goldstein, W. Lippert, and D. Warshauer, Pulmonary Alveolar Macrophage: Defender Against Bacterial Infection of the Lung, *J. Clin. Invest.*, 54: 519-528 (1974).

13. T. P. Stassel, Phagocytosis, *New Engl. J. Med.*, 290: 774-780 (1974).
14. N. Y. Reynolds, Pulmonary Host Defenses in Rabbits After Immunization with Pseudomonas Antigens: The Interaction of Bacteria, Antibodies, Macrophages and Lymphocytes, *J. Infect. Dis.*, 130(Supp.): S134-S142 (1974).
15. P. A. Ward, Leukotaxis and Leukotactic Disorders. A Review, *Amer. J. Pathol.*, 77: 520-538 (1974).
16. H. N. Keller and E. Sarkin, Studies on Chemotaxis. V. On the Chemotactic Effect of Bacteria, *Int. Arch. Allergy*, 31: 505-517 (1967).
17. E. Sorkin, V. S. Stecher, and J. F. Borel, Chemotaxis of Leukocytes and Inflammation, *Ser. Haematol.*, 3: 131-162 (1970).
18. P. A. Ward, J. Chapitis, and M. C. Conroy, Generation by Bacterial Proteinases of Leukotactic Factors from Human Serum and Human C3 and C5, *J. Immunol.*, 110: 1003-1009 (1973).
19. G. Weissman, R. B. Zurier, and S. Hoffstein, Leukocytic Proteases and the Immunologic Release of Lysosomal Enzymes, *Amer. J. Pathol.*, 68: 539-559 (1972).
20. S. Boyden, The Chemotactic Effect of Mixtures of Antibody and Antigen on the Polymorphonuclear Leukocyte, *J. Exp. Med.*, 115: 453-465 (1962).
21. P. A. Ward, Chemotaxis of Mononuclear Cells, *J. Exp. Med.*, 128: 1201-1221 (1968).
22. P. A. Ward, Insubstantial Leukotaxis, *J. Lab. Clin. Med.*, 79: 873-877 (1972).
23. R. Snyderman, L. L. Altman, M. S. Hausman, and S. E. Mergenhagen, Human Mononuclear Leukocyte Chemotaxis: A Quantitative Assay for Humoral and Cellular Chemotactic Factors, *J. Immunol.*, 108: 857-860 (1972).
24. H. U. Keller J. F. Borel, P. C. Wilkinson, M. W. Hess, and H. Cottier, Reassessment of Boyden's Technique for Measuring Chemotaxis, *J. Immunol. Methods*, 1: 165-168 (1972).
25. S. H. Zigmund and J. G. Hirsh, Leukocyte Locomotion and Chemotaxis. New Methods for Evaluation and Demonstration of a Cell Derived Chemotactic Factor, *J. Exp. Med.*, 137: 387-410 (1973).
26. G. A. Warr and R. R. Martin, Chemotactic Responsiveness of Human Alveolar Macrophages: Effects of Cigarette Smoking, *Infect. Immun.*, 9: 769-771 (1974).
27. W. S. Lynn, S. Muñoz, J. A. Campbell, and P. W. Jeffs, Chemotaxis and Cotton Extracts, *Ann. N. Y. Acad. Sci.*, 221: 163-173 (1970).
28. P. Camner, M. Lundborg, and P. A. Hellström, Alveolar Macrophages and 5-μm Particles Coated with Different Metals. *In Vitro* Studies, *Arch. Environ. Health*, 29: 211-213 (1974).
29. V. L. Richmond, *In Vitro* Hydrolase and Phagocytic Activities of Alveolar Macrophages, *J. Lab. Clin. Med.*, 83: 757-767 (1974).
30. D. L. Coffin, D. E. Gardner, R. S. Holzman, and F. J. Wolock, Influence of Ozone on Pulmonary Cells, *Arch. Environ. Health.*, 16: 633-636 (1968).
31. D. E. Gardner, R. S. Holzman, and D. L. Coffin, Effects of Nitrogen Dioxide on Pulmonary Cell Population, *J. Bacteriol.*, 98: 1041-1043 (1969).
32. J. D. Acton and Q. N. Myrvik, Nitrogen Dioxide Effects on Alveolar Macrophages, *Arch. Environ. Health*, 24: 48-52 (1972).
33. C. L. Vassallo, B. M. Domm, R. H. Poe, M. L. Duncombe, and J. B. L. Gee, NO_2 Gas and NO_2 Effects on Alveolar Macrophage Phagocytosis and Metabolism, *Arch. Environ. Health*, 26: 270-274 (1973).

34. D. J. Wilkins and A. D. Bingham, The Effect of Some Metal Ions on *In Vitro* Phagocytosis, *J. Reticuloendothel. Soc.*, 1233-1242 (1964).
35. G. M. Green and D. Carolin, The Depressant Effect of Cigarette Smoke on the *In Vitro* Antibacterial Activity of Alveolar Macrophages, *New Engl. J. Med.*, 276: 421-427 (1967).
36. J. B. L. Gee and C. E. Cross, Drugs Affecting Phagocytosis and Pinocytosis, in *Fundamentals of Cell Pharmacology*, S. Dikstein (Ed.), Chap. 14, pp. 349-372, Charles C Thomas, Publisher, Springfield, 1973.
37. L. J. Casarett, M. G. Casarett, and S. A. Whalen, Pulmonary Cell Responses to Metallic Oxides, *Arch. Intern. Med.*, 127: 1090-1098 (1971).
38. M. D. Waters, D. E. Gardner, C. Aranyi, and D. L. Coffin, Metal Toxicity for Rabbit Alveolar Macrophages *In Vitro*, *Environ. Res.* 9: 32-47 (1975).
39. J. S. Tan, C. WatanakunaKorn, and J. Phair, A Modified Assay for Neutrophil Function: Use of Lysostaphin to Differentiate Defective Phagocytosis from Impaired Intracellular Killing, *J. Lab. Clin. Med.*, 781: 316-322 (1971).
40. H. Y. Reynolds and R. E. Thompson, Pulmonary Host Defenses. II. Interaction of Respiratory Antibodies with *Pseudomonas aeruginosa* and Alveolar Macrophages, *J. Immunol.*, 111: 369-380 (1973).
41. G. A. Laurenzi, L. Berman, M. First, and E. H. Kass, A Quantitative Study of the Deposition and Clearance of Bacteria in the Murine Lung, *J. Clin. Invest.*, 43: 759-768 (1964).
42. G. M. Green and E. Goldstein, A Method for Quantitating Intrapulmonary Bacterial Inactivation in Individual Animals, *J. Lab. Clin. Med.*, 68: 669-677 (1966).
43. E. Goldstein, G. M. Green, and C. Seamans, The Effect of Acidosis on Pulmonary Bactericidal Function, *J. Lab. Clin. Med.*, 75: 912-923 (1970).
44. G. J. Jakab and G. M. Green, Regional Defense Mechanisms of the Guinea Pig Lung, *Amer. Rev. Respir. Dis.*, 107: 776-783 (1973).
45. M. Kim, E. Goldstein, J. P. Lewis, W. Lippert, and D. Warshauer, Murine Pulmonary Alveolar Macrophages: Rates of Bacterial Ingestion, Inactivation and Destruction, *J. Infect. Dis.*, 133(3): 310-319 (1976).
46. G. B. MacKaness, The Phagocytosis and Inactivation of Staphylococci by Macrophages in Normal Rabbits, *J. Exp. Med.*, 112: 35-53 (1960).
47. Z. A. Cohn, The Fate of Bacteria Within Phagocytic Cells. I. The Degradation of Isotopically Labelled Bacteria by Polymorphonuclear Leukocytes and Macrophages, *J. Exp. Med.* 117: 27-42 (1963).
48. F. A. Gill and R. M. Cole, The Fate of Bacterial Antigen (Streptococcal M Protein) After Phagocytosis by Macrophages, *J. Immunol.*, 94: 898-915 (1965).
49. P. Elsbach, On the Interaction Between Phagocytes and Microorganisms, *New Engl. J. Med.*, 289: 846-852 (1973).
50. M. R. Purvis, S. Miller, and R. J. Ehrlich, Effect of Atmospheric Pollutants on Susceptibility to Respiratory Infection, *J. Infect. Dis.*, 109: 233-242 (1961).
51. D. L. Coffin, Study of the Mechanisms of the Alteration of Susceptibility to Infection Conferred by Oxidant Air Pollutants, in *Inhalation Carcinogenesis*, AEC Symposium Series, No. 18; (CONF-691001), pp. 259-269, 1970.
52. G. L. Huber and F. M. LaForce, Comparative Effects of Ozone and Oxygen on Pulmonary Antibacterial Defense Mechanisms, *Antimicrob. Agents Chemother.*, 1: 129-136 (1970).

53. E. Goldstein, W. S. Tyler, P. D. Hoeprich, and C. Eagle, Ozone and the Antibacterial Defense Mechanisms of the Murine Lung, *Arch. Intern. Med.*, 127: 1099-1102 (1971).
54. R. Ehrlich, Effect of Nitrogen Dioxide on Resistance to Respiratory Infection, *Bacteriol. Rev.*, 30: 604-614 (1966).
55. E. Goldstein, M. L. Eagle, and P. D. Hoeprich, Effect of Nitrogen Dioxide on Pulmonary Bacterial Defense Mechanisms, *Arch. Environ. Health*, 26: 202-204 (1973).
56. G. A. Fairchild, P. Kane, B. Adams, and D. Coffin, Sulfuric Acid and Streptococci Clearance from Respiratory Tracts of Mice, *Arch. Environ. Health*, 30: 538-545 (1975).
57. R. Rylander, M. Ohrström, P. A. Hellström, and R. Bergström, SO_2 and Particulates—Synergistic Effects on Guinea Pig Lungs, in *Inhaled Particles III*, W. H. Walton (Ed.), pp. 535-541, Symposium Proceedings, London, September 16—23, 1970, Unwin Brothers Limited, Surrey, England, 1971.
58. D. L. Coffin and E. S. Blommer, Acute Toxicity of Irradiated Auto Exhaust. Its Indication by Enhancement of Mortality from Streptococcal Pneumonia, *Arch. Environ. Health*, 15: 36-38 (1967).
59. A. Spurgesh, R. Ehrlich, and R. Petzold, Effect of Cigarette Smoke on Resistance to Respiratory Infection, *Arch. Environ. Health*, 16: 385-391 (1968).
60. E. Goldstein, G. M. Green, and C. Seamans, The Effect of Silicosis on the Antibacterial Defense Mechanisms of the Murine Lung, *J. Infect. Dis.*, 120: 210-216 (1969).
61. P. A. Shurin, S. Permutt, and R. L. Riley, Pulmonary Antibacterial Defenses with Pure Oxygen Breathing, *Proc. Soc. Exp. Biol. Med.*, 137: 1202-1208 (1971).
62. M. C. Henry, J. Spangler, J. Findley, and P. Ehrlich, Effects of Nitrogen Dioxide and Tobacco Smoke on Retention of Inhaled Bacteria, in *Inhaled Particles III*, W. H. Walton (Ed.), pp. 527-533, Symposium Proceedings, London, September 16—23, 1970, Unwin Brothers Limited, Surrey, England, 1971.
63. E. Goldstein, D. Warshauer, W. Lippert, and B. Tarkington, Ozone and Nitrogen Dioxide Exposure. Murine Pulmonary Defense Mechanisms, *Arch. Environ. Health*, 28: 85-90 (1974).
64. E. Goldstein, C. Eagle, and P. D. Hoeprich, Influence of Ozone on Pulmonary Defense Mechanisms of Silicotic Mice, *Arch. Environ. Health*, 24: 444-448 (1972).

Effects of Cotton Dust on Free Lung Cells

RAGNAR RYLANDER* and MARIE-CLAIRE SNELLA†
*Department of Environmental Hygiene, University of Gothenburg, Sweden, and †Division of Environmental Medicine, Institute of Social and Preventive Medicine, University of Geneva, Switzerland

ABSTRACT

The free lung cells were produced in guinea pigs exposed to cotton dust. An acute exposure caused an increase in the number of polymorphonuclear (PMN) leukocytes in the airways. After subacute exposure, the number of PMN leukocytes decreased after about 5 days. In animals exposed again after 3 days without exposure, the number of macrophages and leukocytes increased at 24 hr but decreased thereafter, whereas the increase persisted in acutely exposed animals. The number of plaque-forming cells after immunization with sheep red blood cells was decreased in animals exposed for 4 and 6 weeks.

Prolonged exposure to cotton dust, particularly in cardrooms, may cause byssinosis, a disease that has been known for several hundred years. The prevalence of byssinosis in cotton mills has been found to correlate to the dust level,[1] but the causative agent and the mechanisms behind the development of the disease are not known in detail. Bouhuys and Lindell[2] demonstrated that cotton dust induced liberation of histamine in in vitro experimental models. The significance of the bacterial contamination of the dust for the development of the disease was suggested by Schneiter, Neal, and Caminita[3] and Cavagna, Foa, and Vigliani.[4] From the different parts of the cotton plant, the highest biological activity has generally been reported from the bract.

In previous work we have demonstrated that an acute exposure to a water extract of cotton dust will cause an increase in the number of polymorphonuclear leukocytes in the airways of guinea pigs.[5]

Further work demonstrated that the magnitude of this increase was related to the amount of gram-negative bacteria in the dust.[6]

Studies of various cotton dusts have demonstrated a high bacterial contamination. When cotton was stored under humid conditions, an increase in the number of bacteria took place with a parallel increase in the leukocyte mobilizing capacity. In the testing of different bacterial strains for their ability to recruit leukocytes into the airways, the strongest reactions were found in animals exposed to *Klebsiella pneumoniae.*[7] A recent epidemiological study in different cotton mills has demonstrated a close correlation between the number of gram-negative bacteria in the air and the prevalence of byssinotic symptoms among the cardroom workers.[8]

Although the acute pulmonary reaction after exposure to cotton dusts and probably also the development of byssinosis is related to the presence of gram-negative bacteria in the air, further information is required concerning the exact mechanisms responsible for the development of the disease before a definite cause–relationship can be established. Results are presented from subacute exposure experiments where animals inhaled cotton bract. The number of free lung cells and their capacity to lyse sheep red blood cells (SRBC's) were assessed after various exposure regimes.

MATERIALS AND METHODS

In the experiments full-grown high-quality guinea pigs of both sexes weighing 250 to 350 g were used. Cotton bract was obtained by hand picking and was micronized in a mechanical grinder. An aerosol of the bract dust was generated with the aid of a RagPe aerosol generator.[9] The apparatus consists of a circular duct with a fan and a perspex tower mounted on top. The fan circulates the dust through the duct, and smaller particles mount into the tower, which is connected to the exposure chamber. The concentration of dust in the chamber was determined by filtering air through Millipore filters, which were weighed. A concentration of about 500 mg/m^3 was used in the experiments. Bract extract was prepared by filtering 60 ml of saline through 5 g of the bract. The liquid was placed in a Collison spray for aerosolization.

The animals were exposed 2 hr daily to the dust aerosol or 40 min daily to the water extract and sacrificed at varying time intervals thereafter. In other experiments, one group of animals was exposed during 10 days, given 3 exposure-free days, and exposed once again the following day. Another group was given one acute exposure only.

After the animals had been sacrificed, the number of free lung cells was determined.[10] Ten milliliters of saline was gently flushed into the lungs and withdrawn. The same fluid was then flushed in again and withdrawn. After the process had been repeated altogether 10 times, a sample of the fluid was transferred into a test tube and stained with Türck's solution. The preparation was studied under the microscope, and the macrophages and polymorphonuclear leukocytes were counted.

In animals that had been exposed to dust extract for 30 and 40 days, the capacity of the free lung cells to lyse SRBC's was determined with the use of the plaque-forming-cell (pfc) technique.[11] The animals were exposed to an aerosol of SRBC's (concentration, 10^8 cells/ml) twice with a 12-day interval between the two exposures and were examined 2 days after the last exposure. The free lung cells obtained with the lavage method earlier described were washed twice in phosphate-buffered saline and resuspended at a concentration of 10^6 cells/ml. A 0.2-ml aliquot of this suspension was added to 0.1 ml of commercial guinea pig complement (1/10) and 0.2 ml of SRBC's (5×10^8).

The preparations were transferred to incubation chambers consisting of a glass slide with cover slides on top of two-faced Scotch tape. The chambers were sealed with Vaseline and incubated at 37°C for 2 hr. Thereafter the number of the SRBC's was counted under the microscope (250 x) and expressed as the number of pfc's per 10^3 cells.

RESULTS

Macrophages and leukocytes found at different times after an acute exposure are illustrated in Table 1. The number of macrophages was slightly increased immediately after the exposure. The value varied at the time intervals thereafter but remained above the control value. The increase was significant at 48 and 96 hr after the exposure. The number of leukocytes was equal to that of the controls immediately after the 40-min exposure. Twenty-four hours afterward, the number had increased about sixfold, and it remained high until 48 hr afterward when a decrease took place. Even at 96 hr after exposure, the level remained increased as compared to the control values.

Macrophages and leukocytes in the lungs of animals 72 hr after exposure to a dust aerosol of bract for a successive number of days are shown in Table 2. As shown in the table, the number of macrophages was not affected in animals exposed for 1 and 3 days.

TABLE 1

MACROPHAGES AND LEUKOCYTES ($\times 1.25 \times 10^4$) IN AIRWAYS OF ANIMALS EXPOSED TO BRACT DUST AT DIFFERENT TIMES AFTER A 2-HR EXPOSURE*

Hours after exposure	No. of animals	Macrophages	Leukocytes
Control	7	86(60.3)	78(60.5)
0	5	128(39.3)	78(24.6)
24	10	103(27.6)	422(142.4)^{xxx}
48	10	171(54.9)^{x}	428(157.2)^{xxx}
72	10	131(57.0)	270(125.0)^{x}
96	5	192(83.5)^{x}	203(142.4)

*Numbers in parentheses indicate the standard deviation. Significance from controls is noted by xxx = $p \leq 0.001$ and x = $p \leq 0.05$.

TABLE 2

MACROPHAGES AND LEUKOCYTES ($\times 1.25 \times 10^4$) IN AIRWAYS OF GUINEA PIGS EXPOSED TO COTTON-BRACT DUST DURING 2 HR FOR DIFFERENT TIMES, 72 HR AFTER CESSATION OF EXPOSURE*

Exposure days	No. of animals	Macrophages	Leukocytes
Control	15	108(33)	76(24)
1	5	85(59)	284(223)^{xx}
3	5	113(13)	239(59)^{xxx}
5	5	199(60)^{xxx}	175(42)^{xxx}
10	5	277(91)^{xxx}	187(73)^{xxx}
15	5	210(61)^{xxx}	181(23)^{xxx}

*Numbers in parentheses indicate the standard deviation. Significance from controls is noted by xxx = $p \leq 0.001$ and xx = $p \leq 0.01$.

After 5, 10, and 15 days of exposure, the value was increased over the controls. The number of leukocytes increased after 1 day of exposure, remained high after 3 days, and decreased somewhat after 5, 10, and 15 days of exposure.

The results from experiments in which animals were exposed to bract dust or bract extract for 10 days followed by 3 exposure-free days and 1 day acute exposure are shown in Table 3 and Fig. 1. In the acutely exposed animals, the number of macrophages increased

TABLE 3

MACROPHAGES (M) AND LEUKOCYTES (L) (x 1.25 x 10^4) IN AIRWAYS OF GUINEA PIGS EXPOSED TO BRACT DUST OR BRACT EXTRACT FOR VARIOUS TIME PERIODS*

Exposure time	Hr after exposure	No. of animals	Bract dust		No. of animals	Bract extract	
			M	L		M	L
Control	24 to 48	7	86(68)	78(61)	10	141(81)	73(41)
1 day	24	10	103(28)	422(142)^{xxx}	5	160(38)	255(104)^{xxx}
	48	10	171(55)^{xx}	428(157)^{xxx}	5	234(52)^{x}	256(87)^{xxx}
10 + (3) days		10	217(81)^{xxx}	244(57)^{xxx}			
10 + (3) + 1 days	24	10	311(113)^{xxx}	440(250)^{xx}	5	432(85)^{xxx}	350(86)^{xxx}
	48	10	222(96)^{xx}	204(53)^{xxx}	5	301(98)^{xx}	137(80)

*Numbers in parentheses indicate the standard deviation. Significance from controls is noted by xxx = $p \leq 0.001$, xx = $p \leq 0.01$, and x = $p \leq 0.05$.

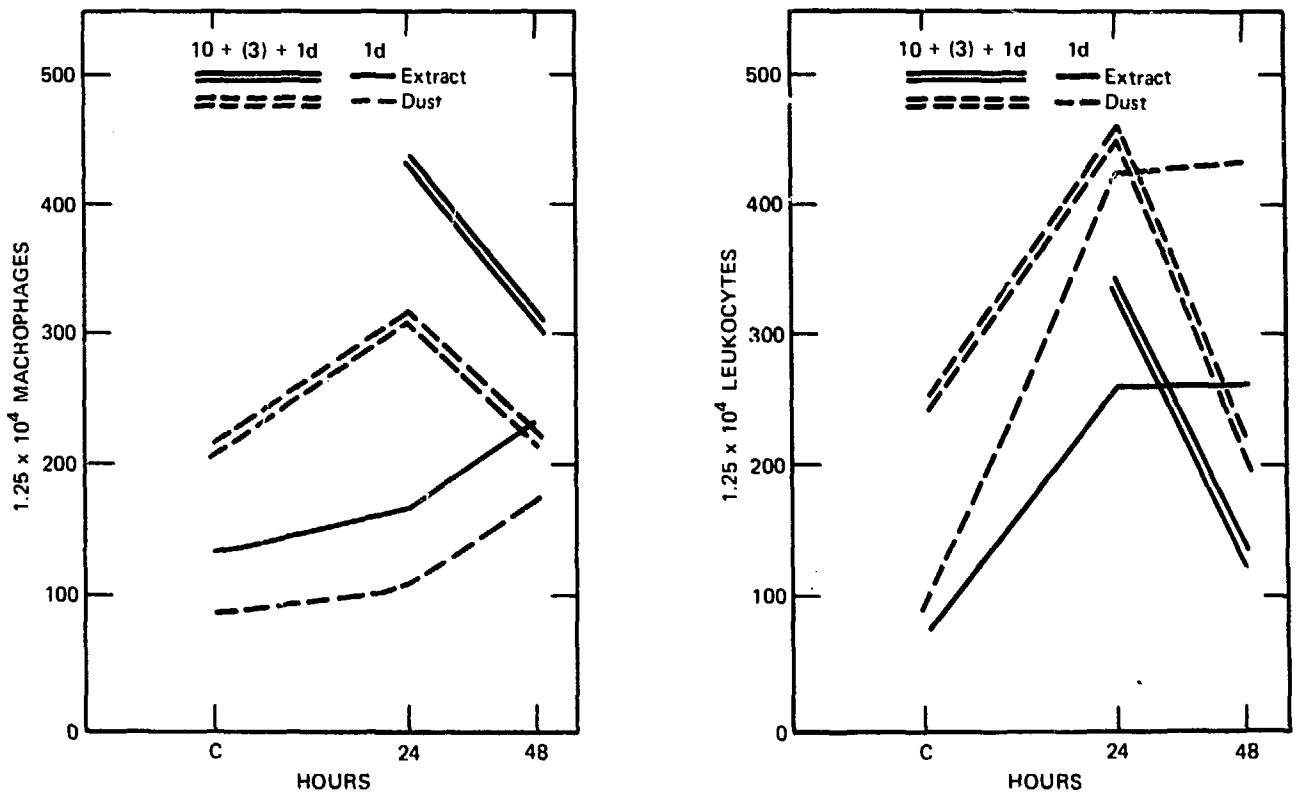

Fig. 1 Macrophages and leukocytes in airways of animals exposed to cotton bract dust and bract extract with and without previous exposure.

slightly above that of the controls at 24 hr after exposure. A further increase took place between 24 and 48 hr. In the animals previously exposed for 10 days, the number at 24 hr was higher than that in the acutely exposed animals. However, between 24 and 48 hr, the number of macrophages decreased. The table further demonstrates that an acute exposure to bract dust or bract extract caused an increase in the number of leukocytes as compared to the controls at 24 hr after the exposure. The level remained the same at 48 hr after exposure. In animals previously exposed for 10 days, the number of leukocytes was increased at 24 hr as compared to the controls but decreased between 24 and 48 hr after exposure.

The pfc's among the free lung cells in the lavage preparation are reported in Table 4. In animals that had been exposed to the bract extract for 4 and 6 weeks, the pfc's were decreased.

TABLE 4

PLAQUE-FORMING CELLS PER 10^3 FREE LUNG CELLS IN PULMONARY LAVAGE PREPARATIONS FROM GUINEA PIGS EXPOSED TO AN EXTRACT OF BRACT DUST FOR VARIOUS TIME PERIODS*

Exposure time	No. of animals	Plaque-forming cells
Control	5	7.1(2.6)
4 weeks	5	2.3(1.1)^{xx}
6 weeks	5	3.7(0.4)^{x}

*Numbers in parentheses indicate the standard deviation. Significance from controls is noted by xx = $p \leq 0.01$ and x = $p < 0.05$.

COMMENTS

The technique used in the present experiments to determine the number of free lung cells has been used on previous occasions and been found to give reproducible results. Effects due to exposure of tobacco smoke, industrial air pollutants, and various components of cotton dust have earlier been demonstrated.

In the present results a fairly large variation was present within both control and exposed animals. A part of this variation is probably due to differences in the technical procedure. It has earlier been shown that an increased number of flushings with the lavage fluid will increase the number of cells present in the fluid.[10]

Although care was taken to standardize the procedure, technical factors have probably accounted for some of the variation present.

The increase in leukocytes after exposure to cotton dust or cotton-dust extract is in line with findings from experiments reported earlier.[5,6,12] The peak increase in acutely exposed animals appears at 24 and 48 hr after the cessation of exposure. Thereafter the number of leukocytes declines. The number of macrophages varies somewhat more irregularly, but a significantly increased number is present at 96 hr after the cessation of exposure.

The leukocyte increase in the airways after exposure to the bract preparation is probably due to the presence of bacteria in the bract preparations. Previous experiments have demonstrated that gram-negative bacteria cause the largest leukocyte reactions.[7] This effect is probably caused by endotoxins acting through activation of complement through the indirect pathway and thus liberating leukotactic factors.[13]

In animals exposed for several days to the cotton-bract dust, the number of leukocytes decreased after the acute increase and remained unchanged at 5, 10, and 15 days exposure. This could indicate the formation of some endotoxin neutralizing agent that was present in the airways, acting by binding the endotoxin molecule and thus preventing the liberation of leukotactic agents. Tolerance to endotoxin appears among humans also and seems to be related to the development of endotoxin antibodies chiefly of the IgM category of immunoglobulins.[13]

In the animals in which the reaction after an acute exposure was compared between nontreated animals and animals previously exposed to the same extract, the number of macrophages and leukocytes fell between 24 and 48 hr after the exposure in animals previously exposed, whereas the number increased in the acutely exposed animals. A rapid decrease in leukocytes was found during the same time period in the subacutely exposed animals, whereas the number remained the same in the acutely exposed animals. The fall in the number of leukocytes in the chronically exposed as compared to acutely exposed animals could imply that, after the initial acute exposure reaction, endotoxin is neutralized, resulting in a decrease in the rate of complement activation and thus the liberation of leukotactic compounds. In animals that are not pretreated, no neutralization takes place, and the complement liberation will therefore continue also at 48 hr after exposure. Data supporting this concept have been presented from an investigation on human byssinotic subjects.[14]

The zone of lysin of SRBC's produced by the free lung cells was considerably smaller than regular plaques formed by immuno-

competent cells. Differences in sizes have previously been described by Rylander and Nordstrand.[5] The majority of the cells producing lysis of SRBC's were found to be typical pulmonary macrophages. This indicates that the exposure to cotton dust interferes with the capacity of pulmonary macrophages to lyse SRBC's.

Since the classification of the free lung cells was made with the aid of a light microscope, it is possible that certain of the cells producing lysis of SRBC's were of other types, such as lymphocytes. The lung contains both B- and T-cells as well as other undifferentiated immunocompetent cells.[15,16] It is known that endotoxins will suppress the activity of B-cells, and the decreased number of pfc's in the preparations could be explained by this mechanism also. The reason for the decrease in the number of cells producing lysis of SRBC's in animals exposed to bract is not clear. Similar effects have been found in animals exposed to silica and manganese dioxide particles.[17] The plaque-forming-cell technique is usually used to estimate the immune capacity of suspensions of immunocompetent cells or homogenates of spleen and lymph nodes.[11] Since the majority of cell-producing lysis of SRBC's in the present experiments were macrophages, it is not likely that the lysis is caused by antibodies produced by these cells. Theoretically the formation of plaques could be explained by antibodies carried on the surface of macrophages or by the release of lysosomal enzymes. Additional experiments are required to elucidate which mechanism is responsible for the lysis of the experimental model used.

In summary, the data from the present experiments indicate that exposure to a bract dust influences the number of free lung cells in the airways and the ability of macrophages to lyse SRBC's. In acutely exposed animals a difference is present between normal animals and those which have previously been exposed for 10 days to bract extract or bract dust.

ACKNOWLEDGMENTS

This work was supported by the U. S. Department of Agriculture with funds made available through Cotton Incorporated.

REFERENCES

1. J. A. Merchant, G. G. Halprin, A. R. Hudson, K. H. Kilburn, W. N. McKenzie, D. J. Hunt, and P. Bermazohn, Responses to Cotton Dust, *Arch. Environ. Health*, 30: 222-229 (1975).
2. A. Bouhuys and S. E. Lindell, Release of Histamine by Cotton Dust Extracts from Human Lung Tissue In Vitro, *Experientia*, 17: 211-220 (1961).

3. R. Schneiter, P. A. Neal, and B. H. Caminita, Etiology of Acute Illness Among Workers Using Low-Grade Stained Cotton, *Am. J. Public Health*, 32: 1345-1352 (1942).
4. G. Cavagna, V. Foa, and E. C. Vigliani, Effects in Man and Rabbits of Inhalation of Cotton Dust or Extracts and Purified Endotoxins, *Br. J. Ind. Med.*, 26: 314-321 (1969).
5. R. Rylander and A. Nordstrand, Pulmonary Cell Reactions After Exposure to Cotton Dust Extract, *Br. J. Ind. Med.*, 34: 220-223 (1974).
6. R. Rylander and M-C. Snella, Acute Inhalation Toxicity of Cotton Plant Dusts, *Br. J. Ind. Med.*, 33: 175-180 (1976).
7. R. Rylander, A. Nordstrand, and M-C. Snella, Effect of Bacterial Contamination of Organic Dust on Pulmonary Cell Reactions, *Arch. Environ. Health*, 30: 137-140 (1975).
8. F. F. Cinkotai, M. G. Lockwood, and R. Rylander, Airborne Microorganisms and Prevalence of Byssinotic Symptoms, *Am. Ind. Hyg. Assoc. J.* (in press).
9. R. Rylander, M. Ohrström, P. A. Hellström, and R. Bergström, SO_2 and Particles—Synergistic Effects on Guinea-Pig Lungs, in *Inhaled Particles*, Vol. III, W. H. Walton (Ed.), pp. 535-541, Unwin Brothers Ltd., 1971.
10. R. Rylander, Free Lung Cell Studies in Cigarette Smoke Inhalation Experiments, *Scand. J. Respir. Dis.*, 52: 121-128 (1971).
11. N. K. Jerne, C. Henry, A. A. Nordin, H. Fuji, A. M.C. Koros, and I. Lefkovits, Plaque Forming Cells—Methodology and Theory, *Transplant. Rev.*, 18: 131-191 (1974).
12. R. F. Walker, G. Edison, and J. D. Hatcher, Influence of Cotton Dust Inhalation on Free Lung Cells in Rats and Guinea-Pigs, *Lab. Invest.*, 33: 28-32 (1975).
13. S. M. Wolff, Biological Effects of Bacterial Endotoxins in Man, in *Bacterial Lipopolysaccharides*, E. H. Kass and S. M. Wolff (Eds.), pp. 251-256, University of Chicago Press, 1973.
14. A. Massoud and G. Taylor, Byssinosis: Antibody to Cotton Antigens in Normal Subjects and in Cotton Card-Room Workers, *Lancet*, 2: 607-610 (1964).
15. R. J. Ford and C. Kuhn, Immunologic Competence of Alveolar Cells, *Am. Rev. Respir. Dis.*, 107: 763-770 (1973).
16. R. P. Daniele, M. D. Altose, and D. T. Rowlands, Jr., Immunocompetent Cells from the Lower Respiratory Tract of Normal Human Lungs, *J. Clin. Invest.*, 56: 986-995 (1975).
17. R. Rylander and R. Bergstrom, University of Gothenburg, unpublished.

Alveolar Macrophages and Teflon Particles Coated with Carbon and Metals

PER CAMNER and MARGOT LUNDBORG
Department of Environmental Hygiene, The Karolinska Institute, and
Department of Environmental Hygiene, The National Environment Protection Board, Stockholm, Sweden

ABSTRACT

Teflon particles (4 to 5 μm) produced by a spinning-disk technique were coated with carbon or various metals. In vitro studies of phagocytosis and toxicity and in vivo studies of lung retention were performed using these particles. The number of particles phagocytized by alveolar macrophages and the number of nonviable macrophages after 1.5 hr of incubation were studied. When serum was added, the number of particles phagocytized was dependent on the coating element, e.g., carbon-coated particles were phagocytized to a greater extent than were silver-coated particles. When serum was not added, the dependence on the coating elements was less. Beryllium-coated particles caused increased numbers of nonviable macrophages and altered appearance of macrophages in the light microscope. Macrophages from rabbits that had inhaled metallic nickel dust for 4 weeks (5 days per week and 7 hr per day) phagocytized more nickel-coated and silver-coated particles than macrophages from control rabbits. Rabbits inhaled metal-coated particles tagged with ^{51}Cr, and then lung retention was followed by external monitoring of radioactivity for about 1 week. In one study the clearance patterns of carbon-coated particles were compared with those of silver-coated particles; in another study the clearance patterns of beryllium-coated particles were compared with those of silver-coated particles. No differences in lung retention were seen in either study.

A general consensus is that a high proportion of inhaled particles deposited in the alveoli is phagocytized by alveolar macrophages.[1-4] However, the importance of macrophages for the elimination of particles or for protection of the lung is not fully understood.

It is known that particle size affects the rate of phagocytosis[5] and that deposition of particles depends on their aerodynamic

diameter.[1,2] Test particles coated with thin layers of different elements might be a useful tool in studying the mechanisms of phagocytosis and elimination of particles from the lung. The rate of phagocytosis could be determined using particles coated with different elements, and the phagocytic rates could be compared with their clearance rates from the lung. Although the elements might differ in density, the coated particles should have about the same physical and aerodynamic diameters. Presented below are original data as well as data from elsewhere.[6-8]

MATERIALS AND METHODS

Teflon particles,[9] 4 to 5 μm in diameter, were produced by a spinning-disk technique[10] and were then coated with metals or carbon by an evaporation-in-vacuum method.[6] In the lung-clearance experiment, the particles were also tagged with ^{51}Cr.[11]

Alveolar macrophages from apparently disease-free rabbits were collected, and their phagocytic activity was studied by a modification of the method of Myrvik, Leake, and Fariss;[12] see also Lundborg and Holma.[13] The coated particles were suspended in 75% Parker 199 solution and 25% autologous rabbit serum, or in 100% Parker 199. Next, 0.5-ml amounts of a suspension of coated particles (6×10^3 particles per cubic millimeter) were added to small Petri dishes containing a monolayer of macrophages. After 1.5 hr of exposure at 37°C, photographs were taken with a light microscope and the macrophages and phagocytized particles were counted. The viability of the macrophages was tested by staining with eosine Y.

Nickel dust was produced with an airstream suspending metallic nickel powder (320 mesh) into the air.[14] The dust was delivered into exposure chambers[5] 0.6 m^3 in volume. The chambers were ventilated with filtered air at a rate of 6 m^3/hr. The mean concentration of nickel dust in the chambers was 3.0 mg/m^3 (standard deviation, 1.2). Measurements were performed daily for 2 hr by sucking air through a Millipore filter. The amount of air was registered, and the filter was weighed. About one-third of the dust was respirable in the sense that the particles (<7 μm in diameter) penetrated the Casella preseparator.

In the clearance experiment an aerosol of coated particles was produced by suspending them in water and spraying the suspension with an airbrush into an exposure chamber.[5] The rabbits were anesthetized with pentobarbital, intubated, placed in a whole-body respirator, and insufflated with the test aerosol. The radioactivity in the lungs was measured by profile scanning of the thorax with NaI

crystals (3 x 2 in.) fitted with collimators.[5] The radioactivity was registered on a recorder, and the total amount of radioactivity was estimated planimetrically.

RESULTS

In Vitro Studies

Table 1 shows the numbers of silver-, lead-, and carbon-coated particles phagocytized per macrophage during 1.5 hr of incubation. The average number of particles per macrophage is about the same for lead- and silver-coated particles but significantly higher for carbon-coated particles, ($p < 0.01$, paired t test). Further details are given in Ref. 6. In another study two samples each of silver-coated and carbon-coated particles suspended in Parker 199 and serum were left undisturbed for 3 hr at 37°C. Particles from one of each pair of samples of silver-coated particles and carbon-coated particles were added to macrophages, and the rate of phagocytosis was studied. The silver- and carbon-coated particles in the other samples were allowed to sediment and the supernatants were removed; the supernatants of the carbon-coated particles were added to the silver-coated particles, and vice versa. The particles were then added to the macrophages, and the rate of phagocytosis was studied. Table 2 shows that the carbon-coated particles were phagocytized faster than the silver-coated particles, regardless of whether or not the supernatants were removed and switched ($p < 0.01$). Thus the difference in phagocy-

TABLE 1

NUMBER OF COATED PARTICLES PHAGOCYTIZED PER MACROPHAGE IN 1.5 hr AT 37°C (SERUM ADDED)*

Rabbit No.	Carbon-coated particles	Lead-coated particles	Silver-coated particles
1	1.08	0.55	0.72
2	1.29	0.99	0.96
3	0.76	0.65	0.43
4	0.83	0.41	0.33
5	1.12	0.46	0.75
6	0.97	0.59	0.58
Mean	1.01	0.61	0.63

*From P. Camner, P.-Å. Hellström, and M. Lundborg, Coating 5-μm Particles with Carbon and Metals for Lung Clearance Studies, *Archives of Environmental Health*, 27: 331-333 (1973).

TABLE 2

NUMBER OF SILVER- AND CARBON-COATED PARTICLES PHAGOCYTIZED PER MACROPHAGE IN 1.5 hr AT 37°C (SERUM ADDED)*

Rabbit No.	Silver-coated particles with supernatant of		Carbon-coated particles with supernatant of	
	Ag-coated particles	C-coated particles	Ag-coated particles	C-coated particles
1	0.62	0.81	1.14	1.01
2	0.50	0.57	0.83	0.75
3	0.66	0.53	1.07	1.02
4	0.62	0.63	1.19	1.15
5	0.57	0.55	1.14	1.06
6	0.65	0.69	1.08	0.93
Mean	0.60	0.63	1.03	0.99

*The particle suspension was first allowed to stand 3 hr at 37°C. The particles were then allowed to sediment, and the particles and supernatants were added to the macrophages.

tosis between carbon-coated and silver-coated particles is not caused by material dissolved from the particles.

The rate of phagocytosis of particles coated with aluminum, chromium, manganese, silver, or uranium was compared. Aluminum-coated and chromium-coated particles (0.7 particle per macrophage) were phagocytized faster than the silver-coated particles (0.6 particle per macrophage; $p < 0.02$). The rate of phagocytosis of silver-, manganese-, or uranium-coated particles did not differ ($p > 0.05$). More details are given in Ref. 7.

In all the experiments previously described, autologous serum was added. The rate of phagocytosis was compared for carbon-, silver-, and aluminum-coated particles by using media devoid of serum. Under these conditions particles were phagocytized more slowly, and the differences among them were smaller (Table 3). Nonetheless, more carbon- and aluminum-coated particles were phagocytized than were silver-coated particles ($p < 0.05$). In all these experiments the number of nonviable macrophages was $\leqslant 4\%$.

Table 4 shows the results of a study in which macrophages were exposed to beryllium- or silver-coated particles for 1.5 hr. After exposure to beryllium-coated particles, a considerable number of the macrophages fell from the glass, died, and had an unusual appearance in the light microscope. For details, see Ref. 7. In another experi-

TABLE 3

NUMBER OF COATED PARTICLES PHAGOCYTIZED PER MACROPHAGE IN 1.5 hr AT 37°C (SERUM NOT ADDED)*

Rabbit No.	Particle coating		
	Carbon	Silver	Aluminum
1	0.53	0.50	0.51
2	0.50	0.45	0.52
3	0.64	0.30	0.34
4	0.37	0.24	0.32
5	0.42	0.38	0.40
6	0.36	0.34	0.34
7	0.42	0.38	0.36
8	0.37	0.33	0.35
9	0.36	0.33	0.33
10	0.55	0.51	0.56
Mean	0.45	0.38	0.40

*From P. Camner, M. Lundborg, and P.-Å. Hellström, Alveolar Macrophages and 5-μm Particles Coated with Different Metals, In Vitro Studies, *Archives of Environmental Health*, 29: 211-213 (1974).

TABLE 4

EXPOSURE (1.5 hr AT 37°C) OF MACROPHAGES TO BERYLLIUM- AND SILVER-COATED 5-μm PARTICLES (SERUM ADDED)*

Rabbit No.	Ag-coated particles		Be-coated particles	
	Percent nonviable macrophages	Number of viable macrophages per picture	Percent nonviable macrophages	Number of viable macrophages per picture
1†	5	41	60	12
2†	5	23	7	6
3	⩽3	120	5	16
4	⩽3	103	17	44
5	⩽3	160	13	34
Mean	⩽4	89	20	22

*From P. Camner, M. Lundborg, and P.-Å. Hellström, Alveolar Macrophages and 5-μm Particles Coated with Different Metals, In Vitro Studies, *Archives of Environmental Health*, 29: 211-213 (1974).

†The macrophages from rabbits 1 and 2 were stored for 2 hr longer than the macrophages from rabbits 3 to 5 before mixture with silver-coated and beryllium-coated particles.

TABLE 5

PERCENT OF NONVIABLE MACROPHAGES AFTER EXPOSURE OF MACROPHAGES (1.5 hr AT 37°C) TO BERYLLIUM- AND SILVER-COATED PARTICLES (SERUM ADDED)*

Rabbit No.	Ag-coated particles with supernatant of Ag-coated particles	Ag-coated particles with supernatant of Be-coated particles	Be-coated particles with supernatant of Ag-coated particles
1	≤3	≤3	20
2	≤3	≤3	8
3	≤3	≤3	12

*The particle suspensions were first allowed to stand 3 hr at 37°C. The particles were then allowed to sediment, and the particles and supernatants were added to the macrophages.

ment two samples of silver-coated particles suspended in Parker 199 and serum and one sample of beryllium-coated particles suspended in the same solution were allowed to stand for 3 hr at 37°C. The particles were allowed to sediment, and the supernatants of one suspension of silver-coated particles and that of the suspension of beryllium-coated particles were removed and exchanged. The particles were then added to macrophages and left undisturbed for 1.5 hr at 37°C. Beryllium-coated particles in the silver-coated particle supernatant produced an increased number of nonviable particles, but silver-coated particles in the beryllium-coated particle supernatant did not (Table 5). Consequently, the toxic effect was not caused by dissolved beryllium.

Four rabbits were exposed to nickel dust for 4 weeks (5 days per week and 7 hr per day). Four control rabbits were kept in similar chambers during the exposure period. Four days after the exposure period, the rabbits were killed and their lung macrophages were washed out. The rate of phagocytosis of nickel- and silver-coated particles was then studied. The macrophages from the exposed rabbits phagocytized both more silver-coated particles and more nickel-coated particles than the macrophages from the control rabbits ($p < 0.01$) (see Table 6).

In Vivo Studies

In one experiment 10 rabbits were exposed to both silver-coated and carbon-coated particles. Five of the rabbits were exposed first to

TABLE 6

NUMBER OF COATED PARTICLES PHAGOCYTIZED PER MACROPHAGE IN 1.5 hr AT 37°C (SERUM ADDED)*

Rabbit No.	Silver-coated particles	Nickel-coated particles
	Unexposed Rabbits	
1	0.81	0.80
3	0.52	0.63
5	0.71	0.66
7	0.76	0.74
Mean	0.70	0.71
Standard deviation	0.13	0.08
	Rabbits Exposed to Nickel Dust	
2	1.07	0.93
4	1.00	1.07
6	1.15	1.00
8	1.13	1.09
Mean	1.09	1.02
Standard deviation	0.07	0.07

*Macrophages from rabbits exposed to nickel dust for 4 weeks (5 days per week, 7 hr per day) are compared with macrophages from unexposed rabbits.

silver-coated particles and 3 weeks later to carbon-coated particles and the other five vice versa. The retentions of silver-coated and carbon-coated particles were quite similar the first day and the first week after inhalation. Further details are given in Ref. 8.

In another experiment eight rabbits were exposed to beryllium-coated particles and eight rabbits to silver-coated particles. The retentions of silver-coated and beryllium-coated particles were quite similar the first day and the first week after inhalation. More information is given in Ref. 8.

DISCUSSION

Results show that the chemical composition of a particle surface is important for its ultimate phagocytosis. The differences in the

number of particles phagocytized were most pronounced in the presence of serum. Earlier studies have shown that serum factors are necessary for an optimal rate of phagocytosis and that those serum factors coat the particles.[15] Differences in the rates of phagocytosis may depend on the ability of the respective element to bind some serum factor. It also seems reasonable to assume that such serum factors are accessible in the alveoli, i.e., the in vitro experiment with serum should be more comparable with the in vivo situation than those in vitro experiments without serum.

The high toxicity of beryllium-coated particles to the macrophages may be of interest. It is known that inhaled beryllium compounds can produce very severe injuries in the lung, acutely as well as chronically.[16] The toxicity of particles to macrophages has been given great attention, especially in the field of silicosis. There seems to be an association between the cytotoxicity of silica dust in vitro and the fibrogenicity in vivo.[17]

Animals exposed previously to nickel dust had macrophages that phagocytized both more silver-coated and more nickel-coated particles in vitro than did macrophages from control animals. Hence the increase was not specific to nickel particles. It is interesting to compare this result with the finding that macrophages from rabbits infected with bacteria ingested both the original infecting organism and unrelated organisms to a greater extent than did macrophages from uninfected animals.[18]

No difference in lung clearance between silver- and carbon-coated particles or between silver- and beryllium-coated particles could be demonstrated during the first week after inhalation although differences in the rates of phagocytosis and toxicity, respectively, were seen in vitro.

REFERENCES

1. T. F. Hatch and P. Gross, *Pulmonary Deposition and Retention of Inhaled Aerosols*, Academic Press, Inc., New York, 1964.
2. Task Group on Lung Dynamics, Deposition and Retention Models for Internal Dosimetry of the Human Respiratory Tract, *Health Phys.*, 12: 173-207 (1966).
3. P. E. Morrow, Alveolar Clearance of Aerosols, *Arch. Intern. Med.*, 131: 101-108 (1973).
4. G. M. Green, Alveolobronchiolar Transport Mechanisms, *Arch. Intern. Med.*, 131: 109-114 (1973).
5. B. Holma, Lung Clearance of Mono- and Didisperse Aerosols Determined by Profile Scanning and Whole-Body Counting: A Study on Normal and SO_2 Exposed Rabbits, *Acta Med. Scand.*, 473(Suppl.): 5-102 (1967).

6. P. Camner, P.-Å. Hellström, and M. Lundborg, Coating 5-μ Particles with Carbon and Metals for Lung Clearance Studies, *Arch. Environ. Health*, 27: 331-333 (1973).
7. P. Camner, M. Lundborg, and P.-Å. Hellström, Alveolar Macrophages and 5-μm Particles Coated with Different Metals. In Vitro Studies, *Arch. Environ. Health*, 29: 211-213 (1974).
8. P. Camner, P.-Å. Hellström, M. Lundborg, and K. Philipson, Lung Clearance of 4-μm Particles Coated with Silver, Carbon or Beryllium, *Arch. Environ. Health*, 32(2): 58-62 (1977).
9. P. Camner, K. Philipson, and J. Svedberg, Production of 7-μ Monodisperse Fluorocarbon Resin Particles Tagged With ^{18}F, *Int. J. Appl. Radiat.*, 22: 349-353 (1971).
10. K. Philipson, On the Production of Monodisperse Particles with a Spinning Disc, *J. Aerosol. Sci.*, 4: 51-57 (1973).
11. K. Philipson, L. Linnman, P.-Å. Hellström, and P. Camner, Labelling Properties of ^{51}Cr in Monodisperse Teflon Particles, *Health Phys.*, 28: 621-622 (1975).
12. Q. N. Myrvik, E. S. Leake, and B. Fariss, Studies on Pulmonary Alveolar Macrophages from the Normal Rabbit: A Technique to Procure Them in a High State of Purity, *J. Immunol.*, 86: 128-132 (1961).
13. M. Lundborg and B. Holma, In Vitro Phagocytosis of Fungal Spores by Rabbit Lung Macrophages, *Sabouraudia*, 10: 152-156 (1972).
14. P.-Å. Hellström, Metal Dust for Experimental Use—Generation and Physical Data (in Swedish), The Swedish Board of Industrial Safety, Stockholm, 1975.
15. D. S. Nelson, *Macrophages and Immunity*, North-Holland Publishing Company, Amsterdam (Netherlands), 1969.
16. H. E. Stokinger (Ed.), *Beryllium: Its Industrial Hygiene Aspects*, Academic Press, Inc., New York, 1966.
17. A. C. Allison, Effects of Silica and Asbestos on Cells in Culture, in *Inhaled Particles III*, W. H. Walton (Ed.), Vol. 1, pp. 437-442, Symposium Proceedings, London, September 16—23, 1970, Unwin Brothers Limited, Surrey, England, 1971.
18. J. D. Johnson, W. L. Hand, N. L. King, and C. G. Hughes, Activation of Alveolar Macrophages After Lower Respiratory Tract Infection, *J. Immunol.*, 115: 80-84 (1975).

Effect of Particle Content of Lung on Clearance Pathways

JURAJ FERIN
Department of Radiation Biology and Biophysics, School of Medicine and Dentistry, University of Rochester, Rochester, New York

ABSTRACT

Inhaled particles evoke in the lung a response that involves several clearance pathways. Titanium dioxide particles were used as a test particle that gave information mainly on the alveolobronchial route of clearance involving alveolar macrophages.

Titanium dioxide lung deposits ranging from 0.1 to 100 mg were achieved in rats by a single inhalation or intratracheal instillation. With increasing lung content, particle translocation to the lymphatic system increased faster than the total clearance rate. The hilar lymph nodes content at day 25 postexposure reached approximately 1 mg TiO_2, which corresponds to a lung content of approximately 30 mg TiO_2. The clearance rate (micrograms per day) at day 25 postexposure increased with larger lung deposits and reached a plateau at a lung load of approximately 40 mg.

It was concluded that increasing lung burdens of TiO_2 affect the alveolar macrophage related lung clearance, which results in greater translocation to the lymphatic system.

Inhaled particles evoke in the lung a response that involves several clearance pathways. Titanium dioxide (TiO_2) particles under certain experimental conditions can be used as a clearance test that gives information mainly on the alveolobronchial route of clearance and on the involvement of alveolar macrophages.[1,2]

The present studies were designed to evaluate the effect of particle concentration in the lungs on the participation of different mechanisms on lung clearance.

MATERIALS AND METHODS

Titanium dioxide lung deposits ranging from 0.1 to 100 mg were achieved in rats by a single inhalation or intratracheal instillation. High deposits above 1 mg per lung were achieved by intratracheal instillations. Low levels, on the other hand, were achieved by both inhalation and instillation.

The technique used for quantitative clearance assessment was as follows: Long–Evans hooded rats were killed in groups of about 10 at days 1, 8, 25, and 130 after TiO_2 deposition, and the excised lungs were analyzed chemically for titanium dioxide content. The lung load at 1 day postexposure represented the amount of TiO_2 deposited in the alveoli. The difference between deposition and retention was the value of particle clearance.

For chemical analysis the lung of each rat was divided into three samples. Sample 1 consisted of the trachea, bifurcation, and portions of the bronchi with attached lymphatic nodes. The airways were rinsed with 20 ml of distilled water. This sample represents the TiO_2 content of the hilar nodes. Sample 2 contained the particles that were washed off from the air surface of the specimen and represents TiO_2 present in the airways. Because of the low TiO_2 content, samples 1 and 2 were pooled within one group. Sample 3 represents the TiO_2 in parenchymal lung.

Titanium dioxide was determined photometrically with the use of 4,4-diantipyryl methane monohydrate. The inhalation exposure lasted 2 to 6 hr at an aerosol concentration of 15 or 100 mg TiO_2/m^3. The mass median aerodynamic diameter of the TiO_2 particles was 1.48 μm with a mean geometric standard deviation of 3.26. The specific surface area of the particles was 7 m^2/g, and the in vitro solubility was approximately 10^{-10} g cm^{-2} day^{-1}. The TiO_2 instillation with 10 different amounts (0.1 to 100 mg in 0.5 ml of saline per rat) was performed directly into the trachea with a syringe and needle.

RESULTS

Lung retentions of TiO_2 at day 1 postexposure ranged from 116 μg per lung through 858 μg per lung. The retention of TiO_2, expressed as percent of the retention, was plotted against time on a semilogarithmic scale. The regression curve can be described as a two-component equation with corresponding biological half-lives

$$Y = 24e^{-0.161t} + 80e^{-0.012t}$$

of 4.3 and 59.5 days, respectively.

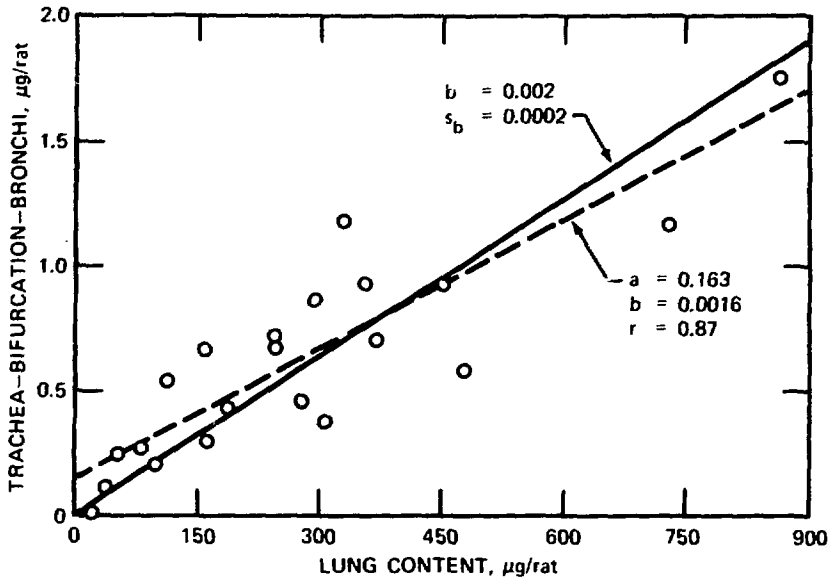

Fig. 1 Particle content at the air surface of the tracheal specimen as a function of the particle lung content at days 1, 8, 25, and 130 postexposure. Each point is an average of approximately 10 rats. a, intercept; b, slope or regression coefficient; s_b, standard deviation of b; r, correlation coefficient.

A correlation was obtained between the tracheal TiO_2 content and the lung TiO_2 content (Fig. 1). It can be postulated that this line should go through the origin since at zero lung content of TiO_2 no particles would be found at the trachea. The untreated line and the line fitted through the origin are shown in Fig. 1. The close correlation and the good fit to the regression line indicate that after exposure the tracheal content decreases at the same rate as the lung content.

In view of these results, as well as of the insignificant amount of TiO_2 in the lymphatic system, the very low solubility of the particles in vitro and in vivo, and the microscopic observations reported earlier,[2] we have stated[1,2] that the main clearance pathway in these experiments was the alveolobronchial route involving mostly the alveolar macrophages.

Figure 2 shows the plot of the hilar lymphatic node content against the lung content, both at day 1 postexposure. At low lung contents, the lymphatic node values are quite scattered with no indication of a slope. At lung contents above 1 mg per lung, there is a steep increase in the TiO_2 amount found in the hilar lymphatics. The increase depends on the lung burden. These results also indicate that at high lung burdens a substantial relocation into the lymphatic

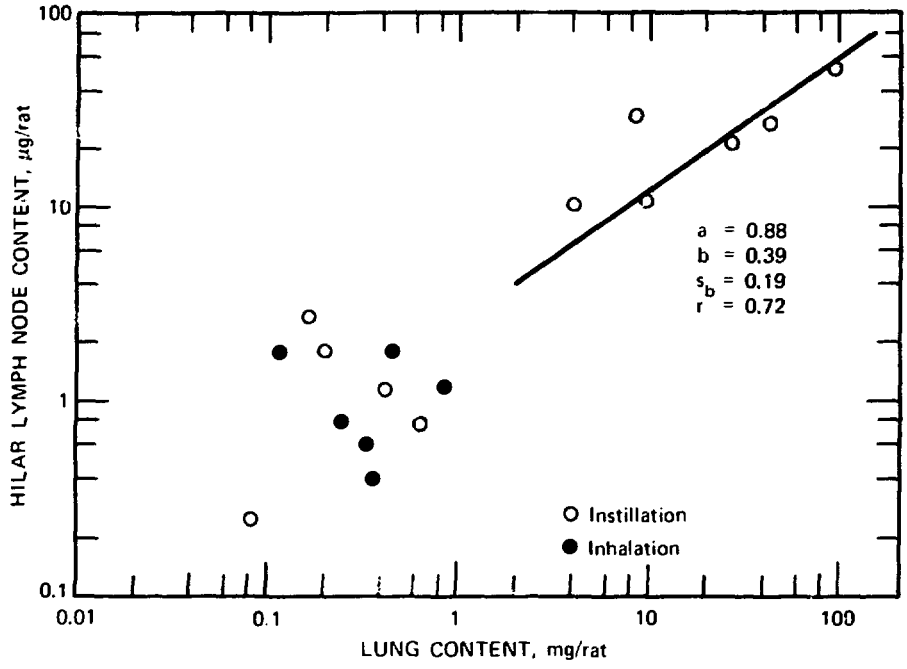

Fig. 2 Titanium dioxide content in the hilar lymph node vs. that in the lung at day 1 postexposure. For meaning of symbols, see Fig. 1.

system can occur within a few hours. The TiO_2 content in the hilar lymph nodes at 25 days postexposure is increased further (Fig. 3). At lung burdens above 30 mg per rat, the lymph nodes contain about 1 mg of TiO_2, which seems to be the saturation level. The nodes are enlarged, white, and appear to be completely filled with particles. The microscopic picture corresponds with the quantitative findings. At day 25 postexposure and at low lung burdens, the alveoli still contain TiO_2 particles that are mostly phagocytized by alveolar macrophages. The hilar lymph nodes, on the other hand, are almost free of particles. At high lung burdens the lung field is qualitatively similar except that the lymphatic nodes contain a very high amount of TiO_2 (Figs. 4 and 5).

Clearance rates were computed from the data and show a good correlation with the lung content (Fig. 6). The linear relation between clearance rate and lung content on the log—log scale is practically linear on a normal scale as well. The experiments with the three highest lung burdens suggest that the clearance rates are approaching a top value and that the clearance-rate curve reaches a plateau. In addition, it may be pointed out that these data did not reveal a difference between inhalation and instillation lung deposition methods.

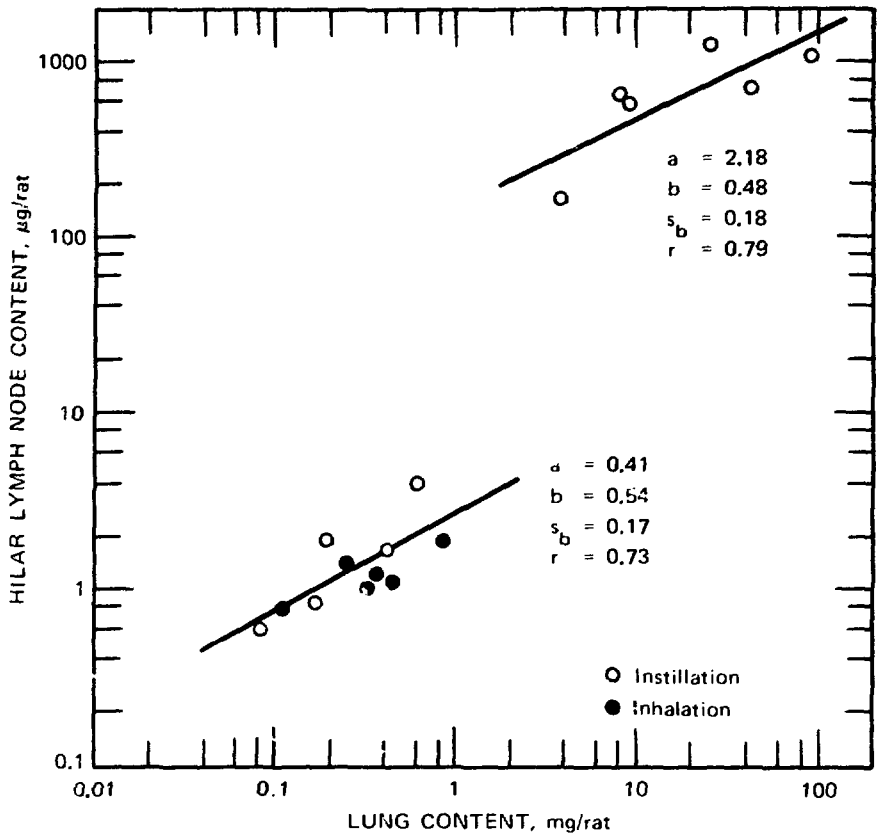

Fig. 3 Titanium dioxide content in the hilar lymph node at day 25 postexposure vs. that in the lung at day 1 postexposure. For meaning of symbols, see Fig. 1.

DISCUSSION

On the basis of the results reported here, we are proposing kinetic curves (Fig. 7) for the translocation of TiO_2 in the early postexposure period. A substantial increase in the TiO_2 content of the hilar lymphatic nodes was observed only at a lung burden above approximately 1 mg per rat. The penetration of the particles into the lymphatic structure can be rapid, as the analysis of the hilar lymph nodes at day 1 postexposure indicates. For the 25-day translocation into the hilar lymph nodes, we are proposing an S-shaped curve. This does not necessarily mean that the upper limit for the intake of the hilar lymph nodes in the rat is about 1 mg of TiO_2. It is conceivable that at different experimental conditions, e.g., repeated exposures, a proliferation of lymphatic tissue and a higher particle load may occur. Our data are plotted in Fig. 8 as 100 times the ratio of hilar lymph node content to the lung content vs. time.[3,4] Kilpper et al.[3]

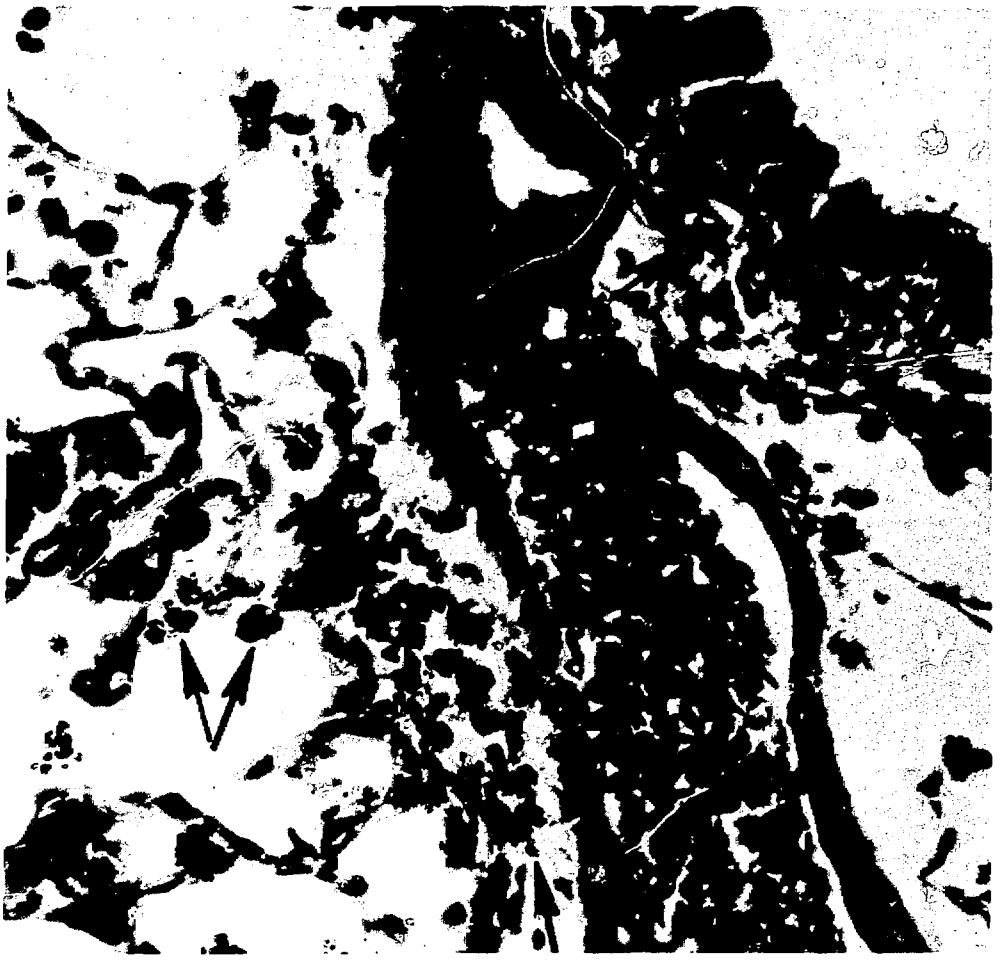

Fig. 4 Lung field from rat with initial deposition of approximately 45 mg per lung 25 days after intratracheal instillation. Many TiO_2 particles (arrows) mostly phagocytized in alveoli and also in the peribronchial and perivascular lymphatic spaces. Hematoxylin and eosin stain. (Original magnification, 100 X, polarized light.)

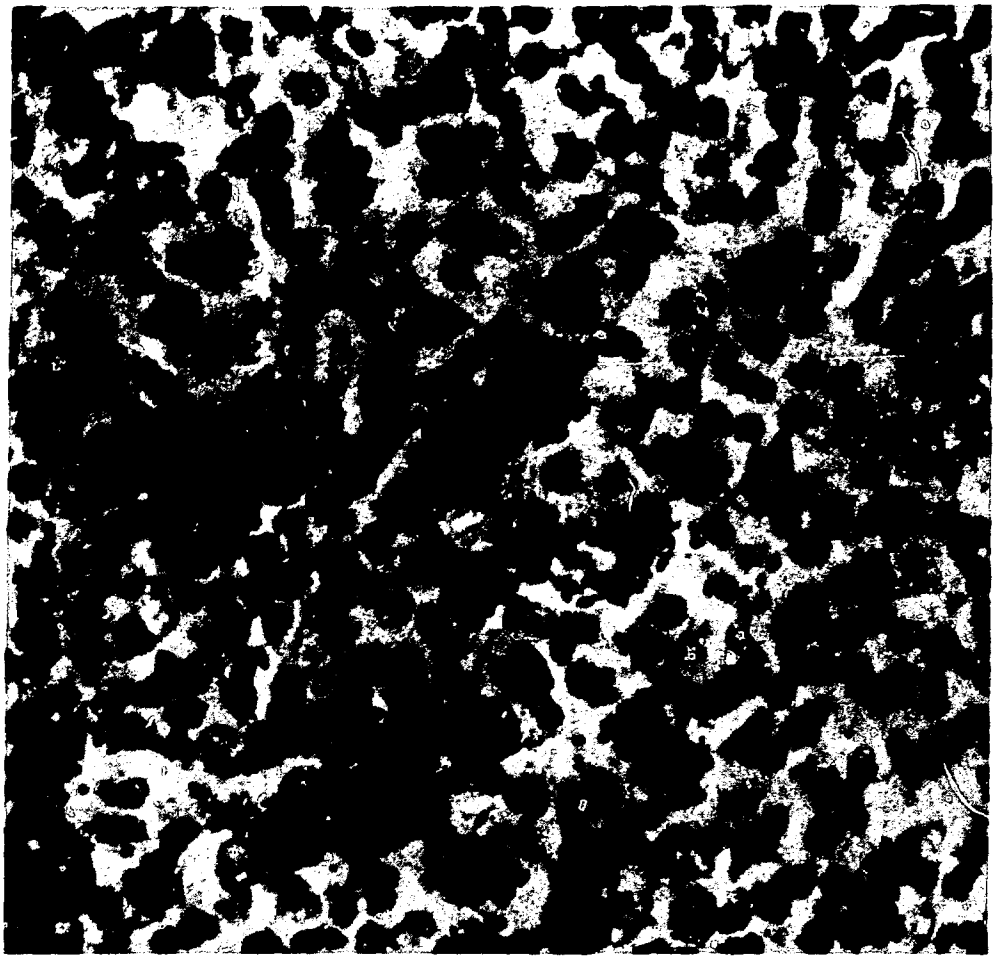

Fig. 5 Hilar lymphatic node from the same rat as in Fig. 4 containing large amount of particles. Hematoxylin and eosin stain. (Original magnification, 160 X.)

and Thomas[4] presented their results from dog experiments. All our data points fall closer to the Kilpper et al.[3] curve than to the Thomas[4] curve.

The experiments show that a large lung burden increases the penetration of particles into the lymphatic nodes. A focal deposit containing a very large amount of particles may similarly affect the translocation processes locally. We used in our experiments both low and extremely high lung burdens. However, local high deposits filling one or more alveoli are possible even at low lung deposits, and a load effect on particle penetration may therefore be operative also under realistic conditions. If the alveolar macrophages are able to phagocytize only a portion of the large number of deposited particles,

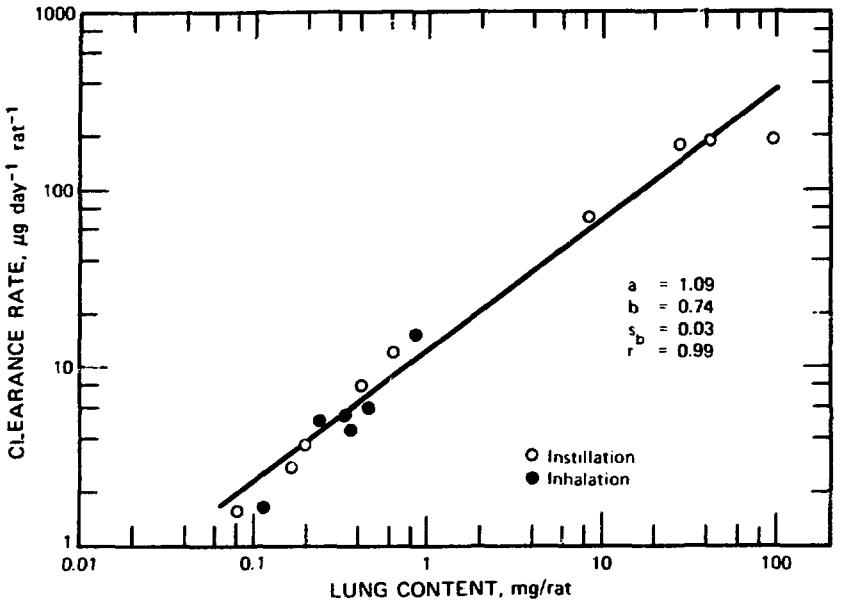

Fig. 6 Regression of clearance rate at day 25 postexposure on particle lung content at day 1 postexposure. For meaning of symbols, see Fig. 1.

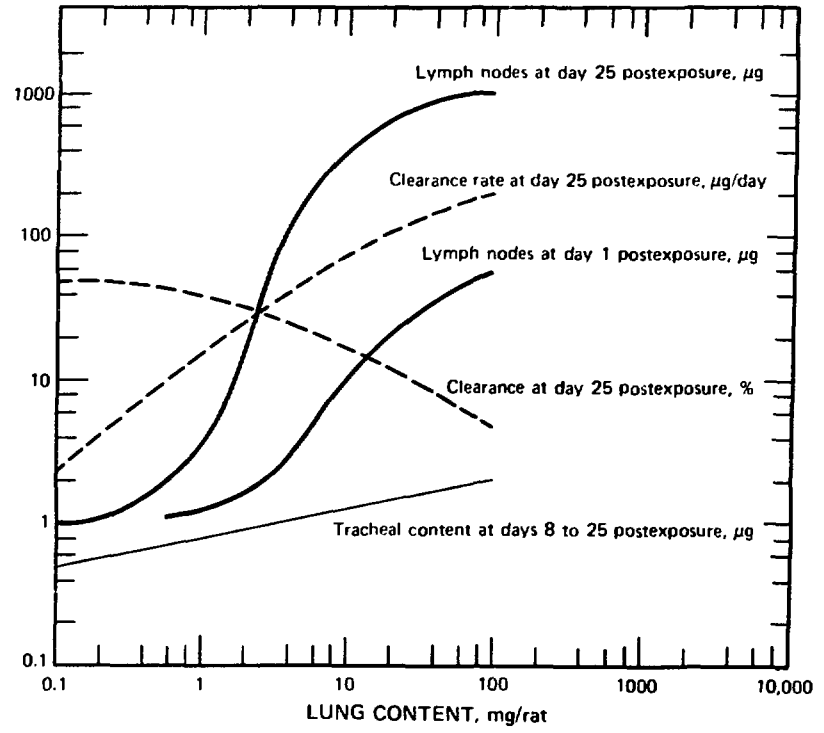

Fig. 7 Dependence of different variables on the particle lung content. (Proposed kinetic curves are based on experimental results.)

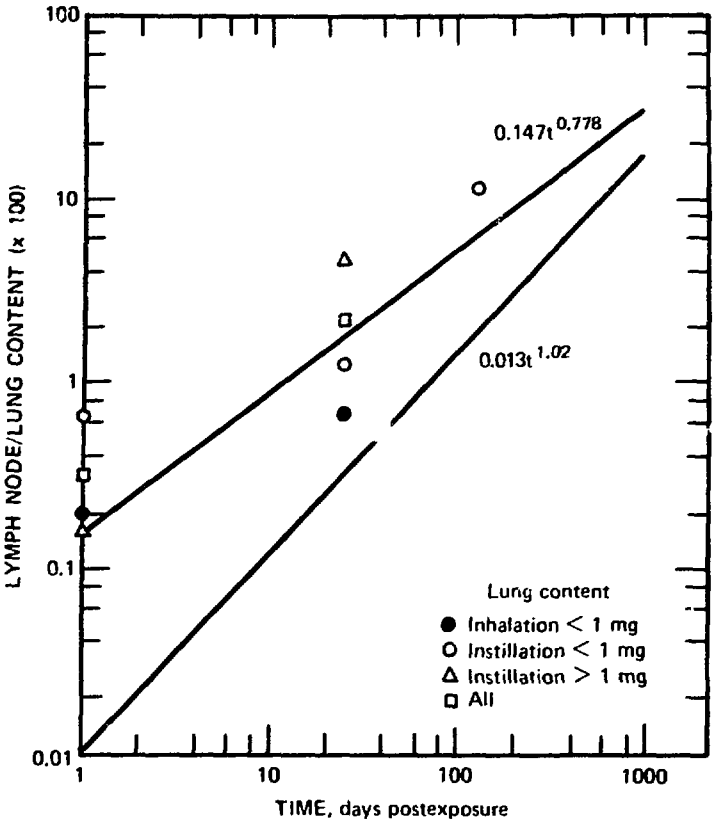

Fig. 8 Lymph node/lung content ratio vs. time. Power curves: $0.147t^{0.778}$ from Kilpper et al.;[3] $0.013t^{1.02}$ from Thomas.[5]

nonphagocytized free particles may be translocated into the lymphatics. We have seen microscopically that, even at very low lung loads, some particles will be found in the lymphatic structures of the lung, probably escaping somehow the phagocytic actions of the alveolar macrophages. Morrow[5] pointed out the important and controversial aspects of this process in relation to particle clearance.

ACKNOWLEDGMENT

This paper is based on work performed under contract with the Energy Research and Development Administration at the University of Rochester Biomedical and Environmental Research Project and has been assigned Report No. UR-3490-1002. Technical collaboration, B. Morehouse and E. Renner.

REFERENCES

1. J. Ferin, Lung Clearance of Particles, in *Air Pollution and the Lung*, Proceedings of the Twentieth Annual "OHOLO" Biological Conference, Ma'alot, Israel, Mar. 16—19, 1975, pp. 64-78, John Wiley & Sons, Inc., New York-Toronto, 1976.
2. J. Ferin and L. J. Leach, The Effects of Selected Air Pollutants on Clearance of Titanic Oxide Particles from the Lungs of Rats, in *Inhaled Particles IV*, 4th International Symposium on Inhaled Particles and Vapours, Edinburgh, U.K., Sept. 22—26, 1975, Pergamon Press, Inc., New York, 1977.
3. R. W. Kilpper, A. Bianco, F. R. Gibb, S. Landman, and P. E. Morrow, Uptake and Retention of Insufflated Tantalum by Lymph Nodes, in *Radiation and the Lymphatic System*, Proceedings of the 14th Annual Hanford Biology Symposium at Richland Wash., ERDA Symposium Series, Sept. 30—Oct. 2, 1974, John E. Ballou (Chairman), pp. 46-53, CONF-740930, NTIS, 1976.
4. R. B. Thomas, An Interspecies Model for Retention of Inhaled Particles, in *Assessment of Airborne Particles*, Third Rochester International Conference on Environmental Toxicity, 1970, pp. 405-420, Charles C Thomas, Publisher, Springfield, Ill., 1972.
5. P. E. Morrow, Lymphatic Drainage of the Lung in Dust Clearance, in Coal Workers Pneumoconiosis, International Conference on Coal Workers' Pneumoconiosis, New York, N.Y., Sept. 13—17, 1971, *Ann. N.Y. Acad. Sci.*, 200: 46-65 (1972).

In Vitro Phagocytosis of Respirable-Sized Monodisperse Particles by Alveolar Macrophages*

F. F. HAHN, G. J. NEWTON, and P. L. BRYANT
Inhalation Toxicology Research Institute, Lovelace Foundation for Medical Education and Research, Albuquerque, New Mexico

ABSTRACT

Phagocytosis by alveolar macrophages of particles deposited deep in the lung may play an important role in the ultimate fate of the particles. An in vitro system for studying the phagocytosis of insoluble monodisperse particles by rabbit alveolar macrophages was developed to study the influence of particle size, particle concentration, and incubation time on phagocytosis. Monodisperse ^{169}Yb-labeled fused aluminosilicate particles and $^{239}PuO_2$ particles ranging from 0.30 to 2.2 μm in real diameter (aerodynamic diameter = 0.55 to 3.4 μm) were incubated with alveolar macrophages, the free particles were separated from the ingested ones, and the number of phagocytized particles was determined. Results indicate that the larger particles are taken up more rapidly and in greater numbers than the smaller ones. In addition, greater numbers of the more dense and rapidly settling $^{239}PuO_2$ particles are taken up than fused aluminosilicate particles of the same real diameter. In vitro studies of the handling of respirable particles by alveolar macrophages may aid in determining the relative importance of phagocytosis in the removal of particles from the deep lung.

A large proportion of inhaled particles deposited in the alveoli are phagocytized by alveolar macrophages. The particle-laden macrophages may migrate to the bronchioles, be transported up the airways by mucociliary flow to the pharynx and thus to the gastrointestinal tract, or they may move via the lymphatics to the pulmonary and tracheobronchial lymph nodes. The exact role of the

*Animals were maintained in facilities accredited by the American Association for Accreditation of Laboratory Animal Care.

macrophages in pulmonary clearance of particles is not fully understood.[1,2]

Particle size is an important determinant of the fate of inhaled particulates. The deposition of inhaled particles in the alveoli is dependent on their aerodynamic diameter.[3] Thus a major portion of the particles in the alveoli are in the 0.05- to 5-μm size range. Further, pulmonary clearance of deposited particles such as plutonium dioxide, uranium oxide, and bacterial spores is also dependent to some extent on particle size.[1,2] Particle size is also a factor in phagocytosis as shown in studies with peripheral leukocytes,[4] phagocytes of the liver,[5] and alveolar macrophages.[6] For example, limited studies suggest that the phagocytosis of radiolabeled polystyrene latex particles by rabbit alveolar macrophages in vitro is less for 6-μm particles than for 3- or 1.5-μm particles.[6] Thus size may also be a factor in phagocytosis of particulates, although definitive in vitro studies with alveolar macrophages have not been conducted. The effect of particle size on in vitro phagocytosis by alveolar macrophages is reported here using particle sizes with aerodynamic diameters that are in the respirable range.

MATERIALS AND METHODS

Fused Aluminosilicate Particles

Monodisperse fused aluminosilicate spheres containing ^{169}Yb were produced as previously described.[7,8] Aerosols were generated from a solution of montmorillonite clay in which ^{169}Yb had been incorporated by cation exchange. The resultant aerosol was passed through an 1100°C heating column and then into a Lovelace aerosol particle separator (LAPS), which separated the particles according to their aerodynamic size and deposited them on a foil. Particles from a particular segment of the LAPS foil had aerodynamic sizes that can be described by a log normal distribution with a geometric standard deviation (σ_g) less than 1.12. Real sizes were calculated from the formula

$$Dr = \frac{Da}{[\rho C(Dr)]^{1/2}}$$

where Dr = real diameter
Da = aerodynamic diameter
C = Cunningham's slip correction
ρ = density (aluminosilicate = 2.2 g/cm^3) (PuO_2 = 8 g/cm^3)

Aerodynamic diameters ranged from 0.55 to 3.37 μm and real diameters from 0.35 to 2.21 μm. Particles used in the phagocytosis

studies were resuspended from the foils in 0.1*N* ammonium hydroxide using ultrasonic agitation. They were relatively insoluble glasslike spheres.

$^{239}PuO_2$ Particles

Monodisperse particles of $^{239}PuO_2$ were made by previously described techniques.[8,9] Aerosols were generated from a solution of plutonium hydroxide in 0.6*N* HCl, passed through two heating columns, maintained at 300 and 1100°C, and collected with a LAPS. The aerodynamic diameters of the particles used were 0.88, 1.62, and 2.12 μm (σ_g = <1.1), and the real diameters were calculated to be 0.30, 0.56, and 0.74 μm, using the density of $^{239}PuO_2$ = 8 g/cm^3. These particles were relatively insoluble and relatively regular in shape. The characteristics of both types of particles are summarized in Table 1.

Alveolar Macrophages

Macrophages were obtained by physiologic saline lavage of excised lungs from New Zealand white rabbits (Keen Ridge Rabbitry, Edgewood, New Mexico) weighing 1.5 to 3.0 kg. Stained smears were made of the lavaged cells, and any samples with more than 15 red blood cells per 100 white blood cells were discarded. Total cell numbers obtained with three lavages of each rabbit ranged from 10^7

TABLE 1

PARTICLE CHARACTERISTICS

Type	Real diameter, μm	AMAD,* μm	Volume, μm^3	Surface area, μm^2	Mass, g/particle	Settling velocity in water, cm/min
Fused aluminosilicate (ρ† = 2.3 g/cm^3)	0.35	0.55	0.034	0.38	5.16×10^{-14}	0.0005
	0.67	1.03	0.157	1.41	3.62×10^{-13}	0.0019
	0.97	1.49	0.478	2.95	1.09×10^{-12}	0.0039
	1.34	2.05	1.26	5.64	2.90×10^{-12}	0.0073
	2.02	3.08	4.32	12.80	9.93×10^{-12}	0.0173
	2.21	3.37	5.65	15.34	1.30×10^{-11}	0.0208
$^{239}PuO_2$ (ρ = 8.0 g/cm^3)	0.30	0.88	0.014	0.28	1.13×10^{-13}	0.0023
	0.56	1.62	0.092	0.99	7.36×10^{-13}	0.0072
	0.74	2.12	0.212	1.72	1.70×10^{-12}	0.0125

*AMAD = activity median aerodynamic diameter.

†ρ = density.

to 10^8 as quantitated using hemocytometer counts; the percentage of macrophages was 96 to 100. Viability of the cells, as determined by the trypan blue dye exclusion method was 92 to 100%. Lavage cells were washed three times by centrifugation and resuspended in medium consisting of Eagle's Minimal Essential Medium (Gibco) enriched with 20% fetal calf serum, 100 units of penicillin–streptomycin, and 200*mM* of glutamine. The same medium was used for all test procedures.

Phagocytic Test Procedures

Particles and cells in 1.0 ml of medium were incubated in a 15-ml plastic centrifuge tube (Falcon Plastics) at 37°C. Triplicate samples were incubated in each test run. At the end of the prescribed time, the samples were cooled in an ice bath, and the particle-laden cells were separated from the free particles by placing the medium over a 30% Ficoll solution in a centrifuge tube. The time for centrifugation varied, depending on the size and density of the particle employed. Each time was calculated and confirmed experimentally and ranged from 4 to 16 hr. After centrifugation, the gradient was removed in three equal layers and each was evaluated for radioactivity. Tubes containing particles only and tubes containing particles and cells served as controls. They were placed in ice at the time of initiation of incubation (0 hr).

Samples containing ^{169}Yb-labeled particles were counted in an auto-gamma counter (Nuclear Chicago). Samples containing plutonium were filtered through a 0.3-μm Millipore filter, sandwiched with zinc sulfide crystals, and counted on a laboratory-constructed zinc sulfide photomultiplier alpha counter.

Calculation of Data

The phagocytosis percentage was determined by the following formula:

$$\frac{[(B_{exp} - A_{exp}) - (B_0 - A_0)] \times 100}{C} = \% \text{ phagocytosis}$$

where A = radioactivity in top third layer
B = radioactivity in middle third layer
C = radioactivity in the bottom third layer of the "particle only" tube
0 = zero time
exp = time after incubation

Absolute numbers of particles ingested were calculated from the net activity in the middle layer and the specific activity of the particles.

RESULTS

Initially, tests were performed to assess the reliability of the methods used. The questions addressed included viability of cells, loss of radioactivity during the course of the experiment, and solubility of the radioactivity in the particles. Viability tests showed that 90 to 95% of the cells were alive after incubation. Pipettes and incubation tubes were analyzed for radioactivity at the end of several tests to determine loss of radioactivity during transfer procedures. Although some activity was lost, it was relatively uniform in all groups. The total radioactivity recovered from each tube was also uniform, again indicating that losses of radioactivity were random in all groups and were less than 15%. The top fraction was filtered through a 0.3-μm Millipore filter to determine whether the radioactivity in that fraction was associated with particles. Most activity passed through the filter, indicating that the activity was in a soluble form and not associated with suspended particles. Autoradiographic electron micrographs of cells from the middle layer showed that particles were ingested (Fig. 1).

The uptake of aluminosilicate particles with increasing time of incubation is shown in Fig. 2. With all four particle sizes, the uptake continues throughout the 5-hr incubation period but tends to lessen at the longer incubation times with the exception of the 0.35-μm particles. In subsequent experiments to compare the effect of particle size on numbers of particles ingested and on the uptake rate, an incubation period of 3 hr was used.

The comparison of uptake rates for different aluminosilicate particle sizes at varied particle concentration is shown in Fig. 3. It shows that the uptake rate is greatest for the 2.02-μm particles and least for the 0.35-μm particles, which indicates that the macrophages have more affinity for the larger particles than the smaller ones.

The effect of particle size on phagocytosis can be seen in Fig. 4. As the particle size increases, the number of particles taken up increase through the size range examined (R_D = 0.35 to 2.2). Included in the plot are both fused aluminosilicate particles and $^{239}PuO_2$ particles. The correlation coefficient for the line through all these points is relatively low, 0.83, compared to that for aerodynamic diameter. The data for $^{239}PuO_2$ fall above the line indicating that, for a given real diameter, more plutonium particles than fused aluminosilicate particles are ingested. If these data are

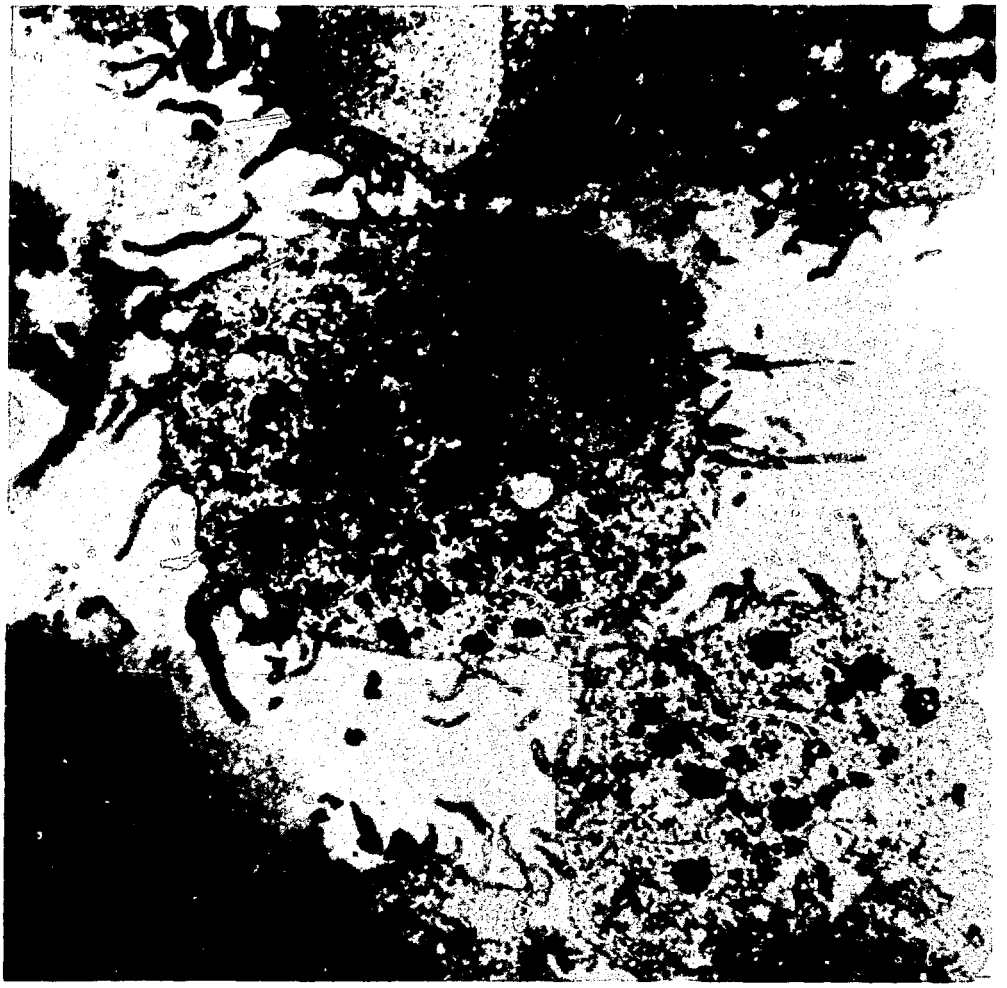

Fig. 1 Autoradiographic electron micrograph of a $^{239}PuO_2$ particle ingested by a rabbit alveolar macrophage.

compared on the basis of aerodynamic diameter, however, instead of real diameter (Fig. 5), a line can be fitted to the data with a correlation coefficient of 0.95, suggesting a relation to density, the main variant between $^{239}PuO_2$ and aluminosilicate particles.

DISCUSSION

The size of a particle has an effect on phagocytosis of that particle, at least in vitro. The number of ingested particles is directly proportional to the size of the particle within the range of 0.30 to 2.2 μm. A similar relation has been shown with the ingestion of

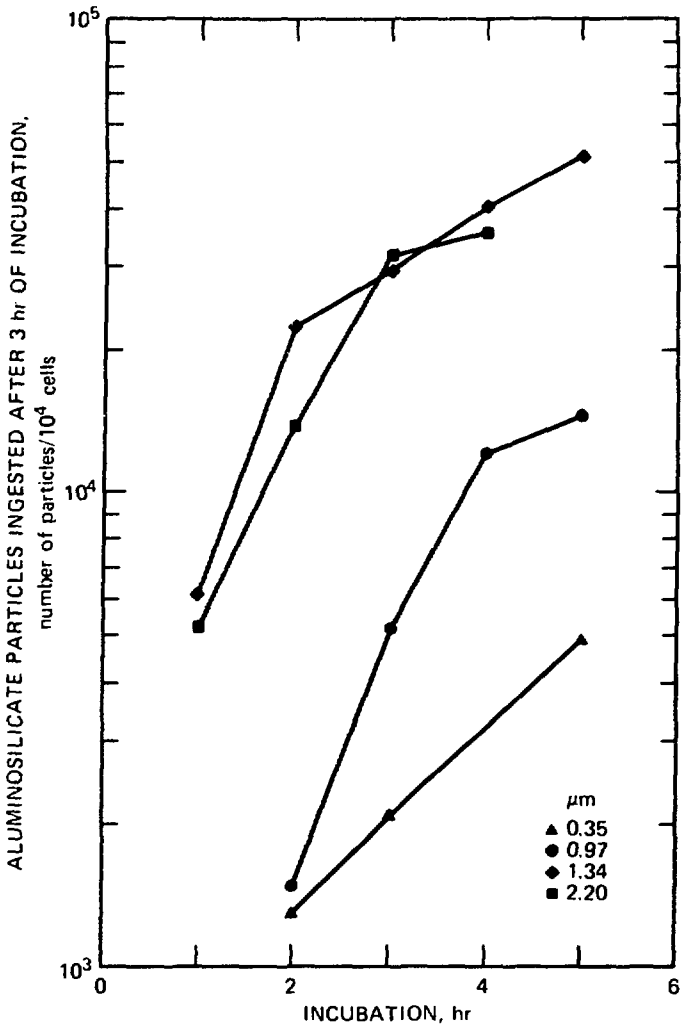

Fig. 2 Uptake of fused aluminosilicate particles by rabbit alveolar macrophages.

0.088- to 1.2-μm latex particles by human neutrophils in vitro.[4] Particles that are 0.26 μm in size or smaller showed scant evidence for ingestion. A difference in the clearance from the blood for 0.51- and 1.17-μm latex particles has also been demonstrated.[5] When injected intravenously, the larger particles were removed from the circulation more rapidly and to a greater extent by the reticuloendothelial cells of the liver and spleen of rabbits.

The degree of in vitro phagocytosis of 1.5-, 3.0-, and 6.0-μm polystyrene particles by rabbit alveolar macrophages has also been reported.[6] Although there were a small number of experiments, they

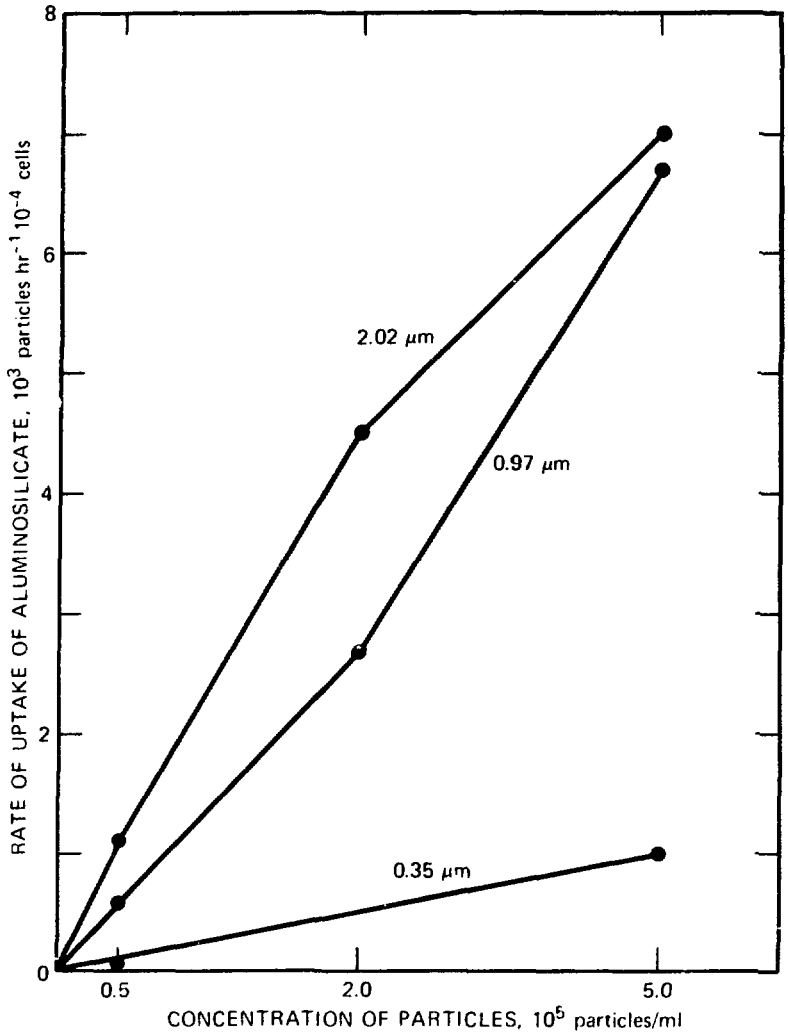

Fig. 3 Uptake rates of fused aluminosilicate particles by rabbit alveolar macrophages.

tended to show that the 6-μm particles were not ingested to the same extent as the 1.5-μm particles. Although it may seem that this result is opposite to ours, one must consider the possibility that there is some particle size at which phagocytosis is optimum and that the direct proportional relation between increasing numbers of ingested particles cannot extend to very large particles. The lower level of phagocytosis of 6-μm particles by rabbit alveolar macrophages[6] indicates that the optimum size is lower than 6 μm. Studies of phagocytosis of cultured spleen cells suggest that dust particles larger than 8 μm are poorly phagocytized.[10]

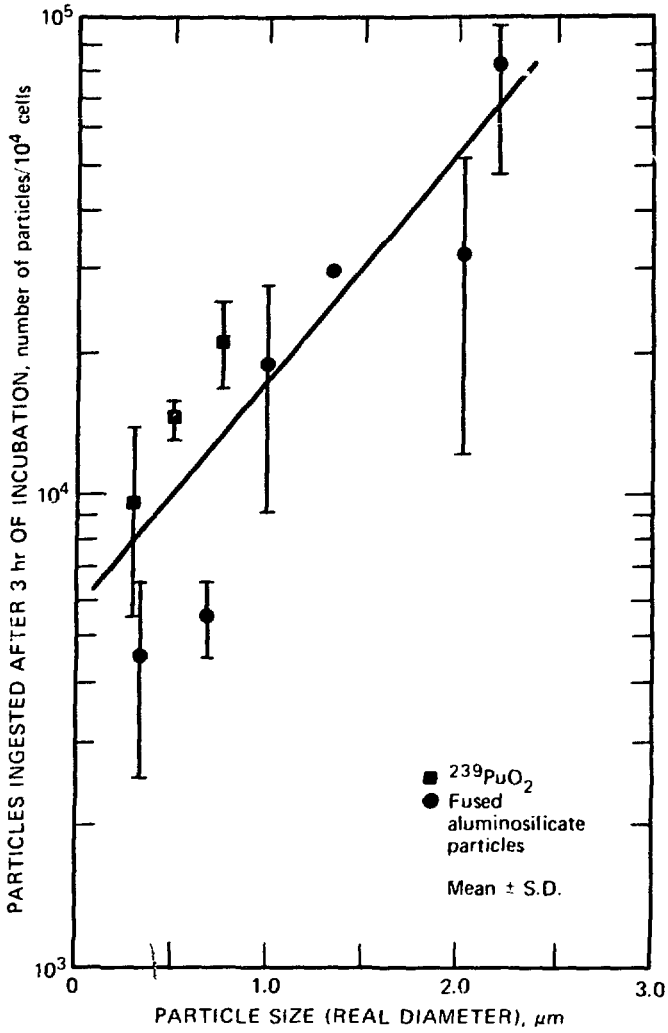

Fig. 4 Effect of particle size (real diameter) on uptake by rabbit alveolar macrophages. S. D. = standard deviation.

The number of particles phagocytized correlates best with the aerodynamic diameter. The other particle parameters examined were real diameter, volume, surface area, mass, and settling velocity. The significance of the correlation between aerodynamic diameter and particle uptake is speculative. It may indicate that the settling velocity of the particle is a factor in this test system since the calculations for settling velocity and aerodynamic diameter both include a factor for the density of the particle. The settling velocity cannot be the only factor, however, since there is a poor correlation between settling velocity alone and particle uptake.

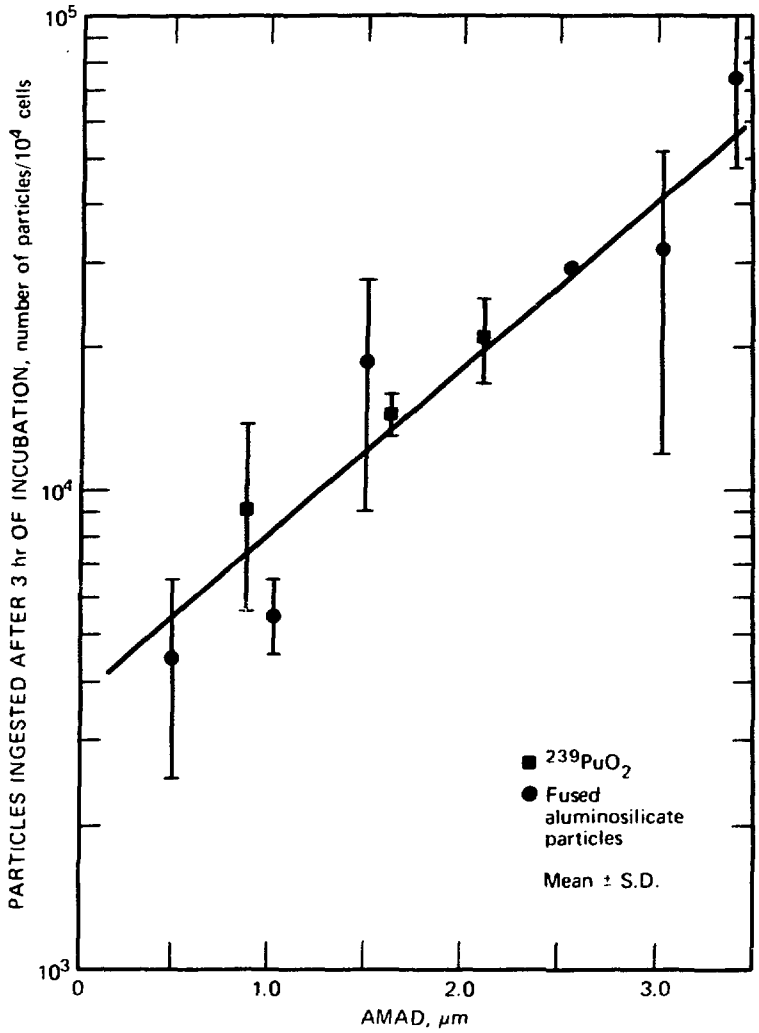

Fig. 5 Effect of particle size (aerodynamic diameter) on uptake by rabbit alveolar macrophages. S. D. = standard deviation.

Further experiments using different physical parameters in the incubation period are required to separate the influence of settling velocity on the number of particles taken up. These additional experiments will also help clarify the optimum size of particles for phagocytosis.

The greater uptake of plutonium particles than aluminosilicate particles of the same real diameter may be due to the chemical or surface differences between the two, or it may be an artifact of the test system. It has been shown that alveolar macrophages in vitro take up carbon,[11] aluminum, or chromium particles better than silver, manganese, or uranium-coated particles.[12] In addition, the

differences in phagocytosis were most pronounced when serum was added to the medium, and the indication was that the ability to bind some serum factor(s) was important in phagocytosis. In the same system, beryllium-coated particles were cytotoxic to the macrophages.[13] The differences in settling velocity of aluminosilicate and plutonium particles may also explain the differences in uptake between these two types of particles. As mentioned previously, additional experiments using different physical parameters during incubation are necessary to eliminate settling velocity as a factor.

The reason for the increase in numbers of particles taken up with increased particle size is also speculative. Previous studies with *Acanthaemoeba* have shown that the kinetics of phagocytosis of latex beads is a function of bead mass or volume.[13] The data indicated that the beads were bound to or accumulated at the cell surface until an optimum volume, approximately the same for all sizes (0.126 to 2.68 μm), was reached, at which time the beads were ingested. Although our study did not show such a relation to particle mass, the kinetics of uptake of aluminosilicate or PuO_2 particles must be related to the selectivity of, or ingestion sites on, the macrophage surface. The macrophage cell membrane has been shown to be a highly organized structure with specific sites reserved for specific functions.[14,15]

These studies do indicate that there are differences in the uptake of respirable-sized particles by alveolar macrophages, and this fact should be considered in studies of the removal of particles from the deep lung.

ACKNOWLEDGMENTS

The work is supported by contract No. EY-76-C-04-1013 between the Lovelace Biomedical and Environmental Research Institute and the Energy Research and Development Administration.

REFERENCES

1. L. F. Casarett, *Essays in Toxicology*, Vol. 3, pp. 1-36, Academic Press, New York, 1972.
2. P. E. Morrow, Alveolar Clearance of Aerosols, *Arch. Intern. Med.*, 131: 101-108 (1973).
3. Task Group on Lung Dynamics: Deposition and Retention Models for Internal Dosimetry of the Human Respiratory Tract, *Health Phys.*, 12: 173-208 (1966).

4. L. J. Krenis and B. Strauss, Effect of Size and Concentration of Latex Particles on Respiration of Human Blood Leucocytes, *Proc. Soc. Exp. Biol. Med.*, 107: 748-750 (1961).
5. M. D. Schoenberg et al., Proliferation of the Reticuloendothelial System and Phagocytosis, *Exp. Mol. Pathol.*, 2: 126-143 (1963).
6. B. Holma, Lung Clearance of Mono- and Di-Disperse Aerosols Determined by Profile Scanning and Whole-Body Counting: A Study on Normal and SO_2 Exposed Rabbits, *Acta Med. Scand. (Suppl)*, 473: 1-102 (1967).
7. O. G. Raabe, G. M. Kanapilly, and G. J. Newton, New Methods for Generation of Aerosols of Insoluble Particles for Use in Inhalation Studies, in *Inhaled Particles III*, Proceedings of an International Symposium, British Occupational Hygiene Association, W. H. Walton (Ed.), London, 1971, Vol. 1, pp. 3-18, Unwin Bros. Ltd., Surrey, England.
8. P. Kotrappa and C. J. Wilkinson, Measurement of the Specific Radioactivity with Respect to Particle Size for Labeled Aerosols, *J. Aerosol Sci.*, 3: 167-171 (1972).
9. O. G. Raabe, H. A. Boyd, G. M. Kanapilly, C. J. Wilkinson, and G. J. Newton, Development and Use of a System for Routine Production of Monodisperse Particles of $^{238}PuO_2$ and Evaluation of Gamma-Emitting Labels, *Health Phys.*, 28: 655-667 (1975).
10. K. W. Jotten and C. Marwyck, The Phagocytosis of Industrial Dusts in Tissue Culture, *Br. J. Ind. Med.*, 9: 173-179 (1952).
11. P. Camner, P. A. Hellstrom, and M. Lundborg, Coating 5 μm Particles with Carbon and Metals for Lung Clearance Studies, *Arch. Environ. Health*, 27: 331-333 (1973).
12. P. Camner, M. Lundborg, and P. A. Hellström, Alveolar Macrophages and 5 μm Particles Coated with Different Metals, *Arch. Environ. Health*, 29: 211-213 (1974).
13. R. A. Weisman and E. D. Korn, Phagocytosis of Latex Beads by Acanthaemoeba 1. Biochemical Properties, *Biochemistry*, 6: 485-497 (1967).
14. M. Tsan and R. D. Berlin, Effect of Phagocytosis on Membrane Transport of Nonelectrolytes, *J. Exp. Med.*, 134: 1016-1035 (1971).
15. F. M. Griffin and S. C. Silverstein, Segmental Response of the Macrophage Plasma Membrane to a Phagocytic Stimulus, *J. Exp. Med.*, 139: 323-336 (1974).

The Fate of Inhaled Asbestos Fibers Deposited in the Rat Lung: A Quantitative Approach

A. MORGAN, A. HOLMES, and R. J. TALBOT
Environmental and Medical Sciences Division, Atomic Energy Research Establishment, Harwell, England

ABSTRACT

Radioactive asbestos was administered to rats by inhalation for 40 min. After exposure, the animals were sacrificed serially and the lungs were subjected to bronchopulmonary lavage. Initial washes were made with a balanced salt solution that removed free fiber and cells from the conducting airways. Subsequent washes were made with physiological saline which recovered cells that were originally present in the alveolar spaces. The number of cells and the amount of fiber recovered in each wash were measured. About 20 μg of fiber was deposited in the lung and appeared to have no significant effect either on the number of free cells in the lung or on their size. Uptake of fiber by alveolar macrophages was effectively complete after 24 hr. Analysis of the results suggests that fibers that are much longer than the diameter of the alveolar macrophage (~12 μm) find their way into the alveolar wall from where they cannot be recovered by lavage. This process is complete within 2 weeks of exposure. The techniques described enable alveolar macrophages with given dust loadings to be recovered from the lung either for study in vitro or for isolation of the associated fiber for characterization by electron microscopy.

The health hazards to humans of occupational exposure to airborne asbestos are well established and include (1) asbestosis, (2) bronchogenic carcinoma, and (3) mesothelial tumors of the pleura and peritoneum. It is perhaps the last of these which gives rise to most concern at the moment since it appears that tumors of this type can be initiated by relatively small doses of fiber and also because they have a long induction period. Examination of lung tissue with the electron microscope[1] showed that more fibers were present in tissue from patients with mesothelioma than in corresponding samples from nonmesothelioma cases. In addition it was noted that fibers of

amphibole asbestos predominate in such cases. In animal experiments, however, in which various types of fibers were administered to rats by intrapleural inoculation,[2] it appeared that chrysotile asbestos could be as effective as amphibole in producing mesothelial tumors. Stanton and Wrench[3] have shown that, in addition to asbestos, fine fibrous glass will also induce mesothelial tumors when introduced into the pleural cavity.

Both epidemiological evidence and the results of animal experiments indicate that thin fibers are more effective than thick ones in inducing mesothelial tumors, and crocidolite (blue) asbestos appears to be particularly potent, possibly because its characteristic fiber diameter is less than that of other amphiboles such as amosite and anthophyllite. Timbrell, Griffiths, and Pooley[4] pointed out that crocidolite mined in the Northwest Cape region of South Africa has an intrinsically smaller fiber diameter than crocidolite from the Transvaal and that this difference may account for the higher incidence of mesothelial tumors in miners from the former region. Clearly, thin fibers have a lower terminal velocity than thick ones and will remain airborne longer. These investigators also postulate that, when inhaled, the thin crocidolite fibers from the Northwest Cape region will reach the periphery of the lung more efficiently than the thicker fibers characteristic of Transvaal crocidolite.

In our own laboratory work with tagged asbestos and autoradiographic techniques [5,6] has demonstrated that asbestos fibers of all varieties are deposited relatively uniformly in the alveolar region of the rat lung. Some months after exposure, however, it is apparent that the fiber remaining in the lung is transported not only to tracheobronchial lymph nodes but also to subpleural foci. Examination of corresponding areas of stained sections shows that these foci consist of groups of alveoli which are filled with histiocytic cells and that nodular fibrosis originates in the same areas. This peripheral movement is not confined to asbestos but has also been observed for plutonium dioxide in the dog[7] and in man[8] and for beryllium in hamsters and rats.[9] It is suggested that this peripheral movement of fibers in the lung is likely to be a more significant factor in the etiology of mesothelial tumors than variations in deposition pattern. It seems probable that the route by which fiber is transported to the periphery of the lung is within the alveolar wall rather than over its surface.

The work described here is in the nature of a preliminary investigation to see how tracer techniques can be combined with bronchopulmonary lavage to study the uptake of asbestos by the alveolar macrophage, the rate of transfer of fiber to the interstitium,

and the significance of fiber dimensions and dosage on lung transport phenomena.

MATERIALS AND METHODS

Preparation of Tagged Asbestos

The asbestos sample used in this experiment was a synthetic nickel chromium fluoramphibole with composition Na_2O, 3 NiO, 2 CrO, 8 SiO_2, F_2. This has a count median diameter of 0.27 μm which falls within the range of the natural amphiboles. The count median length is 5.8 μm. We used this material in our investigation because a relatively high specific activity can be induced with short reactor-irradiation times, but the same procedure can be applied to natural amphiboles. After 2 days of irradiation in the Harwell DIDO reactor (2×10^{14} neutrons cm^{-2} sec^{-1}), the specific activities of ^{51}Cr and ^{58}Co are about 0.2 and 0.02 μCi/mg of fiber, respectively. This enables 0.01 μg of fiber to be quantified nondestructively in tissue samples.

Administration of Tagged Fiber

Fourteen male albino rats, about 5 months old, were exposed in two groups in the type of chamber described by Evans et al.[10] Only the noses of the rats were exposed to the dust cloud. The dust concentrations in the chamber during exposure of both groups were monitored by continuous sampling on Whatman GF/A filters. The time-integrated concentration of airborne fiber in the first experiment was 20.1 and in the second, 17.6 μg $liter^{-1}$ hr^{-1}, so that similar amounts of dust should have been deposited in both exposures.

Lung Lavage

After exposure, one animal from the first group was killed immediately by ether anesthesia and exsanguinated by cutting the dorsal aorta. The trachea was severed just below the larynx, the lungs were dissected out, and the heart, thymus, and any fat were carefully removed. The lungs were washed with saline, dried, weighed, and gamma counted to determine their asbestos content. The bronchopulmonary lavage procedure used was based on that described by Brain and Frank.[11] The trachea was cannulated with the sleeve of an Abocath-G-14 catheter, the lungs were immersed in saline at 37°C, and a negative pressure of 7 in. water gage was applied for 1 min. Eight milliliters of Tyrode's balanced salt solution (BSS) at 37°C was instilled over 1 min., the lungs were massaged gently for 30 sec to

ensure that all lobes were inflated, and the fluid was withdrawn over 30 sec by applying slight suction. This procedure was repeated three further times with BSS and then ten times with physiological saline (PS) at 37°C. The first two washes (1A and 1B) were collected in tared polystyrene containers which were then weighed to determine the volume of fluid recovered. Subsequent washes were combined in pairs (numbered 2 to 7) and the combined volumes measured in the same way. The washes and lavaged lungs were gamma counted immediately to determine their fiber content. The washes were stored in ice until the cell concentrations had been measured. Before the cell concentrations were estimated, the containers were shaken gently to resuspend any cells adhering to the walls. Three replicate cell counts were made on each wash with a Fuchs-Rosenthal hemocytometer (volume, 1.8 mm^3). Free cells were virtually all larger than 10 μm in diameter and could readily be distinguished from red cells in the few instances where the latter were present in small numbers. The mean diameter of a number of cells was measured in selected washes by using a calibrated curtain micrometer eyepiece.

Measurement of Radioactivity

The radioactivity of all tissue samples and washes was measured by gamma counting between two coaxial NaI(Tl) detectors (15 cm ϕ x 7.5 cm). To determine the amount of fiber in any sample, we compared its radioactivity with that of an appropriate standard containing a known weight of irradiated fiber in solution and counted at the same time.

RESULTS AND DISCUSSION

Table 1 gives the times at which the rats were killed, their weights at the time of exposure and at death, their lung weights and the amount of fiber in the lungs before washing and recovered by lavage. It can be seen that the animals continued to gain weight after exposure and that there was no increase in the relative weight of lung. About 20 μg of fiber was deposited in the lower respiratory tract (i.e., alveolar region and smaller conducting airways). The total numbers of free cells recovered from the experimental animals are also included in the table.

Recovery of Free Cells

The numbers of free cells recovered in washes 1A, 1B, and subsequent combined washes are shown in Fig. 1. Included for

TABLE 1

BODY AND LUNG WEIGHTS OF THE EXPERIMENTAL ANIMALS, NUMBER OF FREE CELLS, AND WEIGHT OF FIBER PRESENT IN AND RECOVERED FROM THE LUNGS

Rat No.	Time of death	Body weight, g		Weight of lungs		Weight of fiber, μg		Free cells recovered × 10^6
		Exposure	Death	Grams	Percent of body weight	In lung	Recovered	
1	5 min	360	360	1.70	0.47	15.0	9.0 (60)*	8.7
2	2 hr	358	358	1.51	0.42	26.4	16.4 (62)	8.6
3	3.5 hr	363	363	1.74	0.48	23.4	15.6 (67)	9.8
4	4 hr	341	341	1.57	0.46	25.2	15.3 (61)	8.4
5	1 day	341	341	1.52	0.45	16.5	9.3 (57)	8.2
6	1.2 day	378	378	1.77	0.47	10.0	5.0 (50)	8.1
7	2 days	333	333	1.50	0.45	20.3	8.3 (41)	5.4
8	7 days	334	343	1.57	0.46	10.6	5.5 (52)	8.6
9	9 days	340	352	1.58	0.45	14.6	6.6 (45)	9.0
10	17 days	329	354	1.59	0.45	15.5	7.3 (47)	10.6
11	28 days	345	390	1.68	0.43	9.1	4.3 (48)	10.2
12	50 days	343	387	1.64	0.42	8.5	2.7 (32)	7.0
13	91 days	344	421	1.66	0.39	3.6	1.3 (36)	6.0

*Numbers in parentheses are percentages.

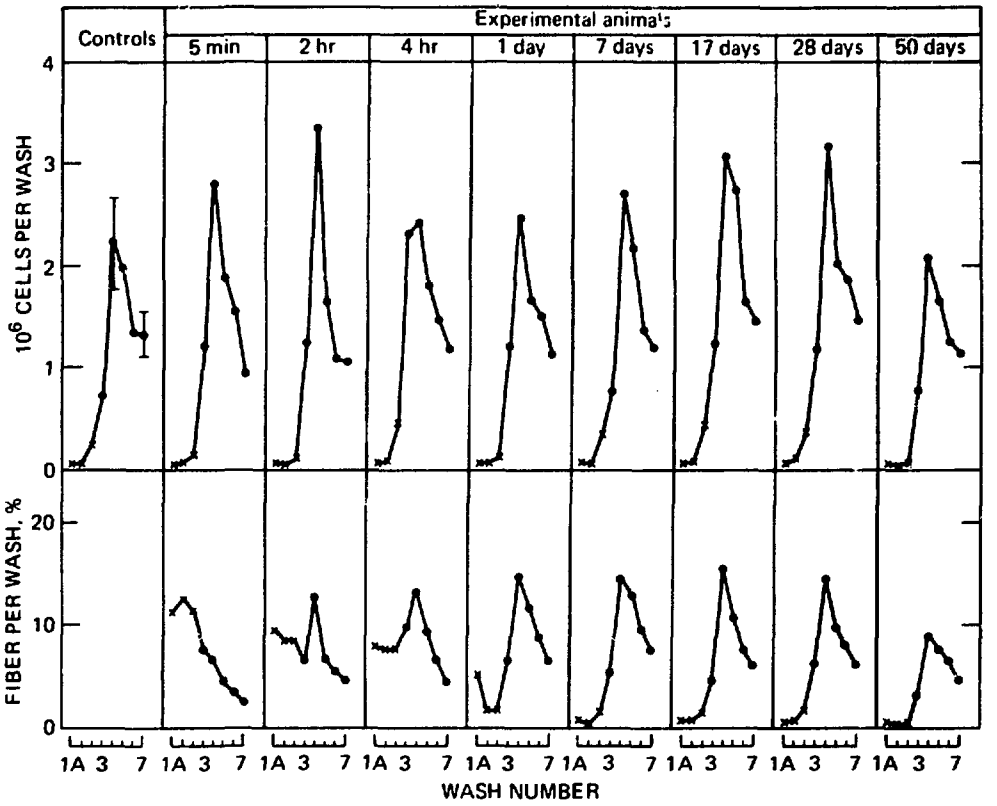

Fig. 1 Recovery of free cells from control and experimental animals and of fiber from experimental animals. Results for individual washes from selected animals are indicated. X, balanced salt solution (BSS). ●, physiological saline (PS).

comparison are the mean results obtained from four unexposed control rats from the same group of animals killed at various times over the duration of the experiment. The patterns of free cell recovery were similar in both experimental and control animals in that few cells were recovered with BSS; but on changing to PS the numbers increased, generally reaching a maximum in the fourth (combined) wash and then declining. This observation is in agreement with that of Brain and Frank[11] who suggested that Ca^{2+} and Mg^{2+} cations influence the forces that cause free cells to adhere to the alveolar wall. In the absence of the divalent cations, it appears that free cells tend to round up and detach themselves from the wall and may thus be recovered by lavage. The total numbers of free cells recovered from rats killed at various times after exposure are shown in Fig. 2. An average recovery of 8.5 (±1.4) x 10^6 was obtained, which does not differ significantly from the mean for the four controls, i.e., 7.9 (±2.3) x 10^6. Examination of histological sections

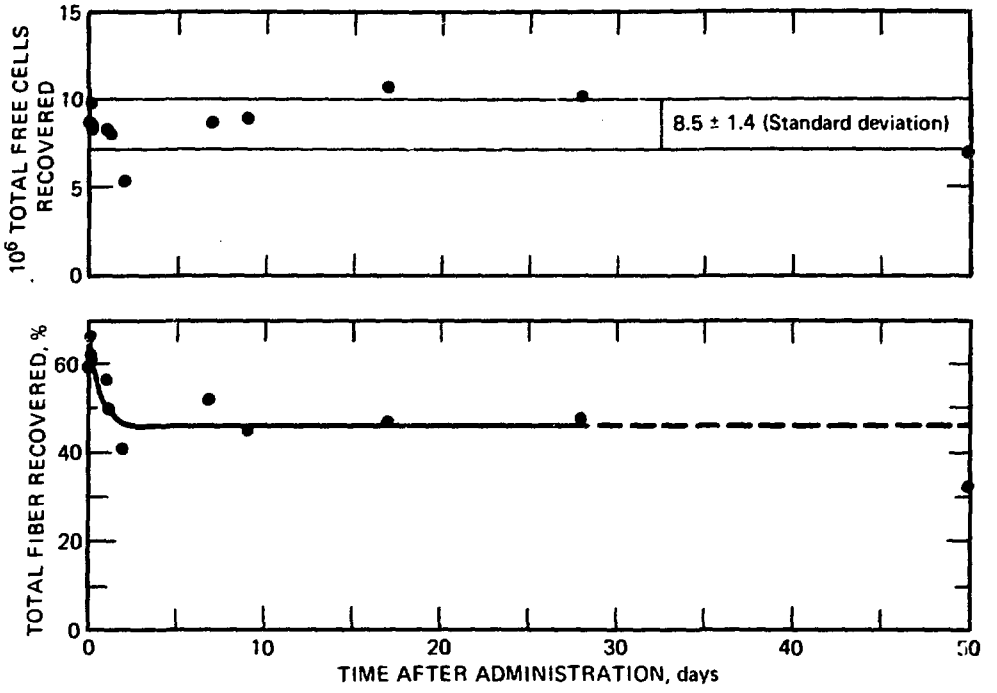

Fig. 2 Total recovery of cells and of fiber from all experimental animals. The dashed line indicates extrapolation for the period between 30 and 50 days.

prepared from lavaged lungs showed that slight damage to the structure of the alveoli was invariably present, and it appeared that the highest recovery of free cells was obtained from lungs in which the damage was minimal. It could also be seen in such sections that no free cells remained on the bronchial epithelium of lavaged lungs but that considerable numbers of rounded-up cells were still present in the alveolar spaces. Brain[12] reported that there was a significant increase in the number of alveolar macrophages recovered from the rat lung following the administration of milligram quantities of various dusts by intratracheal injection, the maximum response being observed after 1 day. In our study, however, there was no evidence to suggest that deposition of 20 μg of fluoramphibole in the lung resulted in any change in the number of free cells.

Size of Free Cells

Brain and Frank[11] reported that cells recovered with BSS tended to be larger and to have more inclusions and vacuoles than cells recovered with PS. They suggested that free cells recovered with BSS may include older macrophages, which have a relatively weak attachment to

the alveolar surface, as well as cells in the mucus carpet in the airways. Our results described later confirm that free cells recovered in the later PS washes are representative of those present in the alveolar spaces, while it seems likely that those in the conducting airways are washed out in the initial BSS washes. In Fig. 3 the size distributions of cells recovered in wash 1A (BSS) and wash 4 (PS) are compared for both the controls and selected experimental animals. Generally in the fourth wash, at least 40% of the cells fell within the 12- to 13-μm size range and few cells exceeded 15 μm in diameter. For cells recovered in wash 1A, the frequency of the smaller cells was reduced, and a higher proportion of cells exceeded 15 μm in diameter. In general, the mean diameter of cells recovered in wash 1A was about 1 μm greater than that of cells in wash 4 which fact confirmed the observation of Brain and Frank. An average dust loading of about one picogram of fiber per cell does not appear to have produced a significant change in the size of free cells recovered either from the airways or from the alveolar spaces.

Recovery of Fiber

The recovery of fiber in each wash, expressed as a percentage of the lung content prior to lavage, is included in Fig. 1. For the rat killed immediately after exposure, the amount of fiber recovered in combined washes (2 to 7 inclusive) declined exponentially. This is shown in Fig. 4 from which it can be seen that there is only a slight indication of an excess of fiber in wash 4, which contained the greatest number of free cells. It is clear that at this time (i.e., 45 min after the start of exposure) very little of the fiber deposited in the lung had been taken up by the free-cell population. Two hours later, however, there was a peak in fiber recovery in wash 4, which showed that a significant fraction of the deposited dust was now associated with free cells. After 24 hr, with the exception of wash 1A, the patterns of cell and fiber recovery were very similar, showing that by this time virtually all the fiber was associated with cells. The excess of fiber in wash 1A can be attributed to the fact that material deposited in the smaller conducting airways is not completely cleared for at least 48 hr and that this is mainly recovered in the initial wash. The total amount of fiber recovered is shown in Fig. 2. Initially between 60 and 70% of the fiber in the lung was recovered. After 48 hr this had fallen to between 40 and 50%, and there was no evidence of any further reduction for at least 1 month. The initial fall in recovery can be attributed to the clearance of fiber deposited in the conducting airways. It is also likely that free fiber can be

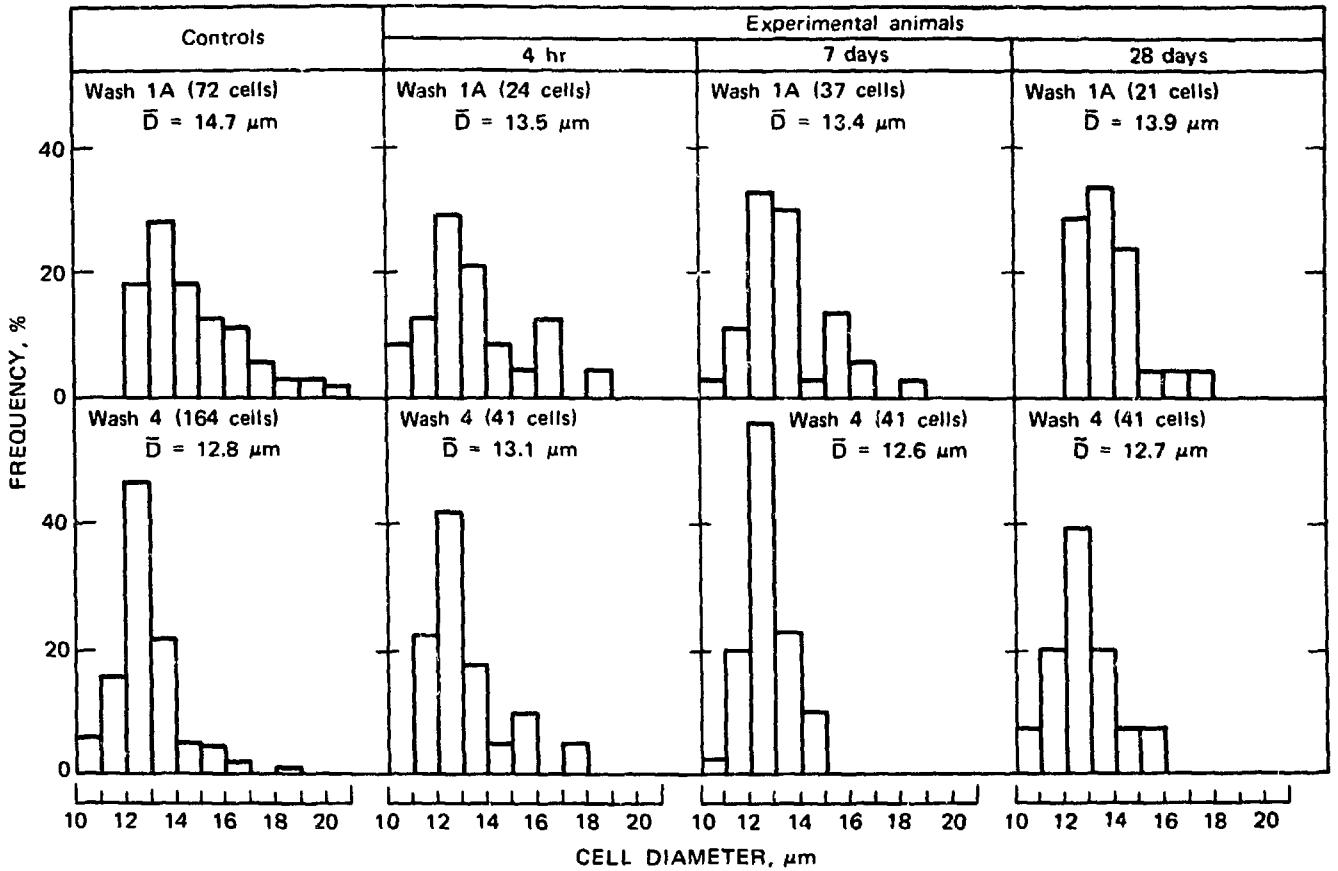

Fig. 3 Diameter of cells recovered in wash 1A (balanced salt solution) and wash 4 (physiological saline). Measurements for controls and selected experimental animals are indicated. $\bar{D}$, average diameter.

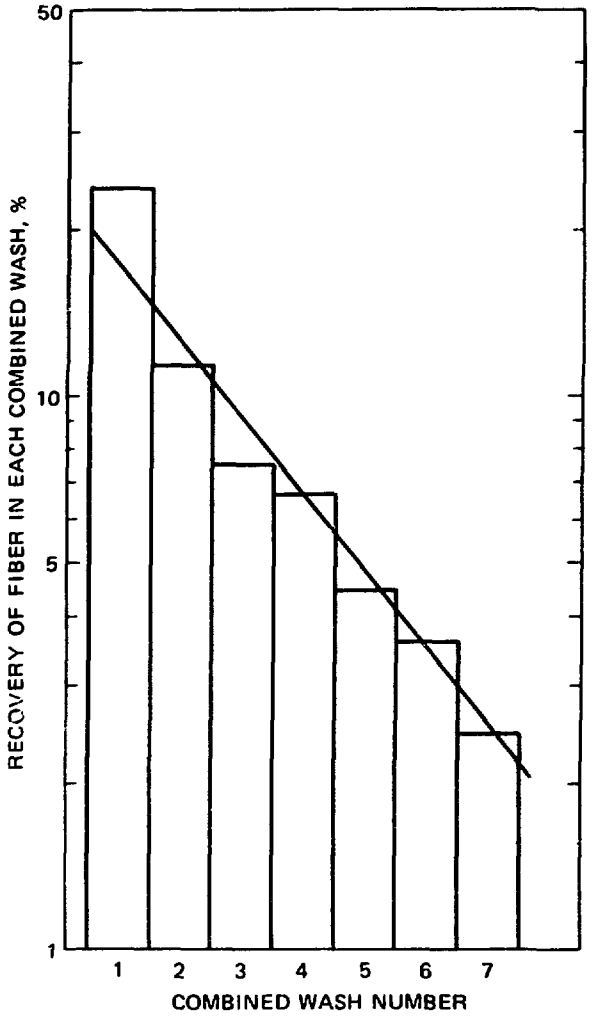

Fig. 4 Recovery of fiber from the lungs of the rat killed 5 min after the termination of exposure.

recovered from the lung more efficiently than fiber contained in free cells.

As shown in Fig. 5, the mean dust content of the free cells rapidly reached a peak value of a little over 1 pg and then declined, as dust-containing cells were removed from the lungs via the airways and replaced with dust-free cells. The fall in the mean dust content of the free cells, over a period of 2 months, can be expressed in terms of a single exponential expression with a half-time of about 30 days. The scatter in the results is due to inevitable variations in the amounts of dust deposited in the different animals during exposure.

To examine the relationship between cell and fiber recovery more closely and to eliminate variations in the dust content of cells

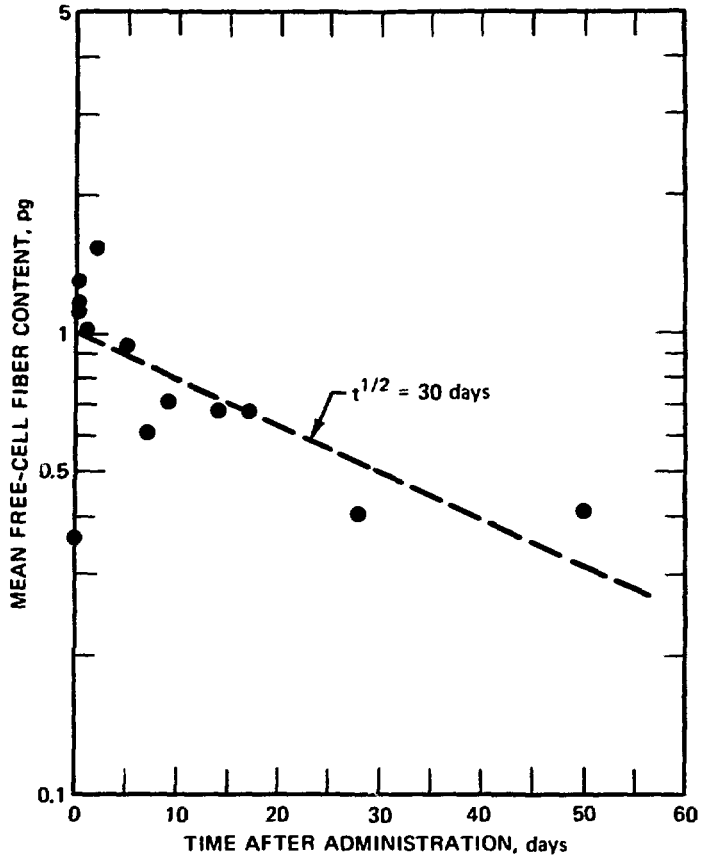

Fig. 5 Mean fiber content of cells recovered in washes 4 to 7 from all experimental animals.

caused by differences in dose, we calculated the *relative* fiber content per cell for each wash by dividing the amount of fiber present (expressed as a percentage of the lung content before lavage) by the corresponding number of free cells. Values for the relative fiber contents of cells recovered in washes from selected animals are shown in Fig. 6. For rats killed shortly after exposure, the relative dust content of cells in the initial BSS washes was very high because of the small number of cells recovered and the presence in these washes of free fiber from the alveolar spaces in addition to fiber deposited in the conducting airways. As free fiber was taken up by cells and the airways were cleared by mucociliary action, the relative dust loading of cells in the initial BSS washes declined. The relative dust content of cells recovered in washes 4 to 7 inclusive was quite constant for each animal, which indicated that the cells were derived from the alveolar spaces. As would be expected, the mean relative dust content of these cells increased initially as the fiber was taken

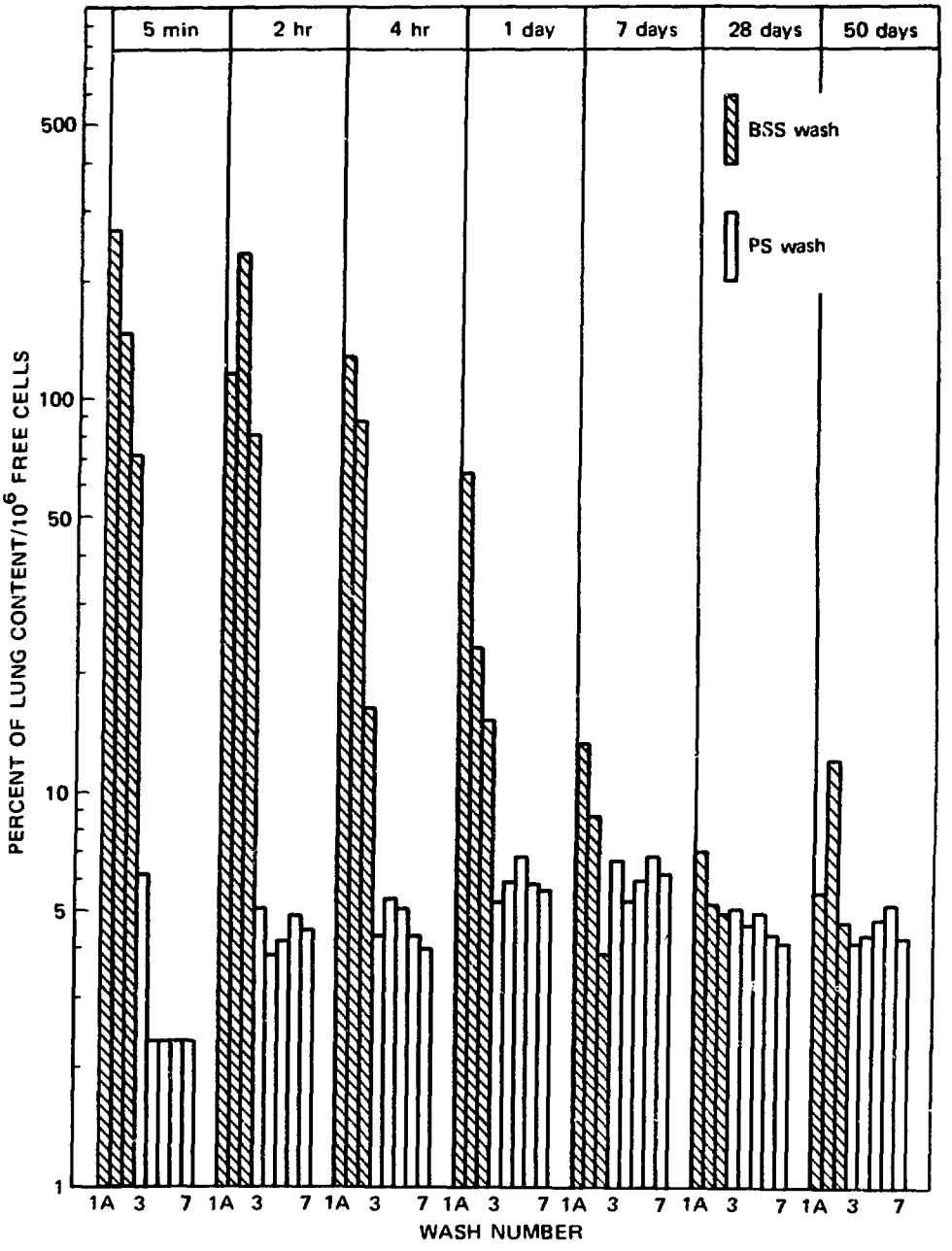

Fig. 6 Relative fiber content of cells recovered in all washes from selected experimental animals.

up. The maximum relative dust loading depends upon the number of free cells in the lung. In the strain of rats used, the maximum relative dust loading observed in a number of experiments was about 7×10^{-6}% per cell. If all the fiber in the lungs at this time is

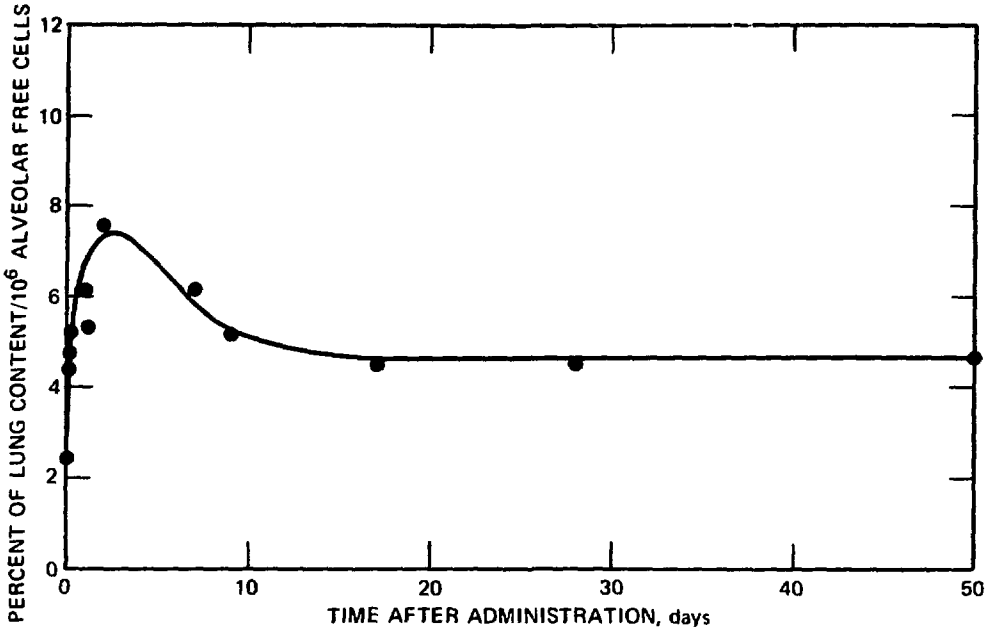

Fig. 7 Mean relative fiber content of cells recovered in washes 4 to 7 for all animals.

associated with the free-cell population, the reciprocal of this number multiplied by 10^2 would be equal to the total number of free cells (i.e., about 14×10^6 for these animals).

Once all the fiber had been taken up by the free cells, their relative mean dust content should remain constant provided (1) there is no transfer of fiber to the alveolar wall and (2) there is no change in the total number of free cells. In Fig. 7 the mean relative dust content of alveolar-derived cells is plotted against time after exposure. It can be observed that the mean relative dust content declined over a period of about 2 weeks after reaching its peak; it then remained relatively constant at about 70% of the maximum value. This fall implies either that there was an increase in the free-cell population (which is not borne out by the results presented in Fig. 1) or that some of the fiber present initially in the free cells was no longer available for recovery at later times. Examination of free cells under the optical microscope showed that shortly after exposure many were impaled upon fibers whose length was considerably greater than the diameter of the alveolar macrophage. After 2 weeks, however, very long fibers were not seen in lung washings. It is suggested that the fall in the relative dust loading of the free cells was due to the loss to the alveolar wall of fibers that were too long to be engulfed by single macrophages. In support of

this it can be stated that in similar experiments with the UICC (Union Internationale Contre le Cancer) standard reference samples of asbestos, which have a shorter fiber-length distribution, the fall in relative dust loading was much less marked. Techniques are being developed to measure with the electron microscope the fiber-length distribution of fiber in lung washes. If the median length of fibers recovered in wash 4 diminishes with time after exposure, this finding should confirm that the longer fibers are being transferred to the alveolar wall more efficiently than the short ones.

CONCLUSIONS

The work described above is in the nature of a preliminary study to assess the potential of tracer techniques and of bronchopulmonary lavage for investigating the fate of fiber deposited in the rat lung. It was possible to show that 20 μg of a synthetic fluoramphibole deposited in the lung had no significant effect either on the total number of free cells (which in these animals was about 14×10^6) or upon their size. It appeared that fibers that were too long (>15 μm) to be contained within free cells were transferred to the alveolar wall over a period of about 2 weeks. The technique described will be exploited to study further the effects of fiber length and dose upon the distribution of fiber between the free-cell population and the interstitium. It also enables free cells to be recovered from the alveolar spaces with precisely known dust loadings for study in vitro or for isolation of the associated fiber for characterization by electron microscopy.

ACKNOWLEDGMENTS

The authors gratefully acknowledge the support of the Institute of Occupational and Environmental Health (Montreal) and contract 127-74-1 ENV UK of the European Economic Community (EEC) Environmental Research Programme.

REFERENCES

1. F. D. Pooley, Mesothelioma in Relation to Exposure, in *Biological Effects of Asbestos*, Proceedings of a Working Conference, Lyon, 1972, pp. 222-225, IARC Scientific Publication No. 8, International Agency for Research on Cancer, Lyon, 1973.
2. J. C. Wagner, G. Berry, J. W. Skidmore, and V. Timbrell, The Effects of the Inhalation of Asbestos in Rats, *Brit. J. Cancer*, 29: 252-269 (1974).

3. M. F. Stanton and C. Wrench, Mechanisms of Mesothelioma Induction with Asbestos and Fibrous Glass, *J. Nat. Cancer Inst.*, 48: 797-821 (1972).
4. V. Timbrell, D. M. Griffiths, and F. D. Pooley, Possible Biological Importance of Fiber Diameters of South African Amphiboles, *Nature (London)*, 232: 55-56 (1971).
5. A. Morgan, J. C. Evans, R. J. Evans, R. F. Hounam, A. Holmes, and S. G. Doyle, Studies on the Deposition of Inhaled Fibrous Material in the Respiratory Tract of the Rat and Its Subsequent Clearance Using Radioactive Tracer Techniques. II. Deposition of the UICC Standard Reference Samples of Asbestos, *Environ. Res.*, 10: 196-207 (1975).
6. A. Morgan, J. C. Evans, and A. Holmes, Deposition and Clearance of Inhaled Fibrous Minerals in the Rat. Studies Using Radioactive Tracer Techniques, in *Inhaled Particles IV*, Symposium Proceedings of a British Occupational Hygiene Society Symposium, Edinburgh, 1975, Pergamon Press, Inc., New York, 1977.
7. W. J. Clarke and W. J. Bair, Plutonium Inhalation Studies. VI. Pathologic Effects of Inhaled Plutonium Particles in Dogs, *Health Phys.*, 10: 391-398 (1964).
8. G. Voelz, J. Umbarger, J. McInroy, and J. Healy, Considerations in the Assessment of Plutonium Deposition in Man, in *Diagnosis and Treatment of Incorporated Radionuclides*, Symposium Proceedings, Vienna 1975, pp. 163-175, International Atomic Energy Agency, Vienna, (1976) (STI/PUB/411).
9. C. L. Sanders and W. C. Cannon, Toxicology of High-Fired Beryllium Oxide Inhaled by Rodents. I. Metabolism and Early Effects, *Arch. Environ. Health*, 30: 546-551 (1975).
10. J. C. Evans, R. J. Evans, A. Holmes, R. F. Hounam, Diane M. Jones, A. Morgan, and M. Walsh, Studies on the Deposition of Inhaled Fibrous Material in the Respiratory Tract of the Rat and Its Subsequent Clearance Using Radioactive Tracer Techniques. I. UICC Crocidolite Asbestos, *Environ. Res.*, 6: 180-201 (1973).
11. J. D. Brain and R. Frank, Alveolar Macrophage Adhesion: Wash Electrolyte Composition and Free Cell Yield, *J. Appl. Physiol.*, 34: 75-80 (1973).
12. J. D. Brain, The Effects of Increased Particles on the Number of Alveolar Macrophages, in *Inhaled Particles III*, W. H. Walton (Ed.), Vol. I, pp. 209-223 Symposium Proceedings, London, September 16—23, 1970, Unwin Brothers Limited, Surrey, England, 1971.

CONF-760927--2

Life History of Plutonium Dioxide in the Lung: From Macrophage to Carcinoma

C. L. SANDERS, R. R. ADEE, K. RHOADS, and R. M. MADISON
Biology Department, Battelle, Pacific Northwest Laboratories, Richland, Washington

ABSTRACT

The pulmonary macrophage exerts a large influence on the distribution of alpha energy from inhaled $^{239}PuO_2$, whereas the pulmonary epithelium serves as the prime "target" cell for neoplastic transformation. In the rat, of the total radiation energy absorbed in the lung, about 80% is delivered to the alveolar septae, 19% to the vascular tissues, and less than 1% to the bronchial epithelium. Of the radiation energy delivered to the alveolar septae, about 10% is absorbed by alveolar epithelium, 10% by macrophage, 10% by endothelium, and 70% by other cellular and noncellular elements. Both the type 2 alveolar epithelium and the bronchiolar epithelium serve as the probable cells of origin for induced adenocarcinoma.

Common mechanisms of lung clearance are involved in determining the fate of inhaled particulates with solubility and intrinsic properties of the particulate being the most significant determinants of toxicity to pulmonary cells. Plutonium-239, which has a physical half-life of 24,400 years and emits 5.1-MeV alpha particles, is the most common plutonium isotope present in nuclear reactor fuel. Plutonium dioxide (PuO_2) is the most common chemical form for ^{239}Pu. This report will attempt to describe the life history of inhaled $^{239}PuO_2$ particles in rats, tracing the fate of inhaled particles from their deposition to the development of pulmonary tumors.

The PuO_2 particles used in these studies were prepared by calcination of plutonium oxalate at either 300 or 700°C. No difference in fate of inhaled $^{239}PuO_2$ was noted between the two calcination temperatures. The larger PuO_2 particles were removed by sedimentation, and the smaller particles were aerosolized. In vitro ultrafiltra-

tion studies and in vivo lung clearance and translocation studies of inhaled $^{239}PuO_2$ in rats clearly demonstrate the relatively insoluble nature of inhaled $^{239}PuO_2$ particles.[1] The $^{239}PuO_2$ aerosol was delivered, nose only, to female albino rats for 30 to 60 min when the animals were about 70 days of age. The exposure techniques have been described.[2] The PuO_2 particles were heterodisperse in size and exhibited count median diameters of about 0.2 μm and activity median aerodynamic diameters of about 2.5 μm. The size distributions were usually log-normal. After suspension in water for over a year, $^{239}PuO_2$ particles did not lose their characteristic X-ray-diffraction patterns.

Alpha particles emitted by ^{239}Pu exhibit an average linear energy transfer of about 100 keV/μm, with alpha particles traveling about 48 μm in tissue of density 1. Alpha particles will travel considerably longer distances and expose much larger numbers of cells in lung than in solid tissue because of intervening air spaces in alveoli and bronchioles.

Clearance of particles from the lung is essential for protection of the lung from the external environment. The pulmonary macrophage system constitutes the major defense mechanism for the removal of inhaled particles deposited in the alveoli. Pulmonary macrophages are active phagocytic cells that are derived from circulating monocytes that probably originate from the bone marrow.[3,4]

The phagocytosis of inhaled $^{239}PuO_2$ by pulmonary macrophages is rapid, occurring within a few hours after inhalation.[5] X-ray diffraction with high-voltage electron-microscopy and electron-microscopic autoradiography has been used to identify and localize inhaled $^{239}PuO_2$ in macrophages and other pulmonary cells.[6,7] The particles are localized within phagolysosomes of macrophages.

Studies using pulmonary lavage and autoradiography of cells isolated from lavages have shown that about 75% of initial alveolar deposition of $^{239}PuO_2$ was present in pulmonary macrophages during the first few weeks after inhalation.[5] Initial alveolar depositions of greater than 50 to 100 nCi ^{239}Pu resulted in early toxicity to macrophages and differences in lung clearance as compared to lower alveolar depositions. At depositions of less than 50 to 100 nCi ^{239}Pu, plutonium particles were not concentrated in individual macrophages. At these lower depositions, the retention half-time for ^{239}Pu in macrophages was about 50 days. A net decrease in macrophage numbers, indicative of cytotoxicity of ^{239}Pu to macrophages, was seen several months after exposure.[8] However, pulmonary macrophages appear to be relatively radioresistant to the effects of ^{239}Pu as compared to other pulmonary cell types.[9]

Plutonium particles that were not phagocytized by pulmonary macrophages were found within the attenuated cytoplasmic arms of type 1 alveolar epithelium during the first few hours to days after inhalation exposure.[10] The mechanism of engulfment of PuO_2 by type 1 alveolar epithelium and its ultimate fate are not known. Type 2 alveolar epithelium contained no engulfed PuO_2. Type 2 alveolar epithelium is thought to be responsible for the production of pulmonary surfactant, which is thought to originate from lamellar, osmiophilic, cytoplasmic inclusions.[11] Once having engulfed PuO_2 particles, type 1 alveolar epithelium may round up and become type 2 cells, finally desquamating from the basement membrane of the alveolar septae. These cells are then cleared from the lung like a macrophage.[12]

Less than 1% of the initial alveolar deposition of ^{239}Pu is found in pulmonary lymph nodes by 30 days after exposure.[13] This indicates that few naked PuO_2 particles or particles within macrophages are penetrating lymphatic endothelium, possibly near terminal bronchioles, and finding their way to pulmonary lymph nodes.

Initially, about 75% of inhaled $^{239}PuO_2$ particles are found in pulmonary macrophages, and most of the retaining particles are found in type 1 alveolar epithelium; less than 1% appear in pulmonary lymph nodes during the first few weeks after exposure.

The clearance of inhaled $^{239}PuO_2$ particles from the alveoli is biphasic (Fig. 1). During the first phase about 75% of deposited ^{239}Pu is cleared from the lung with a half-life of about 30 days. During the second phase the remaining 25% of deposited ^{239}Pu is cleared from the lung with a half-life of about 250 days (Ref. 1). The first clearance phase probably represents removal of PuO_2-laden macrophages from the lung. The much more prolonged retention of ^{239}Pu in the second clearance phase may be due to several factors, perhaps the most important being the engulfment of PuO_2 particles by type 1 alveolar epithelium. Other factors may include cytotoxicity to pulmonary macrophages from phagocytized $^{239}PuO_2$ particles[14-16] and concentration of particles in subpleural and peribronchiolar regions of the lung.[17]

The determination of relevant radiation-dose parameters has been a difficult problem in studies of pulmonary carcinogenesis from inhaled $^{239}PuO_2$. The changing position of the particles in relation to the target cells that are transformed into tumors is caused by (1) inspiration—expiration breathing cycle, which results in inflation and contraction of the alveoli many times a minute; (2) movement of pulmonary macrophages and other pulmonary cells with engulfed $^{239}PuO_2$ particles; cellular infiltrates, such as are seen following in-

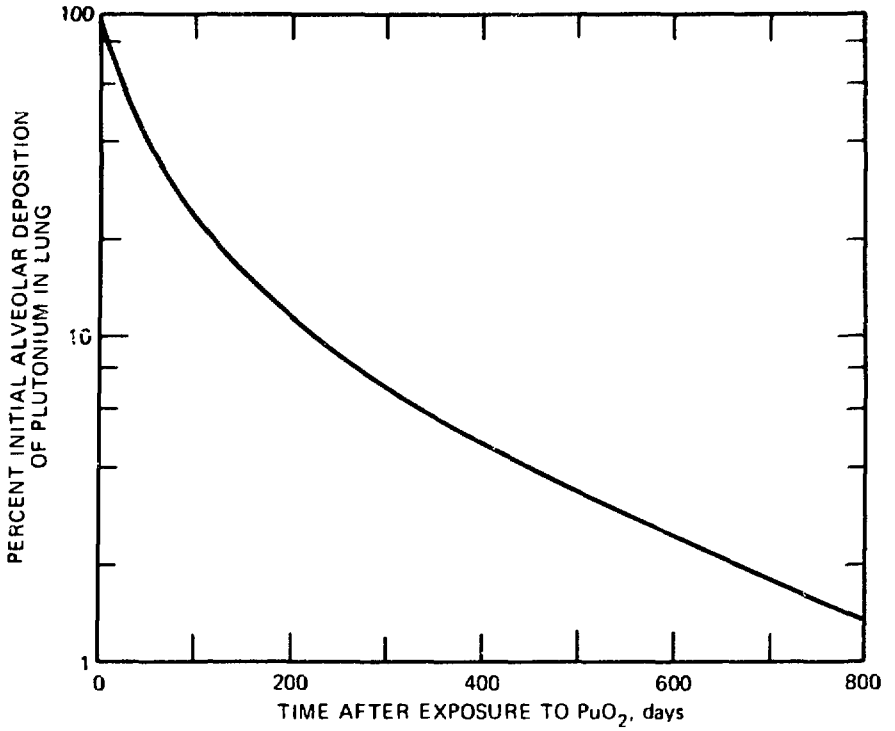

Fig. 1 Alveolar clearance for inhaled $^{239}PuO_2$.

flammation in the lung after PuO_2 inhalation; and (4) cell turnover of target cells either under normal conditions or abnormally during hyperplasia or metaplasia. The varying changing penetration distances of the alpha emissions and the changing linear energy transfer along the Bragg curve further complicate the microdosimetry pattern.

The volume distribution of plutonium in pulmonary tissues was determined at both the light- and electron-microscopic levels with morphometric techniques.[18,19] Lungs were fixed under 20-cm inflation pressure prior to embedding and sectioning. Of the total energy deposited in the alveolar region of the lung from inhaled $^{239}PuO_2$ particles, about 80% is initially absorbed by the alveolar septae, 20% by the vascular areas, and less than 1% by the bronchiolar epithelium. Of the 80% delivered to the alveolar septae, a large part is delivered to the confines of the alveolus containing the PuO_2 particle. With the use of a hybrid computer model of the alveolar region in the lung of rat, it was shown that 60% of the alpha energy was absorbed in the confines of one alveolus when the $^{239}PuO_2$ particle was free within the alveolar air space. The absorbed alpha energy in the alveolus increased to 70% when the same particle was placed

within a pulmonary macrophage of 13-μm diameter.[20] A similar computer method has been used for morphometric studies in human lung.[21] On the basis of the extent of phagocytosis of inhaled $^{239}PuO_2$ particles and the distribution of alpha energy, we can estimate that the average pulmonary macrophage receives about 10% of the total alveolar radiation energy during the first several weeks after exposure, even though the macrophage accounts for only about 1% of the mean alveolar volume (Table 1). At an initial alveolar deposition of 10 nCi ^{239}Pu, only about 10% of the macrophages have

TABLE 1

TISSUE DISTRIBUTION OF ALVEOLAR TISSUE OF UNEXPOSED RATS*

Component	Fraction of total alveolar volume (X 100), %
Alveolar Epithelium	14 ± 3
Type 1	11 ± 2
Type 2	3 ± 2
Interstitium	32 ± 6
Capillary endothelium	13 ± 3
Capillary space	40 ± 7
Alveolar macrophage	1 ± 1

*A morphometric analysis was performed on electron micrographs at a 5300 X magnification with the use of three thin sections per animal and six micrographs per section. Values are reported as mean volume fractions ± standard deviation (%) of total alveolar volume for seven rats.

phagocytized particles.[5] Thus the radiation dose is concentrated only in those macrophages which have phagocytized plutonium particles.

The alveolar epithelium (both types 1 and 2) accounts for 14% of the mean alveolar volume (Table 1). However, because the type 1 epithelium engulfs fewer $^{239}PuO_2$ particles than does the pulmonary macrophage and because the type 2 epithelium does not engulf particles, it is probable that the initial alpha-energy absorption by alveolar epithelium was less than its mean volume fraction of total alveolar tissue. We have estimated this initial alpha absorption as 10% of that delivered to the alveoli, with a larger fraction going to type 1 cells than to type 2 cells.

The capillary endothelium accounts for 13% of the mean alveolar volume (Table 1) but does not appear to retain $^{239}PuO_2$ particles for any length of time since they have not been microscopically

observed in these cells. However, the capillary endothelium should receive an appreciable early radiation dose because of its proximity to $^{239}PuO_2$-laden macrophages and type 1 epithelium. We have estimated that about 10% of the initial alveolar radiation energy is delivered to endothelial cells. The remaining 70% of radiation dose, not absorbed by macrophages, alveolar epithelium, or endothelium, is absorbed by other cellular and noncellular elements in the alveolar septae.

We estimate that, of the total alpha energy deposited from inhaled $^{239}PuO_2$ in the alveolar region of the lung, 80% is initially delivered to the alveolar septae, 20% to the blood vessels, and less than 1% to the bronchiolar epithelium. Of the energy absorbed by the alveolar septae, 10% is initially absorbed by macrophages, 10% by alveolar epithelium, with type 1 epithelium receiving proportionately more dose than type 2 epithelium, 10% by capillary endothelium, and 70% by other septal elements. This energy distribution changes with time at high deposition levels. However, autoradiograms of lung at depositions of about 50 nCi or less do not show an obvious redistribution of PuO_2 particles. The total number of PuO_2 particles does markedly decrease with time. However, their relative distribution within the lung remains unchanged at low to moderate depositions.

Inhaled plutonium is a strong carcinogen in the lungs of rats.[1,22-25] Squamous cell carcinoma and hemangiosarcoma are tumors seen mostly at high radiation doses,[1] both being induced by inhaled $^{239}PuO_2$ at a slower rate than is adenocarcinoma (Fig. 2). Both squamous cell carcinoma and hemangiosarcoma require sufficient numbers of deposited $^{239}PuO_2$ particles to cause subpleural concentration of particles, which results in subpleural and to a lesser degree peribronchiolar fibrosis in these areas of concentration. Squamous cell carcinomas are preceded by squamous cell metaplasia in regions of alveolar fibrosis.[1,17]

The major concern with respect to extrapolation to man is at lower radiation doses where there is limited or no apparent subpleural concentration of $^{239}PuO_2$ particles and no fibrosis over large areas of the lung. The lung-tumor type seen almost exclusively at low radiation doses is the adenocarcinoma (Table 2), which is induced at a faster rate than the other tumor types. A similar pattern has been seen in rats given lower doses of inhaled $^{238}PuO_2$ particles and following inhalation of ^{238}Pu from crushed $^{238}PuO_2$ microspheres. Plutonium-238 is not concentrated in subpleural regions, and the alpha activity for ^{238}Pu is more uniformly distributed in the lung than that for PuO_2. Squamous cell carcinoma and heman-

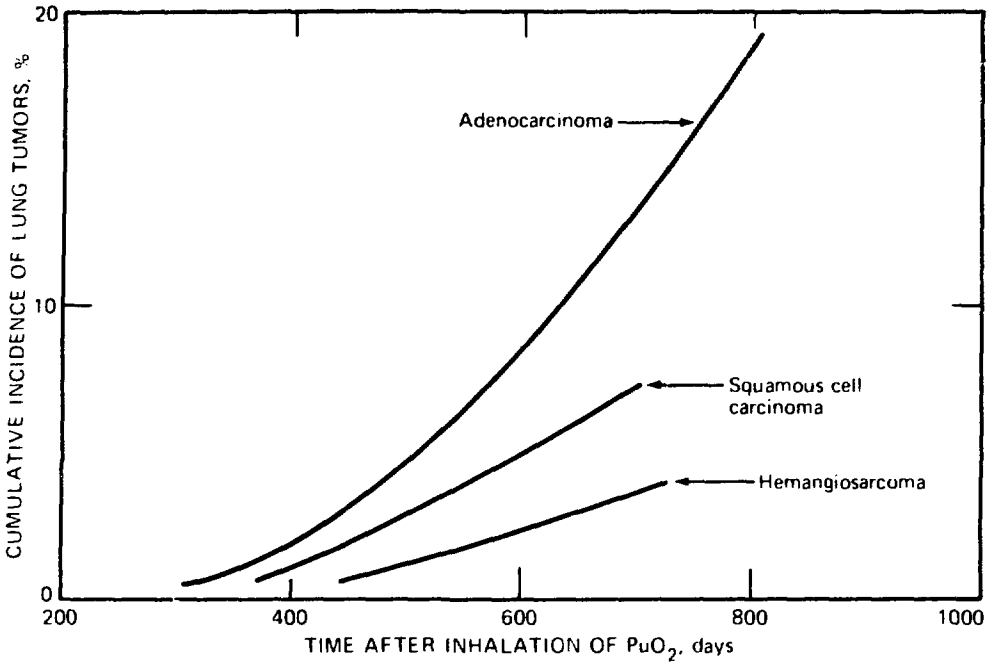

Fig. 2 Cumulative incidences of pulmonary adenocarcinoma, squamous cell carcinoma, and hemangiosarcoma for rats exposed to inhaled $^{239}PuO_2$. Data includes 56 lung tumors induced in 181 rats with initial alveolar deposition of 5.0 nCi, 45 nCi, or 180 nCi ^{239}Pu. Data were taken from Table 2 and Ref. 1.

TABLE 2

INCIDENCE OF LUNG TUMORS AS RELATED TO RADIATION DOSE DELIVERED TO LUNG FROM INHALED $^{239}PuO_2$*

Cumulative dose to lung,† rads	Number of rats	Incidence of pulmonary tumors		
		Total	Adenocarcinoma	Others
0	48	0	0	0
10	131	1.5	0.8	0.8
27 ± 12	51	7.8	3.9	3.9
78 ± 17	26	34.6‡	30.8‡	3.8
255 ± 132	38	44.7‡	36.8‡	7.9
680 ± 120	16	31.3‡	18.8‡	12.6
2100 ± 1210	18	66.7‡	33.3‡	33.3
>10,000	15	46.7‡	6.7	40.0

*Adapted from Ref. 1.

†At 620 days after exposure; mean ± standard deviation.

‡Significantly greater than control at $P < 0.05$ level using Kolmogorov—Smirnov two-sample test.

giosarcoma are not significant tumor types in the lung following inhalation of alpha-emitting transuranics that give a homogeneous dose pattern and are not concentrated in subpleural regions of the lung.[1,3] Thus, for purposes of hazard evaluation (at much lower doses than those required to induce squamous cell carcinoma), the adenocarcinoma type becomes the tumor type of significance.

Histochemical studies were carried out on 16 lung tumors induced by inhaled $^{239}PuO_2$. Formalin-fixed paraffin sections were stained with hematoxylin and eosin, periodic acid-Schiff with and without predigestion with diastase, Fontana Masson, Verhoeff's elastin, Perl's, or methyl green—pyronin Y stains. Half the lung tumors exhibited extracellular and/or intracellular PAS material that was not removed by diastase. This was evidence that these tumors may have originated from mucin-producing bronchiolar epithelium. Most of the lung tumors appeared to originate from peripheral regions of the lung and were usually well differentiated (Fig. 3). The tumor cells were arranged in a glandular or papillary pattern overlapping bands of collagen and elastin fibers. Iron pigments were more concentrated in necrotic areas of the tumor than in other regions of the lung parenchyma. Ribonucleic acid rich cells were concentrated around the periphery of many tumors.

Several lung tumors have been examined with the electron microscope. Some of the tumors were comprised of cells that contained cytoplasmic, osmiophilic, lamellar inclusions characteristic of type 2 alveolar epithelium (Fig. 4). Similar inclusions are seen in human alveolar cell carcinoma.[26] Hyperplasia and metaplasia of type 2 alveolar epithelium were also commonly observed in the lungs of rats exposed to $^{239}PuO_2$ (Ref. 1). Other tumors contained mucin-like vacuoles and a cytoplasm of low electron density, which are characteristic of bronchiolar epithelium. Desmosomes, which are abundant in human cornified epidermoid carcinoma,[27] were not seen in any of our pulmonary adenocarcinomas. Insufficient numbers of lung tumors have been examined to make a statistical comparison with light-level histochemical studies.

In summary, pulmonary adenocarcinoma is the primary tumor type seen in the lung after moderate to low radiation doses. Histochemical and electron-microscopic evidence indicates both a type 2 alveolar epithelial cell and a bronchiolar epithelial cell origin for adenocarcinomas in the lung.

A radiation dose of 78 rads delivered to the whole lung over a period of 620 days after exposure to inhaled $^{239}PuO_2$ induces a significant incidence of pulmonary adenocarcinoma (Table 2). Yet the bronchiolar epithelium receives a small fraction of the total

Fig. 3 Adenocarcinoma of the lung of a rat following inhalation of $^{239}PuO_2$. (Magnification, 17 X.)

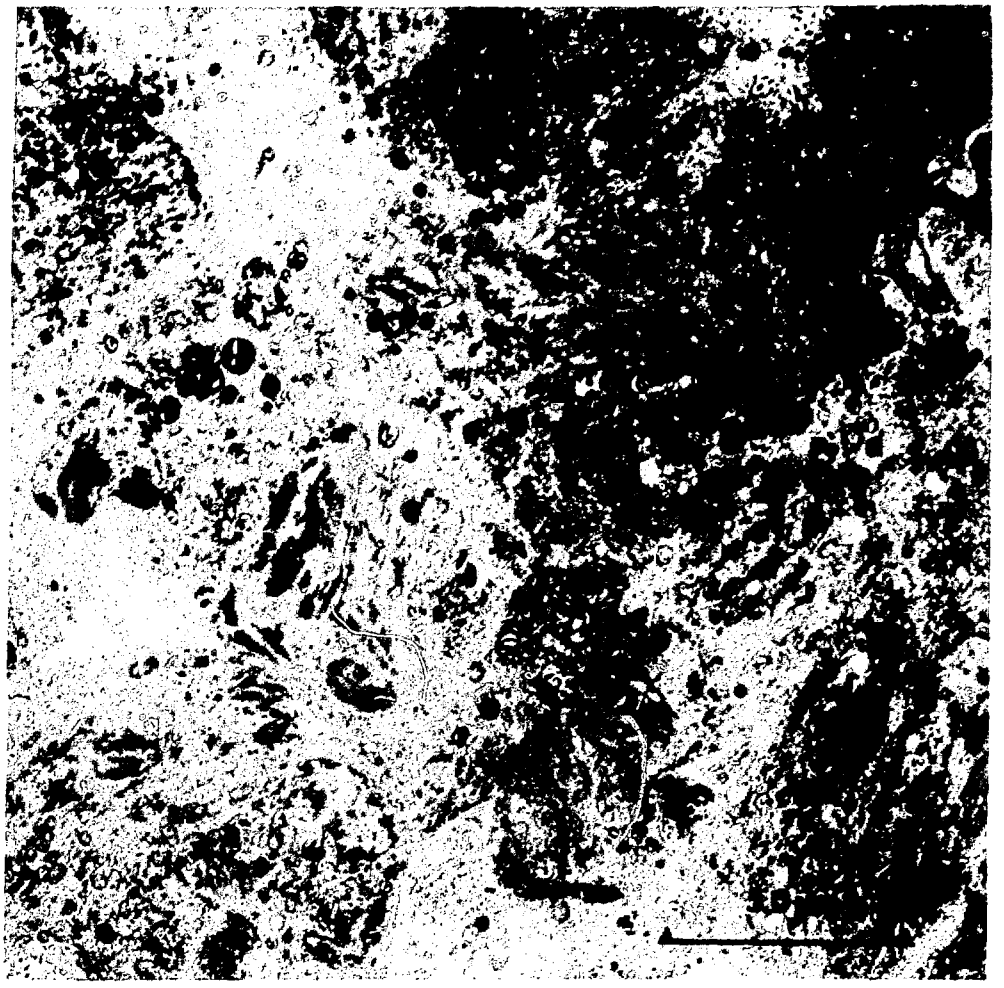

Fig. 4 Electron micrograph of an adenocarcinoma in the lung following inhalation of $^{239}PuO_2$. Note the presence of lamella osmiophilic inclusions in the cytoplasm of the tumor cells.

energy, perhaps less than 1% of the total. Type 2 alveolar epithelium receives a greater fraction, though small, of the total lung energy, amounting to perhaps less than 3% of the total. Can these small amounts of energy cause the cellular evolution needed to transform a normal cell population into a neoplasm? Subpleural and peribronchiolar concentrations of inhaled $^{239}PuO_2$ particles are not apparent at depositions needed to give 78 rads to the lung. Even at radiation doses of 400 rads, only a limited radiation pneumonitis with minimal subpleural concentration of PuO_2 particles is observed. The majority of the lung dose is accumulated during the first few months after exposure. Perhaps it is this early dose that is the most cytotoxic and

carcinogenic in the lung. In any event the total-dose radiation absorbed by all pulmonary epithelial cells is probably substantially less than the dose delivered to the whole lung.

In conclusion, it has been shown that the alveolar macrophage plays a dominant role and type 1 alveolar epithelium a secondary but important role in determining the early dose distribution of inhaled $^{239}PuO_2$ particles. Small fractions of the radiation energy are delivered to the pulmonary epithelial cells, which apparently are the origin of tumors following inhalation of $^{239}PuO_2$ by rats.

ACKNOWLEDGMENT

This paper is based on work performed under Energy Research and Development Administration contract E(45-1):1830.

REFERENCES

1. C. L Sanders, G. E. Dagle, W. C. Cannon, G. J. Powers, and D. M. Meier, Inhalation Carcinogenesis of High-Fired $^{239}PuO_2$ in Rats, *Radiat. Res.*, 68: 349-360 (1976).
2. D. K. Craig and R. L. Buschbom, The Alveolar Deposition of Inhaled Plutonium Aerosols in Rodents, *Am. Ind. Hyg. Assoc. J.*, 36: 172-180 (1975).
3. M. O. Pinkett, C. R. Cowdrey, and P. C. Nowell, Mixed Hematopoietic and Pulmonary Origin of "Alveolar Macrophages" as Demonstrated by Chromosome Markers, *Am. J. Pathol.*, 48: 859-867 (1966).
4. M. Virolainen, Hematopoietic Origin of Macrophages as Studied by Chromosome Markers in Mice, *J. Exp. Med.*, 127: 943-952 (1968).
5. C. L. Sanders, The Distribution of Inhaled $^{239}PuO_2$ Particles Within Pulmonary Macrophages, *Arch. Environ. Health*, 18: 904-912 (1969).
6. R. R. Adee and J. J. Laidler, Subcellular Identification of Exogenous Particles by High-Voltage Electron Microscopy, *Am. Ind. Hyg. Assoc. J.*, 34: 507-511 (1973).
7. R. R. Adee, C. L. Sanders, and J. D. Berlin, Subcellular Localization and Identification of Alpha Emitters by Electron Microscopic Autoradiography, *Health Phys.*, 15: 461-463 (1968).
8. C. L. Sanders, Deposition Patterns and Toxicity of Transuranium Elements in Lung, *Health Phys.*, 22: 607-615 (1972).
9. C. L. Sanders, R. R. Adee, and T. A. Jackson, Fine Structure of Alveolar Areas in the Lung Following Inhalation of 239-PuO_2 Particles, *Arch. Environ. Health*, 22: 525-533 (1971).
10. C. L. Sanders and R. R. Adee, Ultrastructural Localization of Inhaled $^{239}PuO_2$ Particles in Alveolar Epithelium and Macrophages, *Health Phys.*, 18: 293-295 (1970).
11. Y. Kikkawa, E. K. Motoyama, and L. Gluck, Study of the Lungs of Fetal and Newborn Rabbits; Morphologic, Biochemical and Surface Physical Development, *Am. J. Pathol.*, 52: 177-209 (1968).
12. L. J. Casarett and P. S. Milley, Alveolar Reactivity Following Inhalation of Particles, *Health Phys.*, 10: 1003-1011 (1964).

13. C. L. Sanders, Effects of Transuranics on Pulmonary Lymph Nodes of Rodents, in *Radiation and the Lymphatic System*, ERDA Symposium Series, Richland, Wash., Sept. 30—Oct. 2, 1974, J. E. Ballou (Ed.), pp. 225-229, CONF-740930, NTIS, 1976.
14. J. C. Nenot, Study of the Effect of Irradiation on Lung Clearance, in *Inhaled Particles*, Vol. III, W. H. Walton (Ed.), pp. 239-246, Unwin Brothers, Ltd., England, 1972 (in French).
15. R. Masse, Comparative Cytological Study of the Effect of Inhaled Plutonium and Silica on the Behavior of the Alveolar Macrophage, in *Inhaled Particles*, Vol. III. W. H. Walton (Ed.), pp. 247-257, Unwin Brothers, Ltd., England, 1971 (in French).
16. M. Kunzle-Lutz, D. Nolive, G. Petaby, and J. C. Rannaud, Retention and Lung Clearance of Plutonium Dioxide. Structure of Alveolar Macrophages, *Arch. Mal. Prof. Med. Trav. Secur. Soc.*, 31: 185-196 (1970) (in French).
17. C. L. Sanders and G. E. Dagle, Studies of Pulmonary Carcinogenesis in Rodents Following Inhalation of Transuranic Compounds, in *Experimental Lung Cancer: Carcinogenesis and Bioassays*, E. Karbe and J. F. Park (Eds.), Symposium Proceedings, Seattle, Wash., June 23—26, 1974, pp. 422-429, Springer-Verlag, New York, 1974.
18. E. R. Weibel, Morphometric Estimation of Pulmonary Diffusing Capacity. I. Model and Method, *Resp. Physiol.*, 11: 54-75 (1971).
19. E. R. Weibel, Stereological Principles for Morphometry in Electron Microscopic Cytology, *Int. Rev. Cytol.*, 26: 235-302 (1969).
20. P. J. Dionne and C. L. Sanders, A Simulated Model for Determining the Distribution of Alpha Energy in Alveoli from Inhaled Plutonium Particles, USAEC Report BNWL-SA-2282, Battelle, Pacific Northwest Laboratories, NTIS, 1969.
21. R. Johnston, M. D. Levine, and W. M. Thurlbeck, A Computer Model for Counting the Number of Alveoli Per Unit Area of Human Lung Tissue, *IEEE Trans. Bio-Med. Eng.*, 19: 422-428 (1972).
22. H. Lisco, Autoradiographic and Histopathologic Studies in Radiation Carcinogenesis of the Lung, *Lab. Invest.*, 8: 162-170 (1959).
23. J. Lafuma, J. C. Nenot, M. Morin, R. Masse, H. Metivier, D. Nolibe, and W. Skupinski, Respiratory Carcinogenesis in Rats After Inhalation of Radioactive Aerosols of Actinides and Lanthanides in Various Physicochemical Forms, in *Experimental Lung Cancer: Carcinogenesis and Bioassays*, E. Karbe and J. F. Park (Eds.), Symposium Proceedings, Seattle, Wash., June 23—26, 1974, pp. 443-453, Springer-Verlag, New York, 1974.
24. Y. I. Moskalev, ^{239}Pu: Problems of Its Biological Effect, *Health Phys.*, 22: 723-729 (1972).
25. C. L. Sanders, Carcinogenicity of Inhaled Plutonium-238 in the Rat, *Radiat. Res.*, 56: 540-553 (1973).
26. J. S. Adamson, R. M. Senior, and T. Merrill, Alveolar Cell Carcinoma: An Electron Microscopic Study, *Am. Rev. Respir. Dis.*, 100: 550-557 (1969).
27. S. Hattori, M. Matsuda, R. Tateishi, and T. Terazawa, Electron Microscopic Studies on Human Lung Cancer Cells, *Gann*, 58: 283-290 (1967).

The Removal of Macrophages and Plutonium Dioxide Particles by Bronchopulmonary Lavage

J. BRIGHTWELL and M. ELLENDER
National Radiological Protection Board, Harwell, England

ABSTRACT

Bronchopulmonary lavage is a potential technique for treating individuals who have accidentally inhaled insoluble radioactive aerosols. However, the optimum conditions of treatment have yet to be defined. This study has investigated in rodents the use of lavage for removing plutonium dioxide from the lungs and examined the relationship between the amount of radioactive material and the number of macrophages present in the lavage fluid.

Rats and hamsters were exposed to aerosols of plutonium dioxide and subsequently lavaged. Each lavage consisted of a number of saline lung washes, each of 2 or 3 ml. The interval between successive lavages appeared to be critical in the rat, a second lavage generally removing less plutonium than the first lavage. This effect was not apparent in hamsters. Furthermore, it proved feasible to repeatedly lavage hamsters with an extended procedure of 10 lung washes. Rats, however, did not recover from this procedure.

In hamsters about 90% of an initial lung deposit of plutonium was removed by seven 10-wash lavages during the 4 weeks after inhalation. There was a good correlation between the amount of plutonium removed and the number of large mononuclear cells in the individual washes of each lavage. Autoradiographs of smears of lavage fluid also showed that more than 90% of the plutonium removed by lavage 1 week after inhalation was contained within pulmonary macrophages.

Bronchopulmonary lavage is an accepted procedure for the treatment of various obstructive lung diseases in man[1] and has been used in one instance to partially remove plutonium from the lungs of a worker after accidental inhalation.[2] Considerable experimental work primarily with rats, dogs, and baboons has been carried out to determine the optimum use of lavage for removal of inhaled

radioactive particles.[3-5] In these experiments an average of about 50% of an initial lung deposit of plutonium was removed by lung lavage. A similar fraction of inhaled ^{137}Cs in fused clay particles has been removed from hamster lung.[6]

There is some evidence that inhaled particles removed from the lung by lavage are primarily contained within pulmonary macrophages.[2,7,8] The present study has investigated in rodents the use of lavage and examined the relationship between the amount of inhaled plutonium removed and the number of cells present in the lavage fluid.

MATERIALS AND METHODS

Experimental Animals

Male and female rats weighing between 160 and 200 g were used. These animals were an inbred strain from the Medical Research Council's Radiobiological Unit at Harwell and were derived from outbred Alderley Park (Strain 1) specific-pathogen-free rats. The hamsters used were male DSN strain animals weighing between 100 and 140 g, obtained from the Coombehurst Breeding Establishment, Basingstoke. All animals were allowed food and water ad libitum.

Aerosol Exposures

In this study animals were exposed to aerosols of plutonium dioxide generated by an exploding-wire technique as previously described.[9] The aerosol particles had an activity median aerodynamic diameter (AMAD) of about 1.25 μm and a geometric standard deviation of about 1.5. The plutonium used was about 92 wt.% ^{239}Pu with small amounts of ^{238}Pu, ^{240}Pu, ^{241}Pu, and ^{242}Pu. About 5% of the total alpha activity was contributed by ^{241}Am.

During aerosol inhalation the animals were restrained in tapered, open-ended glass tubes to reduce surface contamination. The exposure technique has been described in more detail in Ref. 10. The initial lung content of plutonium averaged about 14 nCi (500 Bq) for rats and about 40 nCi (1500 Bq) for hamsters (1 becquerel = 1 disintegration per second).

Bronchopulmonary Lavage

Hamsters were anesthetized with 3% halothane in oxygen and rats, with 1.5% halothane in oxygen. A polythene tube (external diameter of 1.3 mm for hamsters and 1.6 mm for rats) was passed via the mouth into the trachea, and a volume of warmed normal saline

(2 ml for hamsters and 3 ml for rats) was instilled into the lungs. The saline was then removed by suction and postural drainage. This procedure is referred to as a lung wash. Several lung washes, each with a fresh aliquot of saline, were performed on each animal during one bronchopulmonary lavage. The animal was then resuscitated, using oxygen if necessary, although spontaneous respiration was usually recovered without aid.

Cell Counts

An aliquot of the fluid washed from the lungs was added to an equal volume of 2% acetic acid containing 50 mg of gentian violet per liter. Cells were counted with a hemocytometer, and the cell content of each lung wash was then calculated. Cells were differentiated into large mononuclear cells (primarily macrophages) and others that included epithelial cells and leukocytes.

In some cases an aliquot of lung wash fluid was centrifuged at 3000 *g*-min. The supernatant was removed and analyzed for plutonium, and the remaining cell pellet was resuspended in a small volume of water. This cell suspension was then smeared onto microscope slides and air dried. Autoradiographs of the smears were prepared as described below.

Histology

Animals were anesthetized with methohexitone sodium (0.3 mg/g body weight), the trachea was tied off, and the thoracic contents were removed. The lungs were then fixed in Carnoy's fluid for about 24 hr. Paraffin sections, 5 μm thick, were cut from the left lung and autoradiographs were prepared by coating the sections with Ilford K5 emulsion (Ilford Ltd., Cheshire, England) and exposing them for 4 weeks in lighttight boxes at 4°C. After development the preparations were stained with hematoxylin and eosin. Autoradiographs of smears were prepared and stained in the same way.

Selected autoradiographs were immersed in xylene for about 72 hr before mounting. This procedure partially clears the silver grains constituting the alpha-track stars and enables the underlying plutonium particles to be seen.[11] Free particles could be differentiated from those within cells. The cells containing plutonium particles were identified as macrophages.

Radiochemical Analysis

Samples of lavage fluid and of tissues, including unused histological material, were ashed at 500°C, and the plutonium content

was measured by liquid-scintillation counting after solvent extraction.[12,13]

RESULTS AND DISCUSSION

Interval Between Successive Lavages

In preliminary experiments to study various aspects of the lavage technique in rodents, groups of 4 hamsters were lavaged twice after inhalation of a plutonium dioxide aerosol. The first lavage of three lung washes (the 3-wash lavage) was carried out 3 days after inhalation and the second 3-wash lavage was performed 2, 4, 8, 24, or 48 hr later. The amount of plutonium removed in the second lavage was expressed as a percentage of that removed in the first lavage (Table 1). Although the amount of plutonium removed varied considerably from animal to animal, it can be seen that there is generally no reduction in the efficiency of the second lavages compared with the first. The second lavage is perhaps the more effective although the difference between lavages is only statistically significant ($p < 0.02$) if the data from all five lavage intervals are pooled.

A similar experiment was carried out in which groups of 4 or 5 rats were given two 3-wash lavages a few days after plutonium dioxide inhalation. The interval between lavages was either 2 or 5 hr

TABLE 1

RELATIVE REMOVAL OF INHALED PLUTONIUM DIOXIDE FROM HAMSTER AND RAT LUNGS BY TWO LAVAGES*

Intervals between lavages, hr	$\frac{\text{Pu in lavage 2}}{\text{Pu in lavage 1}} \times 100$, % (N = 4 or 5)
	Hamsters
2	174 ± 91†
4	131 ± 18
8	210 ± 24
24	211 ± 60
48	154 ± 61
	Rats
2	9 ± 2
5	85 ± 40

*Each lavage consisted of three lung washes.
†Mean ± one standard error of the mean.

(Table 1). It is clear that with a 2-hr interval between lavages far less plutonium is removed by the second lavage than by the first.

A further series of experiments was carried out with both rats and hamsters to investigate the relationship between the cell content of lavage fluid and the interval between lavages. Animals not exposed to plutonium dioxide aerosol were given two 3-wash lavages separated by intervals of between 2 and 96 hr. Two animals from each species were used for each time interval.

The ratio of cell counts from the two lavages in hamsters (Table 2) shows that the number of large mononuclear cells is apparently decreased in a second lavage at 2 hr after the first but is generally increased with longer intervals between lavages. Similar counts of cells lavaged from rat lungs (Table 3) show a marked decrease in the number of large mononuclear cells in a second lavage carried out at times up to 96 hr after the first lavage. These results indicate that large mononuclear cells can be more easily washed from hamster lungs than from rat lungs.

The numbers of cells of all types washed from the lungs in these experiments show a considerable increase in the second lavage. This increase is again more marked in hamsters than in rats.

Number of Lung Washes

In the experiment on hamsters exposed to a plutonium dioxide aerosol (Table 1), a total of 40 lavages, each consisting of three lung

TABLE 2

RELATIVE REMOVAL OF CELLS FROM HAMSTER LUNGS BY TWO LAVAGES*

Interval between lavages, hr	$\frac{\text{Cells in lavage 2}}{\text{Cells in lavage 1}} \times 100$, % (N = 2)	
	Large mononuclear cells	All cells
2	39	144
4	202	358
8	82	249
24	171	772
48	172	257
96	174	157

*Each lavage consisted of three lung washes.

TABLE 3

RELATIVE REMOVAL OF CELLS FROM RAT LUNGS BY TWO LAVAGES*

Interval between lavages, hr	$\frac{\text{Cells in lavage 2}}{\text{Cells in lavage 1}} \times 100$, % (N = 2)	
	Large mononuclear cells	All cells
2	29	67
4	15	195
8	48	351
24	41	192
48	24	133
96	51	257

*Each lavage consisted of three lung washes.

washes, was carried out, and in 23 of these lavages the third wash contained more plutonium than either the first or second wash. A further experiment was therefore carried out in rats and hamsters to determine how many washes could be tolerated. Accordingly, each animal was given a single lavage of 10 lung washes. The majority of hamsters survived although recovery from anesthesia was generally slower than it was after three lung washes. Rats, however, could not be resuscitated after this extended lavage procedure.

The pattern of cell removal by 10 lung washes in both rats and hamsters is shown in Fig. 1. The rats used in this experiment did not recover from anesthesia. The greatest numbers of all free lung cells, including large mononuclear cells, were removed in washes 5 to 7 in rats, whereas in hamsters this peak occurred earlier, in washes 3 and 4; again this suggests that large mononuclear cells may be more easily removed from hamster lung than from rat lung. The reasons for these differences in cell removal remain unexplained.

A significant number of cells are removed in the later washes of a 10-wash lavage, which indicates that this procedure does not remove all the available free lung cells. This was further demonstrated by the lavage of a single hamster with 20 lung washes. In this animal about 34% of the total, both of large mononuclear cells and of all cells removed, were in washes 11 to 20. The 20th lung wash still contained about 2% of the total of cells removed.

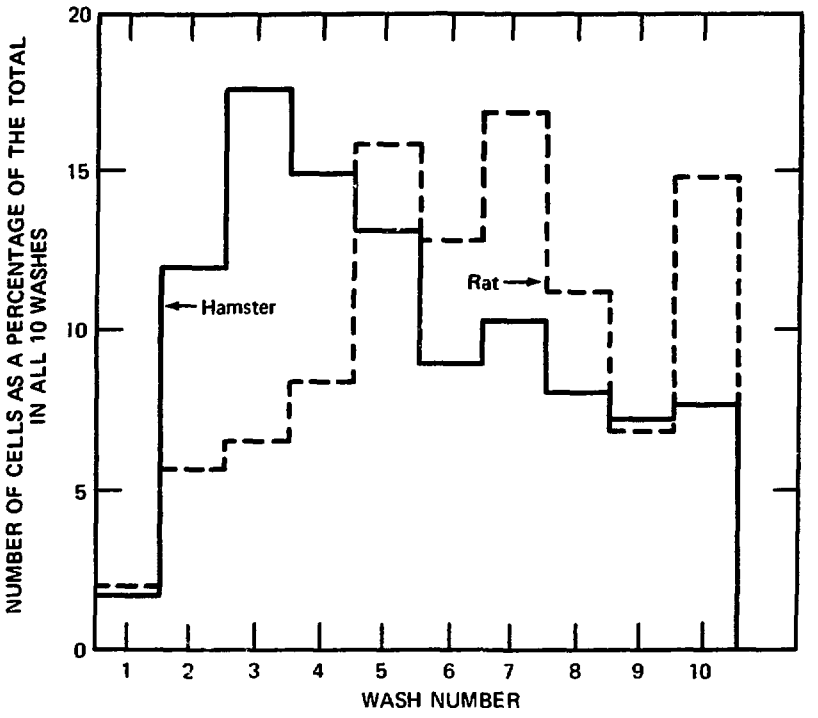

Fig. 1 Pattern of removal of large mononuclear cells from rat and hamster lungs by 10 lung washes.

Effectiveness of Lavage in Removing Inhaled Insoluble Plutonium

Hamsters were chosen for this experiment because of their ability to recover from extended lavage procedures. Fifteen hamsters were exposed to an aerosol of plutonium dioxide. In 5 animals sacrificed immediately after exposure, the mean lung content of plutonium was found to be 50 ± 11 nCi (1800 ± 400 Bq; $\overline{X}$ ± S.E.). The remaining 10 animals were lavaged with 10 lung washes on day 2 after inhalation. Two animals failed to recover from this procedure. The surviving hamsters were divided into two groups of four. One group was given a total of five 10-wash lavages and the other group, seven similar lavages. There were no significant changes in the body weights of these 8 animals during the course of treatment, and no further deaths occurred. The lavages were carried out on days 2, 6, 9, 13, 16, 20, and 23 after inhalation. All animals were killed at 28 days. The lavage fluid from all animals was analyzed for plutonium content, and cell counts of the 7-lavage group were carried out for each wash in lavages 1, 2, 3, 5, and 7.

The amount of plutonium removed by each lavage is shown in Table 4 as a percentage of the estimated mean initial lung content.

TABLE 4

PERCENTAGE OF INITIAL LUNG PLUTONIUM DIOXIDE DEPOSIT REMOVED FROM HAMSTER LUNGS BY SEVEN LAVAGES*

Lavage No.	$\frac{\text{Pu in lavage fluid}}{\text{Initial lung content}\dagger} \times 100$, % (N = 4)
1	45.2 ± 6.0‡
2	19.4 ± 2.4
3	8.7 ± 1.0
4	6.9 ± 0.8
5	4.5 ± 0.6
6	2.6 ± 0.6
7	2.0 ± 0.3
Total	89.3 ± 7.2

*Each lavage consisted of 10 lung washes.

†Initial lung content estimated from 5 animals killed immediately after inhalation.

‡Mean ± one standard error of the mean.

The total removed in all lavages was 89% of the initial lung content with the first lavage containing about 50% of this total. The seventh lavage removed about 2% of the initial lung content, but this still represented about 20% of the plutonium remaining in the lung at that time, which suggests that a significant increase in plutonium removal may be achieved by further lavage treatments.

The plutonium content of the lungs at 28 days after inhalation is shown in Table 5. These results indicate that 89% of the initial lung content had been cleared in animals given five lavages and 92% in those given seven lavages. Experiments on lung retention of inhaled plutonium dioxide aerosols in hamsters not treated by lavage indicated that 41 ± 7% ($\bar{X}$ + S.E.) of the initial lung content remained at 28 days after inhalation (Table 5).

The amount of plutonium and the number of cells removed in each wash of a lavage were also expressed as proportions of the total for that lavage. The values for plutonium content and cell number were then compared, and the correlation coefficient, r, was calculated for each lavage.

There was a significant correlation between plutonium content and large mononuclear cell count in each lavage (Table 6). Some correlation was also seen between plutonium content and the number of cells of all types. This was, however, less significant than

TABLE 5

PERCENTAGE OF INITIAL LUNG PLUTONIUM DIOXIDE DEPOSIT REMAINING IN HAMSTER LUNGS AFTER FIVE OR SEVEN LAVAGES*

Number of lavages	Number of animals†	$\frac{\text{Plutonium content of lungs}}{\text{Initial lung content}‡} \times 100$, %
0	11	40.8 ± 7.0§
5	4	10.8 ± 1.2
7	4	8.2 ± 1.7

*Each lavage consisted of 10 lung washes.

†Animals were killed at 28 days after inhalation.

‡Initial lung content estimated from 5 animals killed immediately after inhalation.

§Mean ± one standard error of the mean.

TABLE 6

CORRELATION BETWEEN PLUTONIUM CONTENT AND THE NUMBER OF LARGE MONONUCLEAR CELLS IN THE INDIVIDUAL LUNG WASHES OF EACH LAVAGE*

Lavage No.	Correlation coefficient, r	Statistical significance
1	0.97†	$p < 0.001$
2	0.87	$p < 0.01$
3	0.86	$p < 0.01$
5	0.95	$p < 0.001$
7	0.85	$p < 0.01$

*Hamsters were given seven lavages, each of 10 lung washes.

†Each value was obtained from 4 animals except in lavage 1 where 8 animals were used.

the correlation seen with large mononuclear cells. The pattern of removal both of cells and plutonium by the 10 washes was very similar in all lavages and approximated that shown for hamsters in Fig. 1.

This correlation between plutonium content and large mononuclear cell number suggests that the plutonium removed from the lung by lavage is largely contained within pulmonary macrophages. A further study was carried out in which the lavage fluid from hamsters given three lung washes at 7 days after plutonium inhalation was

centrifuged and smears of the cell pellet were prepared. The supernatants of the centrifuged material contained about 2% of the plutonium removed for each of the first two lung washes and about 7% in the third wash. Autoradiographs of the smears were cleared in xylene, as described earlier, and the distribution of the alpha-track stars was determined. More than 99% of the plutonium activity in these smears was in particulate form, and more than 95% of these particles were found to be within pulmonary macrophages.

The total number of large mononuclear cells removed by each lavage shows little variation with lavage number (Table 7). However, as in the experiments summarized in Tables 2 and 3, there is a great increase in the number of all cell types in the second and later lavages compared with the first. This increase is largely due to the presence of polymorphonuclear cells in the later lavages. These cells were rarely seen in the fluid from the first lavage, and their increased numbers in later lavages are probably a result of an inflammatory response to the lavage fluid.

The first few washes of each lavage also contained some small groups of epithelial cells. These were more numerous in the early lavages. Such groups of epithelial cells were not included in cell counts.

CONCLUSIONS

From the investigation of the relationship between the removal of large mononuclear cells and plutonium dioxide particles by

TABLE 7

REMOVAL OF CELLS FROM HAMSTER LUNGS BY SEVEN LAVAGES*

Lavage No.	Cell count × 10^6 (N = 4)	
	Large mononuclear cells	All cells
1	2.6 ± 0.3†	3.6 ± 0.3†
2	2.9 ± 0.2	8.4 ± 1.8
3	2.8 ± 0.5	10.3 ± 3.9
5	3.2 ± 0.8	14.6 ± 8.0
7	3.5 ± 0.9	17.2 ± 4.3

*One lavage consisted of 10 lung washes.
†Mean ± one standard error of the mean.

bilateral bronchopulmonary lavage in rats and hamsters, we conclude that

1. Hamsters have proved more suitable than rats as experimental animals for lavage studies.
2. Large mononuclear cells are more easily removed from hamster lungs than from rat lungs by lavage.
3. Inhaled plutonium particles removed from rodent lungs by lavage are primarily contained in pulmonary macrophages.
4. There is no significant difference in the number of large mononuclear cells removed from hamster lungs in any of seven successive 10-wash lavages.
5. About 90% of the initial lung deposit of an inhaled plutonium aerosol can be removed from hamster lung by seven 10-wash lavages carried out between 2 and 23 days after inhalation.

ACKNOWLEDGMENTS

Aerosol exposures were carried out at the Atomic Weapons Research Establishment, Aldermaston, Berkshire, England, with the collaboration of Mr. R. F. Carter. We should also like to thank Dr. H. Smith and Dr. J. W. Stather for critical reading of the manuscript.

REFERENCES

1. R. M. Rogers, M. S. Braunstein, and J. F. Shuman, Role of Bronchopulmonary Lavage in the Treatment of Respiratory Failure. A Review, *Chest*, 62 (Suppl.): 95S-106S (1972).
2. R. O. McClellan et al., Bronchopulmonary Lavage and DTPA Treatment of an Accidental Inhalation ^{239}Pu Exposure Case, in *Fission Product Inhalation Program, Annual Report*, October 1971—September 1972, USAEC Report LF-45, pp. 287-294, Lovelace Foundation, NTIS, November 1972.
3. C. L. Sanders and T. A. Jackson, Removal of Plutonium and Macrophages by Lung Washings, in *Pacific Northwest Laboratory Annual Report for 1970*, USAEC Report BNWL-1550, Part 1, pp. 78-79, Battelle, Pacific Northwest Laboratories, NTIS, October 1971.
4. B. A. Muggenburg, J. A. Mewhinney, J. J. Miglio, D. O. Slauson, and R. O. McClellan, The Removal of Inhaled ^{239}Pu and ^{238}Pu from Beagle Dogs by Lung Lavage and Chelation Treatment, in *Diagnosis and Treatment of Incorporated Radionuclides*, Seminar Proceedings, Vienna, Dec. 8—12, 1975, pp. 341-354, STI/PUB/411, International Atomic Energy Agency, Vienna, 1976.
5. D. Nolibé, J. C. Nenot, H. Metivier, R. Masse, and J. Lafuma, Traitement des inhalations accidentelles d'oxyde de plutonium par lavage pulmonaire in vivo, in *Diagnosis and Treatment of Incorporated Radionuclides*, Seminar Proceedings, Vienna, Dec. 8—12, 1975, pp. 373-384, STI/PUB/411, International Atomic Energy Agency, Vienna, 1976.

6. S. A. Felicetti, B. A. Muggenburg, K. Hall, H. Nelson, and F. F. Hahn, Removal of Inhaled ^{137}Cs in Fused Aluminosilicate Particles from Syrian Hamsters by Bronchopulmonary Lavage, in *Inhalation Toxicology Research Institute Annual Report, 1974-1975*, USERDA Report LF-52, pp. 357-359, Lovelace Foundation, NTIS, 1975.
7. K. E. McDonald, Removal of Plutonium by Pulmonary Lavage, in *Pacific Northwest Laboratory Annual Report for 1972*, USAEC Report BNWL-1750, Pt. 1, pp. 64-65, Battelle, Pacific Northwest Laboratories, NTIS, April 1973.
8. D. Nolibé, Elimination par lavage pulmonaire, in vivo, des particules d'oxyde de plutonium inhalées. Description de la technique utilisée, *Compt. Rend., Ser. D*, 276: 225-228 (1973).
9. J. Brightwell and R. F. Carter, Comparative Measurements of the Short-Term Lung Clearance and Translocation of PuO_2 and Mixed $Na_2O + PuO_2$ Aerosols in Mice, in *Inhaled Particles IV*, W. H. Walton (Ed.), Symposium Proceedings, Edinburgh, September 22—26, 1975, pp. 285-302, Pergamon Press, Inc., Elmsford, N.Y., 1977.
10. J. W. Stather, S. Howden, and R. F. Carter, A Method for Investigating the Metabolism of the Tranportable Fraction of Plutonium Aerosols, *Phys. Med. Biol.*, 20: 106-124 (1975).
11. J. Brightwell, M. Ellender, and P. Rodwell, unpublished data.
12. R. F. Keough and G. J. Powers, Determination of Plutonium in Biological Materials by Extraction and Liquid Scintillation Counting, *Anal. Chem.*, 42: 419-421 (1970).
13. J. W. Stather and S. Howden, The Effect of Chemical Form on the Clearance of 239-Plutonium from the Respiratory System of the Rat, *Health Phys.*, 28: 29-39 (1975).

A Mathematical Model of ^{238}Pu Alpha-Ray Dose-Rate Distribution in the Lung

CARL FELDMAN, PAUL BODOR, LAWRENCE J. PEREZ, JR., and STEVE HENRY
Environmental Safeguards Division, NUS Corporation, Rockville, Maryland

ABSTRACT

A mathematical model was constructed for calculating plutonium-238 alpha-ray dose-rate spatial distribution in the alveolar tissue region of the lung, which had been caused by a randomly placed $^{238}PuO_2$ particle. Input data were obtained through the manual digitization of photomicrographs of the alveolar region of rat lung tissue. The use of such data allows one to perform calculations with greater spatial resolution than does the method obtained through the use of analog computer lung-geometry simulations. Multiparticle averaging simulates the dose-rate distribution for a randomly placed particle. The sampling procedures used allow multiparticle averaging with shorter computer time than does the frequently used Monte Carlo averaging technique. This approach provides a method for estimating spatial dose-rate distributions as a function of $^{238}PuO_2$ particle size and can serve as a tool for investigating the relevance of parameters that may cause biological dose-related effects in the lung.

A mathematical model was constructed for calculating plutonium-238 (^{238}Pu) dose-rate spatial distribution in the alveolar tissue region of the lung, which had been caused by a randomly placed $^{238}PuO_2$ particle. The model allows one to perform calculations with greater spatial resolution than does the method obtained through the use of analog computer lung-geometry simulations.[1] The sampling procedures used allow multiparticle averaging with shorter computer time than does the frequently used Monte Carlo averaging technique.[2]

The model assumes the static placement of $^{238}PuO_2$ particles (limited to 0.73 μm in diameter) within the lung geometry. Only air—tissue geometry is considered, and the tissue sample used is

regarded as typical of the inhomogeneous geometry encountered. Calculations of the dose rate as a function of irradiated tissue mass were performed for $^{238}PuO_2$ particle sizes ranging from 0.1 to 0.73 μm.

This study is a continuation of previous work done at NUS Corporation entitled "Consideration of a Tumor Probability Function and Micro-Dosimetry for the Lower Pulmonary Compartment."[3] In the previous effort a deterministic model was developed of the lung structure, based on a single systematic configuration of air and tissue, which had fixed dimensional characteristics. These dimensions were determined from average dimensions of the lung structure under consideration. However, it was recognized that the large variations in the shape and size of air spaces and in the thickness of tissue walls will cause significant variations in the alpha-ray dose-rate distributions from those calculated for an average lung structure. Accordingly, this study was initiated to develop a method to determine the statistical variation of the dose-rate distribution resulting from the random placement of a $^{238}PuO_2$ particle within actual air—tissue configurations of the alveolar region.

The radiobiological implications of the nonuniform energy deposition (i.e., dose rate) caused by the placement of a hot particle in the lung are the subject of a large number of articles, which were reviewed and summarized in Ref. 4. The present investigation only concerns itself with developing a practical calculational technique for performing microdosimetry in the alveolar region of the lung to provide an estimate of spatial dose-rate distributions as a function of $^{238}PuO_2$ particle size. This work can therefore serve as a tool for investigating the relevance of parameters that may cause biological dose-related effects in the lung.

ANALYTICAL DEVELOPMENT

The development of the analytical expressions required for evaluating the dose rate for a particle placed in inhomogeneous lung tissue will be presented.

Definition of Absorbed Dose

The quantity absorbed dose is defined as the energy imparted by ionizing radiation to an elemental mass/volume of matter. This definition may be expressed as

$$D = \frac{\Delta E}{\Delta m} \tag{1}$$

where D is the absorbed dose, Δm is the mass contained in an elemental volume, and ΔE is the energy imparted to an elemental volume containing a mass, Δm. The special unit of absorbed dose is the rad, where 1 rad = 100 ergs/g.

If D, ΔE, and Δm are expressed in units of rads, MeV, and grams, respectively, Eq. 1 becomes

$$D = 1.6 \times 10^{-8} \frac{\Delta E}{\Delta m} \tag{2}$$

For calculational purposes it is convenient to work with the dose rate, DR. DR is related to D through the relation,

$$D = \int_0^{\tau} DR\, e^{-\lambda t}\, dt$$

where DR is the initial dose rate in rads per second, λ is the decay constant per second, and τ is the residence time in seconds.

The integration gives

$$D = \frac{DR}{\lambda}(1 - e^{-\lambda\tau})$$

Thus, for a particular radioactive decay and specified residence time, the dose is related to the initial dose rate by a multiplicative constant.

Calculation of Absorbed Dose Rate

The method developed for calculating the dose rate is based upon determining a change in energy current over an incremental change of alpha-ray path length. The energy current, J, is defined as the quantity of energy crossing unit area of a surface per unit time. It is a vector quantity directed along the normal to the surface and may be expressed in units of MeV/cm^2-sec. The dose rate at a point can be calculated as

$$DR = -\frac{1}{\rho} \nabla \cdot J \times 1.6 \times 10^{-8} \tag{3}$$

where ρ is the density in grams per cubic centimeter of the absorbing medium. This expression is simply the equation of specific energy continuity through an infinitesimal volume element.

The energy flux, ψ, due to alpha radiation emanating from a spherical particle, at a distance, r, from the center of the particle, can be found from the expression,

$$\psi = S_0 E_\alpha \rho_p \, 3.7 \times 10^{10} \int_v \frac{fe\, r^2}{4\pi r^2} \sin\theta \, dr \, d\theta \, d\phi \tag{4}$$

where S_0 = specific activity, Ci/g
E_α = alpha-ray energy, MeV
ρ_p = density of particle, g/cm^3
v = volume
fe = fraction of alpha-ray energy remaining after traversing a distance, r
ψ = energy flux, MeV/cm^2-sec
r = distance, cm

In general, this is a complicated expression. However, if one assumes that the particle diameter is small compared with the alpha-ray range in the particle, then all the energy escaping the particle will behave as though it originates from a point located at the center of the particle which has a source energy current strength, j_s; j_s is the energy current at the surface of the spherical particle.[3] The energy current, J, is now given by

$$J = j\hat{i}_r$$

$$j = j_s \frac{4\pi r_p^2}{4\pi r_2^2} fe' = j_s \left(\frac{r_p}{r}\right)^2 fe' \tag{5}$$

where because of spherical symmetry J has a component only in the radial direction, $\hat{i}_r$, and fe′ is now the fraction of alpha-ray energy remaining for a trajectory from the surface of the particle to the observation point. Note that the divergence expression in Eq. 3 must be expressed in spherical coordinates to maintain spherical symmetry. Thus the divergence is given by

$$\nabla \cdot J = \frac{1}{r^2} \frac{\partial}{\partial r} (r^2 j) \tag{6}$$

The expression for j_s can be found since j_s comes from the contribution of all alpha-ray trajectories in the observation direction. This introduces an additional cosine factor into the previous expression for j (see Eq. 4). Thus

$$j_s = B \int_v fe(r) \sin\theta \cos\theta \, dr \, d\theta \, d\phi$$

$$= \int_0^{2\pi} d\phi \int_0^{\pi/2} d\theta \sin\theta \cos\theta \int_0^{d_p \cos\theta} fe(r) \, dr \tag{7}$$

where

$$B = \frac{3.7 \times 10^{10}}{4\pi} S_0 E_\alpha \rho_p$$

An expression for fe is needed to proceed further. This is developed through the use of an empirical alpha-ray energy vs. range curve obtained from Evans.[5] The following equation can be used to adequately express the energy—range relationship for limited segments within the energy range 0.1 to 10 MeV:

$$E_\alpha = a\ R\ air^{b} \tag{8}$$

where E_α is the alpha-ray energy (MeV), R air is the range of alpha ray in air (cm), and a and b are the empirical coefficients. Caution must be used in using the above relation near the beginning and the end of a particular alpha-ray energy range. At these extremities the energy vs. range relationship differs from Eq. 8. For finding the range of the alpha ray in any other material, R_m, the Bragg-Kleeman relation is used,

$$R_m = 3.199 \times 10^{-4} \frac{(A_m)^{1/2}}{\rho_m} R\ air \tag{9}$$

where ρ_m is the material density (g/cm^3), and the effective atomic weight of the compound, A_m, is calculated from the relation,

$$(A_m)^{1/2} = \frac{n_1 A_1 + n_2 A_2 + \ldots n_n A_n}{n_1 (A_1)^{1/2} + n_2 (A_2)^{1/2} + \ldots n_n (A_n)^{1/2}} \tag{9a}$$

where n_i is the atomic fraction of element i and A_i is the atomic weight of element i. It should be noted that the range in air, R air, is based upon dry air at 15°C and 760 mm Hg (ρ = 0.001225 g/cm^3; A = 14.48). The range in air at other conditions may be calculated for use in Eq. 9 by considering the effective atomic weight and the density of air at the new conditions. In particular, the air inside the lung is considered to be warm and moist.

For inhomogeneous media such as air and tissue, it is possible to define an effective range, R_e, for the alpha-ray trajectory by using suitably averaged density and atomic weight expressions. The contribution of the densities of tissue and of air (i.e., ρ_t and ρ_a) to the total effective density, ρ_e, is proportional to the respective volume fractions of tissue and air within the trajectory. Similarly, the

contribution of the atomic numbers for tissue and air (A_t and A_a evaluated from Eq. 9a) to the total effective atomic number, A_e, is proportional to the respective mass fractions of tissue and air within the trajectory. This leads to the results

$$\rho_e = \frac{\rho_t r_t + \rho_a r_a}{r_a + r_t} \qquad A_e = \frac{A_t \rho_t r_t + A_a \rho_a r_a}{\rho_t r_t + \rho_a r_a} \tag{10}$$

where r_t and r_a are the total distances the alpha ray travels in tissue and air. When Eqs. 9 and 10 are used, the effective range for inhomogeneous air—tissue media, R_e, is given by

$$R_e = 3.199 \times 10^{-4} \frac{(A_e)^{1/2}}{\rho_e} R_{air} \tag{11}$$

At the end of the range, fe and the dose rate must go to zero. At the beginning of the range, fe must go to unity and the dose rate must be a maximum. By using the above constraints as well as Eqs. 8 and 11, expressions for fe for limited segments of the dose rate vs. distance curve can be obtained. If the analytical expressions for fe in Eqs. 3, 5, 6, 7, 10, and 11 are suitably used, it can be shown (in a nontrivial way) that the dose rate in tissue, at a distance, r, from the center of the particle of radius r_p is given by

$$DR = r_p^2 \, DS \, \overline{DR} \qquad r_p \leqslant 0.3685 \ \mu m$$

The constraint on r_p occurs because of the condition imposed on the expression for j in Eq. 5. The value of DS is found from the relation,

$$DS = 2.963885 \times 10^2 \, \rho_p S_0 E_\alpha d_p \left(1/3 - \frac{d_p}{R_p} \frac{0.630}{8}\right)$$

where d_p is the particle diameter and R_p the alpha-ray range in $^{238}PuO_2$. The parameter η [where $\eta = 1 - (r - r_p)/R_e$] determines $\overline{DR}$ (i.e., $\overline{DR}_i$). $\overline{DR}$ can be evaluated from the modeling parameters Γ_i, b_i, and the limiting values of η given in Table 1 and from the following analytical expressions:

$$\overline{DR}_i = \frac{W}{r^2 R_e} \Gamma_i b_i \eta^{b_i - 1} \qquad i = 1 \text{ to } 5 \tag{12}$$

where

$$W = \frac{\rho_t (3 A_e - A_t)}{2 A_e \rho_e}$$

TABLE 1

INITIAL DOSE-RATE ($\overline{DR}_i$) MODELING PARAMETERS*

i	Γ_i	b_i	Limiting values of η†	
			η_{0a}	η_{0b}
1	11.47185145	1.78	0	0.048885777
2	3.878319188	1.42	0.048885777	0.097771555
3	1.532999698	1.02	0.097771555	0.244428887
4	1.030388690	0.738	0.244428887	0.733286662
5	1.0	0.630	0.733286662	0.995

*For values of $\overline{DR}$ at η_{0b} values (i = 1 to 5), the expression $\overline{DR} = \frac{1}{2}(\overline{DR}_i + \overline{DR}_{i+1})$ is used.

†$\eta_{0a} < \eta < \eta_{0b}$.

In the above expressions the density of tissue is assumed to be the same as water equal to 1 g/cm^3, and all distances are expressed in centimeters.

DESCRIPTION OF ESSENTIAL COMPUTER CODE FEATURES

From an analytical viewpoint, i.e., Eq. 12, it can be seen that the dose-rate calculations are relatively straightforward. However, from an applicational viewpoint, because of complicated search procedures required to describe the inhomogeneous geometry, the calculating of realistic dose-rate distributions becomes a formidable problem. A brief description of the computer codes used to accomplish this task and a general description of the procedures incorporated into the codes to circumvent calculational difficulties follow.

The three codes STAGIN, STAG, and STAGOUT are used to obtain the particulate dose-rate distribution in rat lung. Code STAGIN utilizes the manually reduced photomicrograph lung-geometry data to provide a convenient digitized data access base. In this study a photograph of the alveolar region of normal rat lung tissue, made at Los Alamos Scientific Laboratory, was used. From a 1.7 x 2.1-mm field of this slide, a montage was constructed of dimensions 5 by 6.2 ft (scale, 9 mm : 10 μm). Void edges were approximated by straight lines (of maximum error ± 2 μm), and void vertexes were identified on an overlaid grid system for input to the code.

Code STAG utilizes the data base assembled with code STAGIN to calculate the dose rate and associated irradiated tissue mass for all

single-particle placements that are used to develop multiparticle sampling.

Code STAGOUT utilizes dose rates and associated tissue masses calculated in code STAG to perform the required multiparticle averaging for obtaining a dose-rate distribution with respect to tissue mass for a randomly placed particle in the lung tissue and graphically displays the result.

Various limiting procedures are used in code STAG to keep the computer times reasonable. For the understanding of these procedures, code calculational techniques are briefly described. For a specific particle placement, an initial alpha-ray trajectory (radial) is chosen. Along this radial, calculations at specified tissue increments for the dose rate and its associated mass are performed and sorted into specified dose-rate intervals. When the particle placement is rotated to a different radial (limited by a maximum inputted arc length), the calculations are repeated. When a 360° radial-rotation angle is achieved, the calculations are terminated. This procedure is repeated for each particle placement.

Reasonable estimates for the maximum and minimum dose-rate values expected (DR_{max} and DR_{min}) are made so as to limit the magnitude of the dose-rate calculations for scaling purposes. With these values incremental distances in tissue along a particular radial can be estimated. Use of an equally spaced logarithmic incrementation of DR from DR_{max} to DR_{min} permits values of the distance in tissue, r, and subsequently the change in r to be calculated through inversion of Eq. 12 for the consecutive incrementation. The incrementation index is chosen so that the dose rate between consecutive incrementations decreases by no more than 10% (i.e., about 200 increments) so that the midpoint of the increment can be used to estimate the dose rate for the full increment (i.e., approximately the linear over the incremental distance).

The volume associated with this midpoint dose-rate incremental calculation (or mass) then is also calculated by using a convenient radially symmetric volume element where the distance of arc-length sweep in the working plane (i.e., tissue) is inputted as a parameter. Typically, a 6-μm arc-length limit exhibits enough fine structure to be meaningful. It is assumed that all variations in inhomogeneity of tissue are contained within the photomicrograph data so that the eventual multiparticle averaging performed will give reasonable three-dimensional representation to the basically two-dimensional variation behavior of the volume calculations performed for single particles.

STATISTICAL PROCEDURES

For limited samplings, as performed in these calculations, the use of careful sampling techniques as described in the previous sections attempts to remove sampling bias so that averaging techniques can be relatively efficient.

Consider the dose rates and their associated masses calculated for a single-particle placement. If one divides the dose rates into n dose-rate categories that are equally spaced logarithmically (i.e., from DR_{max} to DR_{min}), a simple mass weighting fraction, $DR_I^{(j)}$, can be used to define the average dose rate for particle j in category I. If there are $n_I^{(j)}$ dose-rate calculations that fall into category I, then

$$DR_I^{(j)} = \frac{\sum_{i=1}^{n_I^{(j)}} m_i^{(j)} DR_i^{(j)}}{\sum_{i=1}^{n_I^{(j)}} m_i^{(j)}}$$

$$m_I^{(j)} = \sum_{i=1}^{n_I^{(j)}} m_i^{(j)} \qquad (13)$$

where $DR_i^{(j)}$ and $m_i^{(j)}$ are the specific calculated values of the dose rate and its associated mass element, which fall into category I for particle j. If one believes in the reasonableness of the sampling procedure, in the sense that a sufficiently fine-structured sampling has been performed to account for the prominent details of the inhomogeneous tissue under consideration, then a multiparticle average should give a proper estimate of a randomly placed particle's values of $DR_I^{(j)}$ and $m_I^{(j)}$ (denoted by $\overline{DR}_I$, $\overline{m}_I$). If it is assumed that the irradiated energy found in the dose-rate category I, $[m_I^{(j)} DR_I^{(j)}]$, is equally likely for each of the particles (i.e., j's), then one finds

$$\overline{DR}_I = \frac{\sum_{j=1}^{k} m_I^{(j)} DR_I^{(j)}}{\sum_{j=1}^{k} m_I^{(j)}}$$

$$\overline{m}_I = \frac{1}{k} \sum_{j=1}^{k} m_I^{(j)} \qquad (14)$$

It is of interest to estimate the density, $\bar{\rho}$, of the inhomogeneous tissue found from the multiparticle averaging. This is given by

$$\bar{\rho} = \frac{1}{k}\sum_{j=1}^{k} \rho_j$$
$$\rho_j = \frac{V_T\rho_T + \rho_a V_a}{V_T + V_a} \tag{15}$$

where V_a and V_T are the respective total volumes of the void and solid matter alpha-ray irradiated from the jth particle source term.

RESULTS

The results of the modeling analysis are shown in Figs. 1 to 4. In presenting these results, we placed emphasis on easily accessible usage for a variety of possible objectives. Accordingly, Figs. 1 to 3 summarize the dose-rate distribution behavior (for multiparticle averages of 25 particles with diameters of 0.1, 0.4, and 0.73 μm, respectively) in terms of distributions as a function of dose rate for irradiated energy and mass as well as the distribution for cumulative energy and mass. Finally, in Fig. 4 the standard deviation from a distribution of the mean (i.e., the confidence interval behavior) is presented for the various distributions presented in Figs. 1 to 3. Depending on one's objective, the dose-rate distributions can be regarded as due to a fictitious random particle placement for which the standard deviation represents the limiting spread in the distributions from specific randomly placed particles. Alternatively, these distributions can be regarded as due to a random placement of noninteracting particles, where now the irradiated tissue mass must be multiplied by the number of particles used. Frequently, wiggly behavior at high dose-rate values can be observed in the distributions. Such behavior is attributed to the low mass available for irradiation at the higher dose rates affecting the volume-sampling procedures used by the computer code. Finer sampling is not warranted at this time since reasonable interpolation of the distributions presented should provide results that will satisfy most objectives.

For all particle diameters the density and the accumulated irradiated mass are approximately the same and have approximate values of 0.36 g/cm^3 and 1.7 x 10^{-6} g, respectively. A comparison of the mass with the energy distribution curves indicates that the energy distribution is more slowly varying and has a broader peak (at the

(Text continues on page 494.)

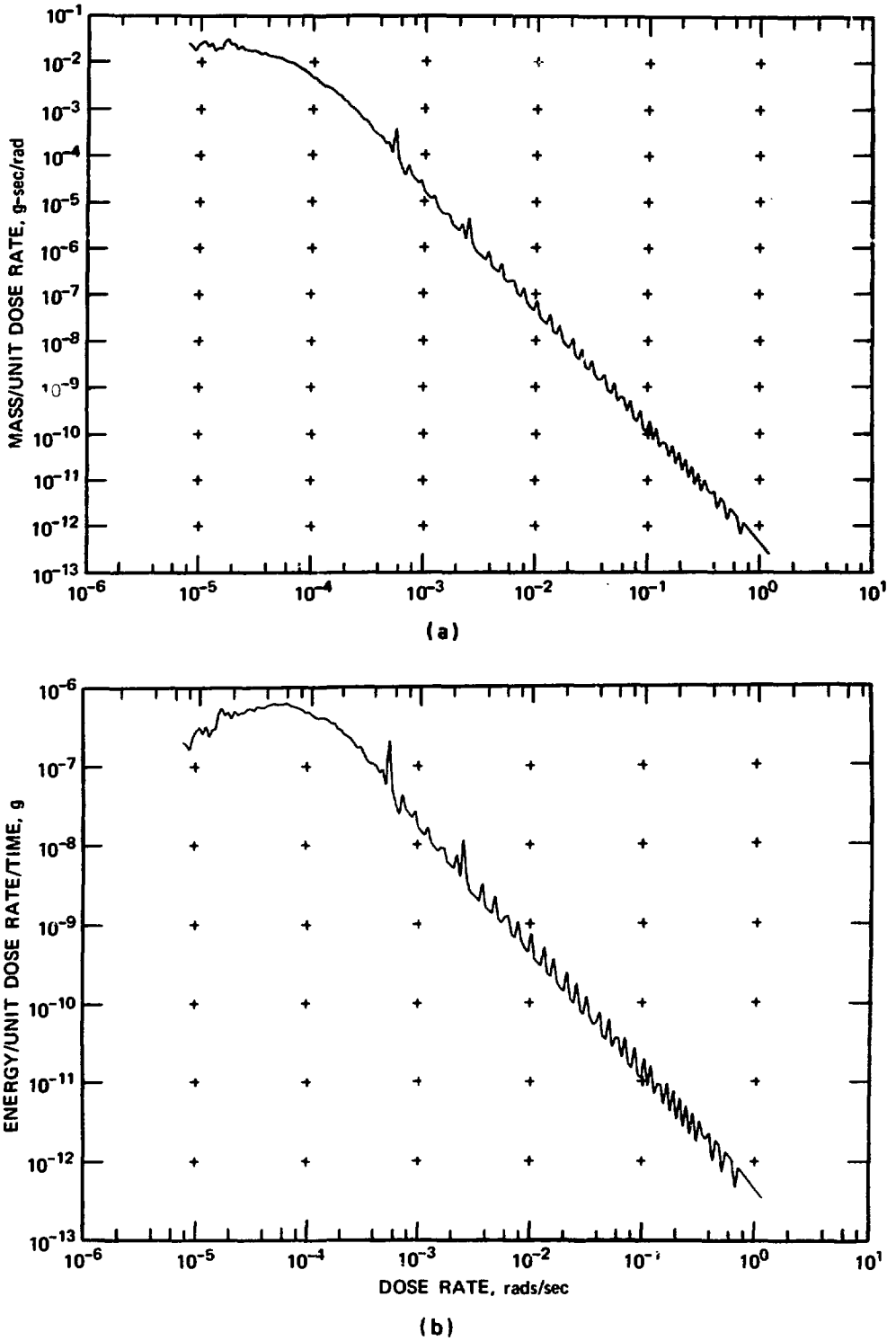

Fig. 1 Modeling results for multiparticle average for 0.1-μm-diameter $^{238}PuO_2$ particles. **(Figure continues on next page.)**

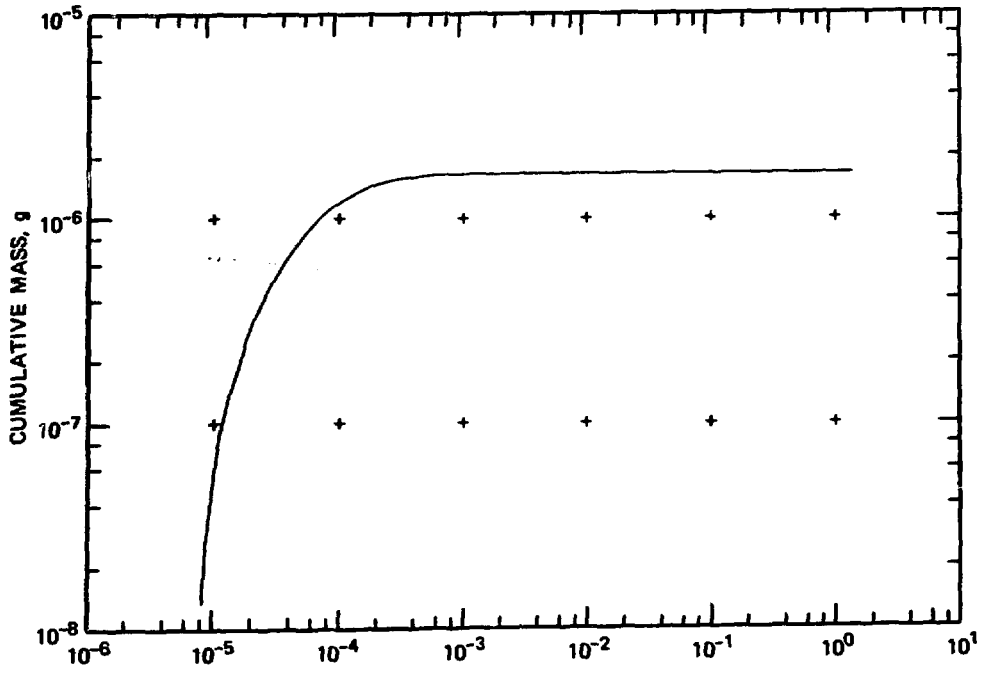

(c)

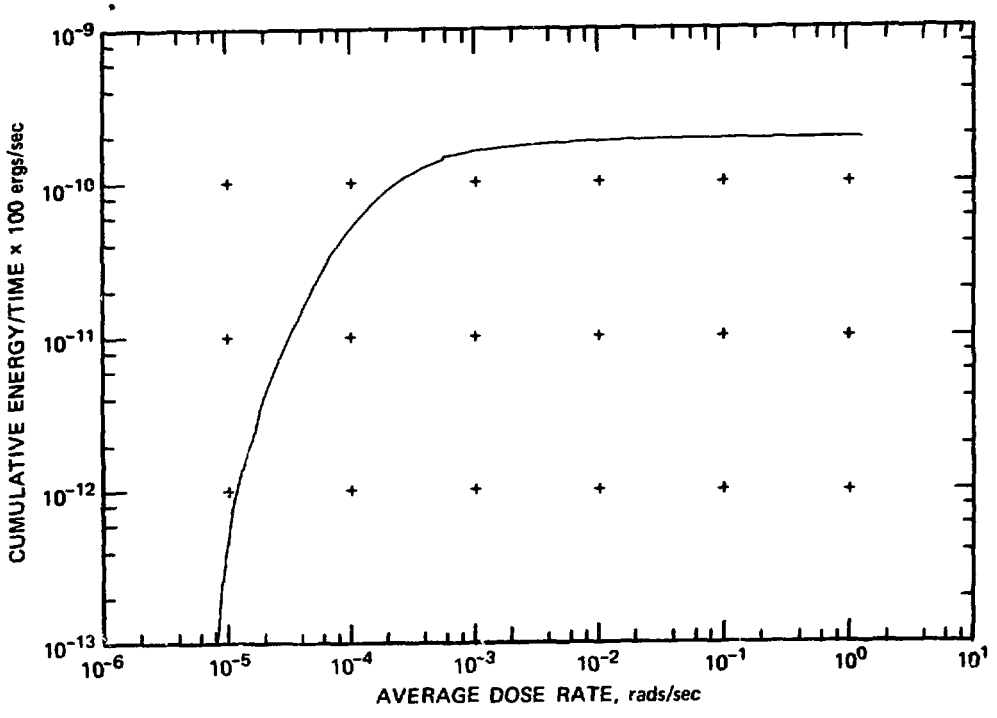

(d)

Fig. 1 (Continued)

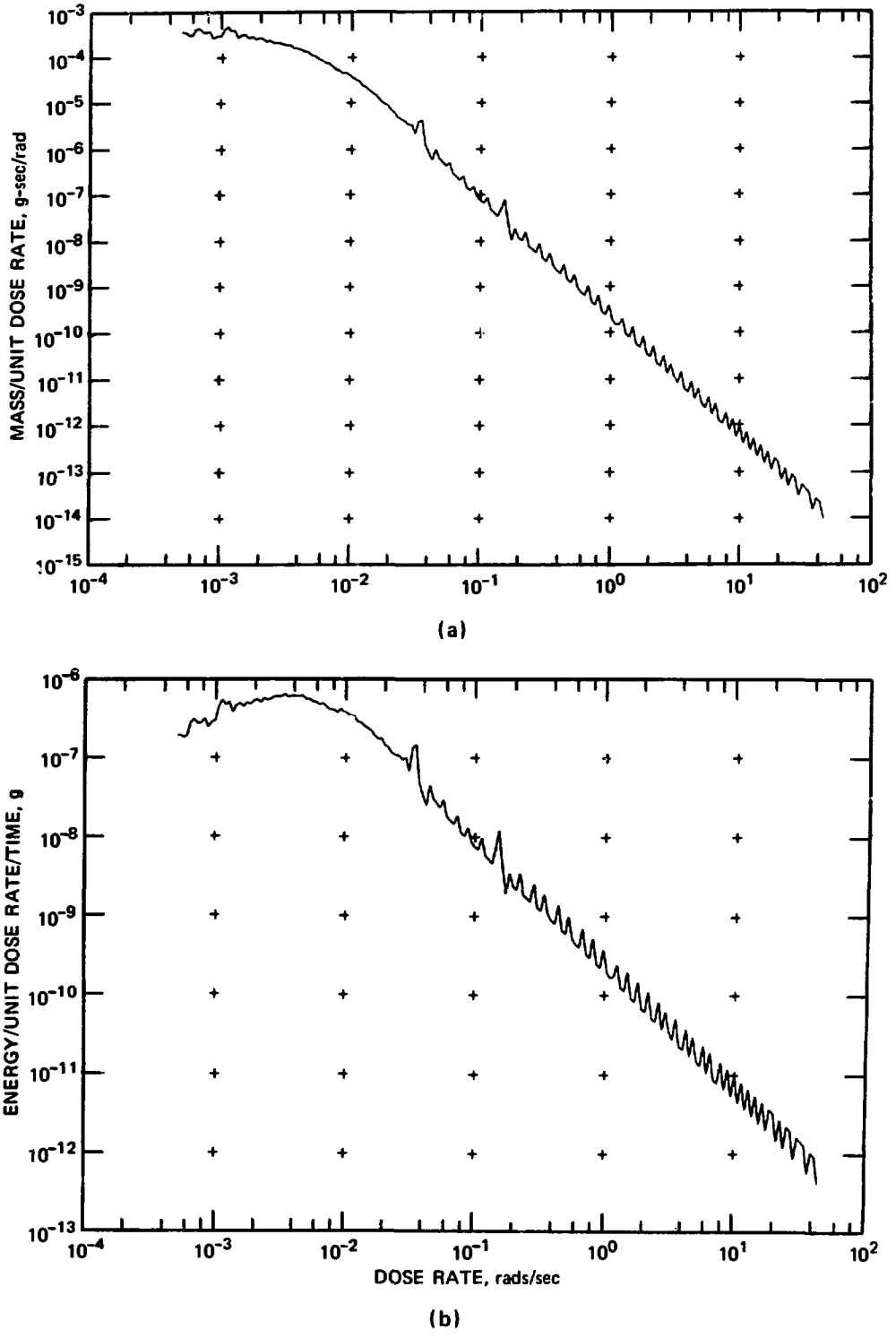

Fig. 2 Modeling results for multiparticle average for 0.4-μm-diameter $^{238}PuO_2$ particles. **(Figure continues on next page.)**

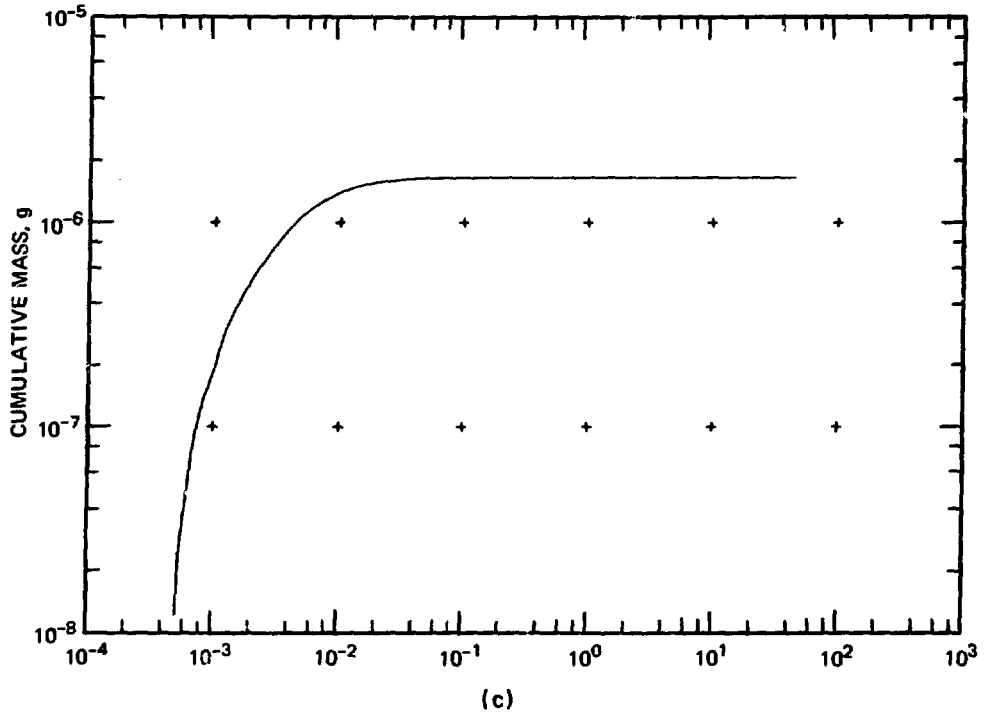

(c)

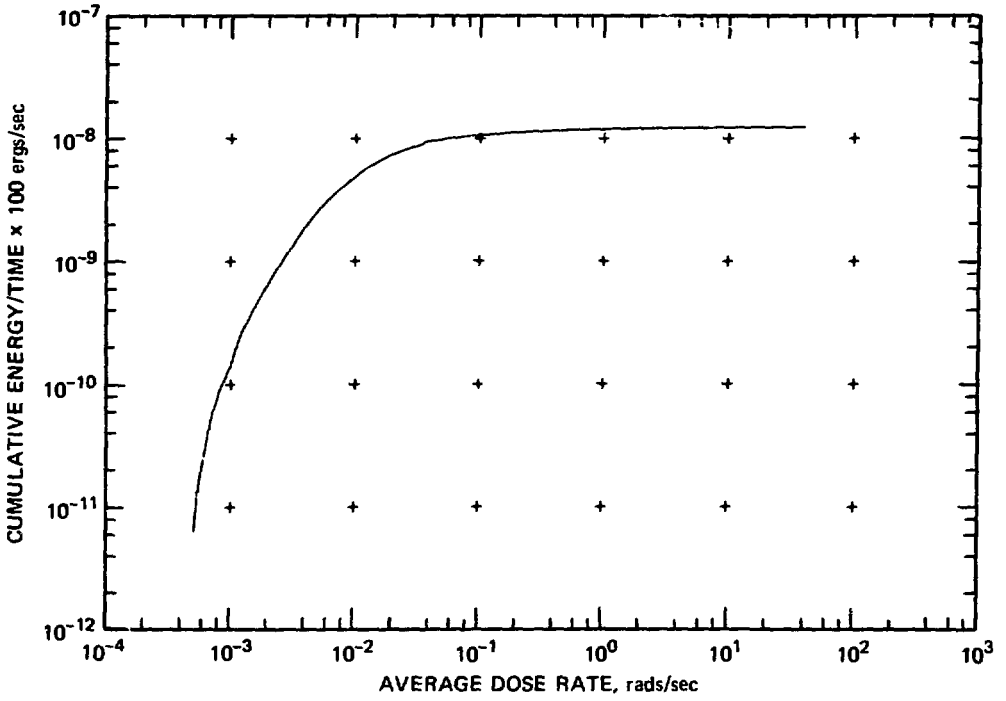

(d)

Fig. 2 (Continued)

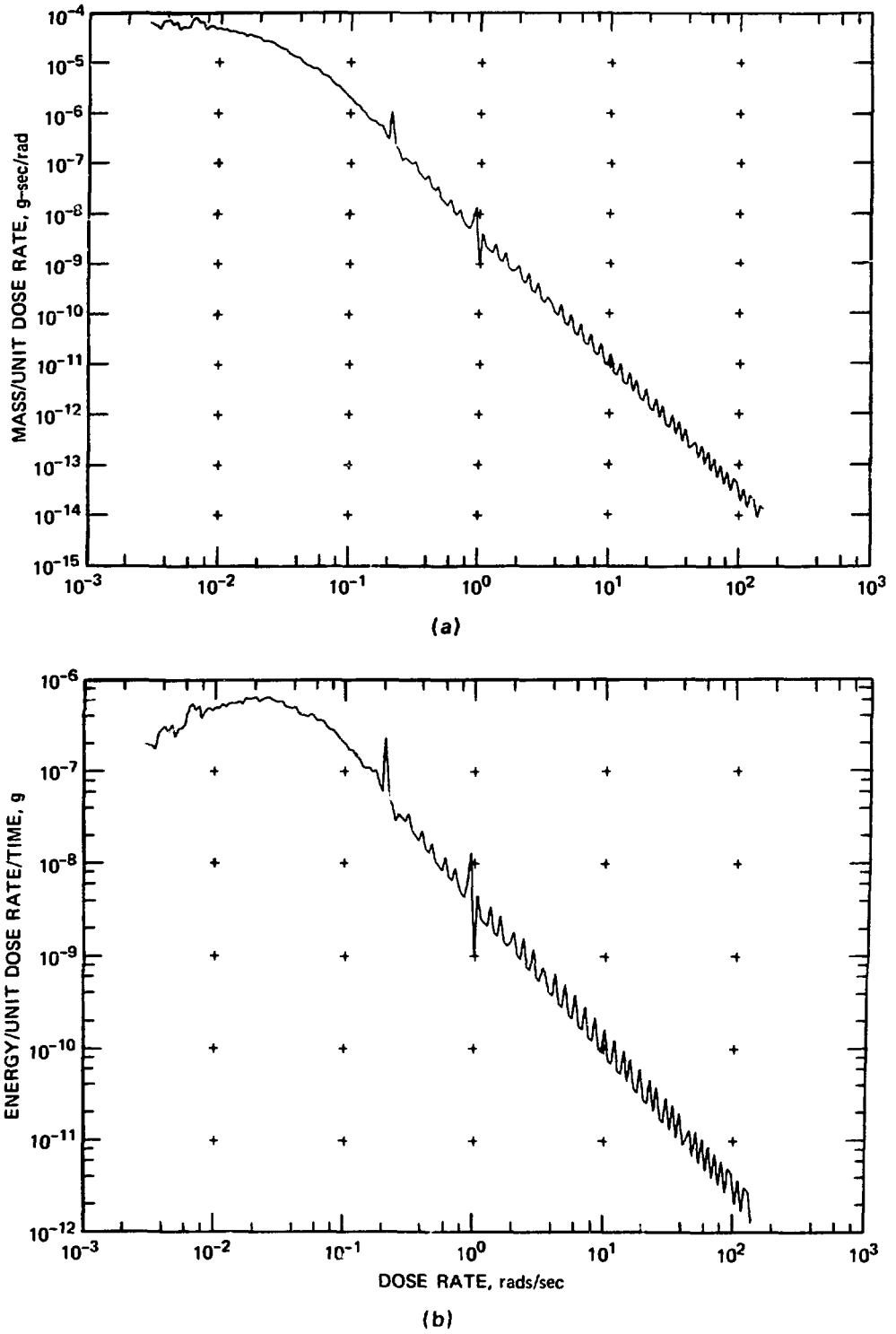

Fig. 3 Modeling results for multiparticle average for 0.73-μm-diameter $^{238}PuO_2$ particles. **(Figure continues on next page.)**

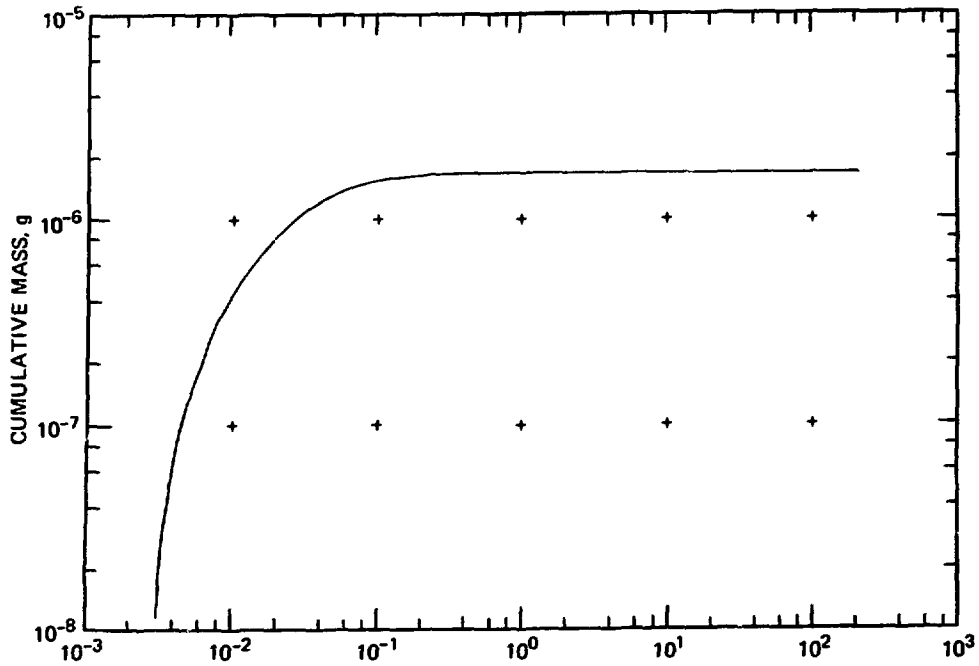

(c)

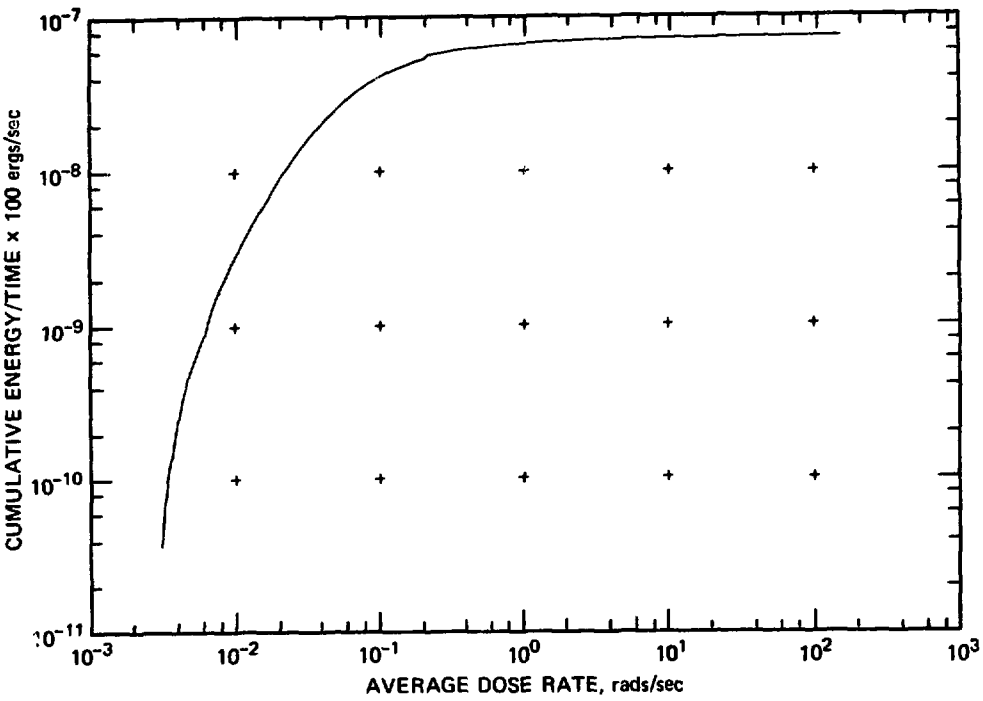

(d)

Fig. 3 (Continued)

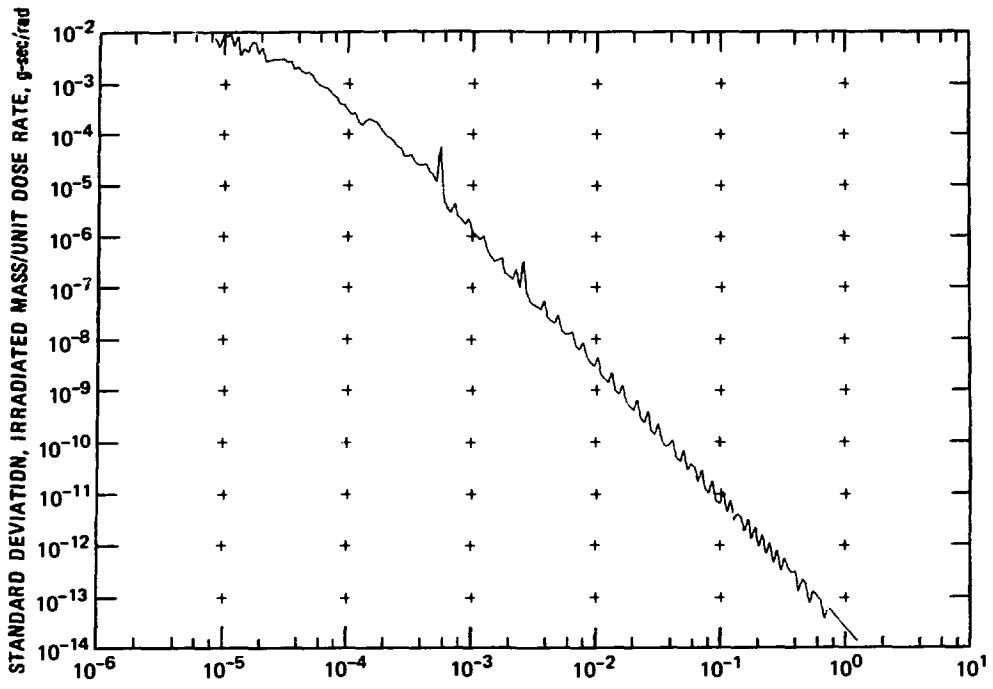

(a)

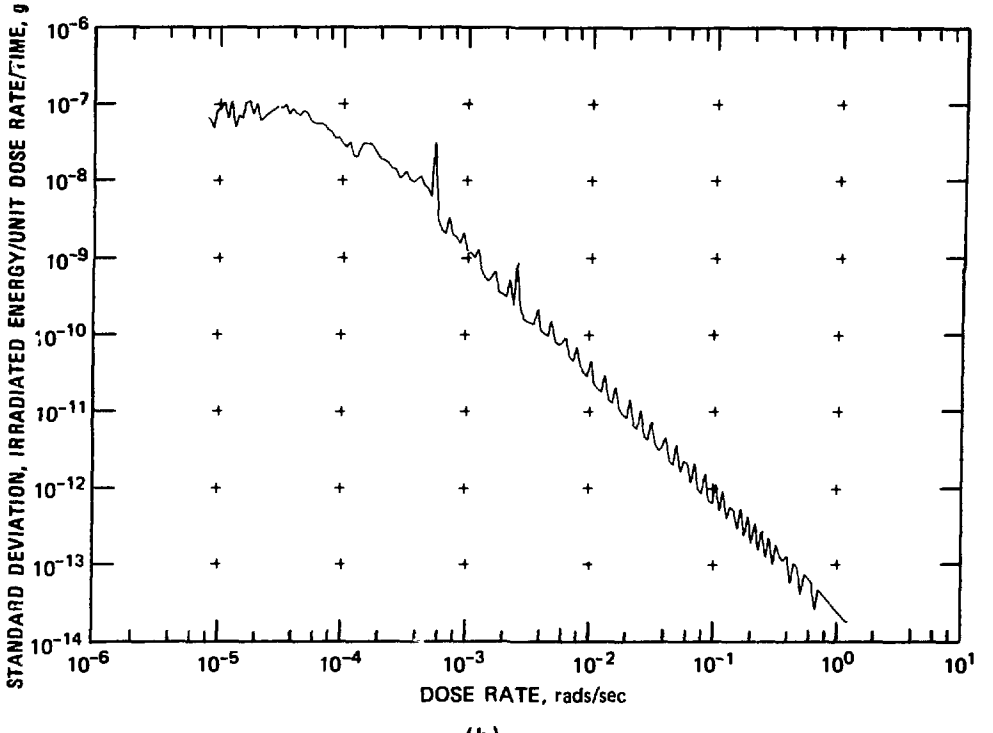

(b)

Fig. 4(a and b) Standard deviations for modeling results for 0.1-μm-diameter $^{238}PuO_2$ particles. (Figure continues on next page.)

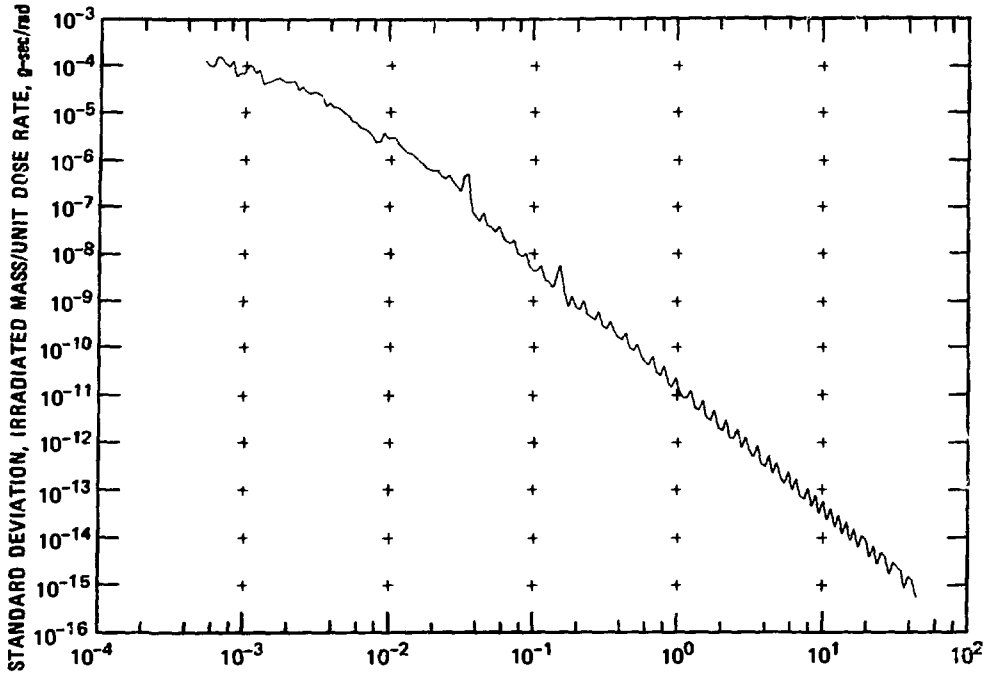

(c)

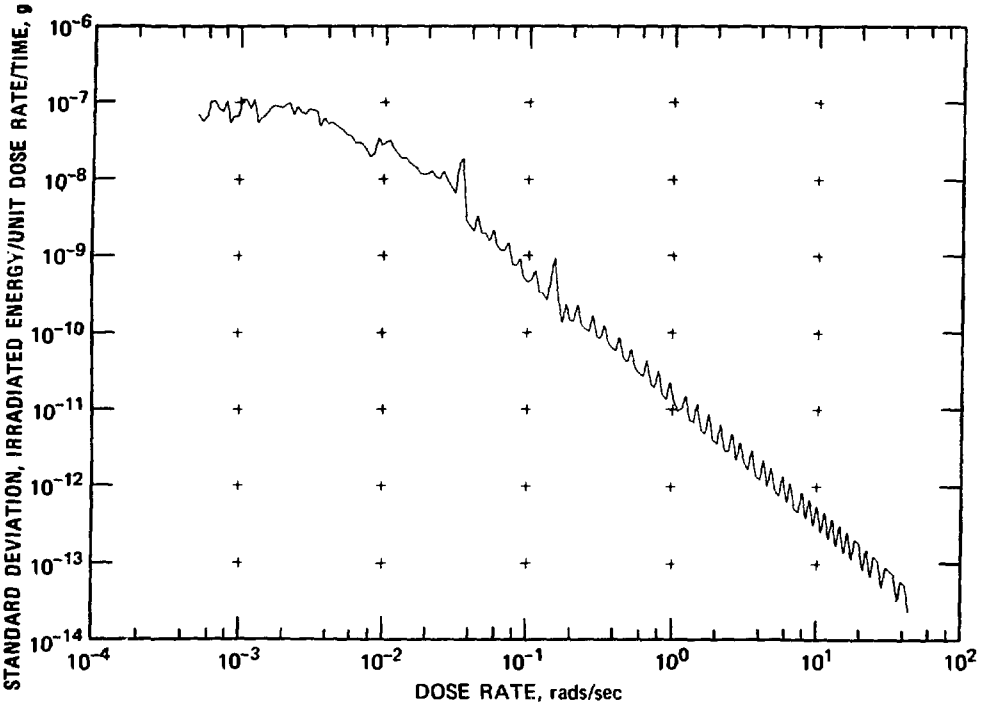

(d)

Fig. 4(c and d) Standard deviations for modeling results for 0.4-μm-diameter $^{238}PuO_2$ particles. (Figure continues on next page.)

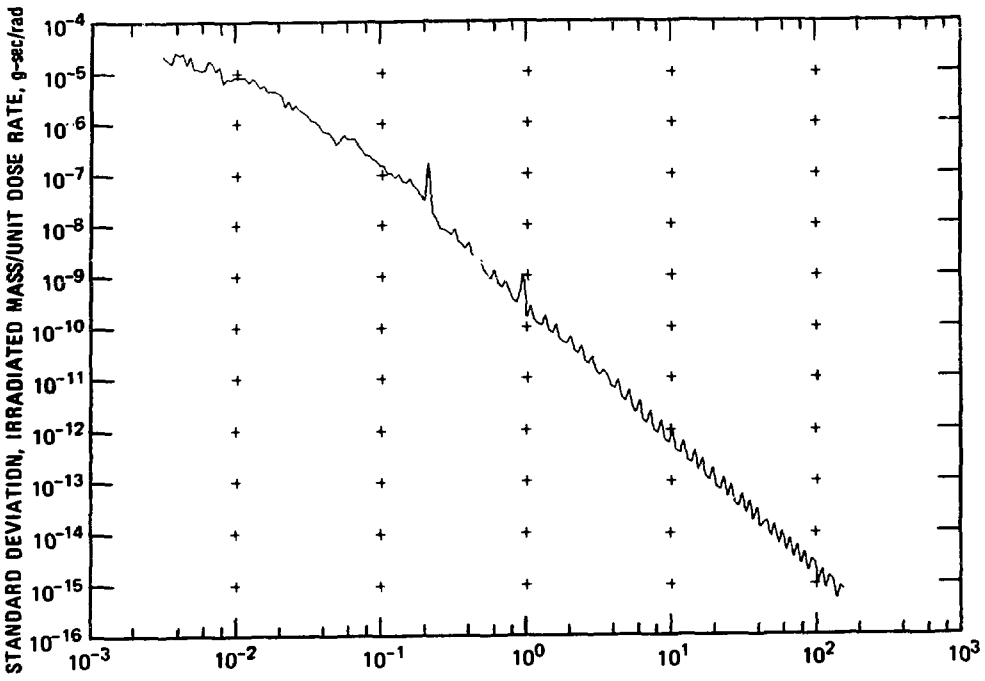

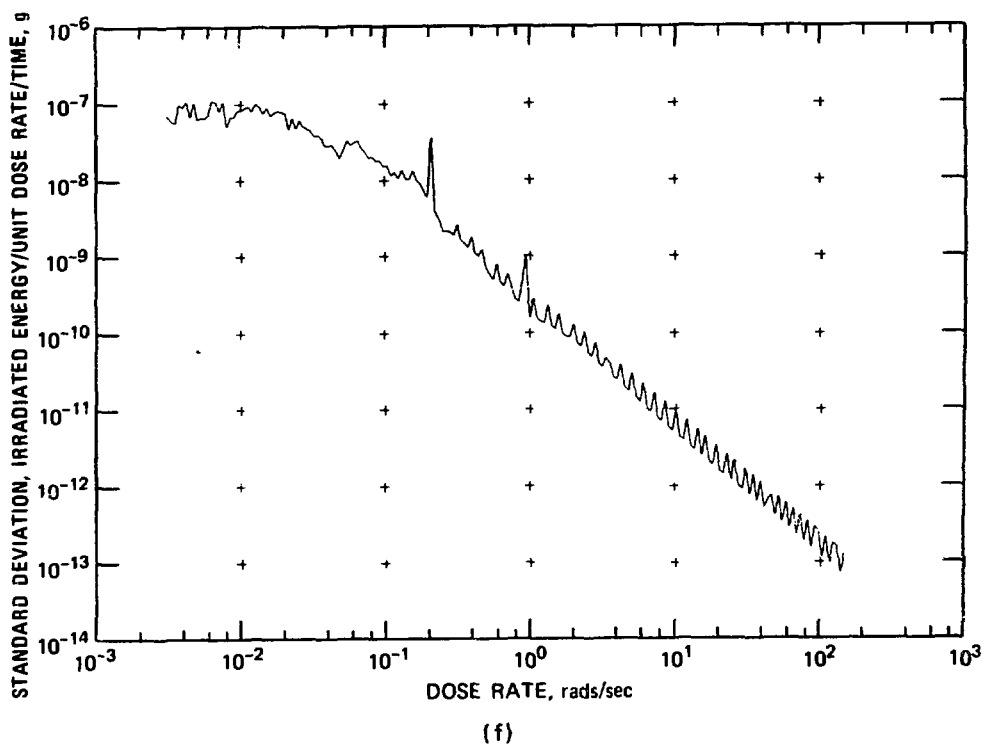

Fig. 4(e and f) Standard deviations for modeling results for 0.73-μm-diameter $^{238}PuO_2$ particles.

lower dose-rate values) than the corresponding mass distribution. This behavior is reflected in the cumulative mass and energy curves, where the latter type of curve accumulates more slowly with increasing dose rate. A comparison of the various distributions with particle size indicates similar shape behavior. As the particle size increases, the cumulative curves accumulate more slowly with increasing dose rate, where again the energy accumulation is slower than the mass accumulation. One can see that the 0.73-μm-diameter distributions do not break as cleanly as the 0.1- and 0.4-μm-diameter distributions at the lower dose-rate values. This is because the lower dose-rate limit was chosen for the scaling. Had a lower limit been used, this break would have been more pronounced. This is not a serious problem, however, because the accumulative mass is about the same for all particle sizes. The wiggly behavior seen at the very low dose rates indicates very little mass available for irradiation. Thus a small extrapolation of the 0.73-μm-diameter distributions at the very low dose-rate values is reasonable. The standard deviations for the various distributions presented in Fig. 4 indicate a small increase in error with decreasing dose rate of about comparable magnitude for the mass and energy distributions.

From an applicational viewpoint, the model is the most realistic available. Flexibility has been incorporated into the computer code input so that examples of dose-rate distributions can easily be obtained for a variety of conditions. Modeling, which removes some of the constraints on the present results such as nonstatic particles, multiparticle overlap, further division of tissue type, and larger diameter particles, may be of interest.

ACKNOWLEDGMENT

The research reported in this study was sponsored by the Energy Research and Development Administration, Division of Nuclear Research and Applications.

REFERENCES

1. P. J. Dionne and C. L. Sanders, A Simulated Model for Determining the Distribution of Alpha-Energy in Alveoli from Inhaled Plutonium Particles, USAEC Report BNWL-SA-2282, Battelle—Northwest, NTIS, January 1969.
2. E. C. Anderson, P. N. Dean, and D. M. Matsakis, Dosimetry, in *Annual Report of the Biological and Medical Research Group (H-4) of the Los Alamos Scientific Laboratory Health Division, January Through December 1972*, USAEC Report LA-5227-PR, pp. 5-9, NTIS, March 1973.

3. J. R. Coleman and L. J. Perez, Jr., Consideration of a Tumor Probability Function and Micro-Dosimetry for the Lower Pulmonary Compartment, NUS Report 654, NUS Corporation, Rockville, Maryland, 1969.
4. W. J. Bair, C. R. Richmond, and B. W. Wachholz, A Radiobiological Assessment of the Spatial Distribution of Radiation Dose from Inhaled Plutonium, USAEC Report WASH-1320, NTIS, September 1974.
5. R. D. Evans, *The Atomic Nucleus*, pp. 649-653, McGraw-Hill Book Company, Inc., New York, 1955.

Macrophages in Culture: Some Properties Relevant to the Study of Emphysema

CHARLES KUHN III, RICHARD WHITE, THOMAS REPPUN, and H. S. LIN
Departments of Pathology and Radiology, Washington University
School of Medicine, St. Louis, Missouri

ABSTRACT

Macrophage proliferation and enzymatic degradation of elastin have been implicated in the pathogenesis of emphysema. Different tissue-culture systems are required for the investigation of alveolar macrophage proliferation and for the demonstration of elastase secretion by macrophages.

For macrophage proliferation in vitro, a serum containing medium supplemented by a source of colony-stimulating (CS) activity is required. In this investigation, cells were obtained by lavage of mouse or hamster lungs and cultured in semisolid agar medium supplemented by L cell or BHK cell conditioned medium as a source of CS factor. After a delay of several days, the cells began to divide and to form colonies. In contrast to peritoneal cells, a high proportion of alveolar cells (up to 20%) formed colonies and did so without "activation." The cells of the colonies have been identified as macrophages on the basis of their morphology, phagocytic activity, cytochemical enzyme staining, and membrane receptors, which bind the Fc regions of immunoglobulins. So that the progenitor of the macrophage colonies could be identified, the population of cells obtained by lavage of the air spaces was fractionated by size and density on isokinetic Ficoll gradients. Fractions enriched in colony-forming cells consisted of large cells classified morphologically as macrophages and possessing phagocytic ability. Fractions of small cells resembling lymphocytes lacked colony-forming cells. Apparently a sizable proportion of typical alveolar macrophages have the capacity for repeated cell division.

Neither peritoneal nor alveolar macrophages store intracellular elastase (detectable by the lysis of elastin suspensions in agar). Peritoneal macrophages secrete little elastase into the culture fluid unless activated as by phagocytosis or thioglycollate. Even without activation alveolar macrophages secrete elastase but do not increase their rate of secretion with phagocytosis of inert particles. Macrophage elastase appears to be a serine protease with a pH optimum of 7.6 to 7.8. It differs from porcine pancreatic and human leukocyte elastase in its behavior toward inhibitors. It is completely inhibited by human serum but only partly inhibited by purified α_1-antiprotease.

The idea that destruction of elastic fibers is a fundamental mechanism in the pathogenesis of emphysema has, for the past 100 years, been a recurrent theme in pathologic studies.[1-4] Although initially the destruction was blamed on mechanical wear, recent clinical and experimental evidence points to enzymatic proteolysis as the mechanism.[5,6] Indeed, intratracheal administration of enzymes with elastolytic activity,[7,8] including pancreatic elastase,[9,10] is effective in producing emphysema in experimental animals, whereas other proteases, including bacterial collagenase,[11] are not.

Inflammatory cells are considered the most likely source of elastases to attack lung elastin. Leukocytes contain an elastase that is inhibited by α_1-antiprotease.[12,13] Experimentally leukocyte homogenates produce emphysema in dogs.[14] However, pathologic studies of early lesions of emphysema[4,15] as well as of the early changes seen in asymptomatic cigarette smokers[16] have stressed the occurrence of increased numbers of macrophages topographically related to the morphologic lesions. Therefore, as part of a comprehensive approach to the pathogenesis of emphysema, it seems pertinent to consider factors that influence alveolar macrophage number and elastase production.

MACROPHAGE NUMBER

Experiments in rats indicate that normally as many as 1 to 3×10^6 macrophages leave the lung hourly and must be replaced.[17] A variety of elegant experiments with radiation-induced chimeras leave little doubt that alveolar macrophages can ultimately be derived from bone marrow.[18-21] In relatively acute inflammatory states, migration of monocytes from blood into air spaces can be demonstrated.[22,23] This does not preclude the possibility that, under steady-state conditions or in response to relatively low-grade stimuli, a locally proliferating pool of cells is a significant source of macrophages. Recent studies have shown that alveolar macrophages can be induced to divide in vitro,[24,25] whereas thymidine uptake and mitosis have been stimulated in alveolar macrophages in vivo by NO_2 and inert particles.[26,27] As a result of these observations, we have begun to study the question of cell division by free alveolar macrophages from the air spaces.

Lin and Stewart[28-30] studied the capacity of mouse peritoneal macrophages to proliferate in semisolid medium and give rise to colonies. Resident peritoneal macrophages were substantially without colony-forming ability, but peritoneal exudates formed in response to thioglycollate or other activating agents could give rise to colonies

of from 50 to several hundred cells.[30] The peritoneal colony-forming cells (PCFC's) were like the well-studied bone-marrow colony-forming cells in that they required media conditioned by other mouse cells as a source of colony-stimulating (CS) factor,[29] but they differed from bone-marrow colony-forming cells in their kinetics. Whereas bone-marrow colony-forming cells begin to divide within 24 hr and the number of colonies reaches a maximum in a week, PCFC's only begin to divide after 10 days in culture and reach a maximum number of colonies after 25 days (Ref. 30).

When the same culture system was applied to cells obtained from hamsters or mice by pulmonary lavage, an appreciable proportion of the lavage cells, up to a maximum of 20%, gave rise to colonies without any additional activation.[31] The kinetics of colony formation were similar to those of PCFC's. Proliferation was delayed for several days, and the maximum number of colonies was not reached until 18 to 24 days (Fig. 1). Again a source of CS factor was required.

The cells that comprised the colonies were typical macrophages morphologically (Fig. 2) and were shown to be phagocytic for yeast and to have Fc receptors.[31] Histochemically they lacked peroxidase activity but had readily demonstrable lysosomal hydrolase activity,

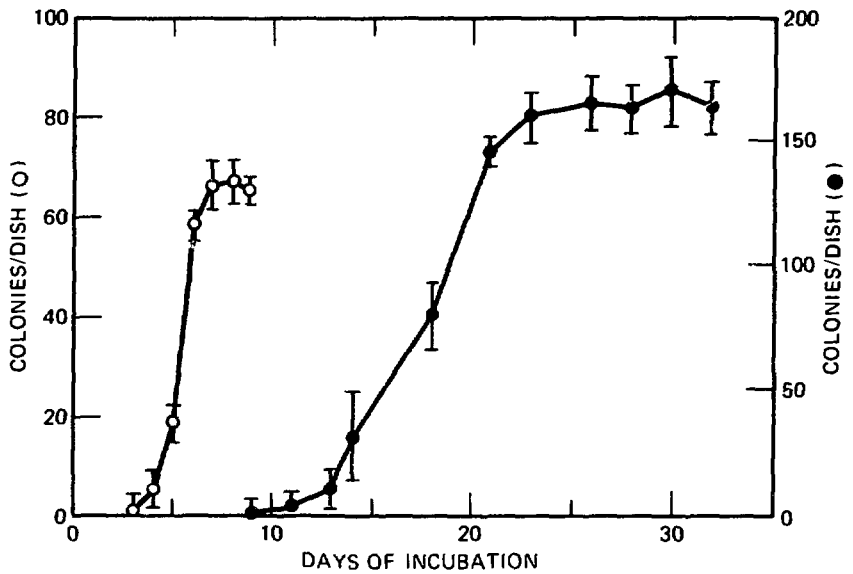

Fig. 1 Appearance of colonies in bone marrow (○) or alveolar cell (●) cultures after various periods of culture. The inoculum was 10^5 bone marrow cells or 10^3 alveolar cells per dish. Vertical bars are standard error of the mean.

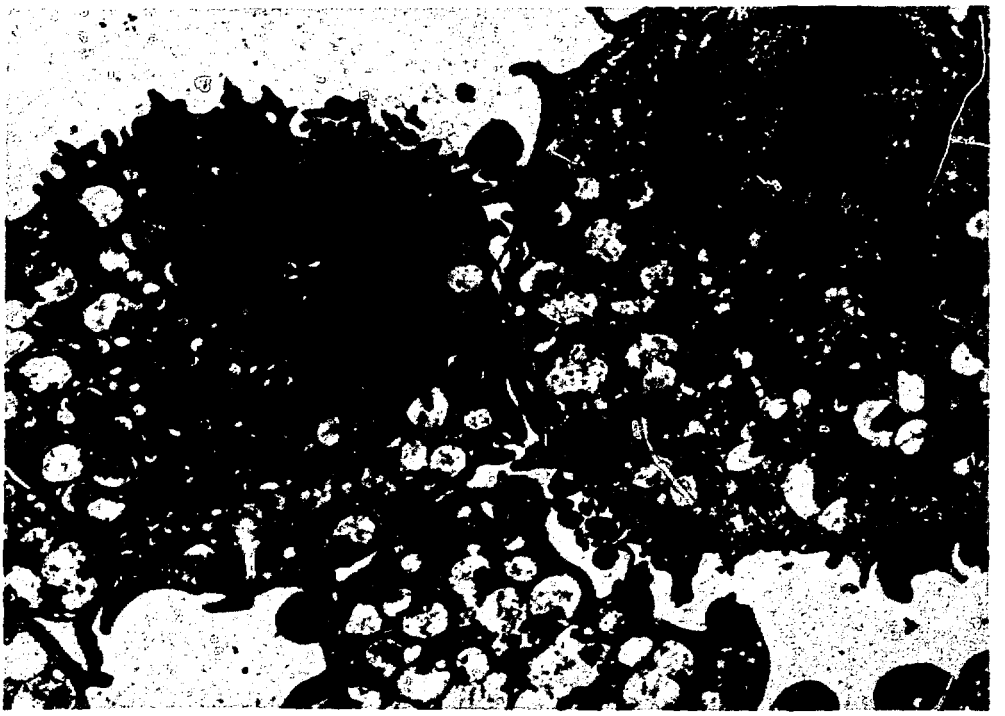

Fig. 2 Ultrastructure of the cells of a 28-day alveolar cell culture. The ruffled border, eccentric nucleus, and distinct cytocenter containing the Golgi apparatus are all features of mature macrophages. The peripheral cytoplasm contains many vacuoles with electron lucent contents, possibly phagocytized agar.

staining for acid phosphatase, β-glucuronidase, and nonspecific esterase. Thus the colonies were clearly macrophages.

The number of colonies formed is linearly related to the number of cells plated.[31] This is consistent with the idea that each colony is a clone derived from a single progenitor. The bone-marrow colony-forming stem cells have been identified as small lymphocyte-like cells.[32-34] In an attempt to characterize the alveolar colony-forming cell (ACFC), alveolar lavages have been fractionated on the basis of the simple physical properties of size and density. Three methods have been used: isopycnic centrifugation in Ficoll, velocity sedimentation at 1 x *g* in albumin,[35] and Pretlow's method of velocity sedimentation by centrifugation in isokinetic Ficoll gradients.[36] In density-gradient experiments, enrichment of the ACFC's occurred in the fractions corresponding to a density of 1.04 to 1.06, but the morphology of the cells in the fractions was too heterogeneous to permit conclusions as to the identity of the ACFC's. The Pretlow method gave uniform separations that resolved the lavage into two

separate peaks, one of large cells and a second one of small lymphocyte-like cells. This procedure produces up to a threefold enrichment of the ACFC's in the large cell peak, whereas the small cell peak is depleted to colony-forming cells (Fig. 3). Thus cell populations of as high as 40 to 50% ACFC's have been obtained. The morphology of the cells comprising the enriched fractions was uniform and typical of differentiated macrophages (Fig. 4). The cells had large eccentric folded nuclei and abundant cytoplasm with pseudopodial extensions of their ectoplasm. The cytoplasm contained numerous endocytic vacuoles as well as large lysosomal granules (Fig. 5). When exposed for 10 min to 1.01-μm latex beads, 85 to 90% of the cells in the most highly enriched fractions engulfed three or more beads. Thus the results of these experiments suggest that morphologically typical alveolar macrophages include cells with extensive proliferative capacity. The PCFC's have not been identified morphologically but have been shown to adhere to plastic surfaces

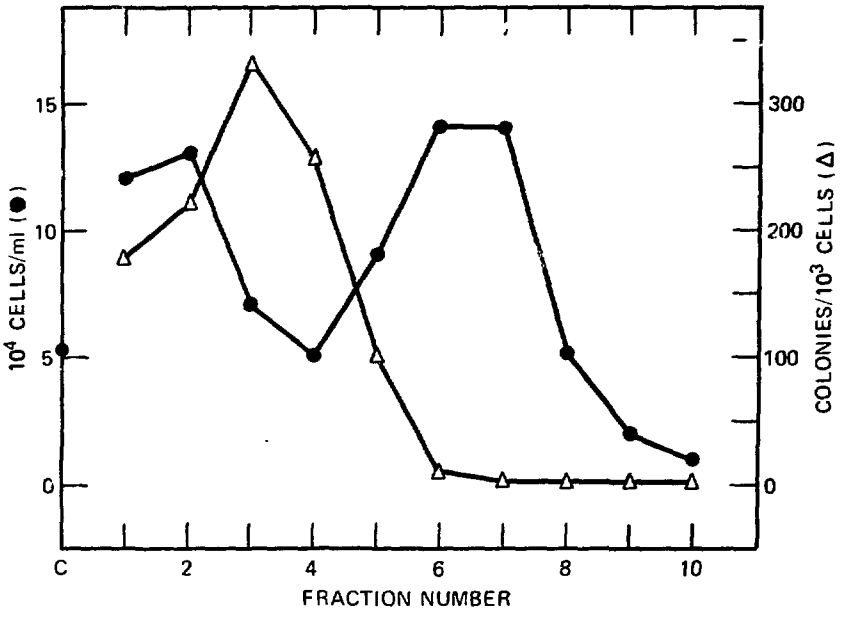

Fig. 3 Separation of alveolar lavage cells by velocity sedimentation on isokinetic Ficoll gradient. Fractions were collected from the bottom of the tube so that fraction 1 is the most dense and fraction 10 the least. The cell population is divided into two peaks; the one with larger cells, sedimenting farther in the gradient, contains the colony-forming cells. Fractions 3 and 4, although small, contain the highest proportion of colony-forming cells. ●, number of cells. △, number of colonies obtained per 10^3 cells seeded.

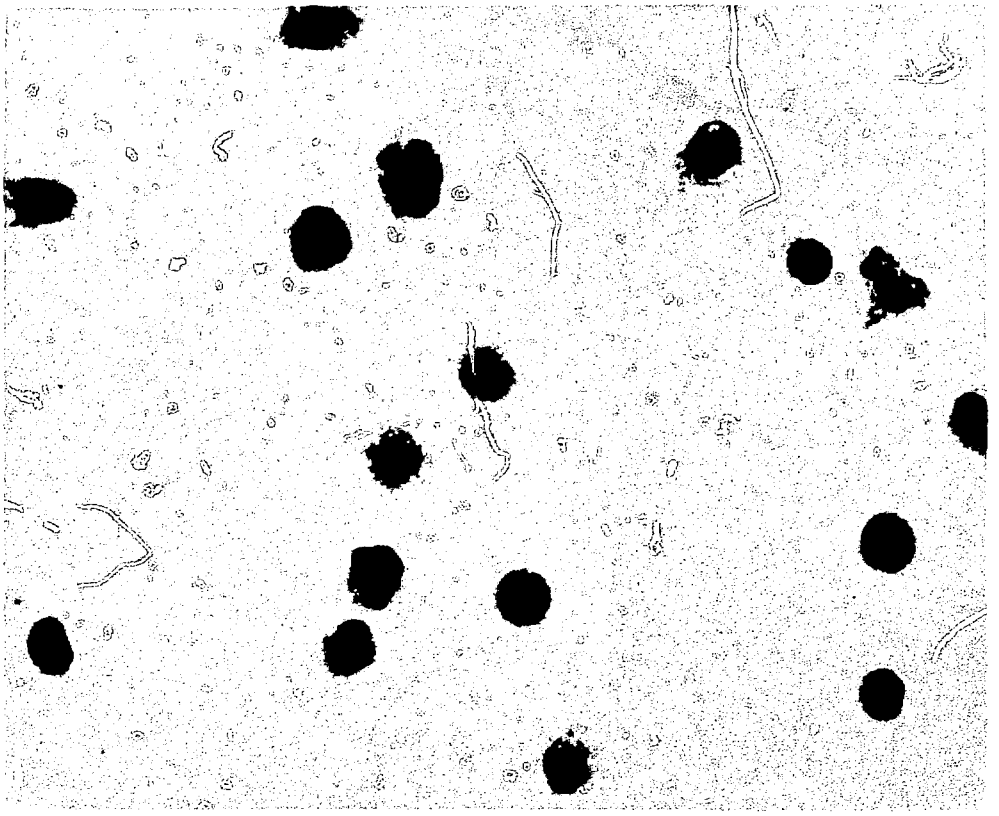

Fig. 4 Light micrograph of a cytocentrifuge preparation from fraction 4 of an experiment similar to that in Fig. 3. Forty percent of the cells in this fraction were ACFC's. The cells have the appearance of mature macrophages.

and to phagocytize iron carbonyl particles[37] so that functionally they too have the properties of macrophages.

As yet little is known about the control of alveolar macrophage proliferation. The ACFC's, like peritoneal and bone-marrow colony-forming cells, require adequate concentrations of specific factors called CS factors, which are released by a variety of cells in tissue culture. Generally the CS factors are species specific, although medium conditioned by mouse strain L cells will support colony formation by hamster as well as mouse alveolar cells.[31] The CS factors for bone marrow have been studied extensively. They are found in serum and urine and some tissues as well as culture fluids. The CS factors from varying sources vary in properties, but most appear to be glycoproteins. The CS factors are active at low concentrations, $10^{-11}M$ in the case of human urinary CS factor, and must be present continuously during the period of culture.[38]

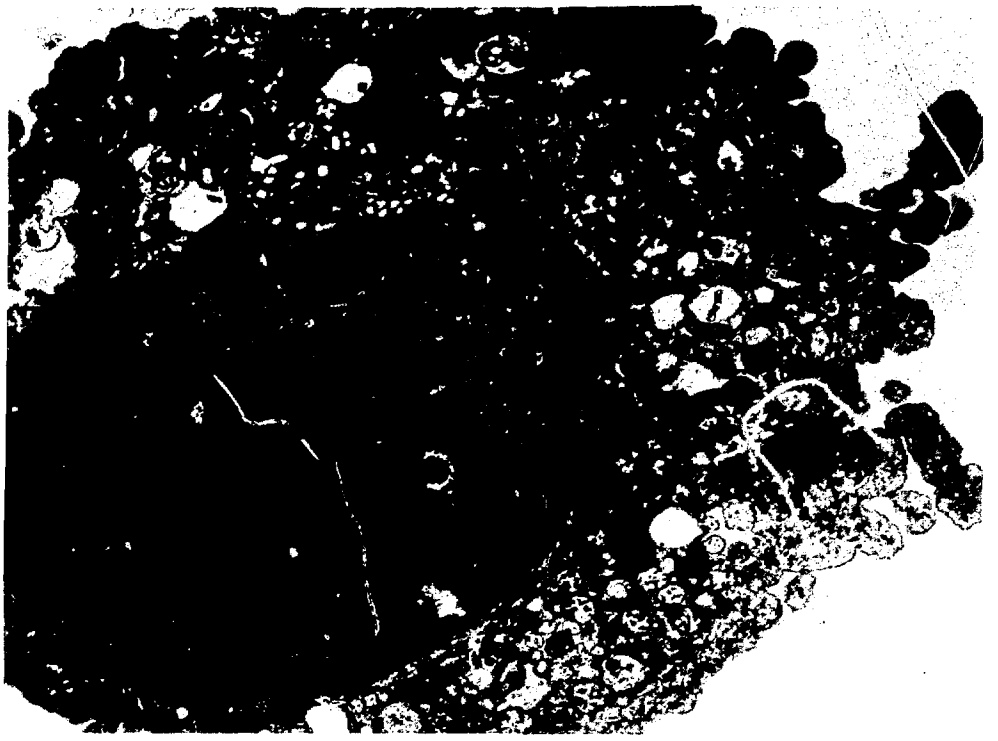

Fig. 5 Electron micrograph of the same fraction as Fig. 4. Cytocentrifuge preparation prepared for electron microscopy. The cell has the configuration and polymorphous granules of a mature macrophage.

Genetic factors also may play a role. In the mouse there are marked differences in the proportion of ACFC's between different strains (Table 1). Moreover, the (C57Bl/6 + DBA/2)F_1 hybrid showed intermediate values compared to the two parental strains. We did not find comparable differences with bone marrow from the same strains. When mouse embryo fibroblasts of the same four strains were used to prepare CS factors, the relative proportion of ACFC's remained the same regardless of the strain of origin of the CS factor, which implies that the strain difference in ACFC's resides in the cell population rather than in strain specificity of particular CS factors.

Although much additional experimentation will be required to determine whether the ACFC's that form colonies in vitro truly represent a pool of cells dividing in vivo, colony formation on semisolid media offers an approach to the investigation of control of macrophage proliferation and to the study of functionally specialized subpopulations among morphologically similar alveolar macrophages.

TABLE 1

STRAIN DIFFERENCES IN ALVEOLAR COLONY-FORMING CELLS

Strain	No. of mice tested	Colonies/10^4 alveolar cells
C3H	28	172 ± 30*
DBA/2	15	190 ± 21
BD_2F_1	14	79 ± 14
C57 Bl/6	26	8 ± 2

*Mean ± SEM.

ELASTASE SECRETION

Studies of macrophages obtained by lavage from cigarette smokers have not only consistently shown an increase in the number of macrophages but also have shown higher levels of granular enzyme activity compared with cells from nonsmokers.[39] Activity of an elastase-like enzyme has been studied in macrophages using synthetic ester substrates such as *t*-butoxylcarbonyl-L (*t*-BOC)-alanine *p*-nitrophenyl ester.[39-41] When Levine, Senior, and Butler[42] attempted to detect elastolytic activity using elastin suspended in agar as substrate or using a newer and more specific synthetic substrate, succinyl-alanyl-alanyl-alanyl-*p*-nitroanilide, they found that granule fractions of macrophages from several species, including man, lacked elastolytic activity, even though they did indeed hydrolyze the *t*-BOC-alanine *p*-nitrophenyl ester. Apparently with the macrophage, unlike the leukocyte, one cannot equate alanyl nitrophenyl esterase activity with elastase.

Several other neutral proteases, including plasminogen activator[43] and collagenase,[44-46] are secreted by macrophages but are not stored by the cells to any appreciable extent and hence cannot be detected in cell lysates. Recently Werb and Gordon[47] found that a similar situation applies to elastase in mouse peritoneal exudate macrophages. They found that peritoneal macrophages could be maintained for extended periods in serum-free medium and would secrete an enzyme that lyses elastin particles suspended in agar and sodium dodecyl sulfate. Activation of the macrophages by thioglycollate or by phagocytosis of nondegradable particles (latex) greatly stimulated elastase secretion.

To investigate elastase production by alveolar macrophages, we cultured the glass-adherent cells obtained by saline lavage of mouse lungs in Dulbecco's medium containing 15% acid-treated serum for 4 days and then washed the cells and replaced the medium with serum-free Dulbecco's medium containing 0.2% lactalbumin hydrolyzate.[47] The amount of elastase in the medium increased for a period of 3 days in culture (Fig. 6). By 4 days in culture, the cells began to show morphologic signs of degeneration, particularly nuclear pycnosis, but the majority would recover if returned to the serum-containing medium. Past 5 days in serum-free medium, the cells began to detach from the culture dish, would not recover with serum-containing medium, and elastase levels in the medium declined. Routinely, therefore, culture fluids and cells were studied on the fourth day.

As with peritoneal exudate cells,[47] alveolar macrophages released elastase into the culture medium, but intracellular levels were undetectable. Although alveolar cells produced more elastase than did peritoneal exudate cells, they did not increase their secretion above resting levels when given a phagocytic load. The release of elastase most probably reflects secretion of newly formed enzyme rather than gradual release of intracellularly stored material. Inclusion of cycloheximide in cultures maintained for 24 hr prevented the appearance of elastase. On the other hand, when washed cells were lysed by sonication, not only was no elastase measurable but also treatment of

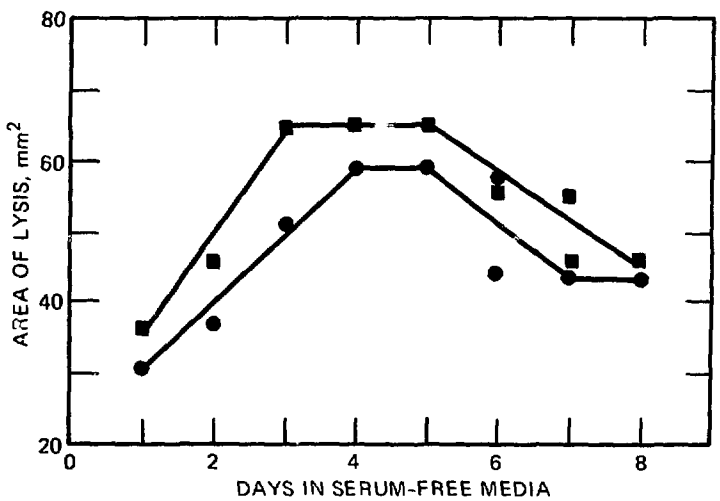

Fig. 6 Elastase activity of fluids obtained from macrophage cultures of varying duration. After 4 days in culture the cells appeared degenerated. ■, alveolar cells. ●, thioglycollate-induced peritoneal cells.

the lysates with trypsin to activate a proenzyme failed to make it appear.

The limited information obtained thus far about the elastase released by alveolar macrophages indicates that its properties are identical to those of the enzyme from peritoneal macrophages but are distinctly different from those of human leukocyte elastase (HLE) and porcine pancreatic elastase (PPE). The pH optimum of macrophage elastase, 7.6 to 7.8, is less alkaline than that of HLE (pH 8.4) or PPE (pH 8.6), and they differ in their susceptibility to several inhibitors (Table 2). Like the other elastases, macrophage elastase is inhibited by sulfonyl fluorides, which indicates the presence of serine at the active site. Of particular interest in the context of emphysema is the observation that elastolysis by the culture fluids is inhibited by human serum but equally so by serum of the Pi MM or Pi Z phenotypes, whereas highly purified α_1-antiprotease only partially inhibited the activity. This suggests that serum proteins other than α_1-antiprotease may be the main biological inhibitor.

Much more work will be required to determine whether elastases are important in the pathogenesis of emphysema in man and which of the many potential sources of elastases contribute. The improvements over the past few years in our ability to culture macrophages under different conditions now give us the means to investigate those

TABLE 2

INHIBITORS OF SEVERAL ELASTASES

Inhibitor	Source*			
	Alveolar macrophage	Peritoneal macrophage	Porcine pancreas	Human leukocyte
Phenyl methane sulfonyl fluoride (10m*M*)	++	++	++	++
P-chloromercuric benzoate (1m*M*)	—	—	—	+
Dithiothreitol (20m*M*)	—	—	+	+
Acetyl (alanyl)$_3$ chloromethyl ketone (2m*M*)	—	—	++	++
Human serum (5%)	++	++	++	++
α_1-antiprotease (60 μg/ml)	+	+	++	++

* —, no inhibition; +, < 50% inhibition; ++, > 50% inhibition.

factors which influence the number and secretory activity of these cells that pathologic studies have implicated in the early stages of emphysema.

ACKNOWLEDGMENTS

This work was supported by U. S. Public Health Service research grants RO1 HL 19746, PO1 HL 16118, and 1 PO2 CA 13053 and training grants ES-00128 and GM-00897. Dr. Lin is the recipient of research career development award CA 70730.

REFERENCES

1. H. Eppinger, Das Emphysem der Lungen, *Vrtljschr. prakt. Heilk. Prag.*, 4: 1-80 (1876).
2. F. Orsos, Über das Elastische Gerüst der Normalen und der Emphysematösen Lunge, *Beitr. Path. Anat.*, 41: 95-121 (1907).
3. R. R. Wright, Elastic Tissue of Normal and Emphysematous Lungs. A Tridimensional Histologic Study, *Am. J. Pathol.*, 39: 355-363 (1961).
4. K. K. Pump, Fenestrae in the Alveolar Membrane of the Human Lung, *Chest*, 65: 431-436 (1974).
5. S. Eriksson, Pulmonary Emphysema and Alpha-1-Antitrypsin Deficiency, *Acta Med. Scand.*, 175: 197-205 (1964).
6. P. Gross, M. A. Babyak, E. Tolker, and M. Kaschak, Enzymatically Produced Pulmonary Emphysema. A Preliminary Report, *J. Occup. Med.*, 6: 481-484 (1964).
7. G. L. Snider, J. A. Hayes, C. Franzblau, H. M. Kagan, P. S. Stone, and A. L. Korthy, Relationship Between Elastolytic Activity and Experimental Emphysema-Inducing Properties of Papain Preparations, *Am. Rev. Respir. Dis.*, 110: 254-262 (1974).
8. C. E. Blackwood, Y. Hosannah, E. Perman, S. Keller, and I. Mandl, Experimental Emphysema in Rats. Elastolytic Titer of Inducing Enzyme as Determinant of the Response, *Proc. Soc. Exp. Biol. Med.*, 144: 450-454 (1973).
9. P. D. Kaplan, C. Kuhn, and J. A. Pierce, The Induction of Emphysema with Elastase. I. The Evolution of the Lesion and the Influence of Serum, *J. Lab. Clin. Med.*, 82: 349-356 (1973).
10. J. A. Hayes, A. Korthy, and G. L. Snider, The Pathology of Elastase-Induced Panacinar Emphysema in Hamsters, *J. Pathol.*, 117: 1-14 (1975).
11. R. M. Senior, P. E. Kaplan, C. Kuhn, and H. E. Linder, Enzyme-Induced Emphysema, in *Fundamental Problems of Cystic Fibrosis and Related Diseases*, John A. Mangos and Richard C. Talamo (Eds.), pp. 183-194, Stratton Intercontinental Medical Book Corp., New York, 1973.
12. K. Ohlsson, Neutral Leukocyte Protease and Elastase Inhibited by Plasma Alpha-1-Antitrypsin, *Scand. J. Lab. Clin. Med.*, 28: 251-253 (1971).
13. A. Janoff, Inhibition of Human Granulocyte Elastase by Serum Alpha-1-Antitrypsin, *Am. Rev. Respir. Dis.*, 105: 121-122 (1972).
14. B. Mass, T. Ikeda, D. R. Meranze, G. Weinbaum, and P. Kimbel, Induction of Experimental Emphysema Cellular and Species Specificity, *Am. Rev. Respir. Dis.*, 106: 384-391 (1972).

15. R. F. McLaughlin and E. E. Tueller, Anatomic and Histologic Changes of Early Emphysema, *Chest*, 59: 592-599 (1971).
16. D. E. Niewoehner, J. Kleinerman, and D. B. Rice, Pathologic Changes in the Peripheral Airways of Young Cigarette Smokers, *New Engl. J. Med.*, 291: 755-758 (1974).
17. A. A. Spritzer, S. A. Watson, J. A. Auld, and M. A. Guetthoff, Pulmonary Macrophage Clearance. The Hourly Rates of Transfer of Pulmonary Macrophages to the Oropharynx of the Rat, *Arch. Environ. Health*, 17: 726-730 (1968).
18. M. O. Pinkett, C. R. Cowdrey, and P. C. Nowell, Mixed Hematopoietic and Pulmonary Origin of Alveolar Macrophages as Demonstrated by Chromosome Markers, *Am. J. Pathol.*, 48: 859-867 (1966).
19. M. Virolainen, Hematopoietic Origin of Macrophages as Studied by Chromosome Markers in Mice, *J. Exp. Med.*, 127: 943-952 (1968).
20. M. A. Brunstetter, J. A. Hardie, R. Schiff, J. P. Lewis, and C. E. Cross, The Origin of Pulmonary Alveolar Macrophages. Studies of Stem Cells Using the Es-2 Marker of Mice, *Arch. Intern. Med.*, 127: 1064-1068 (1971).
21. J. J. Godleski and J. D. Brain, The Origin of Alveolar Macrophages in Mouse Radiation Chimeras, *J. Exp. Med.*, 136: 630-643 (1972).
22. G. P. Velo and W. G. Spector, The Origin and Turnover of Alveolar Macrophages in Experimental Pneumonia, *J. Pathol.*, 109: 7-19 (1973).
23. G. F. Murphy, A. R. Brody, and J. E. Craighead, Monocyte Migration Across Pulmonary Membranes in Mice Infected with Cytomegalovirus, *Exp. Mol. Pathol.*, 22: 35-44 (1975).
24. S. C. Soderland and Y. Naum, Growth of Pulmonary Alveolar Macrophages In Vitro, *Nature (London)*, 245: 150-152 (1973).
25. D. W. Golde, L. A. Byers, and T. N. Finley, Proliferative Capacity of Human Alveolar Macrophage, *Nature (London)*, 247: 373-375 (1974).
26. M. J. Evans, L. J. Cabral, R. J. Stephens, and G. Freeman, Cell Division of Alveolar Macrophages in Rat Lung Following Exposure to NO_2, *Am. J. Pathol.*, 70: 199-208 (1973).
27. S. P. Sorokin and J. D. Brain, Pathways of Clearance in Mouse Lungs Exposed to Iron Oxide Aerosols, *Anat. Rec.*, 181: 581-626 (1975).
28. H. Lin and C. C. Stewart, Colony Formation by Mouse Peritoneal Exudate Cells In Vitro, *Nature (London) New Biol.*, 243: 176-177 (1973).
29. H. Lin and C. C. Stewart, Peritoneal Exudate Cells. I. Growth Requirement of Cells Capable of Forming Colonies in Soft Agar, *J. Cell. Physiol.*, 83: 369-378 (1974).
30. H. Lin, Peritoneal Exudate Cells. II. Kinetics of Appearance of Colony-Forming Cells, *J. Cell. Physiol.*, 84: 159-164 (1974).
31. H. S. Lin, C. Kuhn, and T.-T. Kuo, Clonal Growth of Hamster Free Alveolar Cells in Soft Agar, *J. Exp. Med.*, 142: 877-886 (1975).
32. D. W. Van Bekkum, M. J. Van Noord, B. Maat, and K. A. Dicke, Attempts at Identification of Hemopoietic Stem Cell in the Mouse, *Blood*, 38: 547-558 (1971).
33. A. S. Rubinstein and F. E. Trobaugh, Ultrastructure of Presumptive Hematopoietic Stem Cells, *Blood*, 42: 61-80 (1973).
34 M. A. S. Moore, N. Williams, and D. Metcalf, Purification and Characterization of the In Vitro Colony Forming Cell in Monkey Hemopoietic Tissue, *J. Cell. Physiol.*, 79: 283-292 (1972).
35. R. G. Miller and R. A. Phillips, Separation of Cells by Velocity Sedimentation, *J. Cell. Physiol.*, 73: 191-201 (1969).

36. T. G. Pretlow, E. E. Weir, and J. G. Zettergren, Problems Connected with the Separation of Different Kinds of Cells, *Int. Rev. Exp. Pathol.*, 14: 92-204 (1975).
37. H. S. Lin and P. G. Freeman, Peritoneal Exudate Cells. III. Characterization of Colony Forming Cells, *J. Cell. Physiol.*, 90: 407-414 (1977).
38. E. R. Stanley, G. Hansen, J. Woodcock, and D. Metcalf, Colony Stimulating Factor and the Regulation of Granulopoiesis and Macrophage Production, *Fed. Proc.*, 34: 2272-2278 (1975).
39. J. O. Harris, G. N. Olsen, J. R. Castle, and A. S. Maloney, Comparison of Proteolytic Enzyme Activity in Pulmonary Alveolar Macrophages and Blood Leukocytes in Smokers and Non-Smokers, *Am. Rev. Respir. Dis.*, 111: 579-588 (1975).
40. A. R. Janoff, R. Rosenberg, and M. Galdston, Elastase-Like Esteroprotease Activity in Human and Rabbit Alveolar Macrophage Granules, *Proc. Soc. Exp. Biol. Med.*, 136: 1054-1058 (1971).
41. N. R. Ackerman and J. R. Beebe, Release of β-Glucuronidase and Elastase from Alveolar Mononuclear Cells, *Chest*, 66(Supplement): 215-235 (1974).
42. E. A. Levine, R. M. Senior, and J. V. Butler, The Elastase Activity of Alveolar Macrophages. Measurements Using Synthetic Substrates and Elastin, *Am. Rev. Respir. Dis.*, 113: 25-30 (1976).
43. J. C. Unkeless, S. Gordon, and E. Reich, Secretion of Plasminogen Activator by Stimulated Macrophages, *J. Exp. Med.*, 139: 834-850 (1974).
44. L. M. Wahl, S. M. Wahl, S. E. Mergenhagen, and G. R. Martin, Collagenase Production by Endotoxin Activated Macrophages, *Proc. Natl. Acad. Sci. U.S.A.*, 71: 3598-3601 (1974).
45. Z. Werb and S. Gordon, Secretion of a Specific Collagenase by Stimulated Macrophages, *J. Exp. Med.*, 142: 346-360 (1975).
46. A. L. Horwitz and R. G. Crystal, Collagenase from Rabbit Pulmonary Alveolar Macrophages, *Biochem. Biophys. Res. Commun.*, 69: 296-303 (1976).
47. Z. Werb and S. Gordon, Elastase Secretion by Stimulated Macrophages Characterization and Regulation, *J. Exp. Med.*, 142: 361-377 (1975).

Biochemical Basis of Oxygen Toxicity in Guinea Pig Alveolar Macrophages and Granulocytes

GEORGE S. JOHNSON,* MANFRED RISTER,* COLEEN HIGGINS,* FELICE MANFREDI,† and ROBERT L. BAEHNER*

*Division of Pediatric Hematology-Oncology, Riley Children's Hospital, Indiana University School of Medicine, Indianapolis, Indiana, and †Division of Pulmonary Medicine, Veterans Administration Hospital, Indianapolis, Indiana

ABSTRACT

Superoxide dismutase (SOD) protects organisms from oxygen toxicity by dismutation of superoxide anion (O_2^-) to hydrogen peroxide (H_2O_2), which is metabolized by catalase (cata) and glutathione peroxidase (gluta px). We have previously shown a reproducible pattern of enzyme activities in alveolar macrophages (AM) and polymorphonuclear (PMN) granulocytes of guinea pigs exposed continuously to a fraction of inspired oxygen (FIO_2) of 85% for 90 hr. In both cell types gluta px decreased 50 to 60% below control levels by 18 hr and remained depressed; cata decreased 40% by 66 hr. Total SOD activity increased twofold in AM and PMN granulocytes by 66 hr; however, by 90 hr SOD activity in PMN granulocytes decreased to 50% above control and returned to control levels in AM. Since an FIO_2 of 50% has been shown to be innocuous in humans, we exposed guinea pigs to it continuously for 90 hr and serially quantitated gluta px, cata, and SOD in AM and PMN granulocytes and compared these results with those obtained at 85% FIO_2. Total SOD activity in AM and PMN granulocytes of animals exposed to 50% FIO_2 increased twofold and remained elevated at 90% and 120% above control levels in AM and PMN granulocytes, respectively. In both cell types cata remained at control levels during exposure to 50% FIO_2, but gluta px decreased 50 to 60% below control levels by 66 hr and remained depressed. In vitro exposure of PMN granulocytes 100,000 × *g* supernatant to 20 nmols of O_2^- for 5 min, generated by xanthine and xanthine oxidase, diminished cata and gluta px activities to 65 and 69% of control, respectively; the addition of 100 μg of SOD to the reaction mixtures prevented the decrease in enzyme activities. In summary, these studies support the idea that SOD, gluta px, and especially cata may provide useful biochemical markers of oxygen toxicity and that an FIO_2 of 50% is less toxic than 85%.

Damage to various tissues, such as the lungs, eyes, central nervous system, peripheral ganglia, heart, liver, and adrenal cortex, occurs in mammals on exposure to high concentrations of oxygen;[1-4] it is thought that activated metabolites of oxygen, such as superoxide anion (O_2^-), hydroxyl radical ($OH^\cdot$), oxygen singlet (O_2^*), and hydrogen peroxide (H_2O_2), are the sources of this damage.[5-8] Superoxide anion is generated during the univalent reduction of oxygen. Superoxide dismutase (SOD), an enzyme that is ubiquitous throughout all aerobic organisms but absent in strict anaerobes,[9] protects cells against this highly reactive radical by catalyzing the dismutation of O_2^- to H_2O_2 (Refs. 10 and 11):

$$O_2^- + O_2^- + 2H^+ \xrightarrow{SOD} H_2O_2 + O_2$$

In eukaryotes a copper—zinc form of the enzyme that is cyanide sensitive is localized in the cytosol; a manganese form of the enzyme is found in mitochondria and is cyanide insensitive.[12,13] Hydrogen peroxide is metabolized by catalase (cata) and glutathione peroxidase (gluta px), which protect cells against oxidation by reducing H_2O_2 to water and oxygen.[6,14,15]

Superoxide dismutase has been induced by exposing yeast and bacteria to increased concentrations of oxygen.[16] In mammalian species fractions of inspired oxygen (FIO_2) of greater than 80% induced SOD activity in whole-lung homogenates of rats, guinea pigs, hamsters, and neonatal rabbits.[7,17,18] However, in these studies no attempt was made to isolate the sources of the increased SOD activity in the lung, which is known to contain over 40 different cell types.[19] Consequently Rister and Baehner[20] demonstrated that AM contain five times more SOD activity than peritoneal PMN and concluded that this difference in SOD activity is attributable to the difference in oxygen tension between the lung and peritoneal cavity. In addition, these investigators found a reproducible pattern of SOD, cata, and gluta px activities in AM and PMN following the exposure of guinea pigs to an FIO_2 of 85%. In this study SOD activity increased significantly in AM and PMN. In addition, cata and gluta px activities in AM and PMN were significantly decreased following exposure to 85% FIO_2 (Ref. 21).

Since an FIO_2 of 50% has been shown to be innocuous in humans,[3,4] we exposed guinea pigs continuously to this FIO_2 for 90 hr and assayed for SOD, cata, and gluta px sequentially in isolated guinea pig AM and PMN granulocytes after 18, 42, 66, and 90 hr of oxygen exposure. These results were compared with those obtained previously at 85% FIO_2 to develop a biochemical model of oxygen toxicity.

METHODS

Exposure of Guinea Pigs to 50% FIO_2

Guinea pigs were maintained in a 35-by-40-by-86-cm plastic chamber at a temperature of 24°C and exposed to an FIO_2 of 50%. The oxygen concentration was monitored continuously. Control animals were kept under similar conditions in room air.

Preparations of Polymorphonuclear Leukocytes and Alveolar Macrophages

The AM and PMN granulocytes were obtained by a method previously described.[20] In brief, PMN granulocytes were harvested 18 hr after intraperitoneal injection of 12% casein. The AM were obtained from the same guinea pig by bronchopulmonary lavage. The cell suspensions were washed three times in Krebs Ringer phosphate buffer, pH 7.4. The AM suspension was further purified on a Ficoll—Hypaque gradient,[22] which achieved a purification of 95% viable macrophages. The final red-cell free samples of AM and PMN granulocytes were resuspended in Krebs Ringer phosphate buffer to a concentration of 5×10^6 cells/ml and 2×10^8 cells/ml, respectively. The cells were sonicated at 4°C for 1 min to ensure that all enzyme within the cells was accessible to substrate. The sonicates were centrifuged at 16,000 x *g* for 20 min and the resultant supernatant at 100,000 x *g* for 1 hr in an ultracentrifuge. The 16,000 x *g* and 100,000 x *g* pellets and the supernatant were assayed for cyanide-sensitive and cyanide-insensitive SOD, cata, and gluta px. The protein concentration of each cell fraction was determined with the folin phenol reagent and compared to bovine albumin as a standard.[23]

ENZYME ASSAYS

Superoxide Dismutase

All SOD data reported in this paper were obtained by the assay method of McCord and Fridovich,[10] which depends on the capacity of SOD to inhibit the cytochrome C reduction mediated by O_2^- generated during the oxidation of xanthine catalyzed by xanthine oxidase. Total SOD activity was measured without cyanide. The manganese-containing enzyme was determined by observing the SOD activity remaining after the addition of 1m*M* cyanide. Commercial bovine erythrocyte SOD was used as a standard. The change of the optical density was read at 550 nm. Each reaction mixture contained

1m*M* sodium azide to inhibit cytochrome C reduction.[24] Since one unit of bovine erythrocyte SOD per milliliter of reaction mixture inhibited cytochrome C reduction to 30% of control, we compared the SOD activity found in each sonicate to the amount of protein causing a 30% inhibition and converted this activity to units per milligram of protein. Since the percentage of inhibition was not linear over a wide range of protein concentrations, we used several different protein concentrations of the cell sonicate to obtain the inhibition rate within a few percentage points of 30%. Boiled cell sonicates or apoenzyme preparation did not inhibit cytochrome C reduction.

Catalase

Catalase was assayed by a previously described method by Mandell.[25] The oxygen produced by catalase addition to hydrogen peroxide was measured with a Clark membrane oxygen electrode. The sonicates containing 10 to 50 μg of protein were added to 5 μl of 30% hydrogen peroxide at a final volume of 3 ml, and the linear increase in oxygen concentration was recorded. A standard curve was constructed with the use of commercial purified bovine liver catalase. Catalase activity of the cell sonicate was expressed as units per milligram of protein.

Glutathione Peroxidase

Glutathione peroxidase was determined by the method of Paglia and Valentine,[26] which was modified by Holmes.[27] The reaction mixture contained 500 to 1000 μg of protein, and the change in the optical density was read at 340 nm. The data were expressed as nanomols of NADPH oxidized to NADP per milligram of protein with the use of the extinction coefficient of 6.2×10^3 $mols^{-1}$ cm^{-1} (Ref. 28). All data were corrected for the NADPH oxidation by hydrogen peroxide alone in the absence of enzyme protein.

Calculation of Total Enzyme Activity

Total enzyme activity was calculated by adding the total activity of each cell fraction. This was obtained by multiplying specific activity (units per milligram of protein per minute) times the total protein of each fraction. All enzymes were determined at 18, 42, 66, and 90 hr of exposure to 50% oxygen. The control samples for each enzyme were obtained from normal animals kept in room air for the same time periods. At least five experiments were performed for each

enzyme at the corresponding time period. Cells from several animals were pooled to obtain sufficient material.

Exposure to Superoxide Radical

Each of the enzymes studied was exposed to an O_2^- generating system containing 0.05*M* potassium phosphate buffer at pH 7.8 with 0.1m*M* ethylenediaminetetraacetic acid, 50μM xanthine, and varying amounts of xanthine oxidase. Following exposure to 11 and 20 nmols of O_2^- per 5 min, the enzymes were assayed as described above and compared to the controls containing xanthine or xanthine oxidase and to samples containing 100 μg bovine erythrocyte SOD.

RESULTS

Animal Survival

In these studies all the guinea pigs survived 100 hr of continuous exposure to 50% FIO_2. All animals drank water, ate well, and showed no signs of respiratory distress throughout the entire period of exposure.

Distribution of Protein

During the 90 hr of exposure to hyperoxia, the relative protein distribution was similar in the different cell fractions of AM and PMN granulocytes. In both cell types 48 ± 3% of the total protein recovered was found in the 16,000 x *g* pellet containing membranes, granules, and mitochondria, 12 ± 2% in the 100,000 x *g* microsomal pellet and 40 ± 4% in the 100,000 x *g* supernatant. Although the relative distribution of protein did not differ in both cell types, the AM contained 2.6 times more protein per cell than PMN granulocytes.

Superoxide Dismutase

Total SOD activity in both AM and PMN granulocytes from animals exposed to FIO_2's of 50 and 85% is shown in Fig. 1. Control enzyme activities prior to exposure are set to 100%, and the activities during oxygen exposure are expressed as a percentage of control activity. At both FIO_2's, total SOD activity increased twofold in AM and PMN granulocytes. In AM at 50% FIO_2, activity remained elevated at 31.6 ± 0.5 units per milligram of protein (90% above control) at 90 hr, whereas at 85% FIO_2, SOD activity returned to control levels of 16.8 ± 0.6 units per milligram of protein after 90 hr.

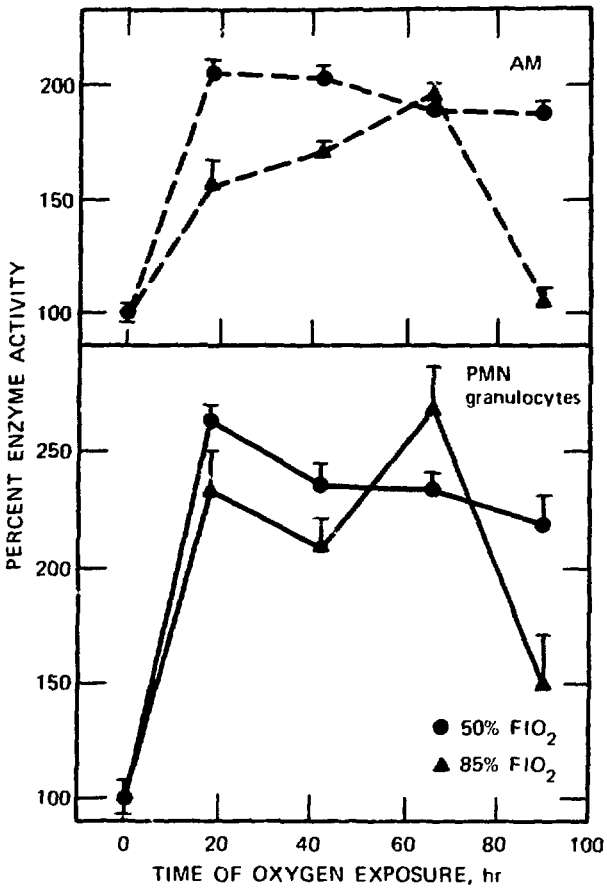

Fig. 1 Percent change in total SOD activity in AM and PMN granulocytes during exposure of guinea pigs to 50 and 85% FIO_2. Control enzyme activities prior to exposure are set to 100%, and the mean enzyme activities during oxygen exposure are expressed as a percentage of control activity ± SEM.

In PMN's at 50% FIO_2, this elevation persisted at 17.7 ± 1.1 units per milligram of protein (120% greater than control levels) for 90 hr. At 85% FIO_2, total activity in PMN granulocytes exhibited only a 50% increase (12.2 ± 1.8 units per milligram of protein) after 90 hr. It should be noted that the mechanism for increased SOD activity at 85% FIO_2 has been saturated in both cell types, as indicated by the fact that maximum SOD activity at 85% FIO_2 is not significantly different from that at 50% oxygen.

Catalase

Catalase is a soluble enzyme located mainly in the 100,000 x *g* supernatant. Total cata activity in AM and PMN granulocytes during

exposure to hyperoxia is shown in Fig. 2. In AM cata activity did not differ significantly from control (245 ± 25 units per milligram of protein per minute) after 90 hr of exposure to an FIO_2 of 50%, whereas at 85% FIO_2 it decreased to 190 ± 12 units per milligram of protein per minute (46% of original activity) at 42 hr and remained persistently diminished. In PMN granulocytes cata activity did not differ significantly from control (245 ± 23 units per milligram of protein per minute) after 90 hr of exposure to an FIO_2 of 50%, whereas at an FIO_2 of 85%, cata activity decreased to 162 ± 24 units per milligram of protein per minute (60% of control activity) at 90 hr.

Glutathione Peroxidase

Glutathione peroxidase is another soluble enzyme located mainly in the 100,000 x *g* supernatant. In AM gluta px activity decreased to 40 and 50% of control activity by 18 hr at 50 and 85% FIO_2,

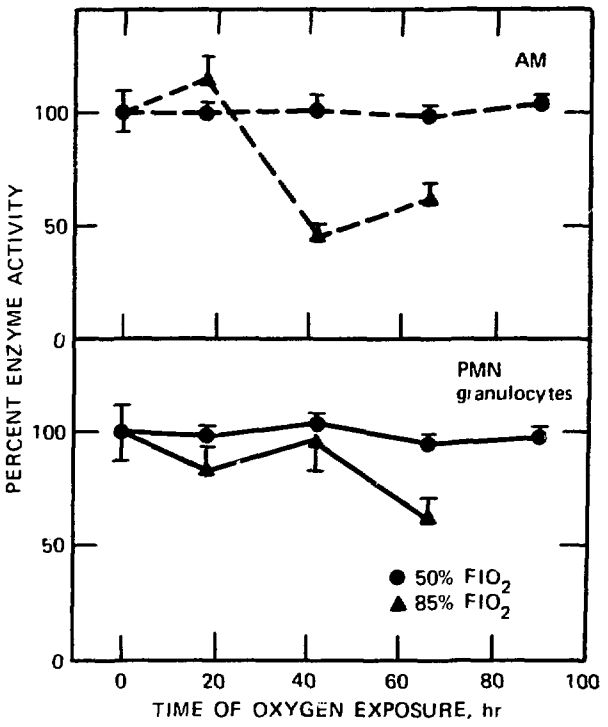

Fig. 2 Percent change in total cata activity in AM and PMN granulocytes during exposure of guinea pigs to 50 and 85% FIO_2. Control enzyme activities prior to exposure are set to 100%, and the mean enzyme activities during oxygen exposure are expressed as a percentage of control activity ± SEM.

respectively, and remained diminished (Fig. 3). In PMN granulocytes, total activity decreased to 60 and 65% of control activity by 42 hr at 50 and 85% FIO_2's, respectively, and remained depressed throughout the entire period of exposure to hyperoxia. The alteration in total SOD, cata, and gluta px activities per milligram of cell protein during hyperoxia is summarized in Table 1.

In Vitro Exposure of Catalase and Glutathione Peroxidase to Superoxide Anion

The extent of inactivation of cata and gluta px was evaluated with an O_2^- generating system in an attempt to simulate the in vivo situation. The 100,000 x *g* supernatant of PMN granulocytes, which contains catalase and glutathione peroxidase, was exposed to either 11 or 20 nmols of O_2^- generated by the reaction of xanthine and xanthine oxidase. Following a 5-min exposure of 20 nmols of O_2^-, catalase and glutathione peroxidase activities fell to 65 ± 7% and

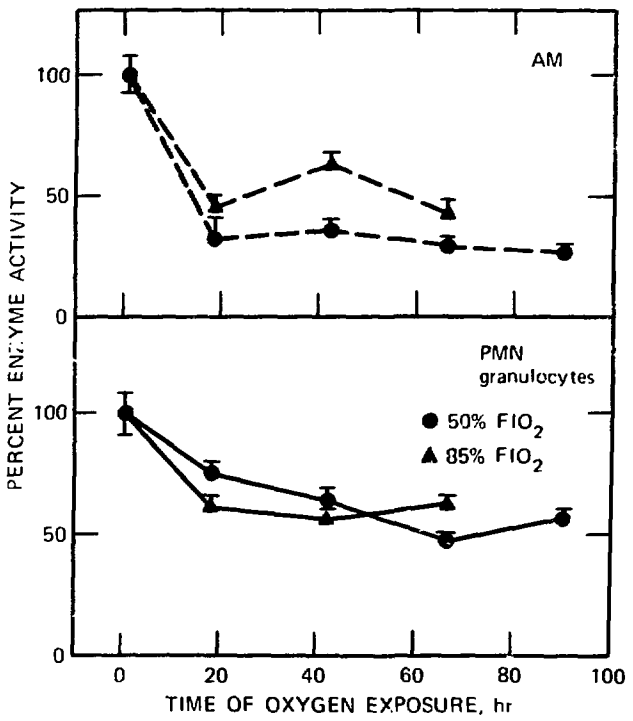

Fig. 3 Percent change in total glutathione peroxidase activity in AM and PMN granulocytes during exposure of guinea pigs to 50 and 85% FIO_2. Control enzyme activities prior to exposure are set to 100%, and the mean enzyme activities during oxygen exposure are expressed as a percentage of control activity ± SEM.

TABLE 1

TOTAL SOD, CATALASE, AND GLUTATHIONE PEROXIDASE ACTIVITIES IN AM AND PMN DURING HYPEROXIA

Hours of exposure to 50% O_2	SOD*	Catalase*	Glutathione peroxidase†
	Alveolar Macrophages		
0	16.8 ± 0.6	245.2 ± 23.0	32.7 ± 2.6
18	34.5 ± 1.0‡	240.8 ± 10.1§	24.9 ± 1.5‡
42	34.1 ± 0.9‡	254.2 ± 9.0§	21.3 ± 1.5‡
66	31.8 ± 0.5‡	234.6 ± 7.2§	15.9 ± 0.9‡
90	31.6 ± 0.5‡	239.0 ± 6.0§	19.2 ± 0.9‡
	Polymorphonuclear Leukocytes		
0	8.1 ± 0.6	368.0 ± 30.0	82.8 ± 6.6
18	21.4 ± 0.6‡	367.0 ± 18.0§	32.9 ± 1.5‡
42	19.1 ± 0.8‡	361.0 ± 21.0§	30.3 ± 1.5‡
66	18.8 ± 0.7‡	361.0 ± 15.0§	24.0 ± 1.2‡
90	17.7 ± 1.1‡	380.0 ± 12.0§	22.2 ± 1.5‡

*Units per milligram of protein; mean ± SEM.
†Nanomoles of NADPH per milligram of protein per minute; mean ± SEM.
‡$p < 0.05$; Student's t-test compared to 0 time.
§Not significant.

69 ± 7% of their original activity, respectively (Table 2). The addition of 100 μg of bovine erythrocyte SOD to the reaction mixtures prevented the decrease in enzyme activity. Exposure to 11 nmols of O_2^- did not decrease enzyme activity significantly. These observations indicate that O_2^- generated in vitro can inactivate catalase and glutathione peroxidase and that these enzymes can be protected from inactivation by SOD.

DISCUSSION

In vivo exposure of guinea pigs to FIO_2's of 50 and 85% significantly increased SOD activity in AM and PMN granulocytes. The greater toxicity of 85% FIO_2's is indicated by less SOD activity at 90 hr than at earlier times and the marked and persistent decrease in catalase activity. In contrast, at 50% FIO_2, SOD activity remained elevated at 90 hr, and catalase activity did not differ significantly from control. However, the toxicity of 50% FIO_2 is evidenced by the

TABLE 2

IN VITRO EXPOSURE OF CATALASE AND GLUTATHIONE PEROXIDASE TO O_2^-

Enzyme	Control activity,%	20 nmols O_2^-/5 min	Percent of original activity
Catalase*	495 ± 48	322 ± 30	65 ± 7
Glutathione peroxidase†	56 ± 4	40 ± 2	69 ± 7

*Units per milligram of protein; mean ± SEM.
†Nanomoles of NADPH oxidized to NADP per milligram of protein; mean ± SEM.

significantly decreased glutathione peroxidase activity in AM and PMN granulocytes, as is the case at 85% FIO_2.

On the basis of these observations, we have proposed a biochemical model for the mechanism of oxygen toxicity in AM and PMN granulocytes (Fig. 4). The univalent reduction of oxygen leads to the generation of O_2^- (Ref. 11), which is then dismutated by SOD to H_2O_2 and O_2 (Ref. 10). Hydrogen peroxide is, in turn, detoxified mainly by cata and gluta px (Refs. 14 and 15). Following exposure to 85% FIO_2, the rate of O_2^- generation increases in vitro and in vivo,[29-31] and, in response, SOD activity is significantly increased.[7,16-18] Similar to other studies in which whole lung homogenates and bacteria are used,[7,16,17] the increased SOD activity in both cell types is attributable to the cyanide-insensitive mitochondrial form of the enzyme. Since SOD generates hydrogen peroxide by dismutation of O_2^-, increased levels of SOD may lead to elevated intracellular concentrations of H_2O_2. Baehner et al.[32] have demonstrated that phagocytized latex particles coated with SOD also increase H_2O_2 concentrations in PMN granulocytes. Others have shown that an increase in the partial pressure of oxygen will raise H_2O_2 concentrations in rat liver and rat liver mitochondria.[33,34] In addition, in vivo exposure of mice to hyperoxia leads to increased H_2O concentrations in erythrocytes.[35] This laboratory[31] has shown that phagocytizing AM and PMN granulocytes of guinea pigs exposed continuously to 85% FIO_2 for 66 hr exhibited significantly increased H_2O_2 release. Another mechanism for the accumulation of H_2O_2 may be the inactivation of H_2O_2 detoxifying enzymes, such as cata and gluta px, which may lead to decreased biodegradation of H_2O_2. At 85% FIO_2 the mechanism for increased SOD activity is saturated, and SOD is unable to dismutate O_2^- to H_2O_2 as rapidly. Conse-

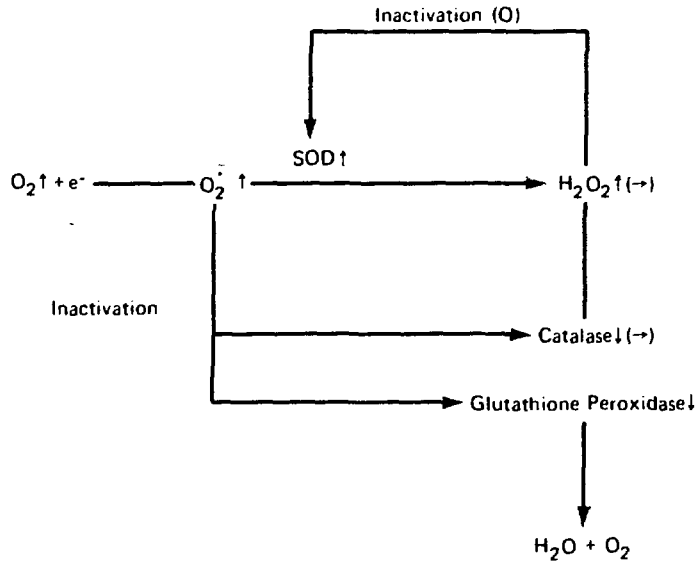

Fig. 4 Interactions among superoxide anion, hydrogen peroxide, catalase, and glutathione peroxidase in AM and PMN granulocytes. See details in text. Changes at 50% FIO_2, which are significantly different from those at 85% FIO_2, are indicated in parentheses.

quently O_2^- may be present in such excess and for adequate duration to partially inactivate cata and gluta px activity; this, in turn, may lead to even greater intracellular concentrations of H_2O_2. It has been shown that H_2O_2 inactivates SOD and that sufficient cata is able to prevent this inactivation.[36,37] The inactivation of SOD by H_2O_2 may occur in vivo and explain the decreased SOD activity noted after 66 hr of oxygen exposure to an FIO_2 of 85%. In addition, it should be noted that diminished SOD and cata activities at 85% FIO_2 and gluta px activities at 50 and 85% FIO_2 may also be partially attributable to the formation of hydroxyl radical (OH·) and oxygen singlet (O_2^*), which can be generated from O_2^- and H_2O_2 via the Haber–Weiss reaction.[38] The loss of SOD activity compromises the first line of defense of the cell against oxygen and its reduction product, O_2^-.

At an FIO_2 of 50%, SOD activity increases and remains significantly elevated at 90 hr of exposure, cata activity remains unchanged, and gluta px activity is significantly decreased throughout the entire period of exposure. Since cata is present in excess, the intracellular concentration of hydrogen peroxidase probably does not increase and therefore is not inactivated, as is the case at 85% FIO_2. Consequently, at 50% FIO_2, SOD, the major defense mechanism of the cell against oxygen and its reduction products, is not compromised. This model is supported by the observation that cata and SOD

together, but not individually, protected red cells against lipid peroxidation induced by oxygen and dialuric acid.[39,40] Since cata activity remained at control levels in both cell types during exposure to 50% FIO_2, it may provide a useful biochemical marker of oxygen toxicity.

Clinical and morphological studies have shown that man is also susceptible to oxygen toxicity.[3,4] Although recent studies of human AM and PMN granulocytes have shown that SOD distribution and activity are similar to guinea pig cells,[41] the application of our model to man must await further studies.

ACKNOWLEDGMENTS

We would like to express our appreciation to Mrs. Debbie Stout and Mrs. Elaine Carroll for their secretarial assistance. This investigation was supported by grant numbers 1RO1 HL 19779-01 and 2RO1-AI 10892-04, awarded by the National Institutes of Health, Department of Health, Education, and Welfare, and a grant from the James Whitcomb Riley Memorial Association.

REFERENCES

1. E. R. Weibel, Oxygen Effect on Lung Cells, *Arch. Intern. Med.*, 128: 54-56 (1971).
2. E. Yamamato, M. Wittner, and R. M. Rosenbaum, Resistance and Susceptibility to Oxygen Toxicity by Cell Types of the Gas—Blood Barrier of the Lung, *Am. J. Pathol.*, 59: 409-420 (1970).
3. J. M. Clark, The Toxicity of Oxygen, *Am. Rev. Respir. Dis.*, 110(40): 40-50 (1974).
4. P. C. Pratt, Pathology of Pulmonary Oxygen Toxicity, *Am. Rev. Respir. Dis.*, 110(40): 51-57 (1974).
5. H. A. Saltzman and I. Fridovich, Oxygen Toxicity, Introduction to a Protective Enzyme:Superoxide Dismutase, *Circulation*, XLVIII: 921-923 (1973).
6. I. Fridovich, Oxygen:Boon and Bane, *Am. Sci.*, 63: 54-59 (1975).
7. A. P. Autor, L. Frank, and R. J. Roberts, Developmental Characteristics of Pulmonary Superoxide Dismutase: Relationship to Idiopathic Respiratory Distress Syndrome, *Pediat. Res.*, 10: 154-158 (1976).
8. J. M. McCord, Superoxide Dismutase in Oxygen Toxicity Oxygen and Physiological Function, in 60th Annual Meeting of Federation of American Societies for Experimental Biology, Anaheim, Calif., Apr. 12—16, 1976, *Fed. Proc.* (in press).
9. J. M. McCord, B. B. Keele, Jr., and I. Fridovich, An Enzyme-Based Theory of Obligate Anaerobiasis: The Physiological Function of Superoxide Dismutase, *Proc. Natl. Acad. Sci. U. S. A.*, 68: 1024-1027 (1971).
10. J. M. McCord and I. Fridovich, Superoxide Dismutase. An Enzyme Function for Erythrocuprein (Hemocuprein), *J. Biol. Chem.*, 241: 6049-6055 (1969).

11. I. Fridovich, Superoxide Radical and Superoxide Dismutase, *Acc. Chem. Res.*, 5: 321-326 (1972).
12. R. A. Weisiger and I. Fridovich, Superoxide Dismutase, Organelle Specificity, *J. Biol. Chem.*, 248: 3582-3592 (1973).
13. J. A. Fee and B. P. Gaber, Anion Binding to Bovine Erythrocyte Superoxide Dismutase. Evidence for Multiple Binding Sites With Qualitatively Different Properties, *J. Biol. Chem.*, 247: 60-65 (1972).
14. L. Flohe, Die Glutathionperoxidase. Enzymologie und Biologische Aspekte, *Klin. Wochenochr.*, 12: 669-683 (1971).
15. J. B. L. Gee, J. Kaskin, M. P. Duncombe, and C. L. Vasallo, The Effects of Ethanol on Some Metabolic Features of Phagocytosis in the Alveolar Macrophage, *J. Reticuloendothel. Soc.*, 15: 61-68 (1974).
16. E. M. Gregory, S. A. Goscin, and I. Fridovich, Superoxide Dismutase and Oxygen Toxicity in a Eukaryote, *J. Bacteriol.*, 117: 456-460 (1974).
17. J. D. Crapo and D. F. Tierney, Superoxide Dismutase and Pulmonary Oxygen Toxicity, *Am. J. Physiol.*, 226: 1401-1407 (1974).
18. M. Rister and R. L. Baehner, Induction of Superoxide Dismutase in Polymorphonuclear Leukocytes and Alveolar Macrophages (Abstract), *Blood*, 46: 1015 (1975).
19. S. Sorokin, The Cells of the Lung, in *Morphology of Experimental Respiratory Carcinogenesis*. ERDA Symposium Series, Gatlinburg, Tenn., May 13–16, 1970, P. Nettesheim, M. G. Hanna, Jr., and J. W. Deatherage, Jr. (Eds.), pp. 3-43, CONF-700501, NTIS, 1970.
20. M. Rister and R. L. Baehner, A Comparative Study of Superoxide Dismutase Activity in Polymorphonuclear Leukocytes, Monocytes, and Alveolar Macrophages of the Guinea Pig, *J. Cell. Physiol.*, 87: 345-355 (1976).
21. M. Rister and R. L. Baehner, The Alteration of Superoxide Dismutase, Catalase, Glutathione Peroxidase and NAD(P)H Cytochrome C Reductase in Guinea Pig Polymorphonuclear Leukocytes and Alveolar Macrophages During Hyperoxia, *J. Clin. Invest.*, 58: 1174-1184 (1976).
22. A. Boyum, Isolation of Mononuclear Cells and Granulocytes from Human Blood, *Scand. J. Clin. Lab. Invest.*, Suppl. 21(97): 77-81 (1967).
23. O. H. Lowry, N. J. Rosebrough, A. L. Farr, and R. J. Randall, Protein Measurement with the Folin Phenol Reagent, *J. Biol. Chem.*, 193: 265-274 (1951).
24. J. M. McCord, C. O. Beauchamp, S. Goscin, H. P. Misra, and I. Fridovich, Superoxide Dismutase, in *Oxidases and Related Redox Systems*, T. O. King, H. J. Mason, and M. Morrison (Eds.), pp. 51-85, University Park Press, Baltimore, London, Tokyo, 1971.
25. G. L. Mandell, Catalase, Superoxide Dismutase, and Virulence of *Staphylococcus aureus*. In Vitro and In Vivo Studies with Emphasis on Staphylococcal-Leukocyte Interaction, *J. Clin. Invest.*, 55: 561-566 (1975).
26. D. E. Paglia and W. N. Valentine, Studies on the Quantitative and Qualitative Characterization of Erythrocyte Glutathione Peroxidase, *J. Lab. Clin. Med.*, 70: 158-169 (1967).
27. B. Holmes, B. H. Park, S. E. Malawista, P. G. Quie, D. L. Nelson, and R. A. Good, Chronic Granulomatous Disease in Females. A Deficiency of Leukocyte Glutathione Peroxidase, *New Engl. J. Med.*, 283: 217-221 (1970).
28. B. L. Horecker and A. Kornberg, The Extinction Coefficient of the Reduced Band of Pyridine Nucleotides, *J. Biol. Chem.*, 175: 385-390 (1948).
29. I. Fridovich, Quantitative Aspects of the Production of Superoxide Anion Radical by Milk Xanthine Oxidase, *J. Biol. Chem.*, 245: 4053-4057 (1970).

30. H. P. Misra and I. Fridovich, The Generation of Superoxide Radical During the Autooxidation of Ferridoxins, *J. Biol. Chem.*, 246: 6886-6890 (1971).
31. M. Rister and R. L. Baehner, Effect of Hyperoxia on Superoxide Anion and Hydrogen Peroxide Production of Polymorphonuclear Leukocytes and Alveolar Macrophages, *Br. J. Haematol.*, 36: 245-252 (1977).
32. R. L. Baehner, S. K. Murrmann, J. Davis, and R. B. Johnston, The Role of Superoxide Anion and Hydrogen Peroxide in Phagocytosis-Associated Oxidative Metabolic Reactions, *J. Clin. Invest.*, 56: 571-576 (1975).
33. A. Boveris and B. Chance, The Mitochondrial Generation of Hydrogen Peroxide. General Properties and Effect of Hyperbaric Oxygen, *Biochem. J.*, 134: 707-716 (1973).
34. N. Oshino, D. Jamieson, and B. Chance, The Properties of Hydrogen Peroxide Production Under Hyperoxic and Hypoxic Conditions of Perfused Rat Liver, *Biochem. J.*, 146: 58-65 (1975).
35. C. H. Mengel, The Effects of Hyperoxia on Red Cells as Related to Tocopherol Deficiency, *Ann. N. Y. Acad. Sci.*, 203: 163-171 (1972).
36. R. C. Bray, S. A. Cockle, E. M. Fielden, P. B. Roberts, and L. Calabrese, Reduction and Inactivation of Superoxide Dismutase by Hydrogen Peroxide, *Biochem. J.*, 139: 43-48 (1974).
37. E. K. Hodgson and I. Fridovich, The Interaction of Bovine Erythrocyte Superoxide Dismutase with Hydrogen Peroxide: Inactivation of the Enzyme, *Biochem. J.*, 14(24): 5294-5299 (1975).
38. F. Haber and J. Weiss, The Catalytic Decomposition of Hydrogen Peroxide by Iron Salts, *Proc. R. Soc. (London) Math. Phys. Soc.*, 147: 332-351 (1934).
39. J. A. Fee, R. Bergami, and R. G. Briggs, Observation of the Mechanism of the Oxygen/Dialuric Acid-Induced Hemolysis of Vit. E. Deficient Rat Red Blood Cells and the Protective Roles of Catalase and Superoxide Dismutase, *Arch. Biochem. Biophys.*, 169: 160-167 (1975).
40. A. Bozzi, I. Mavelli, A. F. Agro, R. Strom, A. M. Wolf, B. Mondovi, and G. Rotilio, Enzyme Defense Against Reactive Oxygen Derivates II. Erythrocytes and Tumor Cells, *Mol. Cell. Biochem.*, 10: 11-16 (1976).
41. G. S. Johnson, M. Rister, C. Higgins, M. O. Farber, F. Manfredi, and R. L. Baehner, A Comparative Study of Superoxide Dismutase Activity in Polymorphonuclear Leukocytes and Alveolar Macrophages in Humans and Guinea Pigs (Abstract), *Clin. Res.*, XXIV: 346A (1976).

Pulmonary Injury and Clearance of MnO_2 Particles

RIKARD BERGSTRÖM and RAGNAR RYLANDER
Department of Environmental Hygiene, University of Gothenburg, Sweden

ABSTRACT

Guinea pigs were exposed to a test aerosol of MnO_2 particles for 24 hr, and the clearance from the lung of these particles was followed up to 7 days after exposure. Certain animals were exposed to an aerosol of *Enterobacter cloacae* for 40 min to induce pulmonary injury. The number of free lung cells and the number of cells containing phagocytosed particles were determined. The deposition of MnO_2 particles was reduced in animals exposed to Enterobacter 1 day prior to exposure to the test aerosol. In this group, clearance of the MnO_2 aerosol was reduced during the first day. Clearance was not altered during the first and second days after bacteria exposure in animals exposed to Enterobacter immediately after the test aerosol. The number of free lung cells and cells containing phagocytosed particles was increased in the group exposed to Enterobacter.

The clearance of inhaled particles from the lung represents an important defense mechanism against airborne pollutants. The pulmonary clearance of different kinds of particles has been extensively studied in experiments on animals and humans.[1] A decrease in the clearance capacity has been demonstrated after exposure to different air pollutants, bacteria, and viruses, and also when host conditions are altered. A decrease in the clearance rate may have a pathological significance for the development of pulmonary disease since the contact time between particles and the lung tissue is prolonged and thus increases their relative toxicity.

Epidemiological studies have demonstrated a relation between exposure to manganese dioxide (MnO_2) dust and the incidence of pneumonia.[2] Studies on the pulmonary clearance of MnO_2 particles

in dogs have yielded half-time values of about 38 days.[3] The relatively long contact time between the pulmonary tissue and MnO_2 may be of importance for the development of the clinical effects. More precise data on how the dust affects different cell systems in the lung are not available.

The experiments described here were undertaken to measure the clearance of MnO_2 particles from the lungs of animals and to study the effect on the clearance after exposing the animals to airborne bacteria.

MATERIALS AND METHODS

Full-grown male and female guinea pigs were exposed to an aerosol of MnO_2 in stainless-steel exposure chambers (volume, 670 liters, throughput volume, 8 m^3/hr) for 24 hr. The dust (MnO_2) aerosol (Mallinckrodt analytical reagent, 99.5%) was generated with a RagPe generator.[4] The apparatus consists of a fan circulating the dust in an airstream through a circular plastic tube. Smaller particles are carried up to the top of a Perspex tower mounted on top of the apparatus and through a connecting tube into the exposure chamber. The concentration of MnO_2 in the exposure chambers was determined by sucking the air through Millipore membrane filters that were then weighed. The mean concentration of MnO_2 was 23 ± 9 mg/m^3, and about 80% of the particles were smaller than 3 μm as determined with an optical particle counter.

In certain experiments the animals were exposed to an aerosol of *Enterobacter cloacae*. A bacteria suspension was placed in a Collison atomizer and aerosolized. For these experiments the animals were exposed in smaller chambers for 40 min. The different exposure regimes used in the experiment are shown in Fig. 1.

At the termination of exposure and at various time intervals thereafter, the animals were killed. The total lung deposition of MnO_2 was determined with atomic-absorption spectrophotometry. The lung and the trachea were removed, weighed, and thereafter dried for 15 hr at 110 to 115°C. The dry weight was determined, and the lungs were ashed for 2 x 15 hr at 445°C. An aliquot of 15 ml of 1*N* HNO_3 was added to the sample, which was left overnight before the analysis. The amount of manganese was expressed as micrograms per gram of dry weight.

The number of free lung cells in the airways was determined by a lavage technique.[5] Ten milliliters of saline was gently flushed into the lungs and withdrawn. The same fluid was then flushed in again and withdrawn. The process was repeated 10 times. A sample of the

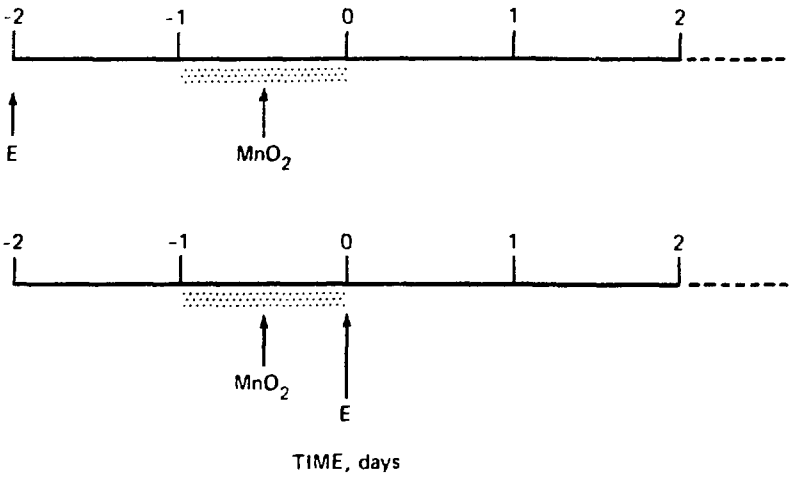

Fig. 1 Timings in days of exposure to Enterobacter (E) and manganese dioxide (MnO_2) in clearance experiments.

fluid was transferred into a test tube and stained with Türcks' solution. The number of macrophages and polymorphonuclear leukocytes was counted in a Bürcker chamber. The number of cells reported in the results should be multiplied by 1.25×10^4 to give the total number of cells in the lavage fluid and hence in the airways.

The number of macrophages and leukocytes containing phagocytosed MnO_2 particles was determined by using stained-smear preparations of the cells in the lavage fluid. Differences among the different groups of animals in the experiments were tested for significance by the two-sided Student's *t* test.

RESULTS

Clearance of Manganese Dioxide

The pulmonary clearance of MnO_2 at various time intervals after the acute exposure is shown in Table 1 and illustrated in Fig. 2. It can be seen that 44% of the MnO_2 initially deposited in the lung remained after 1 day. After 3 days 18% remained, and 4% after 7 days.

In animals exposed to Enterobacter 1 day prior to the MnO_2 exposure (E + MnO_2), 78% of the MnO_2 was found in the lung 1 day after exposure. This was a significantly higher retention than in the group exposed to MnO_2 only ($p \leq 0.01$). At 3 and 7 days the retention was about the same as in animals exposed to MnO_2 only.

TABLE 1

AMOUNTS OF MnO_2 IN LUNGS AT VARIOUS TIME INTERVALS AFTER EXPOSURE EXPRESSED AS MICROGRAMS PER GRAM OF DRY LUNG WEIGHT AND PERCENT OF INITIAL DEPOSITION; EXPOSURES WERE TO MnO_2, ENTEROBACTER 1 DAY PRIOR TO MnO_2 (E + MnO_2), AND ENTEROBACTER IMMEDIATELY AFTER MnO_2 (MnO_2 + E)

(N = number of animals; figures in parentheses indicate standard deviation)

Exposure time	MnO_2			E + MnO_2			MnO_2 + E		
	N	μg/g	%	N	μg/g	%	N	μg/g	%
0 hours	13	613 (197)	100	6	443 (152)	100	13	613 (197)	100
7 hours	6	370 (99)	60 (16)				6	376 (157)	61 (26)
1 day	19	270 (93)	44 (15)	6	347 (162)	78 (37)	6	210 (84)	34 (14)
2 days	14	126 (40)	21 (6)				6	115 (34)	19 (6)
3 days	20	107 (56)	18 (9)	6	103 (34)	23 (8)	6	66 (16)	11 (3)
7 days	6	22 (8)	4 (1)	6	20 (16)	5 (4)			

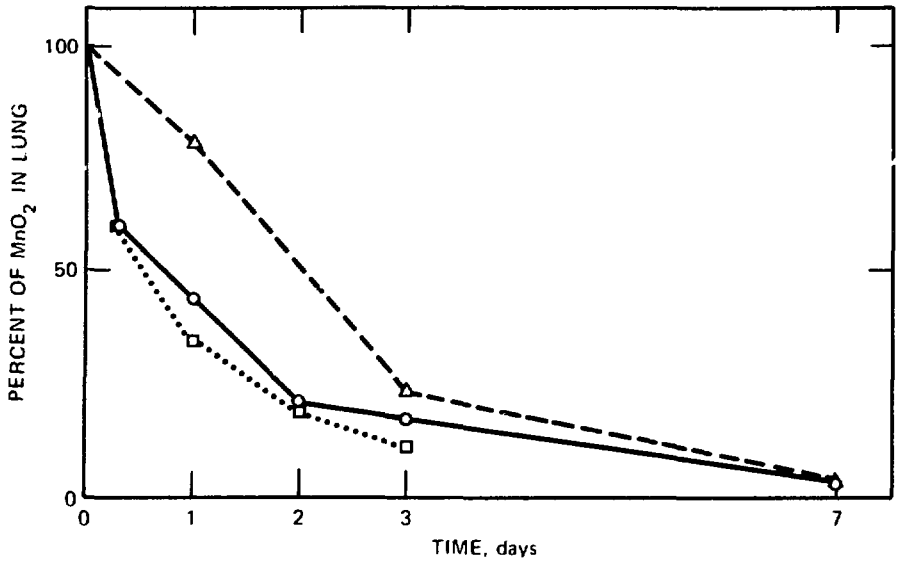

Fig. 2 Clearance of MnO_2 particles at various times after exposure, expressed as percent of initial deposition. ○, exposure to MnO_2. △, exposure to Enterobacter 1 day prior to MnO_2. □, exposure to Enterobacter immediately after MnO_2.

In animals exposed to Enterobacter immediately after the MnO_2 exposure (MnO_2 + E), the retention at 1 day was 34%. The clearance in this group was thus slightly increased as compared with that in animals exposed to MnO_2 only. At 2 days after exposure, the proportional retention was almost the same as in the MnO_2 group, which indicated a tendency to a slower clearance for 1 to 2 days. At 3 days after exposure, the percent of retention was about the same as in the animals exposed to MnO_2.

Number of Free Lung Cells

The number of free lung cells found in animals exposed to MnO_2, Enterobacter, and MnO_2 plus Enterobacter are reported in Table 2. The table demonstrates that the number of macrophages in animals exposed to MnO_2 was significantly reduced immediately after the exposure. Thereafter a successive increase took place during the following 3 days. The number of leukocytes was increased at 1 day after exposure, and this increased level remained up to 3 days after exposure.

In animals exposed to Enterobacter a slight increase in the number of macrophages was noticed 3 days after exposure. The number of leukocytes was significantly increased 1 day after

TABLE 2

MACROPHAGES AND LEUKOCYTES (1.25×10^4) IN ANIMALS EXPOSED TO MANGANESE DIOXIDE (MnO_2), ENTEROBACTER (E), AND ENTEROBACTER IMMEDIATELY AFTER MnO_2 EXPOSURE (MnO_2 + E) AT VARIOUS TIMES AFTER THE EXPOSURE

(Figures in parentheses indicate standard deviation; N = number of animals; x, xx, and xxx indicate a significance of $p \leq 0.05$, $p \leq 0.01$, and $p \leq 0.001$, respectively.)

Time after exposure, days	MnO_2			E			MnO_2 + E		
	N	Macrophages	Leukocytes	N	Macrophages	Leukocytes	N	Macrophages	Leukocytes
Not exposed	24	103 (54)	62 (34)	10	114 (78)	108 (63)	24	103 (54)	62 (34)
0	10	39 (27)^{xx}	57 (28)						
1	16	110 (59)	126 (85)^{xx}	10	141 (123)	507 (283)^{xxx}	5	303 (229)^{xxx}	752 (359)^{xxx}
2	10	121 (57)	113 (46)^{xx}	10	133 (54)	371 (226)^{xx}	6	504 (178)^{xxx}	956 (402)^{xxx}
3	17	169 (85)^{xx}	145 (79)^{xxx}	10	208 (133)	330 (190)^{xx}	6	421 (154)^{xxx}	547 (278)^{xxx}

exposure. A lower increase was found 2 and 3 days after the bacterial exposure.

In animals exposed to Enterobacter immediately after exposure to MnO_2, the number of macrophages was significantly increased 1 day after the exposure to bacteria, even higher at 2 days, and lower thereafter. The number of leukocytes was increased at 1 day after the cessation of exposure. An increased level was also found at 2 and 3 days after exposure. The results show that the increase in the number of free lung cells is higher and appears earlier in animals exposed to both agents.

Number of Macrophages with MnO_2 Particles

The number and proportion of macrophages and leukocytes containing phagocytosed MnO_2 particles is shown in Table 3. It can be seen that the proportion of macrophages containing MnO_2 particles was increased at the cessation of exposure (0 hr). About 50% of all macrophages contained MnO_2 particles as compared with about 8% of the leukocytes. The proportion of macrophages containing particles remained at about the same level until 2 days after exposure, whereafter a slight decrease took place.

The number of macrophages containing phagocytosed MnO_2 particles in animals exposed to Enterobacter immediately after the MnO_2 exposure was significantly increased at 1, 2, and 3 days after exposure as compared with animals exposed to MnO_2 only. However, the proportion of macrophages containing particles was the same as in animals exposed to MnO_2. The number of leukocytes containing particles was increased 1 and 2 days after exposure, but again the proportion was about the same as in animals not exposed to Enterobacter.

CONCLUSIONS

The clearance of MnO_2 from the lungs of guinea pigs takes place rapidly and is almost terminated at 7 days after an acute exposure. This clearance rate is significantly faster than the rate in dogs reported by Morrow, Gibb, and Johnson.[3] In their experiments the biological half-time was given as 38 days. In other experiments on humans,[6] a half-time of 65 days was found during a measurement period of up to 120 days.

The reason for the discrepancy between the present results and those of Morrow, Gibb, and Johnson[3] may be due to methodological differences. In their experiments the particle size (CMD = 0.07) was

TABLE 3

NUMBER OF MACROPHAGES AND LEUKOCYTES CONTAINING MnO_2 PARTICLES AT VARIOUS TIMES AFTER EXPOSURE IN ANIMALS EXPOSED TO MANGANESE DIOXIDE (MnO_2) OR TO ENTEROBACTER IMMEDIATELY AFTER MnO_2 EXPOSURE (MnO_2 + E); DATA ARE PRESENTED AS CELLS WITH PARTICLES (CWP) AND CELLS WITH PARTICLES IN PERCENT OF ALL CELLS (%)

(N = number of animals; figures in parentheses indicate standard deviation; significance is indicated by x, xx, and xxx for $p \leq 0.05$, $p \leq 0.01$, and $p \leq 0.001$, respectively.)

Time after exposure, days	MnO_2					MnO_2 + E				
	Macrophages			Leukocytes		Macrophages			Leukocytes	
	N	%	CWP	%	CWP	N	%	CWP	%	CWP
Not exposed	20	3.8	4 (3)	0.6	0 (0)	12	5.0	5 (3)	0.0	0 (0)
0	9	50.3	20 (16)	7.8	5 (1)					
1	16	44.8	49 (27)	6.5	8 (6)	5	43.6	132 (104)^{xx}	5.5	41 (21)^{xxx}
2	10	49.3	60 (31)	7.5	9 (5)	6	45.2	228 (53)^{xxx}	3.8	36 (23)^{xx}
3	17	38.4	65 (32)	3.8	6 (4)	6	34.9	147 (52)^{xxx}	1.8	10 (9)

smaller than in the experiments reported here. Larger particles favor a deposition in the upper part of the respiratory tree,[7] which can explain the more rapid clearance rate found in these experiments. It is also conceivable that very small particles are not treated by macrophages in a similar manner as larger particles, thus influencing also the clearance from the alveolar region.

In animals exposed to Enterobacter, a large effect on MnO_2 clearance was found in animals that received the bacterial aerosol before MnO_2 exposure. The initial deposition in these animals was lower than in animals exposed to MnO_2 only. If this difference in deposition reflected another distribution pattern in the airways, this could in itself explain the reduced clearance seen during the first day. However, as the proportion of MnO_2 cleared became equal to the control value at 3 days after exposure, this explanation seems less likely.

A reduction in clearance was present between 2 and 3 days after the Enterobacter exposure in animals that received bacteria before MnO_2 exposure and between 1 and 2 days in animals that received bacteria after the MnO_2 exposure. The reason for this difference is not clear, but it is feasible that the presence of MnO_2 in the macrophages when the exposure to Enterobacter took place could be of importance.

Benacerraf and Sebestyen[8] reported that the clearance from the blood of injected carbon particles was decreased in rabbits that had received a small dose of endotoxin. The depression of clearance in their study was maximal at 12 hr after the endotoxin administration, still observed at 1 day, and changed to an increased clearance after 2 days. The depression of pulmonary clearance found in the present experiments appeared about 1 to 2 days later than in Benacerraf's study. This difference could be because the Enterobacter used in this study had a retarded release of endotoxin.

According to the results reported here, exposure to MnO_2 will cause an increase in the number of macrophages and leukocytes appearing at 1 day after exposure. When animals are exposed to an aerosol of Enterobacter immediately after MnO_2 exposure, the increase in the number of macrophages and leukocytes is larger than it is when either of the two agents is given separately. Such synergistic effects on lung reactions have also been demonstrated when MnO_2 and SO_2 aerosols were combined.[4]

No relation was found between the clearance rate and the number of macrophages in the lung. Such relationships have earlier been suggested by LaBelle and Brieger,[9] Ferin, Urbankova, and Vlckova,[10] and others. The exposure to Enterobacter caused a

significantly increased number of macrophages to appear in the airways, and the absolute number of cells containing phagocytosed MnO_2 particles was also significantly increased over the controls. In spite of this, a tendency to reduced clearance was observed. It thus seems that not only the number of macrophages but also other characteristics of these may be of importance for the pulmonary clearance of particles. Further experiments will try to elucidate this problem.

ACKNOWLEDGMENT

This work has been supported by the Swedish Work Environment Fund.

REFERENCES

1. B. Holma, Lung Clearance of Mono- and Di-Disperse Aerosols Determined by Profile Scanning and Whole-Body Counting, *Acta Med. Scand.*, Suppl., 473: 1-102 (1967).
2. T. A. Lloyd Davies, Manganese Pneumonitis, *Br. J. Ind. Med.*, 3: 111-135 (1946).
3. P. E. Morrow, F. R. Gibb, and L. Johnson, Clearance of Insoluble Dust from the Lower Respiratory Tract, *Health Phys.*, 10: 543-555 (1964).
4. R. Rylander, M. Öhrström, P. Å. Hellström, and R. Bergström, SO_2 and Particles—Synergistic Effects on Guinea-Pig Lungs, in *Inhaled Particles III*, W. H. Walton (Ed.), pp. 535-541, Unwin Brothers Limited, Surrey, England, 1971.
5. R. Rylander, Free Lung Cell Studies in Cigarette Smoke Inhalation Experiments, *Scand. J. Respir. Dis.*, 52: 121-128 (1971).
6. P. E. Morrow, F. R. Gibb, and K. Gazioglu, The Clearance of Dust from the Lower Respiratory Tract of Man. An Experimental Study, in *Inhaled Particles and Vapours II*, C. N. Davies (Ed.), pp. 351-358, Pergamon Press, Inc., New York, 1967.
7. Task Group on Lung Dynamics, Deposition and Retention Models for Internal Dosimetry of the Human Respiratory Tract, *Health Phys.*, 12: 173-207 (1966).
8. B. Benacerraf and M. M. Sebestyen, Effect of Bacterial Endotoxins on the Reticuloendothelial System, *Fed. Proc.*, 16: 860-867 (1957).
9. C. W. LaBelle and H. Brieger, Patterns and Mechanisms in the Elimination of Dust from the Lung, in *Inhaled Particles and Vapours*, pp. 356-365, C. N. Davies (Ed.), Pergamon Press, Inc., New York, 1961.
10. J. Ferin, G. Urbankova, and A. Vlckova, Pulmonary Clearance and the Function of Macrophages, *Arch. Environ. Health*, 10: 790-795 (1965).

Irradiation Damage in Hamster Lungs

K. H. WOODRUFF,*† J. T. LEITH,† P. SMITH,† V. HAVENS,† J. T. LYMAN,† J. HOWARD,† and C. A. TOBIAS†
*Department of Pathology, University of California, San Francisco, California, and †Biomedical Division, Lawrence Berkeley Laboratory, and Donner Laboratory of Medical Physics, University of California, Berkeley, California

ABSTRACT

Among the models of pulmonary fibrosis, irradiation injury offers an advantage in that exact doses can be calculated and reproduced. Single doses of 230-kVp X rays or 375-MeV nucleon-accelerated neon ions in the plateau region of ionization were used to study pulmonary injury in hamster lungs. Dose levels ranged from 500 to 1500 rads. Four animals at each dose level were killed 6 months after irradiation. The lungs were evaluated either by scanning electron microscopy or morphometrically by light microscopy.

In contrast to the early postirradiation response, the volume density of inflammatory cells and capillary lumina did not distinguish high linear-energy-transfer heavy-particle irradiation from X-irradiation at 6 months. However, the volume density of inflammatory cells (predominantly macrophages) remained elevated, thus implicating these cells in the progressive injury. The volume density of capillaries was within control value range, but there were fewer capillaries per pulmonary septum since septa were increased in hamsters receiving heavy-particle irradiation. Few changes were observed by scanning electron microscopy. Heavy particles were more efficacious than X-irradiation in producing lung damage.

Although several theories have been proposed concerning the mechanism of injury in irradiation-induced delayed pulmonary fibrosis, the relative importance of different changes remains controversial. In a previous publication[1] we demonstrated that the inflammatory response appears to be of primary importance in the initial stages of lung damage. We also suggested that if inflammatory cells continue to be present in the irradiated lung for long periods,

this condition would represent one mode of irradiation-mediated damage since inflammatory cells are known to contain potent enzymes, particularly elastase and various proteases, which are capable of inducing pulmonary fibrosis.[2-5] To further explore the mechanisms of injury after irradiation-produced damage, we undertook the present study of chronic irradiation damage. This report describes some of the preliminary results from the study.

MATERIALS AND METHODS

Animals

Female golden Syrian hamsters weighing 90 to 100 g (Horton Breeding Laboratories, Los Gatos, Calif.) were irradiated at 10 to 12 weeks of age. Four animals from each dose-level group were housed in the same cage and fed a White Diet (Feedstuffs, Inc., San Francisco, Calif.) and water ad libitum. The animals were examined daily for any fatalities. Hamsters were chosen for this study because they are small, inexpensive, and easily manageable laboratory animals, infrequently contracting chronic respiratory disease[6] (a prime consideration in this type of investigation).

Methods

Irradiation Techniques

Details of X-ray and neon-ion irradiation in the plateau region of ionization have been previously reported.[1] Briefly, for X-irradiation a Phillips therapeutic X-ray machine was used, with the beam in horizontal position. The hamsters were shielded with lead except for the thorax and irradiated two at a time with a beam at 230 kV, 15 mA, with inherent filtration of 1.1 mm Al and with added filtration of 0.25 mm Cu and 1 mm Al. The half-value layer of this filtration was equivalent to 0.83 mm Cu, with a focus-to-skin distance of 40 cm. Exposures were measured with a Victoreen R-meter, and a roentgen-to-rad conversion factor of 0.96 was used to calculate absorbed dose.

For the neon-ion irradiation, the Lawrence Berkeley Laboratory Bevatron and heavy-ion linear accelerator (HILAC) were used in combination (BEVALAC). The beam was initially collimated with a 19- by 24-mm elliptical brass collimator, and either the 22- by 30-mm or the 11.5- by 16-mm half-oval aperture was used for the

actual lung irradiation. After passage through the vacuum windows and dosimetry equipment, the Bragg-peak neon-ion particles had a residual range of 375 MeV/amu or about 14.2 cm in tissue-equivalent material. X-ray films of the 22- by 30-mm field displayed the whole thorax of the animal exposed to the beam. The 11.5- by 16-mm half-oval field included the mediastinum and approximately 50% of the lung field. The smaller field was selected because it may be more relevant to actual clinical application than whole-thorax irradiation would be. These two types of irradiation fields are shown in Fig. 1.

Before irradiation the hamsters were intraperitoneally anesthetized with sodium pentobarbital (90 mg/kg) and placed in 3.8-ID- by 10.5-cm cylindrical Lucite tubes. Single doses of 500, 800, 1000, 1200, or 1500 rads were used for the irradiations.

Histological Techniques

At 6-month intervals postirradiation, four animals from each dose-level and irradiation modality, together with control hamsters, were intraperitoneally anesthetized with sodium pentobarbital. The sacrificed animals were weighed and photographed for radiation-induced skin reactions, and a portion of ventral thoracic skin was placed in neutral-buffered 10% Formalin for routine histological processing. The sternum was removed, and Wright's- or Giemsa-stained touch specimens from sternal bone marrow were prepared. The contents of the thoracic cavity were removed en bloc, and the thymus, esophagus, and heart were rapidly separated from the lungs. Next the heart was weighed; then the thymus, esophagus, and heart were placed in buffered Formalin for routine paraffin sectioning. The lungs and trachea were weighed, and the right lung was tied off and separated from the left lung and trachea. The left lung of every animal was intratracheally perfused at 20-cm water pressure for 30 min with 10% neutral-buffered Formalin; the lung was tied off and subjected to saline volume displacements for lung volume. The left lung was divided into five 0.5-cm transverse sections and standard processed in paraffin. Seven-micrometer sections were stained with hematoxylin and eosin, Masson's trichrome for fibrous tissue, and van Gieson's stain for elastic tissue. For mast cells sections were also stained with toluidine blue. The right lungs from control hamsters and from the 11.5- by 16-mm aperture neon-ion-plateau-irradiated animals were intratracheally perfused with cold fourth-strength Karnovsky's fixative, maintained in fixative overnight, and transferred to cacodylate buffer. Mediastinal portions of the lobes of the right lung were removed and examined by scanning and transmission electron microscopy.

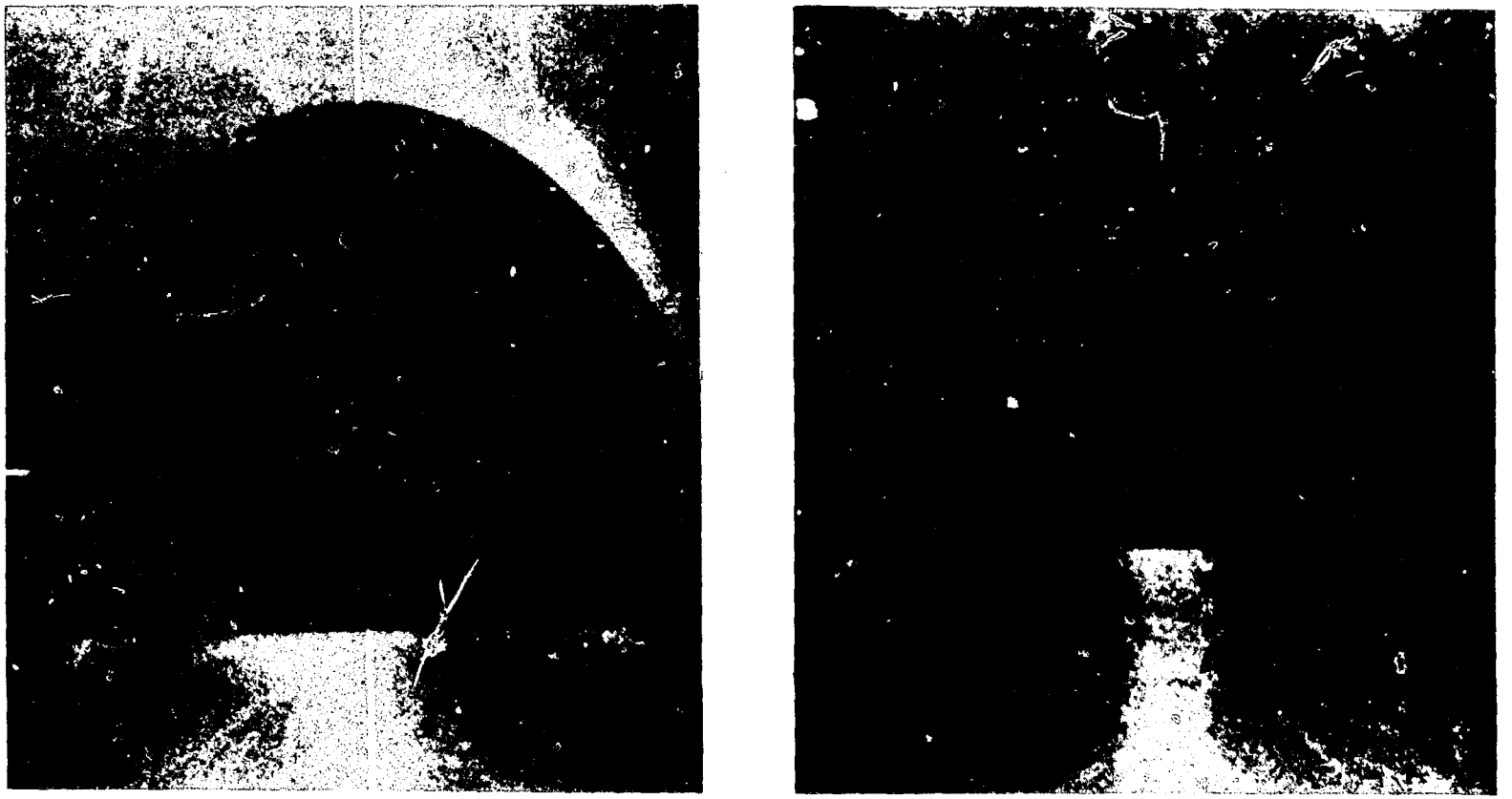

(a) (b)

Fig. 1 Radiographs of neon-plateau beam-field irradiation. (a) The 22- by 30-mm aperture included most of the lung field. (b) The 11.5- by 16.5-mm aperture encompassed the mediastinum and approximately half the lung field.

Morphometric Analysis

Morphometric analyses were conducted on sections from the left lung stained with hematoxylin and eosin or with Masson's trichrome. A 42-point random grid as described by Weibel et al.[7] was used. Three left lungs at each dose level as well as the time of sacrifice and the mode of irradiation were counted. With 25 x magnification 1000 hits were counted to obtain volume densities (number of hits counted on a specific tissue component per total number of hits) of the alveoli, septa, blood-vessel walls and lumina larger than 25 μm in diameter, connective tissue, and airway walls and lumina. With 1000 x magnification and counting 4000 hits, we calculated for each lung the volume densities of the alveolar space, septal cells (alveolar type I, endothelial cells, fibrocytes, and macrophages), alveolar type II cells, macrophages, neutrophils, eosinophils, and lymphocytes. Means and standard deviations were also calculated for each group. Student's *t* test was used to assess statistical significance at the 5% level between groups.

Scanning and Transmission Electron Microscopy

For scanning microscopy, right-lung tissues were subjected to critical-point drying and then coated with gold. The specimens were viewed with a JEOL model JSM scanning electron microscope. Routine photographs of every lung included four 62 X magnification surveys, a 1860 X magnification of a large airway with ciliated epithelium, and a 1860 X magnification of representative alveoli. For any other interesting or abnormal areas, additional photographs were taken. For transmission electron microscopy, mediastinal portions of the right lung were minced in cold cacodylate buffer, postfixed in 1% osmium tetroxide, block stained for 1 hr in uranyl acetate, dehydrated in ascending grades of alcohol, and embedded in Araldite. Further processing of these blocks is currently under way.

Chest X Rays

Chest X rays of the hamster lungs were obtained at the University of California, San Francisco, Department of Radiology. At 3-month intervals, four hamsters from each group were taken from Berkeley to San Francisco where they were anesthetized in the usual intraperitoneal fashion with 0.10 to 0.15 ml of 60 mg/ml sodium pentobarbital. Each animal was then placed with its head in a holder leading to an air inlet, water pressure manometer, and overflow safety valve. Airflow pressures were limited by the overflow valve to less than 13 cm of water. The animals were "overbreathed"

to the point of apnea, during which time standard anterior—posterior and lateral chest X rays were taken. These were enlarged and will be read in a "blind" controlled manner by an experienced radiologist.

RESULTS

The entire right and left lungs of every animal dying spontaneously, and not cannibalized beyond recognition, were histologically evaluated. We could identify no malignant tumors up to 1 year postirradiation. In general, the animals that died 3 months or sooner after irradiation revealed few pulmonary changes. Those dying 6 months or more after irradiation manifested a desquamative interstitial pneumonia with variable fibrosis that increased in severity as the dose level was increased. The lungs of the sacrificed animals were also roughly scored as follows with a system using points for the most frequently observed light-microscopic changes: for mild inflammation, 1 point; for moderate inflammation, 2 points; or for severe inflammation, 3 points; for pneumonia, 1 point; for fibrosis, 1 point; for fibrous pleural plaques, 1 point; and for "bronchiolarization" of alveoli, 1 point. These scores were then multiplied by the numbers of animals demonstrating the change(s) and divided by the total number of animals at that particular dose level and time postirradiation. This type of analysis, however, failed to distinguish X-ray from neon-ion irradiation effects.

Lung weights, left-lung volumes, body weights, lung-to-body-weight ratios, lung-volume to body-weight ratios, and heart-to-lung-weight ratios all proved useless in distinguishing irradiated from control animals as well as distinguishing among the types of irradiation employed.

The major morphometric compartments of the lung, i.e., parenchyma and nonparenchyma, were unchanged at 6 months after irradiation (Table 1, parts A and B). But since parenchyma primarily consists of septa and alveoli, if one of these elements increased at the expense of the other, the volume density of parenchyma would not reflect this change. Indeed, when the volume density of septa was examined and the initial results of septal-cell volume density were evaluated (Table 1, part C), lungs irradiated with 500 rads of neon ions differed significantly from those of the control animals. The volume density of alveoli was correspondingly reduced.

In our first report of the hamster lung response,[1] volume densities of inflammatory cells and capillary lumina proved fairly useful in evaluating the various types of irradiation at 2 weeks and 1 month after treatment. In contrast, at 6 months postirradiation,

TABLE 1

VOLUME DENSITY MEASUREMENTS OF LUNG-TISSUE COMPONENTS AT 6 MONTHS POSTIRRADIATION AS DETERMINED BY MORPHOMETRIC ANALYSIS

Treatment	Dose, rads				
	500	800	1000	1200	1500
		A. Pulmonary Parenchyma*			
X ray	0.746 ± 0.009		0.736 ± 0.003	0.806 ± 0.005	0.801 ± 0.023
Neon plateau Aperture, 30 by 22 mm	0.793 ± 0.022				
Aperture. 11.5 by 16 mm		0.806 ± 0.024	0.804 ± 0.010		
Control, rads 0.782 ± 0.017					
		B. Pulmonary Nonparenchyma*			
X ray	0.254 ± 0.009		0.264 ± 0.003	0.194 ± 0.005	0.199 ± 0.023
Neon plateau Aperture, 30 by 22 mm	0.207 ± 0.022				
Aperture, 11.5 by 16 mm		0.194 ± 0.024	0.196 ± 0.050		
Control, rads 0.218 ± 0.017					

(Table continues on next page.)

TABLE 1 (Continued)

Treatment	Dose, rads				
	500	800	1000	1200	1500
C. Septal Cells† (Fibrocytes, Endothelial Cells, Alveolar Type I Cells, and Septal Macrophages)					
X ray	0.146 ± 0.006				
Neon plateau Aperture, 30 by 22 mm	0.177 ± 0.004‡				
Control, rads 0.151 ± 0.004					
D. Capillary Lumina†					
X ray	0.066 ± 0.001				
Neon plateau Aperture, 30 by 22 mm	0.061 ± 0.009				
Control, rads 0.068 ± 0.002					
E. Inflammatory Cells†					
X ray	0.025 ± 0.005‡				
Neon plateau Aperture, 30 by 22 mm	0.033 ± 0.006‡				
Control, rads 0.010 ± 0.002					

TABLE 1 (Continued)

Treatment	Dose, rads				
	500	800	1000	1200	1500
		F. Alveolar Type II Cells†			
X ray	0.033 ± 0.002				
Neon plateau Aperture, 30 by 22 mm	0.041 ± 0.007				
Control, rads 0.027 ± 0.007					
		G. Collagen*			
X ray	0.063 ± 0.003‡		0.077 ± 0.010‡	0.093 ± 0.001‡	0.087 ± 0.016‡
Neon plateau Aperture, 30 by 22 mm	0.061 ± 0.010				
Aperture, 11.5 by 16 mm		0.073 ± 0.013‡	0.064 ± 0.006‡		
Control, rads 0.037 ±0.003					

*Volume density = mean of the number of hits per 1000 total points of 3 hamster lungs ± 1 standard deviation.

†Volume density = mean of the number of hits per 4000 total points of 3 hamster lungs ± 1 standard deviation.

‡These values differ from those of the control values at $p \leq 0.05$.

these two parameters could not distinguish neon-ion irradiation from X-irradiation since the volume density of capillary lumina had returned to control values in all lungs (Table 1, part D), whereas the amount of inflammation had increased but was similar in degree in all cases (Table 1, part E). These initial results disclosed that the amount of inflammation present in the X-irradiated lungs at 6 months had reached levels comparable to those in neon-ion-irradiated lungs. Special stain (toluidine blue) for mast cells revealed only rare ones, both in irradiated and nonirradiated lungs.

Our initial observations on the volume density of alveolar type II cells (which were stable at 2 weeks and 1 month) were also similar to control values at 6 months (Table 1, part F). This finding was somewhat unexpected, since alveolar type II cells are a basic constituent of pulmonary repair following many kinds of injury and thus might be anticipated to increase in volume density. Nevertheless, the alveolar type II cell response can occur as early as 4 hr after injury, and perhaps our sacrifice schedules were too late to document the peak response.[8]

Probably the most important hallmarks of subacute and chronic irradiation-caused damage are tumor induction and fibrosis. Only one of the 568 animals studied thus far has developed a tumor—a bronchial papilloma—during the first 2-week post-helium-ion Bragg-peak irradiation. Moreover, this was regarded as a spontaneous occurrence. Insofar as fibrosis is concerned, the volume density of collagen was increased for all types of irradiation at 6 months. Lungs irradiated by neon ions and X rays all displayed mild but statistically elevated collagen volume densities (Table 1, part G). Although the collagen in control lungs was predominantly localized in perivascular, peribronchial, or subpleural areas, the irradiated lungs also showed collagen deposition in pulmonary septa (Fig. 2).

With scanning electron microscopy only a few changes distinguished irradiated from control lungs. These alterations consisted of groupings or aggregations of Clara cells (Fig. 3, a and b), enhanced prominence of small airways in the periphery of the irradiated lungs (Fig. 4, a and b), and increased amounts of macrophages in alveoli (Fig. 5, a and b). These abnormalities were present at 600, 800, and 1000 rads of irradiation with neon ions in the plateau region of ionization.

Sequential chest X rays also revealed abnormalities in the irradiated lungs. Although the entire series has not yet been completed, it is subjectively clear that opacification of the lung fields occurs after high doses of either X-ray or neon-ion irradiation compared to the lung fields of nonirradiated control animals (Fig. 6).

(Text continues on page 548.)

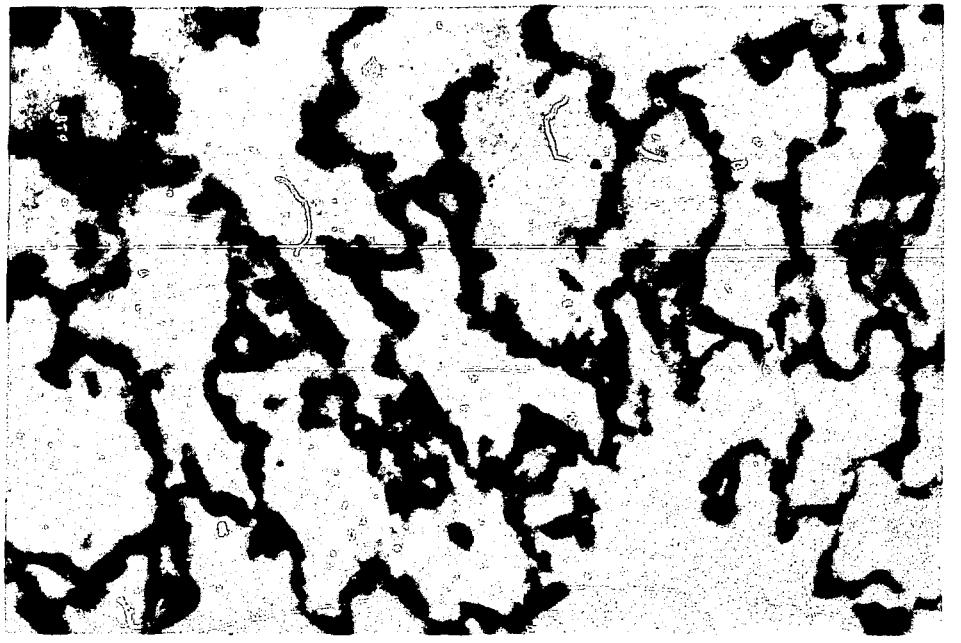

(a)

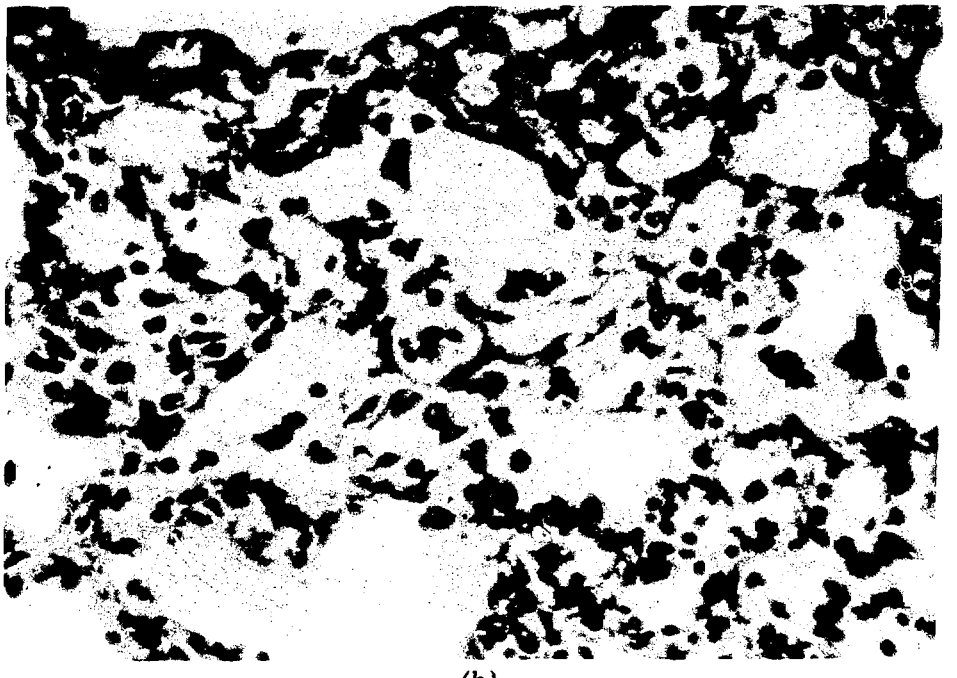

(b)

Fig. 2 In contrast to control hamster lung (a), lungs (b) 6 months after irradiation with 1000 rads of neon ions exhibit pulmonary septal fibrosis. (Masson's trichrome stain for fibrous tissue; 200 X.)

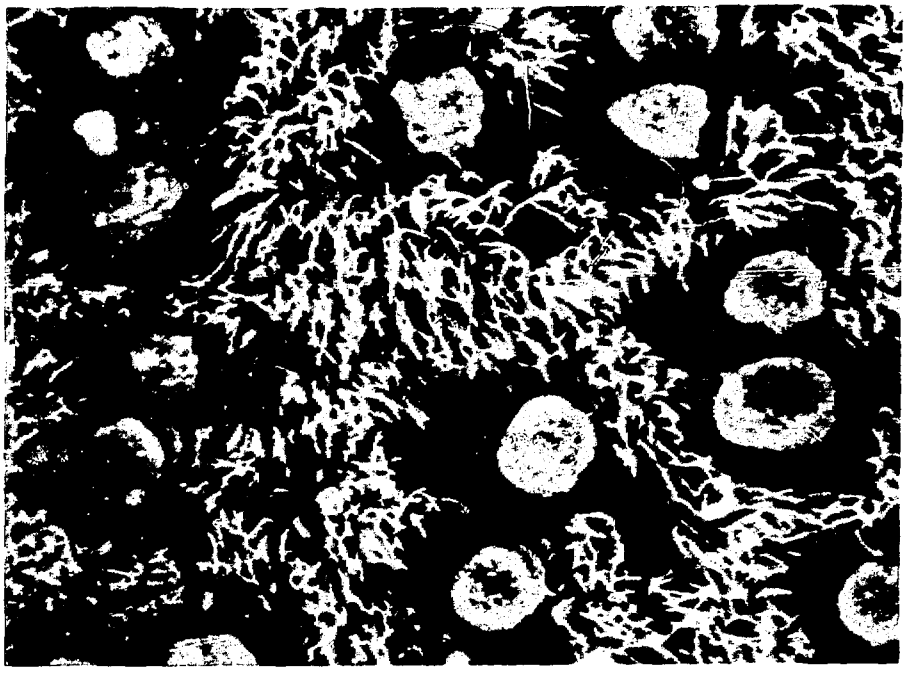

(a)

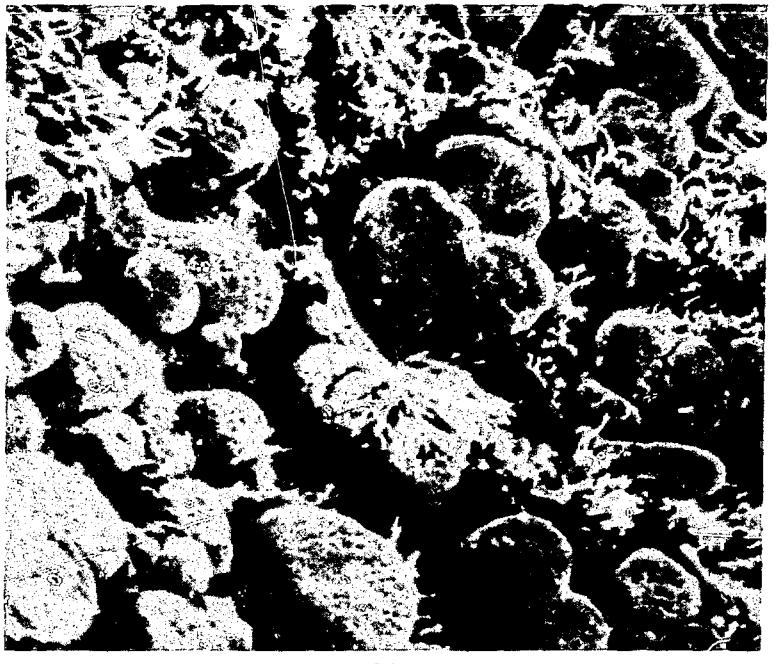

(b)

Fig. 3 Unlike control hamster airways (a) where individual Clara cells are interspersed with ciliated cells, irradiated airways (b) show groupings of the Clara cells. Part b shows an 11.5- by 16-mm aperture neon-plateau-irradiated lung (800 rads, 6 months postirradiation). (Scanning electron microscopy; 930 X.)

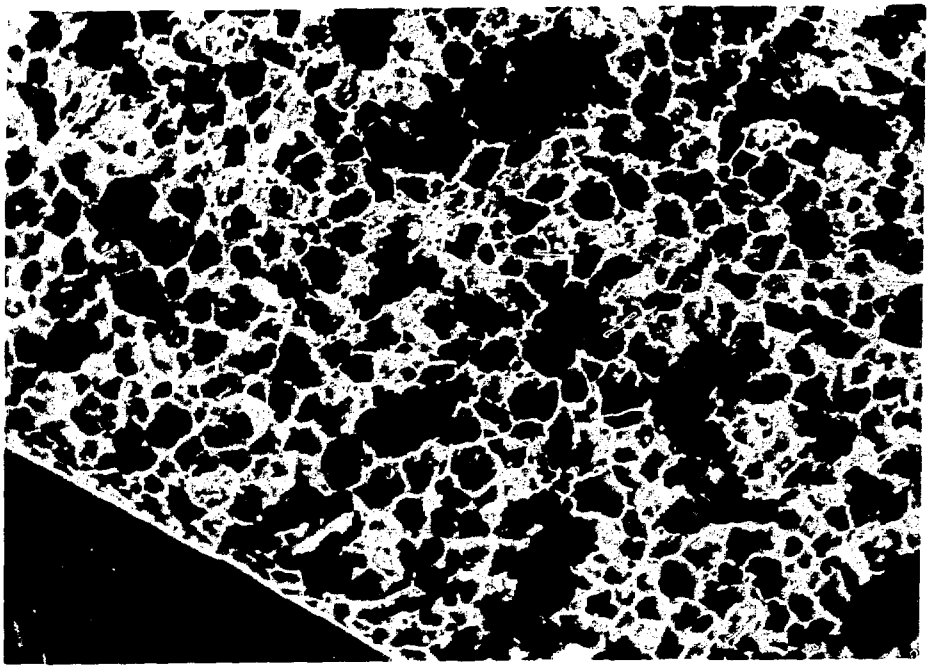

(a)

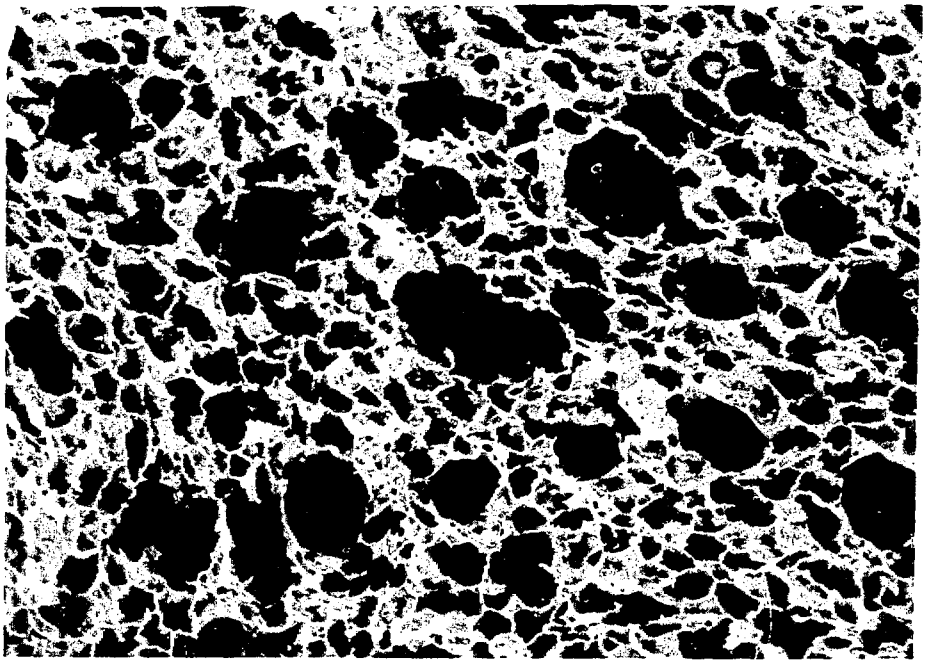

(b)

Fig. 4 Alveolar ducts and terminal bronchioles appear more prominent in irradiated lungs (b) treated with 800 rads of neon ions in the plateau region of ionization 6 months postirradiation than in control hamster lungs (a). (Scanning electron microscopy; 31 X.)

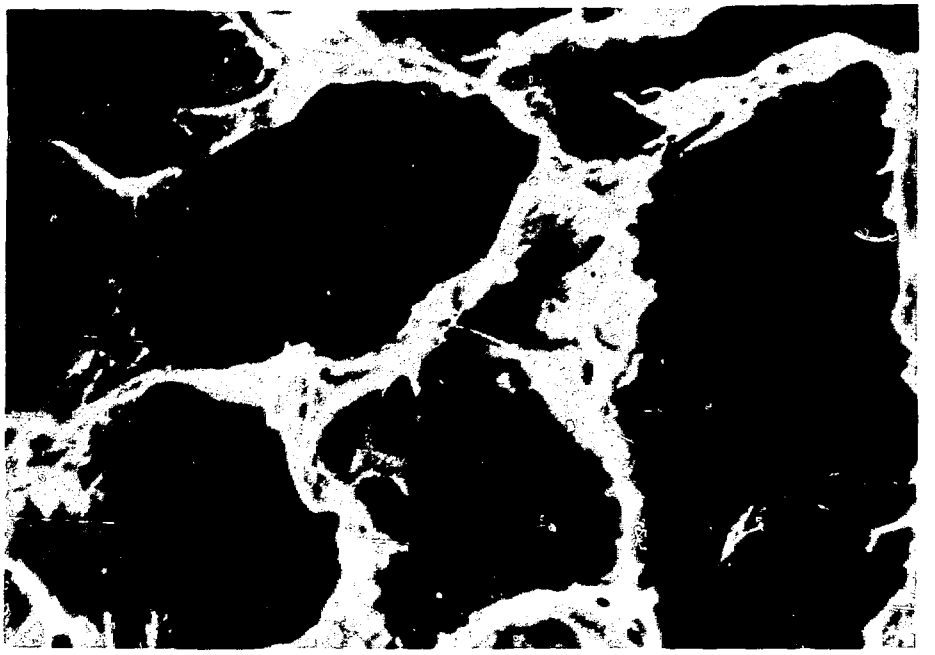

(a)

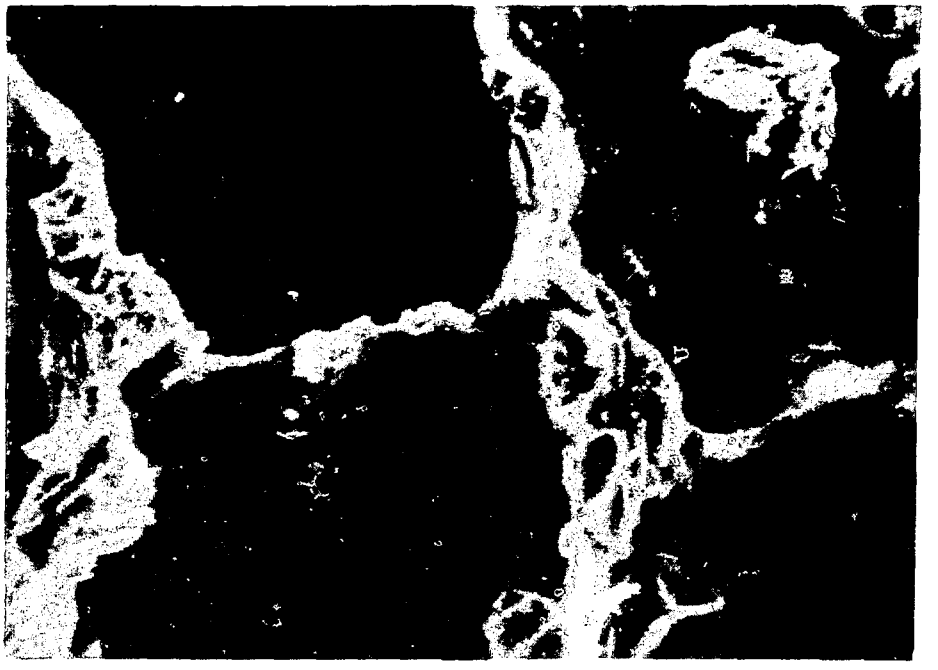

(b)

Fig. 5 Alveoli treated with 800 rads of neon-plateau irradiation disclose more numerous macrophages (b) than those of control animals (a). (Scanning electron microscopy; 930 X.)

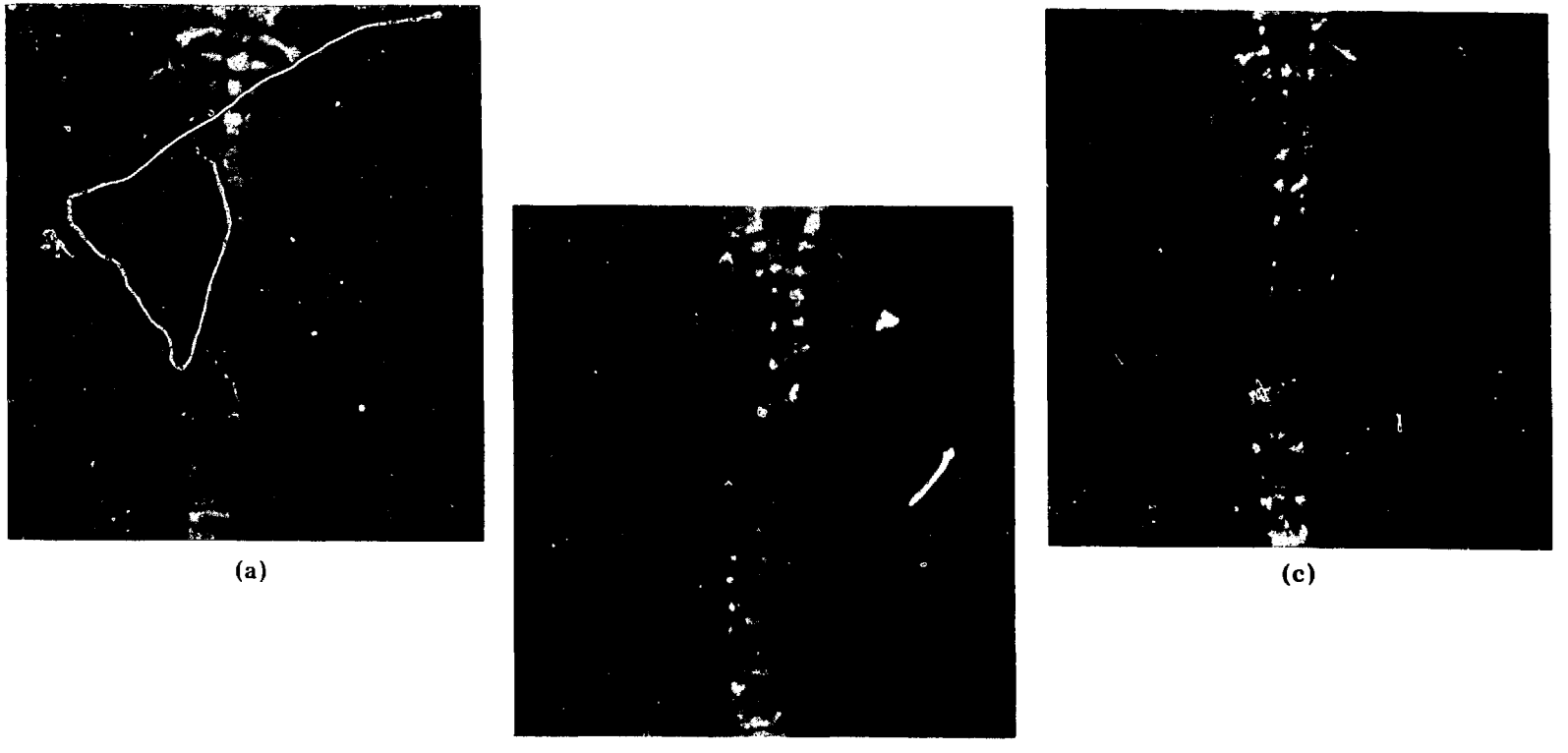

(a) (b) (c)

Fig. 6 Eight months after irradiation, neon-ion-irradiated lungs (b) and X-irradiated lungs (c) demonstrate increased opacification of the lung fields compared to non-irradiated control hamsters (a). Part b depicts the changes observed after 1000 rads of neon, 11.5- by 16-mm aperture. Part c illustrates alterations after 1500 rads of X-irradiation.

Cumulative mortality data covering a period of up to 6 months postirradiation showed a sharp rise in death rates with doses greater than 1200 rads of X-irradiation and 800 rads of neon ion in the plateau irradiation. In comparison with the large-aperture neon-ion-irradiated animals, the small-aperture neon-ion-irradiated animals (at this point in time) show no difference in mortality rates. In groups of irradiated animals, cumulative survival rates are decreased compared to those of control hamsters, even with doses as low as 225 rads of X-irradiation or 300 rads of neon-ion irradiation (Table 2).

DISCUSSION

Studies of irradiation-induced damage to the lung have been somewhat hampered by the rather crude methods of evaluation often used and by certain aspects of experimental design, particularly

TABLE 2

PERCENT CUMULATIVE MORTALITY RATES FOR HAMSTERS AFTER LUNG IRRADIATION

Treatment	Number of animals	Time, months											
		1	2	3	4	5	6	7	8	9	10	11	12
Control	64	0	0	0	0	0	8	9	9	9	12	14	
X ray													
225 rads	30	3	3	3	3	3	3	3	10	17	30	43	
450 rads	32	0	0	0	0	0	0	0	0	6	19	22	
900 rads	30	0	0	0	0	0	0	0	10	10	10	16	
1200 rads	28	11	11	11	14	21	30	39					
1500 rads	28	7	7	7	14	18	32	50					
Neon plateau Aperture, 11.5 by 16 mm													
150 rads	20	0	0	0	5	5	10	10	15	15	25	30	50
300 rads	26	0	0	0	0	4	8	8	19	28	31	31	47
600 rads	48	0	0	0	0	2	2	8	13	14	36	39	46
800 rads	28	0	4	7	7	7	18	25	29	32			
1000 rads	28	11	18	21	29	36	36	53	57	61			
Neon plateau Aperture, 30 by 22 mm													
500 rads	33						18						
1000 rads	33						31						
1500 rads	33						45						

irradiation fields, doses, and the selection of appropriate laboratory animals. We have attempted to overcome some of these problems by using the hamster, a fairly infection-free small animal, with a good potential for the evaluation of radiation-mediated experimental carcinogenesis.[9] In addition, we have utilized and are in the process of assessing methods varying from light-microscopic morphometry (a technique that appears to be very sensitive and discriminating) to the evaluation of cumulative mortality rates. In general, our preliminary results indicate more lung damage at high dose levels of 1000 rads and above of X-irradiation and 800 rads and above of neon-ion irradiation in the plateau region of ionization. Neon-ion doses of 800 rads result in damage quite similar in appearance to that induced by 1000 rads of X-irradiation.

In contrast to other investigators,[10] we were not impressed with the participation of the mast cell in the irradiation response of the hamster lung. Our hamster lungs showed few mast cells before irradiation and no increase in toluidine-blue-stainable mast cells postirradiation. Unlike Madrazo et al.,[11] we did note an inflammatory response, but those workers examined the lungs of their hamsters 2 to 7 days after whole-thorax irradiation with 10,000 rads of X-irradiation. Such a high dose is usually meaningless for clinical purposes. Pickrell et al.[12] also observed only minimal histological changes in hamsters following 2000, 4000, or 6000 rads of hemithorax X-irradiation. Significantly, however, the changes consisted of an increase in macrophages and beginning fibrosis 5 to 5½ months postirradiation. The exposure mortality in Pickrell's experiments was quite high (67 of 185 animals). Phillips and his group, who have studied lung irradiation in both rats and mice,[13-15] attribute early deaths (10 to 20 days postirradiation) to esophageal damage and later deaths to radiation pneumonitis and fibrosis—presumably on the basis of damage to pulmonary endothelial cells. Excessive early mortality has not occurred among our animals, and histological examination of the esophagus only rarely revealed inflammation or fibrosis. The lungs did disclose a late radiation pneumonitis and fibrosis on the basis of most parameters judged. Initial morphometric data suggest that although the absolute volume density of capillary lumina compared favorably with control values 6 months after irradiation, the number of capillaries per pulmonary septum would be diminished since these septa are increased in volume density, which is apparently due to augmentation of fibrocytes, alveolar type II cells, and inflammatory cells. This observation in conjunction with our findings with scanning electron microscopy, i.e., more numerous macrophages, implies that the inflammatory response may be of great importance in chronic, progressing, irradiation-induced

damage to lung tissue and that further exploration of the mechanism of such injury is essential.

ACKNOWLEDGMENTS

The authors express their appreciation to Dr. Ted Phillips, Department of Radiology, University of California, San Francisco, for his support and advice; to Ms. Brook Knowles for technical assistance in scanning electron microscopy; and to the operating crew of the BEVALAC for the production of neon-ion beams.

Dr. Woodruff is supported by the American Lung Association's Grants For Young Investigators. This study was also supported by Grant CA-158401 from the National Cancer Institute, the National Aeronautics and Space Administration, and the U. S. Energy Research and Development Administration.

REFERENCES

1. K. H. Woodruff, J. T. Leith, and C. A. Tobias, Morphologic and Morphometric Analysis of the Early Effects of X-Ray and Heavy-Ion Irradiation of Hamster Lung, *Am. J. Pathol.*, 82: 287-296 (1976).
2. G. M. Turino, J. R. Rodriguez, L. M. Greenbaum, and L. Mandl, Mechanisms of Pulmonary Injury, *Am. J. Med.*, 57: 493-504 (1974).
3. P. M. Henson, Pathologic Mechanisms in Neutrophil-Mediated Injury, *Am. J. Pathol.*, 68: 593-606 (1972).
4. E. A. Levine, R. M. Senior, and J. V. Butler, The Elastase Activity of Alveolar Macrophages: Measurements Using Synthetic Substrates and Elastin, *Am. Rev. Respir. Dis.*, 113: 25-30 (1976).
5. B. Mass, T. Ikeda, D. R. Meranze, G. Weinbaum, and P. Kimbel, Induction of Experimental Emphysema. Cellular and Species Specificity, *Am. Rev. Respir. Dis.*, 106: 384-391 (1971).
6. J. R. Lindsey, H. J. Baker, R. G. Overcash, G. H. Cassell, and C. E. Hunt, Murine Chronic Respiratory Disease: Significance as a Research Complication and Experimental Production with *Mycoplasma pulmonis*, *Am. J. Pathol.*, 64: 675-716 (1971).
7. E. R. Weibel, C. Fisher, J. Gahm, and A. S. Schaefer, Current Capabilities and Limitations of Available Stereological Techniques, *J. Microsc.*, 95: 367-392 (1971).
8. H. Witschi, Proliferation of Type II Alveolar Cells: A Review of Common Responses in Toxic Lung Injury, *Toxicology*, 5: 267-277 (1976).
9. F. Homburger, A. Handler, and C. Land, Unique Properties of Inbred Syrian Hamsters for Carcinogenesis Studies, *Lab. Invest.*, 32: 427 (1975).
10. S. Watanabe, K. Watanabe, T. Ohishi, M. Aiba, and K. Kageyama, Mast Cells in the Rat Alveolar Septa Undergoing Fibrosis After Ionizing Irradiation, *Lab. Invest.*, 31: 555-567 (1974).
11. A. Madrazo, Y. Suzuki, and J. Churg, Radiation Pneumonitis, *Arch. Pathol.*, 96: 262-268 (1973).

12. J. A. Pickrell, D. V. Harris, F. F. Hahn, J. J. Belasich, and R. K. Jones, Biologic Alterations Resulting from Chronic Lung Irradiation. III. Effect of ^{60}Cobalt Irradiation on Upper Pulmonary Collagen Metabolism and Fractionation in Syrian Hamsters, *Radiat. Res.*, 62: 133-144 (1975).
13. T. L. Phillips and L. Margolis, Radiation Pathology and the Clinical Response of Lung and Esophagus, *Front. Radiat. Ther. Oncol.*, 6: 254-273 (1972).
14. T. L. Phillips, S. Benak, and G. Ross, Ultrastructural and Cellular Effects of Ionizing Radiation, *Front. Radiat. Ther. Oncol.*, 6: 21-43 (1972).
15. T. L. Phillips, An Ultrastructural Study of the Development of Radiation Injury in the Lung, *Radiology*, 87: 49-54 (1966).

Early and Late Effects of Fission-Neutron or Gamma Irradiation on the Clearance of Bacteria from the Lungs of $B6CF_1$ Mice

PATRICIA C. BRENNAN and E. JOHN AINSWORTH
Division of Biological and Medical Research, Argonne National Laboratory, Argonne, Illinois

ABSTRACT

Enhanced susceptibility to experimental respiratory infection following chronic exposure to low-level gamma radiation has been reported, but no comparable information exists for neutron-irradiated animals. Such information is needed in view of the apparently greater additivity of repeated low fission-neutron doses. Consequently altered susceptibility to respiratory infection is being examined in the JANUS Neutron and Gamma-Ray Toxicity Program. Some $B6CF_1$ mice of various ages were challenged with *Pasteurella pneumotropica* either by intranasal instillation or by aerosol inhalation following single or fractionated doses of neutrons or ^{60}Co gamma radiation. Clearance of the bacteria from the lungs was assessed 4 days after challenge by a culture technique and by histological and immunofluorescence staining. From 5 to 21 days after a single dose of 288 neutron rads or 740 gamma rads, a ratio equal to the relative biological effectiveness (RBE) for cell killing, there was little repair of the radiation-damaged clearance mechanism evident in neutron-irradiated mice; 85% were unable to clear the organism as long as 21 days after irradiation. Over the same period only 25% of gamma-irradiated mice failed to eliminate *P. pneumotropica*. Immunofluorescent-stained lung sections at all time intervals between 5 and 21 days were strikingly similar among neutron- and gamma-irradiated mice and unirradiated mice. Alveolar macrophages were swollen with fluorescent *P. pneumotropica* cells, and macrophages surrounding the bronchi and in the bronchial exudate were also intensely fluorescent. These data, coupled with the culture data, indicate that pulmonary macrophages in the irradiated host are capable of engulfing *P. pneumotropica* cells but that the ability to kill them is impaired.

The ability to clear a challenge of *P. pneumotropica* following single doses of 240 neutron rads or 807 gamma rads or following the same total doses given in 24 weekly fractions was assessed 2 weeks after the last fraction and 26 weeks after a single dose. Mice given single doses were able to clear the organism; mice that received the same total dose in 24 fractions were not. Interestingly, mice

receiving fractionated gamma radiation were more severely impaired than those receiving fractionated neutron radiation. Consequently, under conditions of protracted irradiation, the RBE of fission neutrons is less than 3.6 on the basis of susceptibility at approximately 300 days of age.

The Neutron and Gamma-Ray Toxicity Program (JANUS) was initiated at Argonne National Laboratory to study the late effects of ionizing radiation. This program seeks to generate new information on late effects of fission-spectrum neutrons and gamma radiations which will contribute eventually to risk assessment. The end points include life shortening and rates of neoplastic and nonneoplastic diseases. Cellular damage and repair are assessed through study of both early and late injury to the hematopoietic system, the immune system, the vascular system, and the pulmonary defense system. Preliminary results of some of these studies have been reported.[1-5]

Increased susceptibility to infectious disease follows acute midlethal exposure to low linear-energy-transfer (LET) radiation;[6,7] however, comparatively little is known about the effect of chronic low-level exposure or about either acute or chronic exposure to high LET radiation. The evaluation of high LET fission-neutron damage assumes added importance in view of the apparently greater additivity of repeated low fission-neutron doses as compared with the sparing effect of gamma-dose fractionation.[2-4] In addition, any evidence of greater injury or slower repair after neutron irradiation would contribute to our understanding of cellular mechanisms of damage and recovery and to acceptance or rejection of the hypothesis that the relative biological effectiveness (RBE) for enhanced disease susceptibility is the same as the RBE for cell killing. With regard to low LET radiation, Hammond, Anderle, and Miller[8] found that susceptibility to *Pseudomonas* infections was related to gamma-radiation dose rate rather than to total dose owing undoubtedly to repair processes during irradiation. Mice exposed at dose rates of 70 to 130 R/day demonstrated increased susceptibility to intraperitoneal challenge, whereas those exposed at 34 R/day showed no significant increase in susceptibility. In later studies[9,10] a slight increase in susceptibility to *Pseudomonas* infection could be demonstrated at a dose rate of 15 R/day gamma radiation but not at 0.5, 1, or 2 R/day.

Information on susceptibility to experimental respiratory infection following continuous low-level gamma radiation is scant. Stewart, Pribnow, and Silverman[11] found increased susceptibility to an aerosol challenge with *Listeria monocytogenes* in mice receiving an accumulated dose of 500 gamma rads at a dose rate of 1 to

1.5 rads/hr. This susceptibility increased thereafter with increasing total dose but was not observed at doses lower than 500 rads. Subsequently Hodge, Leif, and Silverman[12] and Silverman et al.[13] reported enhanced susceptibility and impaired immunity to *Pasteurella tularensis* following total doses of 1000 to 3000 rads gamma radiation at a dose rate of 1.4 rads/hr. Lundgren et al.[14] found enhanced susceptibility to influenza virus following chronic lung exposure to inhaled $^{144}CeO_2$, a beta emitter. In all these studies the mice were exposed to the challenge organism within hours after the radiation was terminated. We believe it is also important to challenge at later times during the early recovery phase and at times long after termination of the radiation sequence to determine residual injury. Previously[2] we reported the results of challenge with *Mycoplasma pulmonis* 5, 11, and 21 days after a single exposure to 288 fission neutrons or 780 gamma rads and 5 days after completion of the same total doses administered in nine fractions over a 3-week period. We found that the RBE for increased susceptibility to *M. pulmonis* infection was of the order of 2.6. Surprisingly, we found the same effect with gamma-dose fractionation over a 3-week period, which indicates total dose dependence for both radiations; the RBE remained at approximately 2.6 under conditions of short-term fractionation. When the mice were challenged 12 to 42 weeks after completion of 6 months of fractionated neutron or gamma radiation at total doses of 240 neutron rads or 855 gamma rads, a sparing effect of gamma-dose fractionation was observed.

In the studies we report here, *P. pneumotropica* was used as the challenge organism because pathogenicity of this organism depends in large part on the functional state of the pulmonary antibacterial mechanism[15] and because of our previous experience with this organism.[16,17]

MATERIALS AND METHODS

Radiation

The source of fission neutrons was the JANUS reactor in the Division of Biological and Medical Research at Argonne National Laboratory. Gamma radiation was delivered with a ^{60}Co source. The reactor, dosimetry, and procedures for irradiating animals have been described elsewhere.[1-3,18,19]

The experimental mice were $B6CF_1$/Anl hybrids [(C57BL6J ♀ x BALB/cJ ♂/Anl)] of both sexes. Radiation was delivered in single doses or in 24 weekly fractionated doses; treatment began when the

mice were 110 to 120 days of age (Table 1). After delivery of the single dose or the last fractionated dose, the mice were held in a "geriatric ward" until challenged with *P. pneumotropica.*

TABLE 1

FRACTIONATED AND SINGLE DOSES USED

	Neutron				Gamma			
	Dose*/ fraction, rads	No. of fractions	Dose rate, rads/min	Total rads	Dose*/ fraction, rads	No. of fractions	Dose rate, rads/min	Total rads
Fractionated	10.0	24†	0.22	240	33.6	24†	0.75	807
doses	3.3	24†	0.074	80				
Single		1	12	240		1	40.4	807
doses		1	13.1	288		1	33.7	740
		1	4	80				

*Factors used to convert kerma to midline tissue dose were 0.80 for JANUS neutrons and 0.934 for ^{60}Co gamma radiation.

†One 45-min exposure per week.

Bacterial Challenge

Pasteurella pneumotropica has been maintained in our laboratory for many years; culture conditions, preparation of inocula, and pathogenicity of our strain have been described.[17]

Mice were administered the bacterial challenge either intranasally or by inhalation with a modified Henderson apparatus[20] similar to that described by Jakob and Green.[21] Briefly, the apparatus consisted, in sequence, of a three-jet impaction nebulizer activated by compressed air, an 8-by-60-cm-long glass tube to mix the nebulized agent with diluting air, a stainless-steel exposure chamber that contained a maximum of six compartmented drawer-like units, each with a capacity for 32 individually separated mice, a fiber glass prefilter, two absolute-type bacterial filters, and a vacuum pump. The entire unit was contained in a Blickman hood, which was also equipped with an absolute bacterial filter.

The mice were challenged with a dose of *P. pneumotropica* that preliminary experiments showed was cleared by approximately 90% of unirradiated control mice in 4 days. Four days after challenge, 10 or 30 mice per group were killed. Their lungs were homogenized in 3 ml sterile 0.9% saline, diluted 10-fold in saline, and the dilutions plated in triplicate on trypticase soy agar. The plates were incubated

for 48 hr at 37°C, and colonies were counted. Results are expressed as viable *P. pneumotropica* per lung.

Immunofluorescence and Histology

The lungs from three or four additional mice in each group were prepared for immunofluorescence and histological staining according to the method of Sainte-Marie.[22] Sections were stained with the indirect fluorescent antibody technique previously described.[17] Duplicate sections were stained with hematoxylin and eosin.

Immunofluorescent-stained sections were examined with a Leitz Dialux ultraviolet microscope with a phase-contrast dark-field fluorescence condenser. The light source was an Asram HBO-200 mercury-arc lamp.

RESULTS

Table 2 gives the clearance data for *P. pneumotropica* from the lungs of mice 5, 11, and 21 days after single doses of 288 neutron rads or 740 gamma rads. These doses were selected because they reduce the surviving fraction of hematopoietic colony-forming units (CFU) equally. Furthermore, this gamma-to-neutron ratio of 2.6 is the RBE for the $LD_{50/30}$. Little repair is evident in neutron-irradiated mice; 85% were unable to clear the organism when challenged as long as 21 days after irradiation as compared to a value

TABLE 2

CLEARANCE OF *PASTEURELLA PNEUMOTROPICA* FROM THE LUNGS OF NEUTRON- OR GAMMA-IRRADIATED MICE

Time of challenge,* days	Radiation dose, rads	Viable *P. pneumotropica* recovered per lung (10^2)†	Percentage of mice unable to clear *P. pneumotropica*
5	fn 288	29.0 ± 12.2	70.4
	γ 740	4.2 ± 2.2	72.0
11	fn 288	280.0 ± 83.0	93.1
	γ 740	5.1 ± 1.8	66.0
21	fn 288	38.0 ± 13.0	85.2
	γ 740	0.27 ± 0.09	25.0
5 to 21	0	0.05 ± 0.005	7.3

*Groups of 30 mice were challenged with 3×10^5 viable *P. pneumotropica*, and their lungs were cultured 4 days later.

†Values are the mean ± 1 SE.

of only 25% in gamma-irradiated mice at 21 days. The number of viable bacterial cells per lung was also significantly higher in neutron-irradiated mice at 11 and 21 days. However, fluorescent-stained lung sections were strikingly similar among neutron-irradiated, gamma-irradiated, and unirradiated mice (Fig. 1). Macrophages surrounding the bronchial epithelium were intensely fluorescent, and alveolar macrophages were swollen with fluorescent *P. pneumotropica* cells. Hematoxylin and eosin stained sections were also similar at all time intervals in both irradiated and unirradiated mice. The microscopic lesions consisted of a severe polymorphonuclear response coupled with moderate lymphocytic infiltration. These lesions were similar to those observed when germ-free mice were infected with *P. pneumotropica.*[17]

The results of challenge with *P. pneumotropica* following single doses of 240 neutron rads or 807 gamma rads or following the same total dose given in 24 weekly fractions are shown in Table 3. Mice challenged 26 or 79 weeks after a single dose had no apparent residual effect of radiation. On the other hand, mice challenged 2 weeks after the termination of fractionated exposure were unable to clear the challenge dose. Interestingly, mice receiving fractionated gamma radiation were more severely impaired than those receiving fractionated neutron exposure. We were not able to challenge mice 56 weeks after the end of fractionated neutron radiation; however, gamma-irradiated mice challenged at that time showed them to be more impaired than mice that received single doses of neutron or gamma radiation 79 weeks earlier.

We also challenged mice that received a total dose of 80 neutron rads as a single dose or in 24 fractions of 3.3 rads at the later time points shown in Table 3. Both groups were able to clear the challenge dose, and there was no significant difference in the bacterial count per lung.

Immunofluorescent-stained lung sections were similar among all groups at both the early and late challenge times. Hematoxylin and eosin stained sections were also similar except for lung sections from mice that had received fractionated gamma radiation. In these mice the amount of lymphocytic infiltration was much more extensive than was observed in lung sections from other groups.

DISCUSSION

The data presented here contribute substantial new information on the susceptibility to *P. pneumotropica* and, by inference, the functional state of the pulmonary antibacterial mechanism following

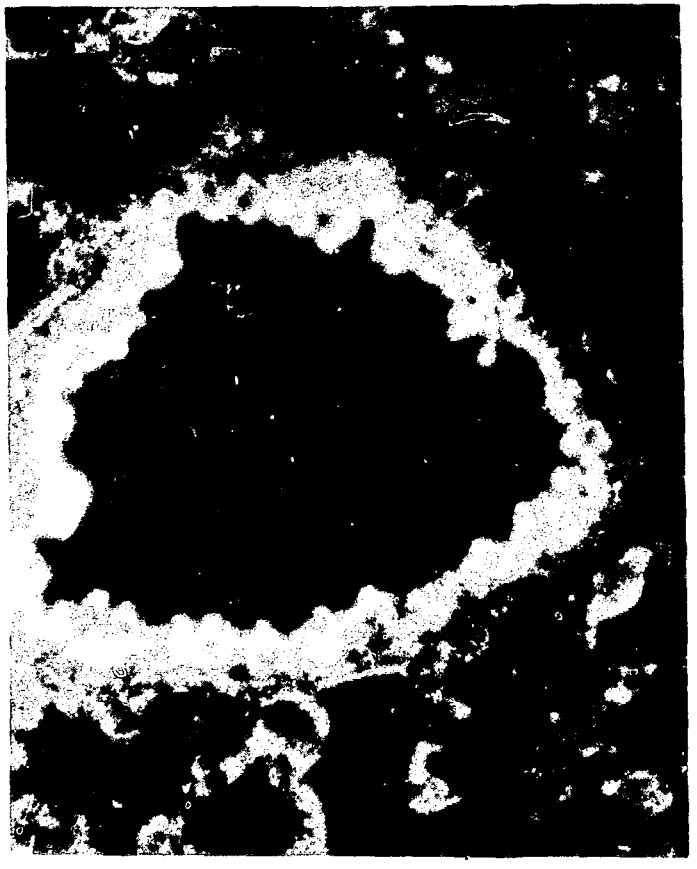

(a)

(a) Lung section from unirradiated control mouse stained with anti-*P. pneumotropica* serum.

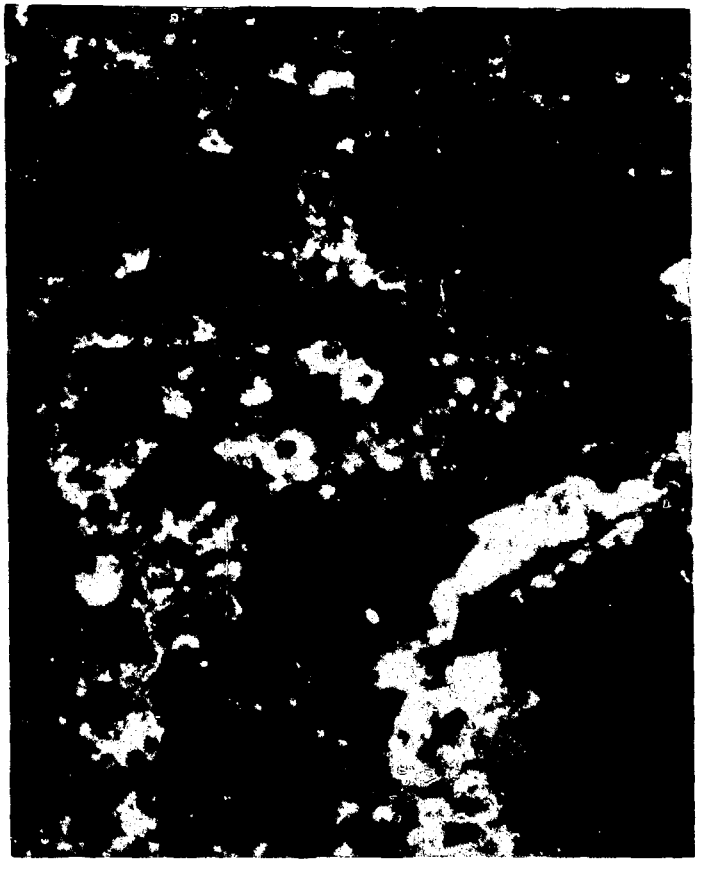

(b)

(b) Lung section from unirradiated control mouse stained with normal rabbit serum.

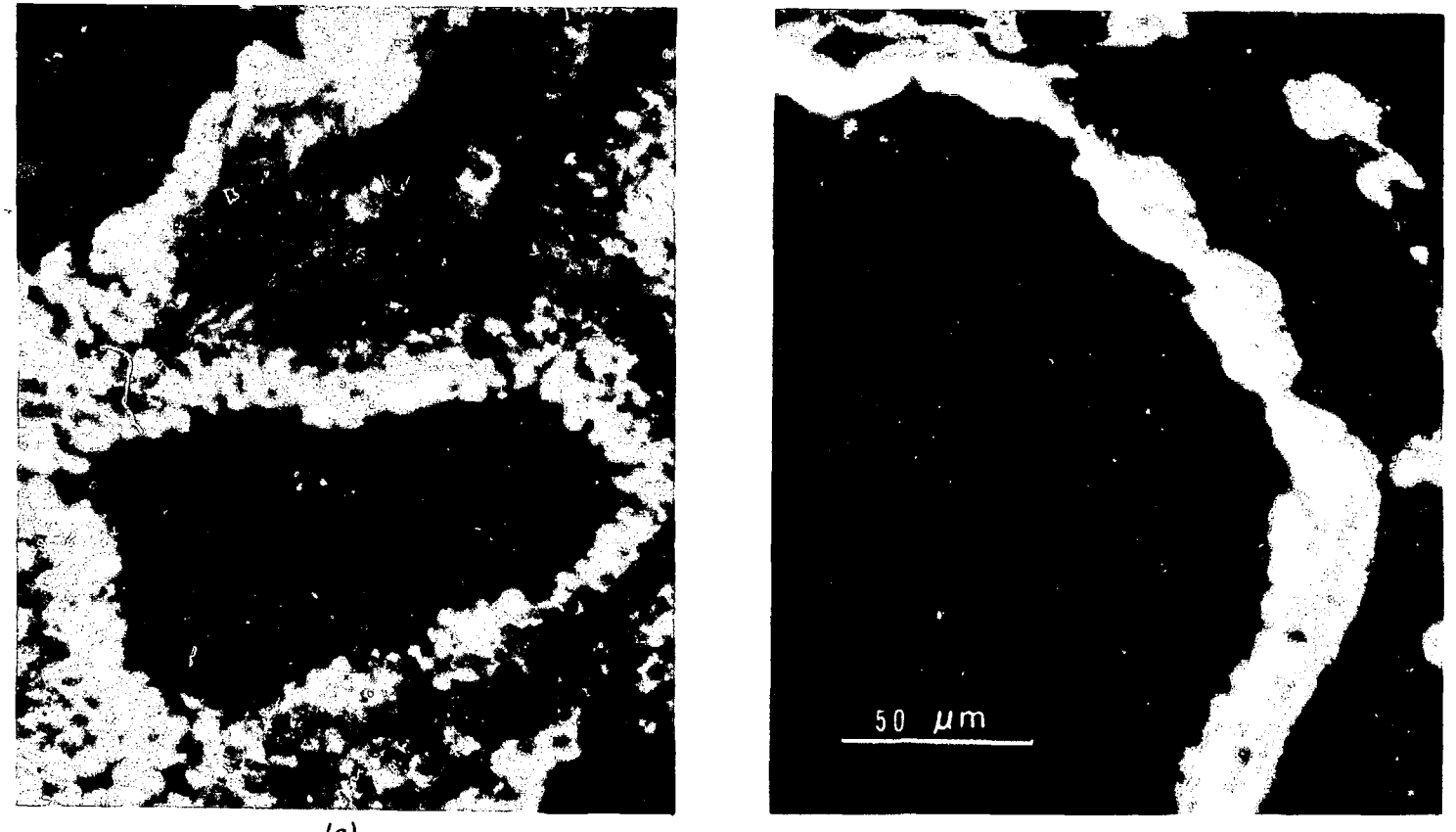

(c) (d)

(c) and (d) Lung sections of neutron- and gamma-irradiated mice, respectively, challenged 11 days after irradiation, stained with anti-*P. pneumotropica* serum.

Fig. 1 Immunofluorescent-stained lung sections of mice challenged with *P. pneumotropica*.

TABLE 3

CLEARANCE OF *PASTEURELLA PNEUMOTROPICA* FROM THE LUNGS OF MICE IRRADIATED WITH SINGLE OR FRACTIONATED DOSES OF NEUTRONS OR GAMMA RAYS

Time of challenge*	Radiation dose, rads	Viable *P. pneumotropica* recovered per lung†	Percentage of mice unable to clear *P. pneumotropica*
26 weeks after a single dose	fn 240	$<10^2$	0
	γ 807	$<10^2$	0
2 weeks after last fraction	fn 240	$2.4 \times 10^3 \pm 2.6$	100
	γ 807	$1.1 \times 10^5 \pm 0.4$	100
Age matched controls	0	$1.2 \times 10^2 \pm 1.7$	40.071
79 weeks after a single dose	fn 240	$6.5 \times 10^1 \pm 3.1$	60
	γ 807	$1.7 \times 10^1 \pm 2.5$	60
56 weeks after last fraction	fn 240	No data	
	γ 807	$2.3 \times 10^3 \pm 5.1$	90
Age matched controls	0	$2.4 \times 10^1 \pm 2.1$	30

*Groups of 10 mice were challenged with 4×10^3 viable *P. pneumotropica*, and their lungs were cultured 4 days later.

†Values are the mean ± 1 SE.

either single or fractionated doses of neutron or gamma radiation. Berlin[2,3] reported a sparing effect of 250 R X-radiation on susceptibility to influenza virus challenge given 1 day after irradiation. He attributed this protection to prevention of the inflammatory response. In a similar study using graded doses of 125 to 500 R X-radiation,[2,4] he found a delay in onset of pneumonia but no effect on susceptibility as measured by infectivity or mortality. In a previous study[2] in which we used *M. pulmonis* as the challenge organism, we found enhanced susceptibility to infection 5 to 21 days after single doses of neutron or gamma radiation. Results with the two radiations did not differ significantly in terms of pneumonia incidence, but there were differences in the severity of the lesions. Mice challenged 5 days after neutron irradiation showed a diminished cellular response and extensive bacterial invasion into the alveolar spaces. In *M. pulmonis* infection, as in influenza infection, the cellular response of the host plays a prominent role in the pathogenesis of the lesions. Clearly, in *P. pneumotropica* infection the inflammatory response plays a less prominent role since the reaction we observed was similar in irradiated and unirradiated mice.

In the present work there was no difference between neutron- and gamma-irradiated mice when they were challenged 5 days after irradiation, but there was at 11 and 21 days when the neutron-irradiated animals had significantly more viable bacteria per lung and a significantly reduced capacity to clear the organism (Table 2). Thus there is at least a delay in recovery of the pulmonary antibacterial mechanism in neutron-irradiated animals, although the initial injury based on hematopoietic CFU survival should be similar. The hypothesis that equal stem-cell killing produces an equal effect on the pulmonary antibacterial mechanism, therefore, is rejected.

The mechanism of radiation injury to the antibacterial system appears to involve impairment of the ability of pulmonary macrophages to kill invading *P. pneumotropica* cells rather than impairment of the ability to engulf them. This conclusion is based on the similarity of the immunofluorescent-stained lung sections between irradiated and unirradiated mice in spite of vast differences in the number of viable bacteria per lung. Similar observations on impaired bactericidal properties of macrophages have been made by other investigators. Donaldson et al.[25] found suppression of intracellular digestion of chicken erythrocytes and *Candida guilliermondi* 6 to 14 days after 350 R whole-body X-irradiation; when the dose was increased to 450 R, digestion did not return to normal until 26 days postirradiation. Nelson and Becker[26] found a reduced ability of mice to kill injected *P. aeruginosa* cells 5 days after 100 to 500 R X-irradiation, and Smith, Fleming, and Wood[27] found a similar reduced ability to kill intramuscularly injected pneumococci 72 hr after 650 R X-irradiation. The increased susceptibility to infection could be correlated with leucopenia. We selected our early challenge times to correspond with the nadir in peripheral neutrophil counts (5 to 11 days) and with the time when both gamma- and neutron-irradiated animals have recovered to control levels (21 days).[28] Although the peripheral count may correlate with the results 5 and 11 days after irradiation, no correlation exists with the results of challenge 21 days after irradiation.

The challenge data 5 to 21 days after single-dose irradiation suggest an RBE of more than 2.6 when the challenge organism is *P. pneumotropica*, in contrast to an RBE of approximately 2.6 when the challenge organism is *M. pulmonis*.[2] The increased RBE at 11 and 21 days may be due in part to delayed repair in neutron-irradiated mice. Increased alveolar macrophage killing in neutron-irradiated animals that would require times longer than 21 days to repair might be involved. This hypothesis gains some support from the observation that repair was complete 26 weeks after single doses

of 240 neutron rads or 807 gamma rads. On the other hand, 79 weeks after these single doses, the percentage of mice unable to clear *P. pneumotropica* was twice that of unirradiated controls. These data thus demonstrate an early effect of neutron and gamma radiation on susceptibility to respiratory challenge with *P. pneumotropica* with an RBE considerably greater than 2.6 and a late effect with an RBE of the order of 3.

The greater susceptibility of gamma irradiated mice to bacterial challenge either 2 weeks or 56 weeks after fractionated exposure is surprising and somewhat difficult to interpret. Our data are consistent with the increased susceptibility to immediate challenge with *L. monocytogenes* and *P. tularensis* observed by Silverman et al.[13] and Stewart, Pribnow, and Silverman[11] following continuous exposure to ^{60}Co gamma radiation. However, the absence of the sparing effect of gamma-dose fractionation, which we have observed in other end points of the JANUS experiment,[3-5] is difficult to understand. We found no sparing effect of gamma-dose fractionation with *M. pulmonis* challenge when the doses were administered over 3 weeks but did find a decrease in susceptibility when the dose was fractionated over 24 weeks.[2] Of equal interest is the observation that mice receiving fractionated doses of neutron radiation were less severely impaired in their ability to clear *P. pneumotropica* than those receiving gamma-dose fractionation when challenged 2 weeks after the last fraction. In fact, there is a two-log increase in the number of viable *P. pneumotropica* cells per lung in the gamma-irradiated group as compared with the neutron-irradiated group. With other end points, including life shortening,[3,4] tumor rates or incidence,[3,5] late changes in the vasculature,[29] and alterations in immune function,[30,31] we have consistently observed an enhancement of damage when the neutron dose is fractionated. A possible explanation for the opposite effect observed here is that fractionated gamma radiation results in accumulated functional sublethal damage, which is perpetuated through successive cell divisions, whereas neutron radiation leaves some residual population that is functionally more intact. In any event, on the basis of susceptibility to *P. pneumotropica* infection at approximately 300 days of age, the RBE for pulmonary antibacterial activity of fission neutrons is less than 3.6 under conditions of protracted irradiation.

ACKNOWLEDGMENTS

We are grateful to Donn L. Jordan for construction and operation of the aerosol apparatus and to Richard C. Simkins for

technical assistance. Work was supported by the Energy Research and Development Administration.

REFERENCES

1. D. Grahn, E. J. Ainsworth, F. S. Williamson, and R. J. M. Fry, A Program to Study Fission-Neutron Induced Chronic Injury in Cells, Tissue and Animal Populations Utilizing the JANUS Reactor of Argonne National Laboratory, in *Radiobiological Application of Neutron Irradiation*, Panel Proceedings, Vienna, 1971, pp. 211-218, STI/PUB/325, International Atomic Energy Agency, Vienna, 1972.
2. E. J. Ainsworth, R. J. M. Fry, D. Grahn, F. S. Williamson, and J. H. Rust, JANUS Late-Effects Studies: Objectives, Plans, Endpoints, Management and Preliminary Results, in *Proceedings of the Second International Symposium on Late Effects of Radiation* (ESLAR TWO), in press.
3. E. J. Ainsworth, R. J. M. Fry, D. Grahn, F. S. Williamson, P. C. Brennan, S. P. Stearner, A. V. Carrano, and J. H. Rust, Late Effects of Neutron or Gamma Irradiation in Mice, in *Biological Effects of Neutron Irradiation*, Symposium Proceedings, Neuherberg, Munich, 1973, pp. 359-379, STI/PUB/352, International Atomic Energy Agency, Vienna, 1974.
4. E. J. Ainsworth, R. J. M. Fry, P. C. Brennan, S. P. Stearner, J. H. Rust, and F. S. Williamson, Life Shortening, Neoplasia and Systemic Injuries in Mice After Single or Fractionated Doses of Neutron or Gamma Radiation, in *Biological and Environmental Effects of Low-Level Radiation*, Symposium Proceedings, Chicago, Ill., 1975, pp. 77-92, STI/PUB/409, International Atomic Energy Agency, Vienna, 1976.
5. R. J. M. Fry, A. G. Garcia, K. H. Allen, A. Sallese, E. Staffeldt, T. N Tamisian, R. L. Devine, L. S. Lombard, and E. J. Ainsworth, Effect of Pituitary Isografts on Radiation Carcinogenesis in Mammary and Harderian Glands of Mice, in *Biological and Environmental Effects of Low-Level Radiation*, Symposium Proceedings, Chicago, Ill., 1975, pp. 213-226, STI/PUB/409, International Atomic Energy Agency, Vienna, 1976.
6. D. M. Donaldson, Responses of Diseased Animals to Ionizing Radiation, in *Ionizing Radiations and Immune Processes*, pp. 245-268, Gordon and Breach, Science Publishers, Inc., New York, 1962.
7. R. D. Stoner, M. W. Hess, and V. P. Bond, *Radiation and Infection. An Annotated Bibliography*, USAEC Report TID-23990, NTIS, 1965.
8. C. D. Hammond, S. K. Anderle, and C. P. Miller, Effect of Continuous Gamma Irradiation of Mice on Their Leucocyte Counts and Susceptibility to Bacterial Infection, *Radiat. Res.*, 11: 242-252 (1959).
9. C. W. Hammond, S. K. Anderle, and C. P. Miller, Effect of Daily Exposure to 15 R Gamma Radiation on Susceptibility of Mice to Experimental Infection, *Proc. Soc. Exp. Biol. Med.*, 104: 261-263 (1960).
10. C. W. Hammond, S. K. Anderle, and C. P. Miller, Attempts to Increase Resistance of Mice to Bacterial Infection by Prolonged Low Dose R-Irradiation, *Proc. Soc. Exp. Biol. Med.*, 105: 1-3 (1960).
11. R. H. Stewart, J. F. Pribnow, and M. S. Silverman, Effect of Chronic Gamma Radiation on Airborne Infection of Mice with *Listeria monocytogenes*, *Radiat. Res.*, 24: 96-107 (1965).
12. F. A. Hodge, W. R. Leif, and M. S. Silverman, Susceptibility to Infection with *Pasteurella tularensis* and the Immune Response of Mice Exposed to

Continuous Low Dose Rate R Radiation, *J. Infect. Dis.*, 120: 356-365 (1969).
13. M. S. Silverman, V. Greenman, A. E. McKee, K. Hadley, F. A. Hodge, and C. Burris, Cellular Response of Mice to Infection with *Pasteurella tularensis* (Live Vaccine Strain) Following Continuous Exposure to Low Dose R Radiation, *J. Infect. Dis.*, 120: 366-371 (1969).
14. D. L. Lundgren, A. Sacher, R. L. Thomas, T. L. Chiffelle, and R. O. McClellan, Effects of Inhaled $^{144}CeO_2$ on Influenza Virus Infection in Mice, *Proc. Soc. Exp. Biol. Med.*, 144: 238-244 (1973).
15. E. Goldstein and G. M. Green, Alteration of the Pathogenicity of *Pasteurella pneumotropica* for the Murine Lung Caused by Changes in Pulmonary Antibacterial Activity, *J. Bacteriol.*, 93: 1651-1661 (1967).
16. P. C. Brennan, T. E. Fritz, and R. J. Flynn, *Pasteurella pneumotropica:* Cultural and Biochemical Characteristics and Its Association with Disease in Laboratory Animals, *Lab. Animal Care*, 15: 307-312 (1965).
17. P. C. Brennan, T. E. Fritz, and R. J. Flynn, Role of *Pasteurella pneumotropica* and *Mycoplasma pulmonis* in Murine Pneumonia, *J. Bacteriol.*, 97: 337-349 (1969).
18. F. S. Williamson, Field Mapping and Depth Dosimetry in the JANUS High Flux Irradiation Room—a Fast Neutron Facility for Biological Research, in *First European Symposium on Neutron Dosimetry in Biology and Medicine*, Symposium Proceedings, Neuherberg, Munich, 1972, pp. 743-755, Report EUR-4896, 1973.
19. F. S. Williamson, *The Digital Computer As an Aid to JANUS Program Operations, Division of Biological and Medical Research Annual Report, 1971*, USAEC Report ANL-7870, Argonne National Laboratory, NTIS, 1971.
20. D. J. Henderson, An Apparatus for the Study of Airborne Infection, *J. Hyg.*, 50: 53-81 (1952).
21. G. J. Jakob and G. M. Green, The Effect of Sendai Virus Infection on Bactericidal and Transport Mechanisms of the Murine Lung, *J. Clin. Invest.*, 51: 1989-1998 (1972).
22. G. Sainte-Marie, A Paraffin-Embedding Technique for Studies Employing Immunofluorescence, *J. Histochem. Cytochem.*, 10: 250-256 (1962).
23. B. S. Berlin, Sparing Effect of X-Rays for Mice Inoculated Intranasally with Egg-Adapted Influenza Virus, CAM Strain, *Proc. Soc. Exp. Biol. Med.*, 117: 864-869 (1964).
24. B. S. Berlin and K. W. Cochran, Delay of Fatal Pneumonia in X-Irradiated Mice Inoculated with Mouse-Adapted Influenza Virus, PR8 Strain, *Radiat. Res.*, 31: 343-351 (1967).
25. D. M. Donaldson, S. Marcus, K. K. Gyi, and E. H. Perkins, The Influence of Immunization and Total Body X-Irradiation on Intracellular Digestion by Peritoneal Phagocytes, *J. Immunol.*, 76: 192-199 (1956).
26. E. L. Nelson and J. R. Becker, The Effect of Whole-Body X-Irradiation on the Bactericidal Activity of Phagocyte Cells. I. Survival of *Pseudomonas aeruginosa* Within Phagocytes from Peritoneal Exudates of Mice, *J. Infect. Dis.*, 104: 13-19 (1959).
27. M. R. Smith, D. P. Fleming, and W. B. Wood, Jr., The Effect of Acute Radiation Injury on Phagocytic Mechanisms of Antibacterial Defense, *J. Immunol.*, 90: 914-924 (1963).
28. E. J. Ainsworth, R. J. M. Fry, D. Grahn, F. S. Williamson, J. H. Rust, P. C. Brennan, A. V. Carrano, D. L. Jordan, M. Miller, K. H. Allen, M. P. Nielsen, E. Cooke, E. Staffeldt, and A. Sallese, *Division of Biological and Medical*

Research Annual Report, 1972, USAEC Report ANL-7970, Argonne National Laboratory, NTIS, 1972.

29. S. P. Stearner, R. L. Devine, and E. J. B. Christian, Late Changes in the Irradiated Microvasculature: An Electron Microscope Study of the Effects of Fission Neutrons, *Radiat. Res.*, 65: 351-370 (1976).
30. P. C. Brennan, D. A. Crouse, and W. T. Kickels, Radiation Effects on Host Immunological Function. I. Response to Mitogens and T-Cell Content, *Radiat. Res.*, 67: 544 (1976).
31. D. A. Crouse, P. C. Brennan, and W. T. Kickels, Radiation Effects on Host Immunological Function. II. Alloantigen Reactivity, *Radiat. Res.*, 67: 545-546 (1976).

Morphological and Stereological Changes in the Parenchyma of the Lungs of Rabbits Following Pneumonectomy and Exposure to Ozone

EDWIN S. BOATMAN
Department of Environmental Health, University of Washington, Seattle, Washington

ABSTRACT

Unilateral pneumonectomy in the adult rabbit causes a stimulus to the growth of the remaining lung such that lung volume is greatly increased. The effects of an environmental stress on this compromised organ were determined by exposing animals to 0.4 ppm of ozone 7 hr per day, 5 days per week, for 6 weeks. Structural changes to the parenchyma of the lung as a result of surgery or ozone or both treatments were investigated by morphometry, light microscopy, and electron microscopy.

The removal of the left lung of a rabbit causes an increase in the volume of the remaining right lung equal to that of total paired-lung volume in about 4 to 8 weeks. There is little, if any, increase in the number of alveoli, but alveolar width and depth increase 40% and the volume density of alveolar ducts increases 20% (average width increased from 166 to 205 μm). The volume density of alveolar wall tissue decreases on the average by 30%; this reduction in septum thickness appears evenly distributed between alveolar type I cells and capillary endothelial cells; alveolar interstitium is unchanged.

Pneumonectomized rabbits exposed to ozone tolerate exposure in a manner similar to ozone-exposed animals without surgery. A comparison of morphometric findings made between these groups shows no substantial differences. By microscopy focal areas of intra-alveolar cellular infiltrates and a moderate degree of interstitial edema with some swelling of the cytoplasm of type I epithelium and endothelium are seen.

It was concluded that pneumonectomy in the rabbit causes structural changes in the remaining lung which ensure a lung comparable in function to normal paired lungs and to paired lungs exposed to ozone. This functional flexibility is due in part to the ability of the remaining lung to use available space by dilatation of existing alveoli and alveolar ducts. It is uncertain at present whether limited replication of alveoli also occurs.

The lungs as the organ of respiration are placed in the hazardous situation of being the prime target for airborne pollutants of a considerable variety and complexity. Of particular importance are the gaseous pollutants like ozone, sulfur dioxide, and nitrogen dioxide.

Ozone, a highly reactive gas, is the principal oxidant formed by photochemical reactions and accounts for more than 90% of the total measured oxidant in Los Angeles; it readily attacks biological tissues, producing changes of varying severity.[1-4] The effect of ozone on the lungs is of some concern, and, should the lungs become compromised by existing disease, the effects of exposure might be even more severe.

The purpose of this study is to evaluate the growth and development of the remaining lung following pneumonectomy and the changes in this development following exposure to ozone. This procedure of unilateral pneumonectomy causes a stimulus to the growth of the remaining lung such that lung volume is greatly increased. The concentration of ozone used was comparable to that found at near peak periods in the urban environment. Changes to the parenchyma of the lung as a result of surgery or ozone or both treatments were characterized by morphometric and morphological techniques using light microscopy and electron microscopy.

MATERIALS AND METHODS

Animals

Male New Zealand white rabbits of between 2.5 and 3 kg in initial body weight were used for the unilateral pneumonectomy procedure, morphometry, and ozone exposure. A further group of rabbits ranging in body weight from 1.1 to 9 kg was used for morphometry only. Animals were kept in a room under a controlled environment and fed a standard pellet diet and water ad libitum.

Unilateral Pneumonectomy

With the animals under sodium pentobarbital anesthesia, the left lungs were removed in toto. Animals were intubated and ventilated by bag inflation with 100% oxygen. The surgical incisions were usually through the fourth interspace. Following isolation of the bronchi and pulmonary vessels, the tissues were ligated and the lungs were removed. The incisions were closed in layers, and about 30 to 40 ml of air was withdrawn by syringe from the left thoracic spaces. The survival rate following pneumonectomy was about 80%,

and animals were usually eating normally within 2 or 3 days. Animals were sacrificed at periods ranging from 2 to 18 weeks following surgery.

Lung Fixation and Processing

Left lungs removed at surgery and the corresponding right lungs removed at various time periods subsequently were fixed and processed in an identical manner. Fixation was accomplished by instillation through the airway of 0.11*M* s-collidine buffered 1.5% glutaraldehyde (pH 7.4; osmolality, 310 mOsm/kg H_2O) maintained at a pressure of 20 cm H_2O with the lungs, or hemilung, immersed in a beaker containing buffered fixative. After 18 to 20 hr fixation at 21°C, the trachea was clamped, and the volume of the lung was estimated by displacement. All lobes were completely sliced transversely. Alternate slices (4 mm thick) were postfixed in s-collidine buffered 1% osmium tetroxide, stained en bloc with uranyl acetate, and dehydrated in ascending concentrations of ethanol starting at 70%. Lung slices were embedded face down in Epon 812 resin and polymerized in flat molds for 48 hr at 60°C. In addition, six random blocks of tissue 2 mm^3 were embedded, and ultrathin sections were cut from each block with a Serval Ultramicrotome II and a diamond knife. Sections for light microscopy were cut at 1 to 2 μm by the method of Boatman and Lowe[5] and stained with azure II—methylene blue.

Tissue slices not postfixed in osmium were stored in buffered glutaraldehyde and used for morphometry for the estimation of the volume density of nonparenchyma.

Morphometry

Light-Microscopic Evaluation

Glutaraldehyde-fixed 4 mm-thick sections superimposed by a plastic grid[6] consisting of rows of points 2 mm apart were observed at 10 x magnification, and point "hits" falling on airways and blood vessels were counted with the use of both sides of the tissue slice.

Resin 1-μm stained sections were evaluated at 200 x and 400 x with a Wild M501 automatic-sampling stage microscope.[7] All sections were systematically covered in steps of 1120 or 1500 μm and the images projected onto a square test-point lattice. Only one point in the center of the test screen was used following the procedure of Burri, Dbaly, and Weibel.[8] From a total of 500 to 700 point hits per section, the relative volume densities of the following components were determined: nonparenchyma (V_{vnp}), alveolar air space (V_{va}),

alveolar septal tissue (V_{vt}), and alveolar duct (V_{vad}). The surface density of air space (S_{va}) and the mean linear intercept (L_m) were estimated by intersection counts.

The number of alveoli in 10 random fields of a standard area was determined on each slide by the method of Dunnill.[6] Absolute values for the number of alveoli per lung (N_a) and the surface area of the air space of the lung (S_a) were obtained by multiplying by the volume of lung parenchyma [total lung volume (V_L) x percent lung parenchyma (V_{vp})].

Electron-Microscopic Evaluation

Ultrathin sections from random blocks of tissue were mounted on 200-mesh carbon-coated grids and photographed in a random manner with a Philips EM 201 in accordance with the procedure described by Weibel, Kistler, and Scherle.[9] An average of 36 to 40 pictures were taken per hemilung on 35-mm film at a magnification of 1120 x. Positives of the films were analyzed on a multipurpose test screen[10] consisting of 84 lines and 168 test points for point and intersection counting. The parameters estimated were the volume densities of epithelium, interstitium, and endothelium and the arithmetic and harmonic mean thicknesses of the air—blood barrier.

Ozone Exposures

Rabbits were placed in stainless-steel and glass exposure chambers (two animals per chamber) of 11.8 ft^3 in volume. Ozone (O_3) was generated with a silent discharge ultraviolet lamp (Ozone Research Corp. model 031 VI) and introduced mixed with filtered air. The concentration of O_3 emitted was monitored directly with a calibrated ozone meter (Mast Development Co.).

Control animals and animals at various periods postpneumonectomy were exposed to 0.4 ppm ± 10% of O_3 7 hr per day, 5 days per week, for up to 6 weeks. Animals were removed from the chambers at noon each day for 1 hr for food and water.

RESULTS

Morphometry

Light Microscopy

The mean volume density of nonparenchyma lung tissue obtained by the analysis of 4-mm-thick transverse slices of lung was 11.89% for left lungs and 10.50% for right.

Estimates of other morphometric parameters for left and right lungs removed from control animals of two distinct body weights are shown in Table 1, and a portion of a typical 1-μm resin section from which such estimates were derived is shown in Fig. 1a. Also included for convenience are volume-density estimates of parenchymal components of a left lung compared with those of a right lung (Fig. 1b) 8 weeks postpneumonectomy. Lung changes as a result of pneumonectomy caused a decrease in V_{va} and V_{vt} and an increase in V_{vad} and L_m.

TABLE 1

MORPHOMETRIC PARAMETERS OF LEFT AND RIGHT LUNGS OF CONTROL ANIMALS*

Rabbits	Lungs	Body wt., kg	V_L, ml	$N_{va} \times 10^6$/cm	$N_a \times 10^6$	L_m, μm	V_{vad}	S_a, m^2
7	Left	2.8	13.7	3.1	43.8	65.9	0.29	0.712
2	Left	4.3	22.5	2.2	47.3	72.9	0.28	1.062
1	Right	2.8	30.1	2.7	80.3	64.6	0.33	1.610
1	Right	4.3	43.2	1.8	79.1	76.4	0.32	1.99

*V_L, lung volume corrected for percent nonparenchyma; N_{va}, number of alveoli/cm^3; N_a, absolute number of alveoli; L_m, mean linear intercept; V_{vad}, volume density of alveolar ducts; and S_a, total air-space surface area.

Overall, it is apparent from Table 1 that an increase in body weight (growth) has a major influence on L_v, L_m, and S_a, all of which increase. The lung volumes of the combined left and right lungs for the two body weights shown (2.8 and 4.3 kg) were 44.0 and 66.0 ml, respectively. In addition, linear-regression calculations (Fig. 2) indicated that N_a and S_a correlated more closely with lung volume than with body weight.

Right Lungs (Control and Postpneumonectomy). The morphometric parameters for these lungs are shown in Table 2. In control right lungs, V_L and L_m increased with gain in body weight, and, except for rabbits 1 kg in weight, the total number of alveoli per right lung remained constant at about 79×10^{-6}. The data for right lungs evaluated at different time periods following left-lung pneumonectomy are shown in the lower part of Table 2, and Fig. 3 is a graphical representation of a portion of the same data. At 8 or more weeks postpneumonectomy, lung volume equaled that of the combined volumes of left and right lungs of animals of a similar body weight.

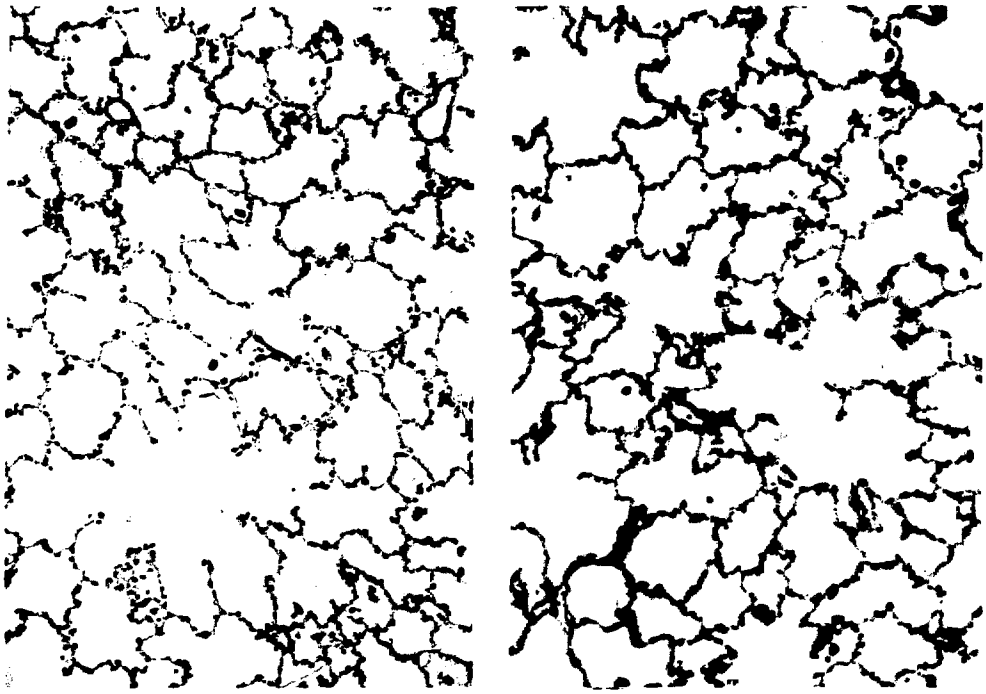

	Body wt., kg	V_{va}	V_{vt}	V_{vad}	L_m, μm
Control	3.4	47.4	21.2	30.2	68.8
Postpneumonectomy	3.6	39.5	15.4	40.8	95.6

Fig. 1 Light microscopy of a random field from a section of control lung (a) and from a section of lung 8 weeks postpneumonectomy (b). Stereological differences derived by morphometric analysis of random fields are shown in Table 1. V_{va}, volume-density percent of alveolar air space; V_{vt}, volume density of alveolar wall tissue; V_{vad}, volume density of alveolar ducts; and L_m, mean linear intercept.

Alveolar number per cubic centimeter of lung and S_{va} decreased with time, and L_m and V_{vad} increased, i.e., the average width increased from 166 to 205 μm. As L_m increased, the volume density of alveolar septal tissue decreased from 18 to 12%.

Ozone-Exposed Lungs. The morphometric parameters of lungs exposed to ozone only and lungs exposed following unilateral pneumonectomy are shown in Table 3.* Ozone-exposed right lungs

*The time periods in weeks postpneumonectomy indicate the total period from surgery to autopsy; in terms of ozone exposure, e.g., line 4, Table 3, exposure was started 2 weeks postpneumonectomy and continued for 2 weeks.

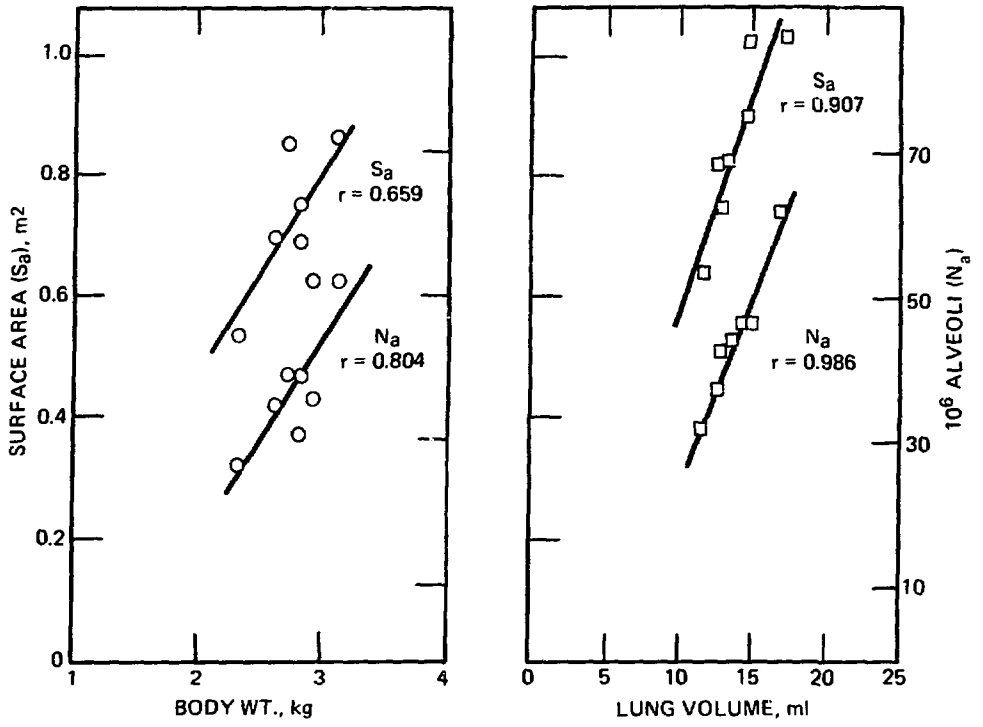

Fig. 2 Linear-regression lines correlating alveolar number and surface area of left lungs with body weight and lung volume.

did not appreciably differ morphometrically from control right lungs; however, following pneumonectomy and whether or not ozone was given, V_L, L_m, and V_{vad} increased. This increase occurred even when ozone was given as early as 2 weeks postpneumonectomy.

Electron Microscopy

Morphometric data derived from a left lung removed at surgery (day 0) and the corresponding right lung removed at autopsy 10 weeks later are shown in Table 4. Changes in the volume densities of different components of the parenchyma are seen as well as differences in air—blood barrier dimensions.

The volume densities of combined air space (alveoli and alveolar ducts) estimated by light microscopy were 0.73 (73%) and by electron microscopy (Table 4) 0.74 (74%). Air-space surface areas calculated by use of electron-microscopy morphometry were larger than those derived by use of light-microscopy morphometry (3.5 m^2 vs. 2.6 m^2). For normal left lungs, the areas were correspondingly 1.1 m^2 vs. 0.76 m^2.

TABLE 2

ESTIMATES OF ALVEOLAR NUMBER AND MEAN LINEAR INTERCEPT FOR RIGHT LUNGS (CONTROL AND POSTPNEUMONECTOMY)*

Body wt., kg	V_L, ml	$N_{va} \times 10^6$/cm	$N_a \times 10^6$	L_m, μm
		Control		
1.0	15.6	1.84	28.6	73.7
2.8	30.1	2.57	80.3	64.6
3.8	47.0	1.40	77.6	66.7
4.3	42.2	1.83	79.1	76.4
		Postpneumonectomy		
3.2	30.1	3.64 (2 weeks)	109.7	67.2
3.1	43.0	2.14 (8 weeks)	92.2	72.7
3.4	34.7	2.03 (9 weeks)	70.5	85.8
3.9	66.0	1.82 (10 weeks)	120.5	87.4
4.0	65.3	1.69 (11 weeks)	98.5	95.3
3.8	77.0	1.30 (12 weeks)	85.4	89.8
4.2	65.0	1.20 (18 weeks)	72.9	96.9

*V_L, lung volume corrected for percent nonparenchyma; N_{va}, number of alveoli/cm^3; N_a, absolute number of alveoli; and L_m, mean linear intercept.

Morphology

Light Microscopy

Of the four groups of lungs observed, i.e., control, ozone-exposed, right lung postpneumonectomy, and pneumonectomy plus ozone, the only lungs that showed morphological differences from the controls were lungs from animals exposed to ozone. In these lungs focal areas of intra-alveolar cellular infiltrates were occasionally seen.

Electron Microscopy

Right lungs from animals subjected to pneumonectomy showed, apart from a few focal areas of swollen cytoplasm of capillary endothelium, relatively normal fine structure. Type I surface epithelium and type II cells with characteristic lamellated bodies were similar to control lungs. Figure 4 is an electron micrograph of a portion of right lung 12 weeks postpneumonectomy. Lungs exposed

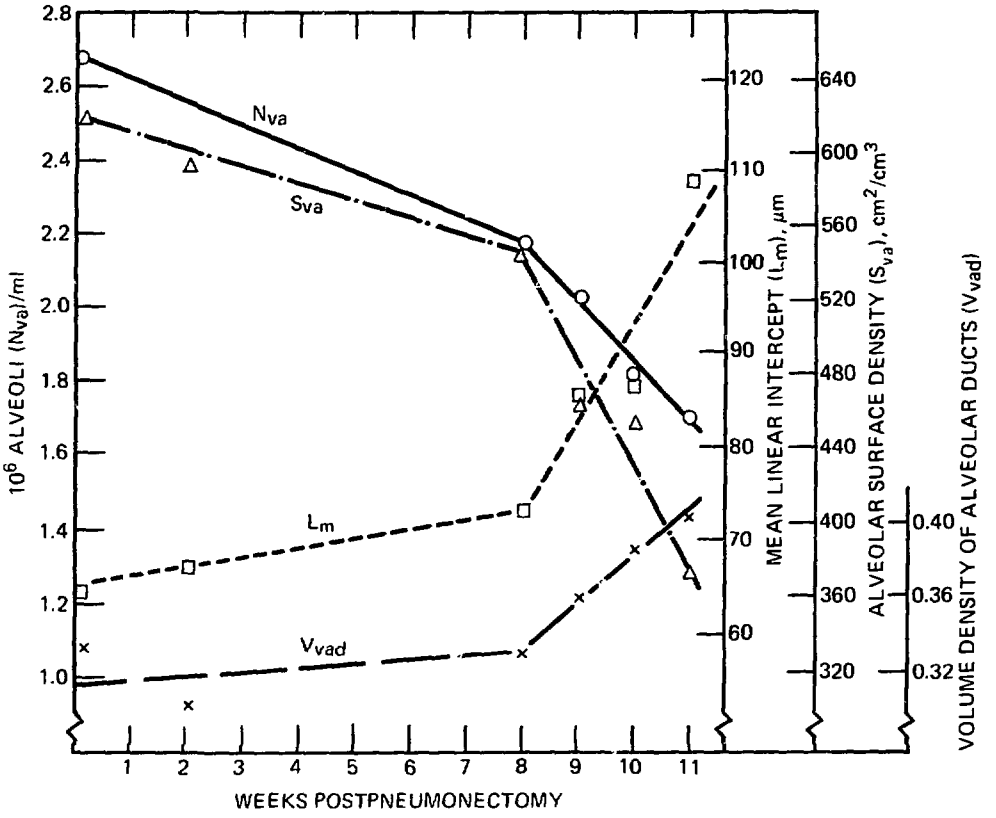

Fig. 3 Graphical representation of morphometric data from a series of right lungs analyzed at different time periods postpneumonectomy. The fall in alveolar number and alveolar surface density and rise in mean linear intercept and volume density of alveolar ducts have a "mirror-image" relationship.

intermittently to 0.4 ppm of ozone for 6 weeks showed interstitial edema of varying severity, focal areas of slightly swollen type I epithelial and capillary endothelial cytoplasm; an example of such changes is shown in Fig. 5. The lungs of animals subjected to unilateral pneumonectomy and exposed subsequently to ozone showed structural changes similar to the paired lungs of animals breathing ozone. Figures 6 and 7 are electron micrographs of lungs in the former category.

DISCUSSION

In a study such as this, the unraveling of the changes taking place following unilateral pneumonectomy with or without subsequent

TABLE 3

MORPHOMETRIC PARAMETERS OF THE RIGHT LUNGS OF RABBITS EXPOSED TO OZONE WITH OR WITHOUT PNEUMONECTOMY*

	Body wt., kg	V_L, ml	$N_{va} \times 10^6$/cm	$N_a \times 10^6$	L_m, μm	V_{vad}
Control	4.3	43.2	1.8	79.1	76.4	0.32
Ozone						
Without pneumonectomy						
0.4 ppm for 6 weeks	3.8	47.0	1.4	77.6	67.0	0.36
Postpneumonectomy						
11 weeks	4.0	65.3	1.6	98.5	95.3	0.40
4 weeks + ozone	4.0	62.0	1.4	91.7	90.3	0.41
18 weeks + ozone	4.2	65.0	1.2	72.9	97.1	0.39

*V_L, lung volume corrected for percent nonparenchyma; N_{va}, number of alveoli/cm^3; N_a, absolute number of alveoli; L_m, mean linear intercept; and V_{vad}, volume density of alveolar ducts.

TABLE 4

MORPHOMETRIC DATA OBTAINED BY ELECTRON MICROSCOPY OF LUNGS PRE- AND POSTPNEUMONECTOMY

Morphometric parameters	Day 0 left lung	10 weeks postpneumonectomy right lung
Volume density		
Air space	0.74	0.84
Capillaries	0.06	0.05
Alveolar wall	0.20	0.11
Epithelium	0.25	0.30
Interstitium	0.40	0.40
Endothelium	0.35	0.30
Surface density, alveoli	854 cm^2/cm^3	588 cm^2/cm^3
Arithmetic mean, alveolar wall	2.9 μm	2.15 μm
Harmonic mean, alveolar wall	0.85 μm	0.85 μm

Fig. 4 Electron micrograph of a portion of an alveolar septum from a right lung 12 weeks postpneumonectomy. The type II cell (T2) and other components of the septum appear normal.

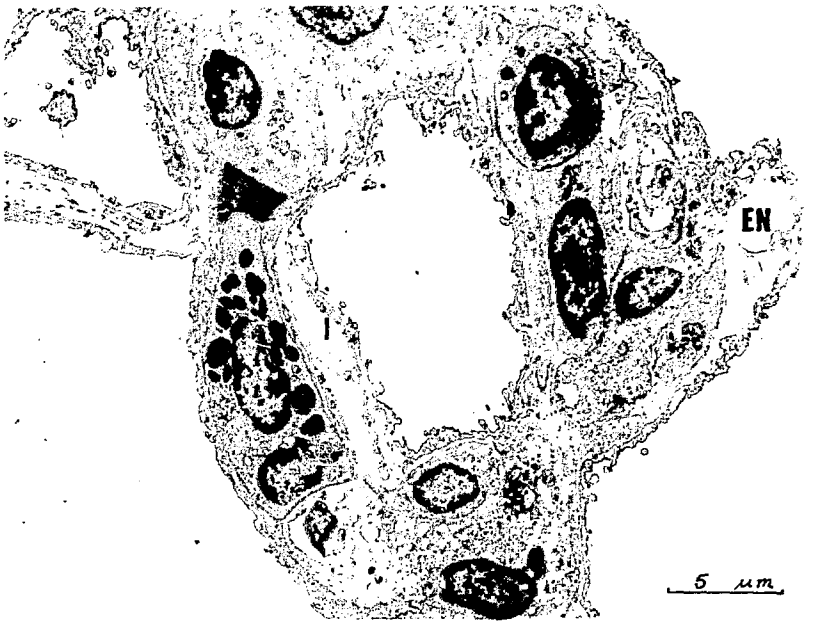

Fig. 5 Electron micrograph of a sectioned alveolus from a lung exposed to ozone (0.4 ppm O_3 for 6 weeks). Interstitial edema (I) is seen along with some damage to capillary endothelium (EN).

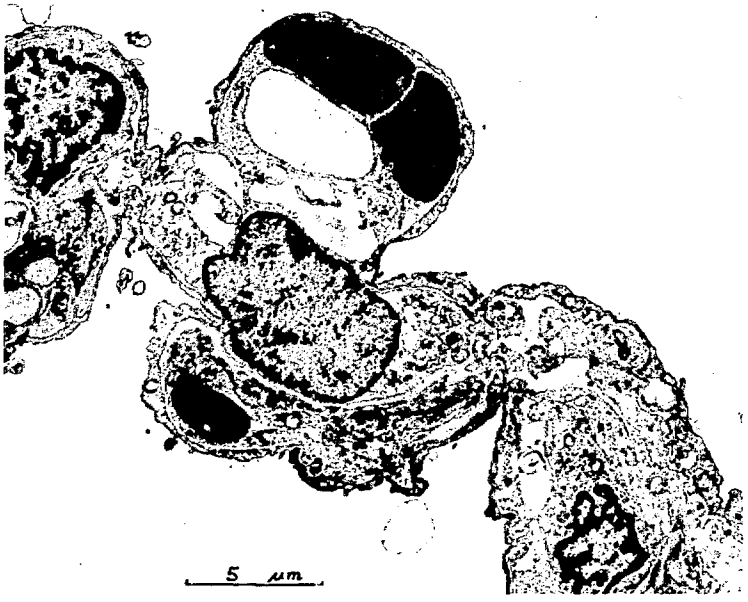

Fig. 6 Portion of an alveolar septum from a lung 2 weeks postpneumonectomy and exposed to ozone for 2 weeks. Changes seen are similar to those in Fig. 5.

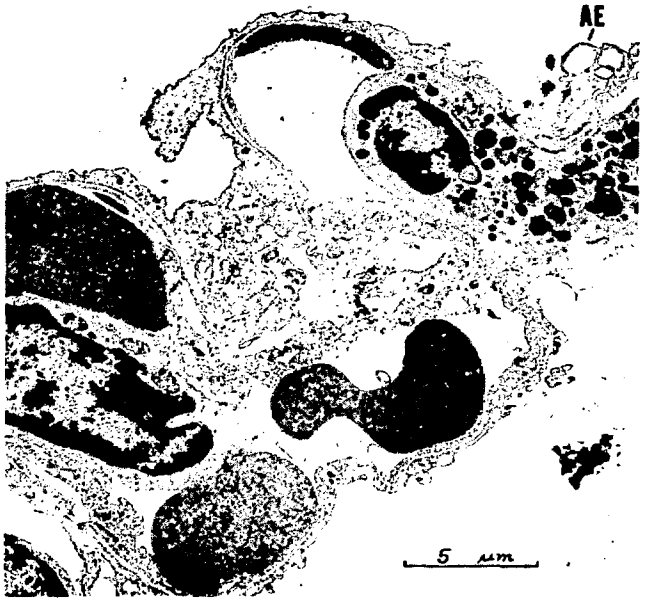

Fig. 7 Portion of an alveolar septum from a lung 9 weeks postpneumonectomy and exposed to ozone for 6 weeks. Changes are similar to those in Figs. 5 and 6 but with some vesiculation of alveolar surface epithelium (AE).

exposure to ozone is complicated by the underlying normal growth and development of the animal.

That considerable variations in alveolar number and other lung parameters occur in both man and animals has been recently discussed by Thurlbeck.[11] In humans, for example, the need for new tissue is met by an increase in both number and size of alveoli until growth of the chest wall is finished.[12] In the rat[13] alveoli may continue to multiply throughout life because continued body growth and growth of the lung are characteristics of this species, whereas in the rabbit[13] differentiation and the formation of new alveoli apparently both cease at 3 months of postnatal development. Šerý and associates[14] came to a similar conclusion. In the present work the data presented in Tables 1 and 2 lend support to this observation. Thus, although both body weight and lung volume increase, the total numbers of alveoli per hemilung remain fairly constant, which suggest that alveolar replication had ceased. The need for an accurate determination of this event, however, is of particular importance in the evaluation of growth stimuli following pneumonectomy and exposure to ozone.

Previous investigators,[14-17] using a variety of animal species, have found that, irrespective of whether the right lung or left lung is removed, the general stimulus to the remaining lung is one of a compensatory increase in lung volume. Generally, the remaining lung doubles in volume or is equal to the combined volume of left and right lungs within 4 to 8 weeks. Our results (Tables 2 and 3) are consistent with this. It should be recalled that, although either lung can be removed, the removal of the right lung abruptly reduces the total lung tissue by about two-thirds. In either event the metabolic needs are apparently met since Nattie, Wiley, and Bartlett[16] found in rats that hypoxia was absent 24 hr after surgery and Cournand et al.[18] noted in humans that alveolar ventilation—perfusion relationships after pneumonectomy indicated that the vascular bed of the remaining lung was able to accommodate a 2 x increase in pulmonary blood flow in a normal manner.

With a rapidly expanding lung, the virtue of the use of morphometry is that relatively small changes not readily detectable by direct examination can be determined. The pictorial and calculated data shown in Fig. 1 support this contention. The overall data (Tables 2 and 3) confirm the findings of Šerý, Kepot, and Obrucnik[14] and indicate that following pneumonectomy the increased volume of the remaining lung is satisfied almost entirely by a substantial increase in mean linear intercept and in the volume density of alveolar ducts. Given such factors as variations in age, body weight, and lung volume, as well as differences in fixation,

sampling, and processing of tissue, the values obtained from the two studies are remarkedly close. In our study, however, the tissues were further evaluated by electron microscopy. In this regard the increase in air-space surface area, as calculated by electron-microscopy morphometry, is due to the increased resolution and the ability to resolve the small undulations of the alveolar wall.

The increase in L_m implies a dilatation of existing air spaces, including alveolar ducts with a corresponding decrease in the volume density of alveolar tissue (Fig. 1). The form this compensatory growth may take is still a subject of considerable controversy.[11,14-17,19] At present it is a matter of alveolar proliferation, alveolar enlargement (or dilatation), or a combination of both. The problem can only be resolved by further careful morphometric analysis.

The magnitude of the effects on the lungs as a result of exposure to ozone is, in part, dependent on the concentration of ozone delivered and the period of exposure.[20]

The fact that normal lungs exposed to ozone did not differ morphometrically from control lungs (Table 3) refers at present to measurements made by light microscopy. Electron micrographs of the parenchyma of ozone-exposed lungs showed varying degrees of interstitial edema and cytoplasmic swelling of Type I surface epithelium and capillary endothelium, changes readily estimated by morphometry at the electron-microscope level. Kistler, Caldwell, and Weibel[21] used this form of analysis in a study of oxygen toxicity in rats, and Plopper, Dungworth, and Tyler[22] studied the lungs of rats after an acute exposure to 3 ppm of ozone for 4 hr. In both instances changes in arithmetic mean thickness of the air—blood barrier were documented which were not discernable by light microscopy.

In respect to lungs exposed to ozone following pneumonectomy, the two examples shown in Table 3 indicate that, whether or not the remaining lung is exposed to ozone 9 weeks or 2 weeks postpneumonectomy, the morphometric analyses of the two are very similar and indeed comparable to postpneumonectomy lungs not exposed to ozone. It is concluded from this that, although electron micrographs of these lungs show changes due to ozone alone, the recognizable increase in lung volume and the enlargement of alveoli and alveolar ducts are not prevented. This is particularly interesting because at 2 weeks postpneumonectomy the remaining lung has yet to reach its full distension. It is, of course, possible that both the concentration of ozone used and the duration of exposure were inadequate. P'an, Beland, and Gegier[23] exposed normal rabbits to 0.4 ppm of ozone for 30 hr per week for 10 months and noted a moderate degree of

emphysema present. Bartlett, Faulkner, and Cook[24] exposed rats to 0.2 ppm of ozone continuously for 30 days, and, although the lungs were histologically normal, lung volume increased by 16% with an increase in mean linear intercept and surface area. It was proposed that the overdistention was due to a decrease in elastic recoil.

In view of these studies, it would seem that exposure to ozone may enhance the progression to higher lung volumes and to larger alveoli by additional tissue changes. At present our data are insufficient to bear on this question. It is provisionally concluded that lung changes as a result of left-lung pneumonectomy and, as analyzed by morphometry at the light-microscope level, are neither enhanced nor inhibited by ozone under the exposure conditions described.

ACKNOWLEDGMENTS

I wish to thank Drs. C. J. Martin and D. Reid for assistance with the surgery and John Boykin and Maria Glaser for technical assistance.

A portion of this work was conducted with the most helpful advice from Professor Ewald Weibel at the Department of Anatomy, University of Bern, during my tenure as a Josiah Macy Scholar. This work was also supported by a grant from the National Institute of Environmental Health Sciences, ES 01049.

REFERENCES

1. L. S. Jaffe, The Biological Effects of Ozone on Man and Animals, *Am. Ind. Hyg. Assoc. J.*, 28: 267-277 (1967).
2. H. E. Stokinger, Ozone Toxicology; a Review of Research and Industrial Experience, 1954—1964, *Arch. Environ. Health*, 10: 719-731 (1965).
3. D. V. Bates, Air Pollutants and the Human Lung, *Am. Rev. Respir. Dis.*, 105: 1-13 (1972).
4. E. S. Boatman, S. Sato, and R. Frank, Acute Effects of Ozone on Cat's Lungs. II. Structural, *Am. Rev. Respir. Dis.*, 110: 157-169 (1974).
5. E. S. Boatman and D. Lowe, Photographic Mapping of a Tissue Surface to Locate Fields for Electron Microscopy, Mouse Lung, *Stain Technol.*, 46: 63-69 (1971).
6. M. S. Dunnill, Quantitative Methods in the Study of Pulmonary Pathology, *Thorax*, 17: 320-328 (1962).
7. E. R. Weibel, An Automatic Sampling Stage Microscope for Stereology, *J. Microsc. (Oxford)*, 91: 1-18 (1970).
8. P. H. Burri, J. Dbaly, and E. R. Weibel, The Postnatal Growth of the Rat Lung. 1. Morphometry, *Anat. Rec.*, 178: 711-730 (1974).
9. E. R. Weibel, G. S. Kistler, and W. F. Scherle, Practical Stereological Methods for Morphometric Cytology, *J. Cell Biol.*, 30: 23-38 (1966).

10. E. R. Weibel, Morphometric Estimation of Pulmonary Diffusion Capacity: 1. Model and Method, *Resp. Physiol.*, 11: 54-75 (1970).
11. W. M. Thurlbeck, Postnatal Growth and Development of the Lung, *Am. Rev. Respir. Dis.*, 111: 803-844 (1975).
12. L. Reid, The Embryology of the Lung, in Development of the Lung, C.I.B.A. Foundation, pp. 109, Little, Brown & Co., Boston, 1967.
13. R. H. D. Short, Aspects of Comparative Lung Growth, *Proc. R. Soc. (London), Sect. B*, 140: 432-441 (1952).
14. Z. Sery, E. Kepot, and M. Obrucnik, Morphometric Analysis of Late Adaptation of the Residual Lung Following Pneumonectomy in Young and Adult Rabbits, *J. Thorac. Cardiovasc. Surg.*, 57: 549-557 (1969).
15. J. M. Cowan and R. G. Crystal, Lung Growth After Unilateral Pneumonectomy: Quantitation of Collagen Synthesis and Content, *Am. Rev. Respir. Dis.*, 111: 267-277 (1975).
16. E. E. Nattie, C. W. Wiley, and D. Bartlett, Jr., Adaptive Growth of the Lung Following Pneumonectomy in Rats, *J. Appl. Physiol.*, 37: 491-495 (1974).
17. M. Gnavi, E. Pansa, and G. Anselmetti, Growth and Regeneration of the Lung, *Minerva Chir.*, 25: 1491-1504 (1970).
18. A. Cournand, R. L. Riley, A. Himmelstein, and R. Austrian, Pulmonary Circulation and Alveolar Ventilation—Perfusion Relationships After Pneumonectomy, *J. Thorac. Surg.*, 19: 80-116 (1950).
19. J. J. Longacre and R. Gohansmann, An Experimental Study of the Fate of the Remaining Lung Following Total Pneumonectomy, *J. Thorac. Surg.*, 10: 131-149 (1940).
20. D. L. Dungworth, C. E. Cross, J. R. Gillespie, and C. G. Plopper, The Effects of Ozone on Animals, in *Ozone Chemistry and Technology—A Review of the Literature: 1961—1974*, Joanne S. Murphy and Janet R. Orr (Eds.), Chap. 11, The Franklin Institute Press, Philadelphia, 1975.
21. G. S. Kistler, P. R. B. Caldwell, and E. R. Weibel, Development of Fine Structural Damage to Alveolar and Capillary Lining Cells in Oxygen-Poisoned Rat Lungs, *J. Cell. Biol.*, 32: 605-628 (1967).
22. G. C. Plopper, D. L. Dungworth, and W. S. Tyler, Morphometric Evaluation of Pulmonary Lesions in Rats Exposed to Ozone, *Am. J. Pathol.*, 71: 395-403 (1973).
23. A. Y. P'an, J. Beland, and Z. Gegier, Ozone-Induced Arterial Lesions, *Arch. Environ. Health*, 24: 229-232 (1972).
24. D. Bartlett, Jr., C. S. Faulkner, and K. Cook, Effect of Chronic Ozone Exposure on Lung Elasticity in Young Rats, *J. Appl. Physiol.*, 27: 92-97 (1974).

Alveolar Epithelial Repair and Changes in Free Airway Cell Populations Following Cadmium Injury

J. A. HAYES, S. ASVADI, R. H. STRAUSS, and K. C. PALMER
Mallory Institute of Pathology and Pathology Department,
Boston University School of Medicine, Boston, Massachusetts

ABSTRACT

The lungs of rats exposed to 0.1% (0.005*M*) $CdCl_2$ aerosol show prominent epithelial damage in peribronchiolar alveoli. Initially there is necrosis of type I cells within 48 hr of exposure. This is followed by marked mitotic activity in type II cells which progresses so that they completely line the affected alveoli by 3 to 4 days. Subsequently, these cells flatten out to reline the surface, and we have interpreted that the flat cells with microvilli and osmiophilic bodies are "intermediate" cells. The necrotic phase of injury coincides with a wave of polymorphonuclear leukocytes (PMLs), whereas type II cell proliferation with conversion to "intermediate" epithelium coincides with an outpouring of alveolar macrophages (AMs). This finding suggests that PMLs indicate active lung-cell necrosis, whereas AMs indicate either a repair phase or one of low-grade activity.

Acute exposure to cadmium fumes produced lesions typical of centrilobular emphysema in man in which the main damage appears to center about respiratory bronchioles.[1,2] Our studies were undertaken to obtain more information on the early stages of injury and repair consequent to an exposure to cadmium chloride ($CdCl_2$) aerosol. Attention was particularly directed to changes in alveolar epithelium and to parallel changes in cells presumed to be exuded into the airspaces as a result of the injury.

MATERIALS AND METHODS

Male Sprague-Dawley rats, 150 to 250 g in weight, were exposed to an aerosol of 0.1% (0.005*M*) $CdCl_2$ in physiologic saline produced

by a DeVilbiss 35A ultrasonic generator. This yields an aerosol concentration of 10 mg of $CdCl_2$ per cubic meter of air in the chamber. A single 2-hr exposure was administered. The generated aerosol was polydisperse, with a mass median particle diameter of 4.5 ± 1.64 μm, and gave a tissue cadmium content of 1 ± 0.5 μg/g wet lung weight.[3] For some animals of each group, colchicine (1.0 μg per gram of body weight) was injected 4 hr before killing. Rats were killed by barbiturate overdose in groups of six at 1 hr and 1, 2, 4, 7, and 10 days after cadmium exposure. Two groups of control animals were used: (1) 36 rats exposed to an aerosol of physiologic saline for the same period and (2) 35 rats not exposed to an aerosol. Both sets of control animals were killed at the same time intervals as the cadmium-exposed rats. Lungs were distended with glutaraldehyde at 25 cm pressure and fixed for 24 hr (Ref. 4). Tissue blocks were taken from the lung periphery and processed for electron microscopy, and appropriate photographs were taken.

In a second experiment rats, either unexposed or exposed to aerosol, were killed at the same time intervals. The lungs were washed out with physiologic saline at room temperature. Washed-out cells were enumerated in a hemocytometer.

RESULTS

The exposure produced multiple lesions of predominantly peribronchiolar distribution. Initially type I cells showed cytoplasmic swelling (Fig. 1a) and necrosis with loss of plasma membranes so that there was exposure of basement membrane (Fig. 1b). This injury apparently triggered proliferation of type II cells in which mitoses were easily identified (Fig. 2) because colchicine was injected 4 hr before killing. Subsequently the damaged alveoli became lined by type II cells between 3 and 4 days after exposure (Fig. 3) although intervening areas showed essentially normal alveolar lining cells. Thereafter the type II cells flattened out to reline the septa with type I cells, although numerous cells intermediate between type I and type II cells were seen. These intermediate cells were flat but showed numerous microvilli and osmiophilic bodies and persisted to at least 7 days after injury (Fig. 4). By 10 days the damaged lungs had regained their normal structure except for some peribronchiolar fibrosis.[5] The alveolar walls sometimes appeared thickened owing to the close apposition of increased numbers of macrophages to the alveolar epithelium (Fig. 5). Apart from the mild cytoplasmic and interstitial edema, at 1 and 2 days saline-aerosol-exposed controls showed the same morphology as unexposed rats.

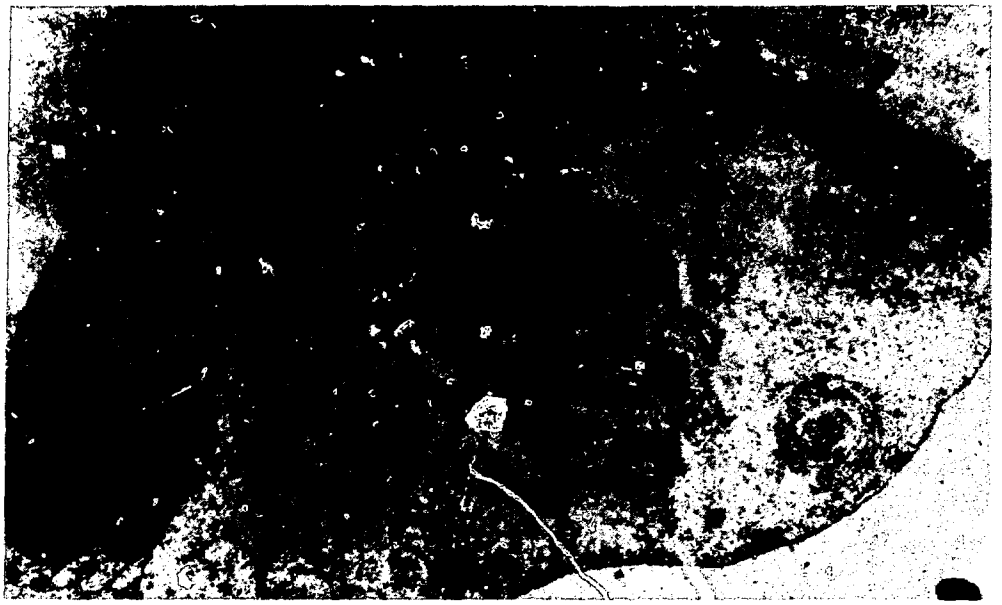

Fig. 1a Lung area 1 day after exposure to $CdCl_2$. Marked cytoplasmic edema of type I alveolar cell. Adjacent alveolus is lined by normal type I epithelium (arrows).

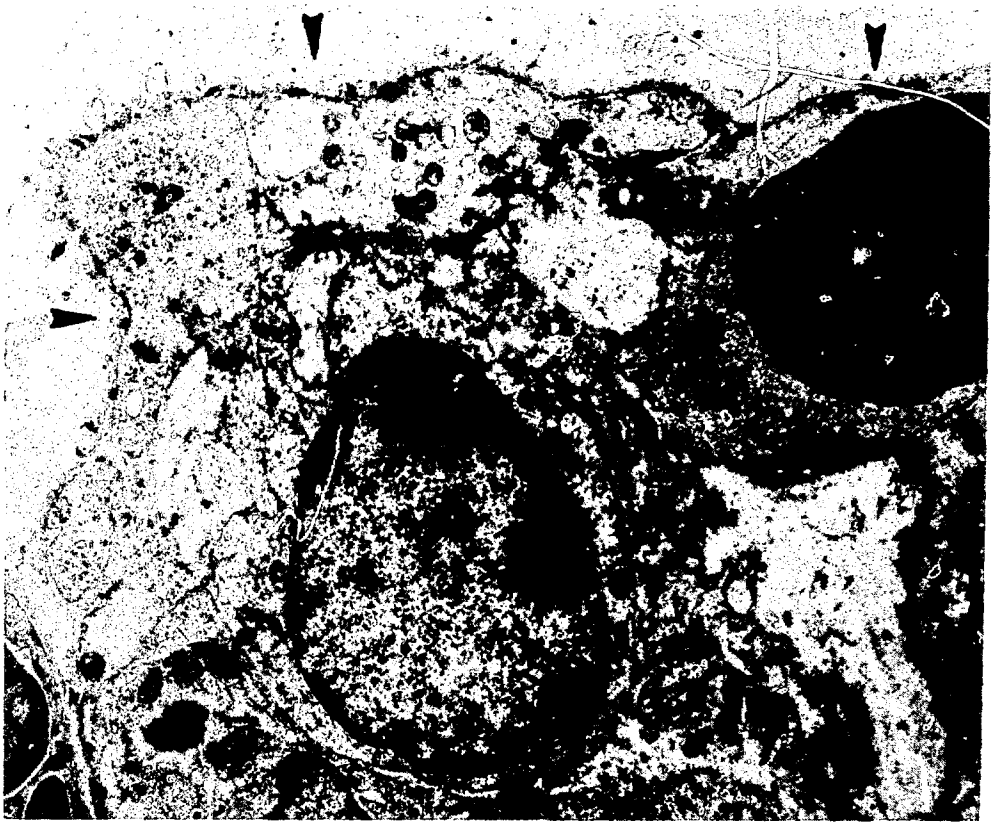

Fig. 1b Different area of same lung showing exposure of basement membrane deep to type I cell after loss of outer plasma membrane.

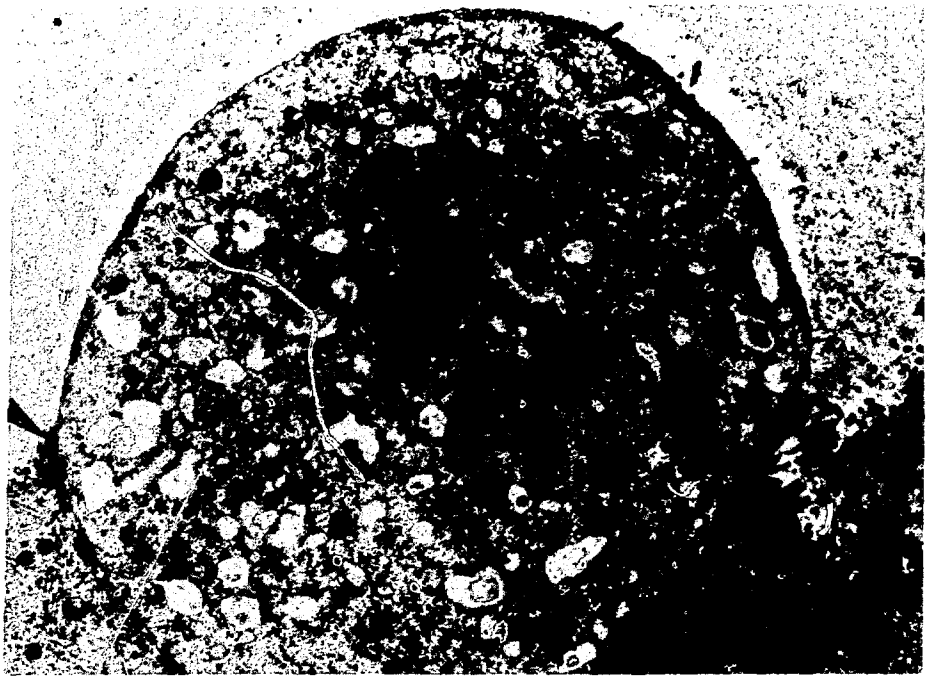

Fig. 2 Typical appearance of colchicine-arrested mitosis in type II cell. Although osmiophilic bodies are not visible, the cell is identified by its epithelial position with junctional complex (arrows) and "corner" location in the alveolus.

Fig. 3 Alveolus 3 days after $CdCl_2$ exposure. It is completely lined by type II cells.

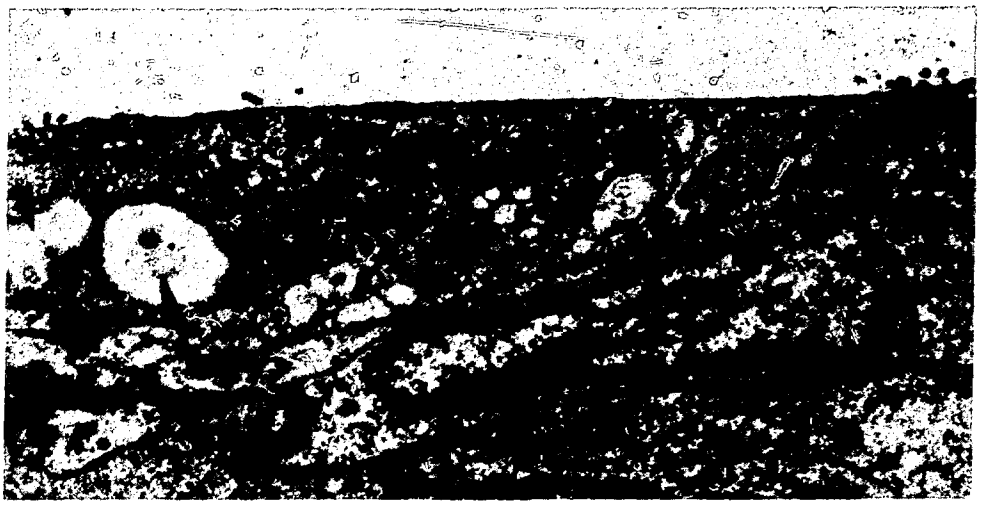

Fig. 4 Seven days after $CdCl_2$ exposure, intermediate type cells line the alveolus. Arrows indicate the presence of microvilli and osmiophilic bodies in clefts which have the attenuated characteristics of type I epithelium.

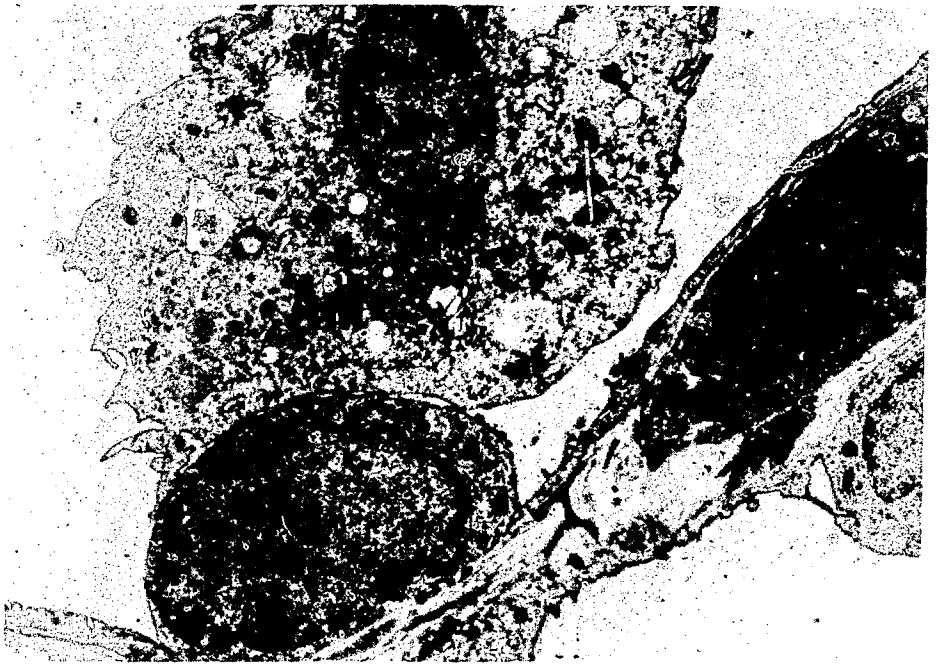

Fig. 5 Ten days after $CdCl_2$ exposure, alveolar walls have regained a normal structure. Close apposition of alveolar macrophages (AMs) may simulate mural hypercellularity.

The lungs as the organ of respiration are placed in the hazardous situation of being the prime target for airborne pollutants of a considerable variety and complexity. Of particular importance are the gaseous pollutants like ozone, sulfur dioxide, and nitrogen dioxide.

Ozone, a highly reactive gas, is the principal oxidant formed by photochemical reactions and accounts for more than 90% of the total measured oxidant in Los Angeles; it readily attacks biological tissues, producing changes of varying severity.[1-4] The effect of ozone on the lungs is of some concern, and, should the lungs become compromised by existing disease, the effects of exposure might be even more severe.

The purpose of this study is to evaluate the growth and development of the remaining lung following pneumonectomy and the changes in this development following exposure to ozone. This procedure of unilateral pneumonectomy causes a stimulus to the growth of the remaining lung such that lung volume is greatly increased. The concentration of ozone used was comparable to that found at near peak periods in the urban environment. Changes to the parenchyma of the lung as a result of surgery or ozone or both treatments were characterized by morphometric and morphological techniques using light microscopy and electron microscopy.

MATERIALS AND METHODS

Animals

Male New Zealand white rabbits of between 2.5 and 3 kg in initial body weight were used for the unilateral pneumonectomy procedure, morphometry, and ozone exposure. A further group of rabbits ranging in body weight from 1.1 to 9 kg was used for morphometry only. Animals were kept in a room under a controlled environment and fed a standard pellet diet and water ad libitum.

Unilateral Pneumonectomy

With the animals under sodium pentobarbital anesthesia, the left lungs were removed in toto. Animals were intubated and ventilated by bag inflation with 100% oxygen. The surgical incisions were usually through the fourth interspace. Following isolation of the bronchi and pulmonary vessels, the tissues were ligated and the lungs were removed. The incisions were closed in layers, and about 30 to 40 ml of air was withdrawn by syringe from the left thoracic spaces. The survival rate following pneumonectomy was about 80%,

and animals were usually eating normally within 2 or 3 days. Animals were sacrificed at periods ranging from 2 to 18 weeks following surgery.

Lung Fixation and Processing

Left lungs removed at surgery and the corresponding right lungs removed at various time periods subsequently were fixed and processed in an identical manner. Fixation was accomplished by instillation through the airway of 0.11*M* s-collidine buffered 1.5% glutaraldehyde (pH 7.4; osmolality, 310 mOsm/kg H_2O) maintained at a pressure of 20 cm H_2O with the lungs, or hemilung, immersed in a beaker containing buffered fixative. After 18 to 20 hr fixation at 21°C, the trachea was clamped, and the volume of the lung was estimated by displacement. All lobes were completely sliced transversely. Alternate slices (4 mm thick) were postfixed in s-collidine buffered 1% osmium tetroxide, stained en bloc with uranyl acetate, and dehydrated in ascending concentrations of ethanol starting at 70%. Lung slices were embedded face down in Epon 812 resin and polymerized in flat molds for 48 hr at 60°C. In addition, six random blocks of tissue 2 mm^3 were embedded, and ultrathin sections were cut from each block with a Serval Ultramicrotome II and a diamond knife. Sections for light microscopy were cut at 1 to 2 μm by the method of Boatman and Lowe[5] and stained with azure II—methylene blue.

Tissue slices not postfixed in osmium were stored in buffered glutaraldehyde and used for morphometry for the estimation of the volume density of nonparenchyma.

Morphometry

Light-Microscopic Evaluation

Glutaraldehyde-fixed 4 mm-thick sections superimposed by a plastic grid[6] consisting of rows of points 2 mm apart were observed at 10 x magnification, and point "hits" falling on airways and blood vessels were counted with the use of both sides of the tissue slice.

Resin 1-μm stained sections were evaluated at 200 x and 400 x with a Wild M501 automatic-sampling stage microscope.[7] All sections were systematically covered in steps of 1120 or 1500 μm and the images projected onto a square test-point lattice. Only one point in the center of the test screen was used following the procedure of Burri, Dbaly, and Weibel.[8] From a total of 500 to 700 point hits per section, the relative volume densities of the following components were determined: nonparenchyma (V_{vnp}), alveolar air space (V_{va}),

alveolar septal tissue (V_{vt}), and alveolar duct (V_{vad}). The surface density of air space (S_{va}) and the mean linear intercept (L_m) were estimated by intersection counts.

The number of alveoli in 10 random fields of a standard area was determined on each slide by the method of Dunnill.[6] Absolute values for the number of alveoli per lung (N_a) and the surface area of the air space of the lung (S_a) were obtained by multiplying by the volume of lung parenchyma [total lung volume (V_L) x percent lung parenchyma (V_{vp})].

Electron-Microscopic Evaluation

Ultrathin sections from random blocks of tissue were mounted on 200-mesh carbon-coated grids and photographed in a random manner with a Philips EM 201 in accordance with the procedure described by Weibel, Kistler, and Scherle.[9] An average of 36 to 40 pictures were taken per hemilung on 35-mm film at a magnification of 1120 x. Positives of the films were analyzed on a multipurpose test screen[10] consisting of 84 lines and 168 test points for point and intersection counting. The parameters estimated were the volume densities of epithelium, interstitium, and endothelium and the arithmetic and harmonic mean thicknesses of the air—blood barrier.

Ozone Exposures

Rabbits were placed in stainless-steel and glass exposure chambers (two animals per chamber) of 11.8 ft^3 in volume. Ozone (O_3) was generated with a silent discharge ultraviolet lamp (Ozone Research Corp. model 031 VI) and introduced mixed with filtered air. The concentration of O_3 emitted was monitored directly with a calibrated ozone meter (Mast Development Co.).

Control animals and animals at various periods postpneumonectomy were exposed to 0.4 ppm ± 10% of O_3 7 hr per day, 5 days per week, for up to 6 weeks. Animals were removed from the chambers at noon each day for 1 hr for food and water.

RESULTS

Morphometry

Light Microscopy

The mean volume density of nonparenchyma lung tissue obtained by the analysis of 4-mm-thick transverse slices of lung was 11.89% for left lungs and 10.50% for right.

Estimates of other morphometric parameters for left and right lungs removed from control animals of two distinct body weights are shown in Table 1, and a portion of a typical 1-μm resin section from which such estimates were derived is shown in Fig. 1a. Also included for convenience are volume-density estimates of parenchymal components of a left lung compared with those of a right lung (Fig. 1b) 8 weeks postpneumonectomy. Lung changes as a result of pneumonectomy caused a decrease in V_{va} and V_{vt} and an increase in V_{vad} and L_m.

TABLE 1

MORPHOMETRIC PARAMETERS OF LEFT AND RIGHT LUNGS OF CONTROL ANIMALS*

Rabbits	Lungs	Body wt., kg	V_L, ml	$N_{va} \times 10^6$/cm	$N_a \times 10^6$	L_m, μm	V_{vad}	S_a, m^2
7	Left	2.8	13.7	3.1	43.8	65.9	0.29	0.712
2	Left	4.3	22.5	2.2	47.3	72.9	0.28	1.062
1	Right	2.8	30.1	2.7	80.3	64.6	0.33	1.610
1	Right	4.3	43.2	1.8	79.1	76.4	0.32	1.99

*V_L, lung volume corrected for percent nonparenchyma; N_{va}, number of alveoli/cm^3; N_a, absolute number of alveoli; L_m, mean linear intercept; V_{vad}, volume density of alveolar ducts; and S_a, total air-space surface area.

Overall, it is apparent from Table 1 that an increase in body weight (growth) has a major influence on L_v, L_m, and S_a, all of which increase. The lung volumes of the combined left and right lungs for the two body weights shown (2.8 and 4.3 kg) were 44.0 and 66.0 ml, respectively. In addition, linear-regression calculations (Fig. 2) indicated that N_a and S_a correlated more closely with lung volume than with body weight.

Right Lungs (Control and Postpneumonectomy). The morphometric parameters for these lungs are shown in Table 2. In control right lungs, V_L and L_m increased with gain in body weight, and, except for rabbits 1 kg in weight, the total number of alveoli per right lung remained constant at about 79×10^{-6}. The data for right lungs evaluated at different time periods following left-lung pneumonectomy are shown in the lower part of Table 2, and Fig. 3 is a graphical representation of a portion of the same data. At 8 or more weeks postpneumonectomy, lung volume equaled that of the combined volumes of left and right lungs of animals of a similar body weight.

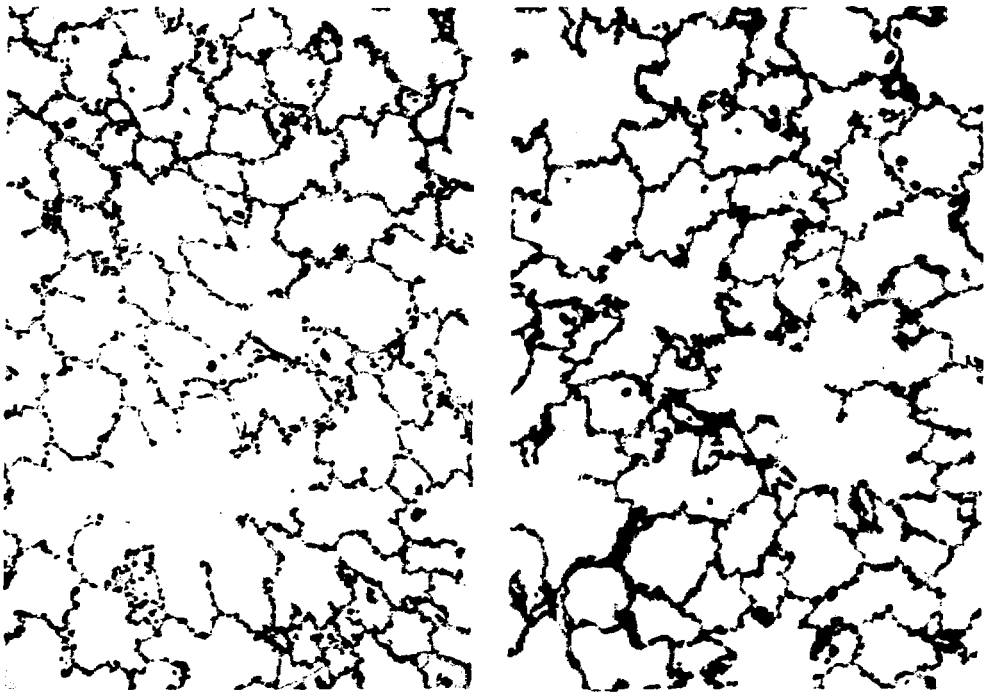

	Body wt., kg	V_{va}	V_{vt}	V_{vad}	L_m, μm
Control	3.4	47.4	21.2	30.2	68.8
Postpneumonectomy	3.6	39.5	15.4	40.8	95.6

Fig. 1 Light microscopy of a random field from a section of control lung (a) and from a section of lung 8 weeks postpneumonectomy (b). Stereological differences derived by morphometric analysis of random fields are shown in Table 1. V_{va}, volume-density percent of alveolar air space; V_{vt}, volume density of alveolar wall tissue; V_{vad}, volume density of alveolar ducts; and L_m, mean linear intercept.

Alveolar number per cubic centimeter of lung and S_{va} decreased with time, and L_m and V_{vad} increased, i.e., the average width increased from 166 to 205 μm. As L_m increased, the volume density of alveolar septal tissue decreased from 18 to 12%.

Ozone-Exposed Lungs. The morphometric parameters of lungs exposed to ozone only and lungs exposed following unilateral pneumonectomy are shown in Table 3.* Ozone-exposed right lungs

*The time periods in weeks postpneumonectomy indicate the total period from surgery to autopsy; in terms of ozone exposure, e.g., line 4, Table 3, exposure was started 2 weeks postpneumonectomy and continued for 2 weeks.

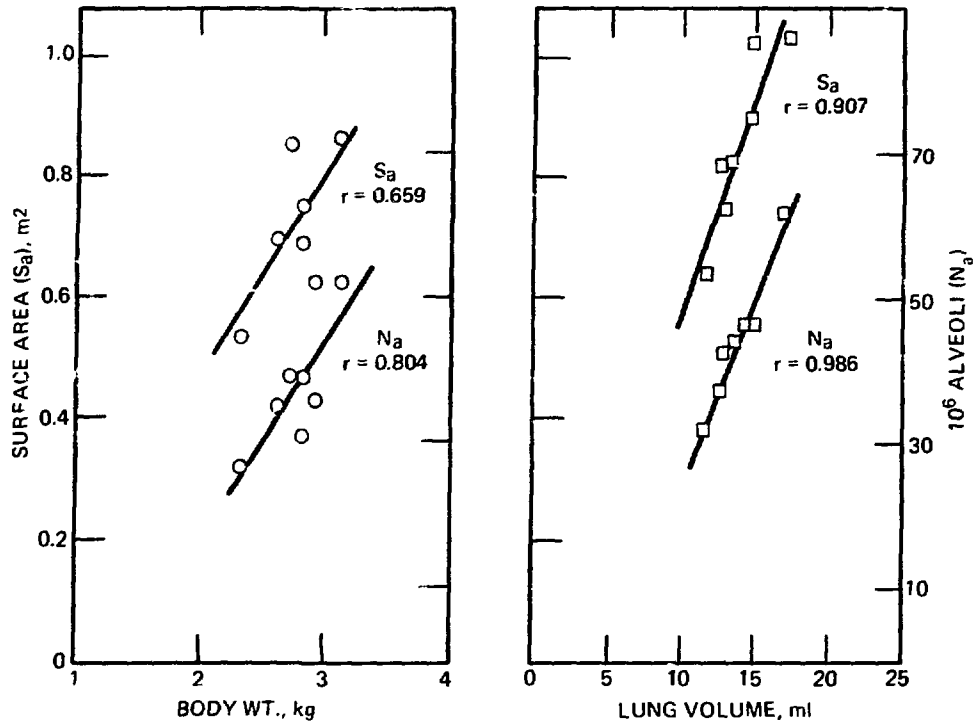

Fig. 2 Linear-regression lines correlating alveolar number and surface area of left lungs with body weight and lung volume.

did not appreciably differ morphometrically from control right lungs: however, following pneumonectomy and whether or not ozone was given, V_L, L_m, and V_{vad} increased. This increase occurred even when ozone was given as early as 2 weeks *postpneumonectomy*.

Electron Microscopy

Morphometric data derived from a left lung removed at surgery (day 0) and the corresponding right lung removed at autopsy 10 weeks later are shown in Table 4. Changes in the volume densities of different components of the parenchyma are seen as well as differences in air—blood barrier dimensions.

The volume densities of combined air space (alveoli and alveolar ducts) estimated by light microscopy were 0.73 (73%) and by electron microscopy (Table 4) 0.74 (74%). Air-space surface areas calculated by use of electron-microscopy morphometry were larger than those derived by use of light-microscopy morphometry (3.5 m^2 vs. 2.6 m^2). For normal left lungs, the areas were correspondingly 1.1 m^2 vs. 0.76 m^2.

TABLE 2

ESTIMATES OF ALVEOLAR NUMBER AND MEAN LINEAR INTERCEPT FOR RIGHT LUNGS (CONTROL AND POSTPNEUMONECTOMY)*

Body wt., kg	V_L, ml	$N_{va} \times 10^6$/cm	$N_a \times 10^6$	L_m, μm
		Control		
1.0	15.6	1.84	28.6	73.7
2.8	30.1	2.67	80.3	64.6
3.8	47.0	1.40	77.6	66.7
4.3	42.2	1.83	79.1	76.4
		Postpneumonectomy		
3.2	30.1	3.64 (2 weeks)	109.7	67.2
3.1	43.0	2.14 (8 weeks)	92.2	72.7
3.4	34.7	2.03 (9 weeks)	70.5	85.8
3.9	66.0	1.82 (10 weeks)	120.5	87.4
4.0	65.3	1.69 (11 weeks)	98.5	95.3
3.8	77.0	1.30 (12 weeks)	85.4	89.8
4.2	65.0	1.20 (18 weeks)	72.9	96.9

*V_L, lung volume corrected for percent nonparenchyma; N_{va}, number of alveoli/cm^3; N_a, absolute number of alveoli; and L_m, mean linear intercept.

Morphology

Light Microscopy

Of the four groups of lungs observed, i.e., control, ozone-exposed, right lung postpneumonectomy, and pneumonectomy plus ozone, the only lungs that showed morphological differences from the controls were lungs from animals exposed to ozone. In these lungs focal areas of intra-alveolar cellular infiltrates were occasionally seen.

Electron Microscopy

Right lungs from animals subjected to pneumonectomy showed, apart from a few focal areas of swollen cytoplasm of capillary endothelium, relatively normal fine structure. Type I surface epithelium and type II cells with characteristic lamellated bodies were similar to control lungs. Figure 4 is an electron micrograph of a portion of right lung 12 weeks postpneumonectomy. Lungs exposed

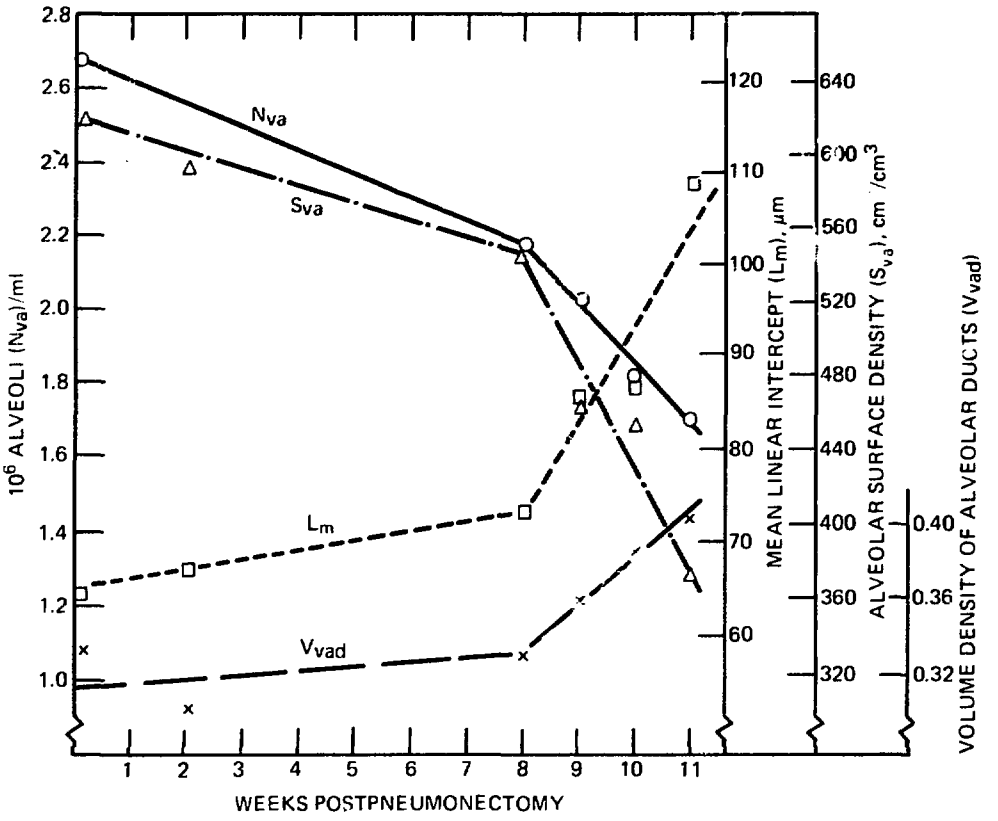

Fig. 3 Graphical representation of morphometric data from a series of right lungs analyzed at different time periods postpneumonectomy. The fall in alveolar number and alveolar surface density and rise in mean linear intercept and volume density of alveolar ducts have a "mirror-image" relationship.

intermittently to 0.4 ppm of ozone for 6 weeks showed interstitial edema of varying severity, focal areas of slightly swollen type I epithelial and capillary endothelial cytoplasm; an example of such changes is shown in Fig. 5. The lungs of animals subjected to unilateral pneumonectomy and exposed subsequently to ozone showed structural changes similar to the paired lungs of animals breathing ozone. Figures 6 and 7 are electron micrographs of lungs in the former category.

DISCUSSION

In a study such as this, the unraveling of the changes taking place following unilateral pneumonectomy with or without subsequent

TABLE 3

MORPHOMETRIC PARAMETERS OF THE RIGHT LUNGS OF RABBITS EXPOSED TO OZONE WITH OR WITHOUT PNEUMONECTOMY*

	Body wt., kg	V_L, ml	$N_{va} \times 10^6$/cm	$N_a \times 10^6$	L_m, μm	V_{vad}
Control	4.3	43.2	1.8	79.1	76.4	0.32
Ozone						
Without pneumonectomy						
0.4 ppm for 6 weeks	3.8	47.0	1.4	77.6	67.0	0.36
Postpneumonectomy						
11 weeks	4.0	65.3	1.6	98.5	95.3	0.40
4 weeks + ozone	4.0	62.0	1.4	91.7	90.3	0.41
18 weeks + ozone	4.2	65.0	1.2	72.9	97.1	0.39

*V_L, lung volume corrected for percent nonparenchyma; N_{va}, number of alveoli/cm^3; N_a, absolute number of alveoli: L_m, mean linear intercept; and V_{vad}, volume density of alveolar ducts.

TABLE 4

MORPHOMETRIC DATA OBTAINED BY ELECTRON MICROSCOPY OF LUNGS PRE- AND POSTPNEUMONECTOMY

Morphometric parameters	Day 0 left lung	10 weeks postpneumonectomy right lung
Volume density		
Air space	0.74	0.84
Capillaries	0.06	0.05
Alveolar wall	0.20	0.11
Epithelium	0.25	0.30
Interstitium	0.40	0.40
Endothelium	0.35	0.30
Surface density, alveoli	854 cm^2/cm^3	588 cm^2/cm^3
Arithmetic mean, alveolar wall	2.9 μm	2.15 μm
Harmonic mean, alveolar wall	0.85 μm	0.85 μm

Fig. 4 Electron micrograph of a portion of an alveolar septum from a right lung 12 weeks postpneumonectomy. The type II cell (T2) and other components of the septum appear normal.

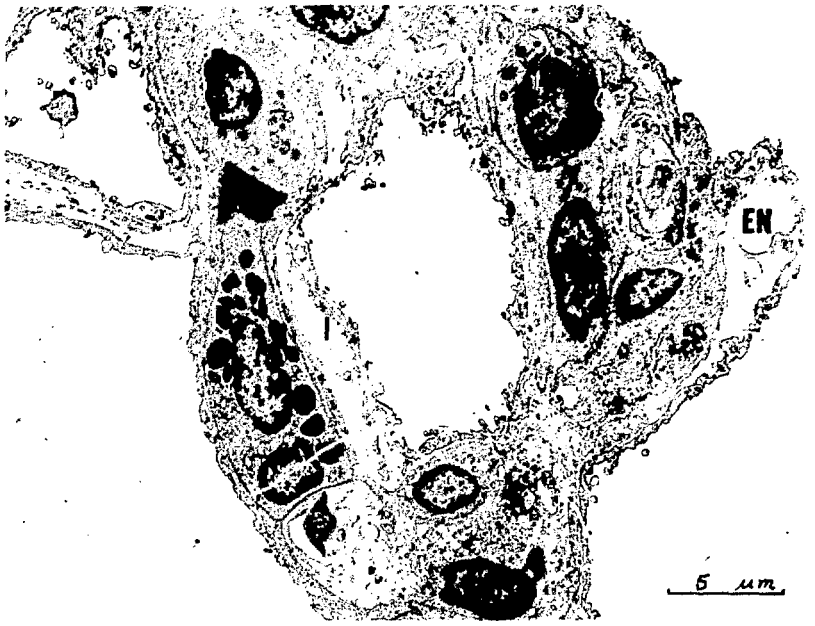

Fig. 5 Electron micrograph of a sectioned alveolus from a lung exposed to ozone (0.4 ppm O_3 for 6 weeks). Interstitial edema (I) is seen along with some damage to capillary endothelium (EN).

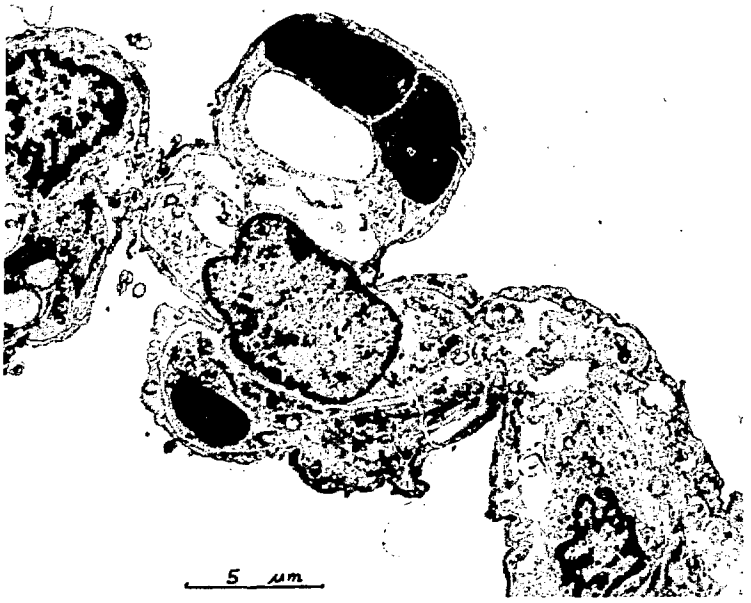

Fig. 6 Portion of an alveolar septum from a lung 2 weeks postpneumonectomy and exposed to ozone for 2 weeks. Changes seen are similar to those in Fig. 5.

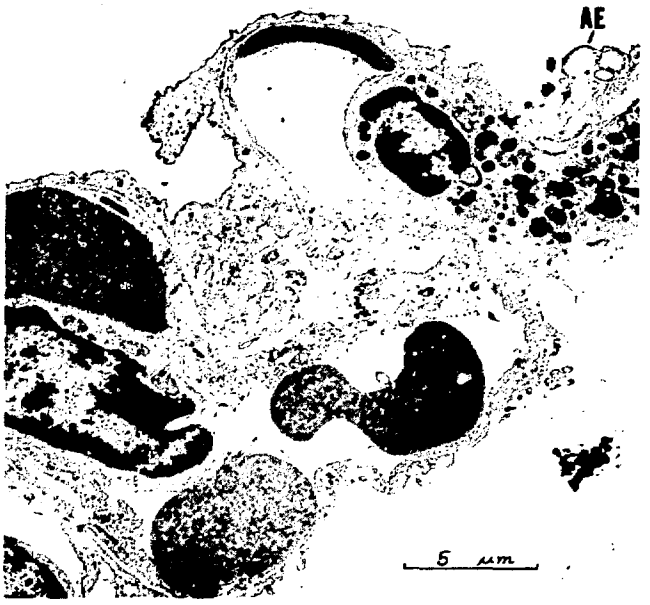

Fig. 7 Portion of an alveolar septum from a lung 9 weeks postpneumonectomy and exposed to ozone for 6 weeks. Changes are similar to those in Figs. 5 and 6 but with some vesiculation of alveolar surface epithelium (AE).

exposure to ozone is complicated by the underlying normal growth and development of the animal.

That considerable variations in alveolar number and other lung parameters occur in both man and animals has been recently discussed by Thurlbeck.[11] In humans, for example, the need for new tissue is met by an increase in both number and size of alveoli until growth of the chest wall is finished.[12] In the rat[13] alveoli may continue to multiply throughout life because continued body growth and growth of the lung are characteristics of this species, whereas in the rabbit[13] differentiation and the formation of new alveoli apparently both cease at 3 months of postnatal development. Šerý and associates[14] came to a similar conclusion. In the present work the data presented in Tables 1 and 2 lend support to this observation. Thus, although both body weight and lung volume increase, the total numbers of alveoli per hemilung remain fairly constant, which suggest that alveolar replication had ceased. The need for an accurate determination of this event, however, is of particular importance in the evaluation of growth stimuli following pneumonectomy and exposure to ozone.

Previous investigators,[14-17] using a variety of animal species, have found that, irrespective of whether the right lung or left lung is removed, the general stimulus to the remaining lung is one of a compensatory increase in lung volume. Generally, the remaining lung doubles in volume or is equal to the combined volume of left and right lungs within 4 to 8 weeks. Our results (Tables 2 and 3) are consistent with this. It should be recalled that, although either lung can be removed, the removal of the right lung abruptly reduces the total lung tissue by about two-thirds. In either event the metabolic needs are apparently met since Nattie, Wiley, and Bartlett[16] found in rats that hypoxia was absent 24 hr after surgery and Cournand et al.[18] noted in humans that alveolar ventilation–perfusion relationships after pneumonectomy indicated that the vascular bed of the remaining lung was able to accommodate a 2 x increase in pulmonary blood flow in a normal manner.

With a rapidly expanding lung, the virtue of the use of morphometry is that relatively small changes not readily detectable by direct examination can be determined. The pictorial and calculated data shown in Fig. 1 support this contention. The overall data (Tables 2 and 3) confirm the findings of Šerý, Kepot, and Obrucnik[14] and indicate that following pneumonectomy the increased volume of the remaining lung is satisfied almost entirely by a substantial increase in mean linear intercept and in the volume density of alveolar ducts. Given such factors as variations in age, body weight, and lung volume, as well as differences in fixation,

sampling, and processing of tissue, the values obtained from the two studies are remarkedly close. In our study, however, the tissues were further evaluated by electron microscopy. In this regard the increase in air-space surface area, as calculated by electron-microscopy morphometry, is due to the increased resolution and the ability to resolve the small undulations of the alveolar wall.

The increase in L_m implies a dilatation of existing air spaces, including alveolar ducts with a corresponding decrease in the volume density of alveolar tissue (Fig. 1). The form this compensatory growth may take is still a subject of considerable controversy.[11,14-17,19] At present it is a matter of alveolar proliferation, alveolar enlargement (or dilatation), or a combination of both. The problem can only be resolved by further careful morphometric analysis.

The magnitude of the effects on the lungs as a result of exposure to ozone is, in part, dependent on the concentration of ozone delivered and the period of exposure.[20]

The fact that normal lungs exposed to ozone did not differ morphometrically from control lungs (Table 3) refers at present to measurements made by light microscopy. Electron micrographs of the parenchyma of ozone-exposed lungs showed varying degrees of interstitial edema and cytoplasmic swelling of Type I surface epithelium and capillary endothelium, changes readily estimated by morphometry at the electron-microscope level. Kistler, Caldwell, and Weibel[21] used this form of analysis in a study of oxygen toxicity in rats, and Plopper, Dungworth, and Tyler[22] studied the lungs of rats after an acute exposure to 3 ppm of ozone for 4 hr. In both instances changes in arithmetic mean thickness of the air—blood barrier were documented which were not discernable by light microscopy.

In respect to lungs exposed to ozone following pneumonectomy, the two examples shown in Table 3 indicate that, whether or not the remaining lung is exposed to ozone 9 weeks or 2 weeks postpneumonectomy, the morphometric analyses of the two are very similar and indeed comparable to postpneumonectomy lungs not exposed to ozone. It is concluded from this that, although electron micrographs of these lungs show changes due to ozone alone, the recognizable increase in lung volume and the enlargement of alveoli and alveolar ducts are not prevented. This is particularly interesting because at 2 weeks postpneumonectomy the remaining lung has yet to reach its full distension. It is, of course, possible that both the concentration of ozone used and the duration of exposure were inadequate. P'an, Beland, and Gegier[23] exposed normal rabbits to 0.4 ppm of ozone for 30 hr per week for 10 months and noted a moderate degree of

emphysema present. Bartlett, Faulkner, and Cook[24] exposed rats to 0.2 ppm of ozone continuously for 30 days, and, although the lungs were histologically normal, lung volume increased by 16% with an increase in mean linear intercept and surface area. It was proposed that the overdistention was due to a decrease in elastic recoil.

In view of these studies, it would seem that exposure to ozone may enhance the progression to higher lung volumes and to larger alveoli by additional tissue changes. At present our data are insufficient to bear on this question. It is provisionally concluded that lung changes as a result of left-lung pneumonectomy and, as analyzed by morphometry at the light-microscope level, are neither enhanced nor inhibited by ozone under the exposure conditions described.

ACKNOWLEDGMENTS

I wish to thank Drs. C. J. Martin and D. Reid for assistance with the surgery and John Boykin and Maria Glaser for technical assistance.

A portion of this work was conducted with the most helpful advice from Professor Ewald Weibel at the Department of Anatomy, University of Bern, during my tenure as a Josiah Macy Scholar. This work was also supported by a grant from the National Institute of Environmental Health Sciences, ES 01049.

REFERENCES

1. L. S. Jaffe, The Biological Effects of Ozone on Man and Animals, *Am. Ind. Hyg. Assoc. J.*, 28: 267-277 (1967).
2. H. E. Stokinger, Ozone Toxicology; a Review of Research and Industrial Experience, 1954—1964, *Arch. Environ. Health*, 10: 719-731 (1965).
3. D. V. Bates, Air Pollutants and the Human Lung, *Am. Rev. Respir. Dis.*, 105: 1-13 (1972).
4. E. S. Boatman, S. Sato, and R. Frank, Acute Effects of Ozone on Cat's Lungs. II. Structural, *Am. Rev. Respir. Dis.*, 110: 157-169 (1974).
5. E. S. Boatman and D. Lowe, Photographic Mapping of a Tissue Surface to Locate Fields for Electron Microscopy, Mouse Lung, *Stain Technol.*, 46: 63-69 (1971).
6. M. S. Dunnill, Quantitative Methods in the Study of Pulmonary Pathology, *Thorax*, 17: 320-328 (1962).
7. E. R. Weibel, An Automatic Sampling Stage Microscope for Stereology, *J. Microsc. (Oxford)*, 91: 1-18 (1970).
8. P. H. Burri, J. Dbaly, and E. R. Weibel, The Postnatal Growth of the Rat Lung. 1. Morphometry, *Anat. Rec.*, 178: 711-730 (1974).
9. E. R. Weibel, G. S. Kistler, and W. F. Scherle, Practical Stereological Methods for Morphometric Cytology, *J. Cell Biol.*, 30: 23-38 (1966).

10. E. R. Weibel, Morphometric Estimation of Pulmonary Diffusion Capacity: 1. Model and Method, *Resp. Physiol.*, 11: 54-75 (1970).
11. W. M. Thurlbeck, Postnatal Growth and Development of the Lung, *Am. Rev. Respir. Dis.*, 111: 803-844 (1975).
12. L. Reid, The Embryology of the Lung, in Development of the Lung, C.I.B.A. Foundation, pp. 109, Little, Brown & Co., Boston, 1967.
13. R. H. D. Short, Aspects of Comparative Lung Growth, *Proc. R. Soc. (London), Sect. B*, 140: 432-441 (1952).
14. Z. Sery, E. Kepot, and M. Obrucnik, Morphometric Analysis of Late Adaptation of the Residual Lung Following Pneumonectomy in Young and Adult Rabbits, *J. Thorac. Cardiovasc. Surg.*, 57: 549-557 (1969).
15. J. M. Cowan and R. G. Crystal, Lung Growth After Unilateral Pneumonectomy: Quantitation of Collagen Synthesis and Content, *Am. Rev. Respir. Dis.*, 111: 267-277 (1975).
16. E. E. Nattie, C. W. Wiley, and D. Bartlett, Jr., Adaptive Growth of the Lung Following Pneumonectomy in Rats, *J. Appl. Physiol.*, 37: 491-495 (1974).
17. M. Gnavi, E. Pansa, and G. Anselmetti, Growth and Regeneration of the Lung, *Minerva Chir.*, 25: 1491-1504 (1970).
18. A. Cournand, R. L. Riley, A. Himmelstein, and R. Austrian, Pulmonary Circulation and Alveolar Ventilation—Perfusion Relationships After Pneumonectomy, *J. Thorac. Surg.*, 19: 80-116 (1950).
19. J. J. Longacre and R. Gohansmann, An Experimental Study of the Fate of the Remaining Lung Following Total Pneumonectomy, *J. Thorac. Surg.*, 10: 131-149 (1940).
20. D. L. Dungworth, C. E. Cross, J. R. Gillespie, and C. G. Plopper, The Effects of Ozone on Animals, in *Ozone Chemistry and Technology—A Review of the Literature: 1961—1974*, Joanne S. Murphy and Janet R. Orr (Eds.), Chap. 11, The Franklin Institute Press, Philadelphia, 1975.
21. G. S. Kistler, P. R. B. Caldwell, and E. R. Weibel, Development of Fine Structural Damage to Alveolar and Capillary Lining Cells in Oxygen-Poisoned Rat Lungs, *J. Cell. Biol.*, 32: 605-628 (1967).
22. G. C. Plopper, D. L. Dungworth, and W. S. Tyler, Morphometric Evaluation of Pulmonary Lesions in Rats Exposed to Ozone, *Am. J. Pathol.*, 71: 395-403 (1973).
23. A. Y. P'an, J. Beland, and Z. Gegier, Ozone-Induced Arterial Lesions, *Arch. Environ. Health*, 24: 229-232 (1972).
24. D. Bartlett, Jr., C. S Faulkner, and K. Cook, Effect of Chronic Ozone Exposure on Lung Elasticity in Young Rats, *J. Appl. Physiol.*, 27: 92-97 (1974).

Alveolar Epithelial Repair and Changes in Free Airway Cell Populations Following Cadmium Injury

J. A. HAYES, S. ASVADI, R. H. STRAUSS, and K. C. PALMER
Mallory Institute of Pathology and Pathology Department,
Boston University School of Medicine, Boston, Massachusetts

ABSTRACT

The lungs of rats xposed to 0.1% (0.005*M*) $CdCl_2$ aerosol show prominent epithelial damage in peribronchiolar alveoli. Initially there is necrosis of type I cells within 48 hr of exposure. This is followed by marked mitotic activity in type II cells which progresses so that they completely line the affected alveoli by 3 to 4 days. Subsequently, these cells flatten out to reline the surface, and we have interpreted that the flat cells with microvilli and osmiophilic bodies are "intermediate" cells. The necrotic phase of injury coincides with a wave of polymorphonuclear leukocytes (PMLs), whereas type II cell proliferation with conversion to "intermediate" epithelium coincides with an outpouring of alveolar macrophages (AMs). This finding suggests that PMLs indicate active lung-cell necrosis, whereas AMs indicate either a repair phase or one of low-grade activity.

Acute exposure to cadmium fumes produced lesions typical of centrilobular emphysema in man in which the main damage appears to center about respiratory bronchioles.[1,2] Our studies were undertaken to obtain more information on the early stages of injury and repair consequent to an exposure to cadmium chloride ($CdCl_2$) aerosol. Attention was particularly directed to changes in alveolar epithelium and to parallel changes in cells presumed to be exuded into the airspaces as a result of the injury.

MATERIALS AND METHODS

Male Sprague-Dawley rats, 150 to 250 g in weight, were exposed to an aerosol of 0.1% (0.005*M*) $CdCl_2$ in physiologic saline produced

by a DeVilbiss 35A ultrasonic generator. This yields an aerosol concentration of 10 mg of $CdCl_2$ per cubic meter of air in the chamber. A single 2-hr exposure was administered. The generated aerosol was polydisperse, with a mass median particle diameter of 4.5 ± 1.64 μm, and gave a tissue cadmium content of 1 ± 0.5 μg/g wet lung weight.[3] For some animals of each group, colchicine (1.0 μg per gram of body weight) was injected 4 hr before killing. Rats were killed by barbiturate overdose in groups of six at 1 hr and 1, 2, 4, 7, and 10 days after cadmium exposure. Two groups of control animals were used: (1) 36 rats exposed to an aerosol of physiologic saline for the same period and (2) 35 rats not exposed to an aerosol. Both sets of control animals were killed at the same time intervals as the cadmium-exposed rats. Lungs were distended with glutaraldehyde at 25 cm pressure and fixed for 24 hr (Ref. 4). Tissue blocks were taken from the lung periphery and processed for electron microscopy, and appropriate photographs were taken.

In a second experiment rats, either unexposed or exposed to aerosol, were killed at the same time intervals. The lungs were washed out with physiologic saline at room temperature. Washed-out cells were enumerated in a hemocytometer.

RESULTS

The exposure produced multiple lesions of predominantly peribronchiolar distribution. Initially type I cells showed cytoplasmic swelling (Fig. 1a) and necrosis with loss of plasma membranes so that there was exposure of basement membrane (Fig. 1b). This injury apparently triggered proliferation of type II cells in which mitoses were easily identified (Fig. 2) because colchicine was injected 4 hr before killing. Subsequently the damaged alveoli became lined by type II cells between 3 and 4 days after exposure (Fig. 3) although intervening areas showed essentially normal alveolar lining cells. Thereafter the type II cells flattened out to reline the septa with type I cells, although numerous cells intermediate between type I and type II cells were seen. These intermediate cells were flat but showed numerous microvilli and osmiophilic bodies and persisted to at least 7 days after injury (Fig. 4). By 10 days the damaged lungs had regained their normal structure except for some peribronchiolar fibrosis.[5] The alveolar walls sometimes appeared thickened owing to the close apposition of increased numbers of macrophages to the alveolar epithelium (Fig. 5). Apart from the mild cytoplasmic and interstitial edema, at 1 and 2 days saline-aerosol-exposed controls showed the same morphology as unexposed rats.

Fig. 1a Lung area 1 day after exposure to $CdCl_2$. Marked cytoplasmic edema of type I alveolar cell. Adjacent alveolus is lined by normal type I epithelium (arrows).

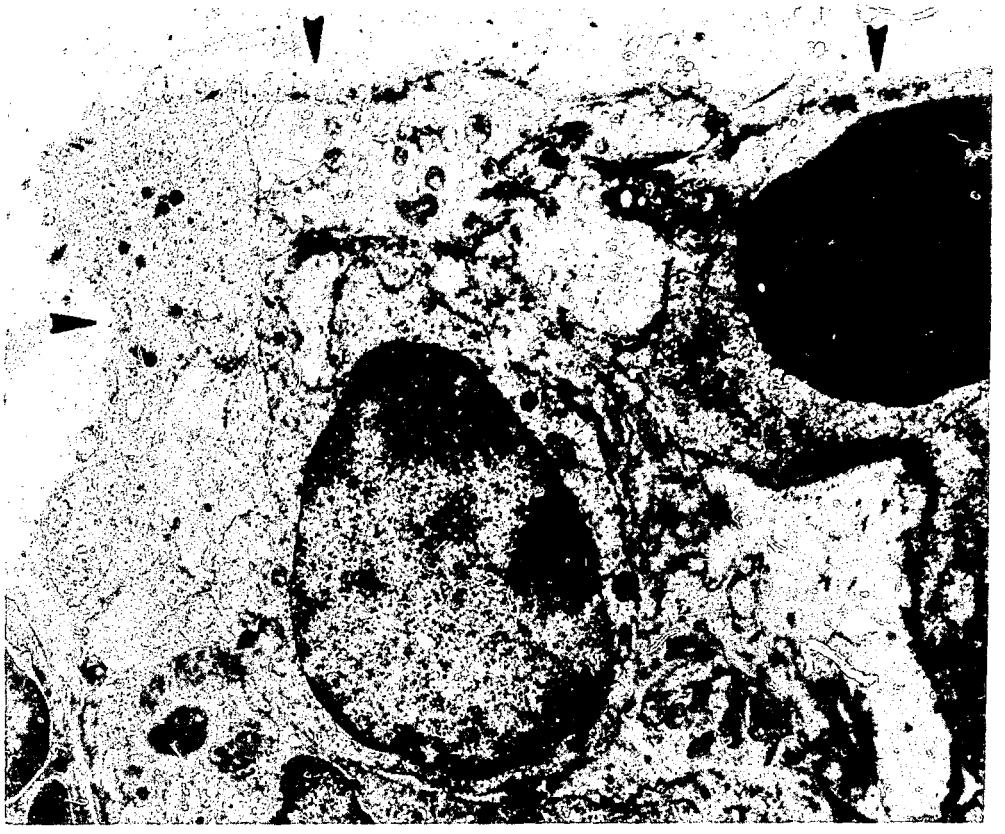

Fig. 1b Different area of same lung showing exposure of basement membrane deep to type I cell after loss of outer plasma membrane.

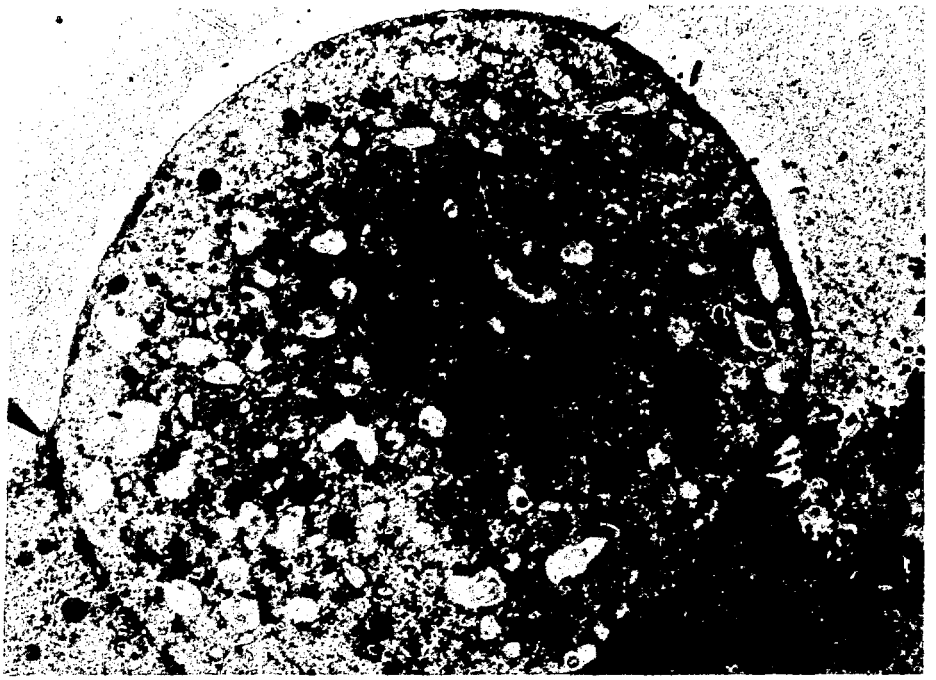

Fig. 2 Typical appearance of colchicine-arrested mitosis in type II cell. Although osmiophilic bodies are not visible, the cell is identified by its epithelial position with junctional complex (arrows) and "corner" location in the alveolus.

Fig. 3 Alveolus 3 days after $CdCl_2$ exposure. It is completely lined by type II cells.

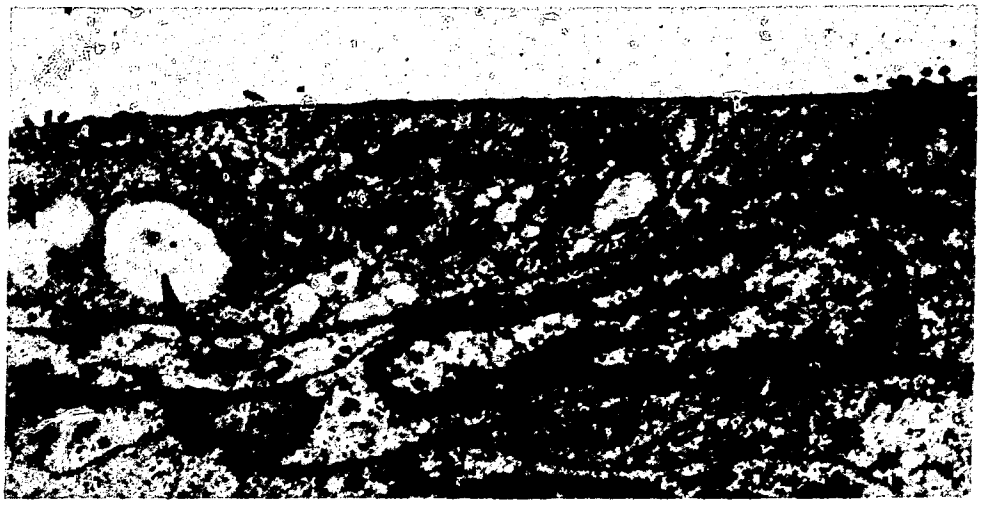

Fig. 4 Seven days after $CdCl_2$ exposure, intermediate type cells line the alveolus. Arrows indicate the presence of microvilli and osmiophilic bodies in clefts which have the attenuated characteristics of type I epithelium.

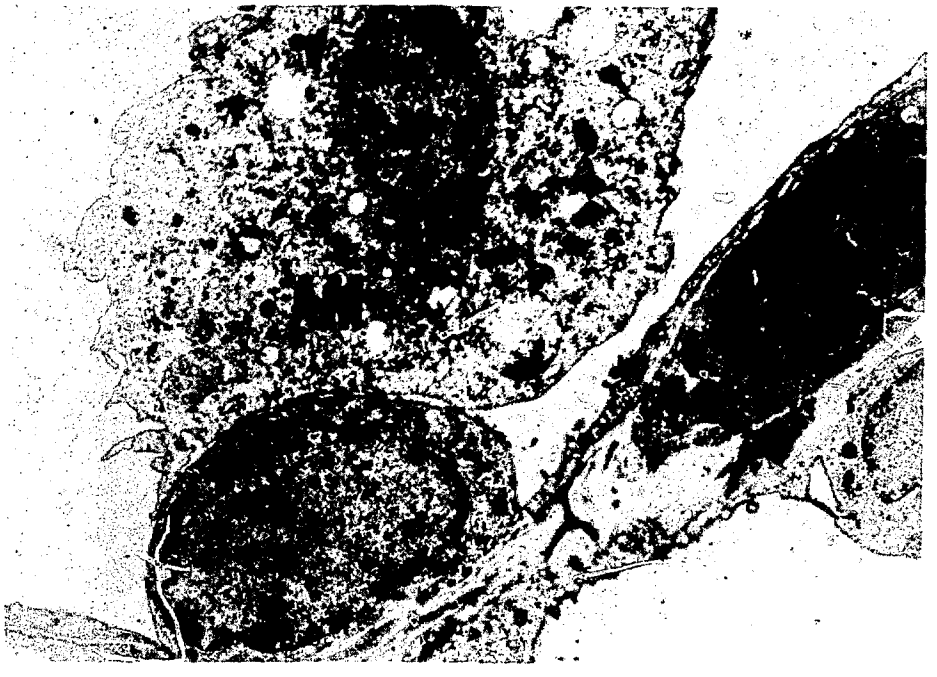

Fig. 5 Ten days after $CdCl_2$ exposure, alveolar walls have regained a normal structure. Close apposition of alveolar macrophages (AMs) may simulate mural hypercellularity.

The parallel studies with lung lavage showed that total free airway cells peak at 4 days in rats exposed to $CdCl_2$ (i.e., $43.2 \pm 0.2 \times 10^6$ cells) which was at least four times the number of cells found in saline-aerosol-exposed controls (i.e., $11.1 \pm 0.1 \times 10^6$ cells/ml). This increase could be resolved into two peaks, one composed of polymorphonuclear leukocytes (PMLs) between 2 and 3 days and a second peak of alveolar macrophages (AMs) between 4 and 5 days postexposure (Fig. 6). Thereafter the number of free cells returned to control values. Saline-aerosol exposure produced a minor increase in AMs at the first day after exposure.

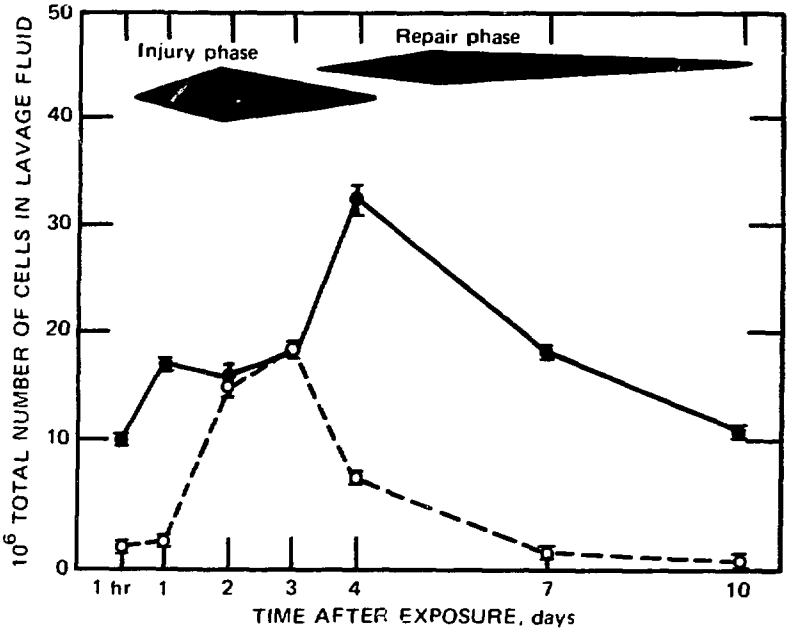

Fig. 6 Total numbers of polymorphonuclear leukocytes and alveolar macrophages in lung lavage fluid from $CdCl_2$-exposed and control groups. ●, alveolar macrophages. ○, polymorphonuclear leukocytes.

DISCUSSION

The pattern of repair following alveolar cell damage by $CdCl_2$, illustrated in Fig. 6, is similar to that produced by ozone,[6,7] nitrogen dioxide,[8] and oxygen[9,10] in that type I cell death is followed by type II cell proliferation and flattening of type II cells to reproduce normal type I cells. Studies of biochemical changes at the same time intervals have shown that wet lung weight, RNA and DNA content, and the activity of lactate, isocitrate, malate, and glucose-

6-phosphate dehydrogenases showed a parallel increase, with a peak at 4 days.[11] We have also shown that there was a very similar increase in uptake of tritiated thymidine in rat lung after a similar $CdCl_2$ exposure.[4] These findings further support the specific timing of the reaction to $CdCl_2$. However, the changes are not identical, as Table 1 shows, and this comparison prompts the question: Do these differences represent a variable cell response to individual agents, or do they merely reflect a variation in site of impact, local concentration, or route of "clearance" of the noxious agent?

TABLE 1

CELL SPECIFIC MITOTIC ACTIVITY INDUCED BY DIFFERENT INHALED AGENTS

	Cells showing proliferation					
Inhaled agent	Bronchioles	Type II	Type I	Endothelium	Interstitial cell	Ref. No.
NO_2	+	+	+	?	?	8
Ozone	?	+	+	?	?	6,7
Oxygen	?	+	+	+	?	9 to 13
Cadmium	?	+	+	?	+	4

+Activity present.
?Activity not recorded.

Correlation of the evolving epithelial change with the pattern of free airway cells as removed by lavage shows that the phase of cell injury coincides with an outpouring of PMLs, whereas the more prominent peak of AMs coincides with replenishment of type I cells and clearance of cell debris. It is not an unreasonable extension to suggest that the free airway cell population is an indicator of the nature of damage to alveolar epithelium; predominance of PMLs indicates an active, possibly acute, process with cell necrosis. In contrast, increased AMs would indicate a healing process or one of low-grade activity with little cell necrosis.

ACKNOWLEDGMENTS

These studies were supported by the Mallory Institute of Pathology Foundation and by National Institutes of Health grants HL 15063 and GRS RR 05569-10.

REFERENCES

1. J. C. Patterson, Studies on the Toxicity of Inhaled Cadmium. III. The Pathology of Cadmium Smoke Poisoning in Man and in Experimental Animals, *J. Ind. Hyg. Toxicol.*, 29: 294-301 (1947).
2. R. E. Lane and A. C. P. Campbell, Fatal Emphysema in Two Men Making a Copper Cadmium Alloy, *Brit. J. Ind. Med.*, 11: 118-122 (1954).
3. K. C. Palmer, G. L. Snider, and J. A. Hayes, Cell Proliferation Induced in the Lung by Cadmium Chloride Aerosol, *Am. Rev. Respir. Dis.*, 112: 173-179 (1975).
4. R. H. Strauss, K. C. Palmer, and J. A. Hayes, Acute Lung Injury Induced by Cadmium Aerosol. 1. Evolution of Alveolar Cell Damage, *Am. J. Pathol.*, 84: 561-578 (1976).
5. K. C. Palmer, G. L. Snider, and J. A. Hayes, An Association Between Alveolar Cell Proliferation and Interstitial Fibrosis Following Acute Lung Injury, *Chest*, 69: 307-309 (1976).
6. C. G. Plopper, D. L. Dungworth, and W. S. Tyler, Pulmonary Lesions in Rats Exposed to Ozone: A Correlated Light and Electron Microscopic Study, *Am. J. Pathol.*, 71: 378-394 (1973).
7. R. J. Stephens, M. F. Sloane, M. J. Evans, and G. Freeman, Early Response of Lung to Low Levels of Ozone, *Am. J. Pathol.*, 74: 31-58 (1974).
8. M. J. Evans, L. J. Cabral, R. J. Stephens, and G. Freeman, Renewal of Alveolar Epithelium in the Rat Following Exposure to NO_2, *Am. J. Pathol.*, 70: 175-198 (1973).
9. Y. Kapanci, E. R. Weibel, H. P. Kaplan, and F. R. Robinson, Pathogenesis and Reversibility of the Pulmonary Lesions of Oxygen Toxicity in Monkeys. II. Ultrastructural and Morphometric Studies, *Lab. Invest.*, 20: 101-118 (1969).
10. I. Y. R. Adamson and D. H. Bowden, The Type II Cell as Progenitor of Alveolar Epithelial Regeneration: A Cytodynamic Study in Mice After Exposures to Oxygen, *Lab. Invest.*, 30: 35-42 (1974).
11. J. A. Hayes, G. L. Snider, and K. C. Palmer, Evolution of Biochemical Damage in the Rat Lung After Acute Cadmium Exposure, *Am. Rev. Respir. Dis.*, 113: 121-130 (1976).
12. D. H. Bowden and I. Y. R. Adamson, Endothelial Regeneration as a Marker of the Differential Vascular Responses in Oxygen-Induced Pulmonary Edema, *Lab. Invest.*, 30: 350-357 (1974).
13. P. C. Pratt, Pulmonary Capillary Proliferation Induced by Oxygen Inhalation, *Am. J. Pathol.*, 34: 1033-1049 (1958).

Light and Scanning Electron Microscopic Observations of Goat Lungs Following 3-Methylindole Infusion

B. J. BRADLEY,* J. R. CARLSON,* and E. O. DICKINSON†
*Department of Animal Sciences, Washington State University, Pullman, Washington, and
†College of Veterinary Medicine, Oregon State University, Corvallis, Oregon

ABSTRACT

Light microscopy and scanning electron microscopy were used to characterize morphologic changes in goat lungs following an infusion of 3-methylindole (3MI). Fifteen yearling goats were given jugular infusions of 0.04 g 3MI per kilogram of body weight in propylene glycol (PG). Three goats were sacrificed at 0.5, 2, 4, 8, or 24 hr. Two noninfused control goats and four PG-infused goats were used as controls. The intact left lung was fixed by airway perfusion with 2% buffered paraformaldehyde for 1.5 hr, then samples were cut from three areas of the caudal lobe and fixed in diluted Karnovsky's fixative. Samples were fixed in 4% buffered paraformaldehyde and stained with hematoxylin and eosin for light microscopy. By 30 min after beginning the infusion, only 25% of the total dose had been infused, but there was mild swelling of alveolar septa accompanied by fibrinous and globular material within the alveolar spaces and on some cilia. Mild distention of blood-vessel adventitia was also observed. By 2 to 4 hr alveolar septa were generally swollen, and connective tissue appeared distended and contained scattered blood cells, primarily lymphocytes. Some alveolar spaces contained a reticulum of fibrinous material suspending blood cells and debris. Bronchial cilia appeared laden with mucus or proteinaceous debris. By 8 and 24 hr, swelling of alveolar septal cells had increased and alveolar spaces appeared to contain a greater infiltration of proteinaceous debris, lymphocytes, and large mononuclear cells. These results indicate that 3MI infusion causes pulmonary alveolar edema within 30 min and that lesions are progressive to 24 hr after the infusion is begun.

Acute pulmonary edema and emphysema (APE) is a disease of adult cattle which develops characteristically in late summer or early fall within 2 to 10 days after a change of pasture from dry grass to lush,

green meadows.[1-4] Orally administered tryptophan has been shown to induce APE in cattle, producing pulmonary lesions similar to those observed in the naturally occurring disease.[5,6] A ruminal metabolite of L-tryptophan, i.e., 3-methylindole (3MI), has been shown[7] to induce APE in cattle,[8,9] sheep,[10] and goats.[11] In these species clinical signs include increased respiratory rate, progressive dyspnea, and forced expiration that is sometimes accompanied with an audible expiratory grunt.[1,9] Gross pulmonary lesions include heavy, dark red lungs that fail to collapse when the thoracic cavity is opened. Interstitial edema and emphysema is apparent following transection of the postmortem lung. Also, foam is contained in the bronchial tree, and hydrothorax is evident in severe cases.

Following administration of tryptophan or 3MI, pulmonary lesions include swollen and some ruptured interalveolar septa, proteinaceous residue in alveolar spaces, and interstitial and perivascular swelling. Foci of hemorrhage are also frequently observed with the light microscope (LM). The luminal epithelia of small bronchioles become swollen, and necrotic and large mononuclear cells are observed in bronchiolar lumina and alveolar spaces. Alveolar epithelia become irregular and somewhat disoriented because of swelling and proliferation. These lesions have been observed within 1 to 4 days in experimental animals.[9]

Three-methylindole is metabolized and cleared rapidly from the peripheral blood of experimental animals.[9-11] By giving an intravenous dose of ^{14}C-labeled 3MI to goats, Hammond[12] has shown that 90% of the radioactive label was excreted in the urine as a metabolite of 3MI and that 0.7% was expired as carbon dioxide over a 3-day period.

Accumulated research data from our laboratory have led us to the hypothesis that damage to lung tissue is initiated soon after 3MI enters the blood. Transmission electron microscopy (TEM) of early lesions (0.5 to 8 hr) induced by 3MI administration to goats shows endothelial and epithelial cell damage and edema accumulation in interstitial spaces. These early lesions are followed by a progressive accumulation of edema in the alveolar spaces.[13] Also under TEM it has been shown that alveolar epithelial cell proliferation, both in the naturally occurring[14] and the 3MI-induced disease,[15] is accounted for by hyperplasia of the type II cells. Since alveolar epithelia appear severely damaged in either the natural or the induced disease, the proliferation of the type II cells seems to be an attempt by the lung to repair the damaged tissue.[16]

The purpose of this experiment was to use the scanning electron microscope (SEM) to characterize surface morphological changes in

lungs within 0.5 to 24 hr after the beginning of 3MI infusion, to determine the time course of these lesions, and to compare these observations with light microscopic (LM) observations of adjacent areas of the same tissues.

METHODS

Fifteen yearling goats were infused via jugular puncture with 3MI dissolved in propylene glycol (0.11 g 3MI per milliliter of PG). Goats given the total dose received 0.04 g 3MI per kilogram of body weight (BW) over a 2-hr period. Goats were killed with sodium pentobarbital injected at 0.5, 2, 4, 8, or 24 hr after beginning the infusion. Three goats were killed at each time period. Animals in the 30-min group received only 25% of the total 3MI dose. Four control goats were sacrificed at 0.5, 2, 8, or 24 hr after the beginning of infusion of an equivalent amount of PG only (0.36 ml per kilogram of body weight), and two noninfused goats were killed. Lungs were removed within 3 to 5 min, and fresh samples from the right lung were fixed in freshly prepared 4% paraformaldehyde in 0.1*M* phosphate buffer (pH, 7.2) for light microscopy. The left whole lung from each animal was perfused through the airways for 1.5 hr with 2% paraformaldehyde in 0.1*M* cacodylate buffer (pH, 7.2) at a column-head pressure of 30 cm. Samples were then cut (10 by 5 by 5 mm) from the fixative-perfused lung, and fixation was continued overnight in diluted (1 : 4.5) Karnovsky's fixative.[17] All samples for light and scanning electron microscopy were cut from three areas of each caudal lobe: the mid-dorsal ridge, mid-lateral edge, and the caudal tip. Tissue for LM was dehydrated through an ethanol series, cleared in xylol, embedded in paraffin, and stained with hematoxylin and eosin. Scanning electron microscopic samples were dehydrated through an ethanol series (30, 50, 70, and 100% 2x), frozen in liquid nitrogen, shaved with a cleaned, single-edged razor blade, and returned to two final rinses in 100% ethanol.[18] Samples were then taken through a graded series of Freon TF (10, 30, 50, 70, and 100% 3x), critical-point dried in Freon 13 (Ref. 19), gold coated, and examined with an Autoscan microscope (Etec Corp.).

RESULTS

Goats dosed with 3MI developed signs of respiratory distress by 1 hr after beginning infusion. These clinical signs became acute by 4 to 6 hr but began to slowly regress by 8 to 10 hr. One animal died of

severe pulmonary edema at 6 hr. No lung lesions were detectable either in carrier-infused or in noninfused control goats. Grossly, the control lungs were light pink in color, soft and pliable; they appeared to collapse completely when the thoracic cavity was opened. The mean control lung weight was 1% of live body weight.

Lungs from the 3MI-infused groups appeared more inflated, darker red in color, and heavier as the experiment progressed. By 30 min after beginning infusion, mean lung weight had increased to 1.2% body weight. The amount of edema grossly detectable increased, as did lung weight, to 1.5, 1.9, 2.4, and 2.2% body weight at 2, 4, 8, and 24 hr, respectively.

Under SEM, the control-lung parenchyma appeared similar to that reported for other mammalian species.[20] Individual alveolar spaces were separated by thin, delicate interalveolar septa in the PG-infused control-goat lungs, and alveolar pores of Kohn were commonly observed in the alveolar walls (Fig. 1). No differences in lung parenchymal tissues were observed between PG-infused control goats and those control goats not infused with propylene glycol. Airways were lined with ciliated and nonciliated cells. The proportion of nonciliated or Clara cells increased at the level of the terminal bronchioles (Fig. 2). The apical surface of most Clara cells in the lungs of control goats appeared covered with mucus droplets ranging in diameter from the size of microvilli to aggregates that appeared to approximate the diameter of the luminal surface of the cells. Cilia appeared clean and erect (Fig. 2). By 30 min the presence of fibrinous debris on the surface of the alveolar walls was observed under SEM (Fig. 3). Foci of hemorrhage were occasionally observed with LM, and these correlate with the erythrocytes seen on the surface of alveolar septa with SEM (Fig. 4). By 2 to 4 hr a fibrinous reticulum filled many alveoli, and swollen alveolar septa were apparent (Fig. 5). Clara cells in the terminal airways appeared swollen (Fig. 6). The apical surfaces of the Clara cells looked uniform, and the variable-sized mucus caps seen in controls were no longer detectable. Cilia appeared to be laden with mucus and debris, and some cilia appeared clumped. Compare Figs. 2 and 6. Interlobular and perivascular swelling were present throughout by 4 hr. By 8 to 24 hr, edema was severe and filled most alveolar spaces. Large mononuclear cells were frequently observed in alveoli, and some hyaline membrane formation was apparent (Figs. 7 and 8). Terminal and respiratory bronchiole lining epithelia appeared more severely swollen than at 2 to 4 hr; some cells appeared to be sloughing into the lumen. Increased numbers of large mononuclear cells in these airways were also seen under light microscopy (Fig. 9). Using SEM,

we observed some cilia on the surface of these airways to be shorter than normal, and macrophages were present in greater numbers than at earlier stages of the disease (Fig. 10).

DISCUSSION

The results of this experiment demonstrate that infused 3MI induces pulmonary lesions in goats within 30 min after beginning infusion. Fibrin and erythrocytes localized in alveoli indicate capillary leakage and cellular damage. Also, changes in the gross appearance and the increase in lung weight (from 1.0 to 1.2% of body weight) by 30 min indicated the presence of edema. These lesions at 30 min were induced by approximately 0.01 g 3MI per kilogram of body weight, but whether the lesions would progress to the severity of those observed following additional 3MI infusion remains to be determined. However, in those animals receiving the full dose of 3MI, it is clear that capillary leakage continues after the half-hour observations. The fibrin strands in the alveoli appear to increase in length, diameter, and number per alveolar space by 2 to 4 hr. Lung weights increased from 1.0% of body weight in controls to 1.5 and 1.9% of body weight by 2 and 4 hr, respectively. This represents approximately 300 g of extra fluid and debris in the lungs at 4 hr.

Under SEM, the amount of fibrin in individual alveoli by 8 to 24 hr appeared similar to that observed at 4 hr, but edema appeared more diffuse by light microscopy. Mean lung weights increased to 2.4 and 2.2% of body weight at 8 and 24 hr, respectively. Alveolar fibrinous strands appeared thicker and clumped by 24 hr, and the number of macrophages and lymphocytes appeared to increase throughout the lung parenchyma. The clumping of these fibrin strands observed with SEM may correspond to the hyaline membranes seen with LM although these observations are not offered as proof. The clinically observed forced expiratory "grunt" characteristically occurring in the natural and 3MI-induced diseases is probably due to the failure of the fibrin-filled alveoli to collapse.

The mechanism by which 3MI initiates pulmonary lesions is not known. The direct effect of 3MI on in vitro membrane systems has been demonstrated. Using nuclear magnetic resonance[21] and electron paramagentic resonance,[22] Bray has shown that 3MI interacts with the polar head of the lecithin molecule and perturbs the structure of the lipid portions of erythrocyte ghost membranes. Endothelial and epithelial cell damage by 30 min after beginning

(Text continues on page 600.)

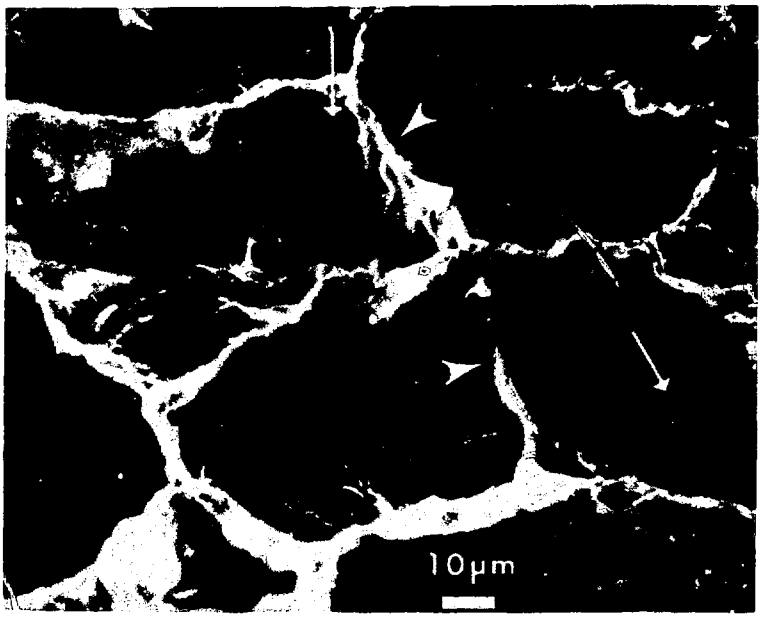

Fig. 1 Control lung infused with PG. Alveolar spaces are separated by thin interalveolar septa (arrow heads). Alveolar pores of Kohn are present in most septa (arrow). Alveolar linings are clean and free of foreign material.

Fig. 2 Control lung infused with PG. Terminal bronchiole showing lining ciliated and nonciliated Clara cells. Clara cell apical surfaces are covered with droplets (solid arrow head) which appear to merge into aggregates that cover the liminal surface of the cell (open arrow head). Cilia appear clean and erect, and microvilli appear to cover the surface of ciliated cells (curved arrow).

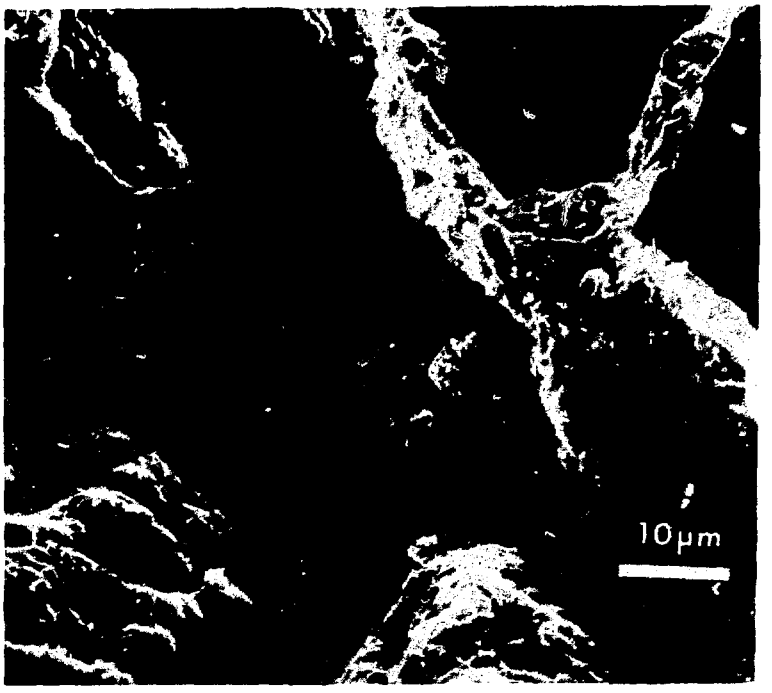

Fig. 3 Lung infused with 3MI, 0.5 hr. Fibrinous debris on the surface of the alveolar septa.

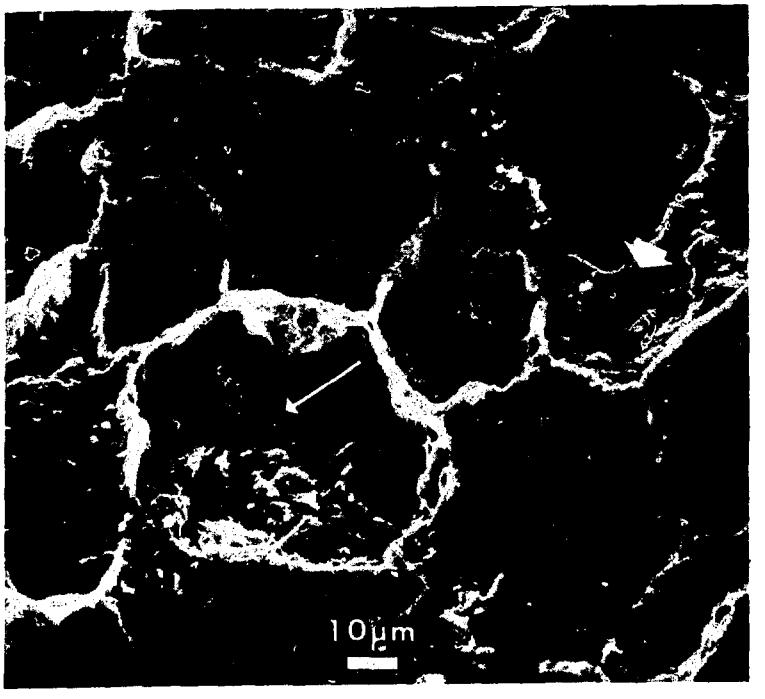

Fig. 4 Lung infused with 3MI, 0.5 hr. Erythrocytes (arrow) scattered in some alveoli with a light scattering of debris (arrow head).

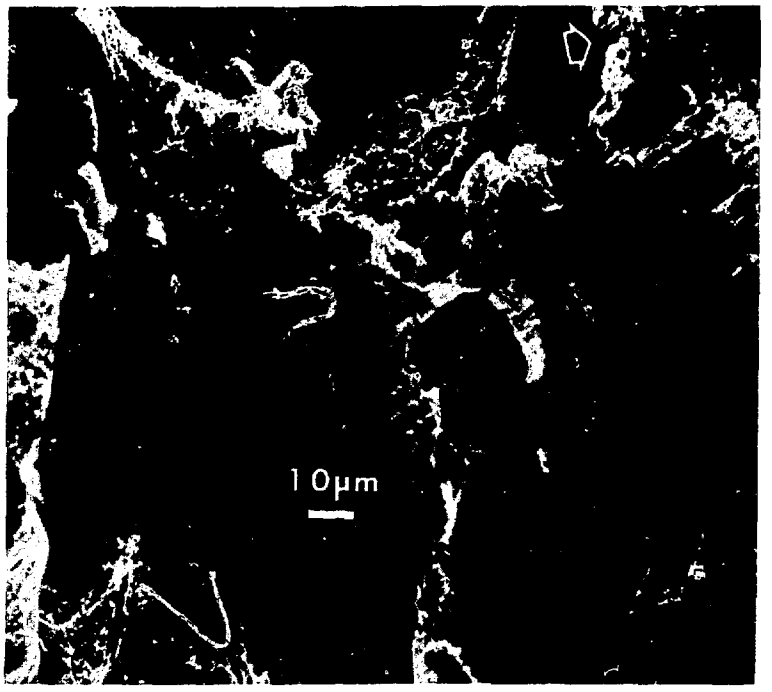

Fig. 5 Lung infused with 3MI, 2 hr. Alveoli are filled with fibrinous reticula. Some interalveolar septa appear swollen or distended (arrow head).

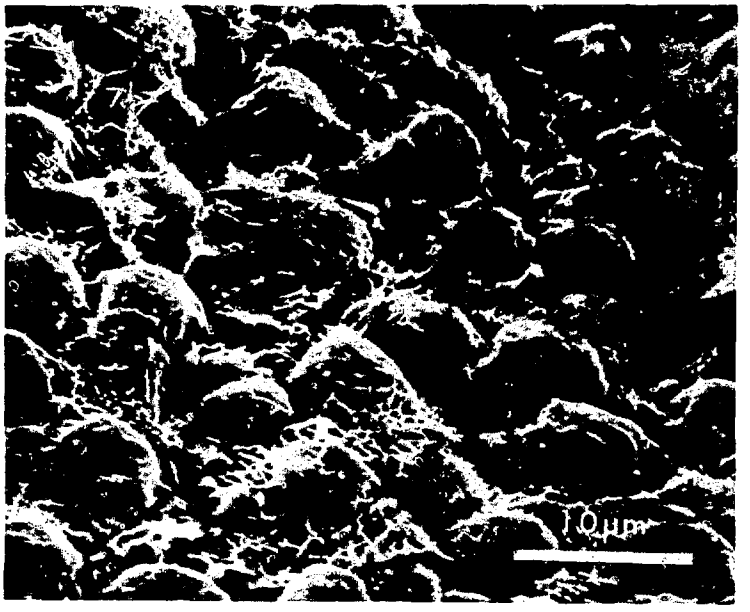

Fig. 6 Lung infused with 3MI, 4 hr. Clara cells are swollen and have lost the variable-sized mucus caps seen in control lungs. Cilia are laden with debris, and some appear clumped.

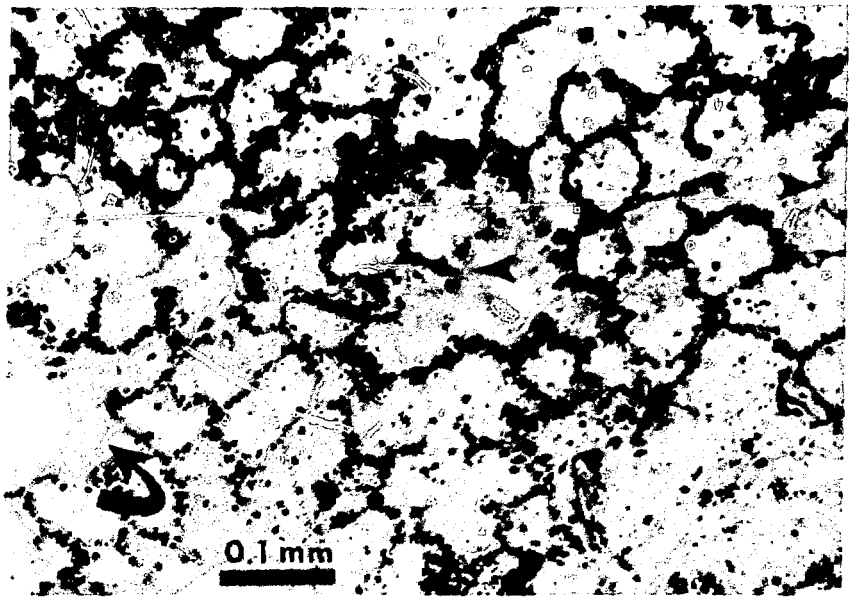

Fig. 7 Lung infused with 3MI, 24 hr. Light micrograph showing proteinaceous material in alveolar spaces. Some interalveolar septa appear ruptured (arrow heads), and hyaline membranes are forming in some areas (curved arrow). Large mononuclear cells are commonly seen in alveolar spaces mixed with lymphocytes and erythrocytes. (Magnification, 140 X.)

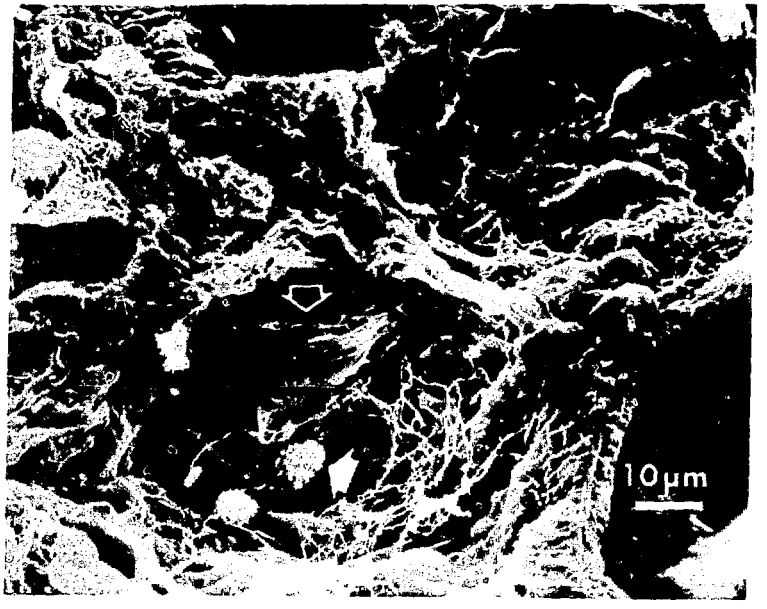

Fig. 8 Lung infused with 3MI, 24 hr. Fibrinous nature of debris in some alveoli appears membranous (open arrow head). This may correspond to what is typically referred to as hyaline membrane seen with LM. Macrophages are frequently seen in these debris-laden alveoli (solid arrow head).

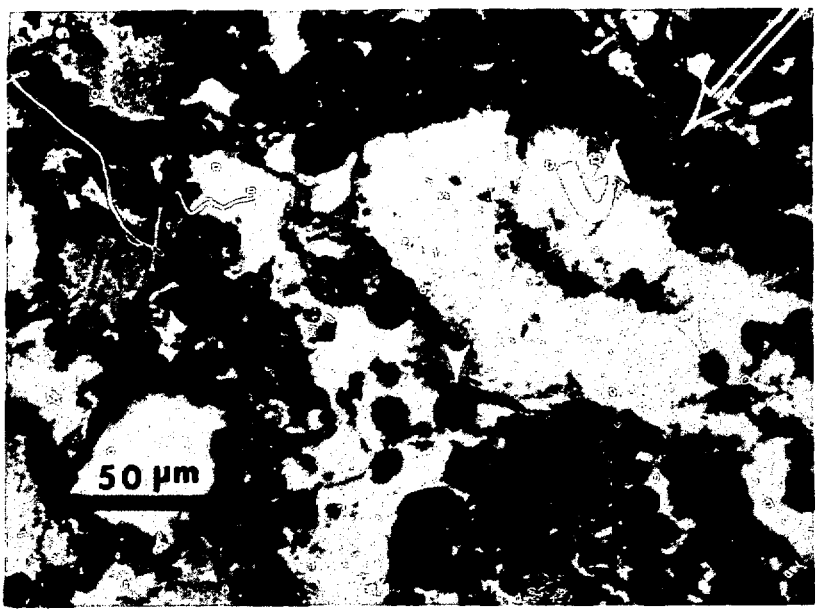

Fig. 9 Lung infused with 3MI, 24 hr. Light micrograph showing swollen lining cells of a respiratory bronchiole (curved arrow) and mononuclear cells in the lumen (arrow heads). Swollen bronchiole submucosa is also evident (arrow). Alveolar septa swelling and debris in alveolar spaces were severe by 24 hr.

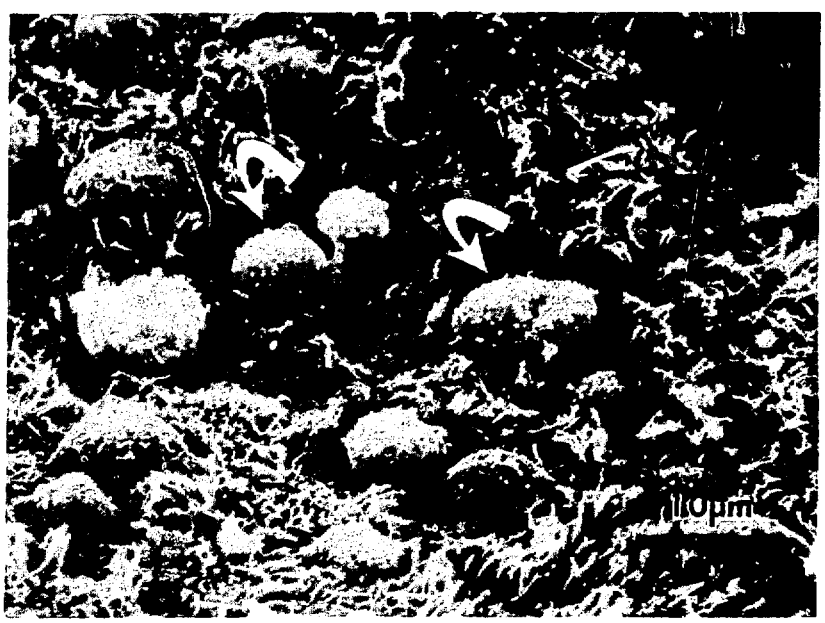

Fig. 10 Lung infused with 3MI, 24 hr. Respiratory bronchiole contains debris-laden cilia. Some cilia appear shorter than normal. Several macrophages are present on the surface of the bronchiole (arrows).

infusion has been observed,[13] and the early onset of fibrin leakage and foci of hemorrhage suggest a possible direct effect of 3MI (or a metabolite) on pulmonary membranes.

Bronchiole epithelia are among the first to show morphological changes and necrosis following 3MI administration. The surfactant-related role of Clara cells is not clear,[23] but it has been shown that total phospholipids are decreased in whole-lung homogenates from cattle with tryptophan-induced APE (Ref. 24), which suggests a decrease in surfactant content. Whether or not these data are related to the hypertrophic terminal bronchiole cells reported here remains to be determined. The sequence of events is not clear, but bronchiolar cells that appear necrotic and sloughing suggest cellular damage regardless of their secretory function.

Proliferation of alveolar lining cells was not observed in this experiment, presumably because 24 hr is short of the time required for these cells to duplicate. The type II proliferation observed by Breeze et al.[14] and Pirie et al.[15] indicates that approximately 4 days are required for these cells to be generally observed in a proliferative state. This is similar to the observations of other researchers,[25,26] who have shown that the type II cells serve as stem cells for type I alveolar lining epithelial cells. This proliferation is apparently a common response to damaged alveolar epithelial lining cells.[16]

The observations seen under LM and SEM mutually support the fact that 3MI when infused directly into the bloodstream of goats can induce APE. Lesions observed by 30 min after beginning infusion demonstrate the short time required for 3MI to affect the lung. Although the initial lesions probably involve the capillary endothelia[13] and result in the capillary leakage observed with SEM and LM, changes in the interstitium and alveolar and bronchiolar epithelia are progressive to 24 hr.

ACKNOWLEDGMENTS

Appreciation is extended to Dr. A. L. Cohen, Director, Electron Microscope Center, Washington State University, for use of the facilities and to Mr. David L. Bentley for technical assistance with the scanning electron microscopy.

This work is supported in part by National Institutes of Health and grant HL-13645. This is Scientific Paper No. 4706, College of Agriculture Research Center, Washington State University, Project 1893.

REFERENCES

1. F. W. Scholfield, Acute Pulmonary Emphysema in Cattle, *J. Am. Vet. Med. Assoc.*, 112: 254-259 (1948).
2. J. T. Blake and D. W. Thomas, Acute Bovine Pulmonary Emphysema in Utah, *J. Am. Vet. Med. Assoc.*, 158: 2047-2052 (1971).
3. I. E. Selman, A. Wiseman, H. M. Pirie, and R. G. Breeze, Fog Fever in Cattle: Clinical and Epidemiological Features, *Vet. Rec.*, 95: 139-147 (1974).
4. M. L. Terry, B. J. Bradley, A. C. Hammond, K. A. Cummins, J. R. Carlson, and E. O. Dickinson, 3-Methylindole and Naturally Occurring ABPE, *Proceedings, West. Sec., Am. Soc. Anim. Sci.*, 27: 330-331 (1976).
5. E. O. Dickinson, G. R. Spencer, and J. R. Gorham, Experimental Induction of an Acute Respiratory Syndrome in Cattle Resembling Bovine Pulmonary Emphysema, *Vet. Rec.*, 80: 487-489 (1967).
6. J. R. Carlson, I. A. Dyer, and R. J. Johnson, Tryptophan-Induced Interstitial Pulmonary Emphysema in Cattle, *Am. J. Vet. Res.*, 29: 1983-1989 (1968).
7. M. T. Yokoyama and J. R. Carlson, Dissimilation of Tryptophan and Related Indolic Compounds by Ruminal Microorganisms In Vitro, *Appl. Microbiol.*, 27: 540-548 (1974).
8. J. R. Carlson, M. T. Yokoyama, and E. O. Dickinson, Induction of Pulmonary Edema and Emphysema in Cattle and Goats with 3-Methylindole, *Science*, 21: 298-299 (1972).
9. J. R. Carlson, E. O. Dickinson, M. T. Yokoyama, and B. J. Bradley, Pulmonary Edema and Emphysema in Cattle after Intraruminal and Intravenous Administration of 3-Methylindole, *Am. J. Vet. Res.*, 36: 1341-1347 (1975).
10. B. J. Bradley, J. R. Carlson, and E. O. Dickinson, Pulmonary Edema and Emphysema in Sheep Induced by Orally Administered 3-Methylindole, in preparation.
11. E. O. Dickinson, M. T. Yokoyama, J. R. Carlson, and B. J. Bradley, Induction of Pulmonary Edema and Emphysema in Goats by Intraruminal Administration of 3-Methylindole, *Am. J. Vet. Res.*, 37: 667-672 (1976).
12. A. C. Hammond and J. R. Carlson, 3-Methylindole Metabolite Excretion in Goats, *Proceedings, West. Sec., Am. Soc. Anim. Sci.*, 27: 332-334 (1976).
13. B. J. Bradley and J. R. Carlson, Effects of 3-Methylindole on Goat Lungs: Electron Microscopy, *Proceedings, West. Sec., Am. Soc. Anim. Sci.*, 27: 335-338 (1976).
14. R. G. Breeze, H. M. Pirie, C. O. Dawson, I. E. Selman, and A. Wiseman, The Pathology of Respiratory Diseases of Adult Cattle in Britain, *Folia Vet. Lat.*, 5: 95-128 (1975).
15. H. M. Pirie, R. G. Breeze, I. E. Selman, and A. Wiseman, Indole-Acetic Acid, 3-Methylindole and Type 2 Pneumocyte Hyperplasia in a Proliferative Alveolitis of Cattle, *Vet. Rec.*, 98: 259-260 (1976).
16. H. Witchi, Proliferation of Type II Alveolar Cells: A Review of Common Responses in Toxic Lung Injury, *Toxicology*, 5: 267-277 (1976).
17. M. J. Karnovsky, A Formaldehyde-Glutaraldehyde Fixative of High Osmolarity for Use in Electron Microscopy, *J. Cell Biol.*, 27: 137A-139A (1965).
18. W. J. Humphreys, B. O. Spurlock, and J. S. Johnson, Ethanol Cryofractography for SEM, in *Scanning Electron Microscopy/1974*, O. Johari and I. Corvin (Eds.), pp. 275-282, Proceedings of the 7th Annual Scanning Electron

Microscopy Symposium, IIT Research Institute, Chicago, April 8—11, 1974, Illinois Institute of Technology Research Institute, Chicago, 1974.
19. A. L. Cohen, Critical Point Drying, in *Scanning Electron Microscopy*, M. A. Hayat (Ed.), Chap. 1, pp. 44-112, Van Nostrand Reinhold Company, New York, 1974.
20. A. T. Mariassy, C. G. Plopper, and D. L. Dungworth, Characteristics of Bovine Lung as Observed by Scanning Electron Microscopy, *Anat. Rec.*, 183: 13-25 (1976).
21. T. M. Bray, J. A. Magnuson, and J. R. Carlson, Nuclear Magnetic Resonance Studies of Lecithin—Skatole Interaction, *J. Biol. Chem.*, 249: 914-918 (1974).
22. T. M. Bray, H. E. Sandberg, and J. R. Carlson, An EPR Study of Structural Perturbations Induced by 3-Methylindole in the Protein and Lipid Regions of Erythrocyte Membranes, *Biochim. Biophys. Acta*, 382: 534-538 (1975).
23. R. G. Breeze, E. B. Wheeldon, and H. M. Pirie, *Cell Function in the Mammalian Lung: The Trachea, Bronchi and Bronchioles*, College of Veterinary Medicine, University of Glasgow, Glasgow, Scotland.
24. F. M. Husby, Phospholipid and Surfactant Changes in Lung Tissue Associated with Tryptophan-Induced Interstitial Pulmonary Emphysema in Cattle, Ph. D. Thesis, Washington State University, Pullman, Washington, 1974.
25. S. L. Kauffman, P. H. Burri, and E. R. Weibel, The Postnatal Growth of the Rat Lung. II. Autoradiography, *Anat. Rec.*, 180: 63-76 (1974).
26. I. Y. R. Adamson and D. H. Bowden, The Type 2 Cell as Progenitor of Alveolar Epithelial Regeneration, *Lab. Invest.*, 30: 35-42 (1974).

INDEX

Prepared by E. Ray Bedford, Science and Technology Branch, Technical Information Center, Energy Research and Development Administration, Oak Ridge, Tennessee.

ERDA SYMPOSIUM SERIES *Available from National Technical Information Service, U. S. Department of Commerce, Springfield, Virginia 22161.*

Reactor Kinetics and Control (TID-7662), 1964, $6.00
Noise Analysis in Nuclear Systems (TID-7679), 1964, $6.00
Radioactive Fallout from Nuclear Weapons Tests (CONF-765), 1965, $6.00
Radioactive Pharmaceuticals (CONF-651111), 1966, $6.00
Neutron Dynamics and Control (CONF-650413), 1966, $6.00
Luminescence Dosimetry (CONF-650637), 1967, $6.00
Neutron Noise, Waves, and Pulse Propagation (CONF-660206), 1967, $6.00
Use of Computers in Analysis of Experimental Data and the Control of Nuclear Facilities (CONF-660527), 1967, $6.00
Compartments, Pools, and Spaces in Medical Physiology (CONF-661010), 1967, $6.00
Thorium Fuel Cycle (CONF-660524), 1968, $6.00
Radioisotopes in Medicine: In Vitro Studies (CONF-671111), 1968, $6.00
Abundant Nuclear Energy (CONF-680810), 1969, $6.00
Fast Burst Reactors (CONF-690102), 1969, $6.00
Biological Implications of the Nuclear Age (CONF-690303), 1969, $6.00
* **Radiation Biology of the Fetal and Juvenile Mammal** (CONF-690501), 1969, $10.00
Inhalation Carcinogenesis (CONF-691001), 1970, $6.00
* **Myeloproliferative Disorders of Animals and Man** (CONF-680529), 1970, $9.00
Medical Radionuclides: Radiation Dose and Effects (CONF-691212), 1970, $6.00
Morphology of Experimental Respiratory Carcinogenesis (CONF-700501), 1970, $6.00
Precipitation Scavenging (1970) (CONF-700601), 1970, $6.00
Neutron Standards and Flux Normalization (CONF-701002), 1971, $6.00
Survival of Food Crops and Livestock in the Event of Nuclear War (CONF-700909), 1971, $9.00
Biomedical Implications of Radiostrontium Exposure (CONF-710201), 1972, $6.00
Radiation-Induced Voids in Metals (CONF-710601), 1972, $9.00
Clinical Uses of Radionuclides: Critical Comparison with Other Techniques (CONF-711101), 1972, $13.60
Interactive Bibliographic Systems (CONF-711010), 1973, $7.60
* **Radionuclide Carcinogenesis** (CONF-720505), 1973, $13.60
Carbon and the Biosphere (CONF-720510), 1973, $10.60
Technology of Controlled Thermonuclear Fusion Experiments and the Engineering Aspects of Fusion Reactors (CONF-721111), 1974, $16.60
Thermal Ecology (CONF-730505), 1974, $13.60
* **The Cell Cycle in Malignancy and Immunity** (CONF-731005), 1975, $13.60
Mammalian Cells: Probes and Problems (CONF-731007), 1975, $7.60
Cooling Tower Environment—1974 (CONF-740302), 1975, $13.60
Mineral Cycling in Southeastern Ecosystems (CONF-740513), 1975, $13.60
* **Radiation and the Lymphatic System** (CONF-740930), 1976, $9.00
Atmosphere–Surface Exchange of Particulate and Gaseous Pollutants (1974) (CONF-740921), 1976, $13.60
Impact of Energy Production on Human Health: An Evaluation of Means for Assessment (CONF-751022), 1976, $6.75
Thermal Ecology II (CONF-750425), 1976, $11.00
Precipitation Scavenging (1974) (CONF-741003), 1977, $10.50
* **Biological Implications of Metals in the Environment** (CONF-750929), 1977, $10.50
* **Pulmonary Macrophage and Endothelial Cells** (CONF-760927), 1977, $12.50

---

* **Annual Hanford Biology Symposiums, Battelle-Northwest, Richland, Washington**